

This electronic thesis or dissertation has been downloaded from the King's Research Portal at <https://kclpure.kcl.ac.uk/portal/>



## Biosensors for the forensic detection of body fluids

Gooch, James Philip

*Awarding institution:*  
King's College London

The copyright of this thesis rests with the author and no quotation from it or information derived from it may be published without proper acknowledgement.

### END USER LICENCE AGREEMENT



**Unless another licence is stated on the immediately following page** this work is licensed

under a Creative Commons Attribution-NonCommercial-NoDerivatives 4.0 International

licence. <https://creativecommons.org/licenses/by-nc-nd/4.0/>

You are free to copy, distribute and transmit the work

Under the following conditions:

- Attribution: You must attribute the work in the manner specified by the author (but not in any way that suggests that they endorse you or your use of the work).
- Non Commercial: You may not use this work for commercial purposes.
- No Derivative Works - You may not alter, transform, or build upon this work.

Any of these conditions can be waived if you receive permission from the author. Your fair dealings and other rights are in no way affected by the above.

### Take down policy

If you believe that this document breaches copyright please contact [librarypure@kcl.ac.uk](mailto:librarypure@kcl.ac.uk) providing details, and we will remove access to the work immediately and investigate your claim.

# **Biosensors for the Forensic Detection of Body Fluids**

***James Gooch MRes***

*September 2018*

*A thesis incorporating publications  
submitted to the University of London for  
the degree of Doctor of Philosophy*

*King's College London*

## Acknowledgments

This work would not have been possible without the contributions made by the Metropolitan Police Forensic Services Directorate, the Home Office and the National Crime Agency.

I would first and foremost like to give sincere thanks to my first supervisor, Dr. Nunzianda Frascione. It is hard to put into words how grateful I am for your unwavering efforts, support and friendship. It has been an honour to work alongside such a brilliant academic and I hope that as the first of many PhD students, I did you proud. *Grazie mille per tutto, non so come avrei fatto senza di te!*

Huge thanks are also given to my second supervisor, Dr. Barbara Daniel. Thank you for always fighting for me and for giving me such a wonderful opportunity. Much like hundreds of previous MSc graduates, I would not be where I am today without your tireless efforts and dedication.

I would also like to thank Dr. Vincenzo Abbate for his expertise, guidance and technical support, Dr. David Ballard for his invaluable genetics advice and the team from DNA Analysis at King's for help with DNA profiling.

Special thanks are also given to all the members of King's Forensics, the Department of Analytical, Environmental and Forensic Sciences and the Institute of Pharmaceutical Science, who have made the last five years a truly wonderful experience, especially the present and past members of the postgraduate office.

Thank you to Dr. Magda Swędrowska. I could not have done this without you. *Jestem bardzo szczęśliwy, że mam Cię w swoim życiu.*

Finally, I would like to say thank you to all my family and friends. To my mother, father, sister and grandfather, who are my personal role models. This thesis is dedicated to my grandmother, who was not able to witness its completion but who always taught me that I can only do my best.

## Abstract

Body fluids may be considered the most important form of trace evidence within forensic analysis. The detection and identification of fluids, such as blood, semen and saliva, can often help advance criminal investigations by providing information on the nature of an offence, as well as a source of genetic material that may be used to construct a scientific link between an individual and a crime through DNA profiling.

However, current techniques used to locate and attribute the identity of fluids deposited at crime scenes are often disadvantaged by issues of low analytical specificity, detrimental effects on DNA recovery and an inability to be performed simultaneously as part of multiplex assays. This project therefore explores the use of fluorescent biosensors as novel strategies for the detection and identification of body fluids. Such sensors may have the potential to reduce overall fluid screening times by producing 'turn-on' fluorescence emissions in response to specific biological interactions with intra-fluidic targets.

As previous investigations into the ability of biosensors to detect analytes *in situ* remain limited, efforts were first made to establish the fluorescent sensing mechanisms exhibiting greatest potential for use as novel fluid analysis strategies. This was achieved by assessing the performance of four commercially available biosensing assays against targets deposited on a range of surfaces commonly encountered within forensic casework.

With biosensors based on enzymatic substrate digestion demonstrating ideal *in situ* detection ability during commercial assay testing, explorations were made into the application of previously reported fluorogenic peptide substrates specific to prostate specific antigen (PSA), kallikrein 8 and thrombin towards the detection of semen, saliva and blood respectively. Attempts to improve upon these assays were then conducted through the construction of custom substrates containing rhodamine-110 and cresyl violet fluorophores, using a novel solid-phase peptide synthesis route.



A displacement immunosensor specific to PSA was also developed via the conjugation of anti-PSA antibodies to highly-fluorescent quantum dot nanoparticles. Emissions from this antibody-nanoparticle complex were initially quenched through the moderate binding of a quencher-labelled peptide analogue to PSA. In the presence of the native PSA protein, this analogue is displaced, relieving quenching effects and restoring quantum dot fluorescence. This immunosensor complex was subsequently used to successfully detect nanomolar amounts of PSA within solution.

Attempts were also made in the construction of a multiplex fluid detection biosensor based on the displacement of fluorescently-labelled aptamers from graphene oxide. In this assay, emissions from three single-stranded DNA sequences, each labelled with a different fluorophore, were initially quenched upon adsorption to the surface of graphene nanosheets. These sequences, specific to the proteins thrombin, PSA and lysozyme, are then individually displaced as a result of target binding, producing emissions at particular wavelengths to indicate the type of target present. Efforts to increase the specificity of this aptasensor were then undertaken through the selection of novel aptamer sequences towards human sperm cells. Analysis of obtained aptamer pools using next generation sequencing and a novel bioinformatics pipeline successfully identified a number of promising sperm-cell binding ligands.

Forensic taggants, materials containing unique coding elements used for the monitoring of contact transfer during a criminal offence, were lastly developed using the fluorophore and peptide components employed for fluorogenic substrate construction. These materials exploit the particular amino acid sequence of incorporated peptides as identifiable 'codes' that may be registered to a specific taggant formulation. It is hoped that such components will eventually allow for the production of 'reactive' taggants containing biosensor molecules, which become fluorescent as a result of handling contact.

## Table of Contents

<b>Acknowledgments</b> .....	II
<b>Abstract</b> .....	III
<b>List of Figures</b> .....	X
<b>List of Tables</b> .....	XV
<b>List of Abbreviations</b> .....	XVI
 <b>Chapter 1 - Introduction</b> .....	 1
1.1 Biological Fluid Testing .....	2
1.2 Current Testing Strategies .....	3
1.3 Current Challenges .....	8
1.4 Recent Advances .....	10
1.4.1 Infrared Spectroscopy .....	11
1.4.2 Raman Spectroscopy .....	13
1.4.3 Hyperspectral Imaging .....	14
1.4.4 RNA Profiling .....	16
1.4.5 DNA Methylation Profiling .....	19
1.4.6 Metagenomic Analysis .....	22
1.4.7 Immunofluorescence .....	23
1.5 Biosensors .....	25
1.5.1 Enabling Biosensors for the Analysis of Biological Fluids .....	27
1.6 Project Aims and Objectives .....	29
 <b>Chapter 2 - Biosensors</b> .....	 32
2.1 Introduction .....	33
2.2 Review of Fluorescent Biosensors .....	34
2.2.1 Environmentally-Sensitive Fluorophores .....	34
2.2.2 FRET-based Biosensing .....	35
2.2.2.1 Intramolecular FRET .....	36
2.2.2.2 Intermolecular FRET .....	38
2.2.3 Static Quenching-based Biosensing .....	40
2.3 Materials and Methods .....	42
2.3.1 Reagents .....	42
2.3.2 Slide Microscopy .....	43

2.3.3 Surface Microscopy .....	44
2.3.4 Image Analysis.....	45
2.3.5 Blood Collection and Storage.....	46
2.3.6 DNA Profiling .....	46
2.4 Results and Discussion.....	47
2.4.1 Commercial Assay Selection .....	47
2.4.2 Slide Microscopy.....	48
2.4.3 Surface Microscopy .....	50
2.4.4 DNA profiling.....	53
2.5 Conclusion .....	54
<b>Chapter 3 - Fluorogenic Substrates .....</b>	<b>56</b>
3.1 Introduction .....	57
3.2 Review of Fluorogenic Substrates .....	58
3.2.1 Transduction Mechanism .....	58
3.2.2 Previously Reported Fluorogenic Substrates .....	60
3.3 <i>Published Article 1: 'Application of Fluorescent Substrates to the in situ Detection of Prostate Specific Antigen'</i> .....	61
3.3.1 Manuscript .....	61
3.4 <i>Published Article 2: 'Solid-phase Synthesis of Rhodamine-110 Fluorogenic Substrates and their Application in Forensic Analysis'</i> .....	73
3.4.1 Manuscript .....	74
3.4.2 Supplementary Information .....	82
3.5 <i>Published Article 3: 'Fluorogenic Substrates for the Detection of Saliva'</i> ....	90
3.5.1 Manuscript .....	90
3.6 Fluorogenic Substrates for the Detection of Blood.....	95
3.6.1 Materials and Methods.....	95
3.6.1.1 Reagents.....	95
3.6.1.2 Body Fluid Collection and Storage .....	96
3.6.1.3 Commercial Substrate Testing.....	96
3.6.1.3.1 Spectrofluorometry.....	96
3.6.1.3.2 Slide Microscopy .....	97
3.6.1.3.3 DNA Profiling .....	97
3.6.1.4 Custom Substrate Synthesis and Testing .....	98
3.6.1.4.1 Resin-CV-NH2 .....	98

3.6.1.4.2 Resin-CV-R(Pbf)-OH.....	98
3.6.1.4.3 Resin-CV-R(Pbf)VF-Bz .....	99
3.6.1.4.4 Ac-CV-RVF-Bz .....	99
3.6.1.4.5 Spectrofluorometry.....	100
3.6.2 Results and Discussion.....	101
3.6.2.1 Commercial Substrate Testing.....	101
3.6.2.1.1 Spectrofluorometry.....	101
3.6.2.1.2 Slide Microscopy .....	102
3.6.2.1.3 DNA Profiling .....	103
3.6.2.2 Custom Substrate Synthesis and Testing .....	104
3.6.2.2.1 Substrate Synthesis .....	104
3.6.2.2.2 Spectrofluorometry.....	107
3.6.3 Conclusion .....	108
<b>Chapter 4 - Immunosensors.....</b>	<b>110</b>
4.1 Introduction .....	111
4.2 Review of Displacement Immunosensors .....	112
4.2.1 Transduction Mechanism .....	112
4.2.2 Quantum Dot Nanoparticles.....	113
4.3 Materials and Methods.....	114
4.3.1 Reagents.....	114
4.3.2 Body Fluid Collection and Storage .....	115
4.3.3 DVCAQV-NH <sub>2</sub> .....	115
4.3.4 Biacore Analysis .....	116
4.3.5 BHQ-3-DVCAQV-NH <sub>2</sub> .....	116
4.3.6 Antibody-QDot Conjugation .....	117
4.3.7 Displacement Assay .....	117
4.3.8 DNA Profiling .....	118
4.4 Results and Discussion.....	118
4.4.1 Immunosensor Design .....	118
4.4.2 Quenching Peptide Synthesis .....	120
4.4.3 Biacore Analysis .....	121
4.4.4 Antibody-QDot Conjugation .....	123
4.4.5 Displacement Assay .....	124

4.4.6 DNA Profiling .....	125
4.5 Conclusion .....	126
<b>Chapter 5 - Aptasensors .....</b>	<b>128</b>
5.1 Introduction .....	129
5.2 <i>Published Article 4: 'Developing Aptasensors for Forensic Analysis'</i> .....	130
5.2.1 Manuscript .....	130
5.3 Graphene Oxide Displacement Multiplex Sensor.....	155
5.3.1 Materials and Methods.....	157
5.3.1.1 Reagents.....	157
5.3.1.2 Body Fluid Collection and Storage .....	157
5.3.1.3 GO Quenching .....	158
5.3.1.4 Buffer Optimisation .....	158
5.3.1.5 Quencher Optimisation .....	159
5.3.1.6 Purified Protein and Whole Fluid Spectrofluorometry .....	159
5.3.1.7 Multiplex Spectrofluorometry.....	160
5.3.2 Results and Discussion.....	160
5.3.2.1 GO Quenching .....	160
5.3.2.2 Buffer Optimisation .....	162
5.3.2.3 Quencher Optimisation .....	164
5.3.2.4 Purified Protein and Whole Fluid Spectrofluorometry .....	166
5.3.2.5 Multiplex Spectrofluorometry.....	170
5.3.3 Conclusion .....	172
5.4 Aptamer Selection against Human Sperm Cells .....	172
5.4.1 Materials and Methods.....	173
5.4.1.1 Reagents.....	173
5.4.1.2 Body Fluid Collection and Storage .....	175
5.4.1.3 Cell Isolation .....	175
5.4.1.4 Incubation and Elution .....	175
5.4.1.5 PCR Amplification .....	176
5.4.1.6 Strand Separation .....	178
5.4.1.7 Flow Cytometry .....	179
5.4.1.8 Next Generation Sequencing and Data Analysis .....	180
5.4.2 Results and Discussion.....	181

5.4.2.1 Aptamer Selection.....	181
5.4.2.2 Flow Cytometry .....	184
5.4.2.3 Next Generation Sequencing and Data Analysis .....	185
5.4.3 Conclusion .....	191
<b>Chapter 6 - Taggants</b> .....	192
6.1 Introduction .....	193
6.2 <i>Published Article 5: 'Taggant Materials in Forensic Science: A Review'</i> ...	194
6.2.1 Manuscript .....	195
6.3 <i>Published Article 6: 'Establishing Evidence of Contact Transfer in Criminal Investigation by a Novel 'Peptide Coding' Reagent'</i> .....	210
6.3.1 Manuscript .....	210
6.4 <i>Published Article 7: 'Monitoring Criminal Activity through Invisible Fluorescent 'Peptide Coding' Taggants'</i> .....	223
6.4.1 Manuscript .....	224
<b>Chapter 7 - Discussion and Conclusion</b> .....	237
7.1 Biosensors .....	238
7.2 Fluorogenic Substrates .....	240
7.3 Immunosensors .....	244
7.4 Aptasensors .....	245
7.5 Taggants .....	248
7.6 Future Work .....	249
7.7 Final Remarks.....	251
<b>References</b> .....	253
<b>Appendix</b> .....	296
A.1 Fluorogenic Substrates for the Detection of Blood .....	297
A.2 'Establishing Evidence of Contact Transfer in Criminal Investigation by a Novel 'Peptide Coding' Reagent' .....	301
A.3 'Monitoring Criminal Activity through Invisible Fluorescent 'Peptide Coding' Taggants' .....	305
<b>Published Articles</b> .....	313

## List of Figures

<b>Figure 1:</b> Typical NIR spectra of urine, semen and vaginal fluid samples.....	12
<b>Figure 2:</b> An illustration of hypercube construction. ....	15
<b>Figure 3:</b> Scheme of body fluid detection using fluorescently-labelled antibodies conjugated to magnetic nanoparticles.....	24
<b>Figure 4:</b> Types of spectral emission change upon sensor-target interaction ..	28
<b>Figure 5:</b> Ideal application of biosensors to the detection of body fluids.. ....	29
<b>Figure 6:</b> Chemical structure of PicoGreen® .....	34
<b>Figure 7:</b> Examples of intramolecular FRET sensing mechanisms. ....	37
<b>Figure 8:</b> Examples of intermolecular FRET sensing transductions.....	39
<b>Figure 9:</b> Examples of static quenching-based sensors.....	41
<b>Figure 10:</b> Instrumental set-up for evaluating <i>in situ</i> sensor performance.....	44
<b>Figure 11:</b> Semi-quantitative analysis of <i>in situ</i> biosensor assay fluorescence using Adobe Photoshop™ software.....	45
<b>Figure 12:</b> Demonstration of <i>in situ</i> commercial assay performance against six concentrations of wet and dry analyte deposits on glass slides. ....	49
<b>Figure 13:</b> Percentage fluorescence increase of commercial assays upon <i>in situ</i> application to analytes on ten forensically relevant surfaces.....	51
<b>Figure 14:</b> STR profiles generated from blood samples after commercial biosensor application. ....	54
<b>Figure 15:</b> Scheme of fluorogenic substrate sensing mechanism. ....	60
<b>Figure 16:</b> PSA fluorogenic substrate structure.....	65
<b>Figure 17:</b> Fluorogenic PSA substrate emission in response to different dilutions of seminal fluid. ....	69
<b>Figure 18:</b> Demonstration of <i>in situ</i> PSA substrate testing against seminal depositions upon glass slides .....	70
<b>Figure 19:</b> Successful detection of human semen across eight forensically relevant surfaces by fluorogenic PSA substrate.....	71
<b>Figure 20:</b> Genetic profiles generated from semen reference profile and semen sample with applied PSA substrate.....	72
<b>Figure 21:</b> Schematic of Rh-110 PSA substrate development .....	76
<b>Figure 22:</b> Fluorescence response of substrate Ac-Rh-110-QLKSSH-Ac to concentrations of PSA protein and seminal fluid dilutions over time. ....	79
<b>Figure 23:</b> Detection of semen across six surfaces by substrate Ac-Rh-110-QLKSSH-Ac.....	80

<b>Figure 24:</b> ESI-MS data demonstrating free Rhodamine-110 presence after cleavage from a solid support. ....	83
<b>Figure 25:</b> ESI-MS data demonstrating successful Resin-Rhodamine-110-Glutamine conjugation after 'soft' cleavage from a solid support .....	84
<b>Figure 26:</b> HPLC data demonstrating purity of substrate product Ac-Rh-110-QLKSSH-Ac.....	85
<b>Figure 27:</b> High-resolution MS data of substrate product Ac-Rh-110-QLKSSH-Ac.....	86
<b>Figure 28:</b> Fluorescence response of Ac-Rh-110-QLKSSH-Ac to concentrations of Proteinase K, Aminopeptidase M, Trypsin and PSA. ....	87
<b>Figure 29:</b> Fluorescence response of substrate Ac-Rh-110-QLKSSH-Ac after incubation with blood and saliva. ....	88
<b>Figure 30:</b> Generated STR profiles from human semen sample treated with substrate Ac-Rh-110- QLKSSH-Ac and reference human semen sample .....	89
<b>Figure 31:</b> KLK8 fluorogenic substrate structure.....	92
<b>Figure 32:</b> Fluorescence response of Boc-VPR-AMC and Ac-VPR-Rh-110-Ac to saliva dilutions deposited on glass slides.....	94
<b>Figure 33:</b> Fluorescence response of substrate Bz-FVR-AMC over time to different dilutions of plasma and whole blood.. ....	102
<b>Figure 34:</b> Demonstration of <i>in situ</i> Bz-FVR-AMC substrate testing of plasma depositions upon glass slides across a range of eight dilutions.....	103
<b>Figure 35:</b> STR profiles generated from whole blood samples containing Bz-FVR-AMC and thrombin triggering solution, and SDW. ....	104
<b>Figure 36:</b> Scheme of solid phase peptide synthesis of cresyl violet based thrombin substrate. ....	105
<b>Figure 37:</b> Confirmation of substrate product Ac-CV-RVF-Bz purity and identity as established by RP-HPLC and ESI-MS respectively. ....	106
<b>Figure 38:</b> Fluorescence response of Ac-CV-RVF-Bz over time to different concentrations of purified thrombin protein.. ....	108
<b>Figure 39:</b> PSA immunosensor assembly. ....	113
<b>Figure 40:</b> Normalised spectral overlap of BHQ-3 absorption compared to 605 and 625 nm QDot emissions.....	119
<b>Figure 41:</b> Structure of quenching peptide BHQ-3-DVCAQV-NH <sub>2</sub> . ....	120
<b>Figure 42:</b> MS of peptide DVCAQV-NH <sub>2</sub> .....	121
<b>Figure 43:</b> Schematic representation of Biacore affinity analysis. ....	122
<b>Figure 44:</b> Agarose gel demonstrating the separation of unconjugated QDots, SMCC-activated QDots and anti-PSA antibody-QDot conjugates. ....	123



<b>Figure 45:</b> Fluorescence emissions of antibody-QDot conjugates before and after incubation with quencher-labelled peptides. ....	124
<b>Figure 46:</b> Fluorescence emissions of antibody-QDot conjugates incubated with quencher-labelled peptide before and after PSA addition. ....	125
<b>Figure 47:</b> STR profiles generated from seminal fluid samples containing immunosensors and sterile distilled water .....	126
<b>Figure 48:</b> Workflow of the Illumina sequencing-by-synthesis approach.....	138
<b>Figure 49:</b> Schema of various aptamer-based sensing formats.....	143
<b>Figure 50:</b> Schema of a FRET-based aptasensor for the detection of thrombin developed by Wang <i>et al.</i> ....	148
<b>Figure 51:</b> Schema of a colorimetric Au-NP aptasensor for the detection of methamphetamine developed by Yarbakht and Nikkhah.....	150
<b>Figure 52:</b> Schema of a graphene-quenching fluorescence aptasensor for the detection of ochratoxin A developed by Sheng <i>et al.</i> ....	151
<b>Figure 53:</b> Schema of an optical fibre-based aptasensor for the detection of TNT developed by Ehrentreich-Förster <i>et al.</i> ....	154
<b>Figure 54:</b> GO multiplex displacement aptasensor design.....	157
<b>Figure 55:</b> Fluorescence emissions of Cy5, 6-FAM and ROX-labeled aptamers before and after the addition of GO.....	161
<b>Figure 56:</b> Fluorescence emissions of aptamers before and after GO addition in the presence of varying concentrations of MgCl <sub>2</sub> .....	163
<b>Figure 57:</b> Fluorescence emission intensities of aptamers after incubation with varying concentrations of GO .....	165
<b>Figure 58:</b> Emission intensities of GO-aptamer complexes after incubation with varying concentrations of relevant purified protein targets.....	167
<b>Figure 59:</b> Emission intensities of GO-aptamer complexes after incubation with varying concentrations of relevant whole fluid targets.....	168
<b>Figure 60:</b> Fluorescence intensities of multiplex GO-aptasensors after incubation with a various protein targets and body fluids.....	171
<b>Figure 61:</b> Microscopic examination of haemotoxylin and eosin-stained sperm cells pre- and post-isolation using density gradient centrifugation .....	181
<b>Figure 62:</b> Gel electrophoresis images of trial and preparative amplifications from the 4th round of aptamer selection. ....	182
<b>Figure 63:</b> Concentrations of ssDNA recovered after strand separation from each round of the Cell-SELEX process.....	183
<b>Figure 64:</b> Flow cytometry histograms of sperm cells incubated with enriched aptamer pools obtained from round 4, 7, 10 and 14 of selection and N40 library template sequences.....	185

<b>Figure 65:</b> Scheme of the developed Cell-SELEX Galaxy pipeline and example data outputs. ....	187
<b>Figure 66:</b> Total number of NGS reads obtained from sequenced aptamer pool samples before and after data processing .....	189
<b>Figure 67:</b> The four main applications of forensic taggants.....	196
<b>Figure 68:</b> The different components of forensic taggants .....	198
<b>Figure 69:</b> The main types of coding used for taggant identification. ....	199
<b>Figure 70:</b> Schematic of peptide-based taggant application and analysis.....	208
<b>Figure 71:</b> Demonstration of peptide taggant recovery and analysis. ....	214
<b>Figure 72:</b> Quantitative analysis of MHF and lubricant transfer rates from forensically relevant surfaces through touch contact. ....	218
<b>Figure 73:</b> Positive ESI-MS spectrum of synthesised peptide Ac-HSSKL.....	219
<b>Figure 74:</b> ESI-MS spectra of Ac-KQQSP-NH <sub>2</sub> , Ac-HSSKL-COOH and Ac-hsskl-COOH samples extracted six weeks after application to paper.....	232
<b>Figure 75:</b> ESI-MS spectrum of Ac-KQQSP-NH <sub>2</sub> and Rhodamine-110 samples applied to glass slides and incubated for six weeks.....	234
<b>Figure 76:</b> Peptide coding reagent successfully transferred upon physical contact .....	235
<b>Figure 77:</b> Schemes of unsuccessful substrate development attempts .....	242
<b>Figure 78:</b> Normalised spectral overlap of haemoglobin absorption compared to CV emissions.....	243
<b>Figure 79:</b> Fluorescence emissions of anti-MUC5B antibody-QDot conjugates after incubation with quencher-labelled peptide.....	245
<b>Figure 80:</b> Thrombin molecular aptamer beacon design.....	247
<b>Figure 81:</b> Confirmation of substrate product $\alpha$ HN-CV-NH <sub>2</sub> purity and identity as established by RP-HPLC and ESI-MS respectively. ....	297
<b>Figure 82:</b> Confirmation of substrate product $\alpha$ HN-CV-R-Fmoc purity and identity as established by RP-HPLC and ESI-MS respectively. ....	298
<b>Figure 83:</b> Confirmation of substrate product $\alpha$ HN-CV-RVF-Bz purity and identity as established by RP-HPLC and ESI-MS respectively. ....	299
<b>Figure 84:</b> Confirmation of substrate product Ac-CV-RVF-Bz purity and identity as established by RP-HPLC and ESI-MS respectively. ....	300
<b>Figure 85:</b> Microscopy images of four chosen media transferred from different surfaces after 0, 6 and 24 hr from application. ....	301
<b>Figure 86:</b> Mass spectra obtained from MHF extracts after primary transfer of reagent containing 5 mg, 2.5 mg and 1 mg of peptide. ....	302

<b>Figure 87:</b> Fluorescence microscopy images obtained after mixing different concentrations of AFC and Rhodamine-110 with MHF. ....	303
<b>Figure 88:</b> Mass spectrum of the reagent containing both fluorophore (Rh-110) and peptide (Ac-HSSKL) after liquid/liquid extraction. ....	303
<b>Figure 89:</b> Mass spectra of peptide reagent samples extracted six weeks after application to surfaces. ....	304
<b>Figure 90:</b> ESI-MS spectra of Ac-KQQSP-NH <sub>2</sub> , Ac-HSSKL-COOH and Ac-hsskl-COOH after synthesis.....	305
<b>Figure 91:</b> ESI-MS spectra of Ac-KQQSP-NH <sub>2</sub> samples extracted six weeks after application to surfaces. ....	306
<b>Figure 92:</b> ESI-MS spectra of Ac-HSSKL-COOH samples extracted six weeks after application to surfaces. ....	306
<b>Figure 93:</b> ESI-MS spectra of Ac-hsskl-COOH samples extracted six weeks after application to surfaces. ....	307
<b>Figure 94:</b> ESI-MS spectra of Ac-KQQSP-NH <sub>2</sub> , Ac-HSSKL-COOH and Ac-hsskl-COOH extracted after exposure to 4°C or 39°C for six weeks .....	308
<b>Figure 95:</b> ESI-MS spectra of Ac-KQQSP-NH <sub>2</sub> , Ac-HSSKL-COOH and Ac-hsskl-COOH extracted after exposure to 70% or 90% humidity for six weeks	308
<b>Figure 96:</b> ESI-MS spectra of Ac-KQQSP-NH <sub>2</sub> and Rhodamine-110 samples extracted after exposure to all experimental conditions. ....	309
<b>Figure 97:</b> ESI-MS spectra of Ac-HSSKL-COOH and Rhodamine-110 samples extracted after exposure to all experimental conditions. ....	310
<b>Figure 98:</b> ESI-MS spectra of Ac-hsskl-COOH and Rhodamine 110 samples extracted after exposure to all experimental conditions .....	311
<b>Figure 99:</b> ESI-MS spectra of Ac-HSSKL-COOH and Rhodamine 110 samples extracted from the surface of a finger after one, two, three, four and five contacts. ....	312

## List of Tables

<b>Table 1:</b> Techniques currently used for the detection of latent body fluids. ....	4
<b>Table 2:</b> Techniques currently used for the attribution of body fluids.....	6
<b>Table 3:</b> mRNA markers used in body fluid identification multiplex assays. ....	17
<b>Table 4:</b> A selection of biosensors developed for use in forensic analysis .....	26
<b>Table 5:</b> Analyte concentrations used for <i>in situ</i> commercial assay testing. ....	43
<b>Table 6:</b> Microscopy parameters used for <i>in situ</i> commercial assay testing. ....	43
<b>Table 7:</b> A list of pro-fluorophores used within fluorogenic substrate assays. ..	59
<b>Table 8:</b> Fluorogenic substrates previously developed for protease detection. ....	61
<b>Table 9:</b> SELEX protocols used to select aptamers .....	135
<b>Table 10:</b> Techniques used to determine the affinity of aptamers. ....	140
<b>Table 11:</b> ssDNAs used to construct a GO displacement aptasensor. ....	157
<b>Table 12:</b> Protein concentrations/ fluid dilutions used for aptasensor tests. ...	159
<b>Table 13:</b> Reaction mixed used for pre, trial and preparative PCRs.....	177
<b>Table 14:</b> Cycling conditions used for pre, trial and preparative PCRs.....	177
<b>Table 15:</b> Cycling conditions used for NGS sample preparation. ....	181
<b>Table 16:</b> Sequences from round 14 of selection exhibiting over 25 reads. ...	190
<b>Table 17:</b> Commercially available forensic taggants .....	200
<b>Table 18:</b> Advantages and disadvantages of commercial taggants.....	206
<b>Table 19:</b> Peptide characteristics obtained from Genscript .....	231

## List of Abbreviations

AFC	- 7-amino-4-trifluoromethylcoumarin
AMC	- 7-amino-4-methylcoumarin
ALS	- Alternate light source
AP	- Acid phosphatase
BHQ-3	- Black hole quencher 3
CE	- Capillary electrophoresis
CP	- Conjugated polymer
CV	- Cresyl violet
ESI	- Electrospray ionization
FRET	- Förster resonance energy transfer
GO	- Graphene Oxide
HSI	- Hyperspectral imaging
HPLC	- High-performance liquid chromatography
HTF	- Human tubal fluid
ICT	- Intramolecular charge transfer
IR	- Infrared
ITC	- Isothermal titration calorimetry
KCL	- King's College London
MALDI-TOF	- Matrix-assisted laser desorption-ionization time of flight
MHF	- Mixed hydrocarbon formulation
MIP	- Molecularly imprinted polymer
MIR	- Mid-infrared
MS	- Mass spectrometry
mRNA	- Messenger RNA
NGS	- Next generation sequencing
NIR	- Near-infrared
PCR	- Polymerase chain reaction
PSA	- Prostate specific antigen
QDot	- Quantum Dot
RPM	- Revolutions per minute
Rh-110	- Rhodamine 110
RT-PCR	- Reverse transcriptase-polymerase chain reaction

SD - Standard deviation

SDW - Sterile distilled water

SELEX - Systematic evolution of ligands by exponential enrichment

SNP - Single nucleotide polymorphism

SPPS - Solid-phase peptide synthesis

SPR - Surface plasmon resonance

STR - Short tandem repeat

# Chapter 1

## Introduction

## 1.1 Biological Fluid Testing

Biological fluids represent one of the most important types of trace evidence in forensic casework. The detection and identification of fluids, such as blood, semen and saliva, may be of enormous evidential value to a case, both in terms of investigative information and personal identification. This importance is reflected by the fact that over 90% of the items submitted each year to the Evidence Recovery Unit of the Metropolitan Police Service (the largest police force in the UK) are tested for the presence of body fluids (Metropolitan Police Service, personal communication, 2013).

Biological fluids may allow investigators to learn more about the specific nature of an offence. For example, establishing the presence of seminal fluid at a scene may help determine if a crime should be investigated as a sexual assault, rather than a physical one. The location and morphology of biological fluid stains can also provide information on the actions and movements of individuals/objects during an offence. In fact, the entire discipline of forensic Blood Pattern Analysis (BPA) is dedicated to the reconstruction of events based on the shape and directionality of bloodstains found at crime scenes.

Body fluids also have significant value in forensic casework as a major source of DNA. The analysis of genetic material contained in fluids can allow investigators to draw scientific links between individuals and an offence with great reliability. In 2016/17, DNA profiling technologies were used to match over 31,000 DNA samples recovered from crime scenes to profiles present on the UK National DNA Database (NDNAD) [1]. DNA analysis techniques have been expanded upon in recent years to also provide phenotypic information directly from fluid samples. Assays based on the analysis of single nucleotide polymorphism (SNP) markers have now been developed for the prediction of an individual's externally visible characteristics (including hair/eye colour and geographic ancestry) and



may be used for the identification of potential fluid donors that cannot be matched via traditional DNA typing [2].

However, obtaining such sources of DNA can be a significant challenge, as fluids left behind during a criminal offence are often difficult to detect. Many fluid traces are deposited at scenes in extremely low amounts (often in microlitre or lower volumes) or may be heavily diluted as a result of mixing with other body fluids or liquid substances. Most fluids (including semen, saliva, urine, vaginal secretions and sweat) are also transparent, making them difficult to observe against black or dark-coloured backgrounds. In some instances, the perpetrators of a crime may attempt to remove, wash or disguise fluid stains to avoid detection [3].

## **1.2 Current Testing Strategies**

The first stage of the body fluid detection process involves the visual inspection of an item for any areas of potential fluid staining. This inspection requires a considerable amount of time to conduct, as every area of the item must be examined in detail using the naked eye and/or optical microscopy. Furthermore, because of the challenges listed in **Section 1.1**, it is still possible for forensic scientists to miss vital fluid evidence during this process.

Several tools have been developed to facilitate fluid detection. Alternate light sources (ALS) are devices that may be used to visualise some latent fluids by providing greater contrast between a stain and the surface on which it is deposited. These devices produce fixed wavelengths of ultraviolet, visible or infrared radiation that can be absorbed by specific molecules present within biological fluids. In some instances (particularly in the case of blood), this absorption will cause stains to appear darker in comparison to their surrounding background. However, some molecules present in semen, saliva and urine, may become excited by ALS radiation and emit their own light (at a longer wavelength than the original source), making the fluids fluorescent [4]. Some of the chemical tests used to establish the identity of a fluid (which are discussed in more detail later

within this section) also possess the ability to detect areas of latent staining. A comprehensive list of the techniques currently used to detect each type of body fluid may be found in **Table 1**.

**Table 1:** Techniques currently used for the detection of latent biological fluid stains.

Fluid	Test	Type	Notes	Ref.
Blood	ALS	Spectroscopic	Blood appears as dark spots when exposed to an ALS wavelength of 415 nm.	[4]
	Luminol	Chemical	Haemoglobin acts as a catalyst in a reaction between luminol and an oxidant (typically H <sub>2</sub> O <sub>2</sub> ) to produce chemiluminescence.	[5]
	Bluestar®	Chemical	A proprietary luminol formulation containing H <sub>2</sub> O <sub>2</sub> and NaOH, offering greater detection sensitivity and signal strength.	[6]
	Fluorescein	Chemical	Reduced fluorescein (fluorescein) is oxidised by H <sub>2</sub> O <sub>2</sub> in the presence of haemoglobin, producing fluorescence at 521 nm.	[7]
	Hemascein®	Chemical	A commercial preparation of fluorescein, NaOH and zinc with greater shelf life than traditional fluorescein formulations.	[8]
	Lumiscene®	Chemical	A proprietary mixture of both luminol and fluorescein, producing chemiluminescence at a wavelength of 525 nm.	[9]
Semen	ALS	Spectroscopic	Choline and Flavin-conjugated proteins cause semen to strongly fluoresce under UV and visible excitation.	[4]
	AP Press Test	Chemical	Moist paper sheets are applied to items and treated with a solution containing α-naphthyl phosphate and brentamine salts, which turns purple in the presence of acid phosphatase (AP).	[10]
Saliva	ALS	Spectroscopic	Fluoresces weakly upon UV and visible excitation. Molecules responsible for emission have yet to be identified.	[4]
	Phadebas® Press Test	Chemical	Commercially available paper sheets impregnated with starch microspheres that can be placed over items. Digestion of spheres by salivary amylase causes a blue dye to be released.	[11]
Vaginal Fluid	None	N/A	No methods currently accepted for use in forensic casework.	N/A
Urine	ALS	Spectroscopic	Exhibits weak fluorescence at multiple ALS wavelengths.	[4]
Sweat	None	N/A	No methods currently accepted for use in forensic casework.	N/A

Several high-profile UK criminal cases have served to highlight the potential miscarriages of justice that can occur as a result of missed fluid evidence. The most prominent of these involved the racially motivated

murder of British teenager Stephen Lawrence by a group of individuals in 1993. As part of the initial investigation, clothing seized from six men accused of the murder was subjected to two forensic screenings (one in 1993 and another in 1995) for the presence of blood, both yielding negative results. However, in a re-examination of all forensic evidence as part of a cold case review started in 2006, a previously missed blood spot was discovered dried into the fibres of a jacket belonging to one of the suspects. Identified through DNA profiling as having originated from Stephen Lawrence, this blood (along with other forensic evidence) was used to convict two of the perpetrators in 2012, almost 20 years after the murder had taken place.

In some cases, characterising the type of body fluid present is equally as important as detection. For example, in an instance of alleged sexual assault in which DNA from a suspect is found on the surface of the victim's skin, a defendant may argue that such DNA may have been indirectly transferred from saliva present on surface of their hands. However, if that DNA is proven to have instead originated from seminal fluid, evidence that a sexual assault did take place will be significantly stronger. Although not always possible, DNA evidence is much more useful to the courts if its origins can be attributed at the 'source-level' (i.e. to a specific biological fluid) [12].

Many assays are available to the forensic scientist for the purpose of body fluid attribution. These tests vary significantly in their mechanism of action as well as their specificity, sensitivity and ease of operation. Assays are often classified as to whether they are 'presumptive' or 'confirmatory' in nature. Presumptive tests are those only able to indicate that a fluid may be present or establish the absence of a fluid from a sample. These assays cannot be used to conclusively identify a fluid species as they may also positively react in the presence of non-body fluid substances or cross react with different fluid types [3]. In contrast, confirmatory tests are able to discriminate fluids with a higher degree of certainty. Presumptive tests are inexpensive and rapid to perform and are

**Table 2:** Techniques currently used within forensic casework for the attribution of body fluids.

Fluid	Test	Type	Specificity	Notes	Ref.
Blood	Hemastix®	Chemical	Presumptive	Plastic test strips coated at one end with H <sub>2</sub> O <sub>2</sub> and Tetramethylbenzidine (TMB) impregnated filter paper. Haemoglobin catalysis causes paper to change blue/green.	[13]
	Kastle-Meyer	Chemical	Presumptive	A colourless reduced form of Phenolphthalein is oxidised by H <sub>2</sub> O <sub>2</sub> in the presence of haemoglobin to produce an intense pink colouration. Usually applied to a swab or filter paper that has been rubbed over the surface of a suspected stain.	[14]
	LMG	Chemical	Presumptive	Oxidation of colourless Leucomalachite Green to Malachite Green by H <sub>2</sub> O <sub>2</sub> occurs in the presence of haemoglobin, resulting in a blue-green colour.	[15]
	ABAcad®	Immunological	Presumptive	Dye-labelled haemoglobin-antibody complexes are formed after the addition of extracted blood-stains to an immunochromatographic cartridge. These complexes migrate through the device to a 'test' zone and are captured by a second anti-haemoglobin antibody. A coloured line produced as a result of dye aggregation is used to indicate a positive result on the surface of the cartridge.	[16]
	HemaTrace®/				[17]
	Hexagon OBTI/				[18]
	SERATEC®				
	HemDirect®				
	RSID™ - Blood	Immunological	Presumptive	Immunochromatographic cartridge targeting red blood cell protein Glycophorin A.	[19]
	Takayama	Crystal	Confirmatory	Heating of a bloodstain treated with pyridine and glucose under alkaline conditions causes the formation of pink, needle-shaped crystals made of pyridine ferroprotoporphyrin. Crystals may be observed using bright-field microscopy.	[20]
	Teichmann	Crystal	Confirmatory	Brown hematin crystals are formed by heating a dried bloodstain in the presence of glacial acetic acid and a halide, which can be observed microscopically.	[21]
	Microscopy	Visual	Confirmatory	The visual identification of red blood cells, white blood cells and fibrin within a liquid fluid sample may be used to confirm the presence of blood.	[3]
Semen	AP Test	Chemical	Presumptive	A reagent containing α-naphthyl phosphate and a diazonium salt is applied to filter paper or swabs that have been rubbed over a suspected semen stain. Hydrolysis of α-naphthyl phosphate by seminal acid phosphatase produces a purple azo dye.	[22]
	ABAcad® p30/	Immunological	Presumptive	Immunochromatographic cartridges targeting the seminal fluid protein prostate specific antigen. Have been shown to cross react with urine, vaginal fluid and breast milk.	[23]
	Biosign® PSA/				[24]
	SERACTEC®				[25]
	PSA Semiquant				

Body Fluid	Test	Type	Specificity	Notes	Ref.
Semen (Cont.)	RSID™ - Semen	Immunological	Presumptive	Immunochromatographic cartridges targeting the seminal fluid protein semenogelin.	[26]
	Microscopy	Visual	Confirmatory	The microscopic identification of spermatozoa may be used to confirm semen presence. Cell staining reagents may be utilised to facilitate observation. These include the Christmas tree and hematoxylin-eosin cytological stains.	[3]
Saliva	Phadebas®	Chemical	Presumptive	A propriety product (produced in tablet or paper form) containing starch microspheres labelled with and insoluble blue dye. Spheres are digested in the presence of salivary $\alpha$ -amylase, releasing the dye, which can be identified visually or by using a spectrophotometer at 620 nm.	[27]
	RSID™ - Saliva/ SERATEC® Amylase	Immunological	Presumptive	Immunochromatographic cartridges targeting the salivary protein $\alpha$ -amylase. Have been shown to cross react with urine, semen and breast milk.	[28] [29]
	SALigAE®	Unknown	Presumptive	A commercially available colorimetric assay for the detection of saliva. The exact mechanism of the test has not been disclosed. Stain extracts are added to a glass vial containing the SALigAE® solution, which turns yellow within 10 minutes in the presence of salivary $\alpha$ -amylase.	[30]
Vaginal Fluids	None	N/A	N/A	No methods currently accepted for use in forensic casework.	N/A
Urine	DMAC	Chemical	Presumptive	Suspected urine stains are extracted onto filter paper using distilled water before a drop of 0.05-0.1% para-dimethylaminocinnamaldehyde (DMAC) solution is applied. Ammonia, released in the breakdown of urea by the enzyme urease, reacts with the DMAC compound, resulting in a pink colour change after 30 min.	[31]
	Uritrace®	Chemical	Presumptive	Lateral flow cartridges containing reagent strips impregnated with picric acid. Creatinine from urine extracts added to the cartridge reacts with the acid, forming creatinine picrate and causing the strips to turn from yellow to orange.	[32]
	RSID™ - Urine	Immunological	Presumptive	Immunochromatographic cartridge targeting the urinary Tamm-Horsfall protein.	[32]
Sweat	None	N/A	N/A	No methods currently accepted for use in forensic casework.	N/A

therefore often initially applied to a suspected fluid stain to determine whether or not a secondary confirmatory test is required.

As previously mentioned, some fluid discrimination tests may also be used for the purpose of stain detection. The luminol assay for the identification of blood relies on iron present within haemoglobin to catalyse the oxidation of the luminol molecule by hydrogen peroxide. A positive reaction results in the luminescence emission of luminol at a wavelength of 431 nm. Consequently, investigators are able to disperse the luminol reagent over surfaces on which blood is suspected to be present to rapidly locate areas of fluid staining (albeit presumptively) through the production of blue-coloured light [5]. However, not all fluid identification assays have the ability to visualise latent stains. Those relying on the generation of colorimetric products (which cannot be observed against most coloured surfaces) or necessitating analytical instrumentation to observe positive signals usually require stains to be located through traditional visual searching methods before tests can be undertaken. A list of fluid identification strategies currently used within forensic casework may be found in [Table 2](#).

### **1.3 Current Challenges**

Many of the assays currently used for the detection and attribution of body fluids have been routinely employed in forensic casework for several decades. In fact, the first use of the Kastle-Meyer reagent for the identification of bloodstains was reported in the late 1920s [14]. However, in recent years, forensic science (and its use within the legal system) has changed significantly. Increases in the DNA profiling capabilities of forensic service providers, as well as mounting pressure on scientists to assure courts of the reliability of analytical tests, has led many members of the forensic and academic communities to question whether or not these fluid testing strategies are still fit for purpose. Several disadvantages associated with current body fluid analysis methods have been identified:

- The impractical length of the fluid detection process.
- The low specificity of presumptive testing assays.
- The inability to multiplex current testing methods.
- The potential interference of assays with DNA profiling processes.

Rapid profiling technologies (such as the IntegenX® RapidHIT® or ParaDNA® systems) are poised to revolutionise forensic DNA analysis by providing full genetic profiles from crime scene samples in less than two hours [33]. However, casework turnaround times are still likely to be constrained by the lengthy fluid detection and identification processes that must be conducted prior to DNA testing. This is largely due to the fact that both processes cannot be conducted simultaneously, as there are no methods currently available to locate latent stains and confirm fluid identity at the same time. As previously mentioned, current attempts to increase search efficiency largely centre upon the use of ALS devices, to exploit the auto-fluorescent properties exhibited by some fluids upon wavelength-specific excitation. However, this fluorescence is highly conditional, with demonstrated signal variability between fluid types and surface materials on which a stain is deposited [34]. Many non-body fluid substances such as laundry detergents, make-up products and skin creams are also highly fluorescent at the ALS wavelengths used for fluid detection [35, 36].

With few exceptions, existing presumptive tests do not demonstrate high degrees of specificity towards target body fluids. Many of these tests have been proven to cross-react between fluid types, as well as with an assortment of non-fluid substances [37-39]. This is especially prevalent with regard to the peroxidation mechanisms exploited in the detection of blood, which may produce false positive results for a range of oxidative products endogenous to the sampling environment [37]. Furthermore, as presumptive tests are generally not based on reactions with species-specific fluid components, the vast majority of fluid-attribution tests are incapable of differentiating human fluids from their non-human analogues.

This low specificity limits the evidential value of presumptive fluid tests, as the potential for false positive or false negative results to occur is well known to the courts [40]. Therefore, any expert witness opinions based on the outcomes of such assays are likely to be contested by defence barristers, who may provide other equally plausible alternative explanations for the test results.

Another limitation of current fluid testing methods is that they cannot be used concurrently in one multiplex reaction. There is no single widely adopted methodology to test for all possible body fluids at the same time. Therefore, in cases where the type of body fluid likely to be present on an item is unknown, investigators may have to perform multiple fluid discrimination tests in sequence on the same stain. This not only increases analysis times, but also reduces the amount of DNA available for downstream profiling applications, as portions of a stain are consumed with every test [41].

Studies have also shown that some presumptive testing reagents may adversely affect the recovery rate of genetic material from fluid stains [37, 42]. The destructive nature of these methods can be extremely detrimental in cases where only limited amounts of biological material are available. In circumstances where minimizing the loss of genetic material is paramount, suspected body fluids may even forgo a presumptive identification step and proceed directly to DNA analysis, prompting a potential loss of investigative information [43]. However, as previously mentioned, there are many times when knowing the type of fluid from which a DNA source has originated is of vital importance, as this information can have a probative value and can strengthen the significance of DNA profiling.

## **1.4 Recent Advances**

The need for the development of new rapid, sensitive, specific and non-destructive body fluid detection and identification strategies is evidenced by the growing research efforts made in the field. These efforts are often



undertaken as part of collaborative partnerships between academia, police organisations and/or private forensic science providers. In recent years, a range of techniques designed to circumvent the issues associated with current fluid tests have been reported. Those techniques that have shown the most promise as replacements for conventional body fluid testing methods are summarised below.

#### **1.4.1 Infrared Spectroscopy**

Infrared (IR) spectroscopy involves the analysis of a sample based on its interaction with IR radiation. This radiation is traditionally divided into three distinct regions based on relative distance from the visible portion of the electromagnetic spectrum: near- (800 - 2500 nm), mid- (2500 - 25000 nm) and far-IR (25000 -  $10^6$  nm). As each of these regions is able to induce different measurable vibrations in covalently bonded atoms and groups, IR spectroscopy may be used to identify unknown compounds by providing information on their molecular structure. IR spectroscopy has become extensively employed in the forensic analysis of drugs [44], explosives [45], inks [46], paints [47], fibres [48] and hairs [49]. Investigations into the identification of biological fluid samples using IR spectroscopy have also been undertaken and have mainly focused on the use of near (NIR) and mid-Infrared (MIR) radiation [34].

NIR is the most energetic form of IR radiation. It is used to detect overtones (electronic transitions of more than one energy level) and combinations (vibrational signals of two identical bonds that appear split due to Fermi resonance), which can provide structural information on bonds involving hydrogen [50, 51]. NIR spectroscopy may be considered particularly amenable as a method of body fluid attribution as it is non-destructive, rapid, requires little-to-no sample preparation and is capable of analysing samples through plastic or glass containers. The NIR spectra of body fluids relevant to forensic investigation have been extensively characterised (**Figure 1**).

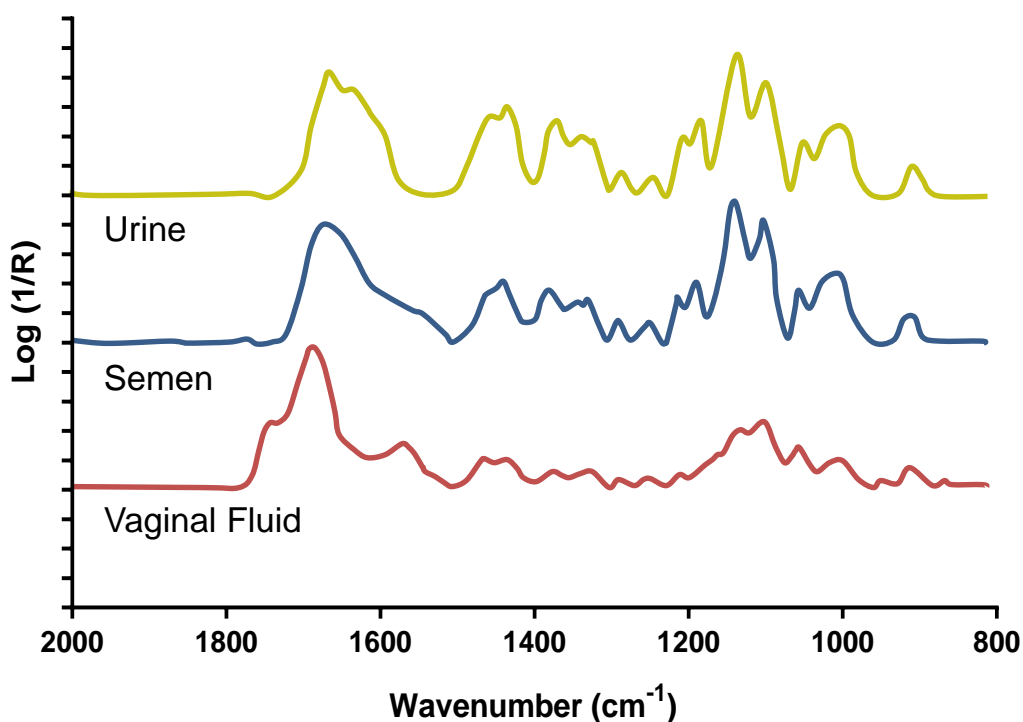


**Figure 1:** Typical NIR spectra of urine, semen and vaginal fluid samples.

Furthermore, advances in instrumental miniaturisation have allowed the development of portable NIR devices, which are already being explored for the analysis of biological fluid stains directly at crime scenes [52, 53]. In one recent study, a handheld NIR device was used to identify bloodstains on a series of surfaces commonly encountered in forensic casework. This device was able to successfully differentiate blood from several blood-like substances (including red wine, ink, tomato sauce, coffee fake blood, food colouring, paint and beetroot juice) in up to 94% of cases [52]. As NIR spectra are often disadvantaged by the presence of broad, overlapping peaks that cannot be distinguished by the naked eye, this study also used a series of chemometric models for the automated interpretation of spectroscopic signals. Such an approach may allow for the operation of the device by police staff or scenes of crime officers that have not been trained in IR spectra interpretation.

Conversely, MIR spectroscopy may be used to detect changes in both the vibrational and rotational states of bonds between carbon and other atoms as a result of IR excitation. MIR analysis has also been

investigated as a method of fluid attribution, with previous studies able to identify patterns of spectral peaks characteristic of macromolecules present in blood, semen, saliva, urine and vaginal secretions [54, 55]. However, all studies conducted so far have relied on the use of benchtop MIR instrumentation, preventing the deployment of this technique directly at crime scenes. Another disadvantage currently associated with MIR-based biofluid analysis includes the prominent spectral bands observed as a result of water molecule presence, which may potentially mask detectable protein analytes.

#### **1.4.2 Raman Spectroscopy**

While most spectroscopic techniques involve observing the amount of radiation absorbed, reflected or emitted by a sample, Raman spectroscopy relies on measuring the inelastic scattering of light to identify molecules. In this technique, samples are irradiated with low-energy monochromatic laser beams, causing the scattering of incident photons. A small percentage of these photons will exhibit a change in frequency in an effect known as a Stokes (or anti-Stokes) shift [56]. The wavenumbers and intensities of these shifts may be used to provide valuable information on the molecular structure, intermolecular interactions and internal environment of a sample. Such information can now be obtained from femtolitre or picogram amounts of liquid and solid samples respectively [57]. As a result, Raman spectroscopy has been extensively studied for the detection and identification of body fluid traces within forensic casework.

The first investigation into the use of Raman spectroscopy for the identification of biological fluids involved the characterisation of whole blood deposited onto glass slides, as well as dried blood particles present on tape lifts [58]. In this study, four laser wavelengths were successfully used to establish blood presence by monitoring the vibrational spectrum of differently oxygenated haemoglobin molecules. However, this technique was unable to distinguish human blood from that obtained from

other mammalian species. This research has been expanded upon in many studies for the identification of multiple body fluids (including peripheral blood, semen, saliva, sweat, vaginal fluid and menstrual blood) based on their Raman signature [59]. In fact, a number of studies have recently demonstrated the extraction of phenotypic information, such as donor age, sex and race directly from fluid samples through Raman spectroscopy [60-62]. Recent efforts to increase the sensitivity of Raman-based fluid attribution methods have also been made through the use of surface enhanced Raman spectroscopy (SERS), in which samples are placed on the surface of metallic sheets or nanostructures to enhance Raman signal strength [63]. This approach is likely to be extremely useful in cases where trace amounts of fluid are present, or for use with portable Raman spectrometers, which are considerably less sensitive than laboratory-based instruments.

One major disadvantage associated with Raman spectroscopy is the potential for signal interference caused by auto-fluorescence from background surfaces on which a fluid is deposited. The intensity of these fluorescence emissions, which are produced through the excitation of substrates by the laser light used to affect photon scattering, is often several orders of magnitude larger than that of Raman signals. Such interference may prevent the identification of a body fluid stain by masking portions of its vibrational signature [64]. However, this issue may be solved by utilising a radiation source from the NIR region of the electromagnetic spectrum.

### **1.4.3 Hyperspectral Imaging**

Originally designed for the purpose of remote sample sensing, hyperspectral imaging (HSI) combines regular imaging and spectroscopy for the simultaneous collection of spatial and spectral information from an object. In this technique, reflectance, absorbance, fluorescence or Raman spectra from tens-to-hundreds of narrow wavebands across the electromagnetic spectrum are obtained for each pixel in a two-

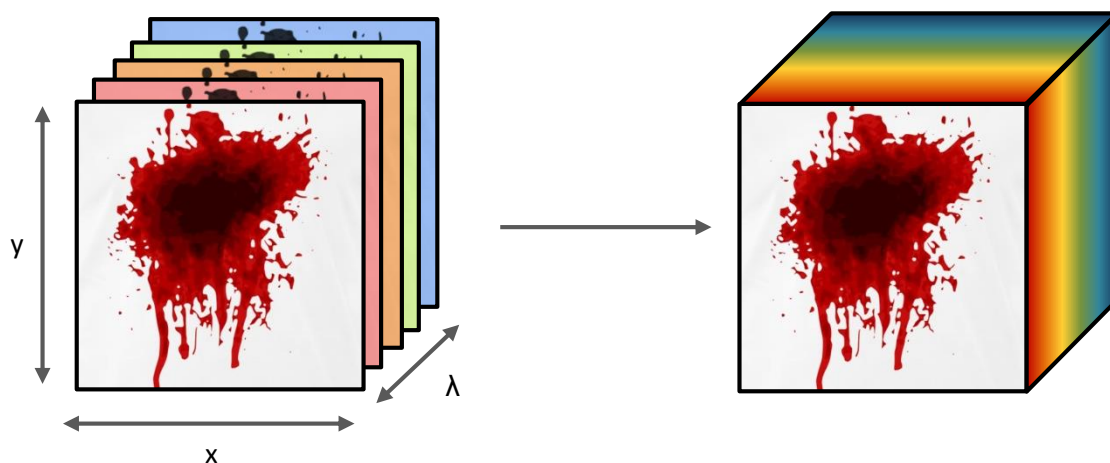


**Figure 2:** An illustration of hypercube construction. Image data from two spatial dimensions ( $x,y$ ) is combined with spectral data from a series of narrow wavebands ( $\lambda$ ) to form a three-dimensional data structure.

dimensional image [65]. These spectra are then used to construct a three-dimensional data structure, comprising two spatial dimensions ( $x$  and  $y$ ) and one wavelength dimension ( $\lambda$ ), known as a hypercube (**Figure 2**). Hypercubes are able to provide users with a complete image for every collected wavelength, as well as a contiguous reflectance spectrum for each image pixel. As such, HSI is emerging as a powerful tool for probing the chemical composition of forensic samples, including biological fluid traces.

A series of studies have recently demonstrated the exceptional performance of HSI techniques in the detection and identification of human bloodstains [66-69]. In these studies, hyperspectral images taken in the visible and NIR regions of the electromagnetic spectrum were used to rapidly identify blood deposited on a range of coloured surfaces, whilst also allowing them to be differentiated from other blood-like substances. HSI has been shown to possess excellent analytical sensitivity with one study being able to detect blood diluted 1:512 deposited on white paper [68]. Furthermore, the use of HSI as a potential method for the estimation of bloodstain time-since-deposition has also been established [66, 67]. Subsequent studies have sought to extend this research by utilising HSI for the identification of other biological fluids, including semen, saliva and vaginal fluid [70, 71].

With the introduction of HSI to the field of forensic analysis remaining relatively recent, extensive validation studies to assess method performance under differing environmental conditions are likely to be required before this technique can be deployed for the analysis of biological fluids in routine forensic casework. Such conditions may include the variability of ambient lighting at crimes scenes (especially those located outdoors), which is known to exert significant influence over the quality of collected HSI spectra [65]. Other challenges to the use of HSI within forensic analysis include the interpretation of complex spectra from mixed or contaminated samples. This is especially important in the testing of biological fluids, which are often found as part of multi-fluid mixtures [65].

#### **1.4.4 RNA Profiling**

In order to fulfil its biological function, each type of cell present within a tissue will exhibit a distinct pattern of gene expression. These patterns can be characterised by measuring the type and/or abundance of RNA transcripts expressed by the cell. As biological tissues contain multiple cellular components, much research has gone into the forensic discrimination of body fluids based on their overall transcriptomic 'signature'. This process is known as RNA profiling. Although several types of RNA molecule have been investigated for fluid identification purposes, most studies have focused on the analysis of messenger RNA (mRNA) [72].

One of the main advantages of mRNA profiling over traditional body fluid identification techniques is that multiple types of body tissues can be tested for simultaneously in a single multiplex reaction. This includes fluids that cannot be identified by conventional means, such as menstrual blood and vaginal fluid [72]. The analysis of multiple mRNA markers per body fluid also ensures a high degree of assay specificity [73]. A list of core mRNA markers used in fluid attribution assays, as well as the proteins with which they are associated, may be found in **Table 3**.

**Table 3:** mRNA markers commonly used in body fluid identification multiplex assays.

Fluid	Gene Name	Associated Protein and Protein Function	Ref.
Blood	ALAS2	Delta-aminolevulinate Synthase 2 - Erythroid protein.	[74]
	ANK1	Ankyrin 1 - Helps attach membrane proteins to cytoskeleton.	[75]
	SPTB	Spectrin Beta Chain - Membrane structure and organisation.	[76]
	CD3G	T-Cell Surface Glycoprotein CD3 Gamma Chain - Immunity	[77]
	CD93	Cluster of Differentiation 93 - Transmembrane receptor.	[78]
	AMICA1	Junction Adhesion Molecule Like - Leukocyte membrane.	[79]
Semen	PRM1	Protamine 1 - Replaces histones in spermatogenesis.	[80]
	PRM2	Protamine 2 - Replaces histones in spermatogenesis.	[80]
	TGM4	Transglutaminase 4 - Reproduction protein.	[75]
	SEMG1	Semenogelin 1 - Dominant semen protein. Forms gel matrix.	[75]
	SEMG2	Semenogelin 2 - Dominant semen protein. Forms gel matrix.	[75]
	KLK3	Kallikrein 3 - PSA. Breaks down seminal matrix.	[75]
Saliva	HTN3	Histatin 3 - Responsible for antimicrobial activity in oral cavity.	[81]
	HTN1	Histatin 1 - Responsible for antimicrobial activity in oral cavity.	[76]
	STATH	Statherin - Limits precipitation of calcium phosphate in saliva.	[81]
	PRB3	Proline Rich Protein BstNI Subfamily 3 - Bacterial receptor.	[81]
	PRB4	Proline Rich Protein BstNI Subfamily 4 - Bacterial receptor.	[75]
	PRH2	Proline Rich Protein Haell Subfamily 2 - Dental enamel.	[82]
	PRB1	Proline Rich Protein BstNI Subfamily 1 - Bacterial receptor.	[81]
	MUC7	Mucin 7 - Gel forming protein. Lubricates oral cavity.	[83]
Vaginal Fluids	CYP2B7P1	Cytochrome P450 Subfamily 2B Member 7 Pseudogene 1.	[84]
	DKK4	Dickkopf WNT Signalling Pathway Inhibitor 4 - Development.	[84]
	FAM83D	Family with Sequence Similarity 83 Member D - Proliferation.	[85]
	CYP2A6	Cytochrome P450 2A6 - Oxidation of nicotine and cotinine.	[85]
	CYP2A7	Cytochrome P450 2A7 - Inactive cytochrome P450 enzyme.	[85]
Menstrual Blood	MMP10	Matrix Metalloproteinase 10 - Breaks down cellular matrix.	[86]
	LEFTY2	Left-right determination Factor 2 - Endometrial bleeding.	[87]
	MMP7	Matrix Metalloproteinase 7 - Breaks down cellular matrix.	[76]
	MMP11	Matrix Metalloproteinase 11 - Breaks down cellular matrix.	[86]
	SFRP4	Secreted Frizzled-related Protein 4 - Uterine morphology.	[87]
Skin	LCE1C	Late Cornified Envelope 1C - Precursor of stratum corneum.	[88]
	CCL27	C-C motif Chemokine 27 - Attracts lymphocytes to skin sites.	[88]
	IL37	Interlukin 37 - Suppresses immunity and inflammation.	[88]
	SERPINA12	Serpin Family A Member 12 - Modulates insulin in tissues.	[85]
	KRT77	Keratin 77 - Epithelial structure in skin and sweat glands.	[89]
	COL17A1	Collagen Type XVII Alpha 1 Chain - Strengthens skin tissue.	[89]

Initial investigations into forensic mRNA profiling involved the use of the reverse transcriptase-polymerase chain reaction (RT-PCR) for the identification of epithelial cells in menstrual blood stains [86]. This technique was subsequently improved upon to allow the analysis of markers from multiple fluids through the incorporation of a capillary electrophoresis (CE)-based detection step [76]. Since then, RT-PCR with CE has largely been accepted as the standard method for mRNA-based fluid attribution in most forensic laboratories. However, a large collaborative exercise recently carried out by the European DNA Profiling group (EDNAP) and EUROFORGEN Network of Excellence has also demonstrated the potential of massively parallel sequencing (MPS) technologies for the targeting of fluid-specific transcripts [82].

These validation studies have cemented mRNA profiling as the most likely candidate to replace conventional body fluid identification methods. In fact, a number of forensic laboratories, including the Netherlands Forensic Institute (NFI) and the Institute of Environmental Science and Research (ESR) in New Zealand have already begun to utilise mRNA profiling methods within their operational casework [83]. However mRNA profiling has yet to be adopted on a global scale. This is likely due to the forensic community's lack of general consensus on how to present mRNA profiling evidence in court. Unlike the analysis of short tandem repeats (STRs) in DNA profiling, there is currently no established framework for the statistical reporting of mRNA results that incorporates a probabilistic measure of uncertainty [90]. However, research in this area is currently underway [91].

A major challenge to the uptake of mRNA profiling by forensic providers is the complex laboratory procedures required for transcriptome analysis. This includes the transcription of mRNA into cDNA by RT-PCR and the removal of contaminating genomic DNA from samples via DNase treatment [92]. Many authors have also expressed concern over the reliability of methods used to quantify total amounts of RNA, which if not



carried out correctly, can result in the production of non-specific profiling artefacts through target over-amplification [92, 93].

One disadvantage of mRNA profiling compared to other recent advances in body fluid testing is that it can only be used for the purposes of fluid attribution and not detection. All fluid stains subjected to mRNA analysis must still be located using the time-intensive searching methods previously listed [34]. However, the use of mRNA profiling in forensic casework is still likely to result in a reduction in fluid analysis times, as both RNA and DNA from stains can be extracted simultaneously [94]. The stability of RNA molecules within body fluid stains is also highly contested [95]. In order to meet the changing demands of protein synthesis, RNA transcripts are rapidly degraded by cells through a number of enzymatic pathways. As a result, these transcripts typically possess much shorter half-lives in comparison to their DNA counterparts (although some specific transcripts have been shown to be more stable than others) [95]. However, several studies have also demonstrated the sufficient recovery of RNA from a range of aged and environmentally compromised body fluid stains [96, 97].

#### **1.4.5 DNA Methylation Profiling**

The unique patterns of gene expression analysed as part of mRNA profiling are regulated in the cell through a number of biochemical pathways. 'Epigenetic' changes in expression are those that do not depend on the nucleotide sequence of DNA, but instead involve alterations to the packaging and structure of the DNA molecule itself. These alterations include histone modification, chromatin structuring and DNA methylation [98]. The latter of these has recently become of great interest to the forensic community, due to the established variability of methylation patterns between body tissues.

In mammalian DNA, methylation is achieved almost exclusively by the addition of a methyl group ( $-\text{CH}_3$ ) at the 5-carbon position of a cytosine base to form 5-methylcytosine. This process is mediated by DNA

methyltransferase enzymes and usually occurs at 'CpG sites', where cytosine nucleotides are directly followed by guanine residues in the linear sequence of bases. Unmethylated CpG sites are often grouped together towards the regulatory region of genes in areas known as 'CpG islands', where they exercise control over transcription activities [98].

In recent years, several forensic applications based on the analysis of DNA methylation have been proposed. Many studies have demonstrated that methylation patterns are altered in response to various lifestyle and environmental stressors, including diet, physical activity, stress and chemical exposure [99]. As a result, DNA methylation analysis has been suggested as a possible method for the genetic differentiation of monozygotic twins, a feat that cannot be accomplished by standard STR typing [100]. Some research groups have also begun to investigate the use of methylation analysis for the estimation of an individual's chronological age directly from biological samples [101].

However, one of the most promising applications of methylation analysis to forensic investigation is as a method of discriminating biological fluids. Much like RNA expression, DNA methylation patterns have been shown to exist in a tissue-dependent manner [102]. Since initial work on epigenetic-based fluid attribution began in 2011 [103], a range of differentially-methylated regions (DMRs) specifically associated with forensically relevant tissues, including peripheral blood, semen, saliva, vaginal fluid and menstrual blood, have been identified. Whilst significantly more research has been undertaken in the identification of fluid stains through mRNA profiling, DNA methylation analysis may be considered an attractive option for use in forensic casework due to the potential for analysing methylation and STR loci in the same reaction, allowing body fluid attribution and DNA profiling processes to be carried out simultaneously [103].

Many techniques have been employed for the detection of fluid-specific DNA methylation. These can be separated into three distinct categories

based on the type of DNA pre-treatment methods used prior to analysis: methylation sensitive restriction enzyme digestion, protein/antibody affinity binding and sodium bisulfite conversion [104]. However, as each of these methods is disadvantaged by issues of either analytical sensitivity or specificity, no assay has been universally recognised by the forensic community as the standard method of fluid methylation analysis. Techniques able to detect many epigenetic markers as part of large multiplexes generally require significant amounts of high-quality input DNA in order to function efficiently, which is likely to be problematic in the profiling of low volume body fluid traces typically found at crime scenes [105]. Conversely, sensitive methods that may be used to analyse sub-nanogram amounts of DNA are currently restricted in the number of methylation markers that can be detected in a single reaction, thereby increasing the potential for erroneous results [105]. However, MPS technologies, such as the Illumina® MiSeq™ platform, have recently shown great promise for the sensitive and reliable multiplex analysis of epigenetic markers [101, 106].

The technical challenges associated with current DNA methylation assays are not the only factor preventing the large-scale adoption of epigenetics-based fluid attribution methods by forensic laboratories. Some studies have demonstrated that tissue-specific methylation markers may be susceptible to change as a result of individual ageing and/or environmental exposure [107]. A more extensive validation of previously reported fluid attribution markers is likely to be required before DNA methylation technologies are accepted for use within operational casework. The Israeli company Nucleix has already conducted one attempt at the commercialisation of a tissue-specific methylation assay; DSI-Semen™ is a 5-loci methylation multiplex for the identification of seminal fluid, analysed using methylation-sensitive restriction enzyme digestion coupled with PCR amplification [108]. However, this product appears to have been later removed from the market.

#### 1.4.6 Metagenomic Analysis

The human 'microbiome' refers to the population of microbes that reside within or on the surface of human bodily tissues. Such microbes, which include bacteria, archaea, fungi, protists and viruses, have been reported to be present in the body in amounts ten times greater than that of human cells (although this number is highly disputed, with some authors claiming the ratio to be closer to 1:1) [109, 110]. Recent studies have shown that despite the variation in microbiomes between individuals (as well as in the same individuals over time), particular body sites tend to be inhabited by distinct microbial communities [110]. As a result, these communities may serve as the basis for the forensic attribution of body fluid stains based on their metagenomic 'signature'.

The most prevalent method of identifying the type of microbes present within a specific community is through the targeted sequencing of the 16S ribosomal RNA gene. This gene is generally present in all microbiota but contains a number of hypervariable regions that may be used for the purpose of species discrimination [111]. Recent improvements in sequencing technologies (as well as reductions in sequencing costs), have also led some forensic researchers to consider the use of whole-genome sequencing for the characterisation of certain microbiomes [112]. Although not yet applied to the field of biological fluid attribution, such techniques may be able to provide investigators with greater levels of taxonomic discrimination, as well as an indication of relative species abundance, by analysing the entire genome of each type of microbe present within a population.

So far, only a small selection of the body fluids commonly found at crime scenes have been able to be identified through metagenomic analysis [72]. Furthermore, those microbial markers that have been reported for the purpose of attribution may only be used to determine the body site from which a fluid has originated, but not the identity of the fluid itself. For example, successful detection of the bacterial species *L. crispatus* or *L.*

*gasseri* within a sample may be able to establish that a fluid is either menstrual blood or vaginal fluid, but cannot distinguish between the two as both originate from the vaginal cavity [113]. Other tissues for which body site-specific markers have been identified include saliva, faeces and skin [72]. Some authors have also stated that microbial profiling is unlikely to be suitable for the analysis of 'sterile' fluids, such as blood and semen, in which bacteria is not usually present in large quantities [114].

Other challenges currently associated with this approach include the potential for a fluid's microbial signature to change after it has been deposited at a crime scene. Changes in the relative abundance of particular microbe species as a result of growth or degradation may make it difficult to identify fluids left at scenes over prolonged periods of time [72]. Inter-individual variation also makes the selection of standardised metagenomic markers problematic, as even some widespread microbe species have been shown to be absent in certain individuals [115]. An established overlap between the microbiome of humans and other mammalian species also means it is unlikely that microbial-based attribution methods will be able to determine whether or not body fluid samples are of human origin [116].

#### **1.4.7 Immunofluorescence**

Two recent studies conducted within the forensic science research group at King's College London have successfully demonstrated the simultaneous detection and confirmatory identification of several biological fluids *in situ*. The first of these involved the visualisation and differentiation of erythrocytes and nucleated leukocytes within blood through interaction with fluorescently-labelled antibodies [117]. In this study, antibodies specific to the erythroid membrane protein Glycophorin A and leukocyte membrane protein CD45 were labelled with the fluorescent dyes Alexa Fluor 568 and Alexa Fluor 488, respectively. These antibodies were then incubated with blood deposited on glass slides and dark-coloured cotton before the visualisation of cells by

fluorescence microscopy. This method was able to detect both erythrocytes and leukocytes at the single cell level. Furthermore, no cross reaction was observed with cells present in semen and saliva, as well as with blood from other mammalian species.

Whilst this method proved suitable in terms of sensitivity and specificity, a series of wash steps were required in order to remove any remaining unbound antibody complexes. Consequently, there is a chance that this technique may negatively affect the recovery of DNA from a biological stain, as minor portions of the fluid are likely to be removed with each successive wash. A follow up study sought to overcome this limitation through the conjugation of iron-oxide nanoparticles to the antibody-fluorophore complex, which allowed unbound fractions to be removed magnetically (**Figure 3**) [118]. The technique was also extended to the detection of saliva using anti-mucin 7 antibody complexes. Despite resolving issues of potential fluid destruction, magnetic removal is considered cumbersome and cannot provide a confirmation that a complete unbound removal has taken place, which may lead to an overestimation of fluid presence.

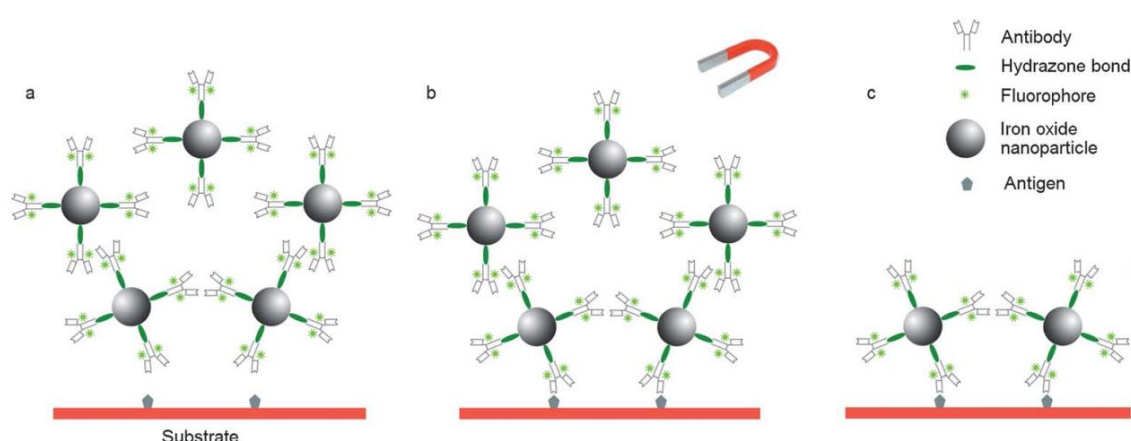


**Figure 3:** Scheme of body fluid detection using fluorescently-labelled antibodies conjugated to magnetic nanoparticles: a) antibody-nanoparticle complexes are deposited over a suspected fluid stain, b) unbound complexes are removed magnetically and c) remaining bound complexes are detected via fluorescence microscopy. Taken with permission from [118].

## 1.5 Biosensors

Biosensors are a group of devices capable of turning biological interactions into observable signal outputs. Such devices have previously demonstrated the delivery of real-time information regarding the presence and activity of specific molecules within complex sample matrices for many biological and medical applications [119]. Biosensing is usually achieved by use of a supramolecular complex comprised of two components; a sensitive biological detection element for the recognition of a testing antigen and a physiochemical transduction element that stimulates the production of an observable output upon successful interaction [120]. Biosensing assays may be regarded as a single integrated system, with direct spatial contact between recognition and transduction elements.

Biosensor construction is facilitated by extensive design flexibility, with a wide range of recognition moieties, signal outputs and intrinsic transduction mechanisms available to meet specific assay requirements. Components such as enzymes, antibodies, peptides, MIPs and nucleic acid sequences may all be utilised for analyte recognition, allowing the detection of almost any molecular target [120]. Sensing outputs also exist in many different formats, including optical, electrochemical, thermal, magnetic or mass-sensitive-based signal detection, which allows analysis to take place over a range of different environments and sample types.

Despite these assets, biosensors have yet to find routine employment within any forms of forensic analysis. In fact, only a small number of sensors have been reported in literature for the detection of targets relevant to criminal investigation (**Table 4**). This is likely due to the challenges associated with both the complexity of biosensor design, as well with the difficult nature of forensic casework samples (which are often subject to contamination and/or environmental exposure), necessitating a meticulous optimisation and validation of all new sensors before they can be deployed for operational use [121].

**Table 4:** A selection of analytical biosensors developed for use in forensic analysis

Field	Target	Recognition	Transduction	Notes	Ref.
Explosives	TNT	Peptide	Absorbance	The UV absorbance of graphene oxide functionalised with peptides specific to 2,4,6-trinitrotoluene (TNT) is increased in the presence of explosive compounds.	[122]
	TNT	MIP	Fluorescence	Quantum dots (QDot) nanoparticles conjugated to molecularly imprinted polymers (MIPs) are quenched through polymer interaction with TNT.	[123]
	Multiple	Antibody	Fibre-optic	Anti-TNT and RDX antibodies present on the surface of a fibre-optic probe are labelled with fluorescent analogues, which are displaced upon analyte binding.	[124]
Illicit Drugs	Cocaine	Antibody	Fibre-optic	Cocaine molecules displace fluorescently-labelled benzoylecgonine bound to antibodies immobilised on the surface of quartz fibres.	[125]
	Cocaine	Aptamer	Electrochemical	Aptamers labelled with a chemiluminescent ruthenium complex interact with the electrode surface on which they are immobilised as a result of cocaine binding.	[126]
	Multiple	Antibody	SPR	Antibodies present on the surface of a protein array chip indicate cocaine, heroin, MDMA or amphetamine presence through surface plasmon resonance (SPR).	[127]
Pathogens, Poisons & Toxins	Anthrax	Aptamer	SWNTs	Aptamers bound to the surface of single-walled carbon nanotubes (SWNTs) are used to detect the anthrax protein, protective antigen (PA) through binding.	[128]
	Cyanide	Enzyme	Electrochemical	The activity of horseradish Peroxidase (HRP) enzymes immobilised on the surface of an electrode is inhibited by cyanide interaction, resulting in a reduced current.	[129]
	Ricin	Antibody	SPR	A handheld sensor employing surface-bound antibody fragments is used to detect the presence of the biological toxin ricin through SPR.	[130]



### 1.5.1 Enabling Biosensors for the Analysis of Biological Fluids

The use of biosensor technology for the simultaneous detection and identification of biological fluid stains may provide an ideal resolution to the disadvantages associated with traditional fluid testing methods [131]. Biosensors may be considered particularly amenable to fluid analysis for a number of reasons. The use of biological elements for the recognition of target analytes ensures that biosensing assays exhibit exceptionally high degrees of analytical selectivity [132]. This selectivity may allow for the development of new body fluid tests that are able to provide an absolute confirmation of tissue identity through interaction with fluid-specific biomarkers.

Locating body fluids within forensic casework generally requires a low-cost detection strategy that employs simple instrumentation applicable to scene analysis. Such qualities may be easily afforded by biosensors employing transduction mechanisms based on fluorescence signalling. These sensors have been extensively employed in the sensitive, versatile and real-time detection of numerous analytes for a variety of biomedical applications [133]. Furthermore, fluorescence biosensing outputs may be easily observed using instrumentation already routinely utilised within body fluid analysis, such as excitation light sources, optical filters and CCD cameras. Forensic investigators are therefore unlikely to require additional specialised knowledge in order to successfully conduct biosensor-based fluid testing.

Unlike the immunofluorescence methods previously described in **Section 1.4.7**, biosensor signals are produced only after a biological interaction event has taken place. As such, there is no prerequisite for the removal of any remaining unbound reagent prior to sample measurement. Detection based on sensing may therefore be considered entirely homogeneous, as it does not require additional sample component processing or enhancement. This lack of extraction, isolation or washing steps is likely

to mitigate the risk of stain destruction during the fluid identification process.

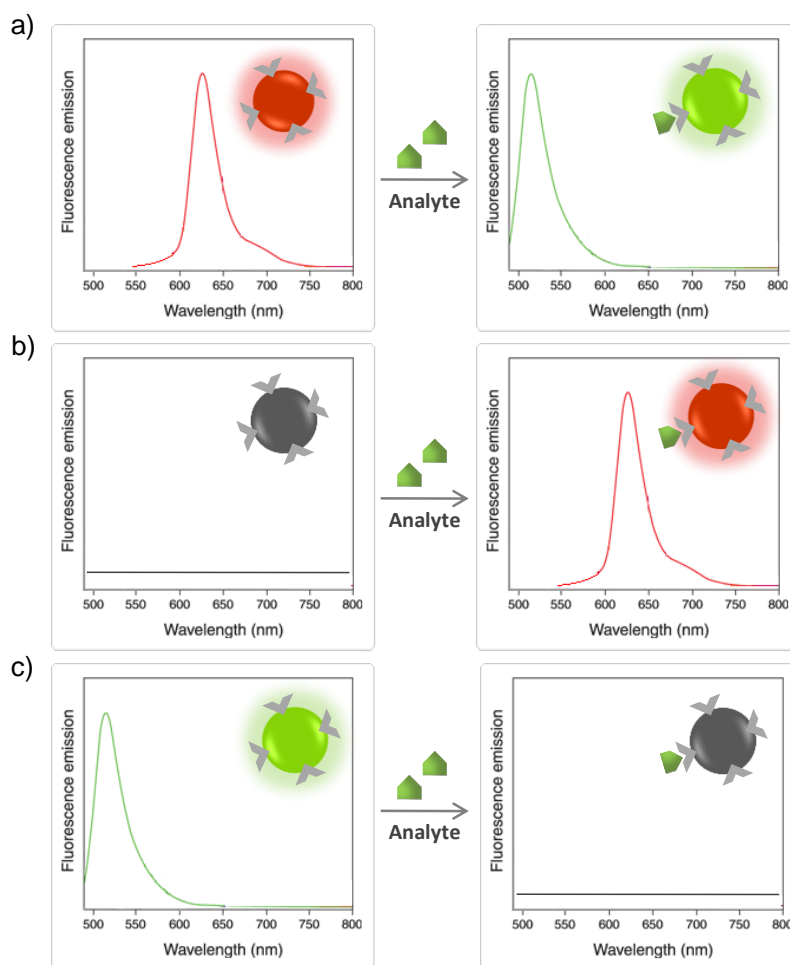


**Figure 4:** Types of spectral emission change upon sensor-target interaction: a) Stokes-shift wavelength change, b) ‘turn-on’ emission production, c) ‘turn- off’ emission quenching. Taken with permission from [131].

One assay based on ‘turn-off’ fluorescent biosensing has already been explored for the purpose of body fluid identification [134]. This study involved the use of an anti-glycophorin A antibody conjugated to a highly fluorescent QDot nanoparticle. In the presence of blood, fluorescence emission from the QDot-antibody complex was quenched in a concentration-dependent manner. However, with the presence of blood indicated through the absence of fluorescence, it is unlikely that this sensor could be used for stain visualisation purposes. Depending on the transduction mechanism employed, biosensors may cause various fluorescence changes during target interaction, either turning a signal on

or off, or shifting its output wavelength (**Figure 4**). For fluid detection purposes, ‘turn-off’ reporting mechanisms may be considered unsuitable as, while potentially allowing for the confirmation of fluid identity in solution, a decrease in observable signal prevents the localisation of fluid deposits *in situ*. Conversely, ‘turn-on’ signals, in which emissions are generated from an initially non-fluorescent sensor, may allow for the visualisation of fluid stains through the production of discrete areas of coloured light.

## 1.6 Project Aims and Objectives

The purpose of this study was to design, develop and test a range of fluorescent biosensors for the location and identification of body fluid traces. This thesis documents the construction of several molecular sensing reagents which, upon interaction with intra-fluidic targets, indicate fluid presence through ‘turn-on’ fluorescence emission.

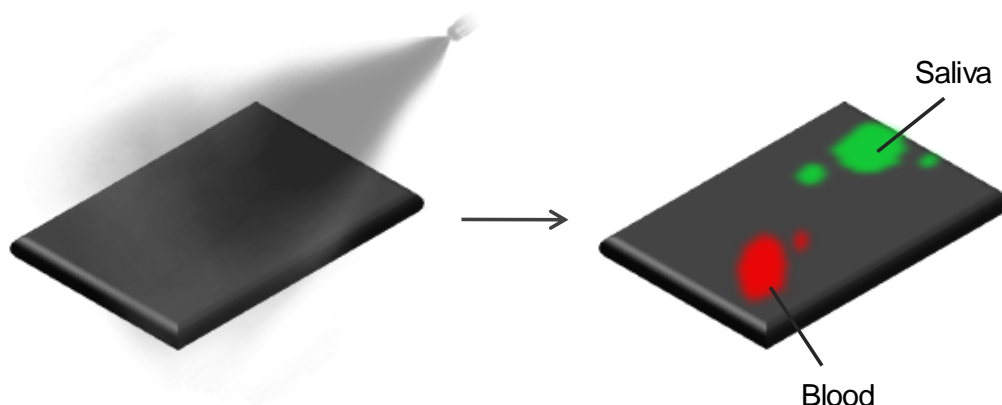


**Figure 5:** Ideal in-situ application of biosensors to the detection of body fluids. Sensing molecules are dispersed across surfaces *via* aerosol spray, generating different fluorescent wavelengths upon multiple fluid target interaction. Taken with permission from [131].

The spray dispersal of these reagents across the surface of large items may allow for the specific and non-destructive localisation of fluid staining areas in real-time. Furthermore, it may eventually be possible to combine several of the biosensing molecules reported within a single multiplex assay (which produces specific wavelengths of light depending on the type of fluid present) for the simultaneous visualisation and attribution of

fluid stains (**Figure 5**). Employment of these reagents within routine forensic casework may lead to a significant reduction in the labour and time expense associated with current manual stain search and identification strategies.

This thesis has been divided into chapters based on the types of sensing mechanisms explored. A chapter outlining the potential incorporation of developed sensors within forensic taggant materials is also provided. A final discussion of results is given in **Chapter 7**:

**Chapter 2 (Biosensors)** - Several commercially available biosensors are tested against their relevant targets within a forensic context. The ability of sensing mechanisms to detect wet and dry analyte deposits *in situ* is explored, as well as effect of each sensor on the production of DNA profiles from biological fluid samples.

**Chapter 3 (Fluorogenic Substrates)** - Three commercially available fluorogenic peptide substrates are utilised to detect human semen, saliva and blood (both in solution and deposited on surfaces relevant to criminal investigation). Attempts to increase assay performance are then made through the production of custom substrates using a novel solid phase peptide synthesis strategy.

**Chapter 4 (Immunosensors)** - A custom displacement immunosensor specific to PSA is constructed. Consisting of an antibody-quantum dot conjugate initially quenched by a moderately bound quencher-labelled peptide analogue, this sensor is shown to successfully detect nanomolar amounts of PSA within solution.

**Chapter 5 (Aptasensors)** - Three different aptamer-based sensing mechanisms are tested against purified protein and whole fluid samples. The discovery of aptamers against human sperm cells is then undertaken using the Cell-SELEX process and next generation sequencing technologies.

**Chapter 6 (Taggants)** - The potential for the incorporation of fluorescent sensing molecules within forensic taggant materials is investigated. Novel taggants are produced for establishing evidence of contact transfer in criminal investigations.

**Chapter 7 (Discussion & Conclusion)** - An overall analysis of the results obtained within each of the previous chapters is presented, along with final conclusions and potential future work.

This thesis will be prepared incorporating publications. Research and review articles that have been produced from this project will therefore be included within the text. These articles will be presented in their final published format and will be accompanied by an appropriate introduction and discussion to place them within the context of the whole thesis.

# **Chapter 2**

## **Biosensors**

## 2.1 Introduction

A significant number of fluorescent biosensors have already been developed for the rapid, sensitive and specific detection of target analytes. These sensors vary drastically in the transduction mechanisms used to indicate positive biological interactions. The vast majority of these biosensors have been designed for the analysis of targets in solution, using spectrofluorometry to monitor changes in fluorescence emission. However, in order to be applied to the analysis of latent body fluids at crime scenes, biosensing reagents must also possess the ability to detect analytes deposited *in situ* on different surface types (or on swabs/paper to which a portion of the stain has been transferred). It may therefore be beneficial to investigate the adaptability of previously developed fluorescent transduction mechanisms towards the *in situ* detection of fluid-specific analytes.

In this chapter, a selection of fluorescent biosensing mechanisms demonstrating potential applicability to the localisation and identification of body fluid stains are first reviewed. The *in situ* detection ability of these mechanisms is then evaluated by testing several commercially available biosensor assays against their relevant analytes deposited on surfaces commonly encountered in forensic investigation. These assays were not selected on the basis of target analyte, but on the unique transduction methods in which 'turn-on' fluorescence signalling is achieved.

The objectives of this particular study were to establish if fluorescent biosensors are still able to generate positive emission signals after application to wet and dry surface-deposited analytes *in situ* and moreover, whether such signals can be observed in the absence of a spectrofluorometer via fluorescence microscopy. The potential interference of different surface types on sensor emission, either as a result of cross-reaction or physical fluorescence screening, is also investigated, along with each sensor's effects on downstream DNA profiling. Those transduction mechanisms displaying greatest *in situ*

detection performance are likely to be utilised for the subsequent development of biosensing assays for the detection and identification of body fluids.

## 2.2 Review of Fluorescent Biosensors

### 2.2.1 Environmentally-Sensitive Fluorophores

One class of sensing transduction mechanism demonstrating potential for use within fluid sensing strategies is that of environmentally-sensitive fluorophores, fluorescent molecules that display variable spectroscopic properties in response to changes in local environment. Such fluorophores include those able to exhibit several energetically favourable conformational isomers whilst free in solution. In these states, quantum yield and fluorescence lifetimes are limited, rendering total fluorescence relatively negligible. However the process of target binding forces these molecules into specific structural conformers, stabilising the arrangement of atomic systems responsible for fluorescence and resulting in an exponential increase in emission intensity [135].

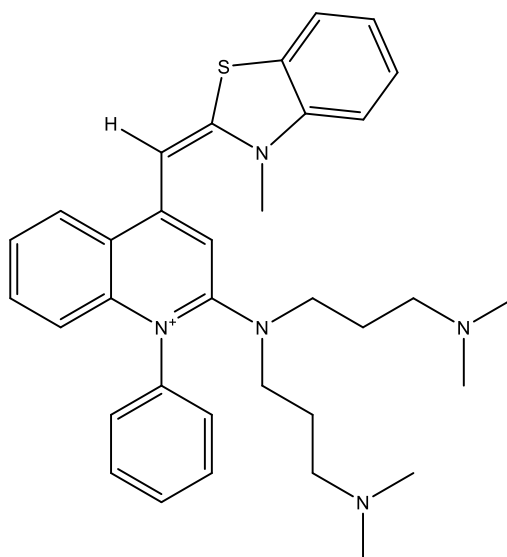


**Figure 6:** Chemical structure of the DNA-intercalating fluorophore PicoGreen®

Many of these molecules are DNA intercalators, which in the presence of nucleic acids undergo non-covalent insertion between helical base pairs as a result of hydrophobic screening and van der Waals interactions [135]. Intercalating dyes such as PicoGreen® (**Figure 6**) have not only



already found common use in the quantitation of double stranded DNA within biological fluid extracts for forensic purposes [136], but have also established a level of *in situ* applicability, aiding in the detection of bacterial biofilms upon historic window glass [137]. However, despite demonstrating usefulness in the visualisation of DNA molecules in general, the lack of sequence selectivity exhibited by such dyes prevents direct application to the identification of tissue-specific DNA sources, such as biological fluid stains.

Instead, the application of environmentally-sensitive fluorophores to the analysis of body fluids may be achieved through the use of conformer-sensitive dyes that suppress isomerisation upon interaction with fluid-specific protein biomarkers. After target binding occurs, the local environment surrounding the fluorophore changes, altering emissions to signify analyte presence. In fact, several previous studies have already explored the biosensing properties of stilbene, a fluorescent dye existing in two isomeric forms, for the detection of monoclonal antibodies. Interactions between antibodies and stilbene molecules results in the formation of a conformer 'exciplex', an excited state heterodimer that allows fluorescence emission [138]. Such work provides a firm basis for the future design of single-molecule sensors with fluorescence sensitivities relative to the macromolecular environment.

### **2.2.2 FRET-based Biosensing**

Förster Resonance Energy Transfer (FRET) refers to the phenomenon of non-radiative energy transfer between two spectrally-active molecules as a result of electrostatic dipole-dipole interactions. This process principally culminates in the quenching of an excited donor fluorophore emission by alternative transmission to a proximate acceptor molecule, which may or may not consequently fluoresce. Energetic transfer is distance-dependent, with fluorophore separation greater than a length of ~10 nm alleviating quenching effects and allowing signal output as either simple

donor emission observation or through ratiometric measurement of an acceptor-donor spectral shift [139].

FRET is often exploited within a number of macromolecular sensing applications for monitoring biological interactions that facilitate a proximity change between two or more chromophore molecules. As FRET occurs across an order of several nanometres, it may be considered ideal for the sensing of biomolecular targets [139]. Furthermore, whilst some FRET methods exploit the spectral properties of organic recognition molecules themselves (such as the intrinsic fluorescence of tryptophan residues in analyte-binding proteins [140]), the additional labelling of non-fluorescent moieties with synthetic dyes allows virtually any bio-recognition element to be used within FRET sensing assays.

Two distinct approaches are applied to the detection of molecular targets through FRET biosensing. The first involves the labelling of a sensor with both donor and acceptor moieties as a single intramolecular complex. Interaction with a testing analyte upon this complex alters the relative proximity of fluorophore molecules through the induction of a structural change within the sensor molecule, resulting in an increase or decrease in energy transfer [141].

The second form of FRET sensing comprises fluorescent labels located upon two separate and independent biological elements, which subsequently unite as a result of binding interactions or disassociate via competitive displacement (the former of which may be impractical for the *in situ* identification of biological fluid residues since it is largely impossible to label the initial testing antigen).

#### **2.2.2.1 Intramolecular FRET**

Recent research has demonstrated the use of intramolecular FRET sensing for the successful detection of enzyme activity *in situ*, with previous studies utilising catabolic events to monitor increased protease expression in wound-infecting bacterial biofilms and during enteroviral pathogenesis [142, 143]. Testing is reliant upon the hydrolysis of a

terminally labelled substrate conjoining two fluorophores to disrupt energy transfer processes (**Figure 7a**). As the specific physiological function of each body fluid necessitates unique enzyme production, similar turn-on fluorescence assays may be potentially developed for the *in situ* detection and identification of biological fluids based on their proteolytic activity.

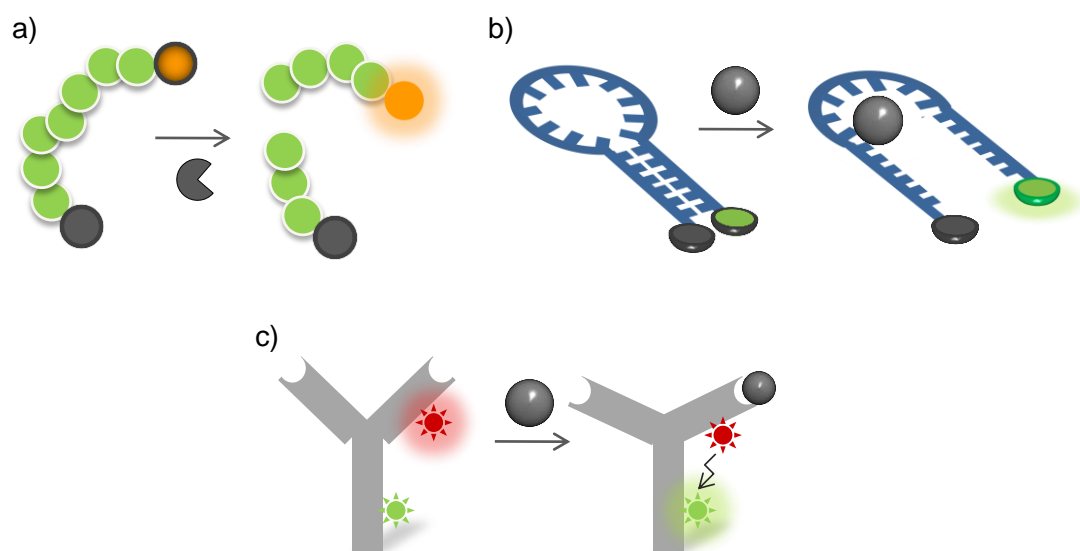


**Figure 7:** Examples of intramolecular FRET sensing mechanisms: a) a terminally labelled fluorogenic substrate is digested by catalytic enzymes, releasing a fluorescent by-product, b) a fluorophore-quencher pair in an initially quenched oligonucleotide hairpin is separated upon binding, restoring fluorescence, c) analyte-induced conformational change upon antibody binding changes donor–acceptor proximity, resulting in a wavelength shift. Taken with permission from [131].

Intramolecular FRET transduction mechanisms have also been integrated into oligonucleotides capable of specific binding to other nucleotide sequences [144], proteins [145] and inorganic molecules [146]. These assays employ a flexible dual-labelled oligonucleotide strand known as a ‘molecular beacon’, that forms a self-complementing hairpin structure in order to bring donor and acceptor dyes within appropriate proximity for FRET quenching to occur. Subsequent hybridization or binding of the probe to the analyte causes separation of the fluorophore moieties to successfully inhibit quenching and enhance fluorescence (**Figure 7b**). Recent research has demonstrated the *in situ* applicability of this technique to detect *Pseudomonas putida* bacteria in activated sludge and

river water [147]. Advances in the use of combinatorial libraries now allow the selection of oligonucleotides with binding capabilities towards virtually any target molecule, potentially allowing for the development of beacon-based sensors for the analysis of body fluid biomarkers.

Intramolecular FRET has also been exploited to induce energy transfer between chromophores located at two specific sites on the surface of antibody moieties (**Figure 7c**). Prior to target interaction, fluorescence signals are produced at the emission wavelength of the donor fluorophore, with limited fluorescence from the acceptor. Analyte binding results in a conformational change in the structure of the antibody, causing a change in fluorophore proximity and switching emission wavelength. Similar systems have already been employed to detect biochemical markers of myocardial infarction [148], as well as bacterial contamination in food products [149]. Immunological-based target recognition makes this type of sensor particularly suitable for body fluid analysis. Antibodies are presently considered a gold standard in protein detection and would ensure high degrees of specificity towards fluid targets with the added value of human species selectivity.

#### **2.2.2.2 Intermolecular FRET**

As previously mentioned, the use of intermolecular FRET processes within fluid sensing assays may be confined to displacement only mechanisms, as unknown testing analytes cannot be pre-labelled. Development of a displacement-based FRET assay involves the preliminary integration of donor fluorophores within a molecular sensing unit, which subsequently binds with moderate affinity to a non-testing substrate alternatively labelled with acceptor moieties, thereby permitting proximal FRET quenching. A positive signal response occurs when moderately bound quenching ligands are competitively removed by a macromolecular target with higher binding affinity (**Figure 8a**).

Sensors for the detection of maltose have been designed on this principle, which utilise the dissociation of a quencher labelled  $\beta$ -

cyclodextrin competitor from an *E. coli* maltose-binding protein [150]. Other studies have produced similar success in the observation of mycotoxin-producing *Amstelodami* fungal spores via the displacement a moderately bound quencher-labelled fungal species from an anti-*Aspergillus* antibody complex [151].

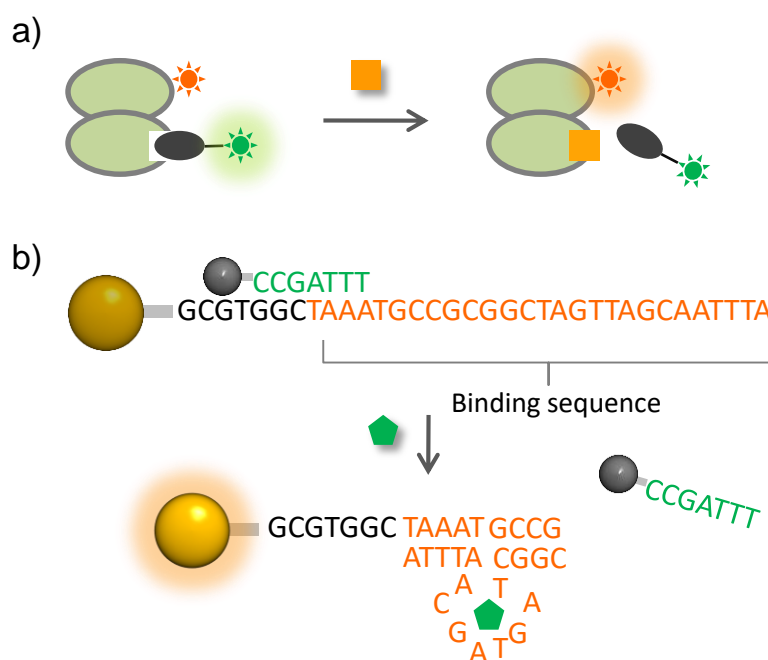


**Figure 8:** Examples of varying intermolecular FRET transductions: a) moderately bound acceptor ligands are displaced via a higher affinity competitive analyte, b) a fluorophore-labelled oligonucleotide sequence is initially hybridized to a complementary quenching strand which is subsequently displaced by a target analyte, producing fluorescence. Taken with permission from [131].

Other assays employ specific oligonucleotide aptamer sequences for fluorescent detection. DNA known to bind to a specific analyte is labelled with a fluorophore and subsequently hybridized to a complementary sequence bearing a quencher molecule, making the system non-fluorescent. The assay exploits conformational changes that aptamers undergo upon target interaction, which displaces the complementary quenching strand and restores fluorescent signal (**Figure 8b**).

Displacement-based FRET biosensors show high adaptability to the analysis of biological fluid depositions, with modifications likely to focus on the replacement of current antibody and aptamer elements with those

able to bind intra-fluidic molecules. Such mechanisms also afford excellent analytical sensitivity, with the majority of sensing macromolecules allowing multiple donor fluorophore labelling, thereby enhancing signal output upon successful interaction. Regardless of the numerable benefits, evaluation into *in situ* the application of FRET-displacement sensors towards any forms of biomedical or industrial analysis currently remains unexplored.

### **2.2.3 Static Quenching-based Biosensing**

Since energetic transfer occurs whilst the donor molecule exists within an excited state, the phenomenon of FRET may be described as a 'dynamic' quenching mechanism. Conversely, a number of spectral processes also exist based on the phenomenon of 'static quenching', in which two fluorophores form a dimeric ground-state intermolecular complex. Physical contact between the fluorescent moieties results in the creation of an entirely new excitation absorption spectrum, thereby inhibiting fluorescence emission [152]. This effect is particularly prevalent when interaction occurs between two identical fluorophores in the formation of homodimers.

Within free solution, fluorophores may aggregate of their own volition due to hydrophobic, electrostatic or steric forces [153]. However, the high fluorescence contribution from remaining unbound dye molecules renders the total reduction in fluorescence intensity negligible. Substantial or even total quenching arises from the integration of the fluorophore moieties into a macromolecular substrate with a significantly high degree of substitution, forcing the majority of dye molecules into dimeric quenching complexes [154].

Efficient substrate-based quenching via homodimeric binding interactions has been utilised in the recent development of analytical biosensors for enzymatic activity. Sensing depends on the initial labelling of numerous dye moieties in a heavy stoichiometric ratio on an individual substrate molecule, with consequent digestion of the substrate backbone by

enzyme activity, allowing the dissociation of dimeric complexes (**Figure 9**). Although the dimerization of all fluorophores results in the diminishment of fluorescence emission, these assays customarily utilise rhodamine or BODIPY derivatives, which display increased aggregation rates compared to other organic dyes [153]. Previous studies employing these substrate-confined dyes have already successfully demonstrated the *in situ* detection of elastase activity associated with dental pellicle production by salivary glycoproteins [155], as well as the proteolytic action of calpain enzymes during cataract formation in sheep [156].

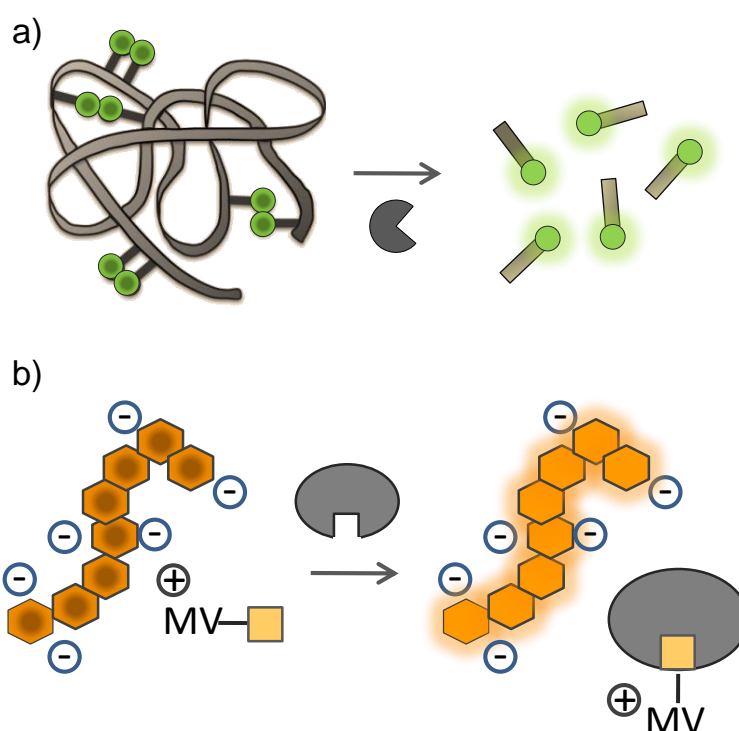


**Figure 9:** Examples of static quenching-based sensors: a) the liberation of dimerized fluorophores from a heavily labelled backbone by digestive enzymes, b) a recognition moiety is conjugated to methyl viologen (MV<sup>2+</sup>), which is electrostatically attracted to the CP, quenching fluorescence. In the presence of the analyte, the recognition moiety and therefore the MV<sup>2+</sup> are pulled away from the CP, restoring fluorescence. Taken with permission from [131].

The modification of previous *in situ* assay technologies for application to the differentiation of biological fluid depositions would largely revolve around the development of a substrate capable of binding, and subsequently separating, a large number of dimerized fluorophores upon interaction with a fluid-specific enzyme. Suitable sensing substrates may



comprise any macromolecule that can be successfully derivatised to include a considerable number of exposed amine binding groups for conjugation with organic dyes via simple covalent chemistry.

The application of fluorescent conjugated polymers (CPs) may also allow for the development of static-quenching based sensors for fluid detection purposes. It has been demonstrated that polyanionic conjugated polymers can be quenched by cationic electron acceptors in aqueous solutions. By conjugating biotin to the cationic acceptor and allowing interaction to take place between the CP and the conjugate, complete quenching of polymer fluorescence can be achieved [157]. In the presence of streptavidin, binding to the biotin molecule ligand takes place, displacing the quencher from the polymer, restoring its fluorescence. Adapting this assay to identify fluid-specific molecules would require the quencher to be linked to an antibody or binding protein. This complex can then be removed from the polymer by interaction with a fluid biomarker. What makes the interaction between CPs and cationic acceptors advantageous over dynamic FRET-based sensing for *in situ* target detection is the complete absence of any background fluorescence, allowing improved localisation of discrete fluid deposition areas.

## **2.3 Materials and Methods**

### **2.3.1 Reagents**

The Quant-iT™ PicoGreen® dsDNA Assay Kit, EnzChek® Protease/Peptidase Assay Kit, FluoReporter® Biotin Quantitation Assay Kit and EnzChek® Ultra Amylase Assay Kit were all purchased from Thermo Fisher Scientific (California, USA). Assay analytes; trypsin from bovine serum, human  $\alpha$ -amylase and biotin were all purchased from Sigma-Aldrich (Dorset, UK), whilst a  $\lambda$  viral DNA source was supplied with the Quant-iT™ PicoGreen® dsDNA Assay Kit.



### 2.3.2 Slide Microscopy

A preliminary demonstration of *in situ* mechanism performance was achieved by testing each commercial assay reagent against its relevant analyte deposited on the surface of glass slides. Reagent concentrations were modified from those given by manufacturers for use in spectrofluorometric assays to account for the decrease in sensitivity associated with observation by fluorescence microscopy.

**Table 5:** Analyte concentrations used for *in situ* testing of commercial assay reagents.

Reagent	Analyte	Deposit Concentrations
Quant-iT™ PicoGreen® dsDNA	λ viral DNA	100, 10, 1, 0.1, 0.01, 0.001 (µg/ml)
EnzChek® Protease/Peptidase	Bovine Trypsin	10, 1, 0.1, 0.01, 0.001, 0.0001 (mg/ml)
FluoReporter® Biotin Quantitation	Biotin	10, 1, 0.1, 0.01, 0.001, 0.0001 (mg/ml)
EnzChek® Ultra Amylase	α-amylase	10, 1, 0.1, 0.01, 0.001, 0.0001 (mg/ml)

Six different concentrations of each analyte solution (**Table 5**) were applied in 5 µl volumes to the centre of glass slides before the direct 5 µl addition of assay reagent. Negative reagent-only controls were also applied on the same slide to measure potential background reagent emission, whilst blank controls consisting of analyte-only applications were used to monitor analyte auto-fluorescence (**Figure 10**). The testing of sensor performance against dry depositions was also undertaken through the application of 5 µl of analyte solutions to slides, which were allowed to dry overnight. Assay reagents were then applied in the same manner as wet deposit testing. Each concentration of both wet and dry analytes was prepared in triplicate.

**Table 6:** Microscopy and reagent parameters used for *in situ* slide and surface testing.

Reagent	[Reagent Increase]	Contrast	Brightness	Exposure
Quant-iT™ PicoGreen® dsDNA	5000%	1023	131	-2
EnzChek® Protease/Peptidase	400%	1023	131	-2
FluoReporter® Biotin Quantitation	75%	1023	131	-1
EnzChek® Ultra Amylase	400%	1023	131	-2

Images were taken immediately after reagent application on an Olympus SZX12 fluorescence microscope (Tokyo, Japan) using an internal CCD

camera. As each assay shared similar excitation and emission wavelengths, GFP optical filtration (Ex460-490/Em510 nm) was utilised throughout testing. Microscopy parameters for each assay (optimised during the first measurement of highest concentration analytes) were also kept constant for all subsequent *in situ* studies in order to restrict result variation ([Table 6](#)).

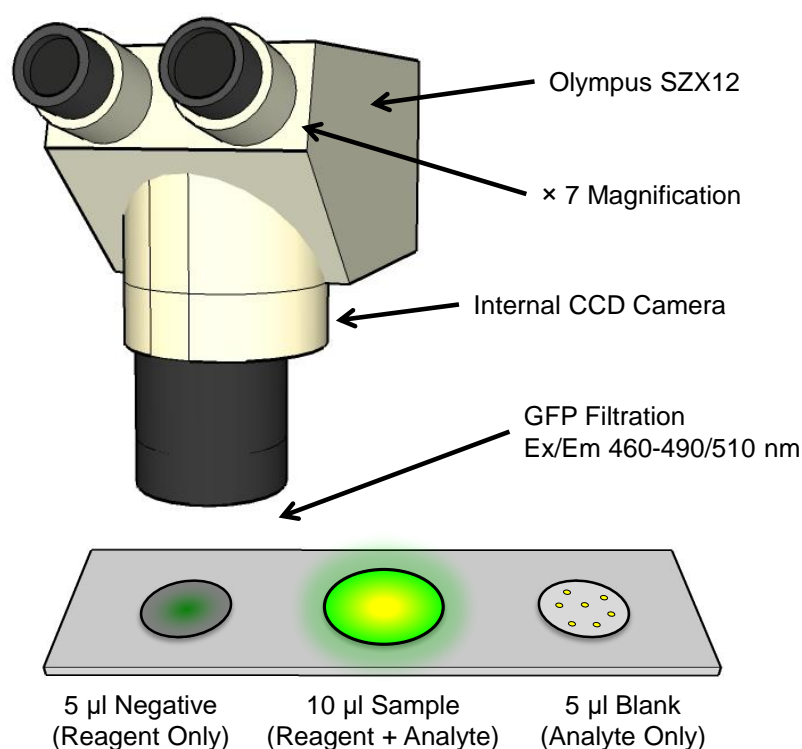


**Figure 10:** Representation of instrumental set-up for evaluating *in situ* sensor performance. An Olympus SZX 12 fluorescence microscope is used to illuminate and observe samples deposited on glass slides or surfaces relevant to forensic casework. Positive samples consist of assay reagent applied to wet or dry analyte deposits. Negative and blank controls were also included.

### 2.3.3 Surface Microscopy

Assays indicating an acceptable level of *in situ* performance during glass slide testing ([Section 2.3.2](#)) were then applied to analytes deposited on a range of different surface types. Ten surfaces, consisting of cardboard (brown), cotton (100%, white), denim (100% cotton, dark blue), felt (100% acrylic, black), leather (black, genuine), paper (white), plastic (dark blue), polyester (black), wood (untreated, brown), and wool (blue) were chosen to reflect those most commonly encountered within criminal investigation.

All surfaces were cut to fit the size of a microscope slide. Analyte concentrations producing the largest fluorescence signal for each assay reagent during dry deposit glass slide testing were applied to surfaces in 5 µl volumes and allowed to dry overnight before reagent addition. Blank and negative controls were also applied in the same manner as previously described (**Section 2.3.2**). Microscopy parameters were kept consistent with those used during glass slide testing (**Table 6**).

### 2.3.4 Image Analysis

Images recorded during surface microscopy testing were subjected to a semi-quantitative measurement of fluorescence intensity using Adobe Photoshop™ (California, USA) imaging software. Deposit areas were first isolated within each image using the magnetic lasso tool, selecting a defined number of pixels. Use of the 'green' channel histogram function subsequently allowed each of these pixels to be assigned a value from 0-255 as a representation of signal intensity.

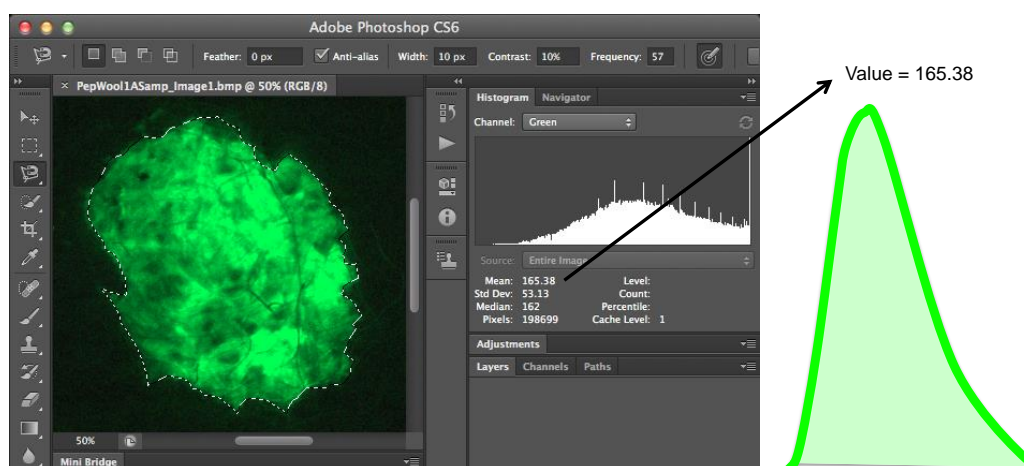


**Figure 11:** Semi-quantitative analysis of *in situ* biosensor assay fluorescence using Adobe Photoshop™ software. Areas of positive signal emission are defined using the magnetic lasso tool before the image histogram function is used to assign a mean intensity value for that area.

An average value for all selected pixels was then recorded as a measurement of mean fluorescence within the entire analyte deposit area (**Figure 11**). Percentage differences between assigned negative control and positive sample values were then plotted for each commercial assay

reagent to establish numerical changes in relative fluorescence intensity against different surface types.

An independent investigation into the accuracy of this processing method was conducted through the deposition and measurement of different concentrations of the fluorophore Alexa Fluor 488 (Thermo Fisher Scientific, California, USA) on glass slides. Software-assigned intensity values were then plotted against fluorophore concentration to determine method linearity.

### **2.3.5 Blood Collection and Storage**

Blood samples were taken upon informed consent from the same healthy donor. Samples were drawn by venipuncture and stored in a BD Vacutainer® Plus tube (Oxford, UK) containing 3.2% sodium citrate coagulation preservative and stored at 4 °C until analysis.

Ethical clearance for the collection of biological fluids for this specific study was granted by the King's College London Biomedical Sciences, Dentistry, Medicine and Natural & Mathematical Sciences Research Ethics Subcommittee (reference number BDM/13/14-26).

### **2.3.6 DNA Profiling**

Potential effects on the recovery of DNA from body fluids after the application of each sensor were observed by adding 50 µl of each reagent at their respective working concentrations to 150 µl of human blood. DNA was extracted using the QIAmp® DNA Mini kit (Qiagen, Manchester, UK) according to the manufacturer protocol and quantified using the Quantifiler™ Human DNA Quantification Kit (Thermo Fisher Scientific, California, USA). Samples were diluted to 0.1 ng/µl prior to amplification (1 ng total DNA) with the AmpFISTR® SGM Plus® PCR Amplification Kit (Applied Biosystems, Paisley, UK) using a Perkin Elmer 9700 thermal cycler (Cambridge, UK). STR amplicons were resolved on an Applied Biosystems® 3130 Genetic Analyser and evaluated using GeneMapper® software (California, USA).

## 2.4 Results and Discussion

### 2.4.1 Commercial Assay Selection

Each of the commercial biosensing assays tested employed one of the sensing transduction mechanisms previously reviewed. These mechanisms were chosen for study based on reported high 'turn-on' emission intensities, instantaneous signal production and a potential adaptability towards the forensic analysis of biological fluids. The commercial assays used for testing were as follows:

- **Quant-iT PicoGreen dsDNA Assay Kit (Environmentally-Sensitive)**  
An initially non-fluorescent probe that intercalates into DNA bases, stabilising thiazol-quinolinium coupled systems and forcing the molecule into a preferred conformational state responsible for fluorescence emission [135].
- **EnzChek Protease/Peptidase Assay Kit (Intramolecular FRET)**  
A substrate comprised of donor and acceptor fluorophores held within close proximity by an amino acid chain, allowing FRET-based quenching to occur. Enzymatic hydrolysis of the chain by a range of proteases separates the pair to relieve quenching effects and produce fluorescence at 528 nm (**Figure 7a**).
- **FluoReporter Biotin Quantitation Assay Kit (Intermolecular FRET)**  
Multiple 2-(4'-hydroxyazobenzene) benzoic acid (HABA) molecules are bound with moderate affinity to avidin labelled with Alexa Fluor 488 dyes, quenching emission via intermolecular FRET. In the presence of biotin, HABA molecules are competitively displaced, resulting in increased fluorescence [158].
- **EnzChek Ultra Amylase Assay Kit (Static Quenching)**  
A substrate comprised of a proprietary starch derivative (DQ™ starch) heavily labelled with self-quenching BODIPY® FL fluorophores to such a degree that emission is quenched. Digestion of the starch backbone by  $\alpha$ -amylase yields numerous fluorescent fragments (**Figure 9a**).

### 2.4.2 Slide Microscopy

Three out of the four transduction mechanisms tested were able to demonstrate a level of *in situ* sensing performance that may be considered suitable for the forensic detection and identification of body fluid stains. Fluorescence increases in response to deposits were exhibited by the EnzChek® Protease/Peptidase, FluoReporter® Biotin Quantitation and EnzChek® Ultra Amylase assay kits and were found to be proportional to analyte concentration (**Figure 12**). Furthermore, these emission changes occurred immediately after reagent application, thereby promising the potential for rapid fluid screening without extended incubation or development times.

In comparison to wet deposits, a small general decrease in fluorescence intensity was observed upon the application of sensors to dried targets, with lower analyte concentrations (1 µg and 100 ng/ml for both EnzChek® Protease/Peptidase and EnzChek® Ultra Amylase assay kits) remaining indistinguishable from negative controls. This phenomenon may be due to the restriction of analyte movement as a result of solute evaporation, which may limit potential target-sensor interaction. However, previous studies investigating differences in the sensitivity of current presumptive testing reagents between wet and dry fluid stains did not find such effects to be statistically significant [38].

Greatest assay sensitivity was shown by the FluoReporter® Biotin Quantitation assay kit, with 100 ng/ml concentrations of biotin differentiated in both wet and dry deposits. This is likely due to the virtually non-existent background emission of the assay reagent, which is achieved through the binding of multiple quencher moieties to a single fluorescently-labelled avidin molecule, resulting in a greater level of intermolecular FRET quenching [158].

Whilst acceptable detection at concentrations of 10 µg/ml and 1 µg/ml for wet and dry deposits respectively was achieved by the EnzChek® Ultra Amylase Kit, this assay also exhibited the highest background



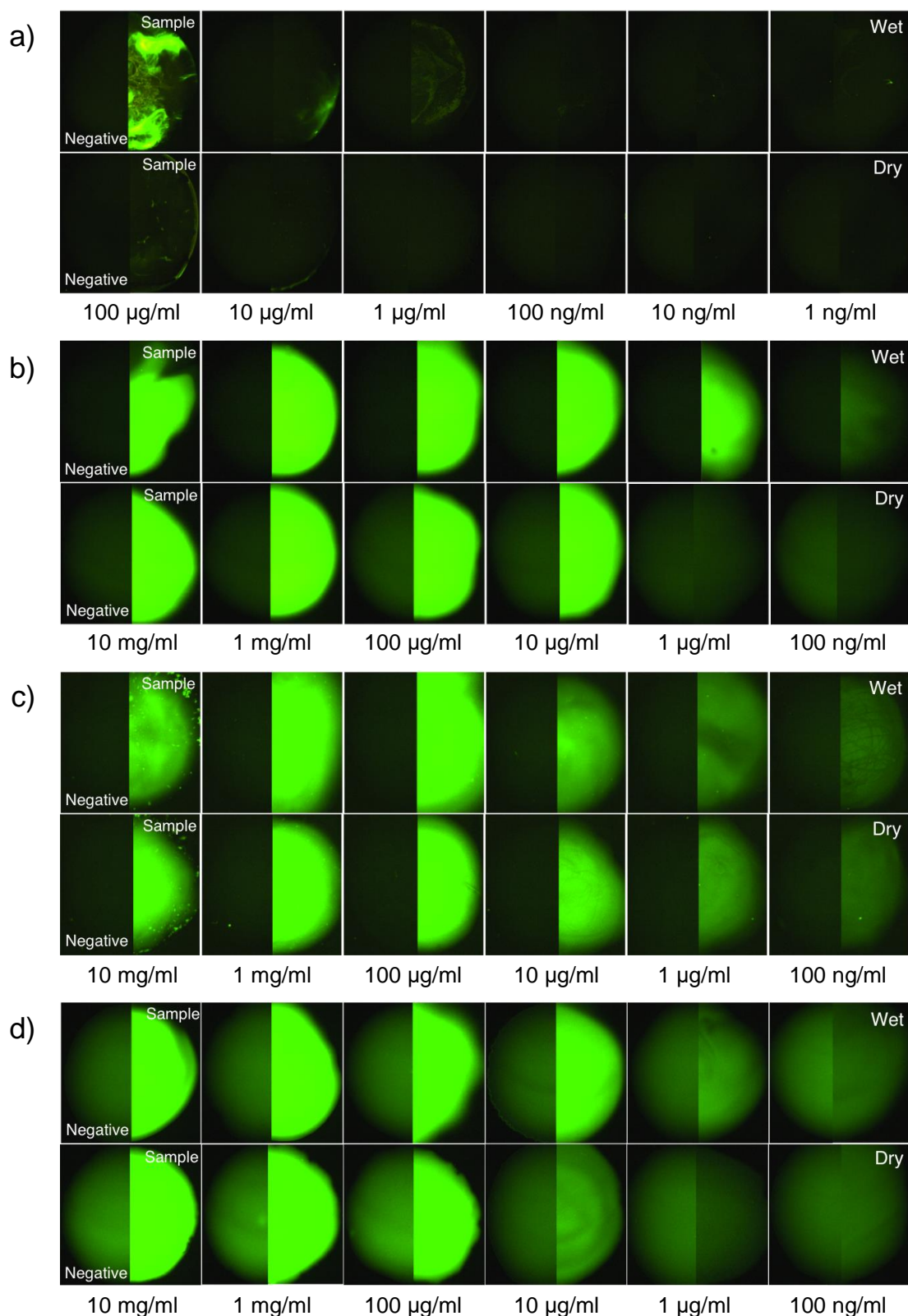


**Figure 12:** Demonstration of *in situ* commercial assay performance against six concentrations of wet and dry analyte deposits on glass slides. Triplicate measurements all displayed similar results: a) Quant-iT™ PicoGreen® dsDNA Assay Kit, b) EnzChek® Protease/Peptidase assay Kit, c) FluoReporter® Biotin Quantitation Assay Kit and d) EnzChek® Ultra Amylase Assay Kit.

fluorescence. This may indicate that the static self-quenching processes of the DQ™ starch substrate are not as effective as those employed within other fluorescence transduction mechanisms, leaving a number of labelled BODIPY dye molecules that have not undergone homodimeric pairing. This high background may potentially inhibit the ability of static-quenching-based sensing mechanisms to visualise areas of fluid staining.

Despite the success of other commercial assays, the Quant-iT™ PicoGreen® dsDNA assay kit failed to generate adequate *in situ* results, with wet and dry depositions under a concentration of 100 µg/ml remaining difficult to distinguish from reagent-only negative controls. The reason for this poor performance is unclear, but may have resulted from the immiscibility of the reagent and analyte deposits. Whilst the exact formulation of assay reagent has not been disclosed by the manufacturers, separation from all aqueous DNA samples was observed upon sensor addition. Such separations are likely to lead to a reduction in overall fluorescence emission signals by restricting interaction of sensing molecules with target analytes. As these effects are likely to have a negative impact on *in situ* fluid analysis, this sensor was excluded from further surface testing.

### **2.4.3 Surface Microscopy**

The 'green' channel of the histogram tool in Adobe Photoshop™ image software was used to assign a value of fluorescence to each of the analyte samples deposited on prepared surfaces. This was performed to augment observations of emissions made by visual inspection and assign a semi-quantitative value of signal strength for the purpose of data comparison. Since emission wavelengths of all assays tested within this study are produced in the 'green' region of the visible spectrum, it may be assumed that these assigned values directly correlate to a measure of fluorescence intensity.

Whilst this approach has already found acceptance in the scientific community for the quantitative analysis of fluorescence emissions in



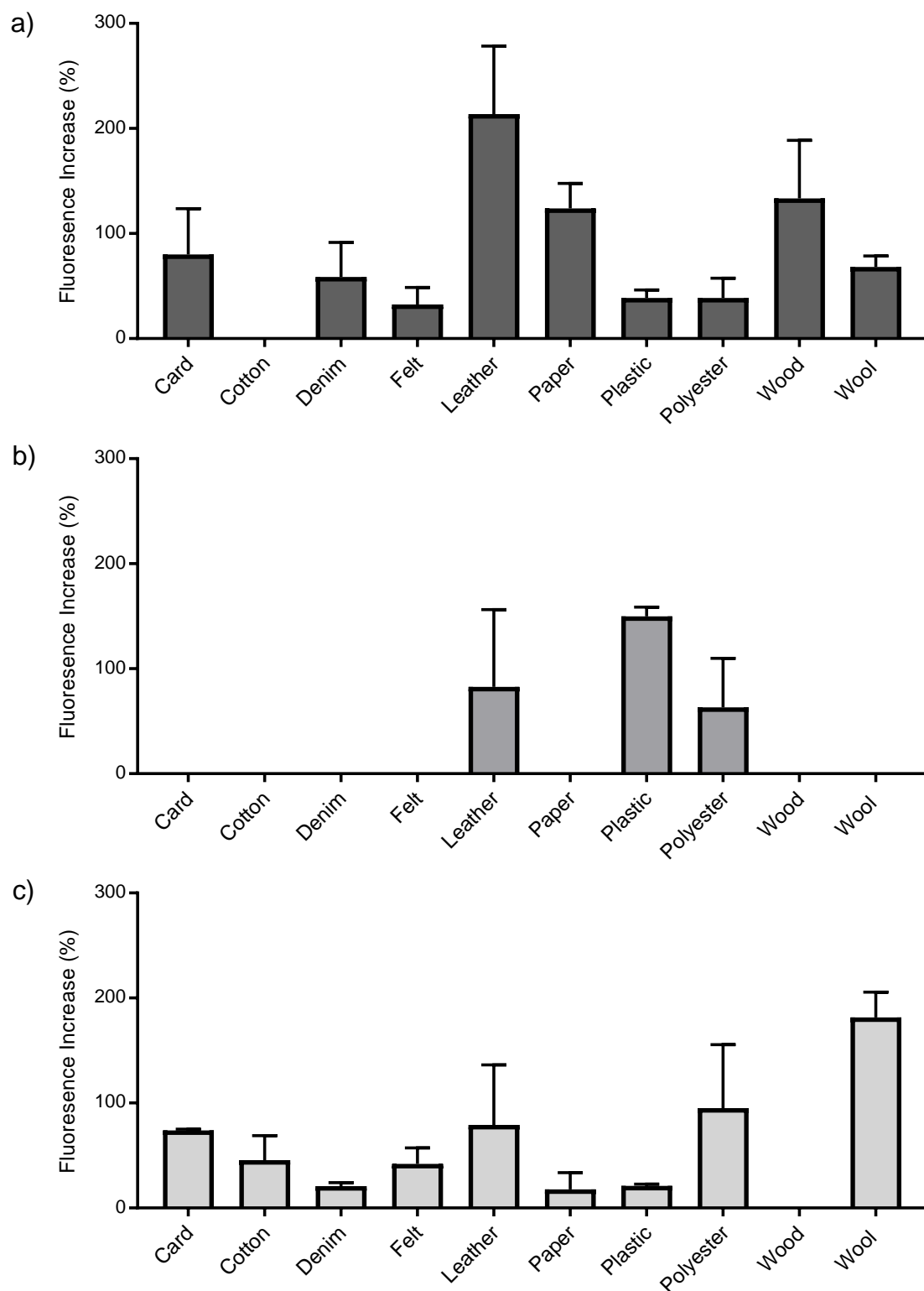


**Figure 13:** Percentage fluorescence increase from reagent-only negative controls of commercial assays upon *in situ* application to analytes on ten forensically relevant surfaces; a) EnzChek® Protease/Peptidase Assay Kit, b) FluoReporter® Biotin Quantitation Assay Kit, c) EnzChek® Ultra Amylase Assay Kit. Data represents the mean  $\pm$  SD, samples performed in triplicate.

digital images [159], an independent assessment of method validity was conducted by depositing serial dilutions of Alexa 488 fluorescent dye onto glass slides. Intensity values given for recorded images were then plotted in a calibration curve against fluorophore concentration, which confirmed technique linearity (results not shown).

Despite established validity, it must be noted that there are several limitations to this method. Whilst reagent and analyte sample volumes remained consistent throughout testing, analyte deposits areas are rarely identical in shape or size. Consequently, the number of pixels chosen to provide average intensity values will be different for each measurement. Furthermore, assay emissions may only be recorded by internal CCD camera up to a maximum light intensity threshold. Samples exhibiting fluorescence above this level will saturate images and will be designated a maximum software intensity value of 255, which will be lower than the actual intensity. However, such saturation occurred only once during testing, resulting in EnzChek® Ultra Amylase assay performance on wood being excluded from plotted results.

Both the EnzChek® Ultra Amylase and EnzChek® Protease/Peptidase assays were able to detect analyte depositions across all surfaces without the need for any further magnification or exposure enhancements (**Figure 13**). These assays both demonstrated high transduction efficiency, utilising the ability of enzymes to interact with multiple substrate molecules, thereby resulting in an amplification of fluorescence signals. Such effects consequently make enzymatic-based signal transduction mechanisms an attractive option for biological fluid sensing.

Despite exhibiting the greatest sensitivity during slide testing, the FluoReporter® Biotin Quantitation assay kit failed to detect analyte deposits on porous surfaces. Absorption of the reagent into these surfaces resulted in the physical screening of fluorescence, preventing emission observation. Enhancements in microscopy magnification and

exposure allowed further detection of analytes deposited on card and denim but still failed to generate results for cotton, felt, paper and wool.

It should also be noted that no fluorescence emission increases were observed from reagent-only negative control samples across all surfaces upon the addition of assay reagent. Such results are likely to indicate the resistance of sensors to cross-reaction with substances endogenous to forensic sampling environments.

#### **2.4.4 DNA profiling**

With previous studies establishing a reduced recovery of high molecular weight STR loci (amplicons that are less likely to undergo successful PCR as a result of DNA degradation) from fluids after some presumptive test applications [37, 42], investigations were undertaken to examine the effects of the fluorescent sensing mechanisms explored in this study on DNA profiling. Such effects may potentially include a reduction in the amount of DNA able to be quantified and/or amplified (which in turn would lead to a decreased number of alleles detected during CE) as a result of sensor-induced PCR inhibition or DNA degradation.

Each of the three commercial reagents used for surface testing were applied to a volume of human blood before DNA was extracted, quantified, amplified and profiled using protocols and techniques standard to most forensic laboratories. Comparisons were then made to a blood reference standard (both in terms of DNA quantification values and electropherogram allele numbers/peak heights), in which distilled water was added in place of assay reagent.

No differences between sensor-added and reference samples outside the limits of normal experimental variation were observed at any stage of the DNA profiling process. DNA extracted from samples containing EnzChek® Protease/Peptidase Assay Kit, FluoReporter® Biotin Quantitation Assay Kit and EnzChek® Ultra Amylase Assay Kit reagents was quantified at 2.09, 2.71 and 5.04 ng/µl respectively, whilst the blood reference sample was found to contain DNA at a concentration of 3.23

ng/μl. Furthermore, full STR profiles were obtained from all samples, with no detrimental effects on high molecular weight loci (**Figure 14**).

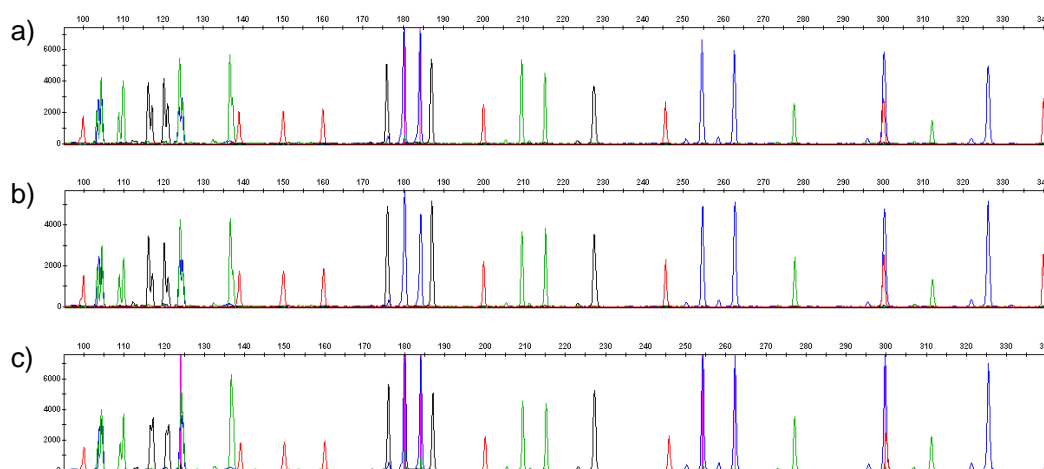


**Figure 14:** STR profiles generated from blood samples after biosensor application: a) EnzChek® Protease/Peptidase Assay Kit, b) FluoReporter® Biotin Quantitation Assay Kit and c) EnzChek® Ultra Amylase Assay Kit. All alleles were observed at each locus compared to a blood reference profile, with relative peak heights also consistent between samples.

## 2.5 Conclusion

In this study, the fluorescent signal transduction mechanisms of four commercial biosensing assays were investigated for their adaptability towards the *in situ* detection and identification of biological fluids. Such sensing mechanisms may potentially provide a number of advantages over current presumptive fluid testing methods, such as increased specificity and a compatibility with downstream DNA profiling processes.

Three out of the four assays tested were successfully able to detect a range of wet and dry analytes deposited in different concentrations on glass slides, each exhibiting ideal increases in fluorescence emission upon target interaction. Two sensors (the EnzChek® Protease/Peptidase Assay Kit and EnzChek® Ultra Amylase Assay Kit) were further able to visualise analytes present on a number of surfaces likely to be found at crime scenes. With the transduction mechanisms of both of these sensors based on the digestion of substrates through enzymatic activity, it was

decided that subsequent efforts in the development of novel fluid analysis methods should first focus on the sensing of intra-fluidic enzyme targets.

Importantly, all sensing mechanisms demonstrating *in situ* detection ability were found to have no effect on downstream DNA profiling processes after application to human blood, thereby allowing the potential for fluids to be identified without sacrificing genetic material.

# **Chapter 3**

## **Fluorogenic Substrates**

### 3.1 Introduction

The two signal transduction mechanisms displaying greatest *in situ* performance during biosensor feasibility tests (**Chapter 2**) both relied upon the hydrolysis of substrates by enzyme activity. Fluorescence transduction based on the selective recognition of enzymes present in bodily tissues is therefore likely to have great potential for use in the development of biosensors for the forensic analysis of biological fluids (although approaches based on static quenching are likely to be less promising, due to the background signals associated with assay reagents).

Although intramolecular signalling via FRET was found to be the most effective method of detecting singular surface-deposited analytes, it may be challenging to combine several sensors based on this mechanism within a single multiplex fluid-biosensing reagent. Assays employing more than one donor-acceptor pair for the analysis of multiple targets within the same sample are often subject to spectral ‘crosstalk’, in which an overlap in the emission wavelengths of commonly utilised fluorophores results in erroneous signal reporting [160].

A solution to this problem may involve the use of fluorogenic peptide substrates, amino acid chains singly-labelled with specific fluorescent molecules that are quenched as part of the conjugation process itself. A range of these molecules, known as ‘pro-fluorophores’, have been produced with emission wavelengths in many areas of the visible spectra and have found wide employment as assays for the measurement of protease activity in biological samples [161].

As each body fluid contains a set of unique protease enzymes (produced in order to fulfil an individual physiological function [162]), fluorogenic substrates may be considered ideal candidates for use as fluid-specific biosensors. Such substrates are often noted for their high target sensitivities, being able to detect proteases at extremely low concentrations within complex biological matrices [163]. The ‘turn-on’

increase in emission intensity exhibited by substrates upon enzymatic digestion is also likely to allow the visualisation of *in situ* body fluid deposits. Furthermore, unlike irreversible antibody-analyte binding interactions, enzymes may react with multiple sensing substrates in succession, resulting in a cumulative amplification of fluorescence signal [164].

This chapter first provides a brief overview of the specific biochemical pathways behind fluorogenic substrate transduction as well as those substrates previously reported for the sensing of various protease enzymes. The application of several commercially available substrates specific to the intra-fluidic proteases prostate specific antigen (PSA), kallikrein 8 (KLK8) and thrombin towards the detection of deposited semen, saliva and blood respectively, is then investigated. Attempts to improve upon these assays are then made through the construction of custom substrates using a novel solid-phase peptide synthesis (SPPS) route.

This chapter contains both published research articles and unpublished work. An introduction to each published manuscript is given explaining the contributions of each listed author. Supplementary material is also provided where available.

## **3.2 Review of Fluorogenic Substrates**

### **3.2.1 Transduction Mechanism**

The capacity of enzymes to distinguish between different molecules is integral to the maintenance of cellular function. Whilst this selectivity is regulated by a range of factors, such as the spatial and temporal location of enzymes (as well as their concentration), protease activity is mainly controlled by the recognition of specific amino acid sequences [165]. In order to study this activity, a wide range of synthetic metabolic substrates have been produced that are able to generate measurable signals, such as a change in absorbance or fluorescence, as a result of protease interaction [166].



Fluorogenic substrate production relies on the attachment of a pro-fluorophore at the C-terminus of a specific peptide chain. Such chains are usually based on the amino acid structure of protein cleavage sites, areas that proteolytic enzymes are able to recognise and bind in order to catalyse the hydrolytic cleavage of peptide bonds [167]. In synthetically produced substrates, this cleavage occurs in the bond between the pro-fluorophore and the P1-position amino acid of the peptide.

**Table 7:** A list of pro-fluorophores commonly used within fluorogenic substrate assays.

Fluorophore	Abbreviation	Ex/Em $\lambda$ (nm)	Type	Ref.
$\beta$ -naphthylamine	$\beta$ NA	330/415	Naphthylamine	[168]
4-methoxy- $\beta$ -naphthylamine	4M $\beta$ NA	340/430	Naphthylamine	[169]
7-amino-4-methylcoumarin	AMC	339/439	Coumarin	[170]
4-methylumbelliferyl	4MU	386/448	Coumarin	[171]
7-amino-4-carbamoylmethylcoumarin	AAC	350/450	Coumarin	[165]
7-amino-4-chloromethylcoumarin	CMAC	353/466	Coumarin	[172]
7-amino-4-trifluoromethylcoumarin	AFC	380/500	Coumarin	[173]
Fluorescein	-	490/514	Xanthene	[174]
Rhodamine-110	Rh-110	498/520	Xanthene	[175]
Resorufin	-	571/585	Phenoxazinone	[176]
Cresyl violet	CV	601/632	Oxazine	[177]

The pro-fluorophores used within these substrates are typically phenoxazinone, coumarin or xanthene-based compounds [178]. Whilst highly fluorescent at specific wavelengths within a free state, conjugation of either coumarin or phenoxazinone derivatives to peptides results in the blue-shifting of fluorophore absorbance and emission via intramolecular charge transfer (ICT) processes [179]. Consequently, fluorescence at the emission wavelengths of the free molecules is suppressed, quenching the entire system [179].

Conversely, xanthene-based fluorophores, such as Rhodamine-110 or fluorescein, are quenched via the internal conversion of molecular structure upon peptide attachment. This conversion, which generally involves the transition of the fluorophores to colour-less lactone forms, results in the disruption of conjugated systems responsible for

fluorescence [180]. A full list of pro-fluorophores commonly used in the production of fluorogenic substrates may be found in **Table 7**.

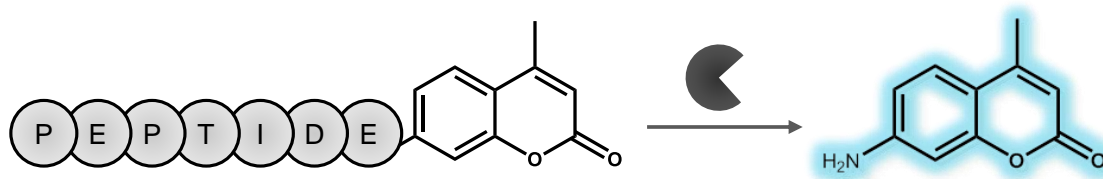


**Figure 15:** A short peptide chain terminally labelled with a fluorescent moiety, creating a non-fluorescent substrate system. Resulting protease activity separates the fluorophore and relieves quenching effects.

Positive ‘turn-on’ emission signals from fluorogenic peptide substrates therefore arise from the liberation of pro-fluorophore leaving groups from peptides as a result of protease digestion (**Figure 15**). This separation causes the fluorophores to revert to their original highly-fluorescent forms, allowing protease activity to be directly observed in real-time.

### 3.2.2 Previously Reported Fluorogenic Substrates

An extensive range of fluorogenic peptide substrates have been developed over the last several decades for the detection of many different proteolytic enzymes. These substrates are prominently employed (in both *in vitro* and *in vivo* settings) to investigate the role of specific proteases in the progression of human disease states, such as cancer, cystic fibrosis and chronic obstructive pulmonary disease [178, 181].

Other substrate applications include the identification and enumeration of microorganisms within microbial communities based on the detection of distinct metabolic enzyme activities [166]. A selection of fluorogenic peptide substrates that have been previously reported in literature is provided in **Table 8**.

**Table 8:** Fluorogenic substrates previously developed for protease activity detection.

Target	Substrate	Leaving Group	Ref.
Aminopeptidase	Leu-AMC	AMC	[182]
DPPIV	[Ala-Pro] <sup>2</sup> -CV	CV	[177]
Caspase 1 & 5	Ac-Trp-Glu-His-Asp-AMC	AMC	[183]
Caspase 2	Ac-Val-Asp-Val-Ala-Asp-AFC	AFC	[184]
Caspase 3 & 7	Ac-Asp-Glu-Val-Asp-Rh-110-MC	Rh-110	[185]
Cathepsin B	Z-Phe-Arg-AMC	AMC	[186]
Cathepsin D	Bz-Arg-Gly-Phe-Phe-Pro-4MβNA	4MβNA	[187]
Cathepsin K	Z-Leu-Arg-AMC	AMC	[188]
Chymotrypsin	Suc-Ala-Ala-Pro-Phe-AMC	AMC	[189]
Elastase	MeO-Suc-Ala-Ala-Pro-Val-AFC	AFC	[190]
Factor Xa	Boc-Ile-Glu-Gly-Arg-AMC	AMC	[191]
Kallikrein 4, 5, 8, 13 & 14	Boc-Val-Pro-Arg-AMC	AMC	[191]
Plasmin	Suc-Ala-Phe-Lys-AMC	AMC	[192]
PSA	Mu-His-Ser-Ser-Lys-Leu-Gln-AFC	AFC	[193]
Thrombin	Bz-Phe-Val-Arg-AMC	AMC	[194]
Trypsin	[Z-Arg] <sup>2</sup> -Rh-110	Rh-110	[175]

### 3.3 Published Article 1: ‘Application of Fluorescent Substrates to the *in situ* Detection of Prostate Specific Antigen’

The content of following section was published as an original research article in: **Gooch, J.**, Daniel, B. and Frascione, N. **Application of fluorescent substrates to the *in situ* detection of prostate specific antigen.** Talanta, 2014. 125: p. 210-214.

All experimental work was performed by the candidate, who also drafted the initial manuscript. Dr. Barbara Daniel and Dr. Nunzianda Frascione provided supervisory and technical support throughout the research and had final approval over manuscript submission.

#### 3.3.1 Manuscript

**Authors:** James Gooch,<sup>a</sup> Barbara Daniel,<sup>a</sup> and Nunzianda Frascione.<sup>a\*</sup>

**Authors Address:** a) Department of Forensic and Analytical Science, King’s College London, Franklin-Wilkins Building, 150 Stamford Street, London SE1 9NH, UK.

**Abstract:** The forensic identification of body fluids frequently presents an important source of genetic material and investigative interpretation. However, presumptive testing techniques presently employed in the discrimination of biological fluids are subject to criticism for poor specificity, lack of fluid localisation ability and detrimental effects on DNA recovery rates. The recognition of fluid-specific biomarkers by fluorogenic substrates may provide a novel resolution to these issues but research has yet to establish any pertinent *in situ* fluid detection applicability. This study therefore utilises a fluorogenic substrate (Mu-HSSKLQ-AFC) specific to the seminal protein prostate specific antigen in an effort to detect human semen deposited on a number of surfaces typical to criminal investigation. The ability of fluorescent fluorogenic substrates to simultaneously identify and visualise biological fluids *in situ* is demonstrated for the first time, whilst the production of complete STR profiles from fluid sources is also confirmed to be completely unaffected by substrate application.

## Introduction

Locating and identifying body fluids such as semen, blood and saliva can often aid the progression of criminal investigation by providing intelligence on the nature and circumstance of an offence and may additionally associate or exonerate a suspect through the isolation of genetic material.

A number of 'presumptive' screening assays exist to rapidly exclude or indicate fluid presence, employing simple biochemical processes in order to generate colorimetric changes within a given substrate. Those indicating the presence of blood rely on the oxidation of haem to catalyse substrate-specific reactions [5, 14, 195] whilst intra-fluidic enzyme activity provides the basis for the testing of semen and saliva [27, 196]. However, previous validation studies have established limitations in the usefulness and evidential strength of these assays. With the exception of the chemiluminescence phenomenon exploited in the detection of blood by

Luminol, presumptive tests cannot be used to localise fluid depositions, thereby necessitating time-consuming visual searches prior to analysis. Furthermore, the molecular targets examined by these tests are not fluid-specific, often leading to false positives between different fluid types and other non-fluid substances [197-199]. Detrimental effects on the recovery of DNA from fluid depositions have also been demonstrated after some presumptive test applications [30, 37].

Currently the most widely used presumptive test for semen identification is the Brentamine assay for the detection of acid phosphatase, an enzyme secreted into semen by the prostate gland [196]. However, the requirement of specialist knowledge and equipment often makes this test problematic. Results are subject to a high level of expert interpretation [200-202], whilst Brentamine toxicity also necessitates use of a fume hood.

Recent improvements in fluid assay specificity have utilised immunological testing strips for the detection of fluid-endogenous protein biomarkers [203-205]. However, these testing processes do not allow for the retention of fluids following application, potentially sacrificing a valuable source of material for genetic profiling [117].

Our research group has made initial efforts in the design of novel body fluid analysis techniques, developing a fluorescent biosensor complex specific to Glycophorin A, an erythrocyte membrane protein used in the identification of human blood [134]. However, whilst demonstrating effective glycophorin detection via decreases in fluorescence intensity, the 'turn-off' nature of signalling restricts the use of this sensor in visualising discrete fluid deposits *in situ*. A 'turn-on' fluorescence based assay is therefore preferable for simultaneous identification and localisation purposes.

The proteolytic digestion of peptide substrates to release fluorescent by-products within the same molecular unit may be considered an attractive signalling mechanism for *in situ* fluid detection. High specificities make

enzyme recognition elements ideal candidates for fluid analysis, whilst 'turn-on' increases in fluorescence intensity upon target interaction may allow the visualisation of *in situ* fluid depositions. Furthermore, unlike irreversible antibody-based reactions, enzyme targets may interact with multiple substrate molecules to amplify signal production. Simultaneous detection of multiple fluid enzymes may also potentially be achieved by exploiting fluorophores of differing wavelengths in a single multiplex assay.

A central appeal of fluorogenic substrates as an alternative to current presumptive assays is that DNA-degrading oxidative processes, such as those exploited by Luminol and Leucomalachite green, are not required to generate a positive response [197]. With research yet to explore the effect of substrates on genetic material, investigation into the possible interference of reagents with DNA amplification, quantitation or profiling may be considered pertinent.

This study therefore explores the use of fluorogenic peptide substrates specific to prostate specific antigen (PSA) for the simultaneous visualisation and identification of human seminal fluid. PSA is a semen-endogenous protein responsible for proteolysis of gel-forming Semenogelin 1 and 2 [206]. The unique expression level of PSA within seminal fluid, often produced in milligram levels per millilitre [206], has established its wide acceptance as a forensic biomarker for semen identification.

Denmeade *et al.* [193] produced 12 peptide substrates for monitoring PSA activity based on amino acid sequences directly adjacent to mapped PSA cleavage sites of Semenogelin 1 and 2. These substrates utilise 7-amino-4-methylcoumarin fluorophores, which after amide bond conjugation to peptides undergo excitation and emission wavelength shifts, restricting fluorescence output. Subsequent separation of the fluorophore from the peptide by serine protease hydrolysis occurs in the presence of PSA and restores fluorescence.

The particular substrate MU-HSSKLQ-AFC (**Figure 16**) displayed the highest specificity for PSA, arising from its resistance to similar proteolytic enzymes found within body fluids. Whilst this substrate has found routine use in the recognition of prostate cancer markers, it has yet to be applied towards the detection of human semen.

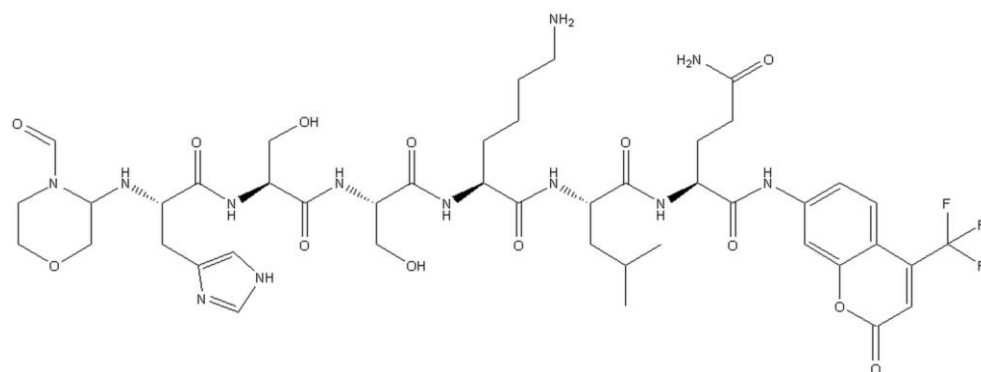


**Figure 16:** PSA fluorogenic substrate - a hexapeptide consisting of amino acid sequence HSSKLQ, terminally labelled with a fluorescent coumarin derivative. Specific digestion of the peptide by PSA yields fluorescent 7-amino-4-trifluoromethylcoumarin.

The fluorescence response of substrate MU-HSSKLQ-AFC to dilutions of semen within solution, as well as to whole semen extracted from *in situ* swabs, was measured via spectrofluorometry to determine the ability of the fluorogenic substrate to detect free PSA within seminal fluid. Further *in situ* detection ability was examined, testing substrate performance against semen deposits on glass slides and a number of surfaces typically encountered within forensic casework. Assay reagent was also applied to depositions of blood, saliva and urine to confirm substrate specificity. MU-HSSKLQ-AFC was lastly applied to semen samples for subsequent SGM plus profiling to assess reagent effect on each stage of the profiling process.

## Materials and Methods

### Reagents

#### *Fluorogenic PSA Substrate*

Lyophilised Prostate Specific Antigen Fluorogenic Substrate (Mu-HSSKLQ-AFC) was purchased from EMD Millipore (Massachusetts,

USA) and dissolved in 109.5  $\mu$ l DMSO to make an 8 mM stock solution before dilution in PBS to a working concentration of 400  $\mu$ M.

### *Body Fluid Collection and Storage*

Blood, semen, saliva and urine samples were taken after informed consent. Blood samples were drawn by venipuncture and stored in a BD Vacutainer® Plus tube (Oxford, UK) containing 3.2% sodium citrate coagulation preservative. All tissue samples were stored at 4 °C until analysis.

## **Instrumentation and Procedures**

### *Spectrofluorometry*

Fluorescence measurements were conducted on a BioTek Synergy HT spectrophotometer (Vermont, USA). Dilution curves were constructed through the addition of 100  $\mu$ l of diluted semen (1:1, 1:2, 1:4, 1:8, 1:16, 1:32, 1:64) in a 96-well microplate to 100  $\mu$ l of 400  $\mu$ M PSA fluorogenic substrate and measured with appropriate blank (200  $\mu$ l PBS) and negative controls (100  $\mu$ l PBS, 100  $\mu$ l assay reagent). Swabs taken from *in situ* semen depositions were extracted in 100  $\mu$ l of PBS and added to 100  $\mu$ l of working concentration substrate. All fluorescence emissions were recorded at room temperature in duplicate using Ex400/Em528 $\pm$ 20 nm wavelengths (for the measurement of emissions at 508 nm) immediately after mixing.

### *Slide Microscopy*

Fluorogenic PSA reagent was tested against seminal dilutions (1:25, 1:50, 1:100, 1:200, 1:500, 1:1000) deposited on glass slides as a demonstration of *in situ* substrate sensitivity. Semen volumes of 10  $\mu$ l were applied to the centre of each slide before the direct 10  $\mu$ l addition of substrate. Duplicates of each dilution were performed. Negative reagent-only controls were applied on the same slide as a measure of background reagent fluorescence, whilst blank controls consisting of semen-only applications were also used to monitor possible analyte auto-



fluorescence. The simulation of dry depositions was achieved through the application of 10 µl of seminal fluid to glass slides, which were subsequently allowed to dry overnight. Reagent was then applied directly at the point of analysis.

Images were taken in the dark immediately after application on an Olympus SZX12 fluorescence microscope (Tokyo, Japan) and internal CCD camera. BV filtration (Ex 400-440 nm) was used for substrate excitation, whilst all additional microscopy parameters were kept constant (hue = 359, saturation = 255, white balance = 64, contrast = 0, brightness = 1023, gamma = 10, magnification = ×8.5) in order to restrict result variation.

Investigations into substrate specificity were also undertaken with application to depositions of whole blood, urine and saliva on slides in order to exclude the possibility of inter-fluidic cross-reaction.

### *Surface Microscopy*

Eight different surfaces consisting of cotton, denim, felt, leather, paper, plastic, polyester and wood were chosen to reflect materials on which body fluids are commonly deposited within criminal investigations. All surfaces were cut to fit the size of a microscope slide. In a similar manner as commercial assay testing, 10 µl depositions of human semen were applied to the surfaces and allowed to dry overnight. PSA substrate was applied directly to depositions in 10 µl volumes with the same negative and blank controls previously described.

Images were once again recorded on an Olympus SZX12 fluorescence microscope utilising BV filtration (Ex 400-440 nm). All measurements were performed in duplicate.

200 µl of working concentration substrate was lastly dispersed directly over a semen deposition on leather using a common atomising spray bottle to reflect ideal future application methods.

## *DNA Profiling*

50 µl of PSA substrate at working concentration was added to 150 µl of human semen to observe effects on DNA recovery after application. DNA was extracted using the QIAmp® DNA Mini kit (Qiagen, Manchester, UK) according to the supplied protocol and quantified with the Quant-iT™ PicoGreen® dsDNA Assay Kit (Invitrogen, Paisley, UK). Samples were diluted to 0.1 ng/µl prior to amplification with the AmpFISTR® SGM Plus® PCR Amplification Kit (Applied Biosystems, Paisley, UK) using a Perkin-Elmer 9700 thermal cycler (Cambridge, UK). STR amplicons were resolved on an ABI3130 genetic analyser and evaluated using GeneMapper® software. Generated profiles were compared to a semen reference profile to examine potential inhibition.

## **Results and Discussion**

### **Spectrofluorometry**

Whilst regularly demonstrating detection of purified PSA protein within solution [193, 207] this fluorogenic substrate has never been used to target the native PSA contained within seminal fluid. The potential for reagent inhibition or physical fluorescence screening by other biomolecules present in a complex matrix makes it pertinent to investigate whether a positive signal can be generated from whole semen.

Appropriate fluorescence intensity changes to varying dilutions of seminal fluid were observed through spectrofluorometry. Constructed calibration curves were found to be consistent with those demonstrated by Niemelä *et al.* [207] for the detection of PSA within solution and established a quantitative linear relationship between semen concentration and substrate fluorescence (**Figure 17**).

A commonplace practice within forensic investigation is to swab potential fluid depositions that require analysis at a later point. It is consequently vital that substrates react to material extracted from these swabs in the same manner as whole fluid. Swabs were therefore taken of semen

deposited on a leather surface prior to extraction in PBS via brief vortexing. The collected material was analysed using the same procedure as whole fluid and did not display any differentiation in fluorescence response from its neat fluid counterpart (results not shown).

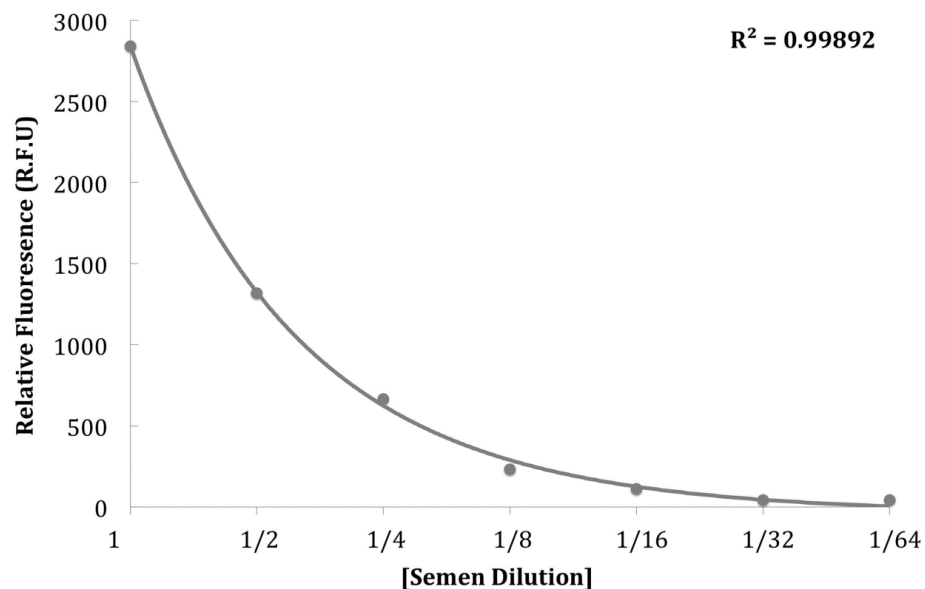


**Figure 17:** Dilution curve demonstrating the relationship between seminal concentration and fluorogenic PSA substrate emission.

### Slide Microscopy

The main benefit of many presumptive tests is their ability to be performed at the point of fluid discovery. It is important that substrate reagents designed to detect biological fluids may do so *in situ* with only basic instrumental assistance for fluorescence observation, such as a portable alternative light source. Human semen was deposited on to glass slides prior to the direct application of PSA substrate. Any changes in fluorescence intensity were observed using standard fluorescence microscopy. Positive substrate reactions successfully identified all semen depositions, even at sensitive 1:1000 dilutions (**Figure 18**). Similar results were obtained using simulated dry depositions. Fluorescence emissions occurred immediately upon substrate application, promising potential for rapid fluid screening without extended incubation times. Background reagent fluorescence was not observed at any point during negative control testing, allowing for the visualisation of discrete fluid areas.

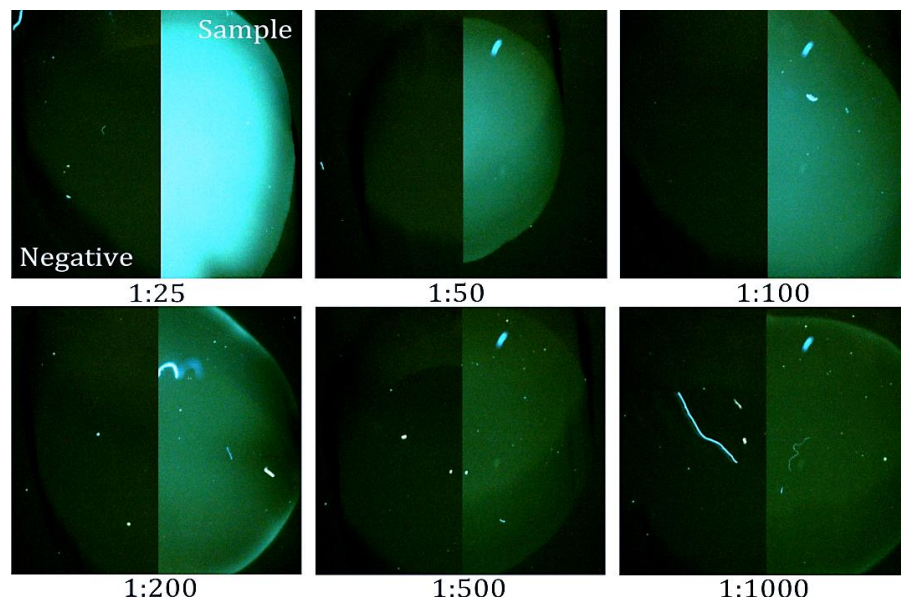


**Figure 18:** Demonstration of in situ substrate testing of seminal depositions upon glass slides across a range of six dilutions. Duplicate measurements were taken and also displayed expected results

Additional studies of inter-fluidic substrate specificity were also undertaken with reagent applied to wet and dry depositions of whole blood, saliva and urine. In all cases, the PSA substrate did not generate a positive reaction, thereby demonstrating both high semen specificity, as well as resistance to proteases that may be present within other body fluids (results not shown).

### Surface Microscopy

The successful detection of semen by this substrate clearly confirms the high performance of fluorogenic substrates in the simultaneous identification and localisation of biological fluids *in situ*. Nevertheless, clean glass slides are not representative of surfaces encountered within forensic casework. Surfaces on which fluids are typically deposited may potentially prevent the success of fluorescent substrates *via* absorption, movement restriction and physical screening effects. Furthermore, surfaces may contain a number of unknown substances that could inhibit substrate–target interaction. Fluorogenic PSA substrate was therefore applied, utilising the same slide testing procedure, to dry semen depositions on eight surfaces relevant to criminal investigation.

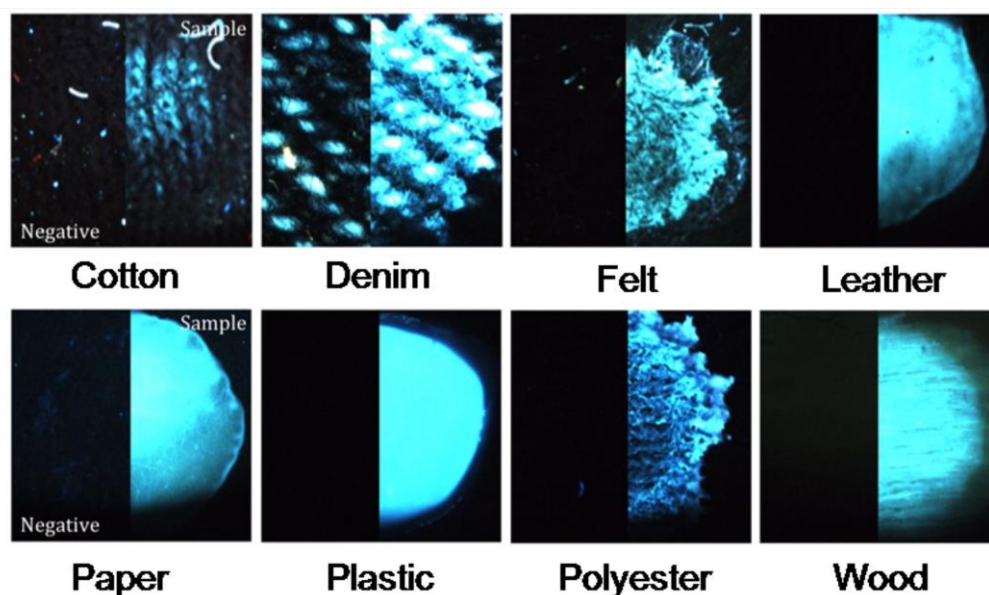


**Figure 19:** Successful detection of human semen across eight forensically relevant surfaces by fluorogenic PSA substrate. Reagent-only negative controls are provided on the left side of each image

Despite the difficult nature of surface testing, positive results were generated on each of the eight surfaces, identifying and visualising all semen deposits (**Figure 19**). Once again, substrate-only negative controls did not exhibit any observable fluorescence upon application. Furthermore, surface material had little effect on the ability of the substrate to generate positive results, with no assay interference occurring during testing.

The direct spray dispersal of reagent over a large evidential surface may be considered the most efficient process of localising fluid deposits. 200 µl of substrate was applied to seminal depositions on leather using a common 1 ml atomising spray bottle in order to examine the *viability* of this method. Positive substrate emissions easily localised all semen depositions, elucidating discrete staining areas and confirming the validity of this technique (results not shown).

### **DNA Profiling**

Validation studies by Tobe *et al.* [37] have previously demonstrated a significantly reduced recovery of high molecular weight STR loci from biological fluids after some presumptive testing applications. Furthermore,

the physical application process of the seminal acid phosphatase test has been shown to limit the amount of spermatozoa, and thus DNA, available for genetic profiling [202].

PSA substrate was applied to semen samples, which underwent extraction, quantification, amplification and profiling according to standard forensic protocols to examine the effects of assay application on the recovery of genetic material from biological fluids. Comparisons were then made to reagent-less semen standard (**Figure 20**).

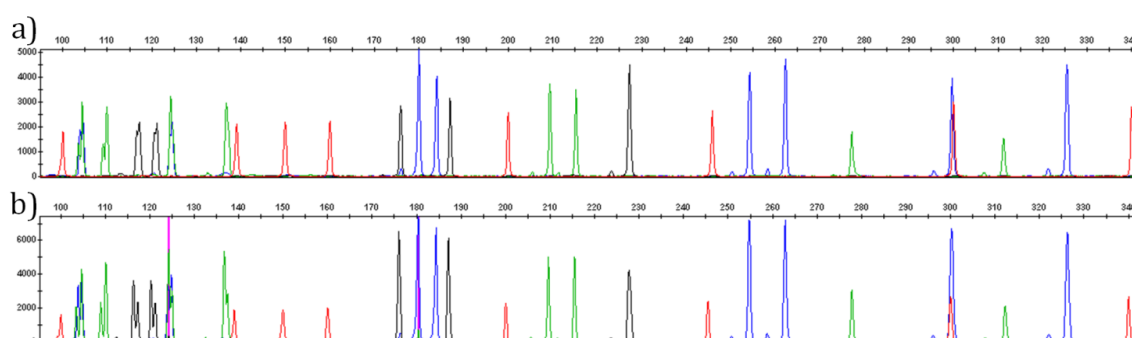


**Figure 20:** Genetic profiles generated from: a) semen reference profile and b) semen sample with applied PSA substrate. Profiles display no significant differences.

Successful genetic recovery from substrate-applied semen was established by Picogreen quantification, with an average concentration of 8.99 ng/μl DNA per sample extraction falling within expected values. Furthermore, full STR profiles were obtained from all assay applications, with no detrimental effects on high molecular weight loci. Differentiation of reagent-applied samples from their reference profiles was not observed at any stage of the profiling process outside the limits of normal experimental variation

## Conclusion

This study successfully demonstrates for the first time the ability of fluorescent substrates to identify biological fluid depositions *in situ*. Human semen was detected across a range of surfaces typical to forensic investigation with additional visualisation via a direct spraying application.

This particular substrate exhibited ideal increases in fluorescence intensity upon target interaction, even at sensitive 1:1000 seminal dilutions, giving opportunity for its use in contaminated fluid depositions or those washed in removal attempts.

Importantly, substrates were found to have no effect on DNA profiling processes after application to biological fluids and thereby negate the potential forfeit of fluid identification in order to maximise genetic material recovery.

An ideal application of fluid-specific substrates would likely exploit a number of different peptide sequences, each with separate emission wavelengths for simultaneous enzyme detection within several fluid types in a multiplex sensing system.

Displaying both an immediate and specific response to analyte presence, fluorogenic substrates have the potential to prevent month-long visual evidence searches by localising fluid depositions within a matter of seconds. Serious thought should therefore be given to the development of fluorogenic substrates as replacements to current presumptive testing techniques.

### **3.4 Published Article 2: 'Solid-phase Synthesis of Rhodamine-110 Fluorogenic Substrates and their Application in Forensic Analysis'**

The content of following section was published as an original research communication in:

**Gooch, J., *et al.*, Solid-phase synthesis of Rhodamine-110 fluorogenic substrates and their application in forensic analysis. Analyst, 2016. 141(8): p. 2392-2395.**

All experimental work was performed by the candidate, who also drafted the initial manuscript. Help with peptide synthesis, as well as access to the Institute of Pharmaceutical Science research laboratories and high-performance liquid chromatography (HPLC) and mass spectrometry



instruments, was provided Dr. Vincenzo Abbate. Dr. Barbara Daniel and Dr. Nunzianda Frascione provided supervisory and technical support throughout the research and had final approval over manuscript submission.

### 3.4.1 Manuscript

**Authors:** James Gooch,<sup>a</sup> Vincenzo Abbate,<sup>b</sup> Barbara Daniel<sup>a</sup> and Nunzianda Frascione.<sup>a\*</sup>

**Authors Address:** a) Analytical & Environmental Sciences Division, King's College London, 150 Stamford Street, Waterloo, SE19NH, London, b) Institute of Pharmaceutical Science, King's College London, 150 Stamford Street, Waterloo, SE19NH, London.

**Abstract:** A novel synthetic route for the rapid and efficient preparation of fluorogenic substrates utilising Rhodamine-110 or similar fluorophores is reported. Applicability of the synthesized peptide substrate within a forensic casework context is also presented.

Last year, over 10,000 exhibits were submitted to the Evidence Recovery Unit (ERU) of the Metropolitan Police Service. Body fluid stains such as blood, semen and saliva are often the most important forms of biological evidence encountered in forensic casework. Determining the identity of such deposits can be used to further a criminal investigation as it may provide information on both the nature of the offence and the genetic origin of the fluid (through DNA profiling) [3]. Consequently, over 90% of these submitted exhibits required examination for the presence of biological fluids.

However, with meticulous visual examination by trained personnel being the most common method of detection, determining the presence and location of any fluid deposits may be very challenging, especially with small, or latent traces on dark backgrounds which may be easily overlooked [3]. Long wave UV or violet light sources may aid detection by exploiting the auto-fluorescent properties of some intra-fluidic molecules



but their use is restricted to a select number of surface types [36]. The colorimetric presumptive assays used in order to identify the type of fluid present are also considered by many in the forensic community to be limited by issues of specificity [208], safety [209] and their detrimental effects on DNA recovery [37]. Developing a fast, dependable and specific method of fluid detection would save time and money. Biosensors that simultaneously detect and identify body fluids could represent a cost and time efficient alternative to present day techniques. The development of fluorogenic peptide substrates specific to each body fluid type could improve body fluid search efficiency through the identification of fluid-specific proteases *in situ* via fluorescence emission [131, 210].

Rhodamine-110 (Rh-110) is a xanthene-based fluorescent dye containing two aromatic amine moieties, the symmetric or asymmetric modification of which may shift the existing equilibrium of the molecule from a highly fluorescent quinoid towards a colourless lactone formation, quenching fluorescence emission [180]. This has cemented Rhodamine-110 as a popular pro-fluorophore for use within many protease substrates *via* the direct attachment of specific amino acid chains (with a positive fluorescence signal achieved *via* the proteolytic separation of peptide and fluorophore in the presence of a target enzyme) [180]. The physical and spectral characteristics of Rh-110 are considered highly desirable for biological fluid detection, as they display a high quantum yield and are relatively pH insensitive. Moreover, Rh-110 based substrates exhibit an almost non-existent emission upon peptide conjugation, preventing background fluorescence and ensuring high enzymatic assay sensitivities [180].

However, all reported symmetric and asymmetrically labelled Rh-110 peptide substrates have so far been synthesized through solution chemistry, a task that is made problematic due to the poor nucleophilicity of the Rh-110 aromatic amines [211], and often leads to inefficient peptide-fluorophore acylations. Final product yields are inevitably very low, as each intermediate must undergo substantial purification [185].

This makes the cost of Rh-110-based substrates high and since the aim of the research is to produce a spray that could be used directly on forensic evidence, this cost would be unacceptable.

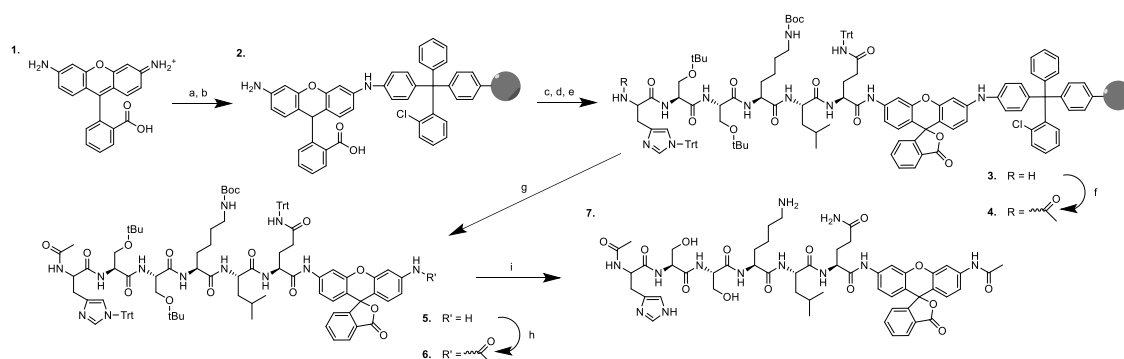


**Figure 21:** Schematic of Rh-110 PSA substrate development: a) 2-ct resin (0.27 mmol), DCM, DIPEA, 24 hrs, b) MeOH, 10 min, c) Fmoc-Gln(Trt)-OH (3 mmol), DMF/pyridine, EDC (2.5 mmol), 24 hrs, x2, d) 20% piperidine/DMF, 30 min, e) 6 x AA, oxyma, DIPCDI, DMF, 1 hr, f) 10 x  $(\text{CH}_3\text{CO})_2\text{O}$ , DIPEA, DMF, 1 hr, g) AcOH : TFE : DCM, 1 hr, h)  $\text{CH}_3\text{COCl}$ , DIPEA, DMF, 48 hrs, i) TFA : TIPS : TA : phenol

We surmised that preparing large quantities of peptide substrates in a rapid and efficient manner could be achieved *via* the direct attachment of Rh-110 to a solid support. In this procedure (**Figure 21**), it is envisioned that one of the aromatic amine groups of Rh-110 may be anchored to a functionalized solid support, keeping the remaining amine group available for the subsequent stepwise incorporation of amino acids by standard Fmoc-SPPS. This route offers advantages over typical solution-phase conjugation techniques by allowing the incubation of fluorophores with large molar excesses of any desired amino acid residue, which may be removed without extensive liquid-liquid extraction and chromatographic purification steps, thereby increasing overall product yield. Instead, excess amino acids, coupling reagents and other by-products may be removed by simple resin wash and filtration processes. Therefore, a fluorogenic substrate for the purpose of detecting seminal fluid within a forensic casework framework was constructed through the sequential coupling of immobilized Rh-110 to amino acids HSSKLQ, a sequence previously reported by Denmeade *et al.* [193] as a proteolytic cleavage site of seminal fluid-specific protease prostate specific antigen (PSA).

Rh-110 was successfully anchored to the 2-chlorotriyl chloride resin (known to react with aromatic amines in the presence of a base such as pyridine or N,N-Diisopropylethylamine (DIPEA)) [212] in the first step towards substrate preparation. Upon reaction, the resin exhibited a deep red coloration that was retained after extensive washing, indicating successful dye incorporation. Cleavage of a small portion of the acid-labile resin, followed by ESI-MS analysis confirmed the presence of free Rh-110 (Supplementary - **Figure 24**).

With a number of workers previously reporting the unsuccessful conjugation of bulky peptides to Rh-110 within solution [213], product **3** was instead assembled *via* the stepwise addition of single amino acids in a series of individual reactions. Multiple large excesses of Fmoc-protected glutamine were first incubated with Rh-110-attached resin **2** in order to ensure complete coupling (which was confirmed *via* ESI-MS analysis after 'soft' cleavage of a small portion of resin (Supplementary - **Figure 25**)), with successive amino acids incorporated through standard SPPS deprotection-wash-coupling-wash cycling to form a PSA-specific peptide backbone. Acetylation of the histidine N-terminus was performed to prevent substrate degradation from environmental aminopeptidase activity [214].

As previously mentioned, many substrates utilising Rh-110 fluorophores are bis-substituted, having been synthesized through the symmetric conjugation of identical peptides to both aromatic amines in order to quench fluorescence. However, in such substrates, a two-step enzymatic hydrolysis is required in order to cleave both peptide chains before a full fluorescence signal is restored, consequently limiting the dynamic linear range of the assay [215]. As a result, the majority of fluorogenic Rh-110 peptide substrates now produced are mono-substituted, with secondary aromatic amines 'capped' through amide, carbamate or urea modifications [180]. This not only permits the assay to be completed within a single hydrolysis step, but also produces the same complete emission quenching effects as bis-peptide modification [216]. Therefore,

a 'soft' cleavage of the resin was performed under mild acidic conditions to generate **5** from the solid support, allowing all tert-butyloxycarbonyl and trityl amino acid side-chain protecting groups to remain intact (preventing accidental amino acid side-chain modification) during the capping of the remaining Rh-110 aromatic amine by acetylation. Liquid-liquid extraction was then performed to separate aqueous-reactive acetyl chloride from organic-soluble products, which were subsequently treated with TFA and precipitated in ether to remove acid-labile side-chain protecting groups. RP-HPLC and high-resolution mass spectrometry were used to confirm the purity and identity of final substrate product **7** respectively (Supplementary - [Figure 26](#) and [Figure 27](#)).

Spectrofluorometry was employed to observe the emission response of **7** quantitatively towards its intended enzymatic target. Whilst the final goal of this substrate is to identify the presence of whole semen, it is important to confirm that a fluorescence response is only elicited as a result of PSA hydrolysis and not from interaction with any other molecule within the seminal fluid matrix. Therefore in addition to dilutions of seminal fluid, substrate **7** was incubated with varying concentrations of purified PSA protein. Immediate fluorescence signal increases upon the addition of both PSA ([Figure 22a](#)) and seminal fluid ([Figure 22b](#)) successfully demonstrated cleavage between Rh-110-Ac and the attached glutamine residue, consequently establishing the potential use of this substrate as a semen-specific biosensor.

Responses generated by seminal fluid were found to be much higher compared to that of tested purified protein concentrations, which was expected considering the significantly larger levels of PSA usually contained within whole semen (approximately 0.5-3.0 mg/ml) [206]. As it is important to determine the proteolytic specificity of fluorogenic substrates prior to their application (especially within the context of forensic casework, in which a false-positive signal may represent an incorrect evidential identification), final substrate **7** was also incubated

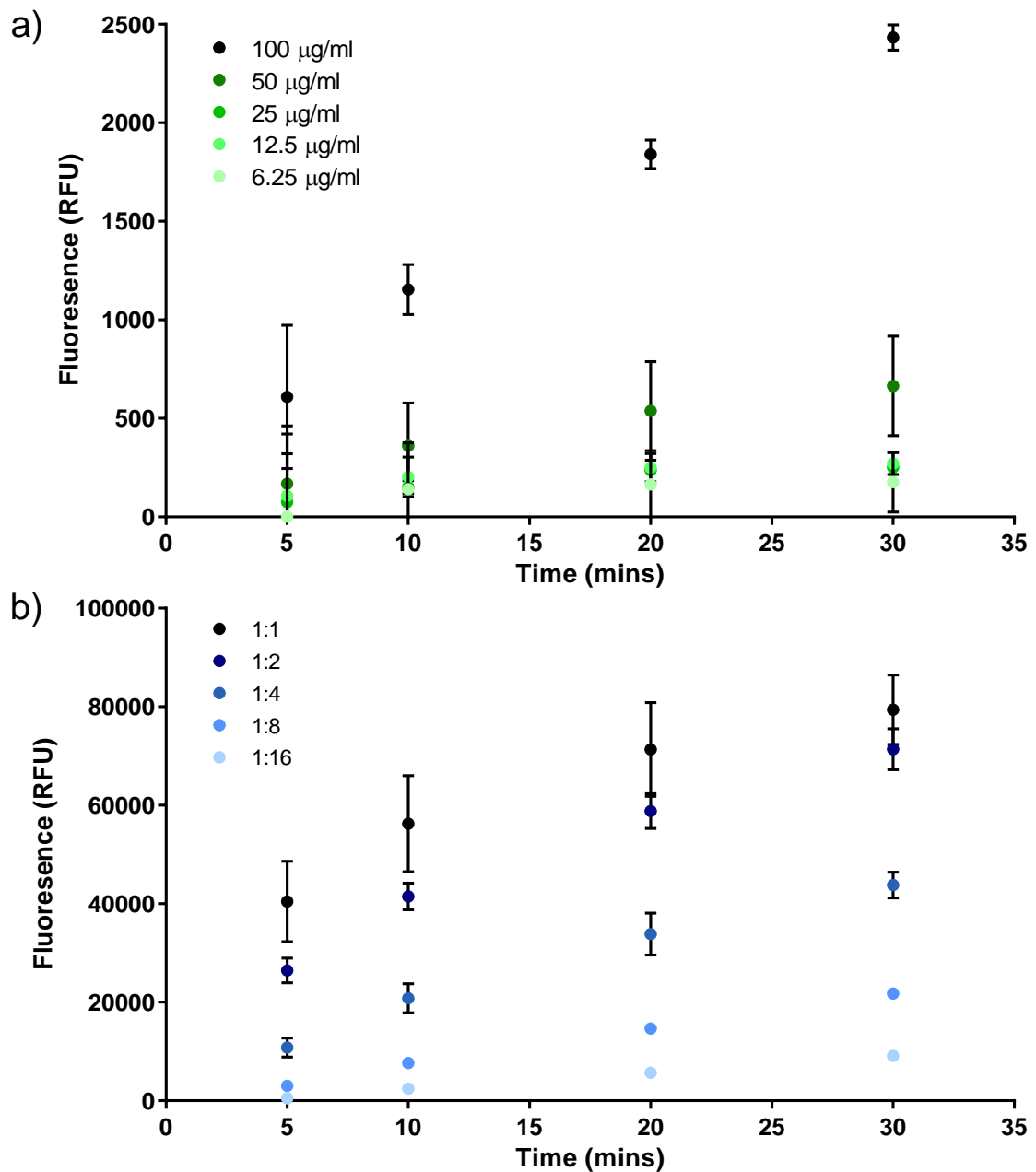


**Figure 22:** Fluorescence response of final substrate 7 to a) concentrations of purified PSA protein and b) seminal fluid dilutions over time.

with identical concentrations of trypsin, proteinase K and aminopeptidase M as a measure of PSA selectivity. In all cases the substrate did not exhibit a positive response, thereby demonstrating a high specificity towards seminal fluid, as well as an inherent resistance to protease enzymes present within other body fluids or the surrounding environment (Supplementary - **Figure 28**). With one of the advantages of this assay over current forensic testing techniques being the ability to simultaneously locate and identify fluid stains *in situ via* fluorescence, it is pertinent to

establish that a positive substrate emission will not be affected by the physical nature of the evidential surface on which a body fluid is deposited. Substrate **7** was therefore applied to small volumes of semen deposited on six surfaces routinely examined within criminal investigation, with subsequent signal responses observed by fluorescence microscopy.

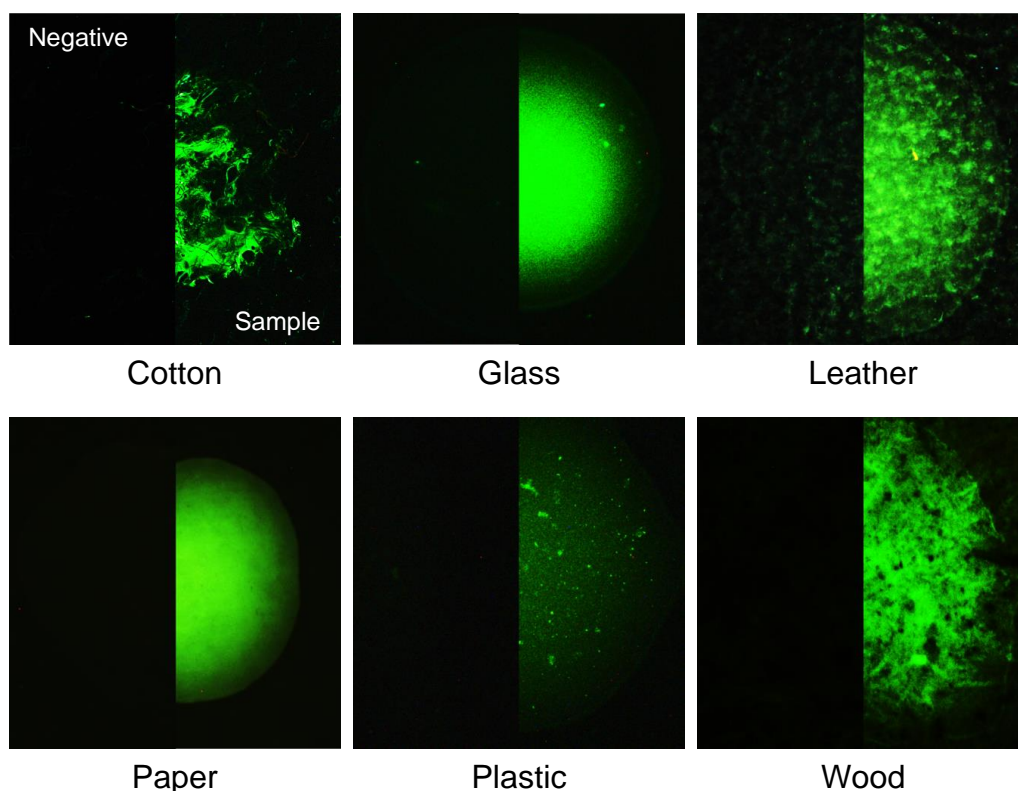


**Figure 23:** Detection of semen across six surfaces by substrate **7**. Reagent-only negative controls are provided on the left side of each image.

Upon reagent application, all deposits were successfully visualised, with surface material displaying little effect on resulting substrate emission (**Figure 23**). Similar visualisation was also achieved *via* the use of a hand-held Crime-lite® portable excitation source (Ex 480-560 nm with 549 nm filter goggles). As an additional method of observing reagent specificity, substrate **7** was also incubated with volumes of blood and saliva *in situ*. No signal was observed upon application (Supplementary - **Figure 29**).

The identification of seminal fluid by PSA detection is currently achieved through absorption of a reconstituted suspect stain onto an

immunochematographic testing strip [217]. However, this technique is not only unable to locate the position of stains upon an evidential item but furthermore, consumes the fluid during the testing process, preventing further DNA analysis. An *in situ* PSA detection assay that allows downstream genetic profiling would consequently be considered advantageous. Therefore, substrate **7** was applied to a volume of seminal fluid deposited on a glass slide, with the resultant mixture being recovered by use of a cotton swab. Samples then underwent standard DNA extraction, quantification, amplification and capillary electrophoresis according to forensic protocols. Comparisons were then made to an untreated but identically processed reference sample to examine the effects of substrate application on genetic recovery. Differentiation of samples was not observed at any stage of the profiling process with the DNA concentrations of reagent-applied fluid and reference sample calculated at 0.66 and 0.61 ng/ $\mu$ l respectively. A full STR profile from both samples was also obtained (Supplementary - **Figure 30**).

In summary, we have described a versatile synthetic route for the simple, rapid and inexpensive preparation of Rh-110-based fluorogenic substrates. Moreover, a substrate produced by this method has already shown great potential as a replacement for currently employed forensic body fluid testing techniques. This substrate allowed the specific detection of seminal fluid traces both within solution and *in situ*, without compromising subsequent genetic profiling processes. Future work will centre on the use of this method to produce fluorogenic substrates towards other biological fluids and latent fingerprints (something that has not currently been achieved). However, with fluorogenic substrates routinely employed in a variety of industrial and biomedical applications, the disclosed synthetic protocol is also likely to have a much larger implication beyond the field of forensic science.

### 3.4.2 Supplementary Information

#### Reagents

All amino acids and peptide coupling reagents were purchased from Sigma Aldrich (Dorset, UK). Rhodamine-110 was obtained from Fisher Scientific Ltd (Loughborough, UK), whilst 2-Chlorotrityl Chloride Resin (1.45 mmol/g loading capacity) was purchased from Cambridge Bioscience (Cambridge, UK). All reagents were used without further modification, except DMF which was kept under constant nitrogen flow.

#### Resin-Rh-110-NH<sub>2</sub>

Chlorotrityl resin (175 mg, 0.27 mmol) was stirred in DCM (1 ml) in the presence of N,N-Diisopropylethylamine (DIPEA, 700  $\mu$ l, 4.11 mmol) for 10 min and subsequently added to a round-bottom flask containing a solution of Rhodamine-110 (136 mg, 0.411 mmol) in DCM (5 ml) and DMF (2 ml). The mixture was gently agitated for 24 hrs before being transferred to an empty fritted polypropylene tube where the resin was filtered and washed with DMF ( $\times 5$ ) and DCM ( $\times 10$ ). Finally, the resin was incubated with methanol for 10 min to cap remaining chloride groups before being re-washed with DMF and DCM. Conjugation was monitored via a 'hard' cleavage of 5 mg of resin to isolate Rhodamine-110 from the solid support via treatment with a 95:0.5:0.5:0.5:0.25 solution of trifluoroacetic acid (TFA): water: phenol: thioanisole (TA): triisopropylsilane (TIPS) for 3 hrs at room temperature. Ice cold diethyl ether was then added to precipitate products, with organic solvent, scavengers and by-products removed by centrifugation. Obtained solids were washed several times with diethyl ether to remove any residual scavenger traces and finally dissolved in 50% acetonitrile (ACN) in water containing 0.1% TFA and freeze-dried for 24 hrs. Correct product mass was verified by ESI-MS on a Waters/Micromass (Manchester, UK) ZQ mass spectrometer (**Figure 24**).



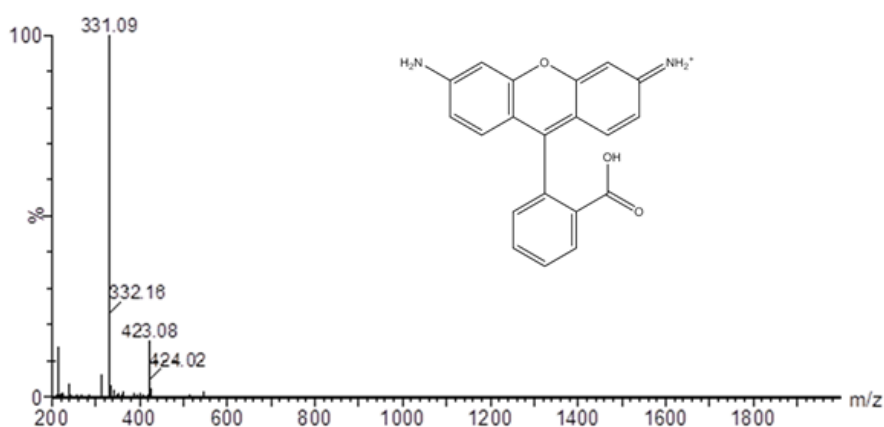


**Figure 24:** ESI-MS data demonstrating free Rhodamine-110 presence after cleavage from a solid support (calculated  $m/z$  for  $[M+H]^+ = 331.11$ ).

### Resin-Rh-110-Gln(Trt)-NH<sub>2</sub>

1.83 g (3 mmol) of Fmoc-Gln(Trt)-NH<sub>2</sub> was added in a round-bottom flask to 8 ml of cold DMF/pyridine (1:1, v/v) and stirred in an ice bath until dissolved. To this was added 479 mg (2.5 mmol) of N-(3-Dimethylaminopropyl)-N'-ethylcarbodiimide (EDC). After 5 min of stirring, 100 mg (0.1 mmol) of Rhodamine-110 resin, suspended in 2 ml of DMF/pyridine (1:1 v/v), was added. Gentle stirring was continued for 24 hrs at room temperature. The resin was transferred to an empty fritted polypropylene tube, filtered and washed with DMF (×5) and DCM (×10) before being re-incubated with additional Fmoc-Gln(Trt)-OH for another 24 hrs using the above-described procedure. Successful amino acid coupling was monitored by a 'soft' cleavage of 5mg of resin to isolate  $^2$ HN-Rh-110-Gln(Trt)-NH<sub>2</sub> from the solid support whilst keeping acid-labile side-chain protecting groups intact. This was achieved by treating the resin with a 1 ml solution of 1:1:8 acetic acid:TFE:DCM for 1 hr at room temperature. Next, the resin was filtered off and washed with cleavage solution, with the collected filtrate concentrated under a stream of nitrogen at 40°C. Hexane (×15 volume excess) was added to precipitate the product, and subsequently removed by rotary evaporation. The obtained products were finally dissolved in 50% ACN in water containing 0.1% TFA and freeze-dried for 24 hrs. The correct mass of the products were once again confirmed via ESI-MS as already outlined (**Figure 25**).

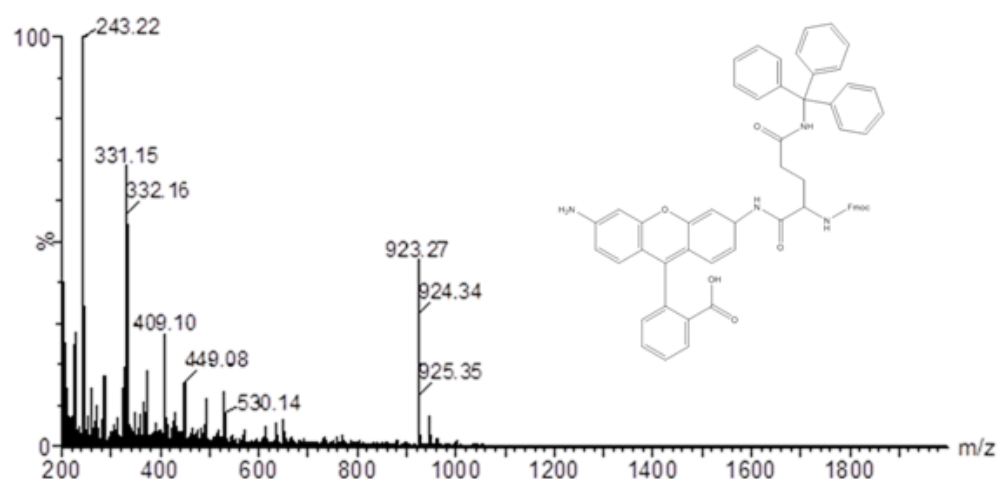


**Figure 25:** ESI-MS data demonstrating successful Resin-Rhodamine-110-Glutamine conjugation after 'soft' cleavage from a solid support (calculated m/z for  $[M+H]^+$  = 923.34).

### Resin-Rh-110-QLKSSH-Ac

Remaining amino acids were added to Rh-110-Gln(Trt)-NH<sub>2</sub>-conjugated resin via a standard Fmoc-Solid Phase Peptide Synthesis (SPPS) strategy. Initial Fmoc deprotection was accomplished by treatment with 20% (v/v) piperidine in DMF for 10 min. The following acylation steps were conducted using six equivalents of Fmoc amino acids, which were pre-activated with ethyl 2-cyano-2-(hydroxyimino)acetate (Oxyma) and N,N'-Diisopropylcarbodiimide (DIPCDI) in DMF in a molar ratio of 1:1:1 of amino acid, Oxyma and DIPCDI, respectively. The N-terminal histidine was acetylated via the addition of ten equivalents of acetic anhydride and twenty equivalents of DIPEA in DMF. All coupling reactions were conducted for at least 1 hr. Excess reagents and impurities were removed by extensive washing with DMF, methanol and DCM. A 'soft' cleavage was once again performed using the above described method to remove <sub>2</sub>HN-Rh-110-QLKSSH-Ac from the solid support.

### Ac-Rh-110-QLKSSH-Ac

To <sub>2</sub>HN-Rh-110-QLKSSH-Ac (7mg) dissolved in DMF (1 ml) were added forty equivalents of DIPEA (28  $\mu$ l) and twenty equivalents of acetyl chloride (5.7  $\mu$ l). The resulting mixture was stirred for 48 hrs before the

addition of 1 ml DCM and 1ml distilled water to isolate a final product by liquid-liquid extraction. The organic phase was isolated prior to the re-extraction of the aqueous layer with 1ml of fresh DCM. The organic layers were combined and washed with 5% NaHCO<sub>3</sub> (1 ml) and brine (1 ml) solutions and dried with sodium sulfate. Following filtration the solvent was removed via rotary evaporation.

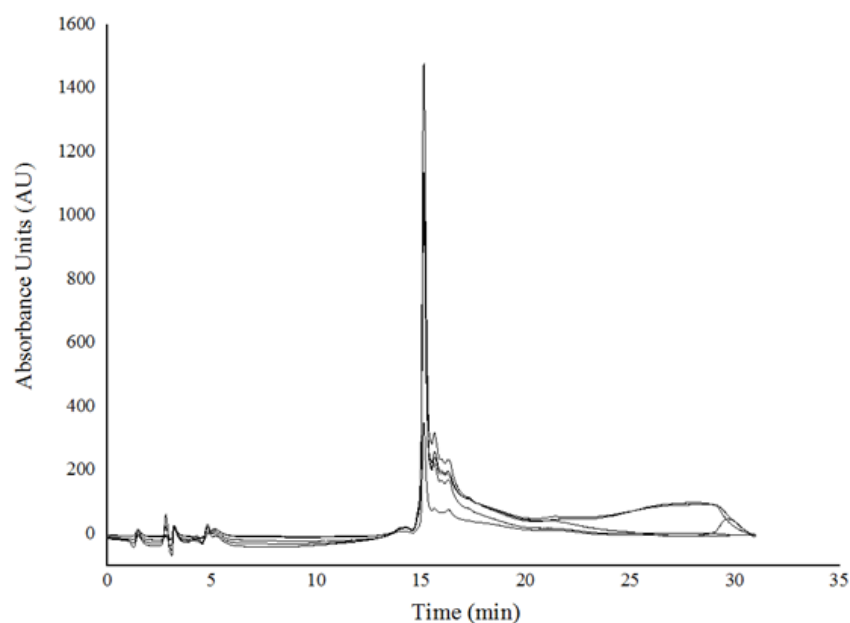


**Figure 26:** HPLC data demonstrating purity of final substrate product Ac-Rh-110-QLKSSH-Ac

To remove acid-labile amino acid side-chain protecting groups, products were treated with using the same ‘hard’ cleavage cocktail solution and precipitation methods as previously outlined. Product purity was examined by analytical RP-HPLC (**Figure 26**), carried out on a HP1050 HPLC system equipped with an autosampler, quaternary pump and Diode-Array Detector and employing a Zorbax SB C-18 2.1mm x 10cm (particle size 3.5 micron) column. A linear gradient of mobile phase B (acetonitrile containing 0.1% TFA) over mobile phase A (0.1% TFA in water) from 0-90% B in 20 min was performed with a flow rate of 0.2 ml/min. Eluents were monitored at wavelengths between 210-280 nm with data collected and analyzed using ChemStation software. Correct product mass was determined by HRMS on an Exactive Plus Orbitrap Mass Spectrometer (**Figure 27**).

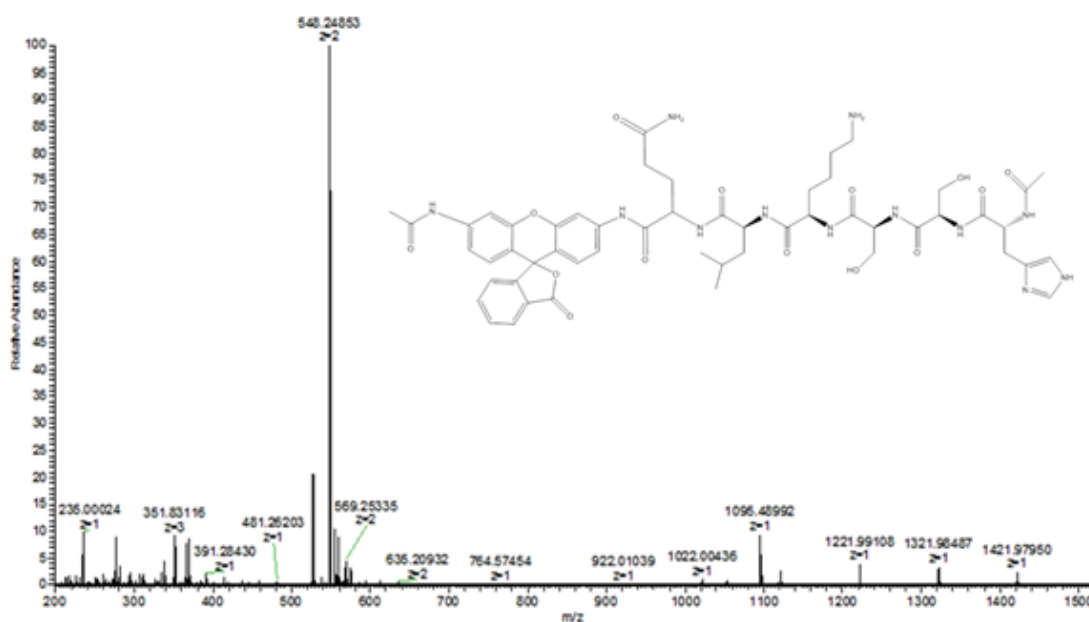


**Figure 27:** High-resolution MS data of final substrate product Ac-Rh-110-QLKSSH-Ac (calculated  $m/z$  for  $[M+H]^+ = 1095.4900$ ) and doubly charged  $[M + 2H]^{2+}$  ion (calculated  $m/z = 548.2489$ )

## Body Fluid Collection and Storage

Semen samples were taken after informed consent and stored at 4 °C until analysis. Tissue collection for this project has full ethical clearance under the King's College London Biomedical Sciences, Dentistry, Medicine and Natural & Mathematical Sciences Research Ethics Subcommittee (Reference number BDM/13/14-26).

## Spectrofluorometry

Final substrate Ac-Rh-110-QLKSSH-Ac (0.9 mg, 0.82  $\mu\text{mol}$ ) was dissolved in DMSO (82  $\mu\text{l}$ ) to make a 10 mM stock solution before dilution in 10 mM Tris reaction buffer to a 50  $\mu\text{M}$  working concentration. Substrate performance was observed via the 100  $\mu\text{l}$  addition of 50  $\mu\text{M}$  Ac-Rh-110-QLKSSH-Ac to 100  $\mu\text{l}$  of both purified PSA protein (100, 50, 25, 12.5, 6.25  $\mu\text{g/ml}$ ) and seminal fluid dilutions (1:1, 1:2, 1:4, 1:8, 1:16) and measured with appropriate negative controls (100  $\mu\text{l}$  10 mM Tris Buffer, 100  $\mu\text{l}$  assay reagent). Additional observations of substrate specificity were undertaken via the incubation of 50  $\mu\text{M}$  Ac-Rh-110-QLKSSH-Ac with 100  $\mu\text{g/ml}$  concentrations of Proteinase K (Fisher Scientific Ltd,

Loughborough, UK), Aminopeptidase M (Merck Millipore, Darmstadt, Germany) and Trypsin (Sigma Aldrich, Dorset, UK) (**Figure 28**). All fluorescence measurements were conducted on a BioTek Synergy HT spectrophotometer (Vermont, USA). Emissions were recorded at room temperature in triplicate using Ex485±20/Em528±20 nm wavelengths (for the measurement of emissions at 535 nm) over the course of 30 min.

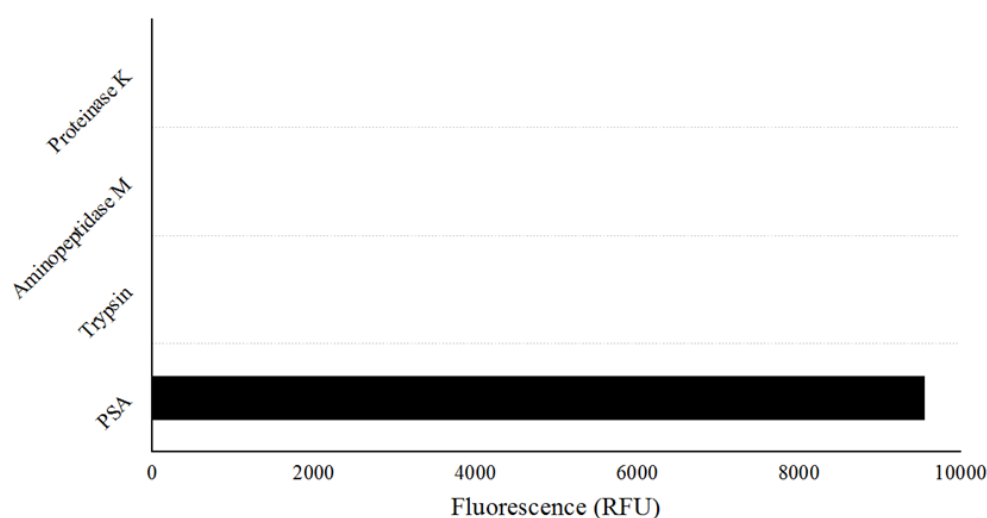


**Figure 28:** Fluorescence response of Ac-Rh-110-QLKSSH-Ac to 100 µg/ml concentrations of Proteinase K, Aminopeptidase M, Trypsin and PSA.

### ***In Situ Microscopy***

Six different surfaces consisting of cotton, glass, leather, paper, plastic and wood were chosen to reflect materials on which body fluids are commonly deposited within criminal investigations. All surfaces were cut to fit the size of a microscope slide. Semen volumes of 5 µl were applied to the centre of each surface before the direct 5 µl addition of substrate Ac-Rh-110-QLKSSH-Ac. Negative reagent-only and blank semen-only controls were used to limit the possibility of background fluorescence. Images were taken in the dark immediately after application on an Olympus SZX12 fluorescence microscope. GFP filtration (Ex 460-490 nm) was used for substrate excitation, whilst all additional microscopy parameters were kept constant (Hue = 359, Saturation = 255, White Balance = 0, Contrast = 1023, Brightness = 0, Gamma = 10, Magnification = ×8.5) in order to restrict result variation.

### ***In Situ Specificity***

An additional observation of substrate specificity against other body fluid types was undertaken via the incubation of 5 µl substrate Ac-Rh-110-QLKSSH-Ac with 5 µl of blood and 5 µl saliva deposited on glass slides. Controls and fluorescence microscopy were utilised in the same manner previously described.

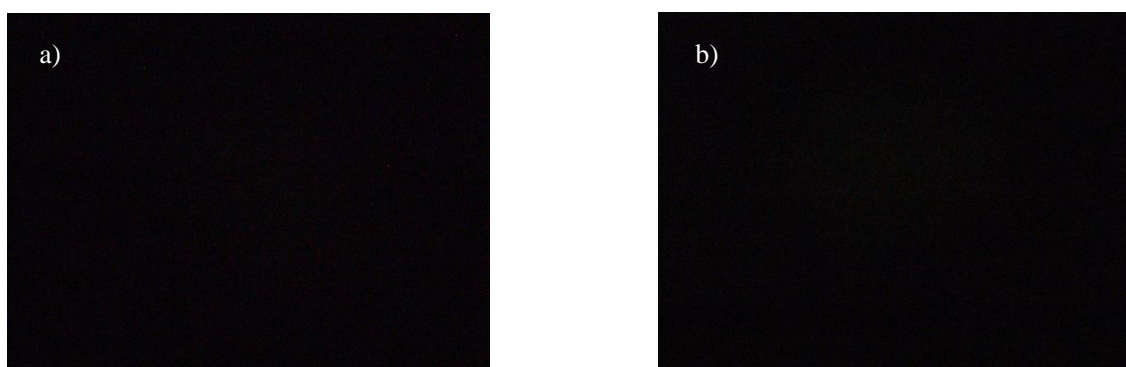
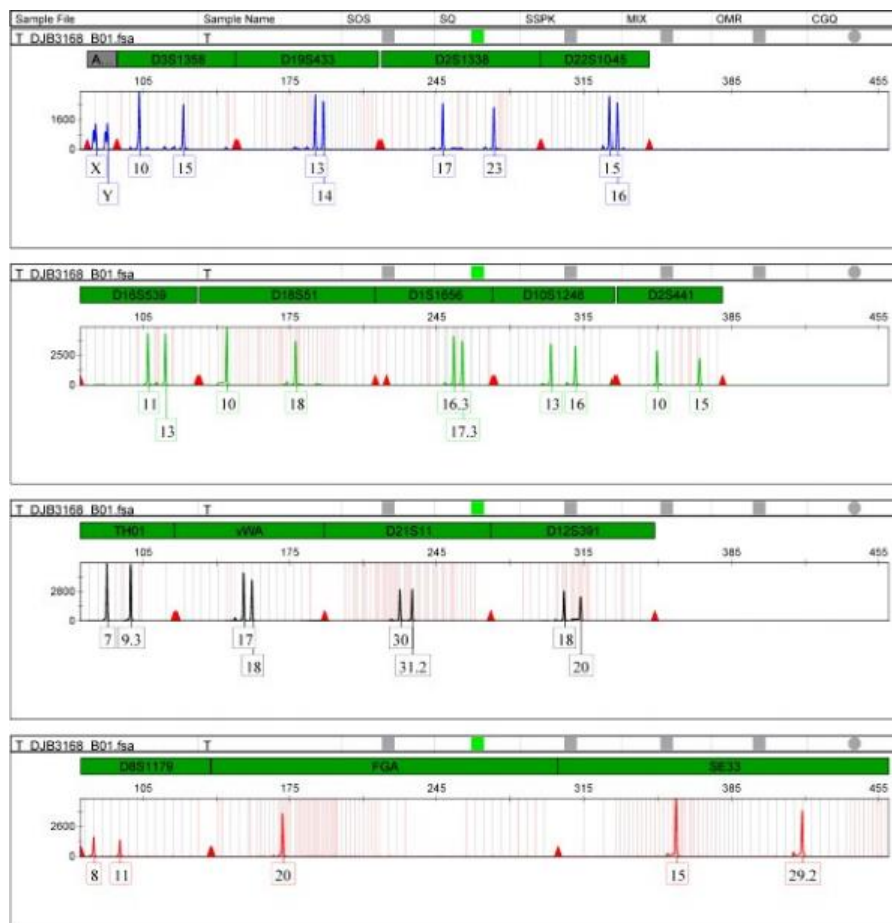


**Figure 29:** Incubation of substrate Ac-Rh-110-QLKSSH-Ac with a) blood and b) saliva. No positive signals were observed upon application.

### **DNA Profiling**

5 µl of Ac-Rh-110-QLKSSH-Ac at working concentration was added to 5 µl of human semen deposited on glass slides to observe effects on DNA recovery after application. The resulting mixture was then recovered via the use of a cotton swab. DNA was extracted using the QIAmp® DNA Mini kit (Qiagen, Manchester, UK) according to the supplied protocol and quantified with the Quantifiler® Human DNA Quantification Kit (Fisher Scientific Ltd, Loughborough, UK). Samples were diluted to 0.5 ng/µl prior to amplification with the PowerPlex® ESI 17 Pro System (Promega, Southampton, UK) using a Perkin Elmer 9700 thermal cycler (Cambridge, UK). STR amplicons were resolved on an ABI3130XL genetic analyser and evaluated using GeneMapper® software. Generated profiles were compared to a semen reference profile (5 µl semen + 5 µl H<sub>2</sub>O to examine potential inhibition (**Figure 30**).

a)



b)

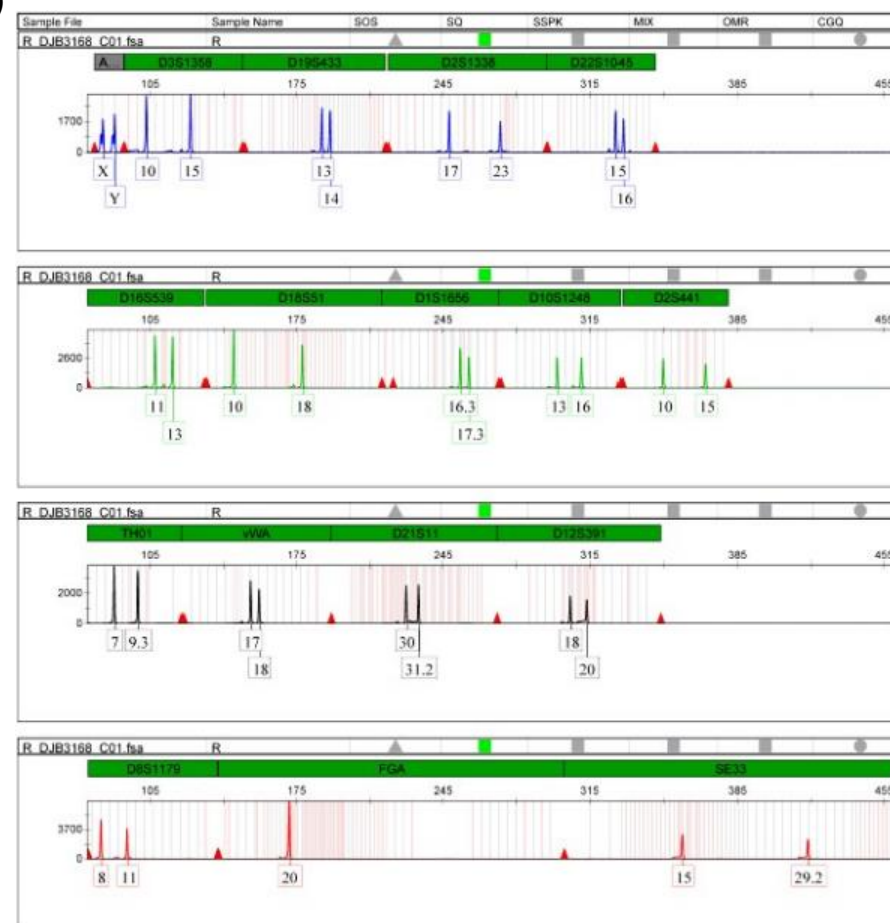


**Figure 30:** Generated STR profiles from a) human semen sample treated with 5  $\mu$ l substrate Ac-Rh-110- QLKSSH-Ac and (b) reference human semen sample treated with 5  $\mu$ l H<sub>2</sub>O. No significant differences between profiles was observed.



### 3.5 Published Article 3: 'Fluorogenic Substrates for the Detection of Saliva'

The content of following section was published as an original research article in:

**Gooch, J., et al., Fluorogenic substrates for the detection of saliva.** Forensic Science International: Genetics Supplement Series, 2017. 6: p. e565-e567.

Experimental work was performed by the candidate with assistance from Chang Rong Chua. The candidate also produced the manuscript. Help with peptide synthesis, as well as access to the Institute of Pharmaceutical Science research laboratories and HPLC and MS instruments, was provided Dr. Vincenzo Abbate. Dr. Nunzianda Frascione provided supervisory and technical support throughout the research.

#### 3.5.1 Manuscript

**Authors:** James Gooch,<sup>a</sup> Chang Rong Chua,<sup>b</sup> Vincenzo Abbate,<sup>a</sup> Nunzianda Frascione.<sup>a\*</sup>

**Authors Address:** a) King's Forensics, Analytical & Environmental Sciences Division, King's College London, 150 Stamford Street, London, SE1 9NH, UK, b) Department of Biological Sciences, National University of Singapore, 14 Science Drive 4, 117543, Singapore.

**Abstract:** The potential of fluorogenic substrates to detect and identify human saliva *in situ* was first explored using commercially available substrate Boc-VPR-AMC. The substrate was applied to a range of saliva dilutions deposited on glass microscope slides. A positive fluorescence response was observed immediately after application against each deposit up to a 1:8 dilution. In an attempt to improve assay sensitivity, a novel substrate Ac-VPR-Rh-110-Ac, utilising a Rhodamine-110 fluorophore, was prepared using a solid-phase peptide synthesis protocol previously reported by our research group. Application of Ac-VPR-Rh-



110-Ac to saliva deposits demonstrated a successful increase in assay sensitivity limits, allowing stains of up to 1 in 128 dilution to be detected.

## Introduction

The Office for National Statistics estimates that in 2016/2017 alone, over 5 million criminal offences occurred within the UK [218]. Of these offences, almost 50% remain unsolved with no recorded suspect [219]. As the vast majority of criminal identifications made by forensic means involve the use of DNA, there is continuing pressure to develop rapid and sensitive techniques capable of detecting and identifying genetic material deposited as biological fluid traces during a criminal act. At present, the most widely used methods to identify deposits of saliva include the Phadebas® test, the RSID™-Saliva test and the SALIgAE® test, all of which exploit reactions with the single most abundant salivary protein,  $\alpha$ -amylase [3]. Although these tests have proven effective within a casework scenario, they often suffer from caveats of low specificity [30] and lack of ability to localise fluids and attribute their tissue type at the same time.

Our research group has recently demonstrated the use of fluorogenic peptide substrates as successful assays for the simultaneous detection and identification of body fluid targets *in situ* [210]. These substrates utilise fluorophores that are quenched as a result of conjugation to an amino acid chain. Incubation of the substrate with a body fluid-specific protease results in the separation of the peptide-fluorophore bond and emission of fluorescence. These assays were shown to possess both high target specificity and sensitivity, whilst a 'turn-on' fluorescence signal allowed for the visualisation of discrete fluid staining areas. Furthermore, this fluorescence approach was shown to be highly compatible with current DNA profiling processes.

In the course of testing a number of commercially available fluorogenic substrates against different biological fluids in solution, it was observed that substrate Boc-VPR-AMC exhibited a strong positive reaction in the presence of saliva. This substrate utilises a 7-amino-4-methylcoumarin

(AMC) fluorophore, which is liberated upon target interaction to produce a fluorescence emission at 440 nm (**Figure 31**).

This study therefore documents the use of Boc-VPR-AMC, to visualise *in situ* deposits of saliva within a forensic context, as well as the synthesis of a novel substrate (Ac-VPR-Rh-110-Ac) based on the same reactive amino acid sequence, in an attempt to increase testing sensitivity.

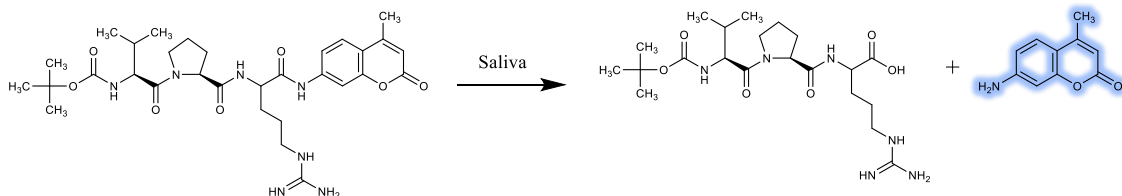


**Figure 31:** Boc-VPR-AMC – A short peptide chain (VPR) terminally labelled with a fluorophore, creating a non-fluorescent substrate system. Resulting protease activity relieves quenching to release highly fluorescent 7-amino-4-methylcoumarin.

## Materials and Methods

### Materials

Saliva was collected upon informed consent from three donors (KCL Ethics BDM/13/14-26). Substrate Boc-VPR-AMC was purchased from R&D Systems (Abingdon, UK) and diluted to a working concentration of 100  $\mu$ M. All amino acids and coupling reagents were purchased from Sigma-Aldrich Ltd (Dorset, UK), while Rhodamine-110 (Rh-110) was purchased from Fisher Scientific Ltd (Loughborough, UK).

### Ac-VPR-Rh-110-Ac Synthesis

Substrate Ac-VPR-Rh-110-Ac was prepared using a solid-phase peptide synthesis protocol previously reported [220]. Electrospray Ionisation Mass Spectrometry (ESI-MS) on a Waters/Micromass (Manchester, UK) ZQ mass spectrometer was used to confirm the identity of the product at each key step of the synthesis (data not shown).

## Microscopy

Saliva dilutions (1:1, 1:2, 1:4, 1:8, 1:16, 1:32, 1:64, 1:128) were applied in duplicate to glass slides in 5  $\mu$ l deposits and allowed to dry overnight. Working concentration Boc-VPR-AMC (100  $\mu$ M) or Ac-VPR-Rh-110-Ac (500  $\mu$ M) was pipetted in 5  $\mu$ l volumes onto the dried saliva. Fluorescence response of the substrates was recorded immediately after application by an Olympus SZX12 fluorescence microscope using UV (Ex 330-385/Em 420 nm) or GFP (Ex 460-490/Em 510 nm) filters for the commercial and synthesized substrates respectively. Negative reagent-only and saliva-only controls were also utilised and recorded in the same manner.

## Results and Discussion

Immediate 'turn-on' signal responses of substrate Boc-VPR-AMC were observed against all saliva deposits up to a 1:8 dilution (**Figure 32a**). Stains beyond this limit could not be visualised successfully. The use of negative controls also demonstrated the inherent lack of fluorescence emission of both saliva deposits and unreacted substrate.

Our research group recently reported the development of a solid-phase peptide synthesis protocol for the construction of fluorogenic substrates using the fluorophore Rhodamine-110 [220]. Such substrates are likely to be more sensitive than those using coumarin dyes due to Rhodamine-110's superior spectral characteristics. Attempts were therefore made to improve assay performance through the construction of a novel substrate Ac-VPR-Rh-110-Ac. After confirming the success of substrate synthesis by mass spectrometry, Ac-VPR-Rh-110-Ac was applied to saliva deposits in the same manner as commercial substrate testing. Successful visualisation of *in situ* saliva samples up to a 1:128 dilution, demonstrated a significant increase in assay detection limits (**Figure 32b**).

During the application of Ac-VPR-Rh-110-Ac, it was noted that the substrate solution exhibited some background fluorescence. However, this was successfully corrected for through changes to microscope

parameters. This background signal is likely to originate from dye molecules that were not completed conjugated during synthesis. Further purification to remove any free Rhodamine-110 from the substrate product should therefore be undertaken to prevent potential limitations to assay sensitivity.

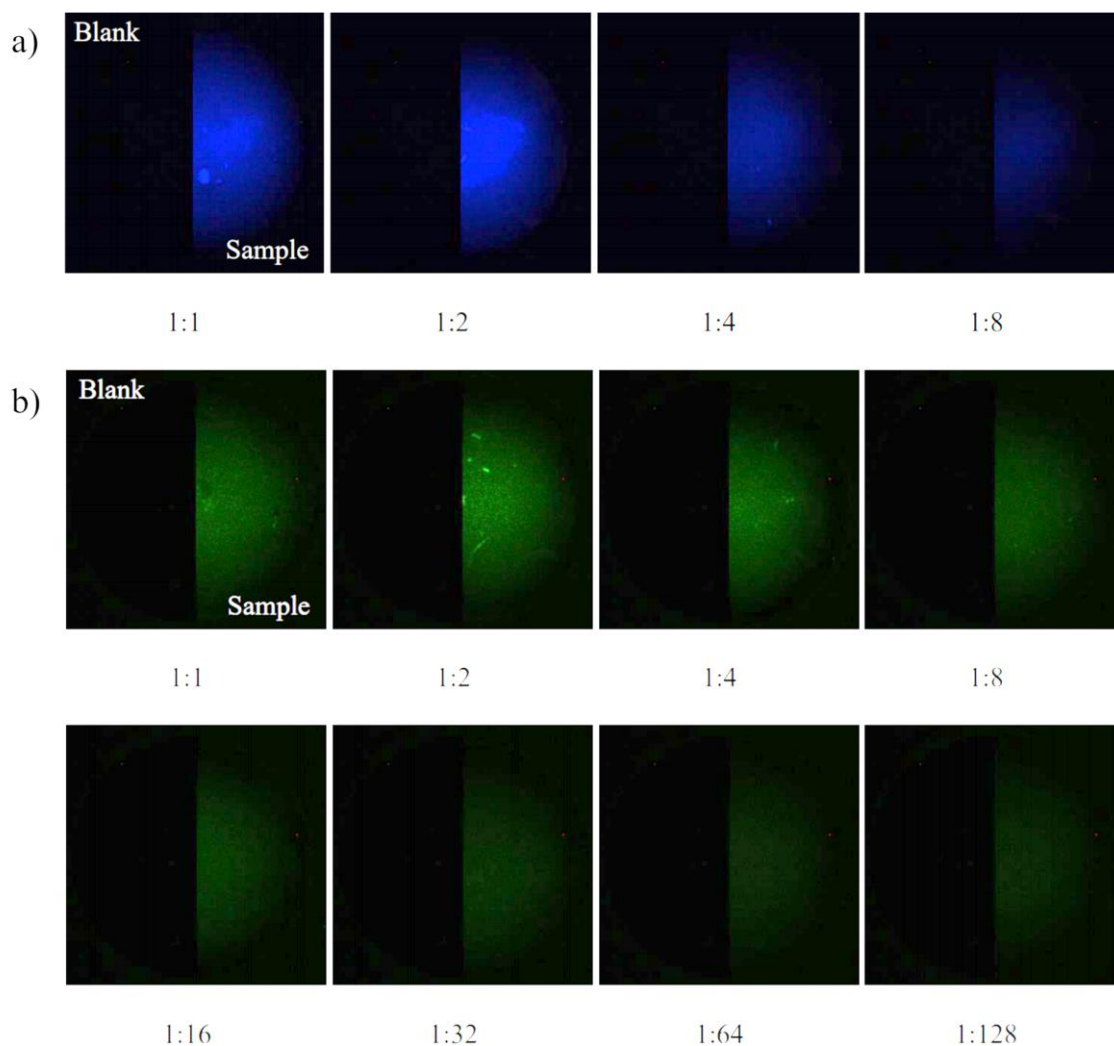


**Figure 32:** Fluorescence response of (a) Boc-VPR-AMC and (b) Ac-VPR-Rh-110-Ac to saliva dilutions deposited on glass slides. Negative reagent-only controls are provided on the left side of each image

## Conclusion

This proof-of-concept study has demonstrated the potential of fluorogenic substrates as a rapid, portable and simple method for the visualisation of saliva. Commercially available Boc-VPR-AMC was first utilised to detect deposited saliva *in situ* before assay sensitivity was increased through the construction of synthetic substrate Ac-VPR-Rh-110-Ac. With substrates

now designed by our group for the detection of both semen and saliva, future work is likely to focus on the development of a multiplex substrate system for the detection of multiple fluid types simultaneously.

### **3.6 Fluorogenic Substrates for the Detection of Blood**

With the successful *in situ* detection of semen and saliva by both commercial and synthesized fluorogenic peptide substrates, similar efforts were also made in the application of substrate-based biosensors towards the forensic analysis of blood.

Initial research focused on the ability of Bz-FVR-AMC, a commercially available peptide substrate commonly employed within coagulation studies [221], to detect samples of plasma and whole blood both in solution and *in situ*. This sensor, originally produced as part of a large substrate development study conducted by Svendsen *et al.* [194], is cleaved in the presence of proteolytic thrombin, which is able to hydrolyse arginine-aromatic amine bonds in small synthetic peptides [222].

Subsequent attempts to develop a custom thrombin-specific substrate employing the pro-fluorophore cresyl violet (CV) were then conducted using the solid-phase synthesis strategy previously developed.

#### **3.6.1 Materials and Methods**

##### **3.6.1.1 Reagents**

Thrombin substrate III (Bz-FVR-AMC) was purchased from Merck Millipore (San Diego, USA) and reconstituted in sterile distilled water (SDW) to a recommended working concentration of 100  $\mu$ M. Ellagic acid was obtained from Flurochem Ltd (Derbyshire, UK) and dissolved in Dimethyl sulfoxide (DMSO) to a concentration of 10 mM. A thrombin triggering solution was produced according to Ramjee [223], through the addition of 0.5  $\mu$ l of 10 mM ellagic acid solution to 20  $\mu$ l of  $\text{CaCl}_2$  (50 mM). Human  $\alpha$ -thrombin was also purchased from Merck Millipore (San Diego, USA).

For custom substrate synthesis, all amino acids and peptide coupling reagents were purchased from Sigma Aldrich (Dorset, UK), with the exception of 2-(7-Aza-1H-benzotriazole-1-yl)-1,1,3,3-tetramethyluronium hexafluorophosphate (HATU), which was purchased from Flurochem Ltd (Derbyshire, UK). Cresyl violet acetate and 2-Chlorotrityl Chloride resin (1.4 mmol/g loading capacity) were obtained from Alfa Aesar (Massachusetts, USA). All reagents were used without further modification, except DMF which was kept under constant nitrogen flow.

### **3.6.1.2 Body Fluid Collection and Storage**

Blood samples were taken upon informed consent from the same healthy donor. Samples were drawn by venipuncture and stored in a BD Vacutainer® Plus tube (Oxford, UK) containing 3.2% sodium citrate coagulation preservative and stored at 4 °C until analysis. Plasma was obtained through the centrifugation of whole blood samples for 10 min at 2000 x g before separation of the supernatant.

Ethical clearance for the collection of biological fluids for this specific study was granted by the King's College London Biomedical Sciences, Dentistry, Medicine and Natural & Mathematical Sciences Research Ethics Subcommittee (reference number HR-17/18-5057).

### **3.6.1.3 Commercial Substrate Testing**

#### **3.6.1.3.1 Spectrofluorometry**

Working concentrations of Bz-FVR-AMC (100 µl) were mixed with 100 µl of both plasma and whole blood dilutions (1:1, 1:2, 1:4, 1:8, 1:16) in a 96-well microplate before the addition of 20.5 µl thrombin triggering solution (as prepared in [Section 3.6.1.1](#)). Fluorescence emission signals were measured on a BioTek Synergy HT spectrophotometer (Vermont, USA) over 60 min using Ex360±40/Em460±40 nm wavelengths (for measurement of emissions at 450 nm). Appropriate negative controls (100 µl water + 100 µl substrate solution) were also utilised. All samples were prepared in triplicate.

### 3.6.1.3.2 Slide Microscopy

The ability of Bz-FVR-AMC to detect *in situ* wet fluid deposits was tested through the application of 5 µl working substrate solution and 0.5 µl of thrombin triggering solution to a range of plasma dilutions (1:1, 1:2, 1:4, 1:8, 1:16, 1:32, 1:64, 1:128) deposited in 5 µl volumes on glass slides. Reagent-only negative and plasma-only blank controls were also used. Images were taken immediately after trigger application using an Olympus SZX12 fluorescence microscope (Tokyo, Japan) and internal CCD camera. UV filtration (Ex 330-385 nm) was used for substrate excitation, with all additional microscopy parameters kept constant throughout testing (Exposure = -2, Hue = 359, Saturation = 255, White Balance = 0, Contrast = 1023, Brightness = 0, Gamma = 10, Magnification = ×8.5).

### 3.6.1.3.3 DNA Profiling

Substrate Bz-FVR-AMC (50 µl + 5 µl of thrombin triggering solution) was added to 100 µl of whole blood to observe effects on DNA recovery after application. A reference DNA sample was then prepared through the addition of 50 µl SDW to a second blood volume in place of substrate reagent. Both samples were then subjected to DNA extraction using the QIAamp® DNA Investigator kit (Qiagen, Manchester, UK) according to manufacturer protocols. Extracts were quantified using the Quantifiler™ Human DNA Quantification Kit (Thermo Fisher Scientific, California, USA), diluted to 0.1 ng/µl and amplified utilising the AmpFLSTR® NGM SElect Express Kit (Thermo Fisher Scientific, California, USA) on a Perkin Elmer 9700 thermal cycler (Cambridge, UK). Amplified STR products were resolved via capillary electrophoresis on an Applied Biosystems® 3130 Genetic Analyser and evaluated using GeneMapper® software (California, USA).



### 3.6.1.4 Custom Substrate Synthesis and Testing

#### 3.6.1.4.1 Resin-CV-NH<sub>2</sub>

A total of 500 mg of 2-chlorotriptyl chloride resin (1.4 mmol/g loading capacity) was swelled using DCM in a SPE fritted polypropylene tube for 30 min. After draining, 112.5 mg (0.35 mmol) of Cresyl Violet and 1.219 ml (7 mmol) of DIPEA in 6ml of DMF were added to the resin. This suspension was incubated on a roller at room temperature for 24 hrs and subsequently washed with DMF and DCM until the filtrate was clear. The resin was then incubated with methanol for 30 min to cap any remaining chloride groups before re-washing with DMF (×5) and DCM (×10). Conjugation was monitored via the 'hard' cleavage of 5mg of resin through treatment with a 1 ml solution of 95:0.5:0.5:0.5:0.25 TFA: water: phenol: TA: TIPS for 3 hrs at room temperature. Ice cold diethyl ether was then added to precipitate products, with organic solvent, scavengers and by-products removed through centrifugation. Obtained solids were washed several times with diethyl ether to remove any residual scavenger traces and finally dissolved in 50% ACN in water containing 0.1% TFA.

Product purity was examined by reverse-phase HPLC (RP-HPLC) on a HP1050 HPLC system (Hewlett Packard, California, USA) equipped with an autosampler, quaternary pump and Diode-Array Detector and using a Zorbax SB C-18 2.1mm x 10cm (particle size 3.5 micron) column. A linear gradient of mobile phase B (A containing 0.1% TFA) over mobile phase A (0.1% TFA in water) from 0-90% B in 37 min was performed with a flow rate of 0.2 ml/min. Eluents were monitored at 280 and 621 nm absorbance wavelengths with data collected and analyzed using ChemStation software. Correct product mass was verified by ESI-MS on a Waters/Micromass (Manchester, UK) ZQ mass spectrometer.

#### 3.6.1.4.2 Resin-CV-R(Pbf)-OH

First, 4.541 g of Fmoc-Arg(Pbf)-OH (7 mmol) was dissolved in 15 ml DMF before the addition of 2.395 g of HATU (6.3 mmol) and 2.438 ml DIPEA (14 mmol). This mixture was stirred for 10 min before addition to the



washed CV-resin. Coupling was allowed to occur for ~96 hrs at room temperature on a roller, whereupon the resin was transferred to an empty fritted polypropylene tube, filtered and washed with DMF (×5) and DCM (×10). Successful coupling was monitored by subjecting 5 mg of resin to the 'hard' cleavage and RP-HPLC and ESI-MS instrumental analysis procedures previously described ([Section 3.6.1.4.1](#)).

#### **3.6.1.4.3 Resin-CV-R(Pbf)VF-Bz**

All remaining amino acids were added to CV-R(Pbf)-OH-conjugated resin via a standard SPPS strategy. Acylation steps were conducted using six equivalents of Fmoc amino acids (1.425 g Fmoc-Val-OH and 1.627g Fmoc-Phe-OH), which were pre-activated with ethyl 2-cyano-2-(hydroxyimino)acetate, potassium salt (K-Oxyma) and DIPCDI in DMF in a molar ratio of 1:1:1 of amino acid, K-Oxyma (756 mg) and DIPCDI (650 µl), respectively. All couplings were allowed to occur for 1 hr at room temperature, whereupon the resin was washed with DMF (×5) and DCM (×10). Fmoc protecting groups were removed through treating the resin with 10 ml of 20:80 v/v Piperidine:DMF for 30 min before further washing with DMF (×5) and DCM (×10). Capping of the N-terminus of phenylalanine residues was achieved through the incubation of de-protected resin for 1 hr with 10 molar equivalents (1.583 g) of Benzoic Anhydride and 20 equivalents of DIPEA (2.438 ml) in 6 ml DMF. A final wash of the resin was then conducted using DMF (×5) and DCM (×10). Coupling success was monitored by subjecting 5 mg of resin to the 'hard' cleavage and RP-HPLC and ESI-MS instrumental analysis procedures previously described ([Section 3.6.1.4.1](#)).

#### **3.6.1.4.4 Ac-CV-RVF-Bz**

A 200 mg portion of the resin was treated with 5 ml of a 'soft' cleavage cocktail of 0.5% TFA in DCM for 1 hr to isolate  ${}_{2}\text{HN-CV-R(Pbf)VF-Bz}$  without disturbing Pbf side-chain protecting groups. Filtrate was collected and allowed to evaporate in a fume hood to a total volume of 1 ml. Products were then precipitated in 10 ml of cold diethyl ether, centrifuged

at 4000 RPM for 20 mins and washed twice with two volumes of 10 ml ether.

To 93.9 mg of  $\text{zHN-CV-R(Pbf)VF-Bz}$  (91.5  $\mu\text{mol}$ ) dissolved in DMF (3 ml) were added twelve equivalents of DIPEA (191  $\mu\text{l}$ ) and six equivalents of acetyl chloride (39  $\mu\text{l}$ ). This solution was allowed to incubate at room temperature for 1 hr before being split into three separate 1ml portions. To each portion, 1 ml DCM and 1 ml distilled water was added to isolate final products by liquid-liquid extraction. Each organic phase was isolated prior to the re-extraction of the aqueous layer with 1 ml of fresh DCM. The organic layers were then combined and washed with 5%  $\text{NaHCO}_3$  (1 ml) and brine (1 ml) solutions before being filtered through a sterile membrane. To remove Pbf side-chain protecting groups, products were treated using the 'hard' cleavage procedures previously described (**Section 3.6.1.4.1**). Instrumental analysis of the final substrate product was also conducted using the RP-HPLC and ESI-MS methods already outlined (**Section 3.6.1.4.1**).

#### **3.6.1.4.5 Spectrofluorometry**

The ability of Ac-CV-RVF-Bz to detect purified thrombin protein, as well as both plasma and whole blood samples, was investigated by dissolving final synthesis products in sterile distilled water to an estimated concentration of 100  $\mu\text{M}$  (based on product weight). Working concentrations (100  $\mu\text{l}$ ) of Ac-CV-RVF-Bz were then mixed with 100  $\mu\text{l}$  of thrombin at a range of concentrations (50, 25, 10, 5, 2.5  $\mu\text{g/ml}$ ) and dilutions of plasma/whole blood (1:1, 1:2, 1:4, 1:8, 1:16) in a 96-well microplate before the addition of 20.5  $\mu\text{l}$  thrombin triggering solution.

Fluorescence signals were measured on a CytoFlour® 4000 spectrophotometer (Applied Biosystems®, California, USA) over the course of 60 min using  $\text{Ex}590\pm20/\text{Em}645\pm50$  nm wavelengths (for the measurement of emissions at 632 nm). Appropriate negative controls (100  $\mu\text{l}$  water + 100  $\mu\text{l}$  substrate solution) were also utilised. All samples were prepared in triplicate.

## 3.6.2 Results and Discussion

### 3.6.2.1 Commercial Substrate Testing

#### 3.6.2.1.1 Spectrofluorometry

Substantial increases in fluorescence signals over time were observed upon the addition of substrate Bz-FVR-AMC to different dilutions of human plasma (**Figure 33a**), demonstrating the potential of peptide substrates for use in the detection of blood-specific components. However, emission intensities were found to be significantly reduced during the application of the same substrate to whole blood samples (**Figure 33b**). Such effects were not unexpected, due to the established spectral overlap between AMC emission and blood absorbance wavelengths. In fact, a similar experiment has already established the quenching of AMC-based substrates in whole blood as a result of fluorescence absorption by haemoglobin at 440-460 nm [223].

It must also be noted that unlike the previous substrates tested against enzymes present in semen and saliva, Bz-FVR-AMC also requires the use of an additional assay component in the form of an enzyme-triggering solution. This is due to the fact that thrombin in circulating blood is largely present as a zymogen precursor, which does not possess enzymatic activity [224]. Whilst this precursor, known as prothrombin, is readily activated by Factor Xa as part of the coagulation cascade during clotting, this process is inhibited in blood containing an anti-coagulant [225]. Enzyme-triggering compounds (as well as calcium ions) are therefore used to overcome anti-coagulative effects within blood samples taken by venipuncture, allowing thrombin generation to take place. In this particular study, ellagic acid, a compound able to enhance the activation of clotting factor XII, was utilised as a pro-coagulant. However, it remains to be seen whether such enzyme-triggering methods would still be required during the application of thrombin substrates to bloodstains deposited at crime scenes, which naturally clot as a result of tissue factor activation during bleeding.

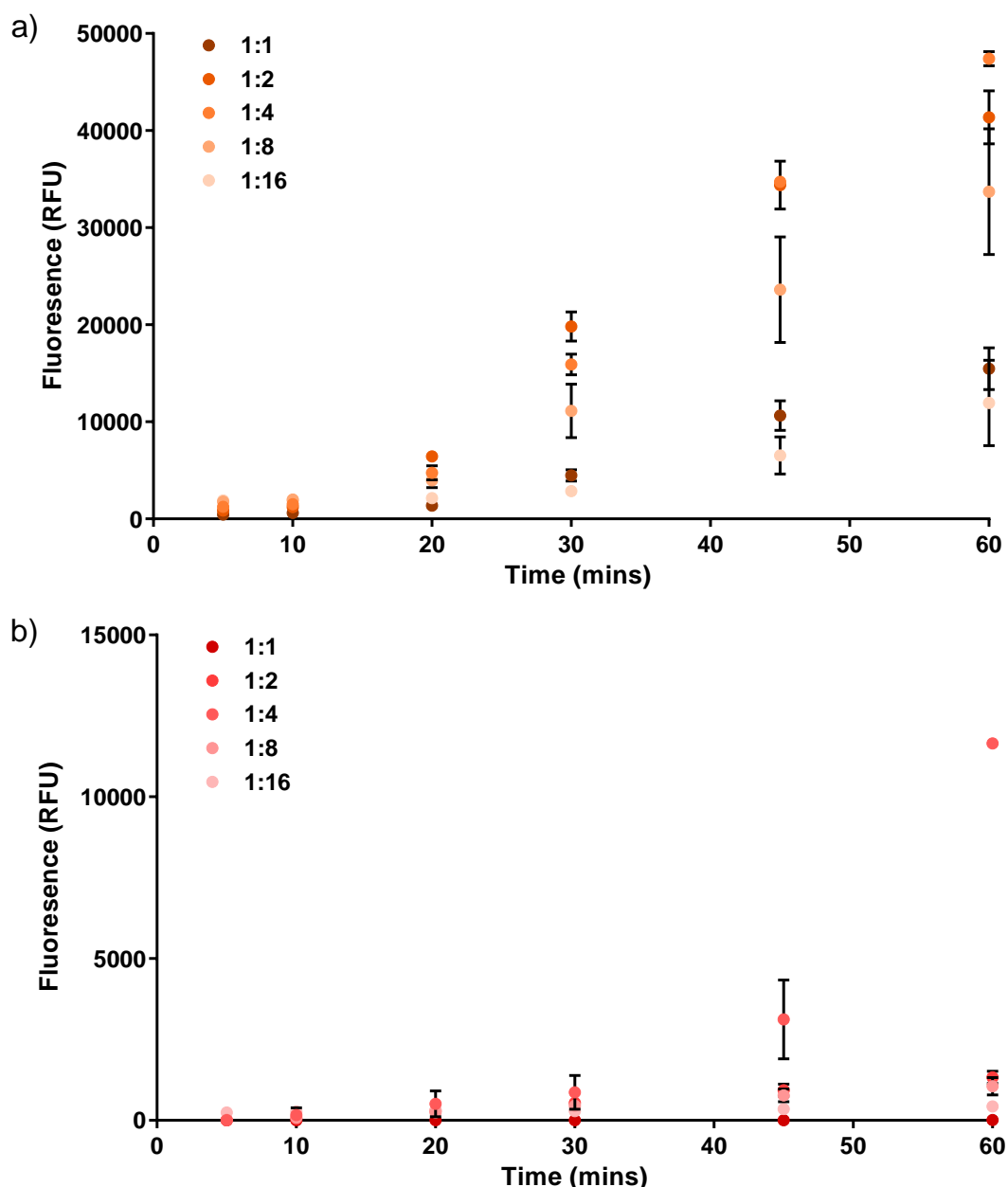


**Figure 33:** Fluorescence response of substrate Bz-FVR-AMC over time to different dilutions of a) plasma and b) whole blood. Data represents the mean  $\pm$  SD, samples performed in triplicate.

### 3.6.2.1.2 Slide Microscopy

Positive fluorescence emissions were observed in all samples during the *in situ* testing of Bz-FVR-AMC against deposits of human plasma on glass slides, even at sensitive 1:128 dilutions (**Figure 34**). Responses were found to be immediate upon the addition of thrombin triggering solution and increased in intensity over the next 60 min. However, no signals were detected from all substrate solutions applied to each whole

blood dilution (data not shown). This is likely due to the haemoglobin AMC-quenching effects already discussed.

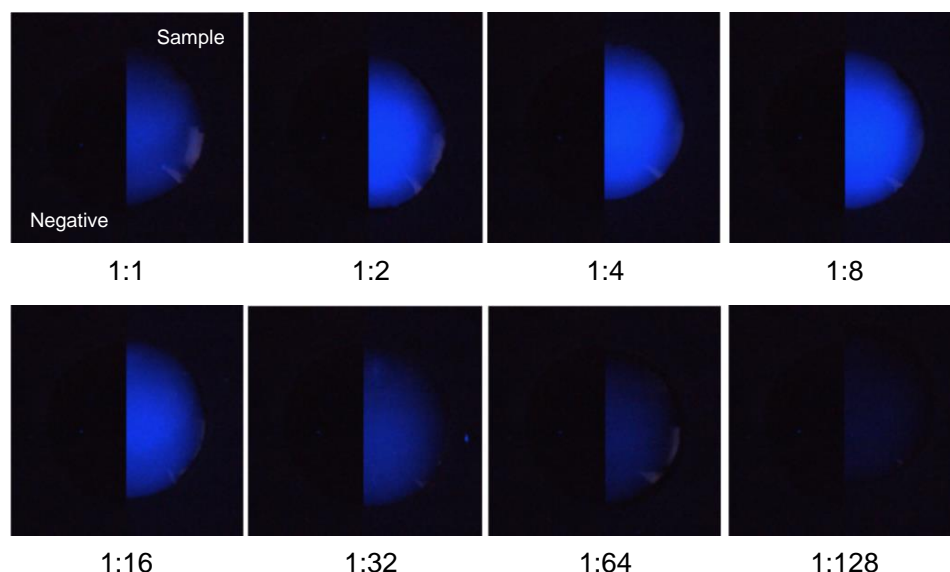


**Figure 34:** Demonstration of *in situ* substrate testing of plasma depositions upon glass slides across a range of eight dilutions. Reagent-only negative controls are provided on the left side of each image. Duplicate measurements were taken and also displayed similar results.

### 3.6.2.1.3 DNA Profiling

To investigate potential interference with downstream DNA profiling processes, Bz-FVR-AMC and thrombin triggering solution were applied to a sample of whole blood, which was then subjected to DNA extraction, quantification, amplification and detection using techniques standard to most forensic casework laboratories. Comparisons (both in terms of DNA quantification values and electropherogram allele numbers/peak heights) were then made to a blood reference standard, in which SDW was added in place of substrate reagent. No differences between substrate-added and reference samples outside the limits of normal experimental variation were observed at any stage of the profiling process. DNA extracted from whole blood containing Bz-FVR-AMC and thrombin triggering solution was quantified at 4.05 ng/μl. Furthermore, a full STR profile was obtained from this sample (**Figure 35**), with no detrimental effects to high molecular weight loci (amplicons less likely to undergo PCR as a result of DNA degradation).

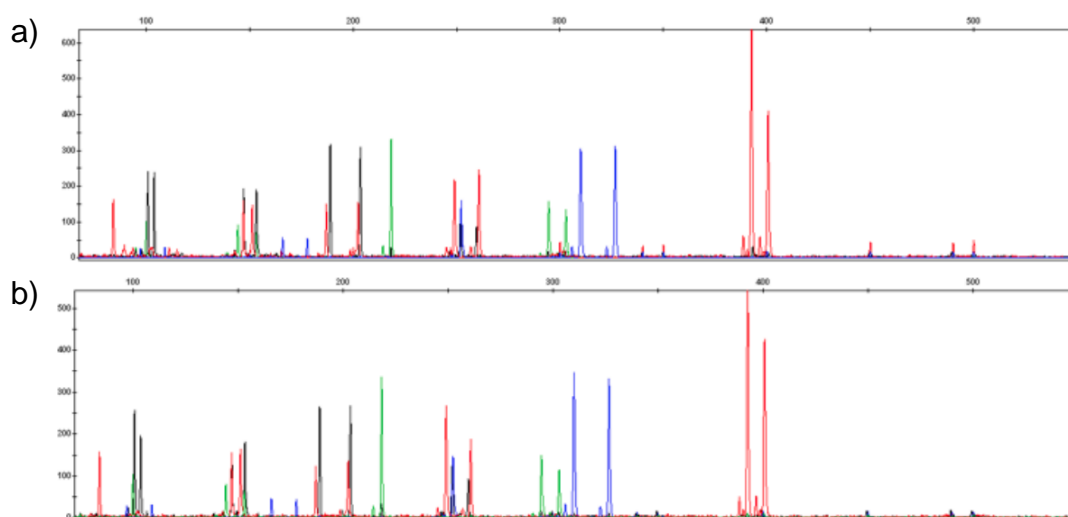


**Figure 35:** STR profiles generated from whole blood samples containing a) Bz-FVR-AMC and thrombin triggering solution and b) SDW.

### 3.6.2.2 Custom Substrate Synthesis and Testing

#### 3.6.2.2.1 Substrate Synthesis

With significant reductions of Bz-FVR-AMC emissions occurring as a result of blood absorption, it was subsequently theorised that a custom thrombin substrate utilising pro-fluorophores emitting within the red region of the visible spectrum (620-750 nm), where haemoglobin does not typically absorb [226], may potentially be used to overcome such quenching effects. Attempts were therefore made to construct a blood-specific sensor based on the amino acid sequence employed within fluorogenic thrombin substrate III (Bz-RVF) and cresyl violet, an oxazine-based fluorophore with an emission maxima of 632 nm (**Figure 36**).

Substrate Ac-CV-RVF-Bz was synthesized using a similar solid-phase strategy to that previously employed in the development of Rh-110-based sensors (**Section 3.4.2**) [220, 227]. This approach was chosen over traditional solution-based preparation due to the higher final product yields and cost-efficiency associated with SPPS. Furthermore, substrates produced using this method are mono-substituted, with amino acids attached at only one site of the pro-fluorophore molecule, allowing production of fluorescent signal through a single enzymatic hydrolysis step.

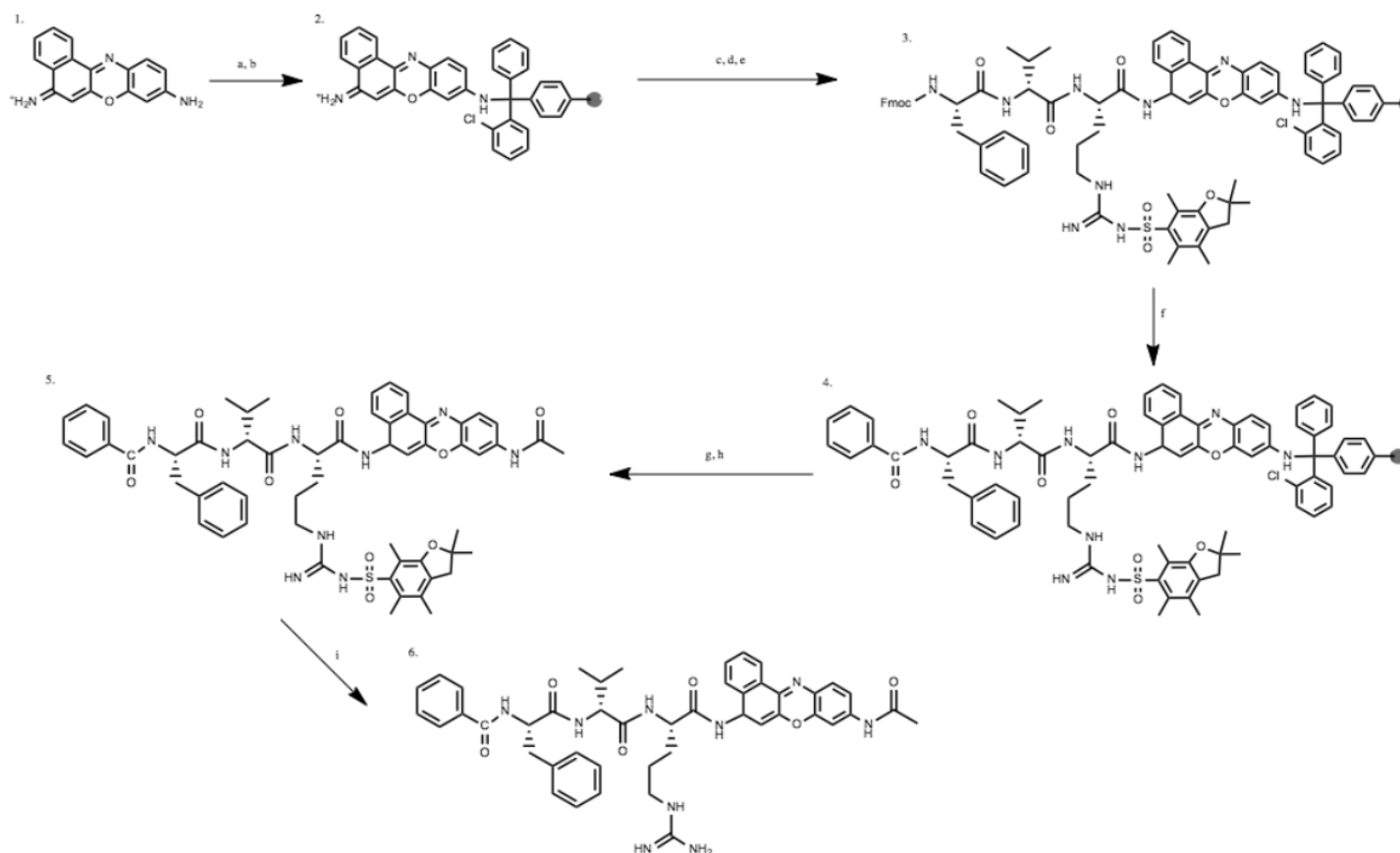


**Figure 36:** Solid phase peptide synthesis of cresyl violet based thrombin substrate: a) 2-ct resin (0.7 mmol), DMF, DIPEA, 24 hrs, b) MeOH, 30 min, c) Fmoc-R(Pbf)-OH (7 mmol), DMF, HATU (6.3 mmol), DIPEA (14 mmol), 96 hrs, d) 20% piperidine/DMF, 30 min, e) 2 x AA, K-Oxyma, DIPCDI, DMF, 1 hr, f) Benzoic anhydride (7 mmol), DIPEA (14 mmol), DMF, 1 hr, g) 0.5% TFA/DCM, 1 hr, h) Acetyl chloride (0.55 mmol), DIPEA (1.1 mmol), DMF, 1 hr, i) TFA:TA:TIPS:water:phenol.

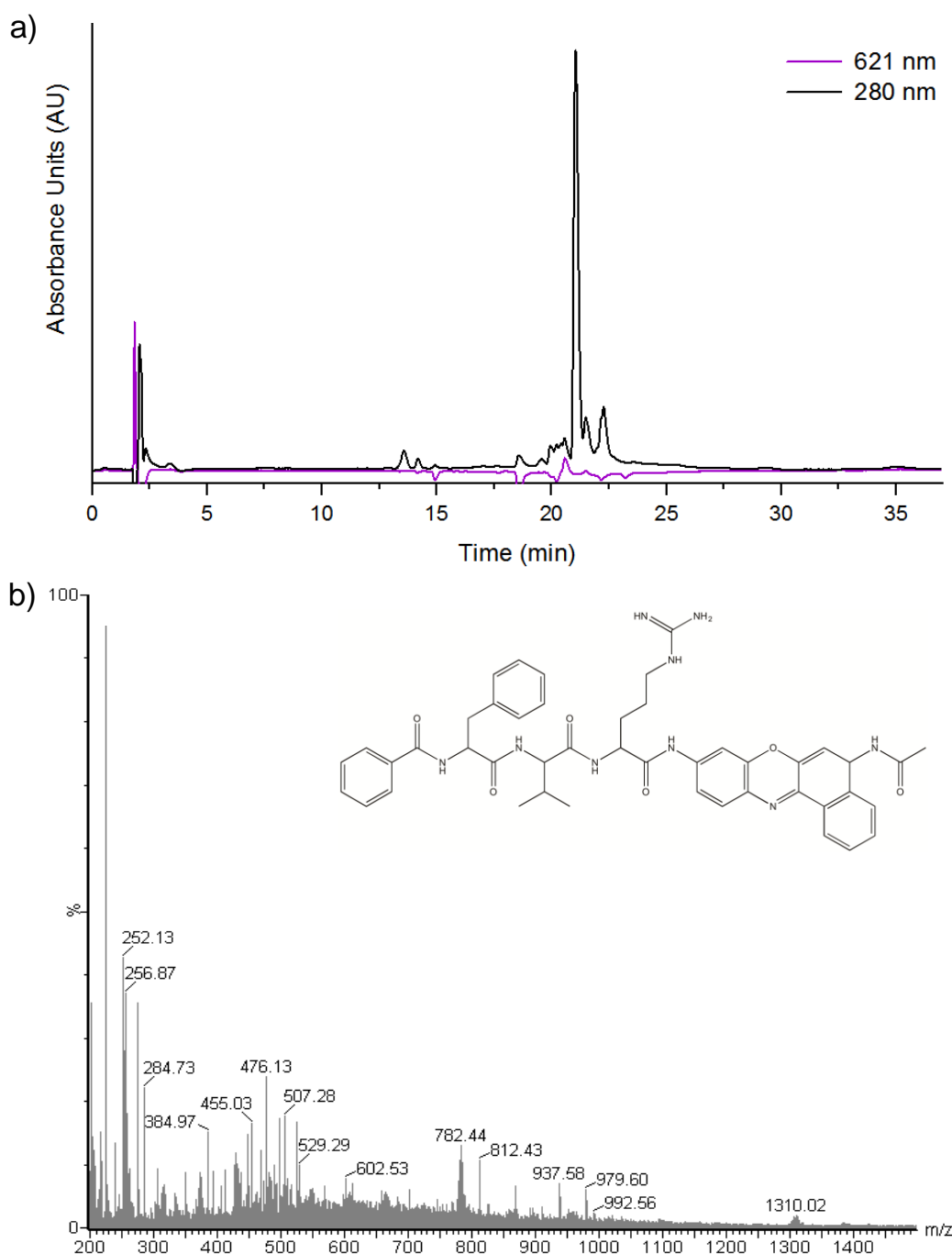


**Figure 37:** Confirmation of final substrate product Ac-CV-RVF-Bz purity and identity as established by a) RP-HPLC and b) ESI-MS (calculated  $m/z$  for  $[M+H]^+ = 812.38$ ) respectively.

Upon attachment of cresyl violet, the 2-chlorotrityl resin displayed a deep-purple colouration that was retained even after extensive washing, indicating successful coupling. A large excess of initial amino acid (Fmoc-Arg-(Pbf)-OH) was used to ensure high final product yields through the comprehensive conjugation of resin-bound pro-fluorophores. Unlike the construction of Rh-110-based substrates, this conjugation was achieved



in the presence of HATU (a peptide coupling agent commonly used to form amide bonds between pro-fluorophores and amino acids during fluorogenic substrate development [228]) and DIPEA, rather than an EDC/pyridine mixture. Subsequent amino acids (as well as an n-terminal benzoyl capping groups) were then added according to the peptide sequence of Bz-FVR-AMC.

After removal from the resin by 'soft' TFA cleavage, the free amine of  $_2\text{HN-CV-R(Pbf)VF-Bz}$  was acetylated to quench the overall emission of the substrate. Pbf protecting groups were lastly removed through treatment of Ac-CV-RVF-Bz using a 'hard' TFA cleavage solution. Analysis by RP-HPLC and ESI-MS was used to confirm the purity and identity of the final substrate respectively (**Figure 37**). RP-HPLC and ESI-MS analysis results from products obtained at each stage of the synthesis process may be found in the appendix (**Section A.1**) of this thesis.

#### **3.6.2.2.2 Spectrofluorometry**

Appropriate increases in fluorescence intensity were exhibited by substrate Ac-CV-RVF-Bz over time in response to different concentrations of thrombin solution (**Figure 38**). In general, these changes occurred much more rapidly than those exhibited by commercial substrate Bz-FVR-AMC in response to plasma and whole blood samples, with saturation of signals occurring in less than 10 min for some higher thrombin concentrations.

However, no fluorescence emissions were observed upon the application of Ac-CV-RVF-Bz to plasma and whole blood dilutions. The reasons behind this lack of signal remain unclear, given the obvious response of the substrate to the purified thrombin protein. Possible explanations may include the prevention of substrate hydrolysis by other components present within plasma and blood matrices (such as fibrin and other clotting factors), which can restrict fluorescence emission [229]. Some authors have also demonstrated a disparity between the concentrations of enzymes required to cleave peptide substrates containing the same

amino acid sequences but utilising different pro-fluorophore leaving groups [165]. As a result, optimisations to increase the sensitivity of this substrate may be required in order to detect the low levels of thrombin present within deposited bloodstains.

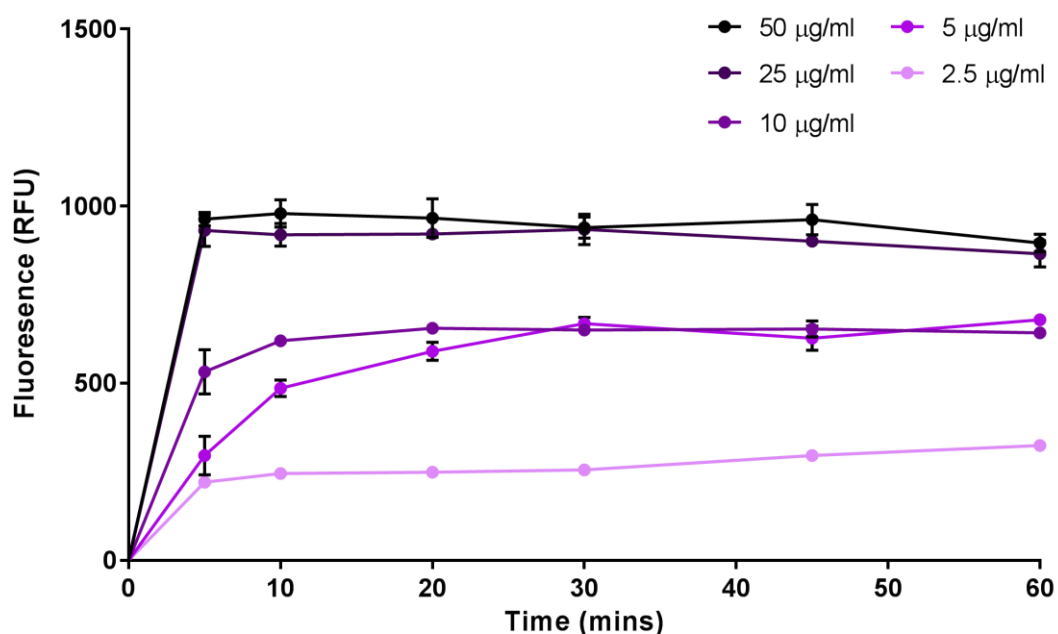


**Figure 38:** Fluorescence response of Ac-CV-RVF-Bz over time to different concentrations of purified thrombin protein. Data represents the mean  $\pm$  SD, samples performed in triplicate.

### 3.6.3 Conclusion

In this study, a commercially available thrombin fluorogenic substrate has been successfully applied for the detection of human plasma both in solution and *in situ*. However, with the quenching of AMC leaving group fluorescence as a result of haemoglobin absorption, it is unlikely that this substrate will have practical use in the analysis of deposited bloodstains within forensic casework. Therefore, the development of a custom thrombin substrate utilising a pro-fluorophore that emits outside the region of haemoglobin absorbance was also conducted.

Substrate Ac-CV-RVF-Bz was constructed using a previously employed SPPS scheme and was found to be responsive to different concentrations of thrombin within solution using spectrofluorometry. However, subsequent attempts to apply this substrate towards the detection of

plasma and whole blood samples were unsuccessful. Further work to optimise this sensor is therefore required before its application to the forensic analysis of biological fluid deposits.

# **Chapter 4**

## **Immunosensors**

## 4.1 Introduction

Whilst fluorogenic substrates were found to be highly effective in the visualisation of semen and saliva deposits, initial attempts in the application of these sensors towards the detection of whole blood samples were met with mixed success. Inhibition of substrate hydrolysis by protein components present within the fluid matrix has been posited as one possible reason for the lack of fluorescence emissions from custom-synthesized thrombin substrates during blood incubation.

Such inhibition may necessitate the construction of an entirely novel fluorogenic peptide substrate towards a different blood-specific target. However, with signal transduction affected only as a result of protease interaction, this is likely to be a significant challenge, as the number of molecules in blood that exhibit proteolytic activity (that are also present in concentrations high enough to cause observable peptide hydrolysis) is limited [230]. Consequently, it may be considered beneficial to also explore the use of other sensing transduction mechanisms that are able to detect non-enzymatic targets towards the forensic analysis of biological fluids.

Despite difficulties in the detection of analyte deposits on porous surfaces during commercial biosensor testing (**Chapter 2 - Section 2.4.3**), the FluoReporter® Biotin Quantitation Assay Kit was shown to exhibit high sensitivity and low background fluorescence, qualities likely essential for effective *in situ* biological fluid sensing. Whilst this assay utilised the highly specific interactions that occur between biotin and avidin molecules to displace a moderately bound quenching ligand, this approach may theoretically be extended to the detection of virtually any target by the replacement of avidin sub-units with other biological recognition moieties, such as antibodies or aptamers.

This chapter therefore documents the design and development of a displacement immunosensor specific to the seminal fluid protein PSA. First, a brief overview of displacement transduction mechanisms is provided, along with an exploration of quantum dots (QDots), fluorescent nanoparticles commonly used in such assays. Construction of a 'turn-on' biosensor employing moderately bound quenching peptide analogues to PSA is then reported.

## **4.2 Review of Displacement Immunosensors**

### **4.2.1 Transduction Mechanism**

Antibody-protein binding generally occurs as result of van der Waals, hydrogen, hydrophobic and ionic bonding between the specific amino acids of the antigenic determinant region of a protein (known as an 'epitope') and the complementarity-determining regions (CDRs) of an antibody molecule. The strength of this binding is usually dependent upon the valency and precise fit of an antigen within these regions [231]. As a result, an antibody may be able to bind to different molecules sharing similar structural characteristics. However, the strength (or 'affinity') of this binding will be distinct for each target.

Furthermore, those antigens exhibiting a low or moderate degree of affinity upon binding to an antibody may be actively displaced by molecules of higher binding strength [232]. This phenomenon has been extensively exploited in many biological assays for indicating the presence of a specific testing antigen by the competitive removal of target analogues labelled with observable reporter moieties (such as radioisotopes, enzymes or fluorescent dyes) [232, 233]. Such analogues may consist of compounds that are structurally similar to the target antigen or analytes that have undergone some form of chemical modification [232]. In some cases, the process of reporter label attachment is often sufficient to decrease the binding affinity of antigenic molecules, allowing their use as moderately bound ligands.

In this study, a displacement immunosensor specific to PSA was constructed via the conjugation of a QDot nanoparticle to an anti-PSA antibody to form an initially fluorescent immunological recognition complex. This complex was subsequently quenched by the moderate binding of an acceptor-labelled peptide (consisting of the amino acids responsible for antibody-PSA interaction). As a result of antibody binding, this peptide is brought within the distance required for the absorbance of the QDot emissions via FRET. However, in the presence of PSA (which has a higher affinity towards the antibody molecule) this peptide is displaced, relieving FRET quenching effects and restoring fluorescence (**Figure 39**).

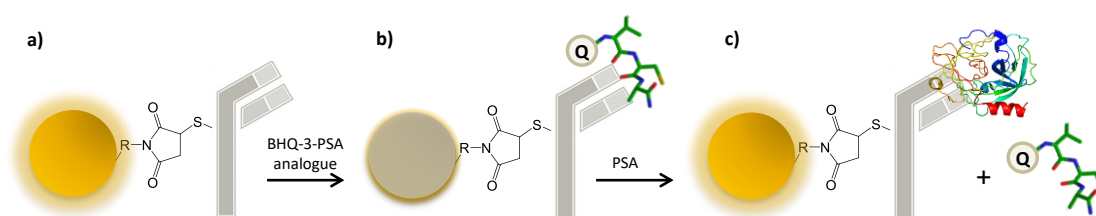


**Figure 39:** PSA immunosensor assembly: a) antibody-QDot conjugates are incubated with a quencher-labelled peptide, b) binding brings QDot and quencher into required FRET proximity and decreases emission, c) PSA protein displaces the peptide and restores fluorescence. Taken with permission from [234].

#### 4.2.2 Quantum Dot Nanoparticles

Several recent studies have demonstrated the excellent performance of QDots as fluorescence reporters within displacement biosensor assays [151, 235, 236]. QDots are nano-sized particles or crystals made from fluorescent semi-conductor materials, such as cadmium selenide, cadmium sulfide and indium arsenide, with diameters of approximately 2-10 nm. These dots exhibit unique spectral properties due to the quantum confinement of excitons within all three spatial dimensions [237]. The most distinctive of these properties is the high emissions intensities exhibited by particles, the wavelengths of which may also be finely tuned by controlling the size of QDots produced during the fabrication process [238].

QDots also possess several key advantages over single-molecule fluorophores in biological labelling applications, such as greater resistance to photobleaching, and the ability to be applied within the aqueous environments required for biological use [239]. Furthermore, the tuneable absorbance and emission properties of QDots can allow for the excitation of multiple nanoparticles, each emitting within entirely different regions of the visible spectrum, using a single illumination wavelength [240]. QDots are therefore ideal for use within assays that require the multiplex detection of several different targets within the same sample.

The possibility to conjugate QDots to biological recognition moieties (such as peptides, aptamers and antibodies) through a variety of labelling chemistries has meant that such nanoparticles have been highly employed in the development of FRET-based biosensing assays [241]. QDot nanoparticles may therefore represent great potential for use within the construction of displacement immunosensors for the analysis of biological fluid targets.

## **4.3 Materials and Methods**

### **4.3.1 Reagents**

Anti-PSA antibody 8301 was purchased from Abcam (Cambridge, UK), whilst the Qdot™ 625 Antibody Conjugation Kit was obtained from Thermo Fisher Scientific (California, USA). Black Hole Quencher-3 (BHQ-3) was obtained from Biosearch Technologies (California, USA). Purified PSA protein was purchased from AbD Serotec (Kidlington, UK).

All amino acids and peptide coupling reagents were purchased from Sigma-Aldrich (Dorset, UK), with the exception of NovaPEG Rink Amide resin (0.4-0.8 mmol/g loading capacity), which was obtained from Merck Millipore (San Diego, USA). All reagents were used without modification, except DMF which was kept under constant nitrogen flow.



### 4.3.2 Body Fluid Collection and Storage

Seminal fluid was obtained upon informed consent from the same healthy donor and stored at 4 °C until the point of analysis. Ethical clearance for the collection and use of body fluids for this specific study was granted by the King's College London Biomedical Sciences, Dentistry, Medicine and Natural & Mathematical Sciences Research Ethics Subcommittee (reference number BDM/13/14-26).

### 4.3.3 DVCAQV-NH<sub>2</sub>

Peptide DVCAQV-NH<sub>2</sub> was synthesized manually via a standard Fmoc-SPPS strategy. NovaPEG Rink Amide resin (100 mg) was first swelled in an empty fritted polypropylene tube for 30 minutes using anhydrous DMF.

All acylation steps were conducted using four equivalents of amino acids, pre-activated for 10 min with a solution of O-(1H-6-Chlorobenzotriazole-1-yl)-1,1,3,3-tetramethyluronium hexafluorophosphate (HCTU) and DIPEA in DMF in a molar ratio of 1:0.95:2 of amino acid: HCTU: DIPEA, respectively.

Coupling reactions were conducted for 1 hr and monitored by the picrylsulphonic acid test. Fmoc deprotection of coupled amino acids was accomplished by treatment with 20% (v/v) piperidine in DMF for 30 min and confirmed by the picrylsulfonic acid test. Excess reagents and impurities were removed by extensive washing with DMF, methanol and DCM.

Cleavage of the peptide from the solid support was achieved by treating the amide resin with a 1 ml solution of TFA: water: phenol: TA: TIPS in a molar ratio of 95:0.5:0.5:0.5:0.25 respectively for 3 hrs at room temperature. The cleavage filtrate was concentrated under a stream of nitrogen at 40 °C to a total volume of 0.5 ml. Ice cold diethyl ether was added to precipitate the peptide product before the removal of organic solvent through centrifugation. The obtained peptide was washed several time with diethyl ether to remove any residual scavenger traces, and

finally dissolved in 50% ACN in water containing 0.1% TFA and freeze-dried for 24 hours.

Product purity was examined by RP-HPLC on a HP1050 HPLC system (Hewlett Packard, California, USA) equipped with an autosampler, quaternary pump and Diode-Array Detector using a Zorbax SB C-18 2.1mm x 10cm (particle size 3.5 micron) column. A linear gradient of mobile phase B (ACN containing 0.1% TFA) over mobile phase A (0.1% TFA in water) from 0-90% B in 26 min was performed with a flow rate of 0.2 ml/min. Eluents were monitored between 210-280 nm with data collected and analysed using ChemStation software. Correct product mass was verified by ESI-MS on a Waters/Micromass (Manchester, UK) ZQ mass spectrometer.

#### **4.3.4 Biacore Analysis**

The interactions of Antibody 8301 with native PSA protein and DVCAQV-NH<sub>2</sub> were monitored using a Biacore T200 SPR instrument (GE Healthcare, Illinois, USA). Approximately 11,000 response units of antibody were immobilised on a carboxy-methylated dextran matrix CM5 sensor chip after activation with EDC and N-hydroxysuccinimide (NHS). Samples were injected at concentrations of 160, 80, 40, 20, 2 and 0.2 nM in HBS-P running buffer (10 mM HEPES pH 7.4, 150 mM NaCl, 0.005% v/v Surfactant P20) with two injections of 10 mM glycine-HCl pH 1.7 used to regenerate the surface of the sensor chip between samples. Antibody interaction signals were analysed using BIAevaluation software.

#### **4.3.5 BHQ-3-DVCAQV-NH<sub>2</sub>**

Coupling of peptide DVCAQV-NH<sub>2</sub> to BHQ-3-N-succinimidyl ester (BHQ-3-NHS) was accomplished following the procedure reported by Stefflova *et al.* [242]. First, DVCAQV-NH<sub>2</sub> was dissolved in DMSO with 1% DIPEA before reacting for 2 hrs with equimolar BHQ-3-NHS (also in DMSO) to produce BHQ-3-DVCAQV-NH<sub>2</sub>. Reaction products were precipitated in ice cold diethyl ether and dried under vacuum. Peptide identity was confirmed through matrix-assisted laser desorption-ionization time of flight

(MALDI-TOF) mass spectrometry using a Bruker Daltonics Autoflex spectrometer (Massachusetts, USA) with Anchorchip™ targets (600 µm/384).

#### **4.3.6 Antibody-QDot Conjugation**

The conjugation of anti-PSA antibody (8301) to amine-functionalised QDots was carried out using protocols and reagents supplied with the QDot™ 625 Antibody Conjugation Kit. Briefly, 300 µg of antibody was first reduced through incubation with a 1 M solution of dithiothreitol (DTT) for 30 min to expose free thiol groups. During this period, a solution of QDot nanoparticles was activated with maleimide crosslinkers through the addition of 10 mM succinimidyl-4-(N-maleimidomethyl) cyclohexane-1-carboxylate (SMCC).

Both reduced antibody and activated QDots were then subjected to buffer exchange using a supplied desalting column before being allowed to react for 1 hr at room temperature. Unreacted functional groups were then blocked through the addition of 10 mM β-mercaptoethanol, with further incubation for 30 min. Antibody-QDot conjugates were finally separated from any unconjugated components through a supplied gel filtration column.

Separation by agarose gel electrophoresis was used to confirm the successful coupling of anti-PSA antibodies to QDot nanoparticles. Collected antibody-QDot conjugates, unconjugated QDots and SMCC activated nanoparticles were diluted to a concentration of 10 nM in SDW and loaded onto a 3% agarose gel in ×0.5 TBE buffer, which was then run at 100 V for ~3 hours.

#### **4.3.7 Displacement Assay**

To investigate the optimal molar ratio of antibody-QDot conjugates to BHQ-3-DVCAQV-NH<sub>2</sub> required for fluorescence quenching, 100 µl of quencher-label peptide at a range of concentrations (5, 10, 20, 40, 80, 160 nM) was incubated with 10 nM solutions of antibody-QDot (100 µl) for

1 hr at room temperature. Emissions were recorded before and after peptide incubation on a Biotek HT spectrofluorometer (Vermont, USA) using  $Ex400\pm30/Em645\pm40$  nm wavelengths (for the measurement of emissions at 625 nm). An appropriate negative control (100  $\mu$ l SDW + 100  $\mu$ l antibody-QDot) was also utilised. The displacement of moderately bound peptides was then achieved through the addition of 160 nM PSA (100  $\mu$ l) to each sample, whereupon spectra were re-recorded. All measurements were performed in triplicate.

#### **4.3.8 DNA Profiling**

To determine the effects of this sensor on DNA profiling, a 50  $\mu$ l volume of 10 nM antibody-QDot-BHQ-3-peptide solution was added to 150  $\mu$ l of seminal fluid. A reference DNA sample was then prepared through the addition of 50  $\mu$ l SDW to a second semen volume in place of substrate reagent. Both samples were then subjected to DNA extraction using the QIAamp® DNA Investigator kit (Qiagen, Manchester, UK) according to manufacturer protocols.

Extracts were quantified using the Quantifiler™ Human DNA Quantification Kit (Thermo Fisher Scientific, California, USA), diluted to 0.1 ng/ $\mu$ l and amplified using the AmpFISTR® NGM SElect Express Kit (Thermo Fisher Scientific, California, USA) on a Perkin Elmer 9700 thermal cycler (Cambridge, UK). Amplified STR products were then resolved through capillary electrophoresis using an Applied Biosystems® 3130 Genetic Analyser and evaluated using GeneMapper® software (California, USA).

### **4.4 Results and Discussion**

#### **4.4.1 Immunosensor Design**

The selection of a suitable quencher-labelled analogue that is able to undergo indefinite antibody binding until it is preferentially displaced in the presence of a target analyte may be considered the most challenging aspect of immunosensor development. Due to their lack of secondary

folding structure, synthetic peptides based on the specific amino acids responsible for protein-antibody interaction are likely to possess a lower binding affinity than their native protein counterparts [243]. These sequences may therefore have ideal use as moderately bound quenching ligands in antibody displacement assays. Furthermore, the small length of most protein epitope-based sequences ensures that acceptor molecules attached to such ligands will be brought within the required distance for the efficient FRET quenching of antibody-bound donor fluorophores.

Antibody and peptide analogue selection were therefore both based on previous research conducted by Piironen *et al.* [244], in which the antigenic epitopes of PSA for a range of monoclonal antibodies were determined. In this study, anti-PSA antibody 8301 (designated in Piironen as E86) exhibited considerable specificity and binding affinity for free PSA protein. Furthermore, this antibody was shown to interact exclusively with amino acids 158-164 (DVCAQV) of PSA, which were subsequently selected as the basis for the construction of a quenching peptide ligand.

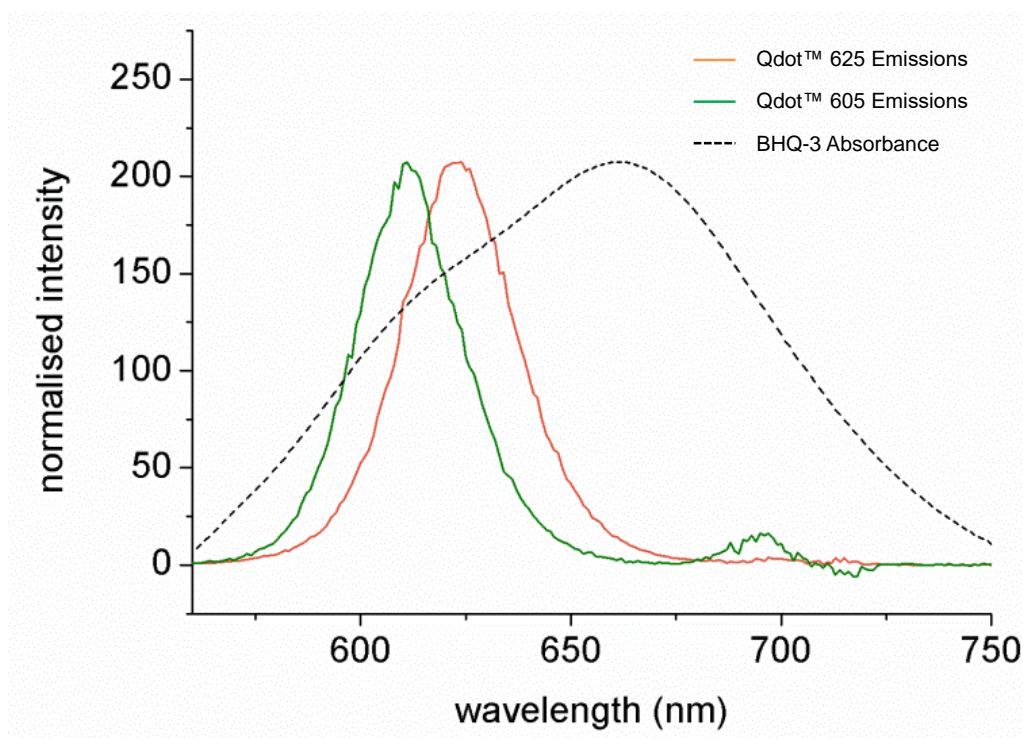


**Figure 40:** Normalised spectral overlap of BHQ-3 absorption compared to 605 and 625 nm QDot emissions. Taken with permission from [234].

With the hope that this sensor may eventually be applied towards the detection and identification of seminal fluid at crime scenes, QDot nanoparticles emitting at 625 nm were specifically chosen for use within this assay in order to prevent the potential quenching of sensor fluorescence by the broad absorption spectrum of human semen [245]. The most suitable quenching partner for QDots was found to be BHQ-3, with suitable absorbance overlap of QDot™ 625 emissions previously demonstrated by Kattke *et al.* [151] (**Figure 40**).

#### 4.4.2 Quenching Peptide Synthesis

The construction of a moderate affinity peptide ligand based around amino acids 158-164 (DVCAQV) of PSA was accomplished using a standard SPPS strategy. Peptide DVCAQV-NH<sub>2</sub> was then labelled with the succinimidyl ester form of BHQ-3 to produce BHQ-3-DVCAQV-NH<sub>2</sub> (**Figure 41**).

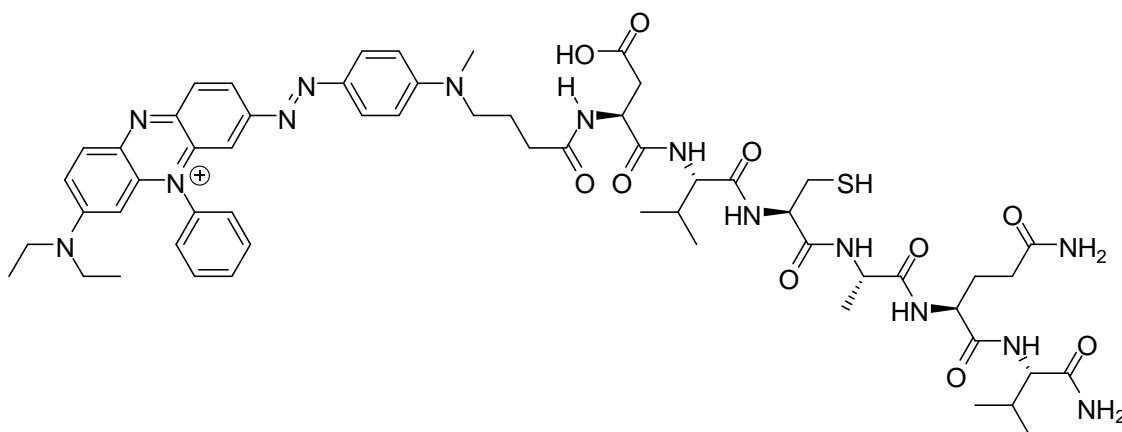


**Figure 41:** Structure of conjugated quenching peptide BHQ-3-DVCAQV-NH<sub>2</sub>. Taken with permission from [234].

This particular quencher was not only chosen due to an efficient spectral overlap of QDot™ 625 emissions, but also for a lack of native fluorescence. Instead, this ‘dark’ quencher dissipates absorbed light via non-radiative processes (such as the generation of heat through molecular bond vibration), allowing its use at higher concentrations in FRET assays without interference on donor emissions [246].

Analysis via ESI and MALDI-TOF mass spectrometry was used to confirm the successful synthesis of DVCAQV-NH<sub>2</sub> and BHQ-3-DVCAQV-NH<sub>2</sub> respectively (**Figure 42**).

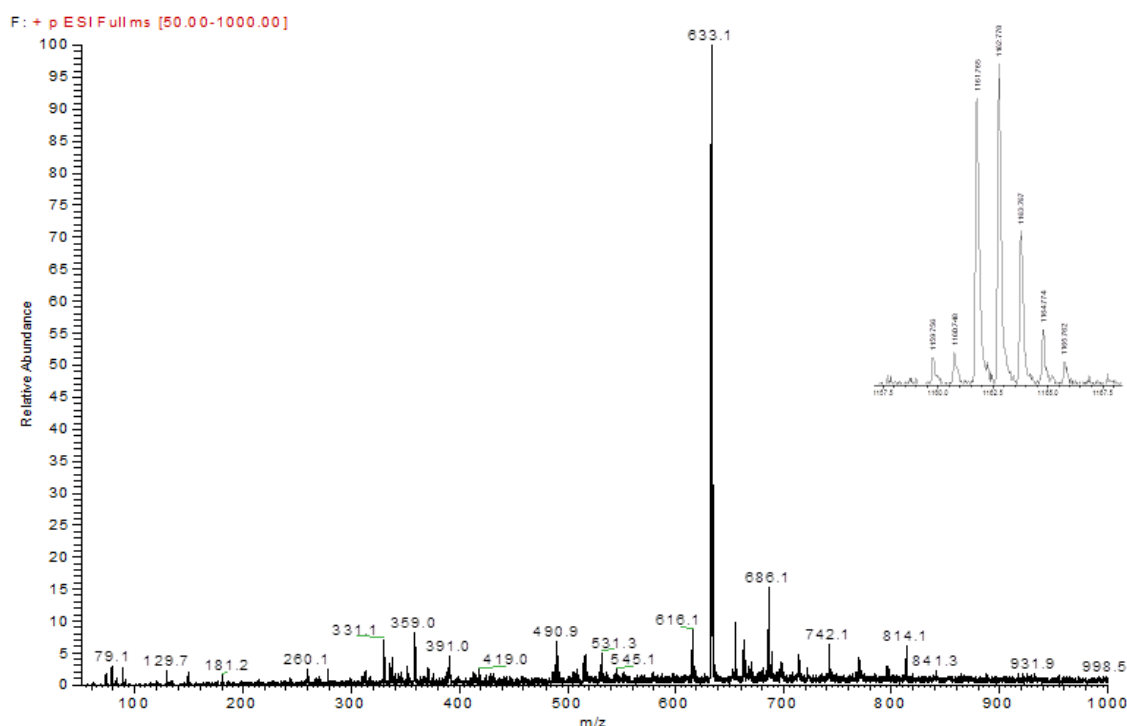


**Figure 42:** ESI-MS of peptide DVCAQV-NH<sub>2</sub> (calculated m/z for [M+H]<sup>+</sup> = 633.3, main peak reported = 633.1). Inset: MALDI-TOF of BHQ-3-DVCAQV-NH<sub>2</sub> (calculated m/z for [M+H]<sup>+</sup> = 1162.5, main peak reported = 1162.770). Taken with permission from [234].

#### 4.4.3 Biacore Analysis

Differences in the binding affinity of anti-PSA antibody 8301 with both native PSA protein and DVCAQV-NH<sub>2</sub> were monitored in real-time using a Biacore SPR instrument. In this technique, antibody ligands are first covalently attached to the surface of a carboxy-methylated dextran-functionalised gold-coated sensor chip. A polarized light source focused through a glass prism is then used to illuminate the chip, causing light to be reflected at a specific angle of incidence ( $\theta$ ). At this angle, light will excite plasmons at the surface of the gold, causing SPR to occur. Analytes are then passed over the surface of the chip within a continuous buffer solution and captured by immobilised ligands. Accumulation of mass as a result of target capture affects a change in resonance angle,



which is measured by the instrument [247]. A schematic overview of this process is provided in (Figure 43).

Small response unit increases observed upon 40 nM peptide injection indicated a successful binding of DVCAQV-NH<sub>2</sub> to immobilised anti-PSA antibodies, whilst the same concentration of PSA showed much larger interaction, requiring three injections of 10 mM glycine-HCl (pH 1.7) to regenerate the surface of the sensor chip. This reflects the significantly large affinity constant of  $1 \times 10^{11}$  L mol<sup>-1</sup> given by the antibody manufacturer.

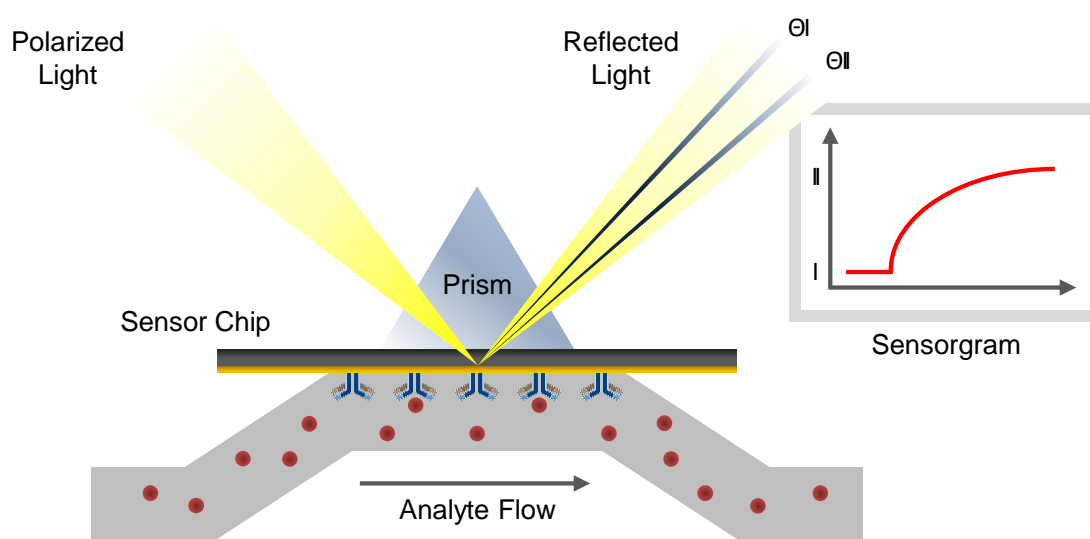


**Figure 43:** Schematic representation of Biacore affinity analysis.

However, attempts to gain a quantitative measurement of peptide binding affinity were unsuccessful. This is usually achieved via the construction of a calibration curve of immobilised antibody resonance responses against a range of different analyte concentrations. Whilst such responses were adequately observed upon peptide injections of 40, 20, 2 and 0.2 nM, concentrations above this level could not be detected, preventing accurate curve plotting. The reason for this lack of signal remains unresolved but may involve the dimerization of peptides at higher concentrations through cysteine residue disulphide bridge formation, which may inhibit antibody binding.



#### 4.4.4 Antibody-QDot Conjugation

Anti-PSA antibodies were conjugated to amine-functionalised QDot nanoparticles using a sulfhydryl-reactive antibody conjugation kit, allowing for the site-specific labelling of hinge region thiols [248]. This approach was chosen over the traditional non-specific labelling of amine groups through EDC chemistry in order to better control the distance between QDots and quenching ligands and ensure that all FRET components are within the 10 nm distance required for quenching.

Many authors have noted the difficulties associated with confirming conjugation between antibodies and QDots [249]. Some studies have found moderate success in the separation of antibody-QDot complexes from unconjugated nanoparticles by agarose gel electrophoresis [250, 251], but with electrophoretic mobility based on both size and charge, results are often unpredictable.

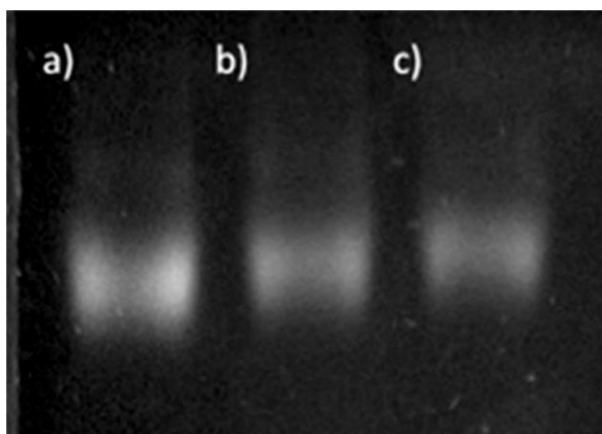


**Figure 44:** A 3% agarose gel demonstrating the separation of a) unconjugated QDots, b) SMCC- activated QDots and c) anti-PSA antibody-QDot conjugates. Taken with permission from [234].

According to the manufacturer protocols supplied with the QDot™ 625 Antibody Conjugation Kit, the ratio of antibodies conjugated to each QDot during labelling is approximately 4:1. Assuming this information is correct, the weight of antibody-QDot conjugates will be ~800 kDa. Such conjugates are therefore likely to run significantly slower on a gel compared to ~200 kDa unconjugated nanoparticles. SMCC-activated QDots would also be expected to travel slightly slower due to the addition

of maleimide cross-linkers. A small amount of separation that reflects these size differences was seen during electrophoresis experiments, which may be taken as an indication of successful antibody-QDot conjugation (**Figure 44**).

#### 4.4.5 Displacement Assay

In a preliminary assay optimisation study, varying concentrations of BHQ-labelled peptide were incubated with 10 nM antibody-QDot conjugates to determine the ideal molar ratio of ligand required to quench biosensor fluorescence. Significant decreases in nanoparticle emission intensities were observed within all samples, even at lower BHQ-3-DVCAQV-NH<sub>2</sub> concentrations, successfully establishing the binding of peptide ligands to the antibody-QDot complex (**Figure 45**). However, a large peptide concentration of 160 nM was required for the complete quenching of QDot signals.

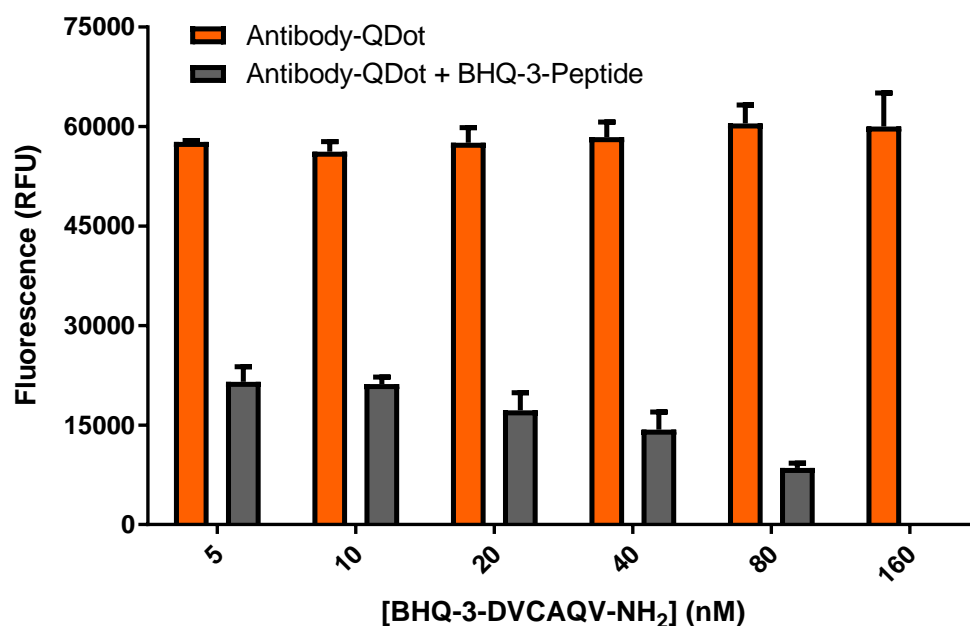


**Figure 45:** Fluorescence emissions of antibody-QDot conjugates before and after incubation with quencher-labelled peptides. Data represents the mean  $\pm$  SD, samples performed in triplicate.

The subsequent addition of 160nM PSA to quenched conjugates resulted in the immediate restorations of antibody-QDot fluorescence comparable

to pre-peptide incubation emission intensities (**Figure 46**), indicating the successful displacement of moderately bound ligands. Statistical analysis of datasets from samples both pre and post-PSA addition across all BHQ-3-DVCAQV-NH<sub>2</sub> concentrations using a Wilcoxon signed-ranks test found these fluorescence increases to be statistically significant ( $p = 0.018$ ).

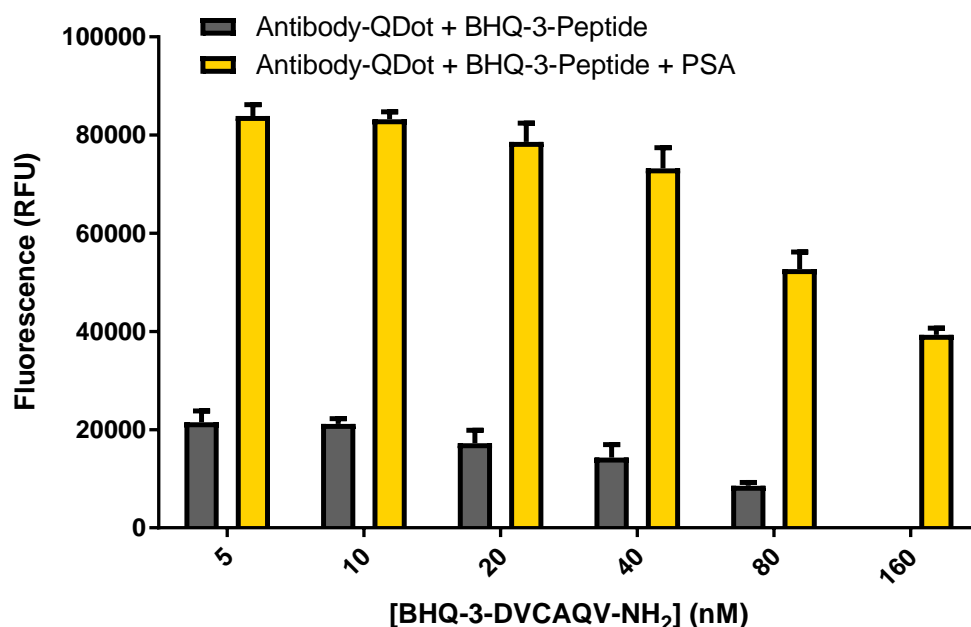


**Figure 46:** Fluorescence emissions of antibody-QDot conjugates incubated with quencher-labelled peptide before and after PSA addition. Data represents the mean  $\pm$  SD, samples performed in triplicate.

#### 4.4.6 DNA Profiling

Whilst no detrimental effects on DNA profiling processes were observed during the application of fluorogenic substrate-based biosensors to body fluid samples, this may not be the case for sensors employing immunological or nanoparticle components. Therefore a solution of antibody-QDot conjugates was applied to a 150  $\mu$ l volume of seminal fluid, which was then subjected to standard forensic DNA extraction, quantification, amplification and electrophoresis procedures. A DNA reference sample was also prepared through the addition of 50  $\mu$ l SDW to a second volume of semen, which was processed in an identical manner.

No differences between immunosensor-added and reference samples outside the limits of normal experimental variation were observed at any

stage of the profiling process. DNA extracted from semen containing immunosensor reagent was quantified at 2.21 ng/μl, whilst the semen reference sample was found to contain DNA at a concentration of 2.33 ng/μl. Furthermore, a full STR profile was obtained from this sample, with no negative effects to high molecular weight loci (**Figure 47**).

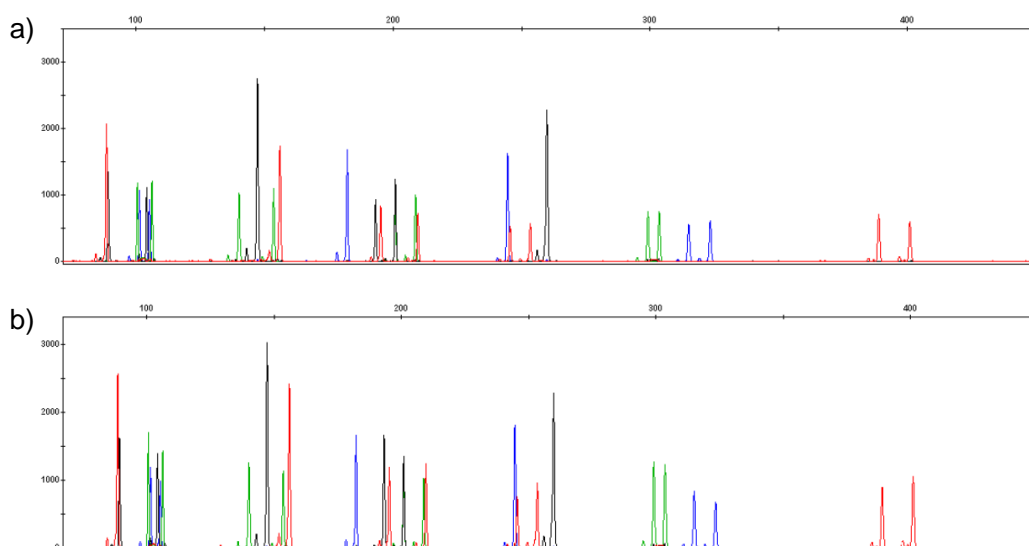


**Figure 47:** STR profiles generated from seminal fluid samples containing a) immunosensors and b) SDW. Taken with permission from [234].

## 4.5 Conclusion

Promising results were demonstrated in the construction of an immunological displacement sensor towards PSA. Fluorescent signal transduction involved the displacement of a moderately bound quenching peptide ligand from an antibody-binding site by native PSA protein to restore labelled nanoparticle fluorescence. This sensor demonstrated an immediate response to PSA within solution, with ‘turn-on’ QDot emission signals easily observed via spectrofluorometry.

Work presented in this chapter primarily focused on the design and development of an entirely novel biosensor rather than its application within a forensic context. As a result, investigations into this sensor were limited to the detection of purified PSA protein within solution. However, the promising performance demonstrated by this assay is likely to justify further exploration of its use within the analysis of whole seminal fluid both in solution and deposited *in situ*.

Future studies are likely to involve modifications to individual sensor components to optimise assay specificity, sensitivity and robustness to varying environmental conditions. This may include alterations to the amino acid sequence of BHQ-3-labelled peptides, which may increase initial biosensor quenching by enhancing binding affinity with antibody-QDot conjugates. Selection of ideal sequences may be achieved via the use of peptide microarrays, such as those exploited within epitope mapping studies, or through computer modelling. An extensive validation of final sensor constructs, encompassing a comprehensive evaluation of cross-reactivity, limit of detection, variability, comparison with other biological fluid tests and performance against mock casework samples should also be undertaken.

An ideal application of this sensor is likely to involve the exploitation of several different antibody-QDot conjugates (each with a separate emission wavelength) for the simultaneous detection of several protein targets within a multiplex fluid sensing system. The interchangeable nature of QDots and antibodies may allow for this application to be realised and would likely depend upon the elucidation of amino acid sequences attributed to antibody interaction with forensically relevant proteins for use as other moderately bound ligands.

# **Chapter 5**

## **Aptasensors**

## 5.1 Introduction

After successfully demonstrating detection of an intra-fluidic target, further efforts to construct displacement-based sensors for the analysis of biomarkers in other fluid types were deemed justified. However, during immunosensor investigation, significant challenges were encountered in the use of antibodies as recognition elements. Protocols required for the site-specific conjugation of nanoparticles to antibody fragments were found to be complex and time-consuming. Furthermore, this conjugation came at significant expense, with each QDot-labelling kit costing approximately £500 (in addition to costly antibody components). Such expense is likely to increase the overall cost of produced assay reagents, limiting potential use in forensic casework to targeted stain identification rather than large volume biological screening.

It was subsequently hypothesised that bio-recognition elements based on nucleic acid aptamers may be a more suitable alternative to antibodies in displacement-based biosensors for the detection of body fluid targets. These molecules usually consist of short strands of single stranded DNA (ssDNA) or RNA raised *in vitro* to bind to virtually any given target [252]. Aptamers possess several advantages that make them ideal for use within fluorescent biosensing assays. Whilst comparable to antibodies in terms of specificity and affinity [253], aptamers are entirely synthetic, making them easy to produce at low a cost with no batch-to-batch variation [254]. Aptamers may also be selected against significantly large targets (such as whole cells and tissues [255]), which may be especially useful in fluid identification assays.

This chapter opens with a comprehensive review on aptamer-based sensors (aptasensors) for the purpose of forensic analysis. This review, which underwent publication in 2017, includes a brief overview of the aptamer selection process, the types of sensors that may be constructed using aptamer recognition moieties and developed aptasensors that have been previously reported for the detection of forensically-relevant targets.

The chapter then explores the construction of a displacement-based multiplex body fluid detection sensor using several different fluorescently-labelled aptamer sequences that are initially quenched through adsorption to graphene oxide (GO) nanosheets. Both the presence and identity of fluids is then indicated through the production of emissions at specific wavelengths (corresponding to each type of fluid) after the liberation of sequences from the GO surface as a result of intra-fluidic protein interaction. Attempts to increase the specificity of this aptasensor through the selection of ssDNA aptamers towards whole cell targets are lastly explored. Aptamers were successfully generated against human sperm cells using a modified Cell-SELEX protocol with sequence elucidation achieved through next generation sequencing (NGS) and a novel bioinformatics pipeline.

## 5.2 Published Article 4: 'Developing Aptasensors for Forensic Analysis'

The content of following section was published as a review article in: **Gooch, J., Parkin, M., & Frascione, N., Developing aptasensors for forensic analysis.** TrAC Trends in Analytical Chemistry, 2017. 94: p. 150-160.

Drafting of the manuscript was performed by the candidate. Dr. Mark Parkin and Dr. Nunzianda Frascione had final approval over manuscript submission.

### 5.2.1 Manuscript

**Authors:** James Gooch,<sup>a</sup> Mark Parkin,<sup>a</sup> Nunzianda Frascione.<sup>a\*</sup>

**Authors Address:** a) Analytical and Environmental Sciences Division, King's College London, 150 Stamford Street, London, SE1 9NH, UK

**Abstract:** Aptamer-based biosensors may be of significant benefit to forensic analysis by allowing the rapid, sensitive and specific detection of molecular targets relevant to criminal investigation. However, despite the production efficiency, stability and cost effectiveness of aptamer



recognition moieties, aptasensors have yet to find commercial employment within any area of forensic science. This review therefore attempts to encourage aptasensor development by initially identifying the methods of selection, sequence analysis and affinity measurement most appropriate for the discovery of suitable aptamers against analytes of forensic interest. A range of optical, electrochemical and mass-sensitive transduction platforms that may be considered amenable to current forensic testing procedures are then discussed. The specific analytical disciplines in which aptasensing technology is likely to be of greatest value, including forensic drug analysis, forensic toxicology and biological evidence and explosives detection are lastly highlighted to stimulate researchers to consider the development of sensors towards these particular target types.

## Introduction

Forensic science may be considered one of the broadest analytical disciplines due to the extensive spectrum of analytes and sample types used to add value to a criminal investigation. For example, in the field of human identification alone, examinable material may range from simplistic visual patterns (e.g. fingerprints) to complex biological molecules (e.g. DNA) [256]. Challenges associated with the growing variety of analytical techniques and instrumentation required by forensic laboratories to meet comprehensive testing demands have prompted the search for new and flexible methods that are able to detect, identify and quantify analytes of forensic interest.

Immunological analysis methods have long been an integral part of forensic serological and toxicological screening processes [3]. However, with the recent discovery of aptamer-based recognition, research groups are beginning to question the efficiency of the ELISA and lateral flow strip testing strategy's currently employed by forensic laboratories. Nucleic acid aptamers are short single-stranded DNA or RNA sequences that are able to undergo selective antigen association as a result of three-

dimensional structure formation [257]. These structures (usually a combination of k-turn, loop, pseudoknot and quadruplex motifs) facilitate intermolecular interaction with targets via van der Waal forces, hydrogen bonding and aromatic ring stacking [258]. Through the *in vitro* enrichment of random oligonucleotide libraries (consisting of approximately  $10^{12}$ - $10^{15}$  individual sequences) aptamers may be developed towards almost any small molecule [259], virus [260], large protein [261] or whole-cell target [262], giving potential for their use as recognition moieties in the analysis of diverse forensic samples.

While analogous to antibodies in terms of binding affinity (often displaying  $K_d$  values in the nanomolar or picomolar range [263]), aptamers possess a number of key advantages over their protein counterparts. Once selected, aptamer sequences can be mass-produced using automated solid-phase synthesis techniques, resulting in the production of highly purified oligonucleotides within a number of hours and at a fraction of the cost of biological antibody generation methods [264]. Aptamers also display greater thermal stability affording long shelf-lives without loss of activity, easy transport and storage and ability to return to a native confirmation being subjected to high-temperature assay conditions [265].

Although demonstrating success as effective therapeutic agents [266], aptamers, since their discovery, have been predominately developed as recognition molecules for use in a range of biological chemical analysis techniques. This has mainly focused on the use of immobilized aptamers within traditional ELISA, western blot, flow cytometry and lateral flow assays as replacements for expensive and cumbersome antibody moieties [264]. In addition, aptamers have also found beneficial application within the field of separation science, having been used to successfully resolve enantiomeric molecules within High Performance Liquid Chromatography (HPLC) systems by the inclusion stereospecific aptamers on solid chromatographic supports [267].

Nevertheless, Hamaguchi *et al.* argue that the most powerful application of nucleic acid aptamers is within analytical biosensing platforms [145]. Biosensors are compact devices capable of the real-time transduction of biological interaction events into a number of measurable signal outputs [268]. Some authors have recently recognized the potential of biosensors to provide the highly specific detection and quantification of forensically relevant materials (such as body fluids, drugs, explosives and toxins) without the need for extensive sample processing steps [121, 131, 234]. Displaying significant conformational changes upon target binding and allowing an extensive range of chemical modifications (including the incorporation of various optical, electrochemical or nanoparticle reporters [269]) at various sites without loss of binding affinity, aptamers may be considered as ideal recognition moieties for use within molecular sensing purposes [270].

Despite great promise, aptasensors (or indeed any form of aptamer technology) have yet to find commercial employment within the field of forensics. This lack of success has been attributed to a number of factors, including the limited number of aptamer sequences raised against analytically relevant targets [270], the need for further investigation into the use of developed sensors within complex matrices [121] and the high investment already made by analytical laboratories in antibody-based testing methods [271]. This review therefore attempts to outline the current state of aptasensor development processes, with a specific focus on those techniques most likely to aid the construction of forensic analyte sensing devices. Recent advances in aptamer selection, sequencing and affinity testing are first explored, along with signal transduction mechanisms most amenable to current forensic testing capabilities. A number of forensic disciplines liable to benefit from aptasensor application are lastly identified in the hope of encouraging experts within the field of biosensor design to produce aptasensors towards valuable evidential targets.

## Aptamer Development

### Aptamer Selection

In recent years, a substantial number of modifications have been made to the SELEX (Systematic Evolution of Ligands by EXponential enrichment) protocol initially developed by Gold's [272] and Szostak's [273] groups. While generally based on the same library incubation, target binding and sequence amplification principles exploited within the original method, these modified techniques differ in their approach to the separation and removal of non-specific ligands [274]. By altering the means in which aptamer-target complexes are partitioned from unbound oligonucleotides, aptamers may be selected against particular target types with a higher specificity and affinity than would be possible using conventional SELEX protocols [275]. As the physical properties of forensically relevant targets are extremely diverse, it is vital that an optimal selection method is chosen and carried out prior to aptasensor development. A summary of SELEX protocols that may be useful in the selection of aptamers against forensically relevant targets can be found in **Table 9**.

.These modifications are especially pertinent in the selection of aptamers towards low-molecular weight forensic analytes (e.g. toxic chemicals and explosives), where separation is problematic due to the similar masses of bound complexes and unbound nucleic acid sequences [253]. The immobilization of such targets to a solid support surface (e.g. sepharose, agarose or magnetic beads) may be used to increase separation efficiency but can also result in the amplification of non-specific sequences that bind to the support matrix or immobilization linkers [259]. Furthermore, the creation of a chemical link between the small molecule target and the solid support can introduce an unfavourable selection bias through the removal of least one potential aptamer binding site. Fortunately, a number of SELEX processes that allow for the selection of aptamers against small-molecules without the need for target immobilization have recently been developed.

**Table 9:** SELEX protocols that may be used to select aptamers against forensic targets

Protocol	Mechanism	Advantages	Ref.
Capillary-Electrophoresis SELEX	Aptamer-target complexes are separated from unbound nucleotide sequences according to electrophoretic mobility.	- Selection may be completed within 2-4 rounds. - Useful for small molecule targets.	[276]
Capture-SELEX	Library sequences are displaced from magnetic beads by target binding. Unbound ligands are then removed magnetically.	- Aptamers display large structural changes. - Useful for small molecule targets.	[277]
Cell-SELEX	A panel of membrane biomarker-specific aptamer sequences is produced as a result of exposure to live cell targets.	- Counter-selection used to increase specificity. - Selection performed on targets in native state.	[278]
FluMag SELEX	Complexes formed between bead-immobilized analytes and fluorescent library sequences are collected magnetically.	- Selection rounds and dissociation values may be quantified by fluorescence measurement.	[279]
Graphene Oxide (GO) SELEX	Graphene oxide is used to adsorb and separate unbound ssDNA sequences from aptamer-target complexes in solution.	- Requires less than 5 rounds of selection. - Useful for small molecule targets.	[280]
<i>In-Silico</i> SELEX	Theoretical oligonucleotide libraries are screened against a target using computational tools to identify potential binders.	- Atomic-level mechanisms of nucleotide-target binding can easily be determined.	[281]
Microfluidic (M) SELEX	Ligands bound to magnetic or sol-gel bead-conjugated targets are purified by continuous washing within a microchannel.	- Lower target molecules and reagent volumes are required as a result of miniaturization.	[282]
MonoLEX	Affinity columns used to partition aptamer-target complexes are physically segregated to elute highest affinity sequences.	- Requires a single round of selection. - Diminishes competition between sequences.	[283]
NanoSelection	High affinity aptamers are detected and recovered via the use of fluorescence and Atomic Force Microscopy (AFM).	- Requires a single round of selection. - Binding affinity may be measured by AFM.	[284]

Capture-SELEX (also known as structure-switching SELEX), involves the conjugation of oligonucleotide libraries themselves to DNA-functionalized magnetic particles by use of a complimentary ‘docking’ sequence [277, 285]. When incubated with a target molecule, sequences that undergo conformational changes as a result of binding are displaced from the beads (which can then be removed with unbound ligands through the application of a magnetic field). Aptamers isolated using this capture

method may be considered particularly attractive recognition moieties for use in analytical biosensing platforms due to their significant structure-switching abilities [286].

Another immobilization-free method, GO-SELEX, makes use of the ability of graphene oxide (GO) to bind single stranded DNA through  $\pi$ - $\pi$  stacking interactions [280]. In this technique, target molecules are first incubated with an oligonucleotide library in solution, allowing binding to occur. Unbound sequences are then adsorbed onto the surface of the graphene oxide, allowing separation from aptamer-target complexes via centrifugation. Ethanol precipitation is finally used to purify and recover bound ssDNA sequences. As partitioning is purely based on interaction between DNA libraries and graphene, GO-SELEX is largely independent of target size (and has already been successfully employed to produce aptamer sequences towards low-molecular weight pesticide compounds [287]).

One class of forensic analytes that may also benefit from aptamer-sensing application is that of whole-cells. The immunological analysis of cellular material is currently undertaken by forensic laboratories as a method of confirming the identity of biological fluid deposits left behind at crime scenes [3]. Unlike conventional SELEX procedures, the selection of aptamers against whole-cells does not require the use of a single highly purified (or even known) target. First described by Morris *et al.*, Cell-SELEX instead involves concurrent binding of library oligonucleotides to multiple biomarkers exposed on the surface of intact live cells [278]. As a result, this approach generates a panel of aptamer sequences (each targeting a particular membrane protein or lipid) that can then be used for cell recognition purposes [288]. The use of live targets within Cell-SELEX ensures that aptamers are raised towards the native conformational structure of such membrane molecules, allowing for the high-affinity binding of natural cellular material during subsequent analysis [262].

In comparison to other selection protocols, the partitioning of unbound nucleotides within Cell-SELEX is relatively simplistic and may be achieved by basic centrifugation or washing steps [289]. A counter-selection stage, in which enriched libraries are incubated with a negative control cell line, is also often included in cell-selection protocols to remove non-specific ligands that bind to universally shared membrane motifs [290]. Cell-SELEX techniques have in fact already been used to produce aptamers against sperm [291] and red-blood cell targets [278], which may already be of potential use within forensic assays for the analysis of biological fluids.

### **Sequence Analysis**

Following sufficient enrichment, aptamer pools are sequenced in order to elucidate the nucleotide structures of high-affinity binders [274]. Conventionally, this process was performed via the ligation of selected sequences into commercially available cloning vectors, which are then transformed into competent bacterial cell colonies. Approximately 50-100 individual clones (each possessing one aptamer sequence) are then recovered before plasmids are extracted and subjected to standard Sanger sequencing [292]. However, whilst able to indicate the most abundant aptamers present within an enriched pool, these cloning techniques only involve the sequencing of a small fraction of the total binders obtained during selection (which may be up to 1,000,000 sequences) [293]. As a result, the majority of new aptamer development protocols now make use of next generation sequencing (NGS) platforms for the comprehensive analysis of potential binding candidates [294]. Such high-throughput methods not only allow the discovery of millions of sequences from enriched pools without laborious cloning processes, but can also be used to shorten selection processes by identifying aptamers during early SELEX rounds [295].

Commercially available NGS platforms previously used for aptamer discovery include Ion Torrent's Personal Genome Machine (PGM) [296]

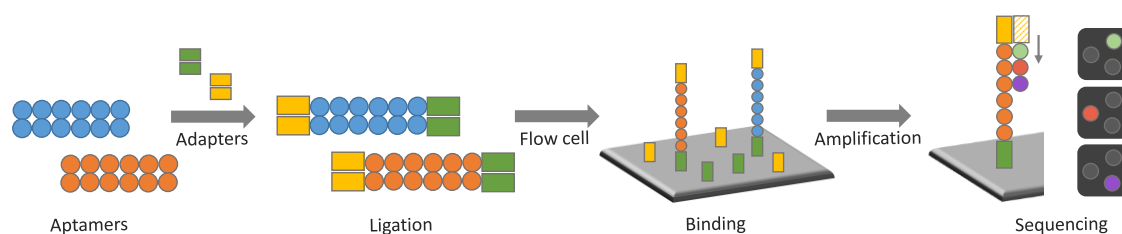


**Figure 48:** Workflow of the Illumina sequencing-by-synthesis approach - Specialist adapter sequences are first ligated to the end of aptamers obtained from SELEX-enriched pools. These adapters aid the anchoring of selected oligonucleotides to the surface of a flow cell, allowing solid-phase bridge amplification. Fluorescently labeled nucleotides are then added to the cell, which is imaged after the incorporation of each base into DNA strands. The emission wavelengths of each nucleotide dye are then monitored in order to determine aptamer sequences.

Illumina's Genome Analyzer/HiSeq system [297, 298], Roche's GS FLX system [299, 300] and Applied Biosystem's SOLiD system [301]. However, with extensive sequence reads and higher total read lengths, a greater level of detail on the structural features of target binders may be provided by Illumina instruments, making them the most preferable choice for aptamer sequencing (**Figure 48**) [292]. Furthermore, these platforms, based upon the principle of cyclic reversible termination, are already widely used within the forensic community for the analysis of human genomic material [302] and may therefore be readily applied by forensic researchers to determine aptamer sequences for the recognition of forensic analytes.

While NGS use may significantly enhance the resolution and sampling depth of enriched aptamer pools, additional computational bioinformatic tools are currently required to process the sheer quantity of raw sequence data obtained [294]. Web-based and offline pre-processing software, such as Galaxy [303], cutadapt [304] and AptaTools [305] are often used to first isolate variable aptamer regions of a defined length by removing adapter and constant region sequences.

Further programs are then employed to filter this data in order to narrow down aptamer candidates for subsequent experimental testing. The FASTaptamer toolkit achieves such filtering by monitoring the relative



enrichment of specific aptamer sequences between selection rounds [306], whereas APTANI examines both the total read counts of each sequence as well as shared structural homology between sequences [307]. After aptamer discovery has taken place, sequences may be further analysed by programs such as *mfold* [308] to provide more information on secondary oligonucleotide structure.

### **Affinity Measurement**

In order to ensure adequate aptasensor performance, it is vital that integrated aptamers demonstrate strong affinity towards target molecules [309]. Aptamer affinity is usually expressed in terms of a dissociation constant ( $K_d$ ), the value of which may be determined by a range of separation-based, mass-sensitive, spectroscopic or other label-free techniques [259]. A summary of methods that may be able to assess the performance of aptamers with potential use in forensic testing may be found in [Table 10](#).

Variations in the size and physical properties of forensically relevant analytes make the evaluation of aptamer-target affinities challenging. Much like similar SELEX processes, measuring  $K_d$  via the separation of unbound ligands from aptamer-target complexes is often problematic for compounds of a smaller molecular weight than nucleotide binding sequences. Other techniques, such as fluorescence polarization or surface plasmon resonance (SPR), are additionally disadvantaged by the chemical labelling or immobilization of aptamers or targets, which may reduce  $K_d$  calculation accuracy by altering binding interactions [259].

A resolution to these issues may be provided by isothermal titration calorimetry (ITC), a label-free solution-based method that allows the characterization of binding energy by monitoring temperature increases during complex formation [310]. ITC methods are currently considered the ‘gold standard’ for quantifying biomolecular interactions and have already been used to assess the affinity of aptamers towards several forensically

**Table 10:** Techniques that may be used to determine the affinity of aptamers.

Technique	Type	Mechanism	Ref.
Affinity Chromatography	Separation	- Binding is measured after labelled aptamers or target molecules are incubated with corresponding components that are conjugated to a solid support (typically agarose or magnetic beads).	[311]
Capillary Electrophoresis	Separation	- Concentrations of aptamers, targets and aptamer-target complexes are determined after size and charge-based separation. Fluorescent labelling of each component is often required for detection.	[276]
Equilibrium Dialysis	Separation	- Unbound ligands within an aptamer-target mixture are allowed to diffuse through a semi-permeable membrane before being quantified.	[312]
Gel Electrophoresis	Separation	- Like capillary electrophoresis, binding components are separated by size and charge but by a non-denaturing agarose or polyacrylamide gel. Visualisation is required to observe isolated components.	[313]
Ultrafiltration	Separation	- Unbound ligands are measured after partitioning across a membrane (typically nitrocellulose) under applied pressure, vacuum or centrifugation.	[314]
Back-Scattering Interferometry (BSI)	Spectroscopic	- Changes in the refractive index of a sample through the association of aptamer-target complexes are detected within a microfluidic channel.	[315]
Circular Dichroism (CD)	Spectroscopic	- Differences in the absorption of left and right circularly polarized light are monitored during the titration of DNA against increasing concentrations of target.	[316]
Fluorescence Intensity	Spectroscopic	- The increase/decrease in fluorescence intensity of targets or labelled aptamers as a result of complex formation is measured via spectrofluorometry.	[317]
Fluorescence Polarization	Spectroscopic	- The rotational diffusion of fluorescent dyes conjugated to aptamers or targets is decreased as a result of binding. Subsequent increases in signal polarization are then monitored.	[318]
UV-Vis Absorption	Spectroscopic	- Affinity is inferred from variations in the wavelength or intensity of UV-Vis absorption of aptamers or targets upon binding.	[261]
Quartz Crystal Microbalance	Mass-Based	- Accumulation of aptamer-target complexes on the surface of functionalized piezoelectric crystals results in a measurable decrease in resonance frequency.	[319]
Surface Plasmon Resonance	Mass-Based	- Ligands immobilized on a sensor flow cell are subjected to an aqueous flow of binding partners. The formation of target complexes then results in a change in refractive index near the sensor surface.	[320]
DNase Footprinting	Other	- The relative levels of aptamers protected from digestion (by association with varying concentrations of target molecules) are determined after treatment with DNase I enzymes.	[321]
Isothermal Titration Calorimetry (ITC)	Other	- The amount of energy required to maintain the temperature of a cell is monitored during exothermic aptamer-complex binding.	[310]

relevant targets, including cocaine [322] and organophosphate pesticides [323].

In this technique, targets are titrated into a cell containing an aptamer of interest and allowed to react. Heat released as a result of exothermic binding processes is monitored and compared to an identical reference cell containing buffer or water. Power required by the calorimeter to maintain equal temperature between the cells at each molar ratio of target/aptamer may then be used to construct a binding isotherm, allowing affinity to be determined [324].

However, while ITC may provide detailed information on the thermodynamic parameters of aptamer-target interactions (such as changes in entropy, enthalpy and Gibb's energy), relatively high amounts of target are required for detectable amounts of heat to be generated [261]. This may be considered problematic for some forensic analytes that are expensive to purchase or only available from commercial providers in low concentrations (although micro and nano-ITC instruments may be utilised to overcome these challenges).

## **Biosensing Platforms**

### **Optical**

Reported by Kleinjung *et al.* in 1998, the first biosensor to use aptamers as moieties for target recognition involved the competitive binding of L-adenosine and FITC-labelled analogues to an RNA ligand immobilized on the surface of an optical fibre [325]. As a result, the vast majority of early aptasensing platforms also focused on the use of optical methods to signal biological interaction occurrence [326]. Such sensing generally relies on the structural transitions that aptamers undergo during target binding to create measurable variations in the spectroscopic properties of optical transduction components [269]. These components (typically organic dyes, luminophores, nanoparticles or conjugated polymers) may be incorporated into conformationally labile regions of oligonucleotide

sequences by covalent attachment or as 'label-free' reporters by indirect intercalation [327]. Subsequent alterations in the microenvironment of these reporters as a result of aptamer folding may then prompt changes in the intensity, wavelength or anisotropy of label emissions [270]. Alternatively, multiple reporters can be used to achieve transduction through distance-dependent fluorescence (FRET) or chemiluminescence (CRET) resonance energy transfer processes [252].

Two popular forms of optical aptasensing include aptamer-beacons and hybridized DNA displacement assays [328]. Based on the conventional molecular-beacon format for the detection of specific DNA molecules, aptamer-beacons are constructed by the addition of short complementary nucleotides (alternately labelled with a fluorophore or quencher) to each end of a specific aptamer sequence [145]. Under normal conditions these nucleotides allow the aptamer to take on a closed hairpin structure, bringing the quencher and fluorophore moieties within close proximity and restricting fluorescence output. However, in the presence of target molecules, aptamer interaction causes the hairpin to unfold, resulting in the production of a 'signal-on' fluorescence emission [328]. Hybridized DNA displacement assays (**Figure 49a**) work via a similar premise but instead employ a separate quencher-labelled antisense sequence bound to fluorescent aptamers through Watson-Crick base pairing that then dissociates in the presence of higher affinity target analytes [329].

One of the main advantages of optical sensing is the ability to offer real-time analyte detection without extensive sample processing steps or specialized equipment [330]. Such advantages may give the potential for optical aptasensors to be used as chemical reagents for the simultaneous detection and identification of latent (i.e. non-visible) evidence deposited at crime scenes or on evidential items. This concept has already been explored within Li *et al.* in which two aptamers labelled with emitting gold nanoparticles (Au-NPs) reassembled in the presence of cocaine doped within latent fingerprints [331]. While the adherence of the nanoparticles themselves to deposited marks was sufficient to visualize identifiable

ridge detail, aggregation of the Au-NPs as a result of cocaine binding also resulted in a shift in emission wavelength of scattered light from 550-580nm.

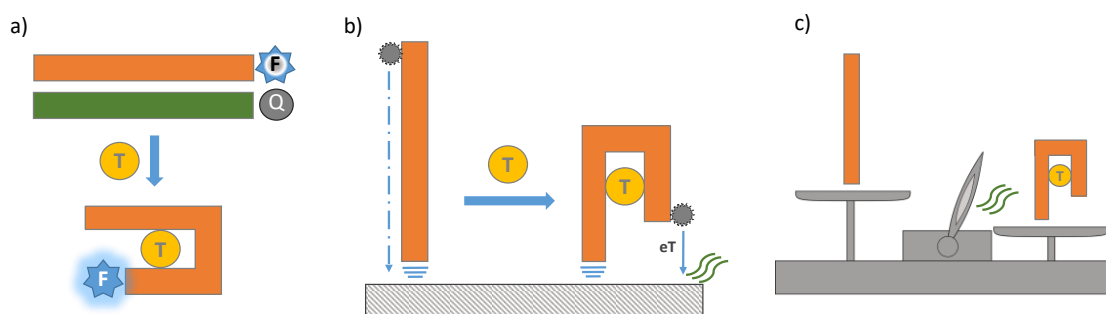


**Figure 49:** Schema of aptamer-based sensing formats - a) Optical transduction. Aptamers labelled with fluorescence reporters (F) are hybridized to quencher (Q)-conjugated DNA sequences, which absorb emission via FRET. Upon binding to targets (T), aptamers separate from complimentary strands, allowing fluorescence to be restored. b) Electrochemical transduction. Changes in aptamer confirmation as a result of target interaction allow redox-active labels to interact with the surface of electrodes to produce an electrical signal. c) Mass-sensitive. An increase in the mass of surface-immobilized binders through aptamer-target complex formation is detected either optically or electrically.

## Electrochemical

Cho *et al.* note that despite the significant amount of optical detection platforms reported during the early stages of aptasensor research, greater attention is now being paid to the use of electrochemical strategies for the transduction of aptamer interactions [270]. Biosensing assays incorporating such methods are becoming increasingly attractive to researchers due to their relative portability, ease of operation, robustness and low cost (to both develop and operate) [332]. Electrochemical aptasensors are further benefitted by excellent sensitivities and can be used in conjunction with a number of electrical signal amplification techniques (such a biocatalytic labelling) to provide extremely low limits of analyte detection [333]. For example, Hanson *et al.* employed the use of a single-step replacement aptasensor exploiting electrochemical nanoparticle stripping-based signal amplification for the measurement of thrombin at ultrasensitive attomole levels [334].

While electrochemical aptasensors may make use of amperometric, potentiometric, conductometric, impedimetric and semiconductor field-effect principles, signals are generally derived from changes in electric current as a result of aptamer-mediated redox reactions occurring at the surface of an electrode [332]. Much like optical aptasensing mechanisms, these reactions are generated by reporter molecules incorporated within aptamer sequences, which are then brought closer to or further away from electrodes as a result of target binding interactions [252]. Popular reporters for electrochemical aptasensors include methylene blue (MB), ferrocene, ferricyanide, ruthenium complexes, enzymes, quantum dots (QDs) and metal nanoparticles [335].

According to Han *et al.*, electrochemical aptasensor assays may be designed in four broad formats: target-induced structure switching (TISS), sandwich, target-induced displacement (TID) or competitive replacement [336]. TISS assays exploit the ability of surface-immobilized aptamers to form rigid tertiary structures in the presence of analytes in order to change the proximity of signalling moieties in relation to an electrode (**Figure 49b**). Sandwich assays conversely involve the assembly of a complex between an immobilized primary aptamer, a target, and a second reporter-labelled recognition molecule (which may be an aptamer or an antibody). In TID sensors, complementary nucleotide sequences are instead immobilized and are used to anchor labelled aptamers to electrodes via base pairing. Upon target interaction these aptamers dissociate, causing a decrease in electron transfer (eT) signals. Competitive replacement lastly involves the incubation of targets with reporter-attached analytes, which then compete for aptamer binding space. As a result, signal intensities obtained from competitive replacement assays are inversely proportional to the amount of target present within a sample.

Electrochemical detection platforms may be considered especially amenable to forensic analysis due to their excellent performance in turbid matrices [337]. Such sensing platforms are able to negate the effects of

optically absorbing and fluorescent molecules present within complex samples (that often interfere with spectroscopic analysis) and therefore represent great potential as toxicological assays for the detection of trace compounds within biological matrices. Work conducted by Baker *et al.* has already proven this capability through the production of an electrochemical TISS aptasensor that was successfully able to detect micromolar concentrations of cocaine in saliva and blood serum samples [338].

### **Mass-Sensitive**

Unlike both optical and electrochemical transduction mechanisms, mass-sensitive aptasensing techniques do not utilise the conformational changes that aptamers undertake in order to indicate biological interaction events [270]. Instead, sequences are tethered to a variety of solid supports and used as simple capture ligands to create discernible increases in mass at sensor surfaces upon target binding (**Figure 49c**). As a result, such methods do not require the use of molecular reporters to generate detectable signals and are therefore classified as 'label-free' techniques [252]. Popular mass-based aptasensing formats include: SPR, surface acoustic wave (SAW), quartz crystal microbalance (QCM) and microcantilever assays [252].

Employing the same principles for the characterization of binding affinity constants, SPR methods have also found use as platforms for the aptamer-based detection of numerous target compounds [339]. One of the most frequently used instruments for SPR sensing is the Biacore™ system manufactured by GE Healthcare [340]. In this system, aptamers are first covalently immobilized onto a thin gold film attached to a glass slide, which is then illuminated by monochromatic p-polarised light. Solutions containing an analyte of interest are then introduced into the sensor at a continuous flow through microfluidic channels. As these analytes interact with aptamer sequences, increases in mass bound to

the film surface cause changes in the refractive index of incident light, which is then registered by the instrument [341].

SAW and QCM-based aptasensors both involve the generation and detection of acoustic waves by electrodes patterned on the surface of aptamer-functionalized piezoelectric crystals [342]. The propagation speed of such waves (either on the surface or in the bulk of crystals for QCM and SAW respectively) is highly influenced by mass associated with the crystal itself. Increases in this mass as a result of aptamer-target binding subsequently cause a reduction in crystal resonance frequencies, which are then observed by electrical means [270]. Whilst these devices are normally only applicable for the sensing of large analytes such as proteins or cells (which provide more measurable mass changes) a number of modified protocols, such as QCM with dissipation monitoring (QCM-D), have been developed to allow the aptamer-based detection of lower molecular weight analytes [253].

Microcantilever assays typically consist of thin silicon or polymer-based micromechanical beams (approximately one micron thick), which respond to changes in physical stress [343]. A gold coating is often applied to one side of the beam in order to allow the immobilization of biological receptors, including aptamers, onto cantilever surfaces [344]. The binding of target molecules to these receptors creates stress differences between the functionalized and non-functionalized sides of the surface, causing the cantilever to bend by a matter of nanometres [345]. The degree of bending (also known as cantilever deflection or  $\Delta x$ ) is then detected optically and compared to a reference cantilever containing non-interacting nucleotide sequences [346]. As this deflection is directly proportional to the amount of target present within a sample, microcantilever methods represent a great opportunity for the quantitative sensing of forensically relevant analytes.



## Aptasensor Applications

### Biological Evidence

Chemical reagents used for the detection and identification of biological evidence (i.e. body fluids and fingerprints) are currently limited by issues of low specificity and sensitivity, environmental and safety concerns, ease of application and effect on downstream DNA profiling processes [131, 347]. Other antibody-based devices (such as immunochromatographic test cartridges) are conversely able to provide absolute confirmation of body fluid identity with a sufficient degree of sensitivity and safety, but cannot be used to locate latent stains on evidential surfaces [117]. As previously mentioned, optical aptasensing strategies may have the opportunity to overcome these challenges by allowing the simultaneous detection and highly specific identification of biological evidence *in situ*.

Furthermore, a number of optical aptasensors have already been constructed towards biomarkers that may be (or currently are) used for the confirmation of body fluid presence. For example, Kong *et al.* recently reported the production of a fluorescent aptasensor towards prostate specific antigen (PSA), a serine protease enzyme already used in forensic analysis for the immunological detection of seminal fluid [348]. In this assay, fluorophore-labelled aptamers adsorbed onto the surface of emission-quenching MoS<sub>2</sub> nanosheets were used to detect sub-nanogram concentrations of PSA after dissociation upon target binding.

Since its isolation by Bock *et al.* in 1992, the thrombin-binding aptamer has become one of the most commonly exploited DNA receptor sequences for the construction of new aptamer-based sensing platforms [349]. As a result, a number of these aptasensing assays may find application in the specific detection of thrombin for the purposes of identifying bloodstains deposited on evidential surfaces. One such sensor, developed by Wang *et al.*, involves the use of aptamer-functionalized upconverting phosphors, which are initially quenched by the binding of carbon nanoparticles to DNA strands through  $\pi$ - $\pi$  stacking

interactions (**Figure 50**). In the presence of thrombin, these nanoparticles dissociate from ligand sequences, relieving FRET quenching effects and producing 'signal-on' fluorescence emission. [350].

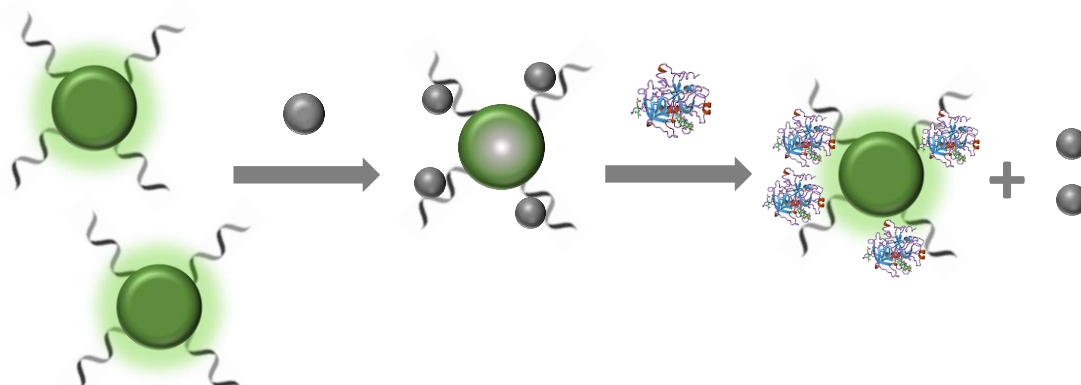


**Figure 50:** Schema of a FRET-based aptasensor for the detection of thrombin developed by Wang et al. [350]. Here, 5' amino-modified aptamer sequences are first covalently linked to poly-acrylic acid (PAA)-functionalized up-conversion phosphors (UCP's). Subsequent incubation with carbon nanoparticles results in quenching of the sensor through aptamer-bridged fluorescence resonance energy transfer (FRET). This sensor demonstrated a linear detection range of 0.5-20 nM and was even used to detect Thrombin concentrations of 0.25 nM within spiked human serum samples.

### Forensic Drug Analysis

Routinely employed methods for detecting trace quantities of illicit drugs include presumptive chemical tests, immunoassays and a wide selection of chromatographic techniques [351]. With a high sensitivity, selectivity and reliability, gas chromatography coupled with mass spectrometry (GC-MS) or liquid chromatography coupled with mass spectrometry (LC-MS) is currently considered the 'gold-standard' for the forensic analysis of bulk drug samples. However, such approaches are costly and may be considered inappropriate for high-throughput analysis due to extensive run times. Rapid, cheap and portable drug-screening assays based on aptasensor technology are therefore likely to be welcomed by the forensic community.

Much like the thrombin-binding sequence previously discussed, a cocaine-specific aptamer constructed by Stojanovic *et al.* [146] has also

been extensively used as a model ligand for proof-of-concept aptasensing assays. Demonstrated by Hilton *et al.*, a particularly sensitive example of such assays involved the target-induced displacement of Dabcyl quencher-attached complementary oligonucleotides from carboxyfluorescein (FAM) labelled aptamers immobilized within microfluidic channels. This assay was subsequently shown to enable the detection of cocaine at picomolar levels, without the need for sample cleanup and derivatization processes required for GC-MS analysis [352].

Beyond cocaine-based assays, initial explorations are also being made into the use of aptasensing platforms for the detection of amphetamine derivatives. Yarbakht and Nikkhah recently exploited the ability of single stranded aptamers to shield Au-NPs from salt-induced aggregation in order to allow the colorimetric signalling of MA and MDMA presence [353]. In this sensor (**Figure 51**), an aptamer able to bind both MA and MDMA is incubated with a given sample. If target molecules are contained within the sample, conformational changes in the aptamer take place as a result of binding. Such changes prevent the association of aptamer sequences with Au-NPs, which then aggregate upon salt addition, turning the colour of sample solutions from red to blue. If target molecules are absent from the sample, aptamers are instead able to interact freely with AuNPs, protecting them from aggregation.

In an alternative transduction approach, Huang *et al.* [354] were able to successfully develop an electrochemical biosensor based on Au-mesoporous silica nanoparticles (Au-MSN) after selecting a 37-mer aptamer sequence against the opiate alkaloid codeine. Here, thiolated codeine aptamers were conjugated to Au-MSN's immobilized on the surface of a glassy carbon electrode. Changes in electrical impedance at the electrode surface associated with aptamer-target binding were used to monitor codeine concentrations across a linear range of 10 pM to 100 nM. Furthermore, denaturation of the aptamer sequences by incubation with heated distilled water allowed the sensor to be reused for subsequent measurements.

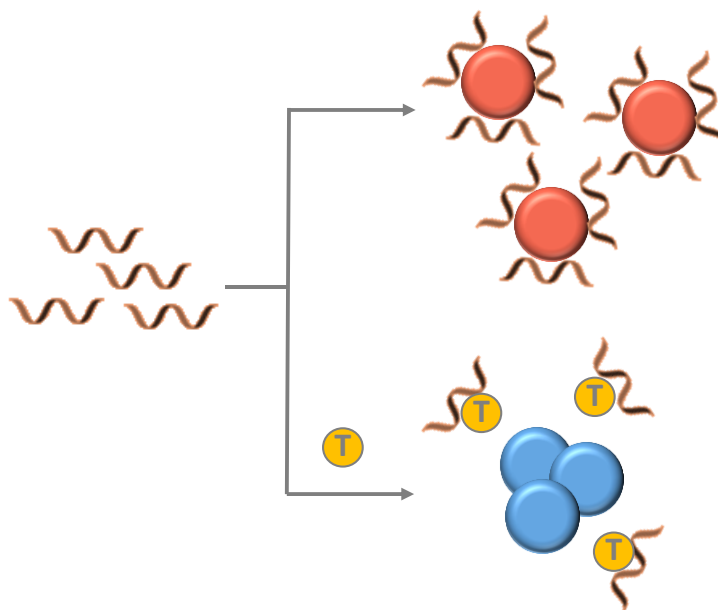


**Figure 51:** Schema of a colorimetric Au-NP aptasensor for the detection of methamphetamine developed by Yarbakht and Nikkhah [353]. In this assay, aptamers are initially adsorbed onto the surface of gold nanoparticles (au-NP's) through hydrophobic and electrostatic interactions to stabilize them within solution. However, in the presence of methamphetamine (MA) or 3,4-Methylenedioxymethamphetamine (MDMA), alterations in the structural conformation of the aptamers allow salt-induced aggregation of the particles to occur, prompting surface plasmon resonance-based colour changes. A purely visual detection of MA was found to occur at concentrations as low as 5 mM.

With relatively fast selection and isolation times compared to antibodies (i.e. a matter of weeks), nucleic acid aptamers also represent a great opportunity to rapidly develop forensic assays for the detection of new psychoactive substances (NPS). These substances (typically scheduled drugs slightly modified to circumvent legal restrictions) are emerging at an unprecedented rate, with over 450 new compounds identified by the EU early warning system since 2005 [355]. At present, the majority of NPS compounds are poorly or not detected by standard immunoassay tests, forcing analysts to rely on mass-spectrometry techniques [356]. Despite the excellent potential of aptasensor platforms as drug-screening assays, aptamers selected towards any NPS target have yet to be reported in the literature.

## Forensic Toxicology

The synthetic nature of SELEX protocols means that aptamer recognition moieties may be selected against toxic compounds that would likely kill animal hosts during standard *in vivo* antibody-generation methods [357]. Such moieties may be therefore of great benefit to toxicology practices, where determining cause of death is often dependent upon the detection and quantitation of hazardous substances. This branch of forensic chemistry heavily relies on the use of expensive and labour-intensive analytical techniques to confirm the identify of various poisons and toxins [358].

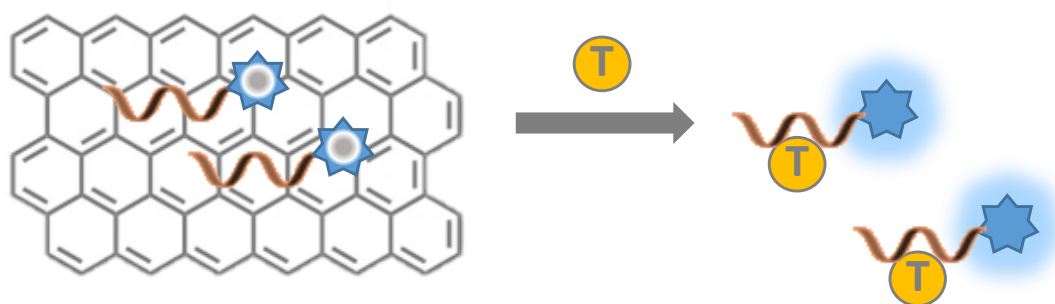


**Figure 52:** Schema of a graphene-quenching fluorescence aptasensor for the detection of ochratoxin A developed by Sheng et al. [359]. Here, aptamers are made initially fluorescent via 5' labelling with 6-carboxyfluorescein (6-FAM). Under normal conditions, these aptamers are readily adsorbed onto the basal plane of PVP-protected graphene oxide, which subsequently quenches 6-FAM emission by energy transfer. However, in the presence of ochratoxin A, antiparallel G-quadruplex formation prevents such adsorption and fluorescence signals are generated. Using this sensor, Sheng et al. were able to monitor ochratoxin A with high selectivity in a liner range from 50-500 nM.

Ochratoxin A (OTA) is a toxic metabolite secreted by *aspergillus* and *penicillium* fungi species that can exert severe nephrotoxic, immunotoxic, and carcinogenic effects [360]. As such toxins represent a threat to health through the contamination of commercialized food systems, significant efforts have been made towards the development of a simple and flexible sensing platform for the detection of OTA compounds [361]. In a strategy designed by Sheng et al. (**Figure 52**), this sensing was achieved by the

use of FAM-modified aptamers which, in the absence of OTA, are adsorbed onto a basal plane of graphene oxide and quenched [359]. However, in the presence of target molecules, aptamers are induced into particular three-dimensional conformations and resist adsorption, allowing fluorescence to be monitored.

In an extension of the Au-NP aggregation assay exploited by Yarbakht and Nikkhah for the detection of amphetamines, Wu *et al.* also utilised an aptamer-based sensor for the detection of arsenic within aqueous solutions [362]. In this method, a cationic surfactant Hexadecyltrimethylammonium bromide (CTAB) was employed instead of salts to stimulate nanoparticle aggregation, allowing the colorimetric detection of arsenic concentrations in the range of 1-500 parts per billion.

Work from Lamont *et al.* resulted in the selection of an aptamer (SSRA1) specific to the B-chain of ricin [363]. Ricin, a cytotoxic protein of biological origin, is considered as a potential threat agent for terrorist use because of its high toxicity and relative availability. The selected aptamer displayed superior detection capabilities compared to a commercially available ELISA kit for ricin. Following this study, attempts have been made in order to embed the SSRA1 aptamer into a biosensing platform for rapid and sensitive ricin detection. Esteban-Fernández de Ávila *et al.* reported a micromotor sensing strategy for the fluorescent detection of ricin [364]. Self-propelled reduced graphene-oxide (rGO)/platinum (Pt) micromotors were synthesized and were modified with the ricin-specific aptamer tagged with a fluorescent dye. The resulting complex is non-fluorescent due to the quenching effect of the graphene surface. In the presence of the target toxin, the aptamer is displaced from the graphene-oxide quenching motor surface and its fluorescence is restored. By this method, real-time detection of trace amounts of ricin toxin could be achieved in biological and environmental samples. Li *et al.* further developed a detection system for ricin based on isothermal strand-displacement polymerase reaction [365]. The ricin-specific aptamer SSRA1 was first hybridized with a single stranded DNA blocker and then immobilized on

the surface magnetic beads. When ricin binds to the aptamer, the blocker is released and then hybridizes with a dye-modified hairpin probe triggering an isothermal strand-displacement polymerase reaction. The fluorescent double stranded DNA product cannot be quenched as it does not interact with the graphene oxide surface, resulting in an increase of the fluorescence intensity.

Scientific efforts have been made in the forensic field towards the development of new methods for the detection of chemical weapon agents with emphasis been placed on the real-time, on-site analysis of nerve agents (e.g. sarin). Zhao *et al.* developed a cantilever-based aptasensor for dimethyl methylphosphonate (DMMP), a nerve agent simulant [366]. The piezoresistive cantilever sensor was designed with four cantilevers (two sensing and two reference cantilevers). A biotinylated anti-DMMP aptamer was immobilized on the surface of the sensing cantilevers. In the presence of DMMP, binding takes place between the immobilised aptamers and the target; this results in a surface stress and a bending of the sensing cantilevers which can be recorded and measured. The method resulted in sensitive (50 nM-1.0  $\mu$ M) and specific detection of DMMP in aqueous solutions.

## **Explosives**

The development of rapid, cost-effective and reliable assays for the detection of explosive molecules in both aqueous and gaseous samples is a high priority for forensic investigators, counter-terrorism agencies and global de-mining projects [367]. Ehrentreich-Förster *et al.* argue that aptamers are likely to make ideal recognition moieties for such assays, as immunological methods are often disadvantaged by the poor specificity of antibodies raised against low molecular weight explosive analytes [368]. Furthermore, aptamers are known to retain their activity in a number of organic solvents (such as methanol and acetonitrile) commonly used for the solubilisation and detection of explosive compounds.

To prove this concept the same group demonstrated the construction of an optical aptasensor towards the detection of 2,4,6-trinitrotoluene (TNT). In this sensing strategy, activated TNT derivatives are first immobilized on the surface of silanised optical fibres. TNT-specific aptamers mixed within sample solutions are then introduced into the flow cell and bind to the surface-bound analytes unless already captured by TNT present within the sample itself (**Figure 53**). Nanobeads covalently attached to these aptamer sequences are then used to report the amount of ligands bound to the fibre (with emission intensities inversely proportional to the concentration of TNT present in measured samples).

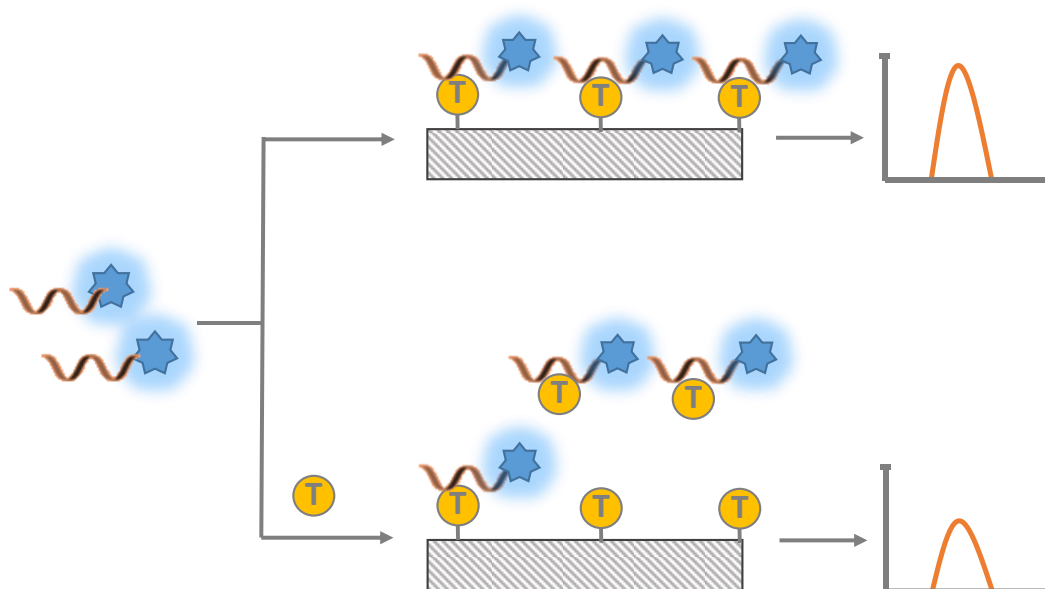


**Figure 53:** Schema of an optical fibre-based aptasensor for the detection of TNT developed by Ehrentreich-Förster et al. [368]. Silanised optical fibres functionalized with TNT competitors are first embedded within the surface of a flow cell. Under normal conditions, a sample solution containing fluorescently labelled aptamers is introduced into the cell, which subsequently bind to the competitive analogues. Excitation by a laser at 480 nm allows the detection of aptamer presence on the fibre. However, a reduction in signal occurs when free TNT molecules present within the sample solution capture available aptamers, preventing interaction with the surface-attached analogues.

Whilst aptasensing assays towards explosive targets other than TNT remain extremely limited, it is hoped that this review will encourage researchers in the field explosives research to consider their use for the



detection for compounds such as hexahydro-1,3,5-trinitro-1,3,5-triazine (RDX).

## Conclusion

Challenges associated with the immunological and instrumental analysis methods currently employed within both crime scene and laboratory-based testing procedures have resulted in the demand for new techniques able to allow the rapid, sensitive and specific detection of forensically relevant analytes. In this review, we have highlighted the potential of biosensing technology that incorporates aptamer recognition moieties to address this demand. Moreover, we have reported on a wide range of aptasensors that, although being successfully developed for use in other analytical disciplines, could be readily adapted to forensic analysis. Whilst research in the development of aptasensors for forensic purposes is extremely limited, it is hoped that recent technological advances (e.g. NGS) will make aptamer-based sensor development more accessible to researchers working within the field of forensic science.

### 5.3 Graphene Oxide Displacement Multiplex Sensor

The above review describes a number of aptasensors that have been produced for the detection of forensically-relevant targets based on the displacement of fluorescently-labelled aptamer sequences from various quenching materials. One particularly prominent example of such materials is GO nanosheets, monolayers of oxidized graphene arranged within a two-dimensional honeycomb lattice [369]. Such nanosheets possess several unique physical and optical properties which may make them ideal for use in fluorescent aptasensing assays for the forensic analysis of biological fluids.

In the presence of high ionic strength buffers, ssDNA is adsorbed to the surface of GO nanosheets as a result of  $\pi$ - $\pi$  stacking interactions between nucleotide bases and GO [370]. The strength of these non-covalent interactions is sufficiently high for ssDNA to be retained on the GO surface over long periods of time, yet weak enough for the rapid

desorption of sequences in response to target binding [370]. Furthermore, as this adsorption is not sequence-specific, multiple different ssDNA molecules may be bound to the surface of single nanosheets, with each liberated independently via interactions with a different type of target molecule.

GO is also noted for its broad fluorescence absorbance capabilities, with several recent studies demonstrating the concurrent quenching of multiple fluorophores emitting at vastly different wavelengths of visible spectrum upon GO adsorption [371, 372]. The exact mechanism behind this quenching is still debated, although reductions in fluorophore emission intensities have been shown to occur in a distance-dependent manner similar to FRET, albeit over a longer range [373].

This combination of non-specific ssDNA adsorption and universal quenching has already resulted in the application of GO nanosheets towards the construction of multiplex fluorescent aptasensing assays [374]. In these assays, several distinct aptamer sequences (each raised against a separate target and labelled with a different fluorophore) are first quenched via adsorption to a graphene monolayer. Displacement of each sequence occurs as a result of higher affinity interaction with corresponding target molecules, relieving quenching effects and allowing the observation of emissions at specific wavelengths (depending on the type of analyte present).

Sensors based on this signal transduction method are therefore likely to possess great potential for use as multiplex biological fluid testing reagents, allowing the simultaneous detection and identification of multiple fluid biomarkers through the production of specific emission wavelengths. Attempts were therefore made in the construction of a displacement-based GO aptasensor, utilising fluorescently-labelled aptamer sequences towards  $\alpha$ -thrombin, PSA and lysozyme for the analysis of blood, semen and saliva respectively (**Figure 54**).

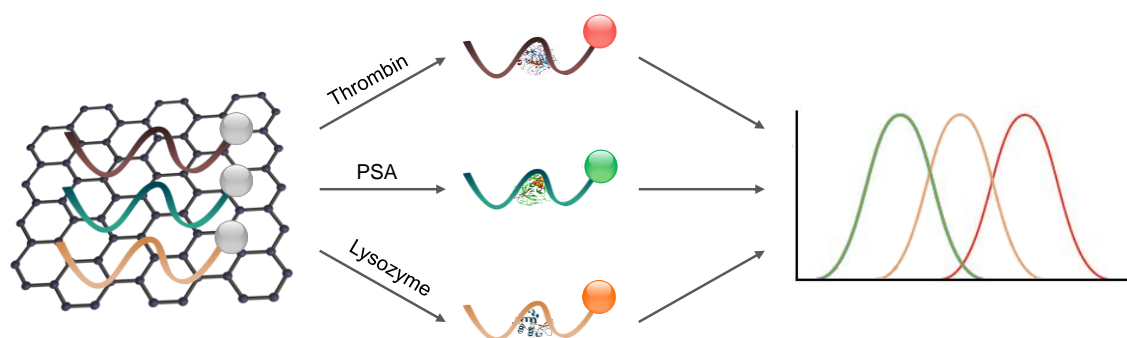


**Figure 54:** GO multiplex displacement aptasensor design. The emission of fluorescently-labelled aptamers is first quenched through adsorption to GO nanosheets. Sequences specific to  $\alpha$ -thrombin, PSA and lysozyme are displaced individually upon interaction with corresponding targets. Emission signals are produced at particular wavelengths to determine which analytes are present within a sample, providing an indication of body fluid identity.

## 5.3.1 Materials and Methods

### 5.3.1.1 Reagents

All fluorescently-labelled ssDNA aptamer sequences (**Table 11**) were purchased from Sigma-Aldrich (Dorset, UK) and reconstituted in SDW to an initial stock concentration of 100  $\mu$ M. GO (4 mg/ml in H<sub>2</sub>O), human  $\alpha$ -thrombin and lysozyme were also obtained from Sigma-Aldrich, whilst PSA was purchased from 2B Scientific (Oxfordshire, UK).

**Table 11:** Fluorescent ssDNAs used to construct a GO displacement aptasensor.

Target	Label	Sequence (5'-3')	Ref.
Thrombin	Cy5	GGTTGGTGTGGTTGG	[375]
PSA	6-FAM	ATTAAAGCTCGCCATCAAATA	[376]
Lysozyme	ROX	ATCTACGAATTCATCAGGGCTAAAGAGTGCAGAGTTACTTAG	[377]

### 5.3.1.2 Body Fluid Collection and Storage

Blood, semen and saliva was obtained upon informed consent from the same healthy donor. Blood samples were drawn by venipuncture and stored in a BD Vacutainer® Plus tube (Oxford, UK) containing 3.2% sodium citrate coagulation preservative. All samples were stored at 4 °C until the point of analysis. Ethical clearance for the collection and use of body fluids for this specific study was granted by the King's College London Biomedical Sciences, Dentistry, Medicine and Natural &

Mathematical Sciences Research Ethics Subcommittee (reference number HR-17/18-5057).

#### **5.3.1.3 GO Quenching**

Investigations into the ability of GO to quench each fluorescently-labelled aptamer were conducted in a similar manner to that reported by Liu *et al.* [378]. GO was first diluted in SDW to a concentration of 1 mg/ml and sonicated for 5 hrs at room temperature to disperse nanosheets in solution, before undergoing centrifugation at 12,000 RPM for 10 min to precipitate un-dispersed graphene powder. The resulting supernatant was then collected for further experimental use.

Measurements of the fluorescence emission spectra of aptamer solutions (1ml), diluted to a working concentration of 50 nM in 50 mM Tris-HCl, 100 mM NaCl, pH 7.4, were made using a Perkin Elmer LS-50B Luminescence Spectrophotometer (Massachusetts, USA), with excitation wavelengths of  $640\pm 7$ ,  $483\pm 7$  and  $575\pm 7$  nm for the measurement of Cy5, 6-FAM and ROX fluorophores respectively. A 20  $\mu$ l volume of previously collected GO dispersion was then incubated with each aptamer solution for 1 hr, followed by a re-measurement of all fluorescence spectra.

#### **5.3.1.4 Buffer Optimisation**

Aliquots (200  $\mu$ l) of each aptamer solution were prepared to a concentration of 50 nM using previously utilised buffer (50 mM Tris-HCl, 100 mM NaCl, pH 7.4) also containing varying concentrations of  $MgCl_2$  (0, 0.1, 1, 5 and 10 mM). All samples were prepared in triplicate. Fluorescence emission intensities of each solution were subsequently measured on a CytoFlour® 4000 spectrophotometer (Applied Biosystems®, California, USA) with Ex/Em  $590\pm 20/645\pm 50$ ,  $485\pm 20/540\pm 30$  and  $560\pm 20/620\pm 40$  nm wavelength filters for the measurement of Cy5, 6-FAM and ROX fluorophores respectively. A 5  $\mu$ l volume of GO at a concentration of 1 mg/ml (prepared using the methods previously described) was then incubated with each sample for 1 hr, whereupon all spectra were re-measured.

### 5.3.1.5 Quencher Optimisation

To determine the optimal concentration of GO required to quench the emission of fluorescently-labelled sequences, a 50 nM working solution of each aptamer was prepared in 50 mM Tris-HCl, 100 mM NaCl, 5 mM MgCl<sub>2</sub> pH 7.4 to a final volume of 200 µl. A 5 µl volume of various concentrations of GO (0, 0.01, 0.025, 0.05, 0.1, 0.25, 0.5, 1, 2, 4 mg/ml), prepared using the methods previously described, was then incubated with each aptamer solution for 1 hr and room temperature. All samples were prepared in triplicate. The emission intensities of aptamer-GO solutions were then recorded in the same manner as buffer optimisation studies.

### 5.3.1.6 Purified Protein and Whole Fluid Spectrofluorometry

Individual displacement aptasensors towards the detection of thrombin, PSA and lysozyme were prepared through the incubation of 10 ml of each respective aptamer solution (100 nM in 50 mM Tris-HCl, 100 mM NaCl, 5 mM MgCl<sub>2</sub> pH 7.4) with 500 µl volumes of GO at a concentration of 0.25 mg/ml prepared using the method previously described ([Section 5.3.1.3](#)) for 1 hr at room temperature.

**Table 12:** Protein concentrations and fluid dilutions used for single aptasensor testing.

Aptamer Target	Protein Concentrations	Whole Fluid Dilutions
Thrombin	0, 0.05, 0.1, 0.25, 0.5, 1, 2.5, 5 (µg/ml)	1:1, 1:2, 1:4, 1:8, 1:16, 1:32, 1:64
PSA	0, 1, 2.5, 5, 10, 25, 50, 100 (µg/ml)	1:1, 1:2, 1:4, 1:8, 1:16, 1:32, 1:64
Lysozyme	0, 0.25, 0.5, 1, 2.5, 5, 10, 25 (mg/ml)	1:1, 1:2, 1:4, 1:8, 1:16, 1:32, 1:64

Aliquots of quenched sensor solutions (100 µl) were then incubated for a further 1 hr with various concentrations of corresponding purified protein (thrombin, PSA and lysozyme) or whole body fluids (plasma/blood, semen and saliva), diluted in SDW to 100 µl volumes. A list of protein concentrations and fluid dilutions used during testing is provided in [Table 12](#). All samples were prepared in triplicate. Emission intensities were then recorded in the same manner as previous buffer and quencher optimisation studies.

### **5.3.1.7 Multiplex Spectrofluorometry**

Construction of a final multiplex aptasensor complex was achieved through the combined incubation of 1 ml of all fluorescently-labelled ssDNA sequences (100 nM in 50 mM Tris-HCl, 100 mM NaCl, 5 mM MgCl<sub>2</sub> pH 7.4) with 150 µl of GO at a concentration of 0.5 mg/ml (prepared using the method previously described) for 1 hr at room temperature. Aliquots of this solution (100 µl) were then incubated with each purified protein and whole body fluid target previously tested (at concentrations or dilutions that provided the largest fluorescence response during individual sensor testing), as well as bovine serum albumin (BSA) at a concentration of 25 mg/ml and SDW. All samples were prepared in triplicate. Emission intensities were then recorded in the same manner as previous buffer and quencher optimisation studies.

## **5.3.2 Results and Discussion**

### **5.3.2.1 GO Quenching**

Multiplex displacement assay design was based on the premise of combining three separate aptamer sequences previously used for the analysis of thrombin [379], PSA [348] and lysozyme [378], in a single aptasensor construct. As these protein targets are present in relatively high concentrations within blood, semen and saliva respectively, this aptasensor may potentially be used as a method for the detection of multiple body fluid types simultaneously. Furthermore, if each of these aptamer sequences is labelled with a different fluorophore, the production of emissions at wavelengths specific for each target may be used to provide an indication of the identity of fluids present within a sample.

Studies have demonstrated that the adsorption of fluorescently-labelled ssDNA to the surface of GO nanosheets (as well as any associated emission quenching) is highly dependent upon both the length of the nucleotide sequence [380] and the position/type of fluorophores employed [371]. As these properties differ between each of the sequences used for sensor construction, a preliminary investigation of the

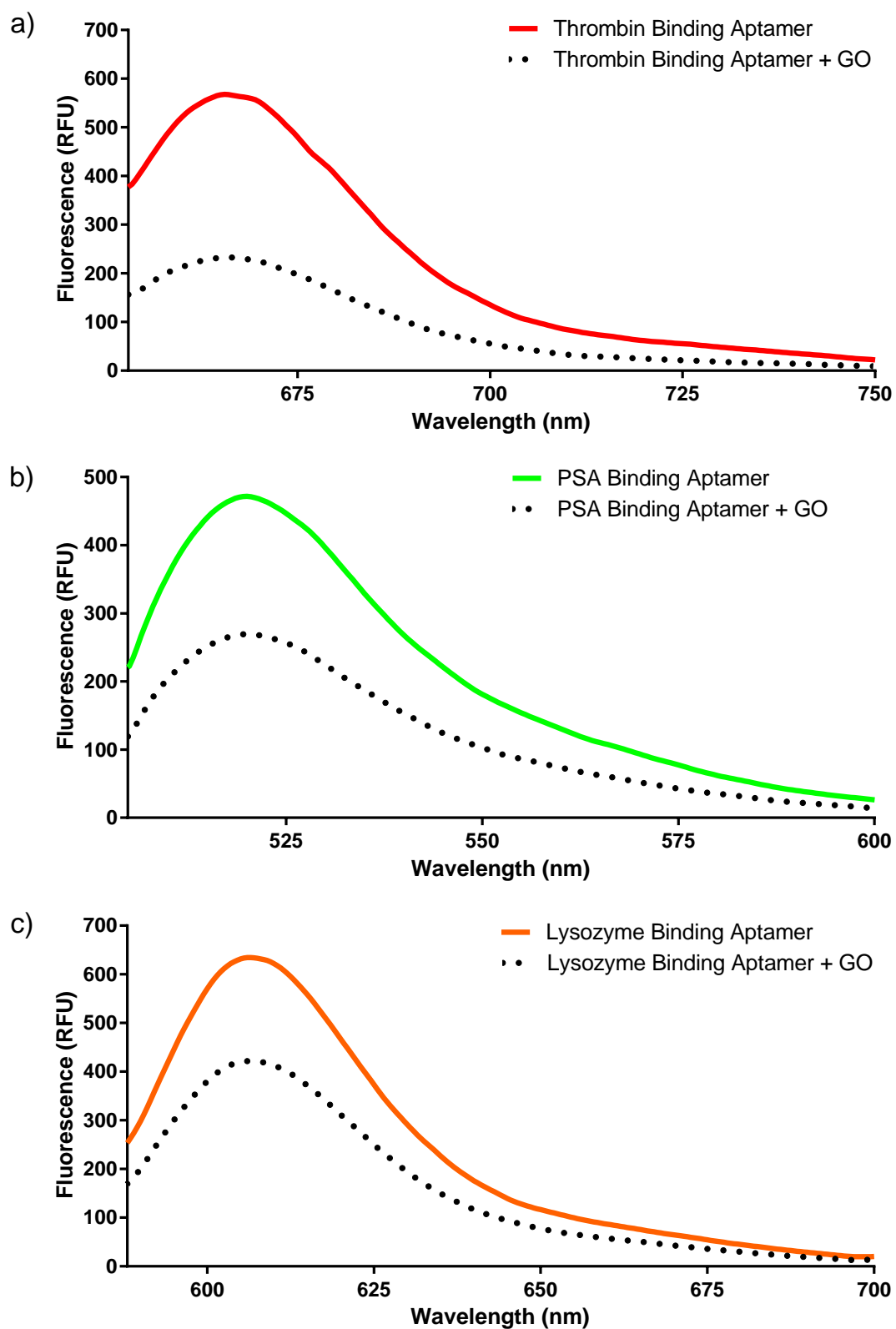


**Figure 55:** Fluorescence emissions of Cy5, 6-FAM and ROX-labeled aptamers specific to a) thrombin, b) PSA and c) lysozyme respectively, before (solid lines) and after (dotted lines) the addition of GO.

relative degree of quenching experienced by each aptamer upon graphene interaction was conducted. This was achieved through the incubation of 50 nM ssDNAs with a standardised concentration (1 mg/ml) of GO.

Different levels of quenching were observed for each of the fluorescently-labelled aptamers upon GO addition, with reductions in emission maxima intensities of 59.9%, 42.6% and 33.7% for thrombin, PSA and lysozyme aptamers respectively (**Figure 55**). Increased levels of emission quenching were found to correlate with a reduction in overall sequence length, which is consistent with results reported in a number of recent studies [371, 380, 381]. This length-dependent quenching phenomenon has been previously attributed to the structure of GO nanosheets, which contain intact crystalline regions that augment ssDNA binding, as well as amorphous areas of anionic functionalization [382]. DNA sequences of significant size are more likely to interact with the latter of these areas, limiting adsorption as a result of electrostatic repulsion [380].

#### **5.3.2.2 Buffer Optimisation**

It should be noted that during the initial investigation of GO-ssDNA interactions, none of the fluorescently-labelled aptamers tested were able to be completely quenched upon graphene addition. As background reagent fluorescence is likely to prevent the application of this biosensor towards the visualisation of body fluid staining *in situ*, attempts were made to increase aptamer emission quenching by enhancing the initial adsorption of ssDNA to GO.

One factor previously established as having a high influence on the interactions between DNA and graphene is the ionic strength of surrounding buffer solutions [383]. High concentrations of mono or divalent salts are often required to screen the long-range electrostatic repulsion effects of GO, in order to bring nucleotide sequences close enough to the nanosheet surface for  $\pi$ - $\pi$  stacking to occur [380]. As



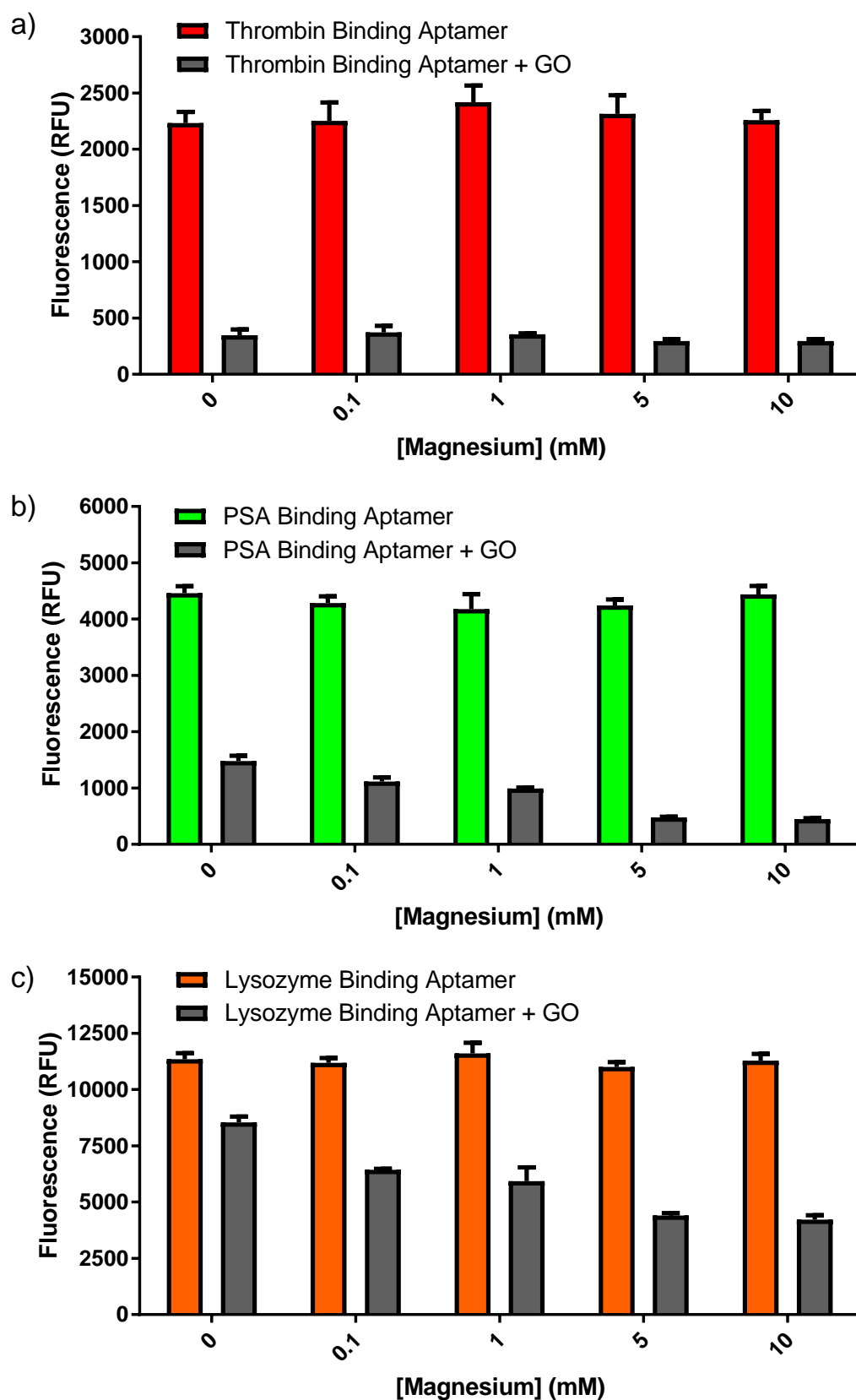


**Figure 56:** Fluorescence emissions of a) thrombin, b) PSA and c) lysozyme aptamers before and after GO addition in the presence of varying concentrations of  $MgCl_2$ . Data represents the mean  $\pm$  SD, samples performed in triplicate.

previous optimization studies have demonstrated that the quenching of fluorescently-labelled aptamers by GO can be significantly enhanced in response to increasing salt concentrations (such as NaCl and MgCl<sub>2</sub>) [380, 383, 384], each of the ssDNA sequences employed in aptasensor construction were incubated with GO in the presence of variable amounts of MgCl<sub>2</sub>.

For all aptamer sequences, a general reduction in fluorescence emission signals was observed with increased MgCl<sub>2</sub>, up until a concentration of 5 mM, beyond which, changes in fluorescence intensity were negligible (**Figure 56**). A one-way analysis of variance (ANOVA) followed by a Dunnett post hoc test, was used to statistically assess the effects of added MgCl<sub>2</sub> concentrations on the quenching of all aptamer sequences compared to negative 0 mg/ml MgCl<sub>2</sub> controls. For both PSA and lysozyme aptasensor complexes, all added magnesium concentrations were found to have a statistically significant effect on signal quenching (p values <0.0001). However, this was not the case for thrombin aptamer samples, where emission intensities were found to be comparable to a magnesium-free negative control. These results may be attributed to the fact that aptasensor complexes employing thrombin-specific ssDNA sequences already exhibited a high degree of quenching compared to PSA and lysozyme aptamers prior to MgCl<sub>2</sub> addition (possibly as a result of reduced sequence length). Therefore, all assay buffers were supplemented with 5 mM MgCl<sub>2</sub> for all further experiments (even in the case of thrombin aptasensors for the sake of testing consistency).

### **5.3.2.3 Quencher Optimisation**

With different degrees of quenching observed across all ssDNA sequences, even after adjustments to buffer ionic strength, it was envisaged that incubation with increased concentrations of GO may be required for each aptamer to undergo further fluorescence reduction. Therefore, varying amounts of GO, ranging from 0.01 to 4 mg/ml, were added to each ssDNA sequence in order to establish the optimal ratios of

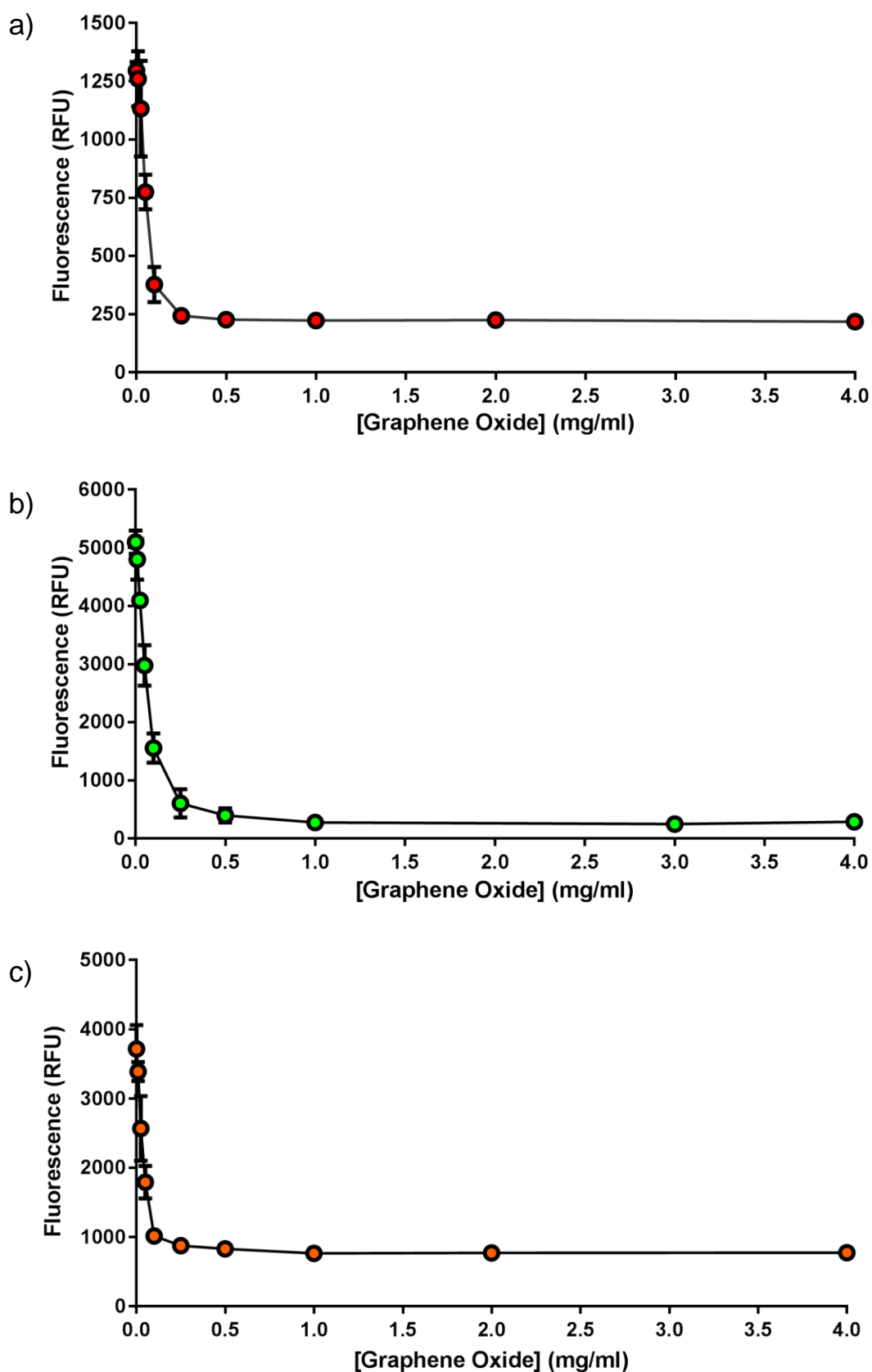


**Figure 57:** Fluorescence emission intensities of a) thrombin, b) PSA and c) lysozyme aptamers after incubation with varying concentrations of GO. Data represents the mean  $\pm$  SD, samples performed in triplicate.

GO:aptamer needed for highest emission quenching. All three aptamer sequences displayed similar patterns of fluorescence intensity reduction in response to increased graphene, all reaching maximum quenching limits upon addition of 0.25 mg/ml GO (**Figure 57**). At this concentration, mean quenching values of 81.2%, 88.1% and 76.4% were shown for thrombin, PSA and lysozyme aptamers respectively. Surprisingly, none of the sequences were able to be fully quenched, even at GO concentrations of 4 mg/ml. Therefore, a ratio of 1.25  $\mu$ g GO (5  $\mu$ l of 0.25 mg/ml) to 10 pmol of ssDNA was used for all further studies.

#### **5.3.2.4 Purified Protein and Whole Fluid Spectrofluorometry**

Before construction of a final multiplex aptasensor, investigations were made into the ability of each ssDNA to be desorbed from the surface of GO in response to target interaction under the assay conditions previously optimised. This involved the initial incubation of 100  $\mu$ l of each aptamer (at concentrations doubled from previous experiments in order to keep the total amount of ssDNA consistent) with 5  $\mu$ l of 0.25 mg/ml GO, before the addition of different concentrations of relevant purified protein targets. Emission changes of thrombin, PSA and lysozyme GO-aptasensor constructs in response to different dilutions of whole blood/plasma, semen and saliva respectively, were also observed.

In the case of purified targets, all GO-aptamers complexes demonstrated distinct increases in emission intensity upon protein incubation (**Figure 58**). Furthermore, these increases were found to correlate with the concentration of analyte added, indicating that fluorescence is restored as a direct result of target interaction. It must be noted that such emission intensities were found to be significantly lower than those exhibited by aptamer sequences prior to GO addition (as seen within previous experiments), suggesting that not all aptamer sequences were able to be desorbed from the graphene surface. Whilst the protein concentration ranges used within this study were limited by the cost and availability of analytes, higher amounts of these targets may be able to liberate a

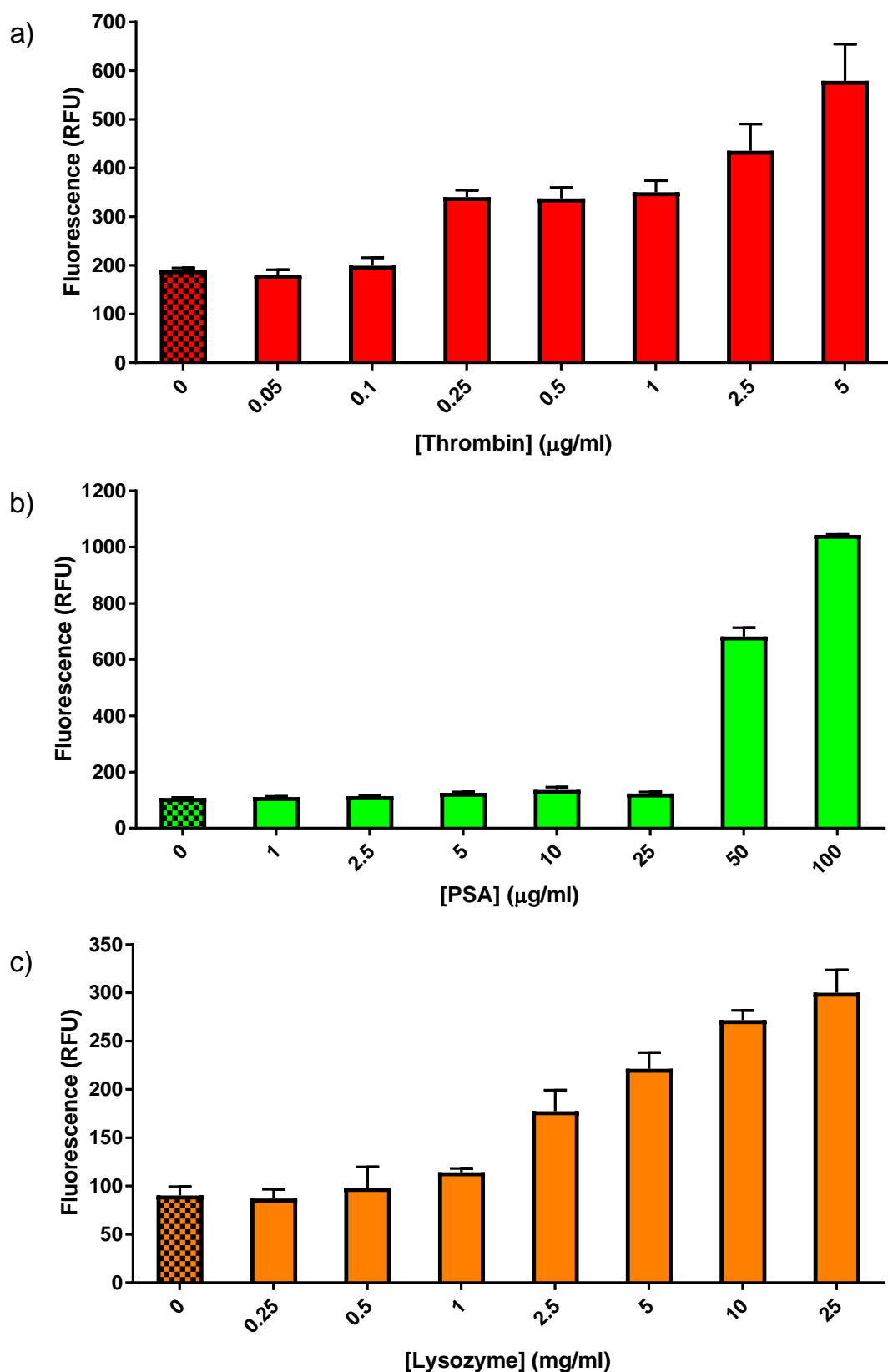


**Figure 58:** Emission intensities of a) thrombin, b) PSA and c) lysozyme GO-aptamer complexes after incubation with varying concentrations of relevant purified protein targets. Data represents the mean  $\pm$  SD, samples performed in triplicate. Negative SDW control = 0 mg/ml.

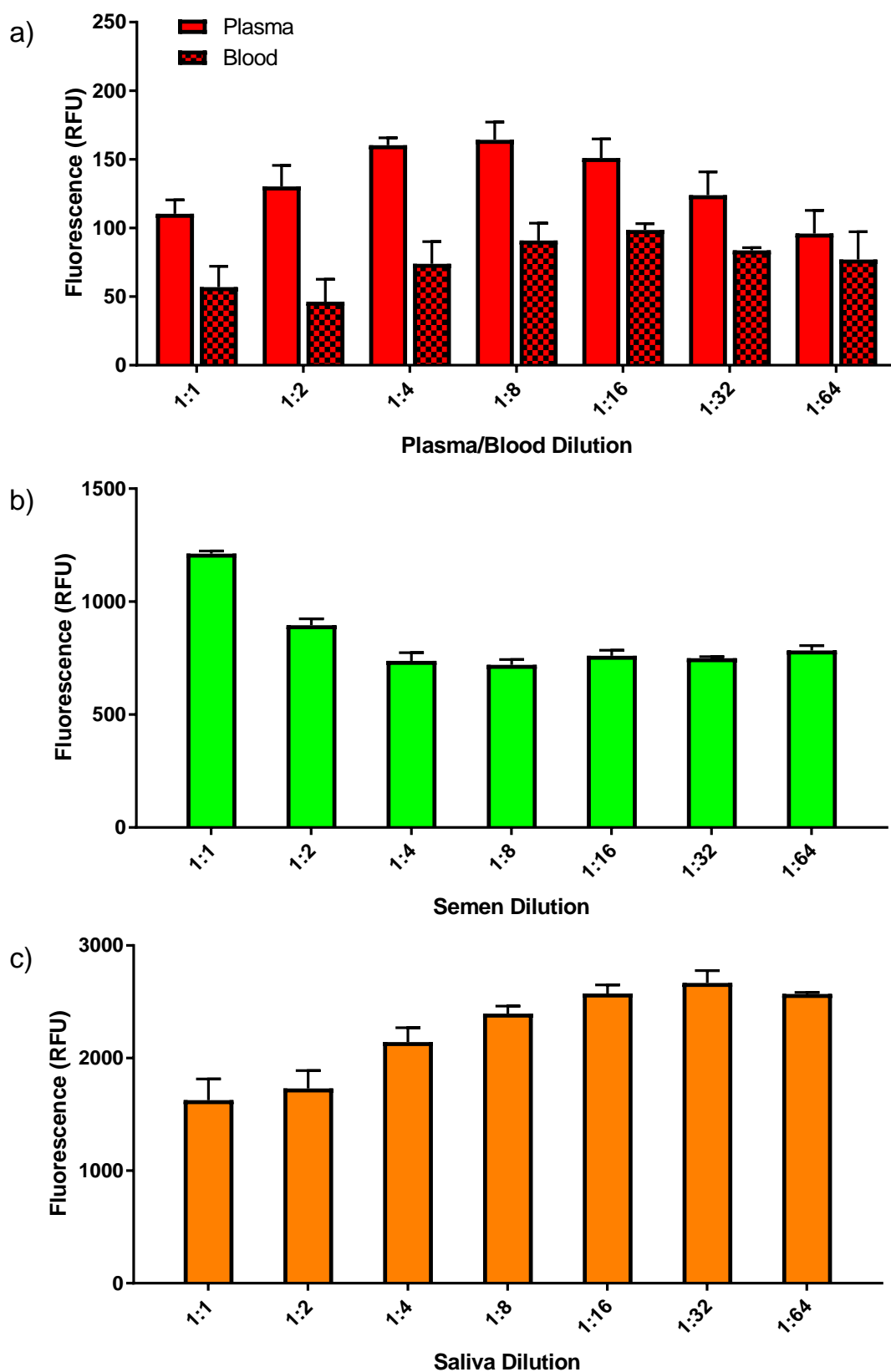


**Figure 59:** Emission intensities of a) thrombin, b) PSA and c) lysozyme GO-aptamer complexes after incubation with varying concentrations of relevant whole fluid targets. Data represents the mean  $\pm$  SD, samples performed in triplicate.

higher number of ssDNA sequences from the GO surface, resulting in increased fluorescence restoration.

Increases in emission signals were also observed from all aptasensor complexes upon the addition of respective fluids. However, the particular patterns of signal exhibited in response to different fluid dilutions were found to vary significantly between each ssDNA sequence (**Figure 59**). Emissions from aptamers specific to PSA were found to be relatively consistent with those gained during purified protein testing, with general decreases in intensity observed as a result of greater fluid dilution.

Conversely, emission patterns for both thrombin and lysozyme-specific aptamers were found to be more complex, with fluorescence intensities first increasing with higher fluid dilutions up to a specific value (1:8, 1:16 and 1:32 for plasma, blood and saliva respectively), after which point signals began to reduce. Such effects may potentially be attributed to the absorption of emissions by other biomolecular components found within the fluid matrices. As fluids are progressively diluted, these components become less concentrated, resulting in lower levels of signal absorbance and greater detectable fluorescence. Further dilution subsequently decreases the amount of target available to desorb ssDNA sequences from the GO surface, thereby reducing aptasensor transduction. Lower emission signals exhibited by thrombin-specific aptamers towards whole blood in comparison to plasma samples (which are likely to contain less highly-absorbing haemoglobin) seem to support this theory.

One other interesting phenomenon encountered during whole fluid aptasensor testing was the large increases in fluorescence intensity displayed by lysozyme-specific aptamer-GO constructs upon whole saliva addition. Such increases were found to be significantly larger than those observed during sensor incubation with protein samples, despite the fact that lysozyme has been shown to be present in human saliva at concentrations between 0.5-4 ng/ml, amounts much lower than those used within previous purified target assay tests. From these results, it

may be inferred that aptamers are potentially being non-specifically desorbed from the GO surface, although the mechanisms behind this effect remain unclear.

#### **5.3.2.5 Multiplex Spectrofluorometry**

Attempts were undertaken to construct a multiplex aptasensing complex for the simultaneous detection of different protein/fluid targets via the incubation of all fluorescently-labelled ssDNA sequences with a previously optimized ratio of GO. Concentrations of purified protein targets (5 µg/ml thrombin, 100 µg/ml PSA and 25 mg/ml lysozyme) or dilutions of fluids (1:8 plasma, 1:16 blood, 1:1 semen and 1:32 saliva) generating the largest fluorescence response during previous single aptamer experiments were then incubated with aliquoted aptasensor constructs. Fluorescence responses were subsequently monitored at the Cy5, 6-FAM and ROX emission wavelengths previously utilised for sensor optimisation studies.

Disappointingly, increases in sensor fluorescence were observed in response to incubation with the majority of both protein and body fluid targets at all measured wavelengths (**Figure 60**). The relative intensities of emissions signals produced for each target were also found to be consistent between Cy5, 6-FAM and ROX wavelengths. Such results are likely to indicate that the non-specific desorption of ssDNA from the GO surface in the presence of general protein molecules is the primary mechanism behind fluorescence restoration, rather than competitive displacement of sequences via higher-affinity target interaction. This hypothesis is supported by the fact that BSA, a target for which all of the aptamers utilised in sensor construction have already been shown to have little affinity towards [385-387], was also able to induce sensor fluorescence at 6-FAM and ROX emissions. In fact, such non-specific desorption effects have already been reported by some research groups in similar aptamer displacement constructs [388, 389].



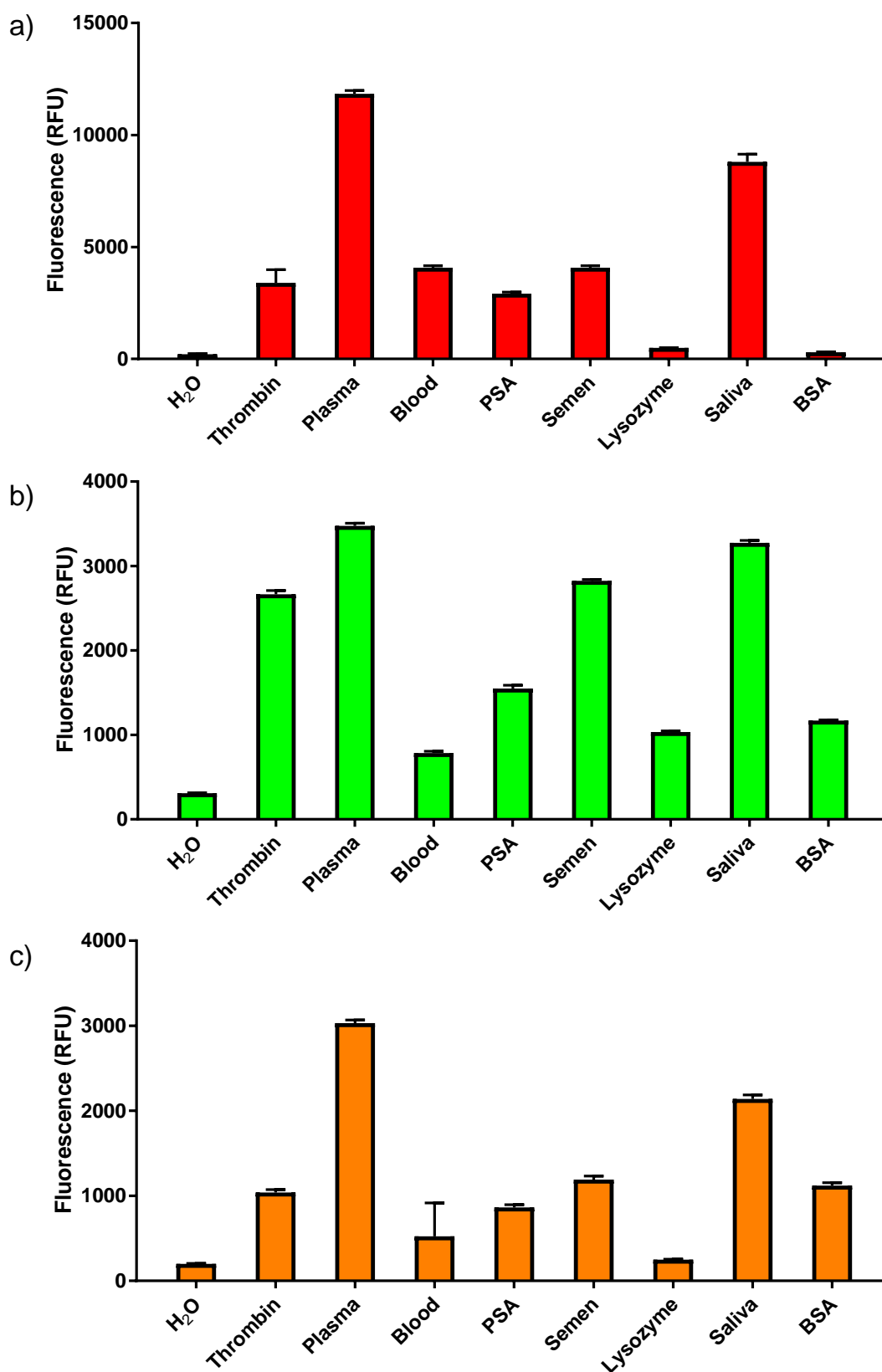


**Figure 60:** Fluorescence intensities of multiplex GO-aptasensors at a) Cy5 (thrombin), b) 6-FAM (PSA) and c) ROX (lysozyme) emission wavelengths after incubation with a various protein targets and body fluids. Data represents mean  $\pm$  SD, samples performed in triplicate.

### 5.3.3 Conclusion

Despite initial promise in the development and optimisation of single aptamer-GO complexes, testing of final multiplex displacement sensor constructs revealed the non-specific nature of protein detection. This lack of selectivity currently prevents the use of this biosensor for the attribution of biological fluid identity based on the production of light at specific wavelengths, as all ssDNA sequences are likely to be desorbed in the presence of each fluid type.

It may be argued that such sensors may still have potential application towards the detection of biological evidence sources in general (either as single or multi-aptamer assays) without providing an indication of cellular origin. However, such assays are unlikely to offer significant advantages over currently utilised forensic body fluid testing strategies.

Efforts to improve aptasensor specificity should therefore be undertaken in order to ensure that ssDNA sequences are only displaced from the surface of GO as a result of binding to intra-fluidic targets. Such improvements are likely to focus on adjustments the sequence or structure of employed aptamer moieties.

### 5.4 Aptamer Selection against Human Sperm Cells

Any new method developed for the analysis of forensic evidence, must be shown to possess a high level of specificity before it can be deployed within operational casework. With demonstrated increases in fluorescent signal upon the addition of non-target proteins, application of the developed displacement-based aptasensor ([Section 5.3](#)) towards the detection of body fluid samples (either as a single or multiplex assay) in operational forensic casework currently remains impractical.

As previously mentioned, several authors have already noted similar restorations of aptasensor fluorescence emission after incubation with proteins other than the target analyte [388, 389]. Recent attempts have also been made to increase the general specificity of such biosensing

methods. These include the use of various blocking agents to prevent non-specific absorption of molecules to the nanosheet surface [388], as well as the hybridization of aptamers to complementary ssDNA sequences immobilised on the quenching material, which are then displaced via target interaction [390]. However, the latter of these may defeat the purpose of using such materials as moderately bound quenchers.

It has been noted that aptamers raised towards single purified protein targets are typically less specific when placed in a biological environment, which is dissimilar from the controlled conditions utilised for selection [391]. Conversely, sequences specific to whole cells (which are mainly raised in conditions best mimicking the physiological environment of a target) are more likely to retain binding selectivity during biological applications [391]. It was therefore theorised that cell-specific aptamer sequences would be less likely to be non-specifically displaced from the surface of GO nanosheets as a result of general protein interaction.

Efforts were therefore made towards the selection of ssDNA aptamers against intra-fluidic cells that may be used for the purposes of body fluid attribution. Initial attempts focused on the elucidation of sequences specific to human sperm cells, the microscopic identification of which is often used for confirming the presence of seminal fluid in forensic casework. This was achieved via a modified version of a popular Cell-SELEX protocol reported by Sefah *et al.* [289].

## **5.4.1 Materials and Methods**

### **5.4.1.1 Reagents**

For sperm cell isolation, Percoll® was obtained from Sigma-Aldrich (Dorset, UK). Human tubal fluid (HTF) was prepared as a ×10 concentrate through the addition of 29.655 g NaCl, 1.75 g KCl, 250 mg MgSO<sub>4</sub>·7H<sub>2</sub>O, 250 mg KH<sub>2</sub>PO<sub>4</sub>, 2.5 g glucose, 2.6 g HEPES, 1 g NaHCO<sub>3</sub>, 1.5 g CaCl<sub>2</sub>·2H<sub>2</sub>O and 3 g human serum albumin (HSA) to 350

ml SDW. This solution was then adjusted to pH 7.4 and made up to a total volume of 500 ml using SDW. Dilution of this concentrate in SDW was used to prepare all  $\times 1$  HTF solutions.

For cell incubation and elution, an ssDNA library comprised of two fixed regions, each 18 nucleotides in length, flanking randomised N40 bases (5'-ATCCAGAGTGACGCAGCA-N40-TGGACACGGTGGCTTAGT-3') was obtained (HPLC purified) from Integrated DNA technologies (Iowa, USA). Aptamer binding buffer was prepared through the addition of 2.25 g glucose, 500 mg BSA and 238 mg  $\text{MgCl}_2$  to 500 ml of  $\times 1$  phosphate-buffered saline (PBS).

All PCR reaction components, including  $\times 10$  PCR buffer, 50 mM  $\text{MgCl}_2$  solution, 10 mM dNTP mixture and Platinum™ Taq DNA polymerase were obtained from Thermo Fisher Scientific (California, USA). Fluorescently-labelled forward (5'-6-FAM-ATCCAGAGTGACGCAGCA-3') and biotin-functionalised reverse (5'-biotin-ACTAAGCCACCGTGTCCA-3') primers were both obtained (HPLC purified) from Integrated DNA technologies (Iowa, USA). Non-labelled versions of both forward and reverse sequences were also procured.

Agarose was obtained from Sigma-Aldrich (Dorset, UK). Tris-Acetate-EDTA (TAE) buffer ( $\times 50$ ) and GelRed nucleic acid gel stain ( $\times 10,000$  in  $\text{H}_2\text{O}$ ) were both purchased from Cambridge Bioscience (Cambridge, UK), whilst HyperLadder™ 25bp (also containing  $\times 6$  loading dye) was obtained from Bioline (Toronto, Canada).

For the separation of double stranded DNA (dsDNA), Pierce™ NeutrAvidin™ agarose resin was purchased from Thermo Fisher Scientific (California, USA). Corning® Costar® Spin-X® and Amicon™ Ultra-0.5 ml (3 kDa MWCO) filter units were both obtained from Sigma-Aldrich (Dorset, UK).

All DNA sequencing reagents, including the NEBNext® Ultra™ DNA Library Prep Kit for Illumina®, NEBNext® Multiplex Oligos for Illumina®

(both New England Biolabs, Massachusetts, USA) and Agencourt AMPure® XP Beads (Beckman Coulter, California, USA), were provided by Dr David Ballard from DNA Analysis at King's, King's College London.

#### **5.4.1.2 Body Fluid Collection and Storage**

Seminal fluid was obtained upon informed consent from the same healthy donor and stored at 4 °C until the point of analysis. Ethical clearance for the collection and use of body fluids for this specific study was granted by the King's College London Biomedical Sciences, Dentistry, Medicine and Natural & Mathematical Sciences Research Ethics Subcommittee (reference number HR-17/18-5057).

#### **5.4.1.3 Cell Isolation**

Isolation of sperm cells from whole seminal fluid was performed using density gradient centrifugation methods outlined by the World Health Organization [392]. First, an isotonic gradient was prepared through the addition of 9 ml of Percoll® to 1 ml of  $\times 10$  HTF. This gradient was separated into two fractions which were then diluted in  $\times 1$  HTF to form 80% and 40% (v/v) Percoll® suspensions. A 2ml volume of the 40% suspension was then layered over the top of 2ml of the 80% suspension in a 15 ml tube to create a discontinuous density gradient. Seminal fluid (1ml) was then added to the top of the gradient and centrifuged for 20 min at 1600 RPM. The ensuing supernatant was removed from the pelleted cells, which were then re-suspended and washed twice with 5 ml of  $\times 1$  HTF. Final pelleted sperm cells were lastly re-suspended in 2 ml of SDW.

Cell concentrations were calculated using a Countess II automated cell counter (Thermo Fisher Scientific, California, USA) after mixing 10  $\mu$ l of suspended cells with 10  $\mu$ l of trypan blue solution.

#### **5.4.1.4 Incubation and Elution**

For the first round of the Cell-SELEX process, 100  $\mu$ l of 100  $\mu$ M (10 nmol) N40 ssDNA library was added to 270  $\mu$ l of aptamer binding buffer, heated to 95 °C for 5 min and allowed to cool to room temperature. During this

period, a volume of sperm cell suspension yielding a total of  $1 \times 10^7$  cells was transferred into a 15 ml tube and centrifuged at 6700 RPM for 3 min. The resulting supernatant was then removed before the re-suspension of pelleted cells in 330  $\mu$ l of aptamer binding buffer. These cells were then added to the 370  $\mu$ l of cooled ssDNA library previously prepared and incubated for 1 hr at 4 °C on a rotary shaker.

After incubation, this mixture was centrifuged at 6700 RPM for 3 min in order to pellet cells and bound ssDNA sequences. The resulting supernatant (comprised of remaining unbound sequences) was removed before cells were re-suspended and washed ( $\times 3$ ) with 1 ml of aptamer binding buffer. Bound ssDNA sequences were then eluted from cells through the addition of 500  $\mu$ l DNase-free SDW with heating at 95 °C for 10 min. A final centrifugation step at 13,100 RPM for 10 min was then used to pellet cells so that eluted sequences could be collected in the ensuing supernatant.

In all subsequent selection rounds (2-14), incubation was achieved through the addition of 200  $\mu$ l ssDNA, diluted to a concentration of 1  $\mu$ M in aptamer binding buffer, to cells also suspended in 200  $\mu$ l of binding buffer. The total number of cells used for incubation was reduced by one million each cycle between SELEX rounds 2-5 (from  $5 \times 10^6$  to  $1 \times 10^6$  cells), in order to increase the stringency of the selection process [289]. A total of  $1 \times 10^6$  cells were used in all further incubations (from rounds 6-14). Elution of sequences from cells in rounds 2 to 14 was also conducted using 600  $\mu$ l of binding buffer, rather than 500  $\mu$ l of SDW.

#### **5.4.1.5 PCR Amplification**

In total, three different types of PCR amplification were performed throughout the SELEX process: 1) pre-PCR, 2) trial PCR and 3) preparative PCR. However, the former of these was only carried out during the first round of selection.

**Table 13:** Reaction mixtures used for pre, trial and preparative PCR during SELEX.

Reagents	Pre-PCR (µl)	Trial PCR (µl)	Prep PCR (µl)
×10 PCR Buffer	100.00	35.00	100.00
dNTP Mixture (10 mM)	20.00	7.00	20.00
MgCl <sub>2</sub> (50 mM)	40.00	14.00	40.00
Forward Primer (100 µM)	5.00	1.75	5.00
Reverse Primer (100 µM)	5.00	1.75	5.00
DNase-free SDW	327.00	254.45	727.00
Platinum <i>Taq</i> Polymerase	3.00	1.05	3.00
Eluted ssDNA Pool	500.00	-	100.00

After the first incubation of N40 ssDNA library with cells, pre-PCR amplification of the entire eluted pool was conducted to create multiple representative copies of all possible bound sequences, thereby avoiding the potential loss of aptamers during subsequent pipetting processes. This was achieved through the addition of 500 µl eluted sequences to 500 µl of a pre-PCR mix (**Table 13**), which was then run as 20 separate 50 µl reactions for 9 cycles on a Perkin-Elmer 9700 thermal cycler (Cambridge, UK) using the temperature programme found in **Table 14**.

**Table 14:** Thermal cycling conditions used for pre, trial and preparative amplification.

Cycle	Temperature (°C)	Time (s)	Cycling stage
Denature	95.0	120	
<i>Denature</i>	95.0	30	
<i>Annealing</i>	56.3	30	
<i>Extension</i>	72.0	30	
Extension	72.0	180	
Hold	4.0	∞	

Trial PCR reactions of ssDNA eluted during each round of selection were carried out in order to determine the optimum number of amplification cycles required for subsequent preparative PCRs. This was conducted through the preparation of a trial PCR reaction mix (**Table 13**), which was then split into six individual 45 µl volumes. To each of these volumes was added 5 µl of eluted ssDNA, with the exception of one sample, to which SDW was instead used in order to act as a negative control. All samples were run using the same thermal cycling methods and temperature

programme previously outlined, with one tube containing eluted ssDNA removed after 6, 8, 10, 12 and 14 cycles. Negative control samples were run for a maximum number of 14 cycles. Amplification products were then loaded alongside a HyperLadder™ 25bp size determination marker onto a 4% agarose gel (made in ×1 TAE and containing 0.01% GelRed), which was then run in ×1 TAE buffer at 80 V for 100 min.

In order to generate the amount of ssDNA required for input into further selection rounds, 100 µl of ssDNA eluted from each incubation was lastly amplified after addition to a preparative PCR mix ([Table 13](#)) using the optimum number of cycles established in trial PCR. Samples were run in 20 separate 50 µl reactions using the thermal cycling methods and temperature programme previously described. Agarose gel electrophoresis was used to confirm successful amplification in the same manner as trial PCR studies.

#### **5.4.1.6 Strand Separation**

With dsDNA generated as a result of the amplification process, strand separation of PCR products from each round of selection was conducted via the use of an avidin-labelled resin to capture biotin-functionalised antisense strands. First, 200 µl Pierce™ NeutrAvidin™ agarose resin was added to two Corning® Costar® Spin-X® filter units, which were then centrifuged at 2730 RPM for 1 min in order to remove storage buffer. Resin beads were then preconditioned for 30 min using 500 µl of 200 mM NaOH to remove any labile avidin molecules, before further centrifugation under the same conditions. Resins were then washed (×5) with 500 µl of ×1 PBS buffer with further centrifugation.

Incubation of resin beads with 500 µl of preparative PCR products obtained from each round of selection was then conducted for 30 min on an orbital shaker to bind dsDNA through biotin-avidin interaction. After this incubation, resins were centrifuged and washed (×5) with PBS in the same manner previously described. A 500 µl volume of 200 mM NaOH was then added to the NeutrAvidin™ beads in order to separate



fluorescently-labeled sense strands, which were then collected via centrifugation at 3800 RPM for 10 min.

To remove NaOH, obtained ssDNA was placed into two Amicon™ Ultra-0.5 ml (3 kDa MWCO) filter units and centrifuged at 14,500 RPM for 30 min. DNase-free H<sub>2</sub>O (450 µl) was then added to the filters, which were then subjected to further centrifugation under the same conditions. De-salted ssDNA was finally collected by placing the filter units upside down in clean microfuge tubes and centrifuging at 3800 RPM for 7 min. The concentration of ssDNA was lastly quantified using a NanoDrop® ND-1000 Spectrophotometer (Thermo Fisher Scientific, California, USA).

#### **5.4.1.7 Flow Cytometry**

The ability of selected aptamer pools to bind sperm cells was monitored between Cell-SELEX rounds via flow cytometry. First, strand-separated ssDNA collected from each round of selection was diluted to a concentration of 500 nM in aptamer binding buffer. A negative control sample, consisting of fluorescently-labelled N40 library template, was also prepared in the same manner. Each of these samples was then added in a 100 µl volume to 100 µl of human sperm cells at a concentration of  $1 \times 10^7$  cells/ml (prepared via the same cell-isolation methods previously described) and incubated at room temperature for 30 min on an orbital shaker. Cells were then centrifuged at 6700 RPM for 3 min before the removal of unbound sequences within the resulting supernatant. Pelleted cells were then washed twice and re-suspended in a final volume of 400 µl aptamer binding buffer.

Analysis of fluorescence emission intensity at 515 nm from cells incubated with either selected aptamer pools or N40 library was conducted using a Beckman Coulter FC 500 flow cytometer (California, USA), measuring 20,000 events. Data analysis was performed using CXP software (version 2.2).

#### 5.4.1.8 Next Generation Sequencing and Data Analysis

Enriched aptamer pools obtained from rounds 1, 2, 3, 8, 9, 10 and 14 of selection were subjected to NGS to elucidate the structure of potential binding sequences. First, dsDNA products were prepared from each pool by PCR amplification using the same reaction mix (with the exception of non-labelled primer sets), number of cycles and temperature programme previously employed during the preparative PCRs for each respective round. Amplified products were then quantified using a NanoDrop® ND-1000 Spectrophotometer (Thermo Fisher Scientific, California, USA) before being diluted in SDW to a concentration of 2 ng/µl.

Samples were then prepared for sequencing using the NEBNext® Ultra™ DNA Library Prep Kit for Illumina®. Briefly, 1.4 µl End Prep Enzyme Mix and 2.9 µl End Repair Reaction Buffer (×10) was added to 25 µl of each dsDNA sample, which were then incubated for 30 min at room temperature and 30 min at 65 °C. Adaptors were then ligated to the ends of dsDNA sequences through the addition of 7.5 µl Blunt/TA Ligase Master Mix, 1.25 µl NEBNext adaptor for Illumina® and 0.5 µl Ligation Enhancer. This mixture was then incubated at room temperature for 15 min before the addition of 2 µl USER™ Enzyme, with further incubation at 37°C for 15 min. A post ligation cleanup was then conducted using AMPure® XP Beads with sequences eluted in 10 µl of 10 mM Tris-HCl, pH 8.5. A further PCR amplification of sequences was performed through the addition of 7.5 µl adaptor-ligated dsDNA to 12.5 µl NEBNext Ultra II Q5 Master Mix, 2.5 µl index primer and 2.5 µl Universal PCR primer. This mixture was run for 8 cycles in a thermal cycler using the temperature programme found in **Table 15**. A final cleanup procedure was lastly conducted using AMPure® XP Beads before elution in ×1 TE buffer. All prepared samples were loaded onto a V2 reagent cartridge and sequenced using the Illumina® Miseq platform (California, USA).

**Table 15:** Thermal cycling temperature programme used for NGS sample preparation.

Cycle	Temperature (°C)	Time (s)	
Denature	98.0	30	
Denature	98.0	10	} Cycling stage
Annealing	65.0	75	
Extension	65.0	300	
Hold	4.0	∞	

Data analysis of raw sequence reads was performed using Galaxy, an open source bioinformatics platform, following a custom-developed pipeline similar to that reported by Thiel *et al.* [303].

## 5.4.2 Results and Discussion

### 5.4.2.1 Aptamer Selection

Aptamers were selected according to a Cell-SELEX protocol previously reported by Sefah *et al.* [289] with several modifications. First, as human sperm cells used for *in vitro* studies are typically obtained from whole seminal fluid, rather than via traditional culture techniques, pre-selection cell growth and preparation methods were substituted with a density gradient centrifugation-based sperm cell isolation process. Microscopic examination of cells pre- and post-centrifugation confirmed the successful separation of spermatozoa from other seminal leukocyte and epithelial cell components (**Figure 61**).

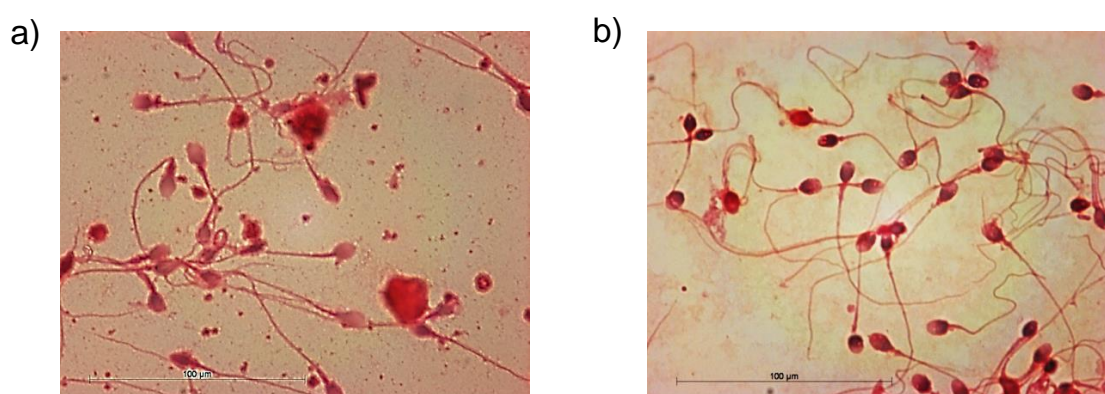


**Figure 61:** Microscopic examination of haematoxylin and eosin-stained sperm cells a) pre- and b) post-isolation using a density gradient centrifugation procedure.

A randomised N40 ssDNA library was incubated with a defined number of sperm cells (which were progressively decreased between SELEX cycles) at the start of each round of selection. Aptamer sequences able to bind to sperm targets were then recovered through centrifugation and eluted from the surface of cells before undergoing PCR amplification (to increase relative representation in subsequent selection rounds).

Trial PCRs were first conducted to determine the number of amplification cycles needed in order to generate the amounts of DNA required for future aptamer-cell incubations. Amplified products were successfully detected across all selection cycles using agarose gel electrophoresis. These products were found to run at approximately the same speed as the 75 bp fragment of a utilised Hyperladder™ DNA standard, which is consistent with the theoretical size (76 base pairs plus additional 6-FAM and biotin functionalisation) of dsDNA sequences (**Figure 62a**).

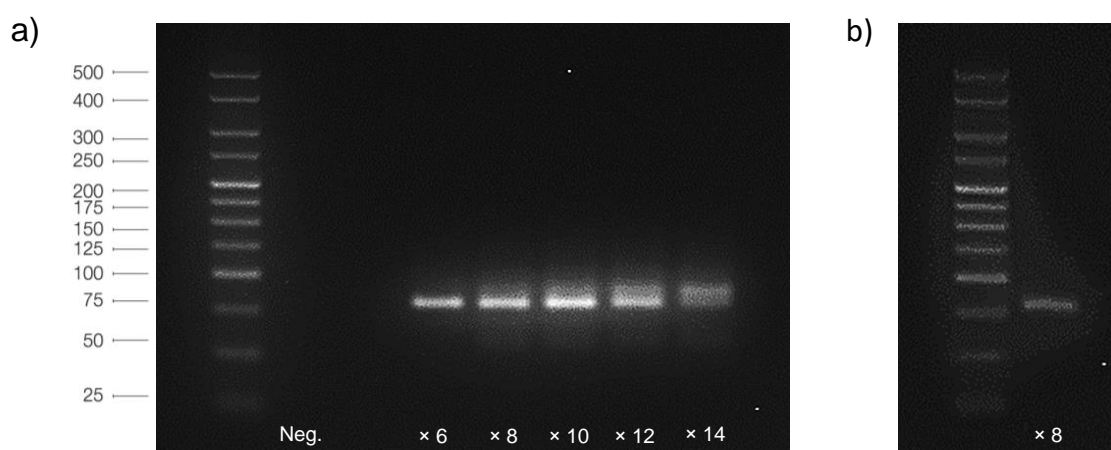


**Figure 62:** Gel electrophoresis images of a) trial and b) preparative PCR amplifications from the 4th round of the sperm cell aptamer selection process. Lane legends represent the number of amplification cycles performed or negative (Neg.) control samples.

One interesting effect observed during trial PCR analysis, was the presence of a secondary DNA band running slightly slower than identified dsDNA products in samples amplified over a certain number of cycles (which were different for each selection round). Previous studies have attributed such effects to the formation of PCR by-products as a result of

the repetitive amplification of randomised ssDNA libraries [393]. These by-products are likely to originate from the hybridization of ssDNA sequences to complementary bases within the random N40 region, which then serve as PCR primers. Extension of sequences at these priming regions by DNA polymerases then results in the formation of longer dsDNA products which run at a marginally reduced speed on electrophoretic gels. Consequently, optimal PCR cycle numbers used for subsequent preparative amplifications were chosen based on the trial PCR samples where only single product bands were observed (**Figure 62b**).

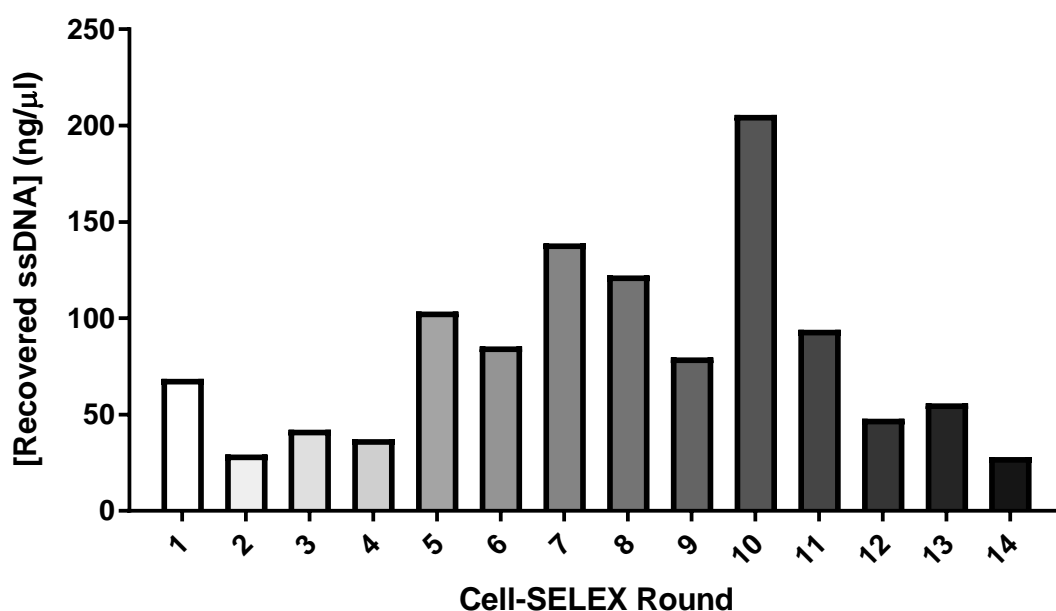


**Figure 63:** Concentrations of ssDNA recovered after strand separation from each round of the Cell-SELEX process.

Double-stranded amplification products were then subjected to strand separation using a Pierce™ NeutrAvidin™ agarose resin and NaOH denaturation to recover sense ssDNA sequences. After desalting, aptamers pools were quantified before being diluted for input into subsequent cell incubations. A general increase in the concentration of recovered ssDNA during each round of selection was observed across the entire Cell-SELEX process (**Figure 63**). This increase may indicate the success of aptamer selection, with greater target-sequence binding

resulting in increased amounts of eluted ssDNA template available for amplification (which in turn results in higher PCR product concentrations). However, this effect was not consistent between all selection rounds, especially between rounds 11-14, where recovered DNA concentrations actually reduced (the reason for which is currently unclear).

#### 5.4.2.2 Flow Cytometry

Attempts to monitor the progress of aptamer selection between SELEX rounds were made using flow cytometry as described in Sefah *et al.* [289]. Samples of enriched ssDNA pools from rounds 4, 7, 10 and 14 of selection, as well as N40 library template (acting as a negative control), were incubated with sperm cells before the measurement of emissions at 515 nm.

Fluorescent signals were observed from each of the selected samples, indicating the occurrence of aptamer cell binding (**Figure 64**). However, signal intensities were found to vary significantly across samples, with no distinct correlation to the amount of SELEX cycles performed. Such results may potentially be attributed to the presence of artefacts or impurities in prepared sperm cell suspensions (such as seminal leukocyte or epithelial components that were not removed during the cell isolation process), which may affect analysis.

This hypothesis is supported by the fact that most of the histograms generated exhibited two discrete peaks, a characteristic of samples containing multiple cell populations [394]. Importantly, no fluorescence emissions were detected for N40 library-incubated cells, giving further indication that sequences contained within enriched pools are present as a result of successful aptamer selection and not non-specific binding.

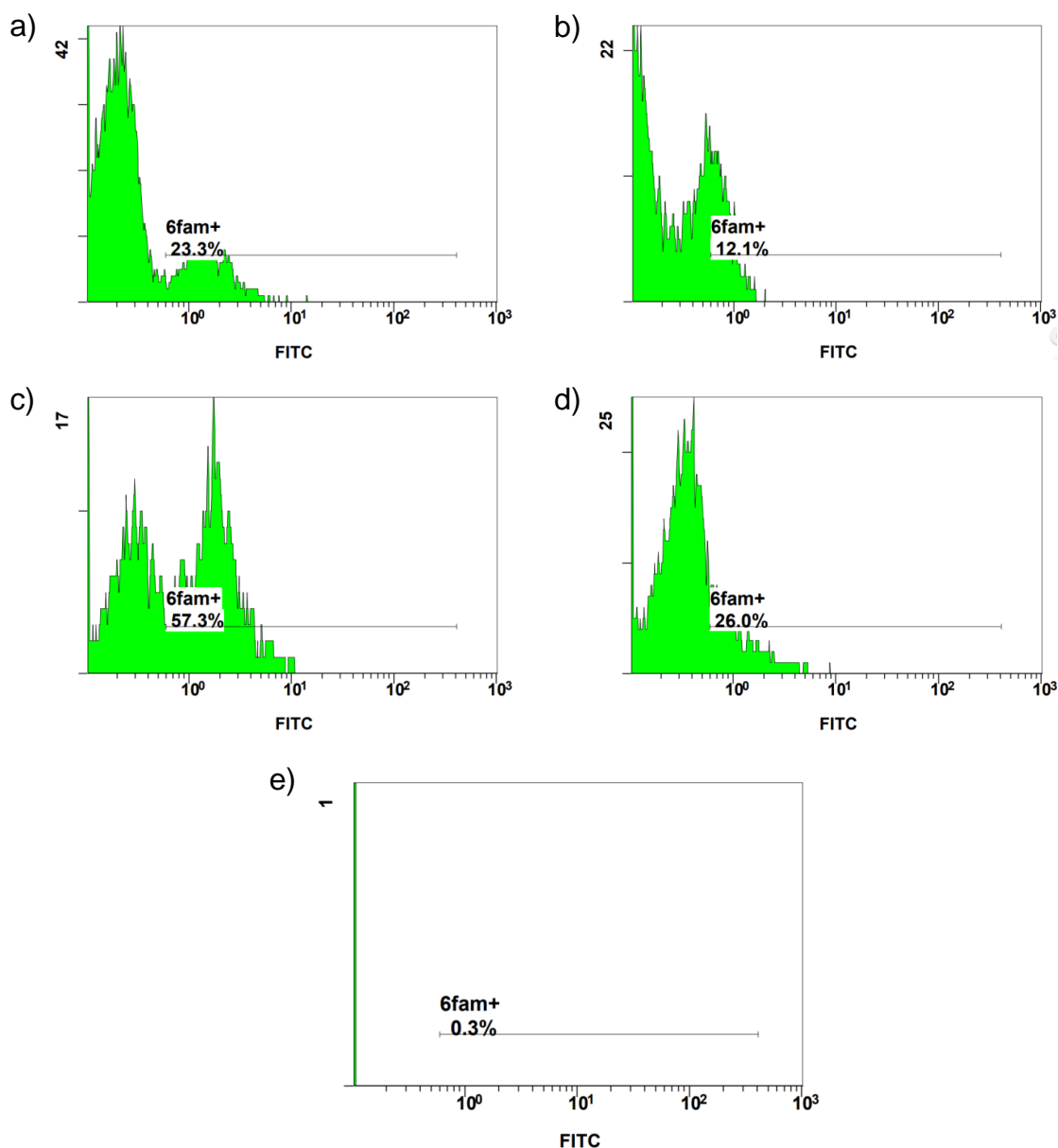


**Figure 64:** Flow cytometry histograms of sperm cells incubated with enriched aptamer pools obtained from a) round 4, b) round 7, c) round 10 and d) round 14 of selection and e) N40 library template sequences.

#### 5.4.2.3 Next Generation Sequencing and Data Analysis

Other modifications made to the employed Cell-SELEX protocol [289] included the use of NGS technologies to elucidate the sequences of potential binding ligands. Such technologies were chosen for use in this study to illicit a greater amount of sequence information from enriched aptamer pools, as well as to avoid the time-intensive cloning and colony-picking methods associated with traditional Sanger sequencing. Although the use of NGS analysis within aptamer selection studies have only



recently begun to be explored, such techniques may allow for both the detection of ligands at earlier rounds of selection and a greater characterisation of the evolution of enriched pools between SELEX cycles [395].

Three separate instances of high-throughput sequencing were conducted using the Illumina® Miseq platform to determine the sequence and relative abundance of ssDNAs contained within early (rounds 1-3), mid (rounds 8-10) and late (round 14) SELEX cycle aptamer pools. As raw sequence reads obtained from these experiments were output as FASTQ sequence files, significant data processing was required to isolate random N40 bases from fixed flanking regions, as well as to remove any undesirable selection and/or sequencing artefacts. Such artefacts include sequences of incorrect length (originating as amplification by-products as already discussed) or those containing mismatched constant regions.

This was achieved using Galaxy, an online bioinformatics management system that allows the construction of custom data processing workflows for the analysis of complex genomics datasets [396]. A Cell-SELEX workflow (made available at <https://usegalaxy.org/u/jamesgooch/w/cell-selex>) for the processing of NGS data obtained from this study was developed according to methods reported by Thiel *et al.* [303]. This automated pipeline is able to provide collated sequence and read count information from a single input of generated raw forward and reverse-read FASTQ files without further user contribution (**Figure 65**). The individual steps of this workflow (as separate Galaxy ‘tools’) were as follows:

- 1) **Upload** - FASTQ files from both forward and reverse sequences reads for a given round of selection are first uploaded to the Galaxy web server.
- 2) **FASTQ.Joiner** - Both forward and reverse paired-end sequence reads are merged together, allowing the simultaneous processing of datasets.





**Figure 65:** Scheme of the developed Cell-SELEX Galaxy pipeline and example data outputs.

- 3) **FASTA-to-Tabular** - Files are then converted to a text-based format that allows for easier sequence manipulation.
- 4) **Cut** - The unique identifier assigned to each read is removed, leaving only raw sequence data.
- 5) **Text Formatting** - Sequences that do not meet specific text-based criteria are removed from the dataset. In this workflow, sequences are retained if both constant flanking regions, as well as a central series of nucleotides of 38-42 bases in length, are present. Longer amplification by-products are removed at this stage.
- 6) **Replace** - A comma character is placed at the end of 5' constant flanking sequences, separating them from central N38-42 base regions.
- 7) **Convert** - Sequences are split based on the position of inserted comma values, placing 5' constant regions into a separate column.
- 8) **Cut** - Columns containing 5' constant region sequences are subsequently removed from the dataset.
- 9) **Replace, convert, cut** - Steps 6-8 of the workflow are repeated in order to remove 3' flanking regions, which are separated by placing a comma character at the beginning of the constant sequence. After this stage, only N38-42 sequences are present within the dataset.
- 10) **Add Column** - An additional column is added to the dataset containing arbitrary '+' character values against each sequence. These values act as sequence identifiers, allowing file conversion to a FASTA format.
- 11) **Tabular-to-FASTA** - Files are converted back from tabular to FASTA file formats, allowing sequences to be collapsed.
- 12) **Collapse** - Repeated identical sequences are reduced into a single read and assigned a count value corresponding to the number of duplicated sequences present within a sample.

The total number of raw sequence reads obtained from NGS analysis was found to vary significantly between samples from each round of selection (**Figure 66**). Such results were unexpected given the fact that all sample DNA concentrations were quantified and normalised both prior to and during NGS library preparation. This variation may potentially be attributed to PCR bias effects, in which samples are differentially enriched during library amplification processes. Previous studies have found that such effects are a major contributor to the established sample-to-sample (as well as run-to-run) variation often exhibited by the Illumina® Miseq platform [397].

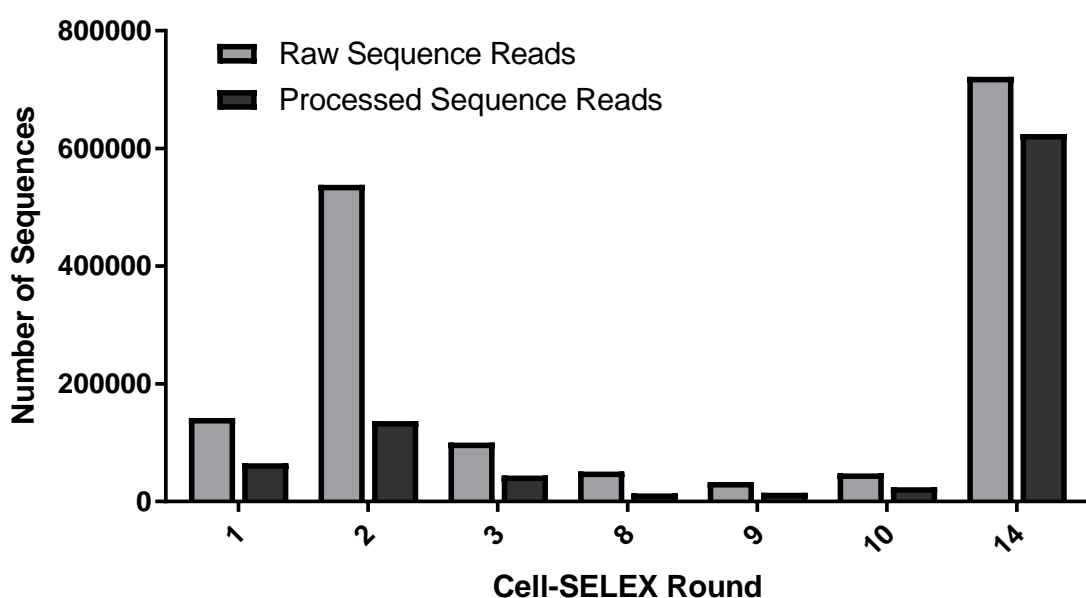


**Figure 66:** Total number of NGS reads obtained from sequenced aptamer pool samples before and after data processing using a custom Galaxy bioinformatics workflow.

Whilst application of the developed Galaxy data processing workflow resulted in a general decrease in the total number of sequence reads in all NGS datasets, this reduction was found to be less significant for the sample obtained from the final round of selection (**Figure 66**). Such results may potentially be taken as an indication of successful selection, with increased enrichment of viable aptamer sequences (that meet data

processing parameters) compared to amplification or sequencing artefacts.

NGS-analysed samples obtained from early (rounds 1-3) and mid (rounds 8-10) Cell-SELEX cycles did not contain any sequences that were repeated more than twice (after data processing). These findings were consistent with the majority of previously reported Cell-SELEX studies, which generally required between 10-20 rounds of positive selection to identify potential ssDNA aptamer candidates [398].

However, a total of 13,138 sequences were found to be repeated multiple times in the NGS dataset obtained from the final round of selection (round 14). In fact, 15 sequences were found to possess read counts greater than 25 (**Table 16**). Many of these showed elements of structural similarity, thereby demonstrating the potential of these sequences for the recognition of human sperm cells.

**Table 16:** Sequences obtained from round 14 of selection exhibiting over 25 total reads.

Seq. ID	Sequence	Reads	Length (bp)
SP1	CACTCTCACCTTCCTGTCACCTTTTTTCACTCTCACTC	252	40
SP2	CACTCACTCTTTCCCTTATCTGCTCACTCTTCATTCACCTC	61	40
SP3	CACCGTCCTTTTCTAGCATCTCTGTCACCTTTTCTCACTC	53	40
SP4	CACTCTCACCTTCCTGTCACCTTTTTTCACTCTCACTC	48	39
SP5	TCACTCGCAATATCCGTCACCTCCTCCTACCTCTTCACCTC	41	40
SP6	TCGACACTCTTTCCCTAACTACTCTGGATTGCTCATCTC	37	40
SP7	CCACTCGTCAACTTCCCTTCATCGTCACTCGCTCACACTC	37	40
SP8	CACTCACTCTTTCCCTTATCTGCTCACTCTTCATTCACCTC	37	40
SP9	CCGACACTCACCTACCTTTATCTCTCTGGATTCCGCACTC	33	40
SP10	CGACCTATCACTCTCTTTTTCACTTGGATTAACTCACTC	30	40
SP11	CCACCCCAACCTTTCGCGTCCTCTTACTCACTCTTCACCTC	29	40
SP12	CGGCACCCTACCCCTTTCTCCTCTCTGGATCGTCTCTC	28	40
SP13	CGCTCATCTCCTTCATTTTTGTCACTCTTCTTTCACTC	28	39
SP14	CGCCGCTCATTCTGGTCACGTCATCTTTTCTTTTCACTC	28	40
SP15	CAACACCATACTCACTCTGCCCTCTCTACTTCTCACTC	26	40

Although not covered within the scope of this study, further work to cluster highly represented sequences should be undertaken using informatics tools such as FASTAptamer [306] or AptaCluster [399] to elucidate the specific structural motifs responsible for aptamer-sperm cell binding.

### 5.4.3 Conclusion

A number of promising ssDNA aptamer candidates have been raised towards the recognition of human sperm cells using *in vitro* Cell-SELEX and NGS methods. A novel data processing pipeline was also constructed using the online informatics workflow management system Galaxy, for elucidating the sequence structure of potential binding ligands. Whilst specifically developed for the analysis of data obtained within this study, this pipeline may have potential use in future SELEX experiments (towards both cellular and non-cellular targets) employing the same N40 library template (and associated constant region sequences).

Whilst these sperm-cell specific sequences were primarily raised for use within displacement-based aptasensing assays, it is also envisioned that such ligands may also have application to other areas of forensic analysis. This may include the incorporation of sequences into solid-phase aptamer-functionalised materials (AFMs) for the capture and isolation of spermatazoa from vaginal epithelial cells. Such materials would be considered extremely useful in sexual assault casework for the separation of male and female cellular components in the biological fluid mixtures, allowing for the complete deconvolution of mixed DNA profiles.

However, further assessments of analyte binding affinities and secondary folding structure are likely to be required before selected ssDNAs may be employed as biological recognition elements. This may be achieved through  $K_d$  measurement techniques (including ITC, SPR or ultrafiltration), with subsequent bioinformatics analysis (using programs such as *mfold* [308]).

# **Chapter 6**

## **Taggants**

## 6.1 Introduction

Biosensors developed within the scope of this study were originally designed to be applied to latent body fluid stains as sprayable liquid reagents. Such reagents would be able to both visualise and identify the type of fluid present on an item, providing investigators with more information about an offence at a 'source' level (i.e. the donor and tissue origin of recovered genetic material).

However, authors have argued that greater emphasis should be placed on the ability of analytical techniques to generate 'activity' level information from biological evidence, such as intelligence on the movements and/or actions of individuals during an offence [400]. This is evidenced by the growth of research in areas such as metagenomic analysis, which may be used to discern the locations an individual has previously visited (as well as any objects they have touched) by examining the presence of specific microbes present on the surface of their skin/clothing [401].

One method of achieving such intelligence (within specific criminal scenarios) is through the use of 'taggants', materials containing encoded marker elements that act as unique identifiers. In locations in which a crime is suspected to potentially occur, these materials may be applied to the surface of an object, which is then handled by an offender, causing the taggant to be transferred. The subsequent detection of the taggant by investigators may then be used to empirically link an individual to a specific offence. A secondary transfer of taggants from a suspect to another surface may also provide additional insights into the movements and actions of an individual.

However, one challenge associated with current taggant materials is evasion by criminals who are familiar with the technology and able to detect areas of reagent application [402]. It was therefore envisaged that fluorogenic substrate biosensors may make for ideal 'reactive' taggant materials that remain completely invisible (even under excitation lighting)

until handling. Such handling may result in the digestion of substrates as a result of interaction with enzymatic moieties present in sweat (or possibly saliva transferred to the surface of the individual's hands), activating a detectable fluorescence signal.

This chapter therefore opens with a review (which underwent publication in 2016) of the prevailing state and future perspectives of taggant technology in forensic analysis. The different potential applications of taggant materials are first outlined before a discussion of the types of unique coding components used for taggant batch identification.

This review is followed by two published original research articles; the first of which involves 'proof of concept' investigation into the use of the peptide and fluorophore moieties previously employed for the construction of custom PSA-specific fluorogenic substrates, as taggant coding and detection components respectively.

A subsequent follow-up study is then reported, which documents a more comprehensive assessment of the developed taggant stability, resistance to varying environmental conditions and secondary transfer ability. An introduction to each published manuscript is given explaining the contributions of each of the listed authors to the work.

## **6.2 Published Article 5: 'Taggant Materials in Forensic Science: A Review'**

The content of following section was published as a review article in: **Gooch, J., Daniel, B., Abbate, V., & Frascione, N., Taggant materials in forensic science: A review.** TrAC Trends in Analytical Chemistry, 2016. 83: p. 49-54.

Drafting of the manuscript was performed by the candidate. Dr. Barbara Daniel, Dr. Vincenzo Abbate and Dr. Nunzianda Frascione had final approval over manuscript submission.



### 6.2.1 Manuscript

**Authors:** James Gooch,<sup>a</sup> Barbara Daniel,<sup>a</sup> Vincenzo Abbate,<sup>b</sup> and Nunzianda Frascione. <sup>a\*</sup>

**Authors Address:** a) Analytical and Environmental Sciences Division, King's College London, 150 Stamford Street, London, U.K., SE1 9NH, b) Institute of Pharmaceutical Science, King's College London, 150 Stamford Street, London, U.K., SE1 9NH.

**Abstract:** The use of taggant technology to mark objects for the purpose of identification is becoming a significant part of national crime reduction strategies. Taggants may be able to prevent or monitor criminal offences by associating an object with a specific piece of information. While the material properties of a taggant will largely vary between application purposes, a specific 'coding' element will generally be incorporated to infer marker uniqueness. With the speed, simplicity and accuracy of coding component analysis largely determining the overall efficacy of taggants, continuing advances in portable in-field analysis, nanotechnology and material science should have allowed for the development of new and improved forensic marking agents. However, the limited amount of recent research in this area suggests that this is not the case. This critical review therefore examines the current state of presently available taggants before attempting to offer insight into the future direction of forensic marking technology.

### Introduction

Costing approximately £24 billion a year, the social and economic effect of organised criminal activity in the UK is substantial. Offences related to the trafficking of illicit drugs (£10.7 billion), organised fraud (£8.9 billion) and acquisitive crime (£1.8 billion) are reported to be the largest sources of criminal revenue [403]. With actual costs likely to be even greater (as such estimates are only based on data from recorded crimes), developing

strategies that are able to prevent or aid in the investigation of these offences is a significant priority of the forensic science community.

Among the number of products made commercially available for the purpose of reducing criminal activity, forensic taggants may be seen as one of the most successfully employed. Taggant materials have been widely accepted for use as evidence within the UK court system since 2008, with certain marking agents having aided in the conviction of over one thousand criminal offenders since that time. Based on statistics published by the Metropolitan Police Service, household burglary across London was decreased by nearly 30% in areas where forensic taggants were applied (i.e. SmartWater®). Taggants are a class of materials that can be applied to or incorporated within an object in order to make it identifiable [402]. This is achieved by producing each 'batch' of taggant in an entirely unique formulation, allowing the particular molecular composition to be registered against a specific piece of information. Once recovered at a later date, this composition can be analysed in order to reveal the identity of the taggant and thus, the object it is marking [404].



**Figure 67:** The four main applications utilising forensic taggants.

A forensic taggant displaying entirely ideal characteristics should be of low cost to produce, have high coding capacity, be non-toxic to individuals and the surrounding environment, be simplistic and

inexpensive to detect and analyse via non-destructive means and be of a complex enough nature to prevent duplication. The majority of taggant manufacturers claim that their products are versatile enough to be applied in a broad range of circumstances. However, forensic marking materials are most extensively utilised for four distinct purposes (**Figure 67**):

- Property marking - Taggants may be applied upon valuable items such as vehicles and electronics in order to associate them with a specific owner. If that property becomes subject to theft but is later recovered, it may be returned to the original purchaser [405, 406]. Property taggants are usually invisible to the naked eye in order to prevent spoiling the item's aesthetic or to avoid detection by offenders.
- Anti-counterfeiting - Industries at risk of counterfeiting activities (pharmaceuticals, clothing, currency, etc.) may choose to incorporate taggants into their products to distinguish them from potential forgeries [407]. Marking agents used for this application are typically non-visible and have replaced traditional barcoding and hologram anti-counterfeit technologies, which are more easily duplicated [408].
- Tracking - Materials used in the manufacture of hazardous or potentially illegal products may be tagged by law enforcement agencies to aid detection or track initial origin. Such marking agents are predominantly applied during the production of industrial explosives that are susceptible to illicit use [409]. Robust taggants able to survive detonation may be detected to reveal information regarding type of explosive, supplier or batch ID. Taggants may also be covertly added to bulk volumes of illegal narcotics, allowing their distribution to be monitored [410].
- Monitoring - Taggants may be placed on exterior surfaces of houses, commercial properties or objects of value. As a result of criminal activity (such as trespassing or out-of-hours burglary),

these taggants may be transferred to an individual, providing strong physical evidence to associate them with that offence [411]. Additional information of the suspect's subsequent activity can also be gained if the taggant undergoes a secondary object-to-person-to-object transfer.

The physical characteristics of a taggant will depend largely upon which of these four purposes it is being used for (**Figure 68**). For example, markers utilised to stain currency stolen during a CViT (Cash-and-valuables-in-transit) robbery should remain permanent after application and should not be easily removed [406]. Conversely, a forensic coating applied to firearms and cartridge casings in an attempt to establish handling, should be designed to be as transferrable as possible [412]. The range of taggant formulations is therefore extensive. Markers may be dispersed within a medium such as grease, paint or ink, sprayed via aerosol, applied directly as a powder or embedded into materials during manufacturing processes [413].

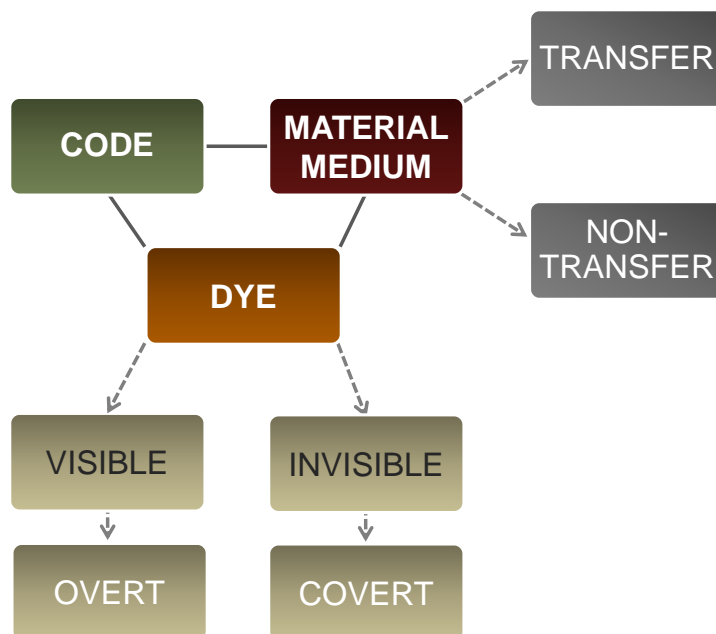


**Figure 68:** Forensic taggants may include different components (i.e. code, dye and material/medium), which can determine its physical characteristics.

Taggants designed to be covertly applied (in order to avoid destruction or discovery by offenders) may also include an additional component to

allow detection at a later time point. Being invisible to the naked eye, these taggants require localization in order to be successfully recovered for analysis. This is most often achieved by adding fluorescent compounds to the taggant, which will then emit light when excited at certain wavelengths of the UV or visible spectrum [414]. Other detection methods involve the inclusion of volatile chemicals for vapour identification [415] or radioactive isotopes [404].

While these detection constituents may not always be required within a taggant, all forensic markers will include a main 'coding' element in order to infer a required statistical uniqueness. By creating a formulation that is unable to be duplicated, a taggant may effectively 'store' information regarding the object it is marking [414].

As the success of a taggant will be largely influenced by the ability of this code to be recovered and analysed, all marker coding methods produced within the UK are subject to validation by the British Standards Institution (BSI) under Publicly Available Specification 820:2012 (PAS 820:2012). In this process, taggants are exposed to a number of accelerated UV light, temperature and humidity conditions in order to simulate the longevity of coding materials within a variety of circumstances.

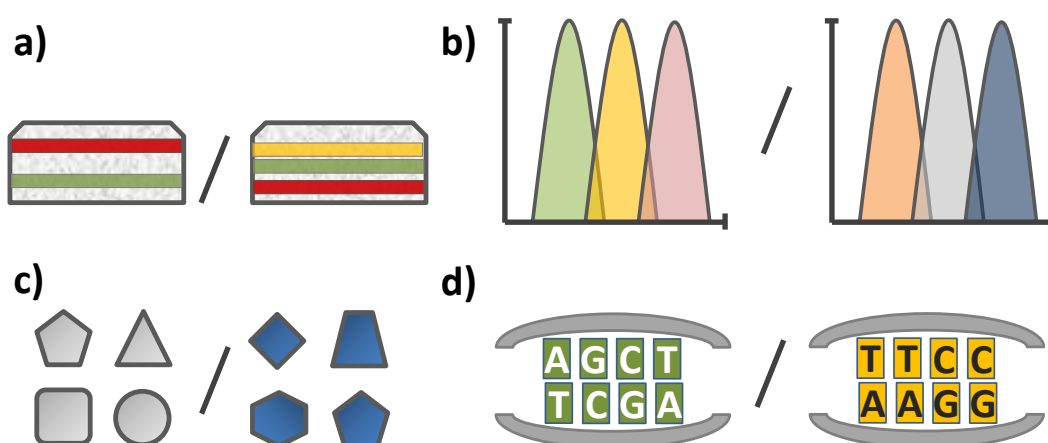


**Figure 69:** Code uniqueness provided by differences in: a) physical characteristics (i.e. multiple coloured layer particles), b) optical spectra, c) chemical composition and d) DNA sequences.

**Table 17:** Commercially available forensic taggants

Coding Type	Manufacturers	Taggants Produced	Analysis Methods	Uses
<b>Physical</b>	Alpha•Dot	Alpha•Dot [416]	Optical microscopy	Property marking, vehicle marking
	DataDot	DataDots® [417]	Optical microscopy	Property marking, anti-counterfeiting
	Microtrace	Microtaggant® [418]	Optical microscopy	Anti-counterfeiting, explosives detection
<b>Spectroscopic</b>	DNA Technologies	SmartDye™[419]	Spectrofluorometry	Anti-counterfeiting
	Luminex	MagPlex® spheres [420]	Flow Cytometry	Anti-counterfeiting, biological labeling
	Microtrace	Spectral Taggant™ [421]	Spectrofluorometry	Currency marking, security printing
	Spectra Systems	SpectraFluor™ [422]	Spectrofluorometry	Currency marking, product tracking
<b>Chemical</b>	Authentix	Authentix [423]	Immunoassay, GC-MS	Fuel Adulteration, anti-counterfeiting
	SmartWater	SmartWater® [405]	LA-ICP-MS	Property Marking, activity monitoring
	Polysecure	Brandproof® [424]	XRF spectroscopy	Anti-counterfeiting
<b>DNA</b>	Applied DNA Sciences	SigNature® [425]	DNA sequencing	Property marking, anti-counterfeiting, CViT
	DataDot	dDotDNA® [426]	DNA sizing analysis	Property marking, anti-counterfeiting
	DNA Technologies	DNA Matrix™ [427]	DNA sequencing	Anti-counterfeiting
	SelectaMark	SelectaDNA® [428]	DNA sequencing	Property marking, activity monitoring
	TraceTag	CypherMark™ [429]	DNA sequencing	Property marking, anti-counterfeiting

Despite the extensive commercialisation of taggant technology ([Table 17](#)), detailed information regarding the synthesis and manufacturing procedures of such marking agents is extremely limited within academic literature. Whilst publishing such protocols within the public domain may result in a decrease in taggant efficiency (by allowing offenders to become familiar with such materials), it is still pertinent to conduct a thorough exploration into the different encoding methods used in commercially established forensic marking agents ([Figure 69](#)). This critical review therefore attempts to examine these coding mechanisms, as well as explore recent research that may indicate how forensic taggant technology is likely to progress within the near future.

## **Current Technology**

### **Physical Taggants**

Renowned for being one of the earliest existing forensic marking materials; physical taggants possess coding systems that are based on the simple morphological properties of their components. These taggants are generally made unique by exploiting solid particles of a specific size, appearance or structural arrangement [430]. Such encoding mechanisms may also be described as 'graphical', as analysis is usually achieved by basic visual methods such as low-power microscopy [414].

One coding element commonly used in physical taggants is the microdot, a small polymer disc between 2-1000  $\mu\text{m}$  in size containing minute photographic information. Text or images etched onto microdots are usually too small to be observed by the naked eye alone but may be revealed upon optical magnification [431]. Although initially developed as a covert means of transferring data during World War II, companies such as DataDot and Microtrace have taken advantage of microdot technology by including them in a number of ink and varnish based suspensions [404]. The dots within these suspensions are then able to act as simplistic tagging mechanisms by being imprinted with a unique numeric code,

which is then registered against a particular owner on an electronic database [417].

Another physical tagging approach pioneered in the 1970's by the US company 3M, focuses on the use of small plastic particles, constructed using a number of different proprietary coloured materials. These materials are combined in a sequence of layers, the order of which will be specific to each formulation of taggant produced [418]. A visual inspection of the layers then reveals the identity of the marker and the batch from which it originated. The robust nature of the materials used in layer construction has resulted in these particles becoming a predominant tagging agent for the identification of post-detonation explosive materials [432].

However, in a number of circumstances the utilisation of physical type taggants may be considered disadvantageous. Marking agents based on graphical identification strategies will generally have very little 'space' in which coding can take place [402]. This consequently limits the amount of statistically unique particles (and thus taggant formulations) that may be produced. Applications such as property marking, which necessitate a continuous stream of distinct codes, may benefit better from the use of molecular-based tagging agents, which have a higher coding capacity. Other drawbacks include the easy observability of physical taggants due to the relatively large size of incorporated solid particles, limiting their use within covert situations [413].

### **Spectroscopic Taggants**

In spectroscopic taggants, a number of molecules possessing differing optical qualities are combined together to create a single mixture with a spectrally unique signature. These taggants utilise multi-component encoding strategies, achieving their individuality from a precise combination of different emission wavelengths or intensities [414]. However, in certain taggant designs, these optically distinct molecules may be enclosed together within solid particles (to increase taggant



stability or simplify analysis) and may thus be described as single-component systems [433]. Determining the identity of these marking agents is usually performed via the analysis of overall emission signature by simple spectrophotometry techniques.

The materials most often utilised within spectroscopic taggants are simple non-toxic organic dyes that fluoresce in different regions of the visible spectrum [434]. Companies such as Luminex and Spectra Systems manufacture a number of marking agents based on the integration of several cyanine, phthalocyanine or squaraine-based fluorophores [420, 422]. The low cost and wide availability of organic dyes ensures that the production of spectroscopic markers remains inexpensive, but may also result in the illegal reproduction of taggants themselves if fluorophores are recognised and acquired by counterfeiters [408]. Organic dyes are also disadvantaged by broad spectral emission overlaps, short fluorescence lifetimes and sensitivity to photobleaching [413].

Industrial and academic research has attempted to overcome these challenges by developing spectroscopic taggants that include more sophisticated optical components. Guillo *et al.* recently reported the development and commercialisation of a large array of spectroscopic coding materials based on non-toxic lanthanide ion complexes [435]. The unique temporal and spectral characteristics associated with these complexes are considered extremely difficult to duplicate by materials available to forgers, which may significantly deter potential attempts at taggant duplication. The narrow emission bands of rare-earth materials may also serve to increase the discriminatory power of a taggant by allowing more optically distinct components to be added to a marker without spectral overlap [414]. As the number of existing lanthanide elements is limited, varying the emission intensity ratios as well as the wavelengths of rare-earth materials is often used to further increase this statistical discrimination.

## Chemical Taggants

Much like spectroscopic markers, inorganic taggants rely on a multiplex of molecules within a specific combination to infer identity. However, instead of optical signature detection, chemical encoding is achieved from a fixed set of trace materials, which may be either present or absent from a mixture [436]. Each of these materials is tested for on an individual basis, essentially creating a form of 'binary string' data in which each position of the string represents a different compound. The presence of a particular trace may be indicated by a "1" in that position of the string, whilst its absence may be denoted by a "0" [437]. Taggant identity is determined by the comparison of binary sequence data generated from trace analysis with a list of strings registered on a database.

The UK's largest manufacturer of forensic marking technology SmartWater, bases the majority of their commercially available reagents on this premise. In these taggants rare-earth lanthanides are also utilised but are identified by their individual mass through laser ablation inductively coupled plasma mass spectrometry (LA-ICP-MS) rather than fluorescence emission [405]. A method of using isotopic materials as chemical encoding components for the authentication of fuels, consumer products and agrochemicals has also been developed by U.S. firm Authentix. These trace elements usually consist of deuterated organic or inorganic compounds that are then detected by either gas-chromatography mass spectrometry (GC-MS) or multiplex immunoassay systems [423, 438]. The increased sensitivity of chemical analysis methods over spectroscopic techniques allows coding materials to be included at much lower quantities (as little as parts per billion) than other taggant types. This in turn prevents the physical properties of a marker from being altered (unlike those containing large insoluble particles, which may appear more 'granular' in nature) and may thus lower the risk of unwanted detection. Once again, these taggant classes are not without limitations. Binary string data can be compromised if one or more

components within a mixture is removed or destroyed, or if extraneous materials are added (for example, by accidental mixing of two different taggant formulations) [436]. Chemical multi-component encoding may also not be compatible with highly transferrable marking agents as the different underlying chemical structures of tracing elements may cause them to be transferred at dissimilar rates, leading to incomplete recovery and subsequent erroneous identification.

### **DNA Taggants**

Discovered in the early 1950's as the foundation of information storage for all known life forms, the immense coding ability of deoxyribonucleic acid (DNA) has been recognised for a considerably long period [439]. Since that time, a range of methods have been developed for the storage of non-genetic data within DNA molecules [414]. As a result, manufacturers such as Selectamark Security Systems [428], TraceTag [429] and Applied DNA Sciences [425] now produce forensic marking agents that can infer identity via the use of unique oligonucleotide sequences. Such sequences may be naturally occurring, entirely synthetic or a combination of both (e.g. botanical DNA shuffled into a random arrangement) [440]. The order of single nucleotide units comprising a sequence will be individual to each formulation of taggant produced, allowing separate batches to be distinguished.

The benefits of near-unlimited coding capacity, straightforward synthesis and low toxicity of genetic material have ensured that DNA taggants are one of the most prevalent forms of forensic marking agents commercially available. However, challenges regarding the application of DNA-based tagging approaches are twofold. Sequencing techniques employed for the analysis of oligonucleotides are typically more cost, reagent and labour-intensive than methods used to identify other types of taggant coding components [441]. As the genetic material recovered from a taggant also requires amplification by the polymerase chain reaction (PCR) prior to testing, this method of analysis can be especially expensive [402].

Furthermore, DNA is a relatively sensitive molecule and can degrade under the normal temperature, oxidation, radiation and chemical and enzymatic activity levels associated with ambient environmental conditions [442, 443]. While DNA damages caused by these stresses may be repaired by a number of processes within living organisms, the same cannot be said of the synthetic oligonucleotides included within forensic taggants. Concerns have therefore been raised over the general stability of DNA-based tagging materials and the subsequent compromise of genetic coding sequences [402, 414, 444]. However, encapsulation of nucleotides within silica microbeads [445] or plant materials [446] may be carried out in order to protect against this potential degradation.

## Future Perspectives

Each of the commercially available taggant mechanisms included within this review displays a distinct set of strengths and weaknesses, either in terms of coding capacity, covert usage, overall stability or method of analysis (**Table 18**). These disadvantages currently prevent a single taggant type from being used as a universal product identification system, necessitating the application of separate marking methods for different purposes [404].

**Table 18:** Summary of the advantages and disadvantages of commercial taggants.

Coding Type	Advantages	Disadvantages
<b>Physical</b>	Simplistic analysis	Limited coding capacity
	Inexpensive	Less covert
<b>Spectroscopic</b>	Simplistic analysis	Subject to counterfeiting
	Inexpensive	Limited coding capacity
<b>Chemical</b>	Analysis sensitivity	Prone to misidentification
	More covert	Incomplete recovery
<b>DNA</b>	High coding capacity	Expensive analysis
	Low toxicity	Possible degradation

However, it must also be noted that major practical innovations in the fields of nanotechnology, material science and analytical instrument portability have occurred since the scientific technologies behind these

coding mechanisms were established. These advances are now being exploited by a number of research groups in an attempt to develop forensic tagging reagents that can identify any object, regardless of situation or circumstance.

Nanoscale particles, wires and tubes all show great potential as next generation tagging mechanisms due to their small size (preventing detection and the physical alteration of marker properties), range of potential analysis methods and ease of formulation within traditional marking reagent media [413]. Semi-conductive quantum dot nanoparticles are currently being utilised to create spectroscopic taggants with optical qualities superior to those employing organic dyes or lanthanide ion complexes [447]. With narrow emission wavelengths, colour-tuneable signals and environmental-independent fluorescence properties, quantum dots may represent an excellent opportunity to improve the multi-component spectral encoding mechanisms presently utilised by spectroscopic taggants [414, 448]. Commercialisation of this technology may have been hindered by the relative cytotoxicity of metal ions used in the synthesis of quantum dot particles [449]. Efforts to reduce these potential damages to human health and the surrounding environment are currently underway through the development of heavy metal-free quantum dots [450].

However, there has been debate over whether fluorescent molecules should be included within tagging materials at all, as many offenders are now familiar with optical anti-counterfeit methods and are able to identify markers with obvious visible emissions [413]. In an attempt to resolve this issue, a number of taggants have recently been produced that can only be analysed via the use of Raman spectroscopy [451, 452]. Much like other forms of spectroscopic coding mechanisms, these reagents comprise compounds mixed in a specific combination to produce a unique spectral signature (which in this case, is generated through the inelastic scattering of monochromatic laser light). The main advantage of

this method is that Raman spectroscopy may also be used for the initial detection of tagging materials as well as identification, avoiding the requirement of additional tracing components that may result in unwanted discovery [413]. The sensitivity of such detection may also be greatly increased through the phenomenon of surface enhanced Raman scattering (SERS) by the direct conjugation of Raman-active compounds to a number of metallic nanoparticles [453].

Another coding technique designed by Duong *et al.* utilises the properties of nanomaterials beyond fluorescence, which involves deriving the individual melting-temperatures of a panel of solid particles within a taggant mixture to provide it with an unique thermal barcode [402]. The presence or absence of these so called ‘phase-change’ nanoparticles within a taggant is assessed using differential scanning calorimetry (DSC) in a linear thermal scan, which generates a specific melting-point peak for each component [408]. However, only a limited selection of nanoparticles has currently been developed for this purpose [454]. It is likely that this number will have to be increased in order for this system to possess the level of statistical differentiation required from a universal tagging system.

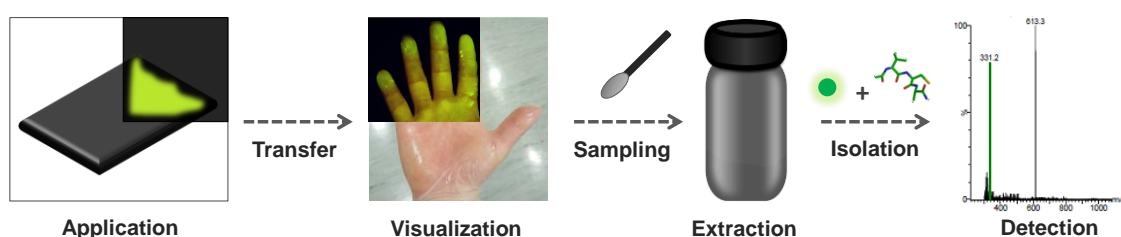


**Figure 70:** Schematic of peptide-based taggant application and analysis. Adapted from [455].

Aside from nanoparticle-based encoding methods, recent developments in novel tagging technology have also been achieved by the use of synthetic polypeptide sequences [456]. The principle of inferring identity through the unique order of successive amino acids has been theorised since the early 1980’s [457]. However, only within the last year have methods been realised for their practical application and analysis within forensic marking materials [455]. **Figure 70** demonstrates this process, in

which an oil-based medium containing hydrophilic peptide molecules is first applied onto the surface of an object. As a result of handling during criminal activity, this reagent is transferred to an individual, associating them with the offence. Detection by added fluorescence tracers is performed to permit recovery of the taggant by targeted swabbing. Hydrophilic peptides may be then isolated from the medium by simple liquid-liquid extraction, allowing their mass (and therefore sequence) to be determined by electrospray ionisation mass spectrometry (ESI-MS).

As an alternative form of single-component biomolecular coding, peptide taggants possess a number of advantages over current commercially available DNA-based marking systems. The statistical coding capacity of polypeptide chains is significantly greater than that of oligonucleotides, owing to the 22 different natural amino acids that may be used as individual sequence units (compared to the four bases possessed by DNA) [458]. Kydd reports that a string of 10 random amino acids can code up to  $4 \times 10^{13}$  unique sequences [457]. ESI-MS methods are also quicker than DNA sequencing (with processes from detection to analysis able to be completed in less than one hour) and are becoming increasingly more portable, which could allow the point-of-care testing of peptide tagging reagents. Peptides are additionally easy to produce at low cost, are environmentally harmless and relatively inert (with stability being further increased by simple chemical modifications) [458].

## Conclusions

By authenticating objects, deterring theft and monitoring illegal activity, forensic taggants continue to play a pivotal role in the reduction of criminal enterprise. This review has attempted to highlight the significant abilities of tagging materials to infer identity in an enormous range of products, as well as document the most prominent commercially available coding mechanisms used for achieving this aim. Whilst it is quite clear that none of the commercial marking methods available currently possess every single one of the qualities demanded of a universally applicable

forensic taggant, the recent research covered within this article demonstrates that concerted efforts towards taggant improvement are occurring. The myriad of surfaces, environments and time-frames in which a taggant may be applied makes the technical innovation and validation of forensic marking materials relatively challenging. Only through continuing advances in material science, nanotechnology and instrumental analysis, can steps be made towards the development of a single versatile platform for object identification. It is hoped that this review will encourage researchers working within the field of analytical chemistry to take interest in taggant technology and engage with this development in order to make universal marking systems a reality.

### **6.3 Published Article 6: ‘Establishing Evidence of Contact Transfer in Criminal Investigation by a Novel ‘Peptide Coding’ Reagent’**

The content of following section was published as an original research article in: **Gooch, J., *et al.*, Establishing evidence of contact transfer in criminal investigation by a novel ‘peptide coding’ reagent.** Talanta, 2015. 144: p. 1065-1069.

Experimental work was performed by the candidate with assistance from Clarissa Koh. The candidate also produced the manuscript. Help with peptide synthesis, as well as access to the Institute of Pharmaceutical Science research laboratories and HPLC and MS instruments, was provided Dr. Vincenzo Abbate. Dr. Barbara Daniel and Dr. Nunzianda Frascione provided supervisory and technical support throughout the research. Additional materials for this article may be found in the appendix of this thesis (**Section A.2**).

#### **6.3.1 Manuscript**

**Authors:** James Gooch,<sup>a</sup> Clarissa Koh,<sup>a</sup> Barbara Daniel,<sup>a</sup> Vincenzo Abbate,<sup>b</sup> and Nunzianda Frascione. <sup>a\*</sup>

**Authors Address:** a) Analytical & Environmental Sciences Division, King’s College London, Franklin Wilkins Building, 150 Stamford Street,



London, SE1 9NH, b) Institute of Pharmaceutical Science, King's College London, Franklin Wilkins Building, 150 Stamford Street, London, SE1 9NH.

**Abstract:** Forensic investigators are often faced with the challenge of forming a logical association between a suspect, object or location and a particular crime. This article documents the development of a novel reagent that may be used to establish evidence of physical contact between items and individuals as a result of criminal activity. Consisting of a fluorescent compound suspended within an oil-based medium, this reagent utilises the addition of short customisable peptide molecules of a specific known sequence as unique owner-registered 'codes'. This product may be applied onto goods or premises of criminal interest and subsequently transferred onto objects that contact target surfaces. Visualisation of the reagent is then achieved via fluorophore excitation, subsequently allowing rapid peptide recovery and analysis. Simple liquid-liquid extraction methods were devised to rapidly isolate the peptide from other reagent components prior to analysis by ESI-MS.

## Introduction

The Home Office estimates that billions of pounds in social and economic costs arise every year as a direct result of organised criminal activity within the UK [459], the majority of which may be attributed to physical crimes, including significant theft and drug trafficking offences. Consequently the reduction of this activity remains a high priority for the UK government and its criminal investigators. This has been recently reflected by the growing number of commercially available forensic 'taggants', chemical reagents which may be applied to a particular surface in order to monitor items of criminal interest or associated activity [402, 445]. These products, usually consisting of a coloured compound mixed within an oil-based medium, are easily transferred onto persons or objects that come into contact with marked surfaces. The subsequent detection of these compounds may then be used to form a logical

association between an individual and the object in question, providing strong evidence of criminal intent. For 'covert' operations, in which indication of transfer should remain hidden from the offender, coloured materials may be replaced by fluorescent ones, the presence of which is only revealed through excitation with specialist light sources [460]. For example, the US based company Sirchie has developed several visible and fluorescent transferrable products designed for home and business owners to protect their property from trespassers and to mark valuable goods that are likely to be the subject of theft. However, the disadvantage of such products is that they are comprised of a single standard formulation and cannot be used to differentiate the source of two separate objects on which the same medium has been applied, thereby limiting investigative potential.

Others have sought to address this problem by inserting a unique 'code' within the medium itself, which may be traced back to the original owner upon analysis. Many of the UV-vis emitting products developed by Cleary [461] contain a mixture of trace metals and organic moieties, with coding achieved by the unique combination in which the materials are present. Subsequent analysis of reagent samples recovered from individuals or stolen goods may then be able to determine the address to which that particular elemental composition is registered [461]. However, the disadvantage of using a large variety of compounds within a single formulation is twofold; first that differences in chemical structure will cause molecules to be transferred at different rates. An incomplete or erroneous code may therefore be given in cases in which only trace amounts of medium are recovered that may not contain a full range of materials added to the formulation. This is further dependant on the type of surface on which the medium has been applied, making the estimation of transfer unpredictable. Furthermore, the relative stability of each molecule is also governed by these same structural differences, which will be different for each additive. Incorrect codes may once again be given if certain compounds break down prior to recovery and analysis. This would

be especially pertinent in scenarios where media have been applied on a long-term basis.

In recent years, Brown and Reichert [428] have made attempts to avoid using a coding system based upon multiple identifying additives by synthesizing a number products that contain a unique synthetic DNA sequence [440]. Despite negating differential transfer rates by using a single molecular identification system, the labile nature of DNA in exposed environmental conditions is well documented [462, 463], making overall reagent stability a cause of concern. Moreover, sequencing DNA to determine its associated address can be expensive and time consuming, requiring trained personnel and large-size laboratory based instrumentation, as well as specific procedures for sample collection and preservation. This also applies to DNA synthesis itself, in which pure sequences are difficult to achieve in a high yield [464]. Although circumvention of this issue may be achieved through the PCR amplification of low amounts of starting material, extensive extraction procedures are likely to be required in order to remove any additional materials that may cause downstream inhibition.

We therefore present the development of a novel reagent used to establish evidence of contact transfer in order to provide a more robust method of monitoring items associated with criminal activity. The proposed reagent, like those previously described, is comprised of a fluorescent compound dispersed within an oil-based medium that is transferred to an offender or object that comes into contact with a marked surface. However, this reagent employs an innovative single molecule coding system based on the addition of a unique synthetic peptide. This peptide, made up of a short known sequence of amino acids, is specific to every formulation of the reagent produced, allowing its registration to an individual or address. Once transferred as a result of criminal activity, this product may be visualised by excitation with a specialist light source to produce fluorescence.

Unlike other DNA based coding systems, peptides can be isolated from the rest of the reagent components via a simpler liquid-liquid workup procedure. Analysis of the sequence may then be rapidly achieved via standard Electrospray Ionisation Mass Spectrometry, with each peptide generating a specific  $m/z$  ratio that can be used to determine its identity (**Figure 71**). Such analysis affords significant advantages over time-consuming and costly DNA sequencing processes. Amino acids are also amenable to a wide array of structural modifications [465], which can either be used to further increase stability or increase the exclusivity of a coded sequence. There are numerous potential applications for this reagent. In addition to linking a person to a target surface via primary transfer (i.e. surface-to-person), it may also be possible to deduce their subsequent activity by tracking secondary transfer (i.e. surface-to-person-to-object). For example, if a person handles a specific item (i.e. a package or document) after coming into contact with the reagent, it may be possible to also link them to that item through secondary transfer.

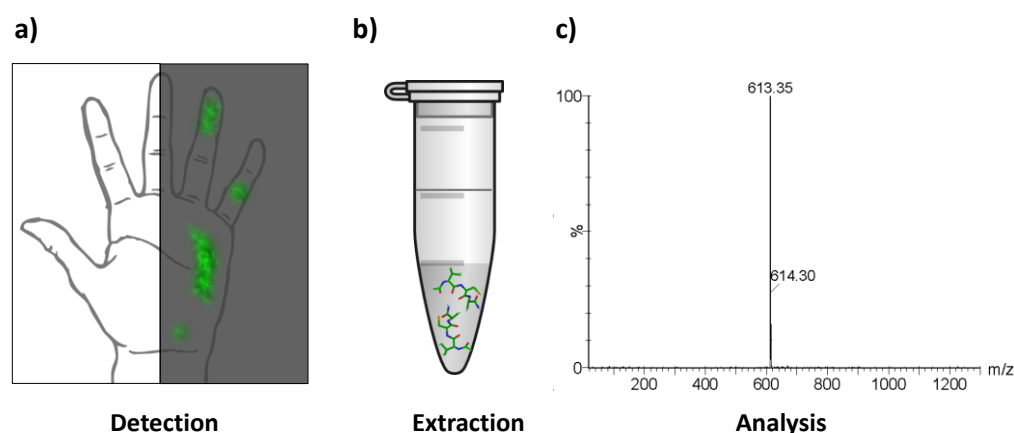


**Figure 71:** Demonstration of peptide recovery and analysis: a) the reagent is visualised through wavelength excitation, b) the collected medium undergoes liquid-liquid extraction to isolate coding peptide, and c) peptides are analysed and unique  $m/z$  value generated to identify sequence.

This study focuses on the reagent design and investigating optimum conditions for its successful detection and analysis. The in-field stability of the final reagent was also monitored over a six-week period via

application to a number of surfaces routinely encountered within forensic casework.

## **Materials and Methods**

### **Medium Selection**

Glycerol (Sigma Aldrich, UK), Castor Oil (Holland and Barrett, UK), a mixed hydrocarbon formulation (MHF) (Vaseline, UK) and a Lithium-based lubricant (Comma, US) were spread evenly in 100 mg amounts on 2.5 cm<sup>2</sup> areas of aluminium foil, ceramic, plastic and glass. Surfaces were contacted after 24 hours with a white vinyl gloved index finger at a standardised force of 30 g. A brief qualitative visual examination was used to establish the two media displaying greatest transfer. A quantitative indication of MHF and lubricant transference was achieved through the process described above but with surfaces weighed before and after contact to calculate deposited media.

### **Peptide Synthesis**

Peptide Ac-HSSKL was manually synthesised by Fmoc-Solid Phase Peptide Synthesis using 2-chlorotritylchloride resin (Sigma Aldrich, UK), which was swollen in dichloromethane (DCM) for 10 minutes prior to coupling. Acylation steps were conducted using six equivalents of Fmoc amino acids, pre-activated with DIPCDI and Ethyl (hydroxyimino)cyanoacetate (Oxyma) in anhydrous N,N-Dimethylmethanamide (DMF). Coupling reactions were conducted for 1 hour and monitored by the picrylsulphonic acid test. Fmoc deprotection of coupled amino acids was achieved by treatment with 20% (v/v) piperidine in DMF for 10 minutes and confirmed by the picrylsulfonic acid test. Impurities and excess reagents were removed by washing at each stage with DMF, methanol and dichloromethane.

Capping acetylation was performed by the addition of ten equivalents of acetic anhydride and twenty equivalents of N,N-Diisopropylethylamine (DIPEA) in DMF. Resin cleavage was achieved through treatment with a

95:0.5:0.5:0.5:0.25 solution of trifluoroacetic acid (TFA): water: phenol: thioanisole (TA): triisopropylsilane (TIPS) for 3 hours at room temperature. Next, the filtrate was concentrated under nitrogen at 40 °C. Ice cold diethyl ether was added to precipitate peptides which were washed several times with diethyl ether, dissolved in 50% acetonitrile in water containing 0.1% TFA and finally freeze-dried for 24 hours. The purity and correct mass of the final peptides were confirmed by analytical reverse-phase high-performance liquid chromatography (RP-HPLC) and ESI-MS, respectively. All peptide synthesis reagents were purchased from Bachem, UK and used as received.

### **Peptide Concentration Selection**

Synthesised peptide in 1 mg, 2.5 mg and 5 mg quantities was mixed into 100mg of MHF, which was subsequently spread evenly on a 2.5 cm<sup>2</sup> area of a glass microscope slide. Slides were contacted with a gloved finger as previously described (refer to the Medium Selection section). Portions of gloves containing transferred media were removed and placed in a 2 ml Eppendorf tube. A liquid-liquid extraction to isolate the peptide for analysis was performed through the addition of 1 ml hexane and 0.5 ml distilled water. Samples were vortexed and glove fragments removed before centrifugation at 13,000 RPM for two minutes. Aqueous phases were placed into a fresh tube. The original sample was then further extracted with an additional 0.5 ml of distilled water. Both aqueous layers were combined before undergoing counter extraction with 1 ml of hexane. After removal of hexane layer, formic acid was added to the aqueous phase at a final concentration of 0.1% v/v prior to ESI-MS analysis using a Waters ZQ micromass 2000 mass spectrometer.

### **Fluorophore Studies**

Rhodamine 110 (Sigma Aldrich, UK) and 7-amino-4-trifluoromethylcoumarin (AFC) (Santa Cruz Biotechnology, US) fluorophores were reconstituted in methanol to concentrations of 10 mg/ml, 1 mg/ml and 0.1 mg/ml. 50 µl of each fluorophore concentration

was added to 100 mg of MHF and mixed thoroughly before being spread evenly on a 2.5 cm<sup>2</sup> area of a glass microscope slide. Samples were visualized in the dark using an Olympus SZX12 fluorescence microscope (Tokyo, Japan) and photographed with an internal CCD camera. Photostability of both fluorophore-containing media was monitored once a week over a six week period. Lastly, 50µl of 0.1 mg/ml rhodamine solution was added to 100mg of peptide-mixed media before extraction and ESI-MS analysis.

### **Stability Studies**

40 mg of peptide-mixed medium was applied to surfaces of aluminium foil, ceramic, plastic and glass, cotton, polyester, leather and denim. Liquid-liquid extractions were performed as previously described in order to isolate peptides for ESI-MS analysis. Extractions were performed from each surface once a week for a period of six weeks.

## **Results and Discussion**

### **Transferability Studies**

The initial priority of every forensic taggant reagent design is the selection of an appropriate medium in which fluorophore and coding additives are dispersed. It is crucial that the medium transfers well by itself so that identification components carried within it will be of a high enough concentration for subsequent analysis. Additionally, media should not dry out, allowing them to be applied over extended periods of time, as well as transparent, to avoid detection within covert investigation.

Glycerol, castor oil, MHF and a Lithium-based lubricant were chosen to be investigated as potential media due to their low volatility, odourless and colourless properties. Each medium was applied to four surfaces that are often encountered within forensic casework (i.e. plastic, ceramic, glass and metal) before being contacted with a gloved finger after a period of 24 hours (Appendix - **Figure 85**). This was carried out to ensure

that the final reagent is able to operate efficiently in a range of environments where it is likely to be applied.

Both castor oil and glycerol samples showed significant decreases in transfer after a 24 hour time period, which was especially evident in samples taken from the glass and metal surfaces. This may be due to the fact that both substances are known to undergo a high degree of hydrogen bonding [466, 467]. Whilst theoretically the high viscosity caused by this bonding should allow for greater transfer, it is possible that the extensive intermolecular interaction also caused molecules to aggregate, leading to a more uneven transfer. In contrast, both semi-solid MHF and lubricant media showed greatest and most consistent transferability over time, likely benefiting from fixed molecular arrangements. These substances were therefore taken forward for further quantitative indication of transfer efficiency, in which the average percentage of media transferred was calculated by recording of surface weight before and after contact (Figure 72).

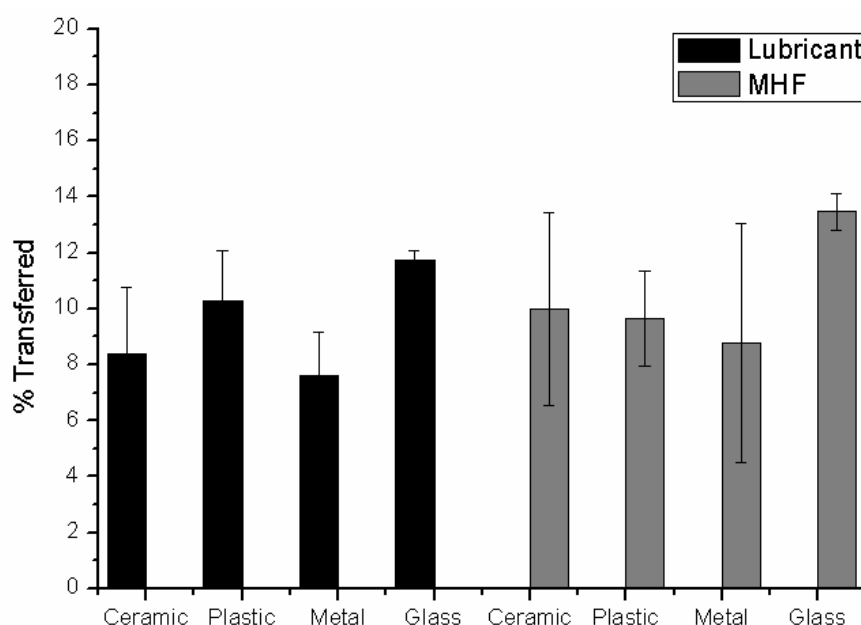


**Figure 72:** Quantitative analysis of MHF and lubricant transfer rates from forensically relevant surfaces through touch contact (error bars represents standard deviation between replicates).



Quantitative studies confirmed transfer efficiency in both semi-solid media. Whilst a two-way ANOVA test determined transfer rates between lubricant and MHF were not statistically significant (P-value = 0.178309), a slightly higher percentage transfer on average across the majority of surfaces selected MHF as the basis for further reagent development. Whilst the use of a gloved finger allowed us to conduct this study within the remit of existing ethical approval, further studies are currently in progress to assess this transfer via skin contact.

### Peptide Sequence Selection

With non-polar hydrocarbon-based MHF chosen as the basis for this reagent, use of a hydrophilic peptide coding sequence would allow for its rapid isolation via a simple liquid-liquid extraction. Amino acid sequence HSSKL was therefore synthesised after GenScript peptide property calculator analysis determined its suitable hydrophilicity through the inclusion of histidine and lysine residues. N-terminal acetylation was also performed to enhance peptide solubility during extraction. This peptide length was chosen such that synthesis would be rapid and inexpensive, while allowing enough variability to ensure unique coding.

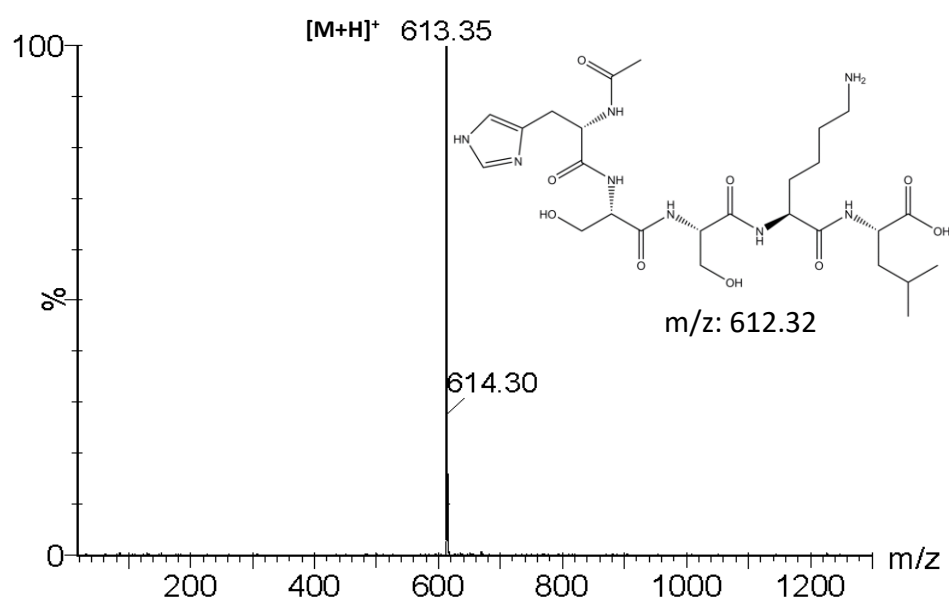


**Figure 73:** Positive ESI-MS spectrum of synthesised peptide Ac-HSSKL and inset: peptide structure and calculated  $m/z$  ratio 612.32.

Additionally, a search of the RCSB Protein Databank yielded no results for this sequence, thus reducing the risk of generating false positive results from naturally occurring peptides. RP-HPLC analysis was performed to check for peptide purity (data not shown) and an analysis via ESI-MS was conducted to confirm that the desired product had been obtained (**Figure 73**). Extraction protocols were subsequently devised with hexane and distilled water selected to isolate the peptide in an aqueous phase and separate the remainder of the non-polar medium prior to further analysis.

### **Peptide Concentration Selection**

With competing interests in designing a reagent that allows for maximum sequence detectability, whilst simultaneously being inexpensive to produce, it is crucial to determine the most suitable concentration of peptide required for successful MS analysis. After confirming identity, 5 mg of synthesised peptide was mixed into MHF (100 mg) and spread on glass slides. Liquid-liquid extraction was conducted on the traces of reagent obtained from primary transfer onto a glove, and the extract was analysed via ESI-MS. All samples and replicates generated positive results with peptides still remaining easily detectable in concentrations reduced to 2.5 mg and even 1 mg (Appendix - **Figure 86**). Based on the results obtained in the transferability studies, following liquid-liquid extraction an aqueous solution of the peptide at a concentration of ~150 µg/ml (corresponding to the lowest amount of peptide employed in the present study) was used for the ESI-MS analysis. Our research group is currently engaged in establishing the lowest amount of peptide that may be added to a reagent in which full detection may be achieved. This is focusing on the application of High Resolution Mass spectrometry, which, in many cases, has detected a number of similar peptides to a femtomolar concentration [468].

## Fluorophore Studies

Ideally, fluorophores incorporated into forensic taggants should allow for easy visualisation as well as an increased resistance to exposed environmental conditions. Rhodamine 110 and AFC, both noted for their fluorescence lifetimes, quantum yield and photostability [173, 180] were therefore investigated as additives for the overall visualisation of the reagent upon transfer. In this study, fluorophores were added independent to peptide concentration to provide end users with more flexibility over how the reagent is applied.

Both fluorophores were mixed in to MHF as stock solutions starting at 10mg/ml concentrations. While all samples displayed an intense emission under appropriate fluorescence microscopy filtration (Appendix - [Figure 87](#)) unexcited formulations still exhibited an obvious visual colouration inappropriate for marking surfaces within a covert scenario. Thus, both solutions were diluted to a concentration of 0.1 mg/ml in which no colour was observed under visible light but fluorescence remained highly detectable. This fluorescence was qualitatively monitored over a period of six weeks and was found to remain detectable.

With appropriate fluorophore concentrations established, Rhodamine 110 was added to a sample of peptide-mixed media to test final reagent performance, before being successfully extracted and analysed by ESI-MS as previously described (Appendix - [Figure 88](#)). Rhodamine is consequently present in the final mass spectrum due to its affinity for the analysed aqueous extraction phase. As an identical fluorophore is added to every formulation of reagent produced, rhodamine presence will not add value to the unique coding system provided by the peptide. However, the detection of a water-soluble fluorophore may infer added confidence that a successful extraction has taken place. Whilst advantageous stability and emission properties selected Rhodamine-110 for use within the scope of this study, any fluorescent compound exhibiting desirable

properties may be used as a replacement detection element, further increasing the versatility of a final reagent for surface application.

### **Stability Studies**

As the majority of forensic taggants are applied to surfaces for extensive periods of time, it is important that coding peptides stored within a reagent remain stable. This is especially pertinent in those that are left within exposed environmental conditions. Samples of peptide-mixed medium were therefore applied once again to aluminium foil, ceramic, plastic and glass, and left without the application of atmospheric or temperature controls (laboratory temperature and humidity:  $23\pm 2$  °C,  $25\pm 5\%$ ) for a period of six weeks before undergoing extraction and analysis at one week intervals. Furthermore, as high coding sequence stability is crucial in the period between surface contact and reagent recovery, the same procedure was repeated on cotton, denim, polyester and leather substrates to simulate typical contact with clothing.

All peptides proved to be detectable over the six week period on all eight surfaces with no evidence of deterioration (Appendix - **Figure 89**). Whilst the scope of this particular study aimed to assess the possibility of peptide breakdown as a result of time, subsequent research examining the effect of temperature and moisture upon reagent persistence is needed to ensure full validation, and is currently being undertaken by our research group. A larger validation study will be able to investigate resistance of the reagent to harsh environmental conditions so that the efficiency of the technique may be fully demonstrated.

### **Conclusion**

We have successfully designed and developed a reagent for the rapid and specific determination of contact transfer arising as a result of criminal activity. When applied to surfaces this reagent becomes virtually undetectable to the naked eye, rendering it particularly useful within covert investigation.

A novel two-step identification system was employed; firstly the area in which the reagent has been deposited is initially visualised through fluorescence excitation, before being subsequently recovered for standard MS analysis to reveal the identity of a unique registered peptide sequence. This process offers extremely rapid results compared to currently available reagents, with recovery, extraction and analysis performed in less than two hours.

Analysis time is further likely to be decreased considering continuing advances in portable MS techniques. Environmental stability of the reagent was also proven over a six-week period. Our research group is currently investigating a number of further refinements to this reagent, including the use of a combination of fluorophores which emit at different wavelengths to confer added discrimination against possible background fluorescence.

This is centred upon the application of compounds emitting in the IR region of the electromagnetic spectrum which offenders, now knowledgeable of UV-based marking, would be unable to detect. While naturally occurring amino acids were used within this study, investigation has been undertaken to examine the benefits of incorporating unnatural or modified peptide sequences. This would not only serve to increase sequence distinctiveness but is also likely to enhance peptide resistance to hydrolytic enzymes present in biological fluids [469].

#### **6.4 Published Article 7: 'Monitoring Criminal Activity through Invisible Fluorescent 'Peptide Coding' Taggants'**

The content of following section was published as an original research article in: **Gooch, J., et al., Monitoring criminal activity through invisible fluorescent 'peptide coding' taggants.** Analytical Chemistry, 2016. 88: p. 4456-4460.

Experimental work was performed by the candidate with assistance from Hilary Goh. The candidate also produced the manuscript. Help with peptide synthesis, as well as access to the Institute of Pharmaceutical

Science research laboratories and HPLC and MS instruments, was provided Dr. Vincenzo Abbate. Dr. Barbara Daniel and Dr. Nunzianda Frascione provided supervisory and technical support throughout the research. Additional materials for this article may be found in the appendix of this thesis ([Section A.3](#)).

#### 6.4.1 Manuscript

**Authors:** James Gooch,<sup>a</sup> Hilary Goh,<sup>b</sup> Barbara Daniel,<sup>a</sup> Vincenzo Abbate,<sup>c</sup> and Nunzianda Frascione. <sup>a\*</sup>

**Authors Address:** a) Analytical and Environmental Sciences Division. King's College London. 150 Stamford Street. London, UK. SE1 9NH, b) Department of Biological Sciences. National University of Singapore. 14 Science Drive 4. Singapore. 117543, c) Institute of Pharmaceutical Science. King's College London. 150 Stamford Street. London, UK. SE1 9NH.

**Abstract:** Complementing the demand for effective crime reduction measures are the increasing availability of commercial forensic 'taggants', which may be used to physically mark an object in order to make it uniquely identifiable. This study explores the use of a novel 'peptide coding' reagents to establish evidence of contact transfer during criminal activity. The reagent, containing a fluorophore dispersed within an oil-based medium, also includes a unique synthetic peptide sequence that acts as a traceable "code" to identify the origin of the taggant. The reagent is detectable through its fluorescent properties, which then allows the peptide to be recovered by swabbing and extracted for ESI-MS analysis via a simple liquid-liquid extraction procedure. The performance of the reagent in variable conditions that mimic the limits of a real world use are investigated.

#### Introduction

Continuing efforts to reduce the substantial costs of crime on society have in recent years produced a number of highly effective criminal prevention

technologies. The invention of forensic ‘taggants’ is a successful example of such advances. Taggants are defined as materials that may act as a means of physically or chemically marking an item in a way that allows it to become uniquely identifiable [405]. Usually consisting of three molecular components, taggants will include: a ‘coding’ element (to infer uniqueness in the taggant), a system that allows the taggant to be visually detected and a medium where these molecules are dispersed.

There are largely four forensic purposes for such materials. The first attempts to combat counterfeiting activities via the addition of a taggant to products (medicines, bank notes, official documents, etc.) to signify that they are of a genuine origin [404]. The second aims at marking valuable property (vehicles, electronic items) to associate them with a particular owner and discourage theft [413]. The third involves the surreptitious addition of taggants into illicit substances (illegal drugs, explosives), so that their distribution or use may be monitored by law enforcement agencies [402]. The last comprises the covert transfer of taggants to individuals during criminal activity in order to link them to a specific offence (e.g. handling firearms, trespassing) [412]. The physical nature of a taggant reagent will be highly dependent on which of the above purposes it is required. For example, taggants employed in covert operations should be invisible to the naked eye, to avoid undesired detection by the offenders [413]. The medium of each taggant will also vary depending on whether it needs to be easily transferred to an individual or remain anchored upon the product it is marking [413]. Only the coding element remains largely consistent across all tagging purposes.

One of the most popular methods to obtain this taggant coding is through the inclusion of unique DNA markers. Companies such as Applied DNA Sciences, Obiex and SelectaDNA produce taggants containing either botanically derived or synthetic DNA oligonucleotides. The specific sequence of these oligonucleotides is then registered to a particular

owner via an internal database [406]. When required, the taggant may be recovered to extract and 'match' DNA to the owner's information. Whilst DNA taggants have been shown to decrease the number of Cash and Valuables in Transit (CViT) offences [406], limitations in their analysis have been identified. The extraction, amplification and sequencing methods employed to isolate and match DNA are expensive and time consuming. Moreover, the labile nature of DNA has raised significant concerns over the general stability of DNA taggants [445]. Research into their use in monitoring fuel adulteration determined that short sequences of DNA within taggants, had poor stability and were often susceptible to erroneous identification [444].

Another recently emerging method of encoding focuses on the use of varying trace elements to identify taggants. Reagents produced by the UK manufacturer Smartwater, contain a number of rare elements that are combined in unique formulations, allowing each taggant to be registered against a specific owner ID. After a reagent is detected (via the use of an incorporated fluorescent dye), laser ablation inductively coupled plasma mass spectrometry (LA-ICP-MS) is used to determine the individual formulation of the taggant and the owner that it is registered to (once again via internal database) [405]. However, much like DNA-based coding systems, these tracer taggants are once again limited in their analysis. The use of multiple elements within a single taggant carries the potential of the formulation being incompletely recovered, which could then lead to erroneous identification. This problem stems from the differing transfer rates and stability of each individual tracer component, resulting from their chemical differences.

The development of a forensic taggant that is stable and can be rapidly and completely recovered is therefore critical to advancing crime reduction. In light of this, our research group recently suggested a novel 'peptide coding' reagent (or peptide taggant) as an alternative to inefficient taggant analysis procedures [456]. This reagent has been



designed to be covert and transferrable so that it may be used to mark an individual or object during criminal activity without the knowledge of the offender. Like the majority of taggants, our reagent comprises three distinct components. The base medium consists of a mixed hydrocarbon formulation (MHF) which is easily transferred to persons or clothing. Detection is achieved by Rhodamine-110 fluorophores, added in such a concentration as to make the taggant invisible under normal lighting conditions but highly fluorescent upon excitation by an appropriate light source.

The specificity of this reagent (and main advantage over currently available taggants) is derived from the insertion of a unique peptide, where the amino acid sequence acts as an identifiable code for that particular taggant. The wide variety of natural and unnatural amino acids available ensures that the peptide may be sufficiently individual, without extensive length. Once the reagent is transferred as a result of criminal activity, it may be easily and rapidly recovered. First, areas of taggant presence may be indicated through fluorescence excitation, allowing complete recovery of the reagent by targeted swabbing. The peptide may then be isolated from the oil-based medium and swab via simple liquid-liquid extraction. The mass-to-charge ratio of the amino acid sequence is then revealed via Electrospray Ionization Mass Spectrometry (ESI-MS), identifying the particular taggant.

Whilst developed as an initial proof of concept, this taggant may have the potential to be used within criminal investigation to establish evidence of primary (object-to-person); and possibly even secondary (object-to-person-to-object) contact transfer. This work therefore involves a comprehensive investigation into the ability of peptide coding reagents to operate effectively within a real-world setting. Significant examination of the transfer, detection, recovery and stability of multiple peptide reagents was undertaken to demonstrate their advantages over currently available forensic taggants.

## Experimental Section

### Peptide Synthesis

Peptides Ac-KQQSP-NH<sub>2</sub> (Sequence 1), Ac-HSSKL-COOH (Sequence 2), and Ac-hsskl-COOH (Sequence 3) were manually synthesized by Fmoc-Solid Phase Peptide Synthesis. NovaPEG rink amide (Merck Chemicals Ltd, UK) and 2-chlorotritylchloride (Sigma Aldrich, UK) resins were used to prepare sequences 1 and 2-3 respectively. Resins were swollen in dimethylformamide (DMF) inside empty fritted polypropylene tubes for 30 minutes prior to coupling. All amino acid coupling steps for sequence 1 were performed using 4 equivalents of Fmoc amino acids with DIPCDI and Ethyl (hydroxyimino)cyanoacetate (Oxyma) in DMF in a molar ratio of 1:1:1 of amino acid, DIC and Oxyma, respectively. The first coupling step for sequences 2-3 was performed using 1 equivalent of Fmoc amino acid with 5 equivalents of N,N-Diisopropylethylamine (DIPEA) in dichloromethane (DCM).

Subsequent coupling steps were performed using the same procedure utilised in the assembly of Sequence 1. Coupling reactions were allowed to take place for 1 hour with successful conjugation monitored by the picrylsulphonic acid test. After coupling, Fmoc de-protection of all amino acids was achieved via treatment with 20% (v/v) piperidine in DMF for 30 minutes and confirmed by the picrylsulphonic acid test. Impurities and excess reagents were removed at each stage via multiple washes using DCM, and DMF. The N-terminus of each peptide was acetylated using ten equivalents of acetic anhydride and twenty equivalents of DIPEA in DMF for 1 hr. Resins were lastly treated with a solution of Trifluoroacetic acid (TFA): distilled water: phenol: thioanisole (TA): triisopropylsilane (TIPS): 2,2'-(Ethylenedioxy)diethanethiol in a 90:5:5:5:2.5:2.5 molar ratio for 3 hrs at room temperature to remove the completed peptides from the solid support. The filtrate was then concentrated under nitrogen at 40 °C before the addition of 10 equivalents of ice cold diethyl ether to precipitate the peptides. The wash and precipitation process was repeated several

times before the final obtained peptide pellets were freeze-dried for 24 hrs. The identities of the synthesized peptides were confirmed using a Waters/Micromass (Manchester, UK) ZQ ESI-mass spectrometer in positive ionisation mode prior to use.

### **Experimental Conditions**

The effects of four experimental conditions: i) surface material, ii) temperature, iii) humidity, and iv) fluorophore addition, on reagent stability were investigated. For monitoring the effect of surface material, peptide sequences 1-3 were mixed into MHF medium (Vaseline, UK) at a concentration of 2.5:100 mg of peptide:medium. Mixtures containing sequence 1 and 3 were then applied in 40 mg deposits onto 10 different surfaces (ceramic, glass, plastic, aluminium foil, wood, paper, denim, polyester, leather, and cotton) cut into 2 cm x 2 cm squares. The mixture in sequence 2 was applied in the same method to surfaces of wood and paper (as the stability of this sequence on the other 8 surfaces was already proven within the previous proof of concept study). The surfaces were then left exposed to standard laboratory conditions (temperature and humidity:  $23\pm 2$  °C,  $40\pm 5\%$ ), constantly monitored using a data logger. Liquid-liquid extractions were then performed to isolate the peptides for ESI-MS analysis at time points of two weeks, four weeks, and six weeks for a total period of six weeks.

For experimental condition studies ii), iii), and iv), the same concentration of peptide-MHF medium was applied to glass slides and exposed to their respective conditions. The effect of temperature was assessed via incubation of slides at both 4 °C and 39 °C and extracted at time points of six hours, 24 hours, one week, and six weeks. For the effect of humidity, surfaces were left in containers of 70% and 90% (as monitored by a hygrometer) and were once again extracted at the same time points as the temperature study. Humidity containers were prepared by enclosing wet paper towels within plastic boxes.

The effect on fluorophore presence on peptide detection was observed through the addition of Rhodamine-110 (Sigma Aldrich, UK) to peptide-MHF at a concentration of 0.25:100 mg fluorophore:peptide-medium. This mixture was then applied in 40 mg deposits on glass slides, which were then exposed to the standard, temperature and humidity conditions previously investigated. Extractions of fluorophore-peptide-MHF reagent were undertaken at time points of three weeks and six weeks for a total period of six weeks.

### **Taggant Extraction and Analysis**

Extraction surfaces were placed into a 30 ml multipurpose container (Greiner Bio-One, UK) before the addition of 1 ml of hexane. Samples were vortexed for 1 minute and the surfaces were removed using sterile forceps prior to the addition of 0.5 ml of distilled water. The samples were vortexed again and allowed to settle before the aqueous phase was removed into a fresh container via pipette. The original organic phase was then further extracted with an additional 0.5 ml of distilled water before both aqueous layers were pooled together. Counter extraction against the pooled aqueous layers was next performed with 1mL of hexane. The final aqueous layer was then isolated into an Eppendorf tube before the addition of 0.1% v/v Formic Acid to enhance ionisation. ESI-MS analysis of the samples was conducted using a Waters ZQ micromass 2000 mass spectrometer in positive ionization.

### **Casework Application**

A thin layer of peptide reagent (containing sequence 2) was spread across a 25 x 25 cm glass tile to mimic a real-world application to a known surface. A transparent latex glove worn over the hand (with the glove pre-weighted) was then used to contact the surface at a standardised force of ~20 N (monitored by analytical balance). Transferred reagent was visualised using a Crime-lite handheld light source (Foster and Freeman, UK) at an excitation wavelength of 460-510

nm and a supplied 495 nm viewing filter. The glove was then reweighed to assess the amount of taggant transferred upon physical contact.

### Depletion Series

To establish the overall sensitivity of the reagent and determine its persistence after multiple contact transfers, a depletion series was prepared. A thin layer of peptide reagent (containing sequence 2) was once again spread over a glass tile before being contacted by a single gloved finger at a standardised force of ~10 N. A series of contacts after the initial reagent transfer were then performed by successively touching either 1, 2, 3, 4 or 5 clean glass slides with the glove. A sterile cotton swab of the entire surface of the finger was used to collect any taggant remaining at the end of each depletion series. Peptide sequence 2 was lastly extracted from all of the swabs and analysed using the methods previously described.

## Results and Discussion

### Peptide Synthesis

Three different peptides were used to demonstrate the flexibility of the reagents coding system. These sequences were chosen due to their hydrophilicity, allowing them to be easily isolated from the non-polar MHF medium by simple liquid-liquid extraction. The properties of each peptide, including hydrophilicity, were derived from GenScript's peptide property calculator ([Table 19](#)). The sequences were also ensured to be non-naturally occurring using UniProt's BLAST function, thereby reducing the possibility of generating false positive results from ubiquitous environmental peptides.

**Table 19:** Peptide characteristics obtained from Genscript's property calculator

Peptide Sequence	GenScript PPC
1: Ac-KQQSP-NH <sub>2</sub> (L-amino acids)	MW = 627.69, attribute = basic (hydrophilic).
2: Ac-HSSKL-COOH (L-amino acids)	MW = 612.68, attribute = basic (hydrophilic).
3: Ac-hsskl-COOH (D-amino acids)	MW = 612.68, attribute = basic (hydrophilic)

Developing a coding system that is able to remain stable and recoverable over extended periods of time is a crucial aspect of taggant design. We therefore decided to explore the effect of a number of modifications on our peptide sequences, with the ideal aim of maximising code detection post taggant recovery. N-terminal acetylation was carried out on all peptides to increase resistance to degradation by aminopeptidase activity [214]. Further protection against enzymatic destruction was conferred by the C-terminal amidation [470] of sequence 1 (Ac-KQQSP-NH<sub>2</sub>) and the introduction of D-amino acids in peptide sequence 3 (Ac-hsskl-COOH). ESI-MS analysis was used to confirm the identity of the synthesized products, which all exhibited correct masses (Appendix - **Figure 90**)

## Experimental Conditions

With popular uses in marking vehicles, objects, fabrics and premises, the nature of the surface on which a taggant may be applied can be highly variable. It is consequently crucial that newly developed taggants demonstrate sufficient robustness to be detected and identified over extended periods of time, without being affected by the material on which they are deposited. The stability of all three peptide-MHF formulations was therefore monitored by their application on 10 different surfaces routinely encountered during forensic casework.

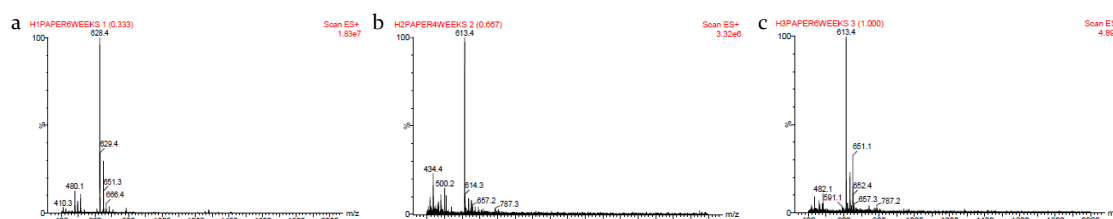


**Figure 74:** ESI-MS spectra of a) peptide sequence 1: Ac-KQQSP-NH<sub>2</sub>, (theoretical [M+H]<sup>+</sup> m/z ratio = 628.34) b) peptide sequence 2: Ac-HSSKL-COOH (theoretical [M+H]<sup>+</sup> m/z ratio = 613.33) and c) peptide sequence 3: Ac-hsskl-COOH (theoretical [M+H]<sup>+</sup> m/z ratio = 613.33) reagent samples extracted six weeks after application to paper. Similar results were seen on all other surfaces

All taggants were then left in standard laboratory conditions (temperature and humidity: 23±2 °C, 40±5%) before being extracted at several time

points over a period of six weeks. **Figure 74** shows the mass spectra of analysed reagent samples containing peptide sequence 1, 2 and 3 from paper at the 6-week time point. The same results were achieved across all peptide, surface and time combinations, with no observable reagent degradation (Appendix - **Figure 91-93**)

Another facet of forensic taggant application that is highly variable is the environmental conditions to which a reagent may be exposed [471]. By marking items both outside and in sheltered locations, taggants are often subjected to a wide range of temperatures and humidities. However, the effect of such conditions on the detection and identification a taggant should ideally remain negligible. To establish the environmental resistance of our peptide coding reagent, formulations containing sequences 1-3 were deposited on glass slides and incubated over six weeks in temperatures of 4°C and 39°C or in humidity's of 70% and 90%. Extraction and analysis of the reagents at various time points demonstrated that all peptides remained detectable despite incubation conditions, with no differentiation in the achieved mass spectra being displayed between samples (Appendix - **Figure 94-95**)

The foremost purpose of Rhodamine-110 addition to the peptide-MHF formulation is to allow taggants to be detected via fluorescence emission after transfer. This fluorescence not only quickly establishes evidence of contact between an object and a suspect but may also be used for a more targeted swabbing by indicating where identifying peptides are likely to be present. Moreover, as water-soluble Rhodamine-110 is co-extracted with peptides into the same aqueous phase, a dual detection of the reagent is provided by the presence of both fluorophore and peptide ion peaks in the ESI-MS spectrum.

To establish this dual-detectability, three final fluorophore-peptide-MHF formulations for each of the peptide sequences utilised were prepared and deposited on glass slides in the same manner previously described. Slides were exposed over six weeks to the standard laboratory,

temperature and humidity conditions already explored and were once again extracted and analysed at a number of time points. **Figure 75** displays both fluorophore and peptide components detected by ESI-MS after extraction of final reagent (containing peptide sequence 1) after six weeks of standard laboratory exposure. In all cases, similar results were achieved regardless of peptide or environmental condition, with no observable fluorophore or peptide degradation (Appendix - **Figure 96-98**).

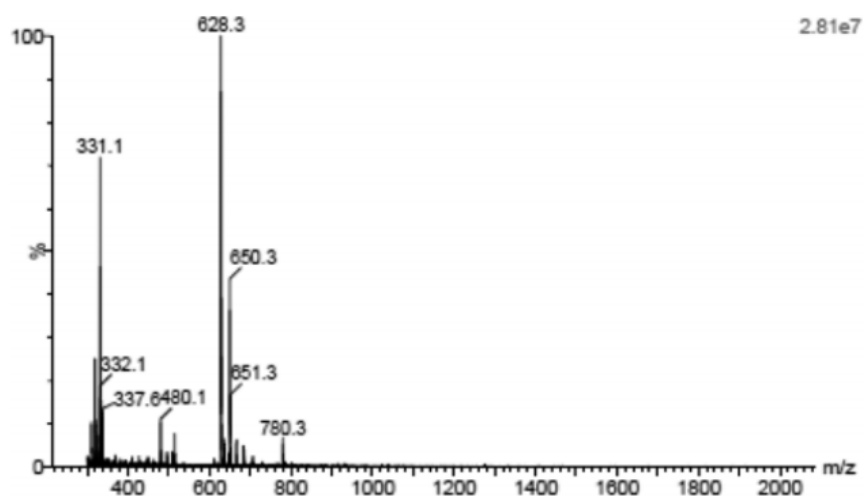


**Figure 75:** ESI-MS spectrum of Sequence 1: Ac-KQQSP-NH<sub>2</sub> (theoretical [M+H]<sup>+</sup> m/z ratio = 628.34, theoretical [M+Na]<sup>+</sup> m/z ratio = 650.32) and Rhodamine-110 (theoretical [M+H]<sup>+</sup> m/z ratio = 331.11) extracted from full reagent samples applied to glass slides and incubated for six weeks in standard laboratory conditions.

### Casework Application and Depletion Series

To successfully operate in the field, touch contacts must result in enough fluorophore and peptide transfer to ensure taggant visualisation and identification respectively. Demonstration of the reagents practical use in a real world scenario was therefore achieved by applying a thin layer of fluorophore-peptide-MHF formulation over a large glass tile, which was subsequently contacted by a transparent glove worn over the hand. As expected, the reagent remained imperceptible under natural light but was easily viewed upon the hand after illumination with a portable light source (**Figure 76**). Approximately 0.44 mg of taggant was transferred to each cm<sup>2</sup> of the glove's surface.





**Figure 76:** Peptide coding reagent successfully transferred upon physical contact. Left: prior to visualization. Right: fluorescence emission upon excitation.

Whilst this rate of transfer may be considered ideal after an initial contact, the amount of taggant recovered in a practical setting may actually be far less, depending upon the subsequent activity of the offender. For example, it is possible that the reagent may be removed if a suspect contacts other surfaces after touching a marked object, thereby diminishing the amount of peptide available for analysis. Designing a taggant to persist on an individual even after multiple contacts is therefore important. A depletion series was created to measure the overall retention of our reagent by contacting the tile previously prepared with a gloved finger. Taggant was then collected and recovered from the entire surface of the finger by direct swabbing and liquid-liquid extraction respectively. This process was then repeated but with additional secondary contacts on clean glass slides (increasing from 1 to 5 contacts) prior to reagent recovery. ESI-MS analysis successfully detected the presence of both peptide and fluorophore ion peaks within all samples, establishing the excellent persistence of our reagent (Appendix - **Figure 99**).

## Conclusions

The ability of a novel 'peptide coding' taggant to monitor contact transfer during criminal activity has been successfully established. The reagent is invisible to the naked eye but highly fluorescent when excited by an appropriate light source. If recovered from an individual, this reagent has the power to physically link a person to a specific object or offence

through uniquely identifying amino acid sequences. The high transferability of the employed medium allows these peptides to persist on a person even after five additional contacts with other surfaces.

Remaining detectable and recoverable over a period of six weeks, our developed peptide taggant has proven to be successfully stable and resistant to all variable experimental conditions. A greater degree of confidence can therefore be given in the taggants efficacy to operate over extended periods of time on different surfaces and in a range of environments.

This reagent promises significant advantages over currently available forensic taggants; liquid-liquid extraction allows coding sequences to be rapidly isolated with little expense. Taggant analysis via ESI-MS is also significantly less time consuming than sequencing techniques used in DNA-based taggants and may be completed within 1 hour of reagent recovery. Continuing advances in portable mass spectrometry technology are likely to result in this time being further reduced, by allowing analysis to be performed at the point of taggant discovery.

Whilst not explored further within this study, this taggant was designed with a high intrinsic flexibility so that it may be easily adapted for application in a variety of crime reduction strategies. This is likely to centre on the substitution of the reagents individual components to suit a specific purpose. For example, the replacement of Rhodamine-110 with a near-infrared fluorophore may provide enhanced contrast against certain coloured or auto-fluorescent surfaces [472]. The discriminatory power of the taggants code may also be further increased by the use amino acids that feature unnatural modifications.

Whilst this reagent was developed for observing physical contact transfer during criminal activity, many taggants are designed to remain immobile upon the object they mark. Our peptide coding system may also be utilised in such an application by a simple change of dispersal media.

# **Chapter 7**

## **Discussion and Conclusion**

## 7.1 Biosensors

Biosensors are fast becoming the molecular detection methods of choice within a variety of analytical disciplines, including pharmaceutical discovery, agricultural quality control and biomedical diagnostics [473-475]. Research efforts in this area have often focused on the development of rapid, low-cost and simple to use biosensing assays that can be utilised for 'in-field' analysis (such as 'point-of-care' testing of hospitalised patients or continuous monitoring of environmental samples [476]). Despite this, only a small number of research groups have explored the use of biosensors for the detection and identification of targets that are relevant to forensic investigation. Furthermore, the vast majority of previously reported biosensors (forensic or otherwise) have largely been designed for the analysis of targets within solution, with limited explorations into the detection of analytes *in situ*.

Initial work in this project was therefore conducted to determine which biosensing transduction mechanisms (with specific emphasis on fluorescence signal outputs) are likely to demonstrate the most potential as methods for the visualisation and attribution of body fluid stains left behind at crime scenes (**Chapter 2**). This was first achieved through an in-depth review of fluorescent biosensors previously reported for use in a variety of comparable *in situ* applications (such as detection of wound-infecting bacteria or biofilms on historic window glass [137, 142]). This review subsequently identified several promising sensing transduction mechanisms, which were based on: 1) the enzymatic digestion of fluorescently-labelled substrates, 2) the competitive displacement of quenched ligands or 3) fluorophores sensitive to changes in local environment.

Four commercial biosensor assays based on these chosen transduction methods were then evaluated on their performance within a forensic context, by examining the ability of each sensor to detect relevant analytes deposited *in situ* on a series of surfaces commonly encountered

within criminal casework. Varying degrees of success were demonstrated by each assay during different stages of testing. The FluoReporter® Biotin Quantitation Assay Kit (intermolecular FRET) was shown to be the most sensitive assay during application to analytes present on glass slides (being able to detect concentrations of biotin as little as 100 ng/ml), but displayed poor performance in forensic surface testing due to reagent absorption by porous surfaces.

Conversely, two biosensors reliant on the enzymatic hydrolysis of fluorescent substrates, the EnzChek® Protease/Peptidase and EnzChek® Ultra Amylase assay kits, were able to detect analytes across all testing phases. These results prompted further investigations into the use of fluorogenic peptide substrates for the *in situ* analysis of body fluid deposits based on digestion by intra-fluidic protease enzymes (as explored within [Chapter 3](#)). The Quant-iT™ PicoGreen® dsDNA assay kit, an environmentally-sensitive DNA detection dye, displayed poor performance during glass slide testing as a result of reagent-analyte immiscibility and was excluded from all further studies.

Importantly, all biosensors selected for further study were found to have no effect on downstream DNA profiling processes after addition to human biological fluids. Such results demonstrate potential for the integration of biosensor technologies within routine casework practices without detrimental effects to the recovery of genetic material contained within biological fluid stains (although a much more comprehensive validation of developed sensors is likely to be required prior to operational deployment).

However, it must be noted that any comparisons made between the fluorescent transduction mechanisms utilised within this study are somewhat limited by both the variability of measured analyte concentrations and the composition of assay reagents. Concentration ranges used for testing were determined based upon the amount of target that could be reasonably purchased. A lower range of 100-0.001 µg/ml

DNA was therefore employed to assess the performance of the Quant-iT™ PicoGreen® dsDNA assay kit compared to other biosensors, which were all tested against relevant analytes at concentrations between 10-0.0001 mg/ml (although these amounts are also not consistent in terms of molarity). This target variation, whilst largely impossible to control, is likely to have some impact on the perceived performance of this sensor and the decision to exclude it from further testing.

The specific preparation of commercial assay reagents is also likely to affect the performance of studied sensors. The poor detection ability demonstrated by both the Quant-iT™ PicoGreen® dsDNA and FluoReporter® Biotin Quantitation assay kits (as a result of reagent immiscibility and surface absorption) may be a result of the solvent/buffers in which sensing components are dissolved, rather than the biosensors themselves. In an ideal experimental set-up, such solutions would be standardised, however this could not be achieved within the scope of this study, as all assays are procured as pre-dissolved stock solutions.

This study represents the first investigations into the use of biosensor technology for the forensic detection and identification of biological fluids. Fluorescent signal transduction mechanisms demonstrating the most promise towards fluid-specific sensing were identified and were subsequently confirmed to possess the ability to detect relevant analytes *in situ*.

## **7.2 Fluorogenic Substrates**

With promising *in situ* detection performance demonstrated across all surfaces by both the EnzChek® Protease/Peptidase and EnzChek® Ultra Amylase assay kits, initial efforts in the development of biosensing assays for the analysis of biological fluid stains focused on the use of enzymatic substrates.

Whilst a myriad of such substrates are already commercially available, many are unlikely to offer any additional specificity advantages over current biological fluid testing strategies. For example, the SensoLyte® MFP Acid Phosphatase Assay Kit, a fluorogenic substrate available from the company AnaSpec, may potentially be used for the detection of acid phosphatase enzymes in seminal fluid stains. However, consisting of a simple phosphate group coupled to the fluorophore 3-O-Methylfluorescein [477], this substrate is likely to be cleaved by other phosphatase enzymes present within the majority of body tissues [478]. Specific emphasis was therefore placed on the application of peptide substrates, which offer increased enzymatic selectivity as a result of sequence-specific hydrolysis [479].

An initial search of commercial peptide substrates that could potentially be used for the forensic detection of intra-fluidic proteases yielded MU-HSSKLQ-AFC, a fluorogenic substrate specific to PSA [193]. Successful 'turn-on' emissions were generated by MU-HSSKLQ-AFC in response to dilutions of seminal fluid (up to 1:1000) both in solution and deposited on glass slides. This substrate was further able to detect semen present on a selection of surfaces commonly encountered within forensic casework and was also shown to have no effect on DNA profiling processes.

With the ideal aim of developing a multiplex fluorogenic substrate assay for the simultaneously sensing of multiple proteolytic targets, efforts were then made in the synthesis of peptide substrates employing fluorophores emitting in different regions of the visible spectrum, starting with the xanthene-based dye Rh-110. Whilst not described within the contents of **Chapter 3**, a series of unsuccessful attempts to conjugate peptides to Rh-110 in solution were first conducted. These involved the direct coupling of a peptide AC-HSSKLQ-COOH to acetylated Rh-110 through the EDC/pyridine chemistry reported by Leytus *et al.* [175] (**Figure 77a**), as well as transformation of Rh-110 amines to more reactive azide groups by incubation with tert-butyl nitrite (*t*BuONO) and azidotrimethylsilane

(TMSN<sub>3</sub>), following Barral *et al.* [480] (**Figure 77b**). However, neither of these procedures resulted in the production of viable fluorophore-peptide products. In the case of in solution peptide coupling, this lack of success may be attributed to the poor nucleophilicity of Rh-110 aromatic amine groups, which often leads to inefficient peptide-fluorophore acylations [211]. Attempts at Rh-110 azide formation instead resulted in the formation of several unidentifiable by-products (as observed by ESI-MS analysis which could not be separated from the transformed Rh-110 molecule via preparative RP-HPLC).

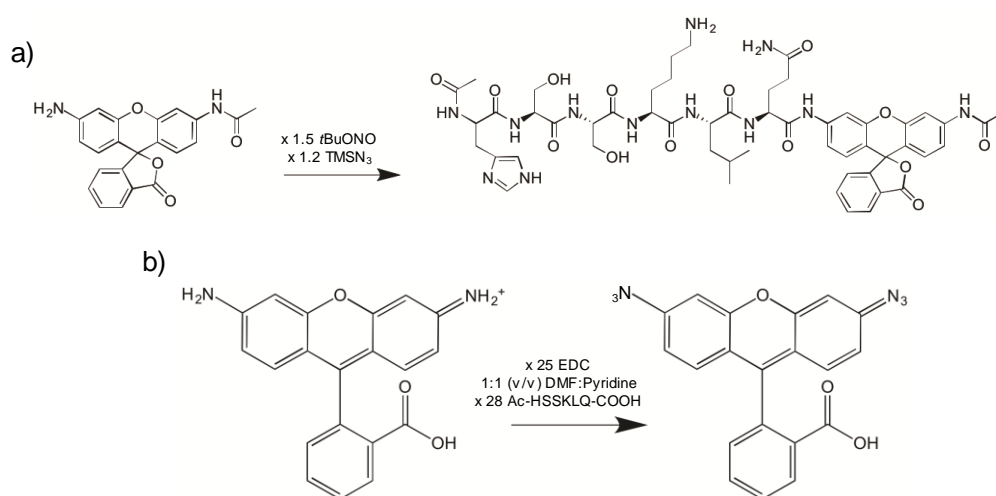


**Figure 77:** Schemes of unsuccessful Rh-110 substrate development attempts: a) Rh-110 is coupled directly to peptide Ac-HSKKLQ-COOH in solution after incubation with EDC/pyridine, b) Rh-110 amine groups are transformed into azides through incubation with *t*BuONO and TMSN<sub>3</sub>.

A novel solid-phase synthesis route was therefore devised, which subsequently led to the successful construction of two Rh-110-based substrates specific to PSA and KLK8 (for the analysis of semen and saliva respectively). This route not only allowed for the production of Rh-110-based substrates in higher quantities, due to the ability to incubate immobilised fluorophores with large amino acid excesses, but also reduced substrate preparation time by preventing the need for extensive reaction purification steps. Both of the substrates prepared using this route were able to detect relevant purified protein and whole biological



fluid targets (both in solution and *in situ*), and were also found to have no detrimental effects on downstream DNA profiling.

This synthetic route was further employed the production of a peptide substrate utilising the fluorophore CV towards the detection thrombin within whole blood. This fluorophore was chosen for use within this assay due to its emission outside the broad absorbance spectrum of haemoglobin (**Figure 78**). Whilst fluorescence signals were observed from this substrate in response to different concentrations of purified thrombin protein within solution, both blood and plasma samples could not be detected.

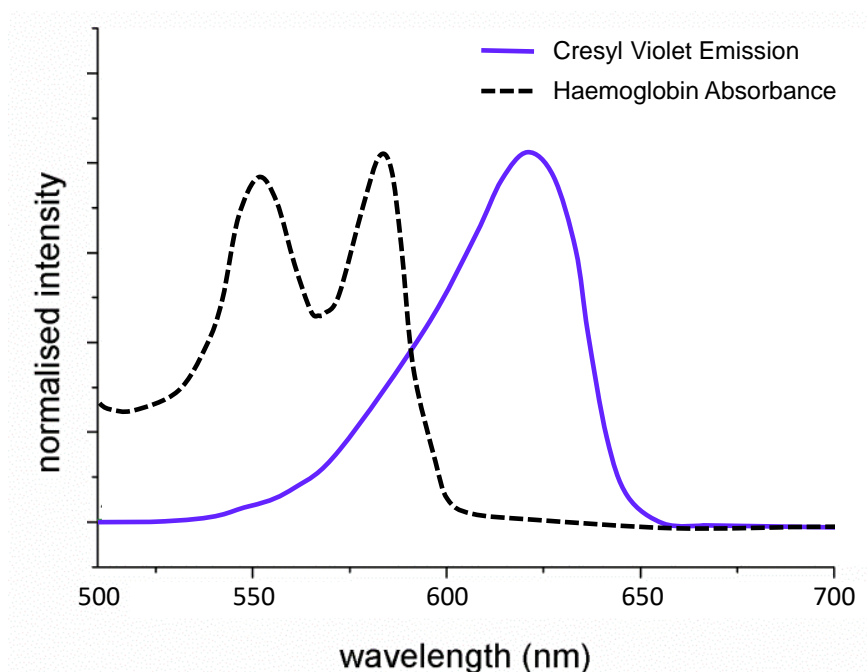


**Figure 78:** Normalised spectral overlap of haemoglobin absorption compared to CV emissions.

Despite the difficulties encountered in the construction of CV-based sensors, the work reported within **Chapter 3** still signifies the first successful application of fluorogenic peptide substrates to the forensic detection of biological fluids. It is further hoped that the novel SPSS routes developed as part of this study may be used for the future synthesis of substrates towards other forensically-relevant protease targets.

### 7.3 Immunosensors

In **Chapter 4**, attempts were made into adapting the displacement-based FRET fluorescence transduction mechanism of the FluoReporter® Biotin Quantitation Assay Kit towards the detection of intra-fluidic protein targets. This was achieved through the use of antibody recognition moieties specific to PSA, rather than the biotin-avidin binding interactions exploited by the commercial assay. These anti-PSA antibodies were conjugated to highly fluorescent QDot nanoparticles, which were utilised for the purpose of emission signalling. An initial quenching of QDot fluorescence was then achieved through the moderate binding of a quencher-labelled peptide sequence consisting of amino acids responsible for antibody-PSA interaction. Immunosensor complexes displayed immediate restorations of emission signals upon the addition of purified PSA protein, indicating successful displacement of quenching ligands by higher affinity targets.

A follow-up to this study was recently conducted in 2017 as part of a three-month research project conducted by a student on the King's College London Forensic Science MSc programme. In this project, a similar immunosensor complex was constructed using antibody recognition elements specific to Mucin 5B (MUC 5B), a protein present at high concentrations within human saliva [481]. Modifications to the original PSA immunosensor design were also made in the use of QDot™ nanoparticles emitting at 525 nm, with black hole quencher-1 (BHQ-1) employed for emission quenching (with absorbance of fluorescence between 480-580 nm).

However, incubation of the antibody-QDot complex with BHQ-1 ligands failed to achieve the same degree of quenching observed in previous PSA immunosensor studies (**Figure 79**). Such results may be attributed to the increased length of the amino acid sequence used for moderate binding (BHQ-1-RNREQVGKF-CONH<sub>2</sub>), which may prevent proximity-based FRET effects. Furthermore, no fluorescence emission signals were

exhibited by antibody-QDot complexes upon the addition of MUC5B protein. A more comprehensive characterisation of factors affecting the performance of this specific immunosensor design is therefore needed.

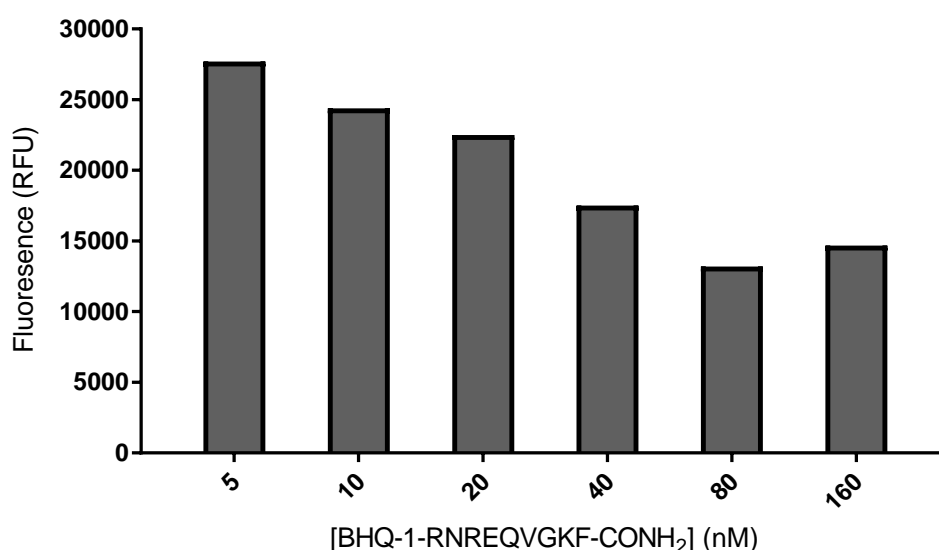


**Figure 79:** Fluorescence emissions of anti-MUC5B antibody-QDot conjugates after incubation with quencher-labelled peptide.

Nevertheless, it must be noted that this particular sensing format represents the first of its kind to be reported. It is hoped that the increased analytical specificity gained from the use of antibody elements for target recognition will make this type of assay format an attractive option in the future development of biosensors for molecular detection purposes (both within and outside of forensic analysis).

## 7.4 Aptasensors

Efforts towards the development of a second FRET displacement-based sensor utilising ssDNA aptamers as target recognition moieties are also described within **Chapter 5**. In this study, three fluorescently-labelled aptamer sequences specific to thrombin, PSA and lysozyme were used to construct a multiplex aptasensing complex for the simultaneous detection of blood, semen and saliva respectively.

This was achieved through the initial absorption of sequences to GO nanosheets (as a result of  $\pi$ - $\pi$  stacking interactions), leading to the quenching of conjugated fluorophore emissions via energy transfer

processes similar to FRET. A series of sensor optimisations were also performed to determine the buffer conditions and GO-aptamer ratios required to achieve maximum fluorescence quenching. Whilst appropriate restorations of fluorescence signal were observed in response to the incubation of single graphene-quenched aptamers with relevant purified proteins, multiplex analysis of both protein and whole fluid targets later demonstrated that such signals are largely due to the non-specific desorption of all ssDNA from the GO surface in the presence of general protein molecules.

Further attempts to increase the analytical specificity of the multiplex aptasensor complex were then conducted through the selection of novel aptamer sequences towards whole human sperm cell targets. A total of 14 rounds of selection were performed following a previously reported Cell-SELEX protocol [289], which was modified to include an additional step for the isolation of sperm cells from human seminal fluid. Selection progress was monitored between SELEX rounds using flow cytometry analysis, with NGS performed on enriched aptamer pools in order to elucidate the sequence structure of potential binding ligands. Whilst relatively unexplored for use within SELEX studies, NGS analysis was chosen for use in this work for its ability to generate greater sequence information from enriched aptamer pools, with the additional possibility of identifying promising aptamer candidates within a reduced number of selection rounds. A custom bioinformatics workflow was also developed using Galaxy for the automated processing of NGS datasets. This data revealed several promising aptamer candidates that may find use not only within GO displacement-based aptasensing assays for the detection of biological fluids, but also within other areas of forensic analysis (such as the separation of sperm and epithelial cell components within body fluid mixtures).

Although not discussed within the contents of [Chapter 5](#), an initial investigation into the application of a thrombin-specific molecular aptamer

beacon towards the detection of whole blood was also conducted. Originally reported by Hamaguchi *et al.* [145], this sensor consisted of a thrombin binding sequence able to undergo self-hybridization as a result of the 5' extension with nucleotides complementary to 3' bases. Such complementarity allowed this sequence to form a stable 'stem-loop' structure that may be used to bring terminally-labelled donor and acceptor fluorophores within the proximity required for FRET. Subsequent incubation with thrombin disrupts this hybridization, relieving quenching effects and generating observable fluorescence emissions (**Figure 80**).

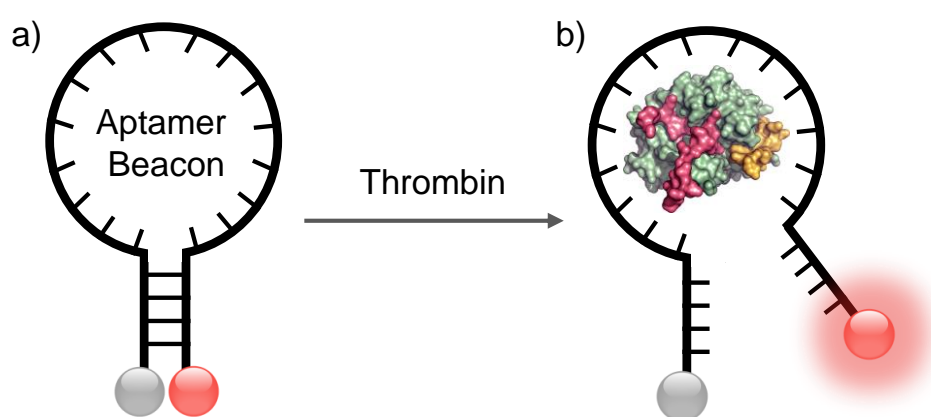


**Figure 80:** Thrombin molecular aptamer beacon design: a) the emission of terminally-labelled donor fluorophores is quenched by acceptor dyes through proximity-based FRET as a result of beacon self-hybridization, b) thrombin-aptamer binding results in a disruption of the beacon's 'stem-loop' structure, separating fluorophores and restoring fluorescence.

To overcome the possible absorption of donor fluorophore emissions as a result of haemoglobin absorbance (as seen in **Chapter 3**), modifications to the reported sensor were also made by replacing the original donor and acceptor fluorophores with Cy5 and Iowa Black® dyes respectively. However, whilst no emissions were observed from this sensor prior to target incubation, no signal increases occurred after addition of thrombin, plasma or whole blood samples. The reason for this lack of detection ability remains unclear but ultimately influenced the decision to exclude this sensor from further studies.

## 7.5 Taggants

Initiated as part of a collaborative project with the National Crime Agency (NCA), investigations were undertaken into the development of novel forensic taggants for the monitoring of contact transfers occurring during a criminal offence (**Chapter 6**). These taggants were comprised of three main components: 1) an amino acid sequence, acting as a unique molecular marker for the identification of particular taggant formulations, 2) a fluorescent dye, allowing for the detection of the taggant and 3) an oil-based medium to facilitate transfer upon contact. With the ultimate aim of developing a 'reactive' taggant only able to be detected after interaction with a biological source (such as sweat or saliva), peptide and fluorophore molecules already utilised within the synthesis of custom fluorogenic substrates (Ac-HSSKL and Rh-110) were used for taggant construction.

An optimisation of taggant components was first undertaken to determine both the type of medium needed to achieve greatest contact transfer, as well as the concentrations of incorporated peptide and fluorophore molecules required for maximum taggant detectability. The stability of selected taggant constituents, both over time and in response to changes in environmental conditions (including temperature and humidity) was then assessed in a subsequent validation study. In all cases, taggant samples were able to be detected (even after an application period of six weeks) through ESI-MS analysis, demonstrating the potential use of this reagent within long-term criminal monitoring activities.

Such materials are likely to offer additional advantages over currently available taggants, including a simplistic detection, extraction and analysis procedure, as well as an increased coding ability through the use of unique amino acid chains.

## 7.6 Future Work

Work conducted during the course of this project represents the first application of biosensor technology towards the detection and identification of biological fluid stains. However, further efforts in the optimisation and validation of all developed sensors is likely to be required in order to bring this technology beyond an initial 'proof of concept' stage and allow sensors to be deployed within an operational casework setting. This optimisation may be achieved through the modification of individual sensing components to enhance the specificity, stability and detection limit of each assay. Comprehensive validation studies should then be undertaken to assess sensor performance within a variety of environmental conditions (such as different temperature, humidity and pH ranges), as well as towards biological fluid stains aged over extended periods of time. Studies examining the potential for false negative or positive signals to occur as a result of sensor inhibition and cross-reactivity (both between fluid types and with other non-fluid substances) respectively, should also be conducted.

Another important aspect of validating new technologies for the analysis of biological fluids is assessing the performance of techniques against fluid samples from different donors. This is particularly pertinent for methods that base detection on the presence/absence or quantification of single biomarkers, which may be differentially expressed between individuals. For example, PSA protein concentrations within human seminal fluid are known to exist over a significant range (from 0.2-5 mg/ml [217]). Such differences in expression may affect the analytical robustness of a fluid detection technique, thereby limiting its usefulness. The sensors reported within the scope of this study were all developed from a 'proof-of-concept' perspective and were therefore only qualitatively tested against samples from one fluid donor. Future work should therefore focus on establishing the ability of each sensor to detect and identify respective fluids from an extensive range of different individuals.

With unsuccessful detection of whole fluids demonstrated by both commercially available and custom-synthesized thrombin assays, future investigations into the use of fluorogenic substrate-based sensors are likely to involve additional efforts to adapt this signal transduction mechanism towards the detection of blood. This may potentially be achieved through the use of novel pro-fluorophores emitting with the NIR region of the electromagnetic spectrum, such as QCy7 [482]. With emission signals able to penetrate through greater depths of organic tissue [482], such fluorophores may be able to compensate for the low concentration of free-thrombin enzymes present within blood by increasing the overall sensitivity of the substrate.

Further investigations are also warranted into the application of constructed PSA-specific immunosensor complexes towards the detection of whole seminal fluid, both in solution, as well as deposited on surfaces commonly encountered within criminal investigation. This may be achieved following experimental procedures similar to those utilised in fluorogenic substrate testing. Furthermore, if adequate *in situ* detection performance is demonstrated by such complexes, subsequent attempts in adapting this transduction mechanism towards the analysis of other intra-fluidic targets (beyond the MUC5B-specific sensor discussed within [Section 7.3](#)) may also be justified.

As demonstrated within [Chapter 5](#), construction of a multiplex GO displacement-based aptasensor for the simultaneous detection of blood, semen and saliva was hindered by the non-specific desorption of ssDNA from graphene in the presence of all protein targets. An attempt to prevent this desorption should therefore be explored. Possessing a lower surface charge density compared to traditional GO nanosheets, reduced graphene oxide (rGO) may provide an ideal resolution to this issue by enhancing the strength of initial ssDNA adsorption to the graphene surface (as a result of decreased electrostatic repulsion effects) [389].



A selection of aptamer sequences towards whole human sperm cell targets using a modified Cell-SELEX protocol was also conducted for the purpose of improving aptasensor specificity. Whilst NGS analysis of enriched selection pools revealed a number of promising aptamer candidates, subsequent efforts are still required to identify the particular structural motifs responsible for sperm-cell interaction, as well as to determine the binding affinities of selected sequences. Further work in the selection of aptamers towards cellular targets present within other body fluids (such as blood and saliva) should also be undertaken in order to identify ssDNA sequences that may have potential use in multiplex fluid detection aptasensors.

Developed as part of two initial 'proof of concept' studies, forensic taggants for monitoring contact transfer during a criminal offence were constructed utilising fluorophores and amino acid sequences previously employed within fluorogenic substrate synthesis. However, with both of these components originally included within taggants as separate molecules, future investigations should be conducted into the development of 'reactive' taggants containing whole substrates, which allow detection only on contact with a biological source, such as sweat or saliva.

## **7.7 Final Remarks**

A substantial number of new biosensing formats are reported within the literature every year. Many of these assays offer analytical specificities and detection limits that significantly outperform those of current forensic body fluid testing strategies. However, despite such performance, biosensors have yet to be fully integrated within any area of forensic analysis. The reason for this lack of sensor use is not clear but may be potentially attributed to the disruptive nature of adopting novel analysis methods within forensic laboratories. It is therefore hoped that the results gained from this project, originally designed as a joint enterprise between King's College London and the Metropolitan Police Forensic Service

Directorates, realises the first step towards the use routine use of biosensor technology in enhancing the detection and identification of biological fluid stains within criminal casework.

# **| References**

1. Home Office, *National DNA Database Strategy Board Annual Report 2016/17*. 2018.
2. Kayser, M., *Forensic DNA Phenotyping: Predicting human appearance from crime scene material for investigative purposes*. Forensic Science International: Genetics, 2015. **18**: p. 33-48.
3. Virkler, K. and I.K. Lednev, *Analysis of body fluids for forensic purposes: From laboratory testing to non-destructive rapid confirmatory identification at a crime scene*. Forensic Science International, 2009. **188**(1–3): p. 1-17.
4. Lee, W. and B. Khoo, *Forensic light sources for detection of biological evidences in crime scene investigation: a review*. Malaysian Journal of Forensic Science, 2010. **1**: p. 17-28.
5. Specht, W., *Die Chemilumineszenz des Hämins, ein Hilfsmittel zur Auffindung und Erkennung forensisch wichtiger Blutspuren*. Deutsche Zeitschrift für die Gesamte Gerichtliche Medizin, 1937. **28**(1): p. 225-234.
6. Dilbeck, L., *Use of Bluestar Forensic in lieu of luminol at crime scenes*. Journal of Forensic Identification, 2006. **56**(5): p. 706-720.
7. Monk, J.W., *Fluorescent bloodstain detection: A replacement for luminol*. 1991, California Criminalistics Institute: California, USA.
8. Lowis, T., et al., *Determining the Sensitivity and Reliability of Hemascein*. Journal of Forensic Identification, 2012. **62**(3): p. 204-214.
9. Radacher, M., et al., *Luminol im Vergleich mit Fluorescein und Blue Star, Blue Star Forensic Magnum im Vergleich mit Lumiscene*. Kriminalistik, 2011. **3**: p. 180-184.
10. Kind, S.S., *The use of the acid phosphatase test in searching for seminal stains*. The Journal of Criminal Law, Criminology, and Police Science, 1956. **47**: p. 597-600.
11. Hedman, J., K. Gustavsson, and R. Ansell, *Using the new Phadebas® Forensic Press test to find crime scene saliva stains suitable for DNA analysis*. Forensic Science International: Genetics Supplement Series, 2008. **1**(1): p. 430-432.

12. Gill, P., *Analysis and implications of the miscarriages of justice of Amanda Knox and Raffaele Sollecito*. Forensic Science International: Genetics, 2016. **23**: p. 9-18.
13. Leonards, J.R., *Simple test for hematuria compared with established tests*. JAMA, 1962. **179**(10): p. 807-808.
14. Glaister, J., *The Kastle-Meyer Test for the Detection of Blood: Considered from the Medico-Legal Aspect*. British Medical Journal, 1926. **1**(3406): p. 650-652.
15. Adler, O. and R. Adler, *Über das Verhalten gewisser organischer Verbindungen gegenüber Blut mit besonderer Berücksichtigung des Nachweises von Blut*. Hoppe-Seyler's Zeitschrift für Physiologische Chemie, 1904. **41**(1): p. 59-60.
16. Johnston, S., J. Newman, and R. Frappier, *Validation study of the Abacus Diagnostics ABACard® HemaTrace® membrane test for the forensic identification of human blood*. Canadian Society of Forensic Science Journal, 2003. **36**(3): p. 173-183.
17. Hochmeister, M.N., et al., *Validation studies of an immunochromatographic 1-step test for the forensic identification of human blood*. Journal of Forensic Sciences, 1999. **44**(3): p. 597-602.
18. Misencik, A. and D.L. Laux, *Validation study of the seratec hemdirect hemoglobin assay for the forensic identification of human blood*. MAFS Newsletter, 2007. **36**(2): p. 18-26.
19. Schweers, B.A., et al., *Developmental validation of a novel lateral flow strip test for rapid identification of human blood (Rapid Stain Identification™-Blood)*. Forensic Science International: Genetics, 2008. **2**(3): p. 243-247.
20. Takayama, M., *A method for identifying blood by hemochromogen crystallization*. Kokka Igakkai Zasshi, 1912. **306**: p. 463-481.
21. Teichmann, L., *Ueber die Krystallisation des orpnischen Bestandtheile des Blutes*. Rational Medicine, 1853. **3**: p. 375-388.
22. Walker, J.T., *A new test for seminal stains*. New England Journal of Medicine, 1950. **242**(3): p. 110-111.

23. Kearsey, J., H. Louie, and H. Poon, *Validation study of the "Onestep Abacard® PSA Test" kit for RCMP Casework*. Canadian Society of Forensic Science Journal, 2001. **34**(2): p. 63-72.
24. Maher, J., et al., *Evaluation of the BioSign (TM) PSA membrane test for the identification of semen stains in forensic casework*. New Zealand Journal of Medicine, 2002. **114**(1147): p. 48-49.
25. Gartside, B.O., K.J. Brewer, and C.L. Strong, *Estimation of Prostate-Specific Antigen (PSA) extraction efficiency from forensic samples using the seratec PSA Semiquant Semiquantitative Membrane test*. National Criminal Justice Reference System, 2003. **2**: p. 1-4.
26. Old, J., et al., *Developmental Validation of RSID™ - Semen: A Lateral Flow Immunochromatographic Strip Test for the Forensic Detection of Human Semen*. Journal of Forensic Sciences, 2012. **57**(2): p. 489-499.
27. Willott, G.M., *An Improved Test for the Detection of Salivary Amylase in Stains*. Journal of the Forensic Science Society, 1974. **14**(4): p. 341-344.
28. Old, J.B., et al., *Developmental Validation of RSID™ - Saliva: A Lateral Flow Immunochromatographic Strip Test for the Forensic Detection of Saliva*. Journal of Forensic Sciences, 2009. **54**(4): p. 866-873.
29. Barbaro, A., et al., *Evaluation study about the SERATEC® rapid tests*. Forensic Science International: Genetics Supplement Series, 2015. **5**: p. e63-e64.
30. Pang, B.C. and B.K. Cheung, *Applicability of two commercially available kits for forensic identification of saliva stains*. Journal of Forensic Sciences, 2008. **53**(5): p. 1117-1122.
31. Ong, S.Y., et al., *Forensic identification of urine using the DMAC test: A method validation study*. Science & Justice, 2012. **52**(2): p. 90-95.
32. Akutsu, T., K. Watanabe, and K. Sakurada, *Specificity, Sensitivity, and Operability of RSID™ - Urine for Forensic Identification of Urine: Comparison with ELISA for Tamm - Horsfall Protein*. Journal of Forensic Sciences, 2012. **57**(6): p. 1570-1573.

33. Romsos, E.L. and P.M. Vallone, *Rapid PCR of STR markers: Applications to human identification*. Forensic Science International: Genetics, 2015. **18**: p. 90-99.
34. Zapata, F., I. Gregório, and C. García-Ruiz, *Body fluids and spectroscopic techniques in forensics: a perfect match?* Journal of Forensic Medicine, 2015. **1**(1): p. 101-108.
35. Pollitt, E.N., et al., *Alternate Light Source Findings of Common Topical Products*. Journal of Forensic Nursing, 2016. **11**(3): p. 97-103.
36. Vandenberg, N. and R.A.H. van Oorschot, *The Use of Polilight® in the Detection of Seminal Fluid, Saliva, and Bloodstains and Comparison with Conventional Chemical-Based Screening Tests*. Journal of Forensic Sciences, 2006. **51**(2): p. 361-370.
37. Tobe, S.S., N. Watson, and N.N. Daeid, *Evaluation of six presumptive tests for blood, their specificity, sensitivity, and effect on high molecular - weight DNA*. Journal of Forensic sciences, 2007. **52**(1): p. 102-109.
38. Vennemann, M., et al., *Sensitivity and specificity of presumptive tests for blood, saliva and semen*. Forensic Science, Medicine, and Pathology, 2014. **10**(1): p. 69-75.
39. Wornes, D.J., S.J. Speers, and J.A. Murakami, *The evaluation and validation of Phadebas® paper as a presumptive screening tool for saliva on forensic exhibits*. Forensic Science International, 2018. **288**: p. 81-88.
40. Koen, W.J. and C.M. Bowers, *Forensic science reform: protecting the innocent*. 2016: Academic Press.
41. Zapata, F., M.Á. Fernández de la Ossa, and C. García-Ruiz, *Emerging spectrometric techniques for the forensic analysis of body fluids*. TrAC Trends in Analytical Chemistry, 2015. **64**: p. 53-63.
42. Sloots, J., et al., *Kastle–Meyer blood test reagents are deleterious to DNA*. Forensic Science International, 2017. **281**: p. 141-146.
43. Mozayani, A. and C. Noziglia, *The forensic laboratory handbook procedures and practice*. 2010: Springer Science & Business Media.

44. Schneider, R.C. and K.-A. Kovar, *Analysis of ecstasy tablets: comparison of reflectance and transmittance near infrared spectroscopy*. Forensic Science International, 2003. **134**(2-3): p. 187-195.
45. López-López, M. and C. García-Ruiz, *Infrared and Raman spectroscopy techniques applied to identification of explosives*. TrAC Trends in Analytical Chemistry, 2014. **54**: p. 36-44.
46. Silva, C.S., et al., *Classification of blue pen ink using infrared spectroscopy and linear discriminant analysis*. Microchemical Journal, 2013. **109**: p. 122-127.
47. Zięba-Palus, J. and R. Borusiewicz, *Examination of multilayer paint coats by the use of infrared, Raman and XRF spectroscopy for forensic purposes*. Journal of Molecular Structure, 2006. **792**: p. 286-292.
48. Meleiro, P.P. and C. García-Ruiz, *Spectroscopic techniques for the forensic analysis of textile fibers*. Applied Spectroscopy Reviews, 2016. **51**(4): p. 278-301.
49. Manheim, J., et al., *Forensic hair differentiation using attenuated total reflection fourier transform infrared (ATR FT-IR) spectroscopy*. Applied Spectroscopy, 2016. **70**(7): p. 1109-1117.
50. Reich, G., *Near-infrared spectroscopy and imaging: basic principles and pharmaceutical applications*. Advanced Drug Delivery Reviews, 2005. **57**(8): p. 1109-1143.
51. Ozaki, Y., *Near-Infrared Spectroscopy; Its Versatility in Analytical Chemistry*. Analytical Sciences, 2012. **28**(6): p. 545-563.
52. Morillas, A.V., J. Gooch, and N. Frascione, *Feasibility of a handheld near infrared device for the qualitative analysis of bloodstains*. Talanta, 2018. **184**: p. 1-6.
53. Pereira, J.F.Q., et al., *Evaluation and identification of blood stains with handheld NIR spectrometer*. Microchemical Journal, 2017. **133**: p. 561-566.
54. Orphanou, C.-M., *The detection and discrimination of human body fluids using ATR FT-IR spectroscopy*. Forensic Science International, 2015. **252**: p. e10-e16.



55. Elkins, K.M., *Rapid presumptive "fingerprinting" of body fluids and materials by ATR FT-IR spectroscopy*. Journal of Forensic Sciences, 2011. **56**(6): p. 1580-1587.
56. Chalmers, J.M., H.G. Edwards, and M.D. Hargreaves, *Infrared and Raman spectroscopy in forensic science*. 2012: John Wiley & Sons.
57. Sikirzhytski, V., A. Sikirzhytskaya, and I.K. Lednev, *Multidimensional Raman spectroscopic signatures as a tool for forensic identification of body fluid traces: a review*. Applied Spectroscopy, 2011. **65**(11): p. 1223-1232.
58. De Wael, K., et al., *In search of blood--detection of minute particles using spectroscopic methods*. Forensic Science International, 2008. **180**(1): p. 37-42.
59. Muro, C.K., et al., *Forensic body fluid identification and differentiation by Raman spectroscopy*. Forensic Chemistry, 2016. **1**: p. 31-38.
60. Doty, K.C. and I.K. Lednev, *Differentiating Donor Age Groups Based on Raman Spectroscopy of Bloodstains for Forensic Purposes*. ACS Central Science, 2018. **4**(7): p. 862-867.
61. Muro, C.K., L. de Souza Fernandes, and I.K. Lednev, *Sex Determination Based on Raman Spectroscopy of Saliva Traces for Forensic Purposes*. Analytical Chemistry, 2016. **88**(24): p. 12489-12493.
62. Mistek, E., et al., *Race Differentiation by Raman Spectroscopy of a Bloodstain for Forensic Purposes*. Analytical Chemistry, 2016. **88**(15): p. 7453-7456.
63. Samantha Boyd, B., et al., *Highly Sensitive Detection of Blood by Surface Enhanced Raman Scattering*. Journal of Forensic Sciences, 2013. **58**(3): p. 753-756.
64. Sikirzhytski, V., K. Virkler, and I.K. Lednev, *Discriminant analysis of Raman spectra for body fluid identification for forensic purposes*. Sensors, 2010. **10**(4): p. 2869-2884.
65. Edelman, G.J., et al., *Hyperspectral imaging for non-contact analysis of forensic traces*. Forensic Science International, 2012. **223**(1): p. 28-39.

66. Edelman, G., T.G. van Leeuwen, and M.C. Aalders, *Hyperspectral imaging for the age estimation of blood stains at the crime scene*. Forensic Science International, 2012. **223**(1-3): p. 72-77.
67. Li, B., et al., *The age estimation of blood stains up to 30 days old using visible wavelength hyperspectral image analysis and linear discriminant analysis*. Science & Justice, 2013. **53**(3): p. 270-277.
68. Li, B., et al., *The application of visible wavelength reflectance hyperspectral imaging for the detection and identification of blood stains*. Science & Justice, 2014. **54**(6): p. 432-438.
69. Edelman, G.J., T.G. Leeuwen, and M.C. Aalders, *Visualization of Latent Blood Stains Using Visible Reflectance Hyperspectral Imaging and Chemometrics*. Journal of Forensic Sciences, 2015. **60**(s1): p. S188-S192.
70. Zapata, F., F.E. Ortega-Ojeda, and C. Garcia-Ruiz, *Revealing the location of semen, vaginal fluid and urine in stained evidence through near infrared chemical imaging*. Talanta, 2017. **166**: p. 292-299.
71. Silva, C.S., et al., *Detecting semen stains on fabrics using near infrared hyperspectral images and multivariate models*. TrAC Trends in Analytical Chemistry, 2017. **95**: p. 23-35.
72. Sijen, T., *Molecular approaches for forensic cell type identification: On mRNA, miRNA, DNA methylation and microbial markers*. Forensic Science International: Genetics, 2015. **18**: p. 21-32.
73. Park, J.-L., et al., *Forensic Body Fluid Identification by Analysis of Multiple RNA Markers Using NanoString Technology*. Genomics & Informatics, 2013. **11**(4): p. 277-281.
74. Juusola, J. and J. Ballantyne, *mRNA profiling for body fluid identification by multiplex quantitative RT-PCR*. Journal of Forensic Sciences, 2007. **52**(6): p. 1252-1262.
75. Fang, R., et al., *Real-time PCR assays for the detection of tissue and body fluid specific mRNAs*. International Congress Series, 2006. **1288**: p. 685-687.
76. Juusola, J. and J. Ballantyne, *Multiplex mRNA profiling for the identification of body fluids*. Forensic Science International, 2005. **152**(1): p. 1-12.

77. Noreault-Conti, T.L. and E. Buel, *The use of real-time PCR for forensic stain identification*. Profiles in DNA, 2007. **10**(1): p. 3-5.
78. Lindenbergh, A., et al., *A multiplex (m) RNA-profiling system for the forensic identification of body fluids and contact traces*. Forensic Science International: Genetics, 2012. **6**(5): p. 565-577.
79. Zubakov, D., et al., *Stable RNA markers for identification of blood and saliva stains revealed from whole genome expression analysis of time-wise degraded samples*. International Journal of Legal Medicine, 2008. **122**(2): p. 135-142.
80. Bauer, M. and D. Patzelt, *Protamine mRNA as molecular marker for spermatozoa in semen stains*. International journal of legal Medicine, 2003. **117**(3): p. 175-179.
81. Juusola, J. and J. Ballantyne, *Messenger RNA profiling: a prototype method to supplant conventional methods for body fluid identification*. Forensic Science International, 2003. **135**(2): p. 85-96.
82. Ingold, S., et al., *Body fluid identification using a targeted mRNA massively parallel sequencing approach—results of a EUROFORGEN/EDNAP collaborative exercise*. Forensic Science International: Genetics, 2018. **34**: p. 105-115.
83. Haas, C., et al., *RNA/DNA co-analysis from human saliva and semen stains – Results of a third collaborative EDNAP exercise*. Forensic Science International: Genetics, 2013. **7**(2): p. 230-239.
84. Hanson, E.K. and J. Ballantyne, *Highly specific mRNA biomarkers for the identification of vaginal secretions in sexual assault investigations*. Science & Justice, 2013. **53**(1): p. 14-22.
85. Hanson, E., et al., *Messenger RNA biomarker signatures for forensic body fluid identification revealed by targeted RNA sequencing*. Forensic Science International: Genetics, 2018. **34**: p. 206-221.
86. Bauer, M. and D. Patzelt, *Evaluation of mRNA markers for the identification of menstrual blood*. Journal of Forensic Sciences, 2002. **47**(6): p. 1278-1282.
87. Roeder, A.D. and C. Haas, *mRNA profiling using a minimum of five mRNA markers per body fluid and a novel scoring method for body*

*fluid identification*. International Journal of Legal Medicine, 2013. **127**(4): p. 707-721.

88. Hanson, E., et al., *Specific and sensitive mRNA biomarkers for the identification of skin in 'touch DNA' evidence*. Forensic Science International: Genetics, 2012. **6**(5): p. 548-558.
89. Ingold, S., et al., *Association of a body fluid with a DNA profile by targeted RNA/DNA deep sequencing*. Forensic Science International: Genetics Supplement Series, 2017. **6**: p. e112-e113.
90. de Zoete, J., J. Curran, and M. Sjerps, *A probabilistic approach for the interpretation of RNA profiles as cell type evidence*. Forensic Science International: Genetics, 2016. **20**: p. 30-44.
91. Dørum, G., et al., *Predicting the origin of stains from next generation sequencing mRNA data*. Forensic Science International: Genetics, 2018. **34**: p. 37-48.
92. Lindenbergh, A., P. Maaskant, and T. Sijen, *Implementation of RNA profiling in forensic casework*. Forensic Science International: Genetics, 2013. **7**(1): p. 159-166.
93. Harbison, S. and R. Fleming, *Forensic body fluid identification: state of the art*. Research and Reports in Forensic Medical Science, 2016. **6**: p. 11-23.
94. Alvarez, M., J. Juusola, and J. Ballantyne, *An mRNA and DNA co-isolation method for forensic casework samples*. Analytical Biochemistry, 2004. **335**(2): p. 289-298.
95. Vennemann, M. and A. Koppelkamm, *mRNA profiling in forensic genetics I: Possibilities and limitations*. Forensic Science International, 2010. **203**(1-3): p. 71-75.
96. Kohlmeier, F. and P.M. Schneider, *Successful mRNA profiling of 23 years old blood stains*. Forensic Science International: Genetics, 2012. **6**(2): p. 274-276.
97. Zubakov, D., et al., *New markers for old stains: stable mRNA markers for blood and saliva identification from up to 16-year-old stains*. International Journal of Legal Medicine, 2009. **123**(1): p. 71-74.
98. Goldberg, A.D., C.D. Allis, and E. Bernstein, *Epigenetics: A Landscape Takes Shape*. Cell, 2007. **128**(4): p. 635-638.

99. Alegria-Torres, J.A., A. Baccarelli, and V. Bollati, *Epigenetics and lifestyle*. Epigenomics, 2011. **3**(3): p. 267-277.
100. Li, C., et al., *Identical but not the same: the value of DNA methylation profiling in forensic discrimination within monozygotic twins*. Forensic Science International: Genetics Supplement Series, 2011. **3**(1): p. e337-e338.
101. Vidaki, A., et al., *DNA methylation-based forensic age prediction using artificial neural networks and next generation sequencing*. Forensic Science International: Genetics, 2017. **28**: p. 225-236.
102. Ehrlich, M., et al., *Amount and distribution of 5-methylcytosine in human DNA from different types of tissues or cells*. Nucleic Acids Research, 1982. **10**(8): p. 2709-2721.
103. Frumkin, D., et al., *DNA methylation-based forensic tissue identification*. Forensic Science International: Genetics, 2011. **5**(5): p. 517-524.
104. Vidaki, A. and B. Daniel, *Forensic DNA methylation profiling—potential opportunities and challenges*. Forensic Science International: Genetics, 2013. **7**(5): p. 499-507.
105. Vidaki, A. and M. Kayser, *From forensic epigenetics to forensic epigenomics: broadening DNA investigative intelligence*. Genome Biology, 2017. **18**(1): p. 238-251.
106. Naue, J., et al., *Proof of concept study of age-dependent DNA methylation markers across different tissues by massive parallel sequencing*. Forensic Science International: Genetics, 2018. **36**: p. 152-159.
107. Christensen, B.C., et al., *Aging and Environmental Exposures Alter Tissue-Specific DNA Methylation Dependent upon CpG Island Context*. PLoS Genetics, 2009. **5**(8): p. e10006020-e1000615.
108. Wasserstrom, A., et al., *Demonstration of DSI-semen--A novel DNA methylation-based forensic semen identification assay*. Forensic Science International: Genetics, 2013. **7**(1): p. 136-142.
109. Sender, R., S. Fuchs, and R. Milo, *Are We Really Vastly Outnumbered? Revisiting the Ratio of Bacterial to Host Cells in Humans*. Cell, 2016. **164**(3): p. 337-340.

110. Turnbaugh, P.J., et al., *The human microbiome project*. Nature, 2007. **449**(7164): p. 804-810.
111. Lane, D.J., et al., *Rapid determination of 16S ribosomal RNA sequences for phylogenetic analyses*. Proceedings of the National Academy of Sciences, 1985. **82**(20): p. 6955-6959.
112. Khodakova, A.S., et al., *Random Whole Metagenomic Sequencing for Forensic Discrimination of Soils*. PLoS ONE, 2014. **9**(8): p. e104996-e105011.
113. Choi, A., et al., *Body fluid identification by integrated analysis of DNA methylation and body fluid-specific microbial DNA*. International Journal of Legal Medicine, 2014. **128**(1): p. 33-41.
114. Hanssen, E.N., et al., *Body fluid prediction from microbial patterns for forensic application*. Forensic Science International: Genetics, 2017. **30**: p. 10-17.
115. Benschop, C.C., et al., *Vaginal microbial flora analysis by next generation sequencing and microarrays; can microbes indicate vaginal origin in a forensic context?* International Journal of Legal Medicine, 2012. **126**(2): p. 303-310.
116. Dewhirst, F.E., et al., *The Canine Oral Microbiome*. PLoS ONE, 2012. **7**(4): p. e36067-e36079.
117. Thorogate, R., et al., *A novel fluorescence-based method in forensic science for the detection of blood in situ*. Forensic Science International: Genetics, 2008. **2**(4): p. 363-371.
118. Frascione, N., et al., *Detection and identification of body fluid stains using antibody-nanoparticle conjugates*. Analyst, 2012. **137**(2): p. 508-512.
119. Banica, F.-G., *Chemical sensors and biosensors: fundamentals and applications*. 2012: John Wiley & Sons.
120. Van Dorst, B., et al., *Recent advances in recognition elements of food and environmental biosensors: A review*. Biosensors and Bioelectronics, 2010. **26**(4): p. 1178-1194.
121. Yáñez-Sedeño, P., et al., *Biosensors in forensic analysis. A review*. Analytica Chimica Acta, 2014. **823**: p. 1-19.

122. Zhang, Q., et al., *Graphene oxide-based optical biosensor functionalized with peptides for explosive detection*. Biosensors and Bioelectronics, 2015. **68**: p. 494-499.
123. Stringer, R.C., S. Gangopadhyay, and S.A. Grant, *Detection of Nitroaromatic Explosives Using a Fluorescent-Labeled Imprinted Polymer*. Analytical Chemistry, 2010. **82**(10): p. 4015-4019.
124. Bakaltcheva, I.B., et al., *Multi-analyte explosive detection using a fiber optic biosensor*. Analytica Chimica Acta, 1999. **399**(1): p. 13-20.
125. Devine, P.J., et al., *A fiber-optic cocaine biosensor*. Analytical Biochemistry, 1995. **227**(1): p. 216-224.
126. Li, Y., et al., *Electrogenerated chemiluminescence aptamer-based biosensor for the determination of cocaine*. Electrochemistry Communications, 2007. **9**(10): p. 2571-2575.
127. Klenkar, G. and B. Liedberg, *A microarray chip for label-free detection of narcotics*. Analytical and Bioanalytical Chemistry, 2008. **391**(5): p. 1679-1688.
128. Cella, L.N., et al., *Nano Aptasensor for Protective Antigen Toxin of Anthrax*. Analytical Chemistry, 2010. **82**(5): p. 2042-2047.
129. Smit, M.H. and A.E. Cass, *Cyanide detection using a substrate-regenerating peroxidase-based biosensor*. Analytical Chemistry, 1990. **62**(22): p. 2429-2436.
130. Feltis, B.N., et al., *A hand-held surface plasmon resonance biosensor for the detection of ricin and other biological agents*. Biosensors and Bioelectronics, 2008. **23**(7): p. 1131-1136.
131. Frascione, N., J. Gooch, and B. Daniel, *Enabling fluorescent biosensors for the forensic identification of body fluids*. Analyst, 2013. **138**(24): p. 7279-7288.
132. Bhalla, N., et al., *Introduction to Biosensors*. Essays in Biochemistry, 2016. **60**(1): p. 1-8.
133. Demchenko, A.P., *Introduction to fluorescence sensing*. 2008: Springer Science & Business Media.

134. Frascione, N., V. Pinto, and B. Daniel, *Development of a biosensor for human blood: new routes to body fluid identification*. Analytical and Bioanalytical Chemistry, 2012. **404**(1): p. 23-28.
135. Dragan, A., et al., *Characterization of PicoGreen interaction with dsDNA and the origin of its fluorescence enhancement upon binding*. Biophysical Journal, 2010. **99**(9): p. 3010-3019.
136. Nicklas, J.A. and E. Buel, *Quantification of DNA in forensic samples*. Analytical and Bioanalytical Chemistry, 2003. **376**(8): p. 1160-1167.
137. Müller, E., et al., *In situ analysis of biofilms on historic window glass using confocal laser scanning microscopy*. Journal of Cultural Heritage, 2001. **2**(1): p. 31-42.
138. Simeonov, A., et al., *Blue-Fluorescent Antibodies*. Science, 2000. **290**(5490): p. 307-313.
139. Stryer, L. and R.P. Haugland, *Energy transfer: a spectroscopic ruler*. Proceedings of the National Academy of Sciences, 1967. **58**(2): p. 719-726.
140. Ghisaidoobe, A.B. and S.J. Chung, *Intrinsic tryptophan fluorescence in the detection and analysis of proteins: a focus on Förster resonance energy transfer techniques*. International Journal of Molecular Sciences, 2014. **15**(12): p. 22518-22538.
141. VanEngelenburg, S.B. and A.E. Palmer, *Fluorescent biosensors of protein function*. Current Opinion in Chemical Biology, 2008. **12**(1): p. 60-65.
142. Schultz, G.S. and D.J. Gibson, *Measurement of Biomarkers for Impaired Healing in Fluids and Tissues*, in *Measurements in Wound Healing: Science and Practice*, R. Mani, M. Romanelli, and V. Shukla, Editors. 2013, Springer London: London. p. 243-258.
143. Hsu, Y.Y., et al., *In vivo dynamics of enterovirus protease revealed by fluorescence resonance emission transfer (FRET) based on a novel FRET pair*. Biochemical and Biophysical Research Communications, 2007. **353**(4): p. 939-945.
144. Tyagi, S. and F.R. Kramer, *Molecular beacons: probes that fluoresce upon hybridization*. Nature Biotechnology, 1996. **14**(3): p. 303-308.



145. Hamaguchi, N., A. Ellington, and M. Stanton, *Aptamer beacons for the direct detection of proteins*. Analytical Biochemistry, 2001. **294**(2): p. 126-131.
146. Stojanovic, M.N., P. de Prada, and D.W. Landry, *Aptamer-Based Folding Fluorescent Sensor for Cocaine*. Journal of the American Chemical Society, 2001. **123**(21): p. 4928-4931.
147. Lenaerts, J., H.M. Lappin-Scott, and J. Porter, *Improved fluorescent in situ hybridization method for detection of bacteria from activated sludge and river water by using DNA molecular beacons and flow cytometry*. Applied and Environmental Microbiology, 2007. **73**(6): p. 2020-2023.
148. Grant, S.A., et al., *Effects of immobilization on a FRET immunosensor for the detection of myocardial infarction*. Analytical and Bioanalytical Chemistry, 2005. **381**(5): p. 1012-1018.
149. Ko, S. and S.A. Grant, *A novel FRET-based optical fiber biosensor for rapid detection of Salmonella typhimurium*. Biosensors and Bioelectronics, 2006. **21**(7): p. 1283-1290.
150. Medintz, I.L., et al., *A fluorescence resonance energy transfer sensor based on maltose binding protein*. Bioconjugate Chemistry, 2003. **14**(5): p. 909-918.
151. Kattke, M.D., et al., *FRET-Based Quantum Dot Immunoassay for Rapid and Sensitive Detection of Aspergillus amstelodami*. Sensors, 2011. **11**(6): p. 6396-6410.
152. Johansson, M.K. and R.M. Cook, *Intramolecular dimers: a new design strategy for fluorescence-quenched probes*. Chemistry, 2003. **9**(15): p. 3466-3471.
153. Bergström, F., et al., *Dimers of dipyrrometheneboron difluoride (BODIPY) with light spectroscopic applications in chemistry and biology*. Journal of the American Chemical Society, 2002. **124**(2): p. 196-204.
154. Jones, L.J., et al., *Quenched BODIPY dye-labeled casein substrates for the assay of protease activity by direct fluorescence measurement*. Analytical Biochemistry, 1997. **251**(2): p. 144-152.
155. Hannig, C., et al., *Intrinsic enzymatic crosslinking and maturation of the in situ pellicle*. Archives of Oral Biology, 2008. **53**(5): p. 416-422.

156. Robertson, L.J., et al., *Calpain may contribute to hereditary cataract formation in sheep*. Investigative Ophthalmology & Visual Science, 2005. **46**(12): p. 4634-4640.
157. Chen, L., et al., *Highly sensitive biological and chemical sensors based on reversible fluorescence quenching in a conjugated polymer*. Proceedings of the National Academy of Sciences, 1999. **96**(22): p. 12287-12292.
158. Batchelor, R.H., et al., *Fluorometric assay for quantitation of biotin covalently attached to proteins and nucleic acids*. BioTechniques, 2007. **43**(4): p. 503-507.
159. Kirkeby, S. and C.E. Thomsen, *Quantitative immunohistochemistry of fluorescence labelled probes using low-cost software*. Journal of Immunological methods, 2005. **301**(1-2): p. 102-113.
160. Grant, D.M., et al., *Multiplexed FRET to image multiple signaling events in live cells*. Biophysical Journal, 2008. **95**(10): p. L69-L71.
161. Yaron, A., A. Carmel, and E. Katchalski-Katzir, *Intramolecularly quenched fluorogenic substrates for hydrolytic enzymes*. Analytical Biochemistry, 1979. **95**(1): p. 228-235.
162. Barrett, A.J., N.D. Rawlings, and J.F. Woessner, *Handbook of Proteolytic Enzymes*. 1998: Academic Press.
163. Haugland, R.P. and I.D. Johnson, *Detecting enzymes in living cells using fluorogenic substrates*. Journal of Fluorescence, 1993. **3**(3): p. 119-127.
164. Tung, C.H., *Fluorescent peptide probes for in vivo diagnostic imaging*. Peptide Science: Original Research on Biomolecules, 2004. **76**(5): p. 391-403.
165. Harris, J.L., et al., *Rapid and general profiling of protease specificity by using combinatorial fluorogenic substrate libraries*. Proceedings of the National Academy of Sciences, 2000. **97**(14): p. 7754-7759.
166. Orenge, S., et al., *Enzymatic substrates in microbiology*. Journal of Microbiological Methods, 2009. **79**(2): p. 139-155.
167. Diamond, S.L., *Methods for mapping protease specificity*. Current Opinion in Chemical Biology, 2007. **11**(1): p. 46-51.

168. Green, M.N., et al., *The colorimetric determination of leucine aminopeptidase activity with L-leucyl- $\beta$ -naphthylamide hydrochloride*. Archives of Biochemistry and Biophysics, 1955. **57**(2): p. 458-474.
169. Rosenblatt, D.H., M.M. Nachlas, and A.M. Seligman, *Synthesis of m-Methoxynaphthylamines as Precursors for Chromogenic Substrates*. Journal of the American Chemical Society, 1958. **80**(10): p. 2463-2465.
170. Zimmerman, M., E. Yurewicz, and G. Patel, *A new fluorogenic substrate for chymotrypsin*. Analytical Biochemistry, 1976. **70**(1): p. 258-262.
171. Jameson, G., et al., *Determination of the operational molarity of solutions of bovine  $\alpha$ -chymotrypsin, trypsin, thrombin and factor Xa by spectrofluorimetric titration*. Biochemical Journal, 1973. **131**(1): p. 107-117.
172. Rosser, B.G., S.P. Powers, and G.J. Gores, *Calpain activity increases in hepatocytes following addition of ATP. Demonstration by a novel fluorescent approach*. Journal of Biological Chemistry, 1993. **268**(31): p. 23593-23600.
173. Smith, R., et al., *Direct photometric or fluorometric assay of proteinases using substrates containing 7-amino-4-trifluoromethylcoumarin*. Thrombosis Research, 1980. **17**(3): p. 393-402.
174. Guilbault, G.G. and D. Kramer, *Fluorometric Determination of Lipase, Acylase, Alpha-, and Gamma-Chymotrypsin and Inhibitors of These Enzymes*. Analytical Chemistry, 1964. **36**(2): p. 409-412.
175. Leytus, S.P., L.L. Melhado, and W.F. Mangel, *Rhodamine-based compounds as fluorogenic substrates for serine proteinases*. Biochemical Journal, 1983. **209**(2): p. 299-307.
176. Kramer, D.N. and G.G. Guilbault, *Resorulin Acetate as a Substrate for Determination of Hydrolytic Enzymes at Low Enzyme and Substrate Concentrations*. Analytical Chemistry, 1964. **36**(8): p. 1662-1663.
177. Van Noorden, C.J.F., et al., *Ala-Pro-Cresyl Violet, a Synthetic Fluorogenic Substrate for the Analysis of Kinetic Parameters of Dipeptidyl Peptidase IV (CD26) in Individual Living Rat Hepatocytes*. Analytical Biochemistry, 1997. **252**(1): p. 71-77.

178. R Drake, C., D. C Miller, and E. F Jones, *Activatable optical probes for the detection of enzymes*. Current Organic Synthesis, 2011. **8**(4): p. 498-520.
179. Boonacker, E. and C.J. Van Noorden, *Enzyme cytochemical techniques for metabolic mapping in living cells, with special reference to proteolysis*. Journal of Histochemistry & Cytochemistry, 2001. **49**(12): p. 1473-1486.
180. Beija, M., C.A.M. Afonso, and J.M.G. Martinho, *Synthesis and applications of Rhodamine derivatives as fluorescent probes*. Chemical Society Reviews, 2009. **38**(8): p. 2410-2433.
181. Hu, H.Y., et al., *FRET - based and other fluorescent proteinase probes*. Biotechnology journal, 2014. **9**(2): p. 266-281.
182. Kanaoka, Y., T. Takahashi, and H. Nakayama, *A New Fluorogenic Substrate for Aminopeptidase*. Chemical & Pharmaceutical Bulletin, 1977. **25**(2): p. 362-363.
183. Rano, T.A., et al., *A combinatorial approach for determining protease specificities: application to interleukin-1 $\beta$  converting enzyme (ICE)*. Chemistry & Biology, 1997. **4**(2): p. 149-155.
184. Tang, Y., J.A. Wells, and M.R. Arkin, *Structural and enzymatic insights into caspase-2 substrate recognition and catalysis*. Journal of Biological Chemistry, 2011. **286**(39): p. 34147-34154.
185. Wang, Z.-Q., J. Liao, and Z. Diwu, *N-DEVD-N'-morpholinecarbonyl-rhodamine 110: novel caspase-3 fluorogenic substrates for cell-based apoptosis assay*. Bioorganic & Medicinal Chemistry Letters, 2005. **15**(9): p. 2335-2338.
186. Barrett, A.J., *Fluorimetric assays for cathepsin B and cathepsin H with methylcoumarylamide substrates*. Biochemical Journal, 1980. **187**(3): p. 909-912.
187. Dingle, J.T., *Lysosomes in biology and pathology*. 1975: North Holland Pub. Co.
188. Bossard, M.J., et al., *Proteolytic activity of human osteoclast cathepsin K expression, purification, activation, and substrate identification*. Journal of Biological Chemistry, 1996. **271**(21): p. 12517-12524.

189. Oshima, G., *Stimulation by phospholipid vesicles of proteolysis of egg white lysozyme by chymotrypsin*. Journal of Biochemistry, 1983. **94**(5): p. 1615-1620.
190. Castillo, M.J., et al., *Sensitive substrates for human leukocyte and porcine pancreatic elastase: A study of the merits of various chromophoric and fluorogenic leaving groups in assays for serine proteases*. Analytical Biochemistry, 1979. **99**(1): p. 53-64.
191. Morita, T., et al., *New fluorogenic substrates for alpha-thrombin, factor Xa, kallikreins, and urokinase*. Journal of Biochemistry, 1977. **82**(5): p. 1495-1488.
192. Pierzchala, P.A., C. Dorn, and M. Zimmerman, *A new fluorogenic substrate for plasmin*. Biochemical Journal, 1979. **183**(3): p. 555-559.
193. Denmeade, S.R., et al., *Specific and efficient peptide substrates for assaying the proteolytic activity of prostate-specific antigen*. Cancer Research, 1997. **57**(21): p. 4924-4930.
194. Svendsen, L., et al., *Synthetic chromogenic substrates for determination of trypsin, thrombin and thrombin-like enzymes*. Thrombosis Research, 1972. **1**(3): p. 267-278.
195. Grodsky, M., K. Wright, and P.L. Kirk, *Simplified Preliminary Blood Testing. An Improved Technique and a Comparative Study of Methods*. The Journal of Criminal Law, Criminology, and Police Science, 1951. **42**(1): p. 95-104.
196. Kaye, S., *The Acid Phosphatase Test for Seminal Stains: A Study of Reliability of Aged Stains*. Journal of Criminal Law and Criminology, 1951. **41**(6): p. 834-835.
197. Cox, M., *A study of the sensitivity and specificity of four presumptive tests for blood*. Journal of Forensic Sciences, 1991. **36**(5): p. 1503-1511.
198. Castelló, A., F. Francés, and F. Verdú, *Bleach interference in forensic luminol tests on porous surfaces: More about the drying time effect*. Talanta, 2009. **77**(4): p. 1555-1557.
199. Bancirova, M., *Black and green tea—Luminol false-negative bloodstains detection*. Science & Justice, 2012. **52**(2): p. 102-105.

200. Redhead, P. and M.K. Brown, *The acid phosphatase test two minute cut-off: an insufficient time to detect some semen stains*. Science & Justice, 2013. **53**(2): p. 187-191.
201. Schiff, A., *Reliability of the acid phosphatase test for the identification of seminal fluid*. Journal of Forensic Sciences, 1978. **23**(4): p. 833-844.
202. Davidson, G. and T. Jalowiecki, *Acid phosphatase screening—Wetting test paper or wetting fabric and test paper?* Science & Justice, 2012. **52**(2): p. 106-111.
203. Pang, B. and B. Cheung, *Identification of human semenogelin in membrane strip test as an alternative method for the detection of semen*. Forensic Science International, 2007. **169**(1): p. 27-31.
204. Casey, D.G. and J. Price, *The sensitivity and specificity of the RSID™-saliva kit for the detection of human salivary amylase in the Forensic Science Laboratory, Dublin, Ireland*. Forensic Science international, 2010. **194**(1-3): p. 67-71.
205. Turrina, S., et al., *Validation studies of rapid stain identification-blood (RSID-blood) kit in forensic caseworks*. Forensic Science International: Genetics Supplement Series, 2008. **1**(1): p. 74-75.
206. Yokota, M., et al., *Evaluation of prostate-specific antigen (PSA) membrane test for forensic examination of semen*. Legal Medicine, 2001. **3**(3): p. 171-176.
207. Niemelä, P., et al., *Sensitive and specific enzymatic assay for the determination of precursor forms of prostate-specific antigen after an activation step*. Clinical Chemistry, 2002. **48**(8): p. 1257-1264.
208. Quickenden, T.I. and J.I. Creamer, *A study of common interferences with the forensic luminol test for blood*. Luminescence, 2001. **16**(4): p. 295-298.
209. Webb, J.L., J.I. Creamer, and T.I. Quickenden, *A comparison of the presumptive luminol test for blood with four non-chemiluminescent forensic techniques*. Luminescence, 2006. **21**(4): p. 214-220.
210. Gooch, J., B. Daniel, and N. Frascione, *Application of fluorescent substrates to the in situ detection of prostate specific antigen*. Talanta, 2014. **125**: p. 210-214.

211. Wysocki, L.M., et al., *Facile and General Synthesis of Photoactivatable Xanthene Dyes*. *Angewandte Chemie International Edition*, 2011. **50**(47): p. 11206-11209.
212. Park, J.G., et al., *Improved Loading and Cleavage Methods for Solid-Phase Synthesis Using Chlorotriyl Resins: Synthesis and Testing of a Library of 144 Discrete Chemicals as Potential Farnesyltransferase Inhibitors*. *Journal of Combinatorial Chemistry*, 2004. **6**(3): p. 407-413.
213. Jixiang, L., et al., *Fluorescent molecular probes V: A sensitive caspase-3 substrate for fluorometric assays*. *Bioorganic & Medicinal Chemistry Letters*, 1999. **9**(22): p. 3231-3236.
214. Carvalho, K.M., et al., *A Highly Selective Assay for Neutral Endopeptidase Based on the Cleavage of a Fluorogenic Substrate Related to Leu-Enkephalin*. *Analytical Biochemistry*, 1996. **237**(2): p. 167-173.
215. Zhang, H.-Z., et al., *N-Ac-DEVD-N'-(Polyfluorobenzoyl)-R110: Novel Cell-Permeable Fluorogenic Caspase Substrates for the Detection of Caspase Activity and Apoptosis*. *Bioconjugate Chemistry*, 2003. **14**(2): p. 458-463.
216. Lavis, L.D., T.-Y. Chao, and R.T. Raines, *Fluorogenic Label for Biomolecular Imaging*. *ACS Chemical Biology*, 2006. **1**(4): p. 252-260.
217. Hochmeister, M.N., et al., *Evaluation of prostate-specific antigen (PSA) membrane test assays for the forensic identification of seminal fluid*. *Journal of Forensic Sciences*, 1999. **44**(5): p. 1057-1060.
218. *Home Office, Crime in England and Wales: year ending March 2017*. 2017, Office for National Statistics.
219. *Home Office, Crime Outcomes in England and Wales 2016/17*. 2017, Home Office.
220. Gooch, J., et al., *Solid-phase synthesis of Rhodamine-110 fluorogenic substrates and their application in forensic analysis*. *Analyst*, 2016. **141**(8): p. 2392-2395.
221. Lottenberg, R., et al., *Assay of coagulation proteases using peptide chromogenic and fluorogenic substrates*. *Methods in Enzymology*, 1981. **80**: p. 341-361.

222. Cho, K., et al., *Active-site mapping of bovine and human blood coagulation serine proteases using synthetic peptide 4-nitroanilide and thio ester substrates*. Biochemistry, 1984. **23**(4): p. 644-650.
223. Ramjee, M.K., *The Use of Fluorogenic Substrates to Monitor Thrombin Generation for the Analysis of Plasma and Whole Blood Coagulation*. Analytical Biochemistry, 2000. **277**(1): p. 11-18.
224. Krishnaswamy, S., *The transition of prothrombin to thrombin*. Journal of Thrombosis and Haemostasis, 2013. **11**: p. 265-276.
225. Mann, K., et al., *Citrate anticoagulation and the dynamics of thrombin generation*. Journal of Thrombosis and Haemostasis, 2007. **5**(10): p. 2055-2061.
226. Zijlstra, W.G., A. Buursma, and O.W. van Assendelft, *Visible and near infrared absorption spectra of human and animal haemoglobin: determination and application*. 2000: VSP.
227. Gooch, J., et al., *Fluorogenic substrates for the detection of saliva*. Forensic Science International: Genetics Supplement Series, 2017. **6**: p. e565-e567.
228. Kasperkiewicz, P., et al., *Design of a selective substrate and activity based probe for human neutrophil serine protease 4*. PLoS ONE, 2015. **10**(7): p. e0132818-e0132830.
229. Réger, B., et al., *Detection of high-risk thrombophilia with an automated, global test: the Coagulation Inhibitor Potential assay*. Blood Coagulation & Fibrinolysis, 2018. **29**(5): p. 435-441.
230. Palta, S., R. Saroa, and A. Palta, *Overview of the coagulation system*. Indian journal of anaesthesia, 2014. **58**(5): p. 515-523.
231. Thompson, N.E., et al., *Identification, Production, and Use of Polyol-Responsive Monoclonal Antibodies for Immunoaffinity Chromatography*, in *Methods in Enzymology*, R.R. Burgess and M.P. Deutscher, Editors. 2009, Academic Press. p. 475-494.
232. Ngo, T.T., *Ligand Displacement Immunoassay*. Analytical Letters, 2005. **38**(7): p. 1057-1069.
233. Darwish, I.A., *Immunoassay Methods and their Applications in Pharmaceutical Analysis: Basic Methodology and Recent Advances*. International Journal of Biomedical Science, 2006. **2**(3): p. 217-235.



234. Frascione, N., et al., *Fluorogenic displacement biosensors for PSA detection using antibody-functionalised quantum dot nanoparticles*. RSC Advances, 2015. **5**(9): p. 6595-6598.
235. Goldman, E.R., et al., *A Hybrid Quantum Dot–Antibody Fragment Fluorescence Resonance Energy Transfer-Based TNT Sensor*. Journal of the American Chemical Society, 2005. **127**(18): p. 6744-6751.
236. Medintz, I.L., et al., *Self-assembled nanoscale biosensors based on quantum dot FRET donors*. Nature Materials, 2003. **2**(9): p. 630-638.
237. Michler, P., *Single quantum dots: Fundamentals, applications and new concepts*. 2003: Springer Science & Business Media.
238. Alivisatos, A.P., *Semiconductor clusters, nanocrystals, and quantum dots*. Science, 1996. **271**(5251): p. 933-937.
239. Rosenthal, S.J., et al., *Biocompatible quantum dots for biological applications*. Chemistry & Biology, 2011. **18**(1): p. 10-24.
240. Jin, S., et al., *Application of quantum dots in biological imaging*. Journal of Nanomaterials, 2011. **2011**: p. 1-13.
241. Medintz, I.L., et al., *Quantum dot bioconjugates for imaging, labelling and sensing*. Nature Materials, 2005. **4**(6): p. 435-446.
242. Stefflova, K., et al., *Targeted photodynamic therapy agent with a built-in apoptosis sensor for in vivo near-infrared imaging of tumor apoptosis triggered by its photosensitization in situ*. Molecular Imaging, 2006. **5**(4): p. 520-532.
243. Jemmerson, R. and R.M. Hutchinson, *Fine manipulation of antibody affinity for synthetic epitopes by altering peptide structure: Antibody binding to looped peptides*. European Journal of Immunology, 1990. **20**(3): p. 579-585.
244. Piironen, T., et al., *Determination and analysis of antigenic epitopes of prostate specific antigen (PSA) and human glandular kallikrein 2 (hK2) using synthetic peptides and computer modeling*. Protein Science, 1998. **7**(2): p. 259-269.
245. Stoilovic, M., *Detection of semen and blood stains using polilight as a light source*. Forensic Science International, 1991. **51**(2): p. 289-296.

246. Le Reste, L., et al., *Characterization of Dark Quencher Chromophores as Nonfluorescent Acceptors for Single-Molecule FRET*. Biophysical Journal, 2012. **102**(11): p. 2658-2668.
247. Olaru, A., et al., *Surface plasmon resonance (SPR) biosensors in pharmaceutical analysis*. Critical Reviews in Analytical Chemistry, 2015. **45**(2): p. 97-105.
248. Jennings, T.L., et al., *Reactive Semiconductor Nanocrystals for Chemoselective Biolabeling and Multiplexed Analysis*. ACS Nano, 2011. **5**(7): p. 5579-5593.
249. Pathak, S., M.C. Davidson, and G.A. Silva, *Characterization of the functional binding properties of antibody conjugated quantum dots*. Nano Letters, 2007. **7**(7): p. 1839-1845.
250. Ag, D., et al., *Biofunctional quantum dots as fluorescence probe for cell-specific targeting*. Colloids and Surfaces B: Biointerfaces, 2014. **114**: p. 96-103.
251. Zdobnova, T.A., et al., *Self-assembling complexes of quantum dots and scFv antibodies for cancer cell targeting and imaging*. PLoS ONE, 2012. **7**(10): p. e48248-e48256.
252. Song, S., et al., *Aptamer-based biosensors*. TrAC Trends in Analytical Chemistry, 2008. **27**(2): p. 108-117.
253. Ruscito, A. and M.C. DeRosa, *Small-Molecule Binding Aptamers: Selection Strategies, Characterization, and Applications*. Frontiers in Chemistry, 2016. **4**(14): p. 1-14.
254. O'Sullivan, C.K., *Aptasensors—the future of biosensing?* Analytical and Bioanalytical Chemistry, 2002. **372**(1): p. 44-48.
255. Lakhin, A., V. Tarantul, and L. Gening, *Aptamers: problems, solutions and prospects*. Acta Naturae, 2013. **5**(4): p. 34-43.
256. Thompson, T. and S. Black, *Forensic human identification: An introduction*. 2006: CRC Press.
257. Hermann, T. and D.J. Patel, *Adaptive recognition by nucleic acid aptamers*. Science, 2000. **287**(5454): p. 820-825.
258. Strehlitz, B., et al., *Aptamers for pharmaceuticals and their application in environmental analytics*. Bioanalytical Reviews, 2012. **4**(1): p. 1-30.

259. McKeague, M. and M.C. DeRosa, *Challenges and opportunities for small molecule aptamer development*. Journal of Nucleic Acids, 2012. **2012**: p. 1-20.
260. Balogh, Z., et al., *Selection and versatile application of virus-specific aptamers*. The FASEB Journal, 2010. **24**(11): p. 4187-4195.
261. Jing, M. and M.T. Bowser, *Methods for measuring aptamer-protein equilibria: a review*. Analytica Chimica Acta, 2011. **686**(1): p. 9-18.
262. Guo, K.-T., et al., *CELL-SELEX: Novel Perspectives of Aptamer-Based Therapeutics*. International Journal of Molecular Sciences, 2008. **9**(4): p. 668–678.
263. Iliuk, A.B., L. Hu, and W.A. Tao, *Aptamer in bioanalytical applications*. Analytical Chemistry, 2011. **83**(12): p. 4440-4452.
264. Song, K.M., S. Lee, and C. Ban, *Aptamers and their biological applications*. Sensors, 2012. **12**(1): p. 612-631.
265. Sun, H. and Y. Zu, *A highlight of recent advances in aptamer technology and its application*. Molecules, 2015. **20**(7): p. 11959-11980.
266. Keefe, A.D., S. Pai, and A. Ellington, *Aptamers as therapeutics*. Nature Reviews Drug Discovery, 2010. **9**(7): p. 537-550.
267. Michaud, M., et al., *A DNA Aptamer as a New Target-Specific Chiral Selector for HPLC*. Journal of the American Chemical Society, 2003. **125**(28): p. 8672-8679.
268. Turner, A.P., *Biosensors: sense and sensibility*. Chemical Society Reviews, 2013. **42**(8): p. 3184-3196.
269. Hong, P., W. Li, and J. Li, *Applications of aptasensors in clinical diagnostics*. Sensors, 2012. **12**(2): p. 1181-1193.
270. Cho, E.J., J.W. Lee, and A.D. Ellington, *Applications of aptamers as sensors*. Annual Review of Analytical Chemistry, 2009. **2**: p. 241-264.
271. Bruno, J.G., *Predicting the uncertain future of aptamer-based diagnostics and therapeutics*. Molecules, 2015. **20**(4): p. 6866-6887.

272. Tuerk, C. and L. Gold, *Systematic evolution of ligands by exponential enrichment: RNA ligands to bacteriophage T4 DNA polymerase*. Science, 1990. **249**(4968): p. 505-510.
273. Ellington, A.D. and J.W. Szostak, *In vitro selection of RNA molecules that bind specific ligands*. Nature, 1990. **346**(6287): p. 818-822.
274. Stoltenburg, R., C. Reinemann, and B. Strehlitz, *SELEX-a (r) evolutionary method to generate high-affinity nucleic acid ligands*. Biomolecular Engineering, 2007. **24**(4): p. 381-403.
275. Gopinath, S.C.B., *Methods developed for SELEX*. Analytical and Bioanalytical Chemistry, 2007. **387**(1): p. 171-182.
276. Mendonsa, S.D. and M.T. Bowser, *In vitro evolution of functional DNA using capillary electrophoresis*. Journal of the American Chemical Society, 2004. **126**(1): p. 20-21.
277. Nutiu, R. and Y. Li, *In vitro selection of structure-switching signaling aptamers*. Angewandte Chemie International Edition, 2005. **44**(7): p. 1061-1065.
278. Morris, K.N., et al., *High affinity ligands from in vitro selection: Complex targets*. Proceedings of the National Academy of Sciences, 1998. **95**(6): p. 2902-2907.
279. Stoltenburg, R., C. Reinemann, and B. Strehlitz, *FluMag-SELEX as an advantageous method for DNA aptamer selection*. Analytical and Bioanalytical Chemistry, 2005. **383**(1): p. 83-91.
280. Park, J.-W., et al., *Immobilization-free screening of aptamers assisted by graphene oxide*. Chemical Communications, 2012. **48**(15): p. 2071-2073.
281. Chushak, Y. and M.O. Stone, *In silico selection of RNA aptamers*. Nucleic Acids Research, 2009. **37**(12): p. e87-e87.
282. Lou, X., et al., *Micromagnetic selection of aptamers in microfluidic channels*. Proceedings of the National Academy of Sciences, 2009. **106**(9): p. 2989-2994.
283. Nitsche, A., et al., *One-step selection of Vaccinia virus-binding DNA aptamers by MonoLEX*. BMC Biotechnology, 2007. **7**(1): p. 1-12.

284. Peng, L., et al., *A combined atomic force/fluorescence microscopy technique to select aptamers in a single cycle from a small pool of random oligonucleotides*. Microscopy Research Technology, 2007. **70**(4): p. 372-381.
285. Stoltenburg, R., N. Nikolaus, and B. Strehlitz, *Capture-SELEX: selection of DNA aptamers for aminoglycoside antibiotics*. Journal of Analytical Methods in Chemistry, 2012. **2012**: p. 1-14.
286. Martin, J.A., et al., *A Method for Selecting Structure-switching Aptamers Applied to a Colorimetric Gold Nanoparticle Assay*. Journal of Visualized Experiments, 2015. **96**: p. e52545-e52557.
287. Nguyen, V.-T., et al., *Multiple GO-SELEX for efficient screening of flexible aptamers*. Chemical Communications, 2014. **50**(72): p. 10513-10516.
288. Kim, Y., C. Liu, and W. Tan, *Aptamers generated by Cell SELEX for biomarker discovery*. Biomarkers in Medicine, 2009. **3**(2): p. 193-202.
289. Sefah, K., et al., *Development of DNA aptamers using Cell-SELEX*. Nature Protocols, 2010. **5**(6): p. 1169-1185.
290. Ohuchi, S., *Cell-SELEX Technology*. Biores Open Access, 2012. **1**(6): p. 265-272.
291. Katilius, E., et al., *Sperm Capture Using Aptamer Based Technology*. 2014.
292. Ozer, A., J.M. Pagano, and J.T. Lis, *New Technologies Provide Quantum Changes in the Scale, Speed, and Success of SELEX Methods and Aptamer Characterization*. Molecular Therapeutics Nucleic Acids, 2014. **3**: p. e183-e201.
293. Conrad, R.C., S. Baskerville, and A.D. Ellington, *In vitro selection methodologies to probe RNA function and structure*. Molecular Diversity, 1995. **1**(1): p. 69-78.
294. Yüce, M., N. Ullah, and H. Budak, *Trends in aptamer selection methods and applications*. Analyst, 2015. **140**(16): p. 5379-5399.
295. Blind, M. and M. Blank, *Aptamer Selection Technology and Recent Advances*. Molecular Therapeutics Nucleic Acids, 2015. **4**: p. e223-e230.

296. Riley, K.R., et al., *Combining capillary electrophoresis and next-generation sequencing for aptamer selection*. Analytical and Bioanalytical Chemistry, 2015. **407**(6): p. 1527-1532.
297. Schütze, T., et al., *Probing the SELEX Process with Next-Generation Sequencing*. PLoS ONE, 2011. **6**(12): p. e29604-e29614.
298. Cho, M., et al., *Quantitative selection of DNA aptamers through microfluidic selection and high-throughput sequencing*. Proceedings of the National Academy of Sciences, 2010. **107**(35): p. 15373-15378.
299. Van Simaey, D., et al., *Study of the Molecular Recognition of Aptamers Selected through Ovarian Cancer Cell-SELEX*. PLoS ONE, 2010. **5**(11): p. e13770-e13777.
300. Wilson, R., et al., *Single-Step Selection of Bivalent Aptamers Validated by Comparison with SELEX Using High-Throughput Sequencing*. PLoS ONE, 2014. **9**(6): p. e100572-e100583.
301. Bawazer, L.A., et al., *Efficient Selection of Biomineralizing DNA Aptamers Using Deep Sequencing and Population Clustering*. ACS Nano, 2014. **8**(1): p. 387-395.
302. Børsting, C. and N. Morling, *Next generation sequencing and its applications in forensic genetics*. Forensic Science International: Genetics, 2015. **18**: p. 78-89.
303. Thiel, W.H. and P.H. Giangrande, *Analyzing HT-SELEX data with the Galaxy Project tools – A web based bioinformatics platform for biomedical research*. Methods, 2016. **97**: p. 3-10.
304. Martin, M., *Cutadapt removes adapter sequences from high-throughput sequencing reads*. EMBnet.journal, 2011. **17**(1): p. 10-12.
305. Hoinka, J., et al., *Large scale analysis of the mutational landscape in HT-SELEX improves aptamer discovery*. Nucleic Acids Research, 2015. **43**(12): p. 5699-5707.
306. Alam, K.K., J.L. Chang, and D.H. Burke, *FASTAptamer: A Bioinformatic Toolkit for High-throughput Sequence Analysis of Combinatorial Selections*. Molecular Therapeutics Nucleic Acids, 2015. **4**(3): p. e230-e240.

307. Caroli, J., et al., *APTANI: a computational tool to select aptamers through sequence-structure motif analysis of HT-SELEX data*. Bioinformatics, 2015. **32**(2): p. 161-164.
308. Jo, M., et al., *Development of Single-Stranded DNA Aptamers for Specific Bisphenol A Detection*. Oligonucleotides, 2011. **21**(2): p. 85-91.
309. Chang, A.L., et al., *Kinetic and equilibrium binding characterization of aptamers to small molecules using a label-free, sensitive, and scalable platform*. Analytical Chemistry, 2014. **86**(7): p. 3273-3278.
310. Sokoloski, J.E., S.E. Dombrowski, and P.C. Bevilacqua, *Thermodynamics of ligand binding to a heterogeneous RNA population in the malachite green aptamer*. Biochemistry, 2012. **51**(1): p. 565-572.
311. Sassanfar, M. and J.W. Szostak, *An RNA motif that binds ATP*. Nature, 1993. **364**(6437): p. 550-553.
312. Lorsch, J.R. and J.W. Szostak, *In vitro selection of RNA aptamers specific for cyanocobalamin*. Biochemistry, 1994. **33**(4): p. 973-982.
313. Fried, M. and D.M. Crothers, *Equilibria and kinetics of lac repressor-operator interactions by polyacrylamide gel electrophoresis*. Nucleic Acids Research, 1981. **9**(23): p. 6505-6525.
314. Hall, B., et al., *In vitro selection of RNA aptamers to a protein target by filter immobilization*. Current Protocols in Molecular Biology, 2009. **24**: p. 1-24.
315. Olmsted, I.R., et al., *Measurement of aptamer-protein interactions with back-scattering interferometry*. Analytical Chemistry, 2011. **83**(23): p. 8867-8870.
316. Nagatoishi, S., Y. Tanaka, and K. Tsumoto, *Circular dichroism spectra demonstrate formation of the thrombin-binding DNA aptamer G-quadruplex under stabilizing-cation-deficient conditions*. Biochemical and Biophysical Research Communications, 2007. **352**(3): p. 812-817.
317. Baugh, C., D. Grate, and C. Wilson, *2.8 Å crystal structure of the malachite green aptamer*. Journal of Molecular Biology, 2000. **301**(1): p. 117-128.

318. Cruz-Aguado, J.A. and G. Penner, *Fluorescence Polarization Based Displacement Assay for the Determination of Small Molecules with Aptamers*. Analytical Chemistry, 2008. **80**(22): p. 8853-8855.
319. Hianik, T., et al., *Influence of ionic strength, pH and aptamer configuration for binding affinity to thrombin*. Bioelectrochemistry, 2007. **70**(1): p. 127-133.
320. Chang, A.L., M. McKeague, and C.D. Smolke, *Facile characterization of aptamer kinetic and equilibrium binding properties using surface plasmon resonance*. Methods in Enzymology, 2014. **549**: p. 451-466.
321. Connaghan-Jones, K.D., A.D. Moody, and D.L. Bain, *Quantitative DNase footprint titration: a tool for analyzing the energetics of protein-DNA interactions*. Nature Protocols, 2008. **3**(5): p. 900-914.
322. Neves, M.A.D., et al., *Defining the secondary structural requirements of a cocaine-binding aptamer by a thermodynamic and mutation study*. Biophysical Chemistry, 2010. **153**(1): p. 9-16.
323. Kwon, Y.S., et al., *Detection of Iprobenfos and Edifenphos using a new Multi-aptasensor*. Analytica Chimica Acta, 2015. **868**: p. 60-66.
324. Velázquez-Campoy, A., et al., *Isothermal Titration Calorimetry*, in *Current Protocols in Cell Biology*. 2001, John Wiley & Sons, Inc. p. 1-24.
325. Kleinjung, F., et al., *High-Affinity RNA as a Recognition Element in a Biosensor*. Analytical Chemistry, 1998. **70**(2): p. 328-331.
326. Hianik, T. and J. Wang, *Electrochemical aptasensors—recent achievements and perspectives*. Electroanalysis, 2009. **21**(11): p. 1223-1235.
327. Feng, C., S. Dai, and L. Wang, *Optical aptasensors for quantitative detection of small biomolecules: A review*. Biosensors and Bioelectronics, 2014. **59**: p. 64-74.
328. Kim, Y.S. and M.B. Gu, *Advances in aptamer screening and small molecule aptasensors*, in *Biosensors Based on Aptamers and Enzymes*. 2013, Springer. p. 29-67.



329. Tang, Z., et al., *Aptamer switch probe based on intramolecular displacement*. Journal of the American Chemical Society, 2008. **130**(34): p. 11268-11269.
330. Long, F., A. Zhu, and H. Shi, *Recent Advances in Optical Biosensors for Environmental Monitoring and Early Warning*. Sensors, 2013. **13**(10): p. 13928-13948.
331. Li, K., et al., *Nanoplasmonic Imaging of Latent Fingerprints and Identification of Cocaine*. Angewandte Chemie International Edition, 2013. **52**(44): p. 11542-11545.
332. Hayat, A. and J.L. Marty, *Aptamer based electrochemical sensors for emerging environmental pollutants*. Frontiers in Chemistry, 2014. **2**(41): p. 1-9.
333. Torres-Chavolla, E. and E.C. Alocilja, *Aptasensors for detection of microbial and viral pathogens*. Biosensors and Bioelectronics, 2009. **24**(11): p. 3175-3182.
334. Hansen, J.A., et al., *Quantum-Dot/Aptamer-Based Ultrasensitive Multi-Analyte Electrochemical Biosensor*. Journal of the American Chemical Society, 2006. **128**(7): p. 2228-2229.
335. Sassolas, A., L.J. Blum, and B.D. Leca - Bouvier, *Electrochemical aptasensors*. Electroanalysis, 2009. **21**(11): p. 1237-1250.
336. Han, K., Z. Liang, and N. Zhou, *Design Strategies for Aptamer-Based Biosensors*. Sensors, 2010. **10**(5): p. 4541-4557.
337. Grieshaber, D., et al., *Electrochemical Biosensors - Sensor Principles and Architectures*. Sensors, 2008. **8**(3): p. 1400-1458.
338. Baker, B.R., et al., *An electronic, aptamer-based small-molecule sensor for the rapid, label-free detection of cocaine in adulterated samples and biological fluids*. Journal of the American Chemical Society, 2006. **128**(10): p. 3138-3139.
339. Weng, C.-H., C.-J. Huang, and G.-B. Lee, *Screening of Aptamers on Microfluidic Systems for Clinical Applications*. Sensors, 2012. **12**(7): p. 9514-9529.
340. Gopinath, S.C., *Biosensing applications of surface plasmon resonance-based Biacore technology*. Sensors and Actuators B: Chemical, 2010. **150**(2): p. 722-733.

341. Schuck, P., *Use of surface plasmon resonance to probe the equilibrium and dynamic aspects of interactions between biological macromolecules*. Annual Review of Biophysics, 1997. **26**(1): p. 541-566.
342. Voinova, M.V., *On Mass Loading and Dissipation Measured with Acoustic Wave Sensors: A Review*. Journal of Sensors, 2009. **2009**: p. 1-13.
343. Datar, R., et al., *Cantilever sensors: nanomechanical tools for diagnostics*. MRS Bulletin, 2009. **34**(06): p. 449-454.
344. Mok, W. and Y. Li, *Recent Progress in Nucleic Acid Aptamer-Based Biosensors and Bioassays*. Sensors, 2008. **8**(11): p. 7050-7084.
345. Hou, H., et al., *Aptamer-Based Cantilever Array Sensors for Oxytetracycline Detection*. Analytical Chemistry, 2013. **85**(4): p. 2010-2014.
346. Vashist, S.K., *A review of microcantilevers for sensing applications*. Journal Nanotechnology, 2007. **3**: p. 1-15.
347. Wood, M., et al., *Selective targeting of fingerprints using immunogenic techniques*. Australian Journal of Forensic Sciences, 2013. **45**(2): p. 211-226.
348. Kong, R.-M., et al., *A novel aptamer-functionalized MoS<sub>2</sub> nanosheet fluorescent biosensor for sensitive detection of prostate specific antigen*. Analytical and Bioanalytical Chemistry, 2015. **407**(2): p. 369-377.
349. Deng, B., et al., *Aptamer binding assays for proteins: The thrombin example -A review*. Analytica Chimica Acta, 2014. **837**: p. 1-15.
350. Wang, Y., et al., *Aptamer biosensor based on fluorescence resonance energy transfer from upconverting phosphors to carbon nanoparticles for thrombin detection in human plasma*. Analytical Chemistry, 2011. **83**(21): p. 8130-8137.
351. Smith, F., *Handbook of forensic drug analysis*. 2004: Academic Press.
352. Hilton, J.P., et al., *A microfluidic affinity sensor for the detection of cocaine*. Sensors and Actuators B: Chemical, 2011. **166**(2): p. 241-246.

353. Yarbakht, M. and M. Nikkhah, *Unmodified gold nanoparticles as a colorimetric probe for visual methamphetamine detection*. Journal of Experimental Nanoscience, 2016. **11**(7): p. 593-601.
354. Huang, L., et al., *A label-free electrochemical biosensor based on a DNA aptamer against codeine*. Analytica Chimica Acta, 2013. **787**: p. 203-210.
355. Cunningham, A., *European Monitoring Centre for Drugs and Drug Addiction: New psychoactive substances in Europe: An update from the EU early warning system*. 2015.
356. Bell, C., et al., *Development of a rapid LC - MS/MS method for direct urinalysis of designer drugs*. Drug Test and Analysis, 2011. **3**(7 - 8): p. 496-504.
357. Thiviyanathan, V. and D.G. Gorenstein, *Aptamers and the Next Generation of Diagnostic Reagents*. Proteomics - Clinical Applications, 2012. **6**(0): p. 563-573.
358. Smith, M.L., et al., *Modern Instrumental Methods in Forensic Toxicology*. Journal of Analytical Toxicology, 2007. **31**(5): p. 237-239.
359. Sheng, L., et al., *PVP-coated graphene oxide for selective determination of ochratoxin A via quenching fluorescence of free aptamer*. Biosensors and Bioelectronics, 2011. **26**(8): p. 3494-3499.
360. Cooper, G. and A. Negrusz, *Clarke's analytical forensic toxicology*. 2013: Pharmaceutical Press.
361. Ha, T.H., *Recent advances for the detection of ochratoxin A*. Toxins, 2015. **7**(12): p. 5276-5300.
362. Wu, Y., et al., *Ultrasensitive aptamer biosensor for arsenic (III) detection in aqueous solution based on surfactant-induced aggregation of gold nanoparticles*. Analyst, 2012. **137**(18): p. 4171-4178.
363. Lamont, E.A., et al., *A single DNA aptamer functions as a biosensor for ricin*. Analyst, 2011. **136**(19): p. 3884-3895.

364. Esteban-Fernández de Ávila, B., et al., *Aptamer-modified graphene-based catalytic micromotors: off-on fluorescent detection of ricin*. ACS Sensors, 2016. **1**(3): p. 217–221.
365. Li, C.H., et al., *A graphene oxide-based strand displacement amplification platform for ricin detection using aptamer as recognition element*. Biosensors and Bioelectronics, 2017. **91**: p. 149-154.
366. Zhao, R., et al., *Cantilever-based aptasensor for trace level detection of nerve agent simulant in aqueous matrices*. Sensors and Actuators B: Chemical, 2017. **238**: p. 1231–1239.
367. Singh, S., *Sensors—An effective approach for the detection of explosives*. Journal of Hazardous Materials, 2007. **144**(1–2): p. 15-28.
368. Ehrentreich-Förster, E., et al., *Biosensor-based on-site explosives detection using aptamers as recognition elements*. Analytical and Bioanalytical Chemistry, 2008. **391**(5): p. 1793-1800.
369. Zhu, Y., et al., *Graphene and graphene oxide: synthesis, properties, and applications*. Advanced Materials, 2010. **22**(35): p. 3906-3924.
370. Liu, B., et al., *DNA adsorbed on graphene and graphene oxide: Fundamental interactions, desorption and applications*. Current Opinion in Colloid & Interface Science, 2016. **26**: p. 41-49.
371. He, S., et al., *A graphene nanoprobe for rapid, sensitive, and multicolor fluorescent DNA analysis*. Advanced Functional Materials, 2010. **20**(3): p. 453-459.
372. Liu, X., et al., *Multiplexed aptasensors and amplified DNA sensors using functionalized graphene oxide: application for logic gate operations*. ACS Nano, 2012. **6**(4): p. 3553-3563.
373. Wu, X., et al., *Study of Fluorescence Quenching Ability of Graphene Oxide with a Layer of Rigid and Tunable Silica Spacer*. Langmuir, 2018. **34**(2): p. 603-611.
374. Zhang, M., et al., *A versatile graphene-based fluorescence “on/off” switch for multiplex detection of various targets*. Biosensors and Bioelectronics, 2011. **26**(7): p. 3260-3265.

375. Bock, L.C., et al., *Selection of single-stranded DNA molecules that bind and inhibit human thrombin*. *Nature*, 1992. **355**(6360): p. 564-566.
376. Savory, N., et al., *Selection of DNA aptamer against prostate specific antigen using a genetic algorithm and application to sensing*. *Biosensors and Bioelectronics*, 2010. **26**(4): p. 1386-1391.
377. Kirby, R., et al., *Aptamer-based sensor arrays for the detection and quantitation of proteins*. *Analytical Chemistry*, 2004. **76**(14): p. 4066-4075.
378. Liu, X., et al., *Highly Sensitive Fluorometric Turn-On Detection of Lysozyme Based on a Graphene Oxide/ssDNA Assembly*. *IEEE Sensors Journal*, 2017. **17**(17): p. 5431-5436.
379. Chang, H., et al., *Graphene fluorescence resonance energy transfer aptasensor for the thrombin detection*. *Analytical Chemistry*, 2010. **82**(6): p. 2341-2346.
380. Wu, M., et al., *Adsorption and desorption of DNA on graphene oxide studied by fluorescently labeled oligonucleotides*. *Langmuir*, 2011. **27**(6): p. 2731-2738.
381. Pei, H., et al., *A graphene-based sensor array for high-precision and adaptive target identification with ensemble aptamers*. *Journal of the American Chemical Society*, 2012. **134**(33): p. 13843-13849.
382. Gomez-Navarro, C., et al., *Atomic structure of reduced graphene oxide*. *Nano Letters*, 2010. **10**(4): p. 1144-1148.
383. Lu, C., et al., *Comparison of MoS<sub>2</sub>, WS<sub>2</sub>, and Graphene Oxide for DNA Adsorption and Sensing*. *Langmuir*, 2017. **33**(2): p. 630-637.
384. Park, J.S., N.-I. Goo, and D.-E. Kim, *Mechanism of DNA adsorption and desorption on graphene oxide*. *Langmuir*, 2014. **30**(42): p. 12587-12595.
385. Pagba, C.V., et al., *Direct detection of aptamer-thrombin binding via surface-enhanced Raman spectroscopy*. *Journal of Biomedical Optics*, 2010. **15**(4): p. 47006-47014.
386. Argoubi, W., et al., *Label-free electrochemical aptasensing platform based on mesoporous silica thin film for the detection of prostate specific antigen*. *Sensors and Actuators B: Chemical*, 2018. **255**: p. 309-315.

387. Wang, J. and B. Liu, *Fluorescence resonance energy transfer between an anionic conjugated polymer and a dye-labeled lysozyme aptamer for specific lysozyme detection*. Chemical Communications, 2009. **0**(17): p. 2284-2286.
388. Geldert, A., et al., *Enhancing the sensing specificity of a MoS<sub>2</sub> nanosheet-based FRET aptasensor using a surface blocking strategy*. Analyst, 2017. **142**(14): p. 2570-2577.
389. Lu, C., et al., *Comparison of graphene oxide and reduced graphene oxide for DNA adsorption and sensing*. Langmuir, 2016. **32**(41): p. 10776-10783.
390. Gao, L., et al., *Highly sensitive protein detection via covalently linked aptamer to MoS<sub>2</sub> and exonuclease-assisted amplification strategy*. International Journal of Nanomedicine, 2017. **12**: p. 7847-7853.
391. Mallikaratchy, P., *Evolution of complex target SELEX to identify aptamers against mammalian cell-surface antigens*. Molecules, 2017. **22**(2): p. 215-232.
392. World Health Organization, *WHO laboratory manual for the examination and processing of human semen*. 2010.
393. Tolle, F., et al., *By-product formation in repetitive PCR amplification of DNA libraries during SELEX*. PLoS ONE, 2014. **9**(12): p. e114693-e114705.
394. Shapiro, H.M., *Practical flow cytometry*. 2005: John Wiley & Sons.
395. Nguyen Quang, N., G. Perret, and F. Ducongé, *Applications of High-Throughput Sequencing for In Vitro Selection and Characterization of Aptamers*. Pharmaceuticals, 2016. **9**(4): p. 76-91.
396. Goecks, J., A. Nekrutenko, and J. Taylor, *Galaxy: a comprehensive approach for supporting accessible, reproducible, and transparent computational research in the life sciences*. Genome Biology, 2010. **11**(8): p. R86-R99.
397. Aird, D., et al., *Analyzing and minimizing PCR amplification bias in Illumina sequencing libraries*. Genome Biology, 2011. **12**(2): p. R18-R32.

398. Lyu, Y., et al., *Generating cell targeting aptamers for nanotheranostics using cell-SELEX*. *Theranostics*, 2016. **6**(9): p. 1440-1452.
399. Hoinka, J., et al., *AptaCluster—A Method to Cluster HT-SELEX Aptamer Pools and Lessons from Its Application*. *Research in Computational Molecular Biology*, 2014. **8394**: p. 115-128.
400. Meuwly, D. and R. Veldhuis. *Forensic biometrics: From two communities to one discipline*. in *Proceedings of the International Conference of the Biometrics Special Interest Group 2012*. IEEE.
401. Metcalf, J.L., et al., *Microbiome tools for forensic science*. *Trends in Biotechnology*, 2017. **35**(9): p. 814-823.
402. Duong, B., et al., *Covert thermal barcodes based on phase change nanoparticles*. *Science Reports*, 2014. **4**: p. 5170-5175.
403. Mills, H., S. Skodbo, and P. Blyth, *Understanding organised crime: Estimating the scale and the social and economic costs*. 2013.
404. Plimmer, J.J., *Choosing the correct forensic marker(s) in currency, document, and product protection*. *Proceedings of SPIE*, 2006. **6075**: p. 60750-60759.
405. Wise, S.H. and J.R. Almirall, *Chemical taggant detection and analysis by laser-induced breakdown spectroscopy*. *Applied Optics*, 2008. **47**(31): p. G15-G20.
406. Mead, B.K., et al., *The Role of DNA-Stained Currency in Gang Robberies within the United Kingdom*. *Journal of Forensic Sciences*, 2014. **59**(1): p. 264-267.
407. Bae, H.J., et al., *Biomimetic Microfingerprints for Anti-Counterfeiting Strategies*. *Advanced Materials*, 2015. **27**(12): p. 2083-2089.
408. Duong, B., et al., *Printed Multilayer Microtaggants with Phase Change Nanoparticles for Enhanced Labeling Security*. *ACS Applied Materials & Interfaces*, 2014. **6**(11): p. 8909-8912.
409. Grate, J.W., R.G. Ewing, and D.A. Atkinson, *Vapor-generation methods for explosives-detection research*. *TrAC Trends in Analytical Chemistry*, 2012. **41**: p. 1-14.

410. Kaish, N., et al., *Method for remote detection of volatile taggant*. 2000.
411. Smith, C., S. Strauss, and L. DeFrancesco, *DNA goes to court*. Nature Biotechnology, 2012. **30**(11): p. 1047-1053.
412. Sermon, P.A., et al., *Deterring gun crime materially using forensic coatings*. Forensic Science International, 2012. **221**(1–3): p. 131-136.
413. Wang, M., et al., *Nanomaterial-based barcodes*. Nanoscale, 2015. **7**(26): p. 11240-11247.
414. Paunescu, D., W.J. Stark, and R.N. Grass, *Particles with an identity: Tracking and tracing in commodity products*. Powder Technology, 2016. **291**: p. 344-350.
415. Perr, J.M., K.G. Furton, and J.R. Almirall, *Solid phase microextraction ion mobility spectrometer interface for explosive and taggant detection*. Journal of Separation Science, 2005. **28**(2): p. 177-183.
416. Loving, C.D., *Composite microdot and method of forming the same*. 1994.
417. Swiegers, G.F., B.W. Bootle, and G.M. George, *Method and system for identifying items*. 2012.
418. Lee, P.K., *Method of tagging with color-coded microparticles*. 1977.
419. Outwater, C., *Product authentication system*. 2002.
420. Chandler, D.J., et al., *Precision fluorescently dyed particles and methods of making and using same*. 2003.
421. Kerns, W.J., B. Brogger, and J.L. Esterberg, *Identification particles and system and method for retrospective identification using spectral codes*. 2006.
422. Lawandy, N., et al., *Multi wavelength excitation/emission authentication and detection scheme*. 2014.
423. Wilkinson, T.G. and E. Dorland, *Marking fuel for authentication*. 2010.



424. Baque, T., *Method of authenticating and/or identifying an article*. 2013.
425. Jung, L., J.A. Hayward, and M.B. Liang, *DNA marking of previously undistinguished items for traceability*. 2014.
426. George, G.M., *Article Marking System*. 2009.
427. Butland, C.L. and B. Baggot, *Labeling technique for countering product diversion and product counterfeiting*. 2000.
428. Brown, J. and B. Reichert, *Compositions for use in security marking*. 2012.
429. Sleat, R. and G. Van Lint, *A marking apparatus for nucleic acid marking of items*. 2012.
430. Deisingh, A.K., *Pharmaceutical counterfeiting*. *Analyst*, 2005. **130**(3): p. 271-279.
431. Whitehead, M.R. and R. Peakall, *Microdot technology for individual marking of small arthropods*. *Agricultural and Forest Entomology*, 2012. **14**(2): p. 171-175.
432. Husáková, L., et al., *Characterization of industrial explosives based on the determination of metal oxides in the identification particles by microwave digestion and atomic absorption spectrometry method*. *Forensic Science International*, 2008. **178**(2–3): p. 146-152.
433. Pham, H.H., et al., *Polymer nanostructured material for the recording of biometric features*. *Journal of Material Chemistry*, 2007. **17**(6): p. 523-526.
434. Finkel, N.H., et al., *Barcoding the Microworld*. *Analytical Chemistry*, 2004. **76**(19): p. 352-359.
435. Guillou, O., et al., *A Long Journey in Lanthanide Chemistry: From Fundamental Crystallogeneses Studies to Commercial Anticounterfeiting Taggants*. *Accounts of Chemical Research*, 2016. **49**: p. 844–856.
436. Przybylowicz, P., *Black and Smokeless Powders, Technologies for Finding Bombs and the Bomb Makers*. 1998: National Academy Press, Washington DC.

437. Cleary, M., *Method of identifying a surface*. 1998.
438. Britton, D.W. and M.J. Wraith, *Detection of chemicals by immunoassay*. 1999.
439. Hood, L. and D. Galas, *The digital code of DNA*. *Nature*, 2003. **421**(6921): p. 444-448.
440. Hayward, J.A. and J. Meraglia, *DNA to safeguard electrical components and protect against counterfeiting and diversion*. *Proceedings of ISTFA*, 2011. **4**: p. 238-241.
441. Cox, J.P.L., *Long-term data storage in DNA*. *Trends in Biotechnology*, 2001. **19**(7): p. 247-250.
442. Paunescu, D., et al., *Reversible DNA encapsulation in silica to produce ROS-resistant and heat-resistant synthetic DNA 'fossils'*. *Nature Protocols*, 2013. **8**(12): p. 2440-2448.
443. Lindahl, T., *Instability and decay of the primary structure of DNA*. *Nature*, 1993. **362**(6422): p. 709-715.
444. Glover, A., et al., *Evaluation of DNA as a taggant for fuels*. *Fuel*, 2011. **90**(6): p. 2142-2146.
445. Puddu, M., et al., *Magnetically Recoverable, Thermostable, Hydrophobic DNA/Silica Encapsulates and Their Application as Invisible Oil Tags*. *ACS Nano*, 2014. **8**(3): p. 2677-2685.
446. Reep, P., M.H. Liang, and J.J. Sheu, *System and method for authenticating multiple components associated with a particular product*. 2006.
447. Zhou, M., S. Chang, and C.P. Grover, *Cryptography based on the absorption/emission features of multicolor semiconductor nanocrystal quantum dots*. *Optics Express*, 2004. **12**(13): p. 2925-2931.
448. Williams Jr, G.M., et al., *Optically coded nanocrystal taggants and optical frequency IDs*. *Proceedings of SPIE*, 2010. **7673**: p. 76730-76744.
449. Hardman, R., *A Toxicologic Review of Quantum Dots: Toxicity Depends on Physicochemical and Environmental Factors*. *Environmental Health Perspectives*, 2006. **114**(2): p. 165-172.

450. Li, H., W.Y. Shih, and W.-H. Shih, *Non-heavy-metal ZnS quantum dots with bright blue photoluminescence by a one-step aqueous synthesis*. *Nanotechnology*, 2007. **18**(20): p. 205604-205610.
451. Li, R., et al., *Dual-Mode Encoded Magnetic Composite Microsphere Based on Fluorescence Reporters and Raman Probes as Covert Tag for Anticounterfeiting Applications*. *ACS Applied Materials & Interfaces*, 2016. **8**(14): p. 9384-9394.
452. Osberg, K.D., et al., *Dispersible Surface-Enhanced Raman Scattering Nanosheets*. *Advanced Materials*, 2012. **24**(45): p. 6065-6070.
453. Natan, M., et al., *Nanoparticles As Covert Taggants In Currency, Bank Notes, And Related Documents*. 2007.
454. Hyun, D.C., et al., *Emerging Applications of Phase-Change Materials (PCMs): Teaching an Old Dog New Tricks*. *Angewandte Chemie International Edition*, 2014. **53**(15): p. 3780-3795.
455. Gooch, J., et al., *Monitoring Criminal Activity through Invisible Fluorescent "Peptide Coding" Taggants*. *Analytical Chemistry*, 2016. **88**(8): p. 4456-4460.
456. Gooch, J., et al., *Establishing evidence of contact transfer in criminal investigation by a novel 'peptide coding' reagent*. *Talanta*, 2015. **144**: p. 1065-1069.
457. Kydd, P.H., *Polypeptides as chemical tagging materials*. 1982.
458. Dollinger, G., *Nonbiological Applications*, in *The Polymerase Chain Reaction*, K. Mullis, F. Ferre, and R. Gibbs, Editors. 1994 Springer: Boston, USA. p. 265-274.
459. Levi, M., *Thinking about Organised Crime*. *The RUSI Journal*, 2014. **159**(1): p. 6-14.
460. Li, L., *Technology designed to combat fakes in the global supply chain*. *Business Horizons*, 2013. **56**(2): p. 167-177.
461. Michael, C., *Improvement in security systems*. 1998.
462. Alaeddini, R., S.J. Walsh, and A. Abbas, *Forensic implications of genetic analyses from degraded DNA—A review*. *Forensic Science International: Genetics*, 2010. **4**(3): p. 148-157.

463. Bender, K., M.J. Farfán, and P.M. Schneider, *Preparation of degraded human DNA under controlled conditions*. Forensic Science International, 2004. **139**(2–3): p. 135-140.
464. Carlson, R., *The changing economics of DNA synthesis*. Nature Biotechnology, 2009. **27**(12): p. 1091-1094.
465. Baslé, E., N. Joubert, and M. Pucheault, *Protein Chemical Modification on Endogenous Amino Acids*. Chemistry & Biology, 2010. **17**(3): p. 213-227.
466. Ogunniyi, D.S., *Castor oil: A vital industrial raw material*. Bioresource Technology, 2006. **97**(9): p. 1086-1091.
467. Chelli, R., et al., *Glycerol condensed phases Part II. A molecular dynamics study of the conformational structure and hydrogen bonding*. Physical Chemistry Chemical Physics, 1999. **1**(5): p. 879-885.
468. Kiyonami, R., M. Zeller, and V. Zabrouskov, *Quantifying Peptides in Complex Mixtures with High Sensitivity and Precision Using a Targeted Approach with a Hybrid Linear Ion Trap-Orbitrap Mass Spectrometer*. The FASEB Journal, 2011. **25**: p. 926-926.
469. Frackenpohl, J., et al., *The Outstanding Biological Stability of  $\beta$ - and  $\gamma$ -Peptides toward Proteolytic Enzymes: An In Vitro Investigation with Fifteen Peptidases*. ChemBioChem, 2001. **2**(6): p. 445-455.
470. Rink, R., et al., *To protect peptide pharmaceuticals against peptidases*. Journal of Pharmacological and Toxicological Methods, 2010. **61**(2): p. 210-218.
471. Penn, S.G., et al., *Nanobarcodes particles as covert security tags for documents and product security*. 2004.
472. Umezawa, K., D. Citterio, and K. Suzuki, *New trends in near-infrared fluorophores for bioimaging*. Analytical Sciences, 2014. **30**(3): p. 327-349.
473. Yu, D., et al., *Biosensors in drug discovery and drug analysis*. Analytical Letters, 2005. **38**(11): p. 1687-1701.
474. Velasco-Garcia, M.N. and T. Mottram, *Biosensor technology addressing agricultural problems*. Biosystems Engineering, 2003. **84**(1): p. 1-12.

475. Song, S., H. Xu, and C. Fan, *Potential diagnostic applications of biosensors: current and future directions*. International Journal of Nanomedicine, 2006. **1**(4): p. 433-440.
476. Zarei, M., *Portable biosensing devices for point-of-care diagnostics: Recent developments and applications*. TrAC Trends in Analytical Chemistry, 2017. **91**: p. 26-41.
477. Hill, H.D., G.K. Summer, and M.D. Waters, *An automated fluorometric assay for alkaline phosphatase using 3-O-methylfluorescein phosphate*. Analytical Biochemistry, 1968. **24**(1): p. 9-17.
478. Gomori, G., *Distribution of acid phosphatase in the tissues under normal and under pathologic conditions*. Archives of Pathology & Laboratory Medicine, 1941. **32**: p. 189-199.
479. Gershkovich, A.A. and V.V. Kholodovych, *Fluorogenic substrates for proteases based on intramolecular fluorescence energy transfer (IFETS)*. Journal of Biochemical and Biophysical Methods, 1996. **33**(3): p. 135-162.
480. Barral, K., A.D. Moorhouse, and J.E. Moses, *Efficient conversion of aromatic amines into azides: a one-pot synthesis of triazole linkages*. Organic letters, 2007. **9**(9): p. 1809-1811.
481. Frenkel, E.S. and K. Ribbeck, *Salivary mucins in host defense and disease prevention*. Journal of Oral Microbiology, 2015. **7**(1): p. 29759-29768.
482. Karton-Lifshin, N., et al., *A Unique Paradigm for a Turn-ON Near-Infrared Cyanine-Based Probe: Noninvasive Intravital Optical Imaging of Hydrogen Peroxide*. Journal of the American Chemical Society, 2011. **133**(28): p. 10960-10965.

# | Appendix

## A.1 Fluorogenic Substrates for the Detection of Blood

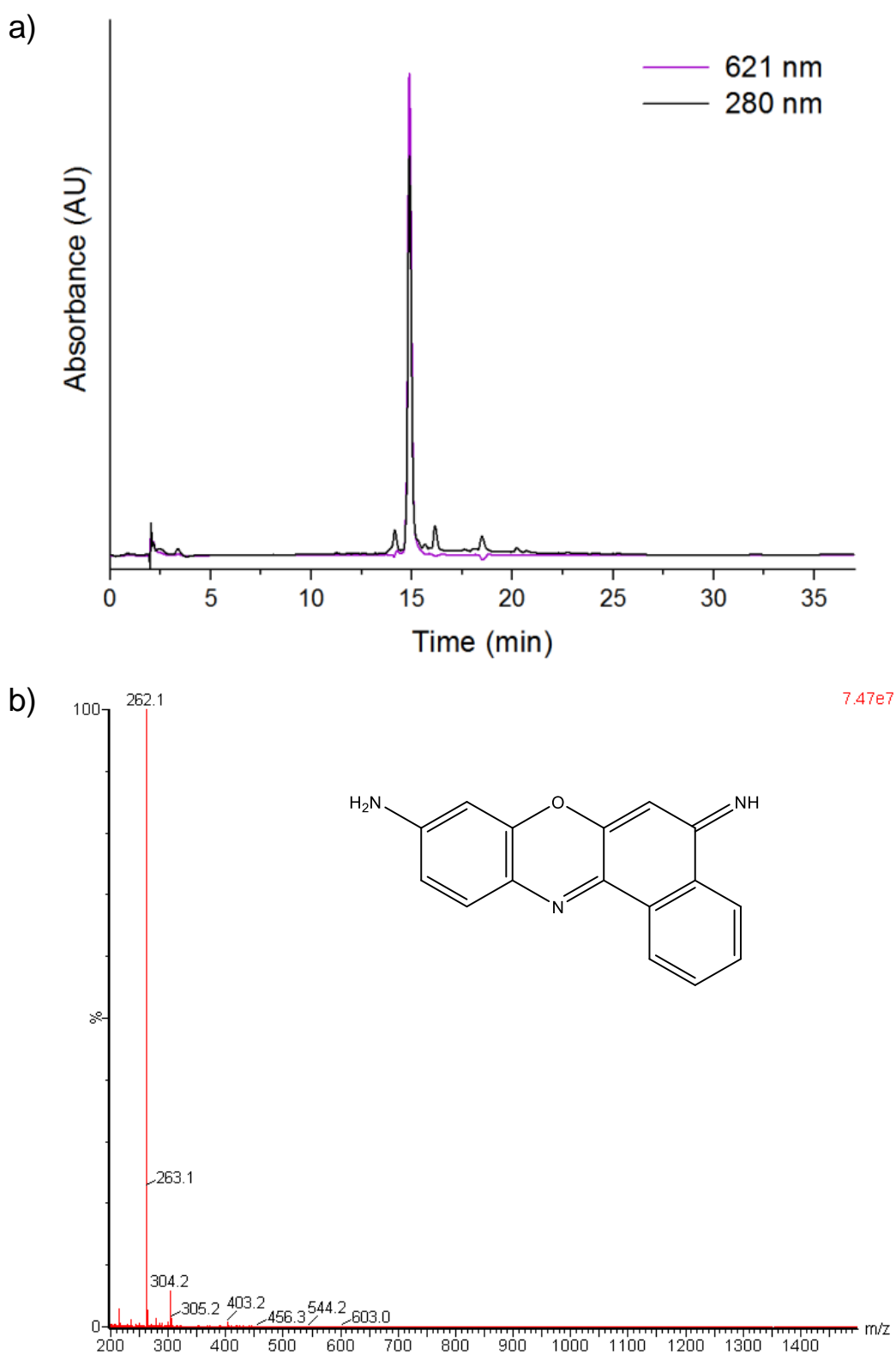


**Figure 81:** Confirmation of substrate product  ${}_2\text{HN-CV-NH}_2$  purity and identity as established by a) RP-HPLC and b) ESI-MS (calculated  $m/z$  for  $[\text{M}+\text{H}]^+ = 262.09$ ) respectively.

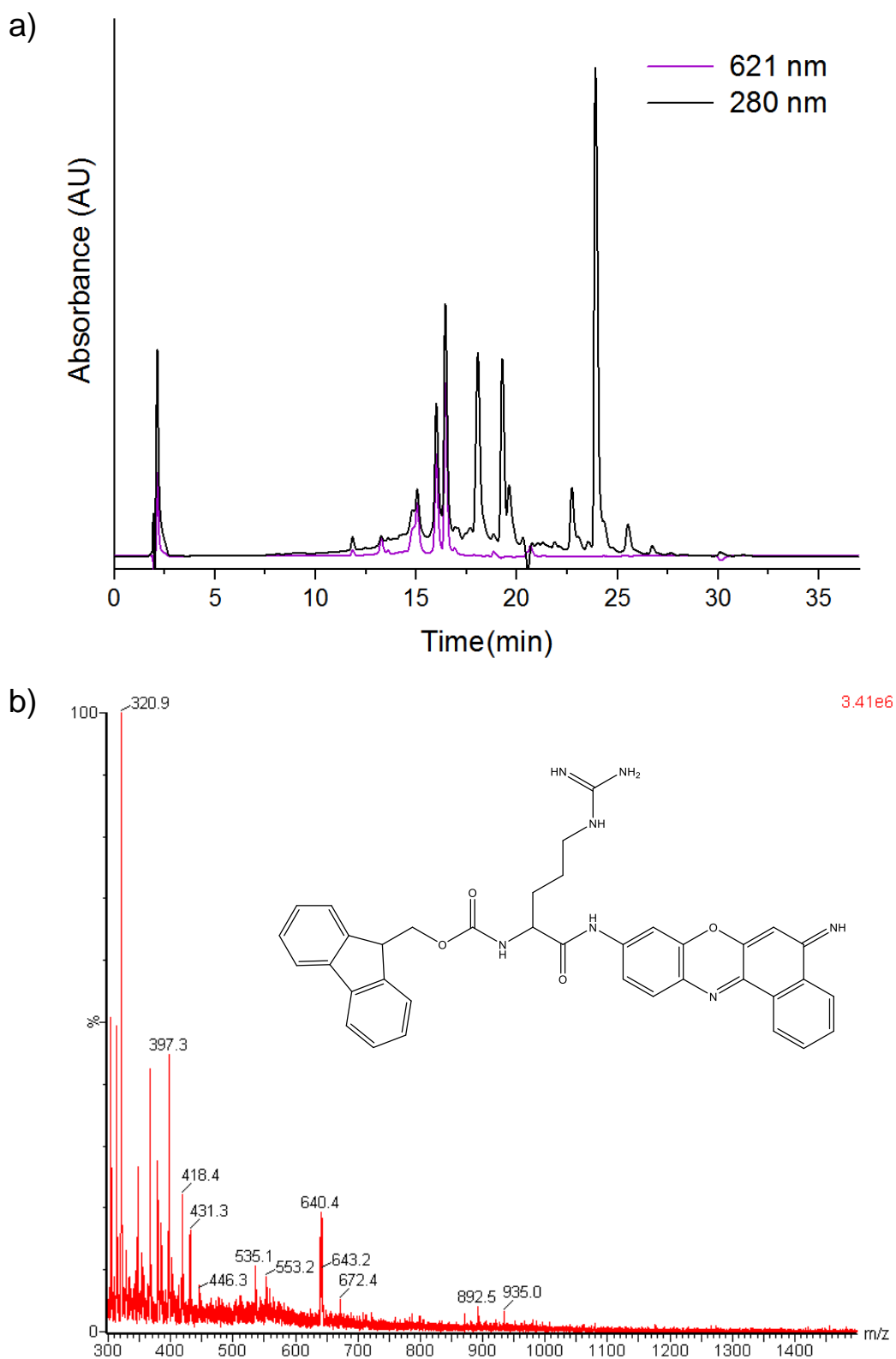


**Figure 82:** Confirmation of substrate product  ${}_{2}\text{HN-CV-R-Fmoc}$  purity and identity as established by a) RP-HPLC and b) ESI-MS (calculated  $m/z$  for  $[\text{M}+\text{H}]^{+} = 640.26$ ) respectively.



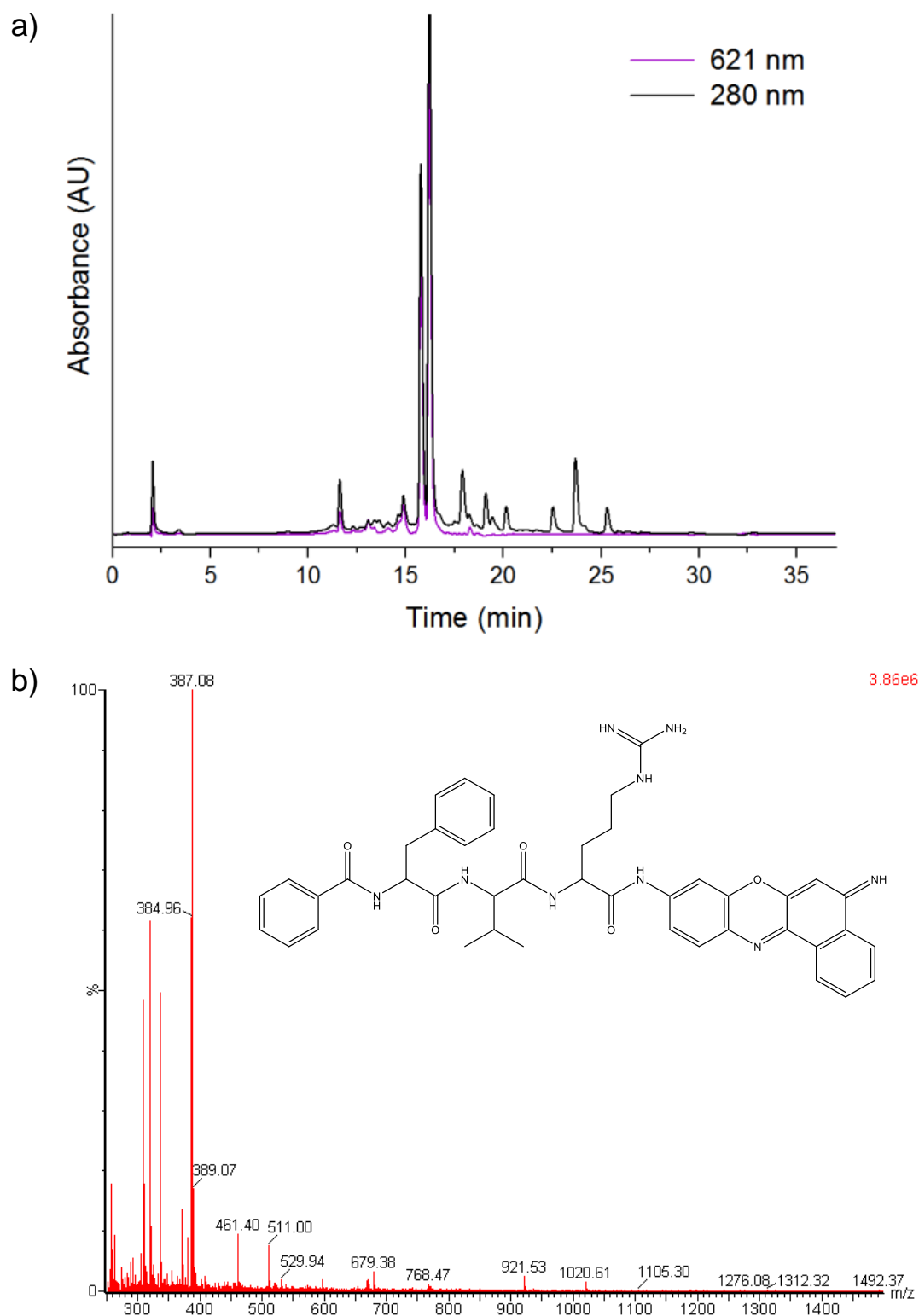


**Figure 83:** Confirmation of substrate product  ${}^2\text{HN-CV-RVF-Bz}$  purity and identity as established by a) RP-HPLC and b) ESI-MS (calculated  $m/z$  for  $[\text{M}+\text{H}]^+ = 767.35$ ) respectively.

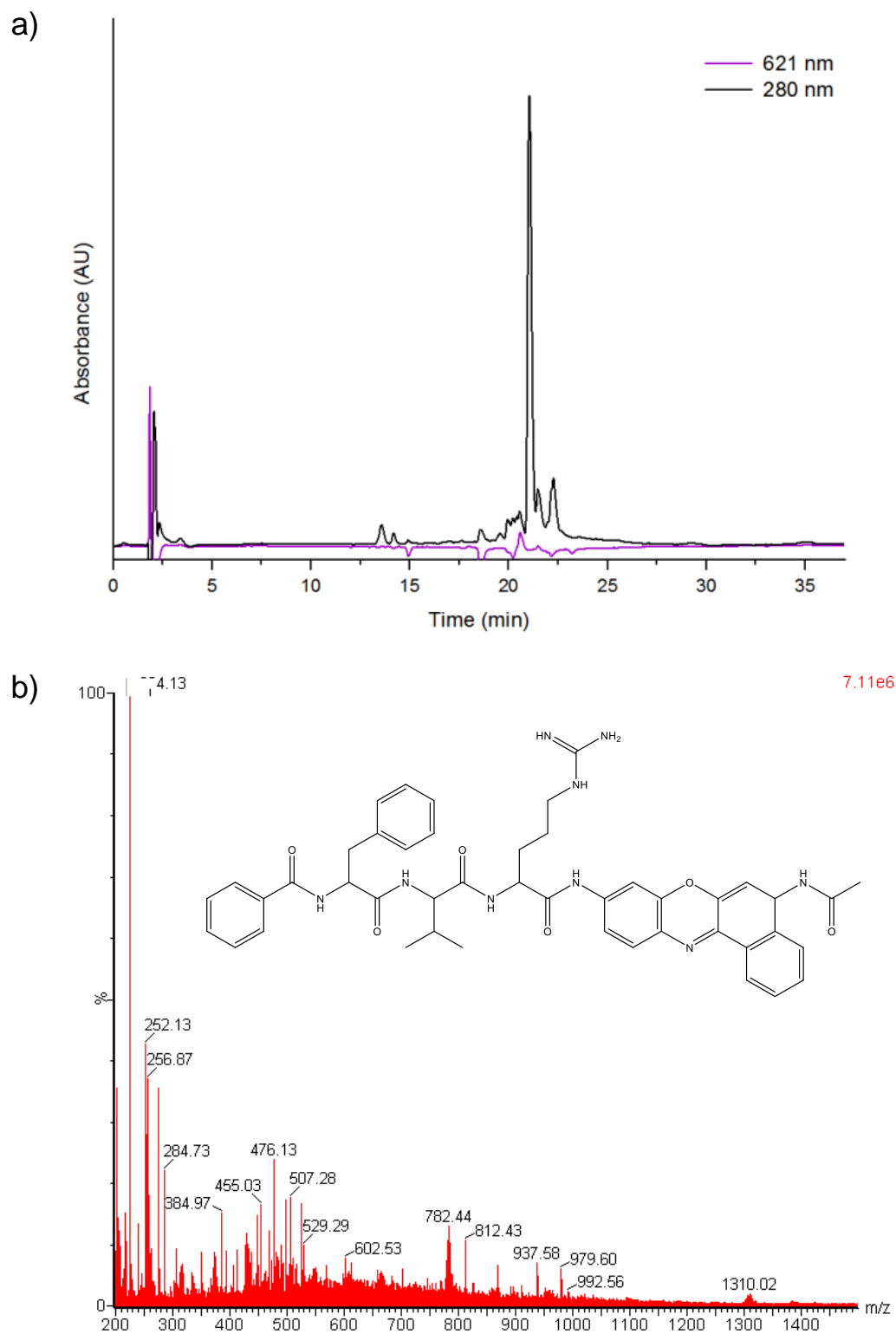


**Figure 84:** Confirmation of substrate product Ac-CV-RVF-Bz purity and identity as established by a) RP-HPLC and b) ESI-MS (calculated  $m/z$  for  $[M+H]^+ = 812.38$ ) respectively.

## A.2 'Establishing Evidence of Contact Transfer in Criminal Investigation by a Novel 'Peptide Coding' Reagent'

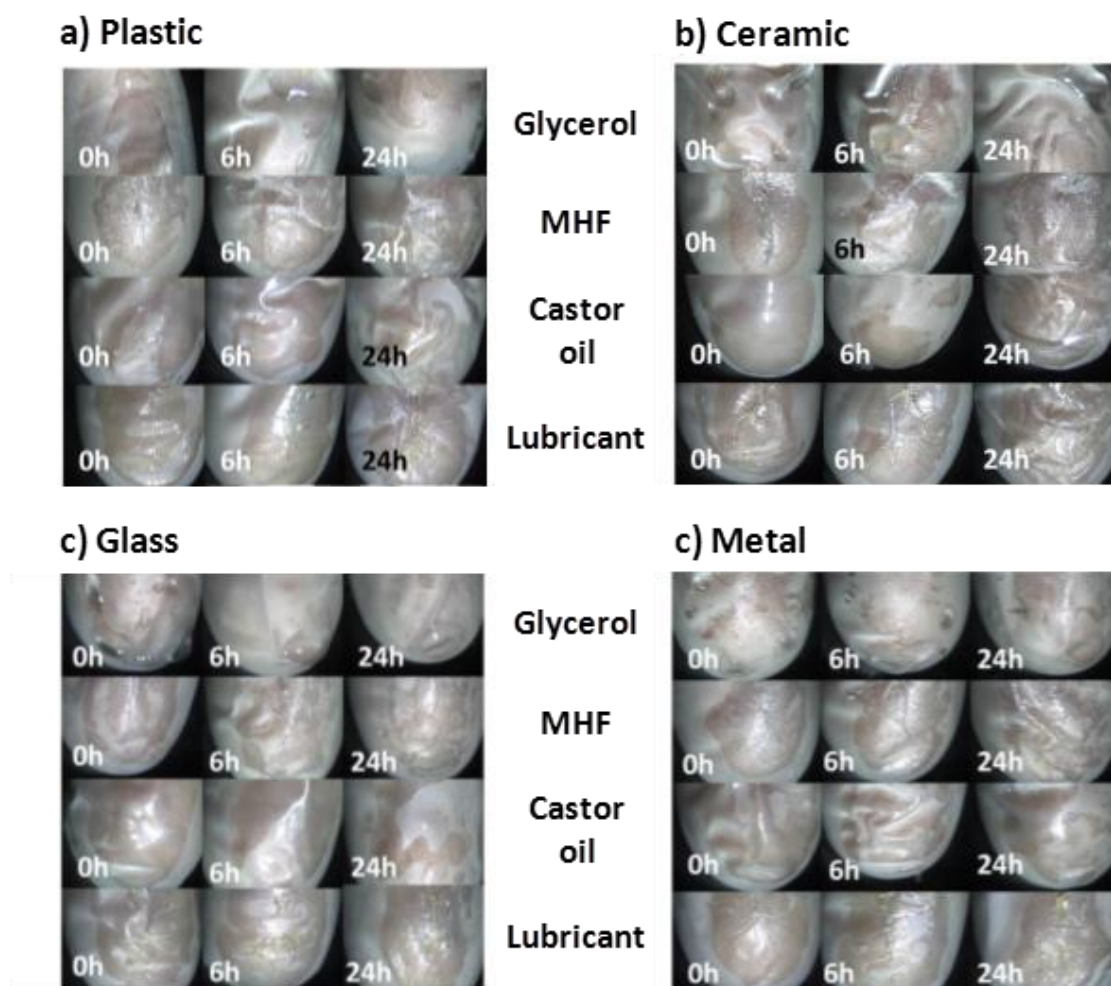


**Figure 85:** Microscopy images of four chosen media transferred from different surfaces a) plastic, b) ceramic, c) glass and d) metal to a gloved finger after 0, 6 and 24 hr from application.

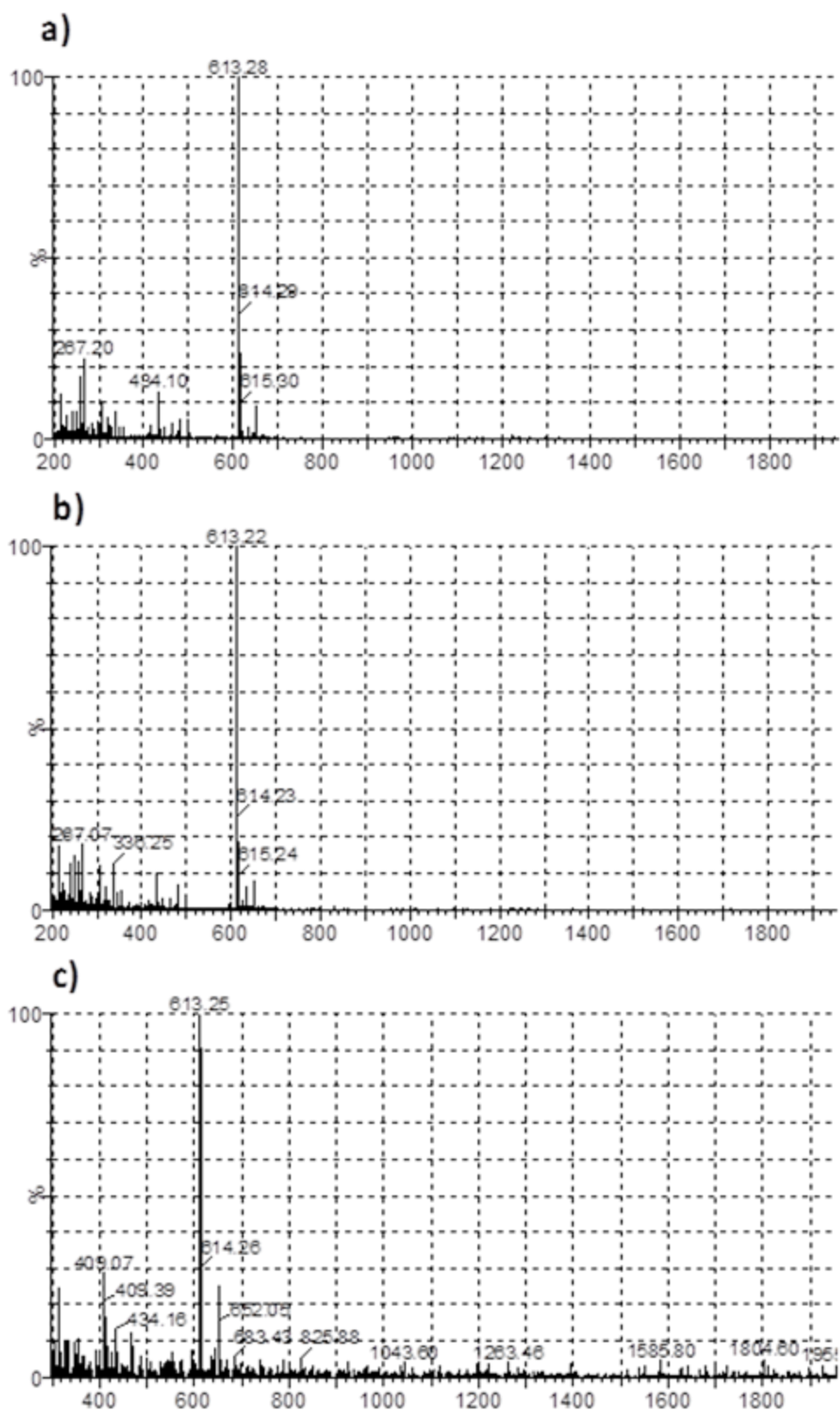


**Figure 86:** Mass spectra obtained from MHF extracts after primary transfer of reagent containing a) 5 mg, b) 2.5 mg and c) 1 mg of peptide.

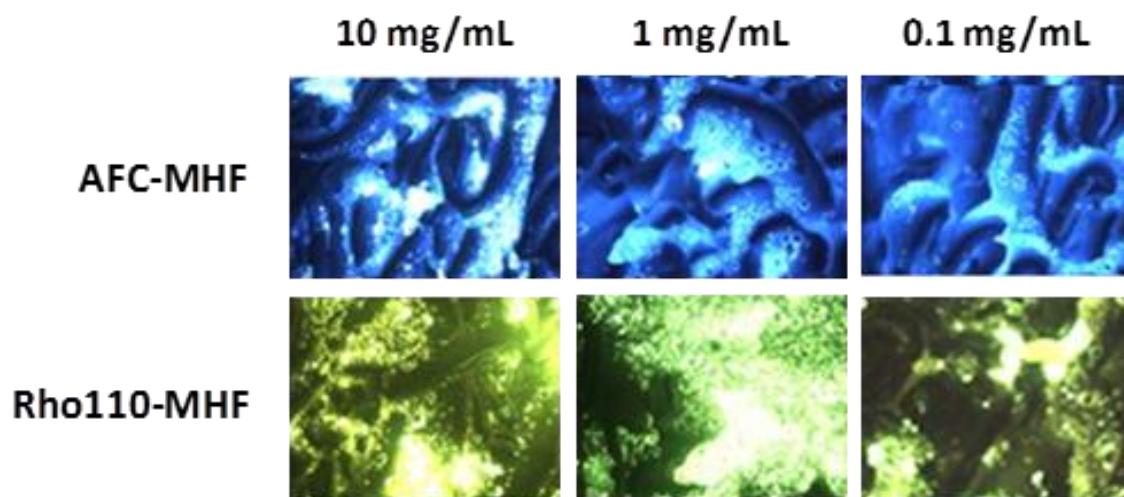


**Figure 87:** Fluorescence microscopy images obtained after mixing different concentrations of AFC and Rhodamine-110 with MHF.

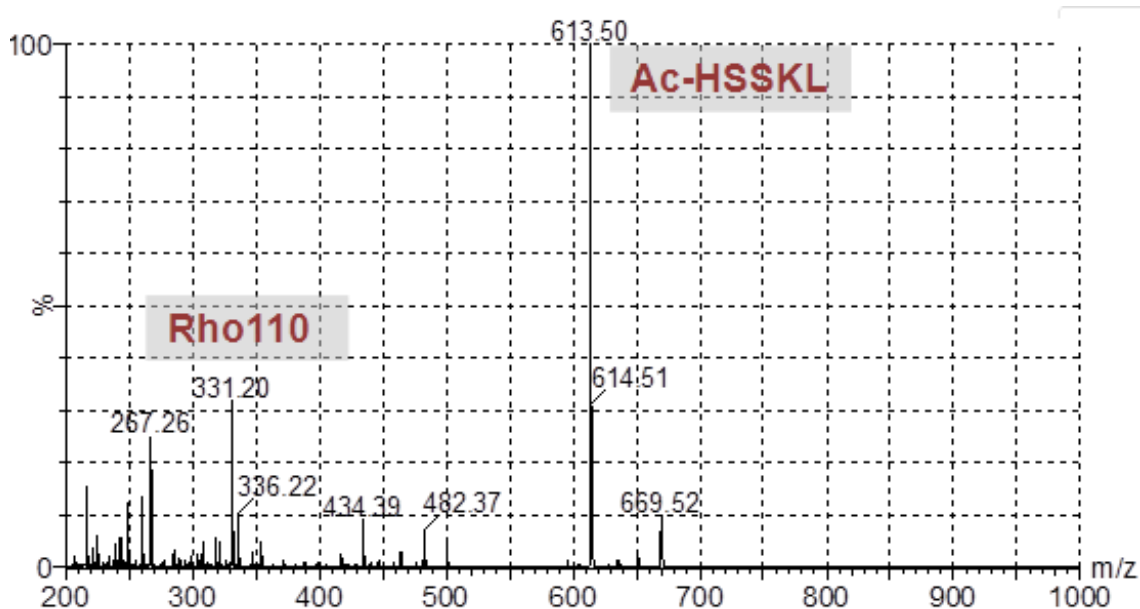


**Figure 88:** Mass spectrum of the reagent containing both fluorophore (Rh-110) and peptide (Ac-HSSKL) after liquid/liquid extraction.

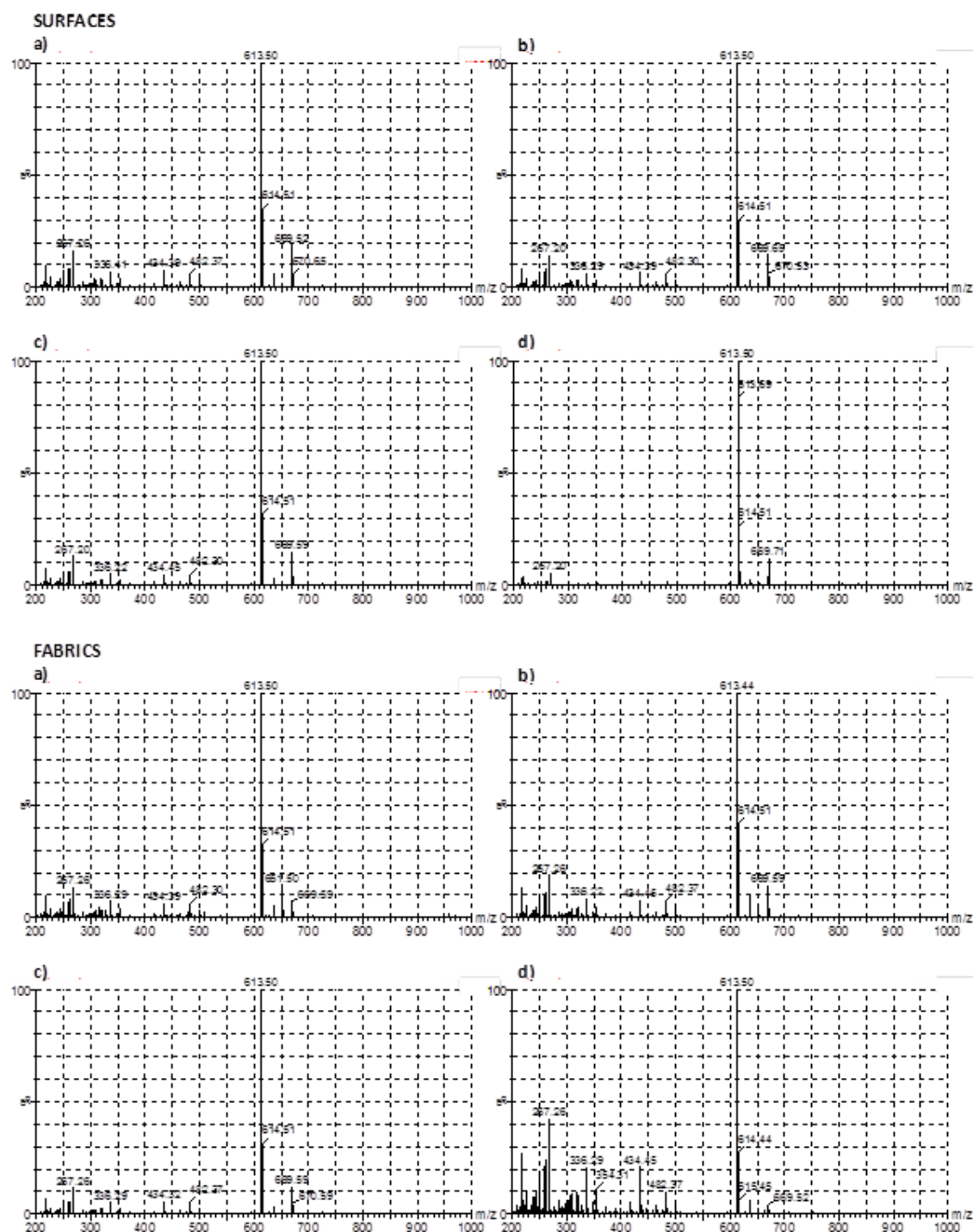


**Figure 89:** Mass spectra of reagent samples extracted six weeks after application to surfaces (upper panel; a) ceramic; b) glass; c) plastic; d) aluminium) and fabrics (lower panel; a) denim; b) polyester; c) leather; d) cotton). Similar results were obtained for all the previous time points analyzed (week 1-5).

### A.3 'Monitoring Criminal Activity through Invisible Fluorescent 'Peptide Coding' Taggants'

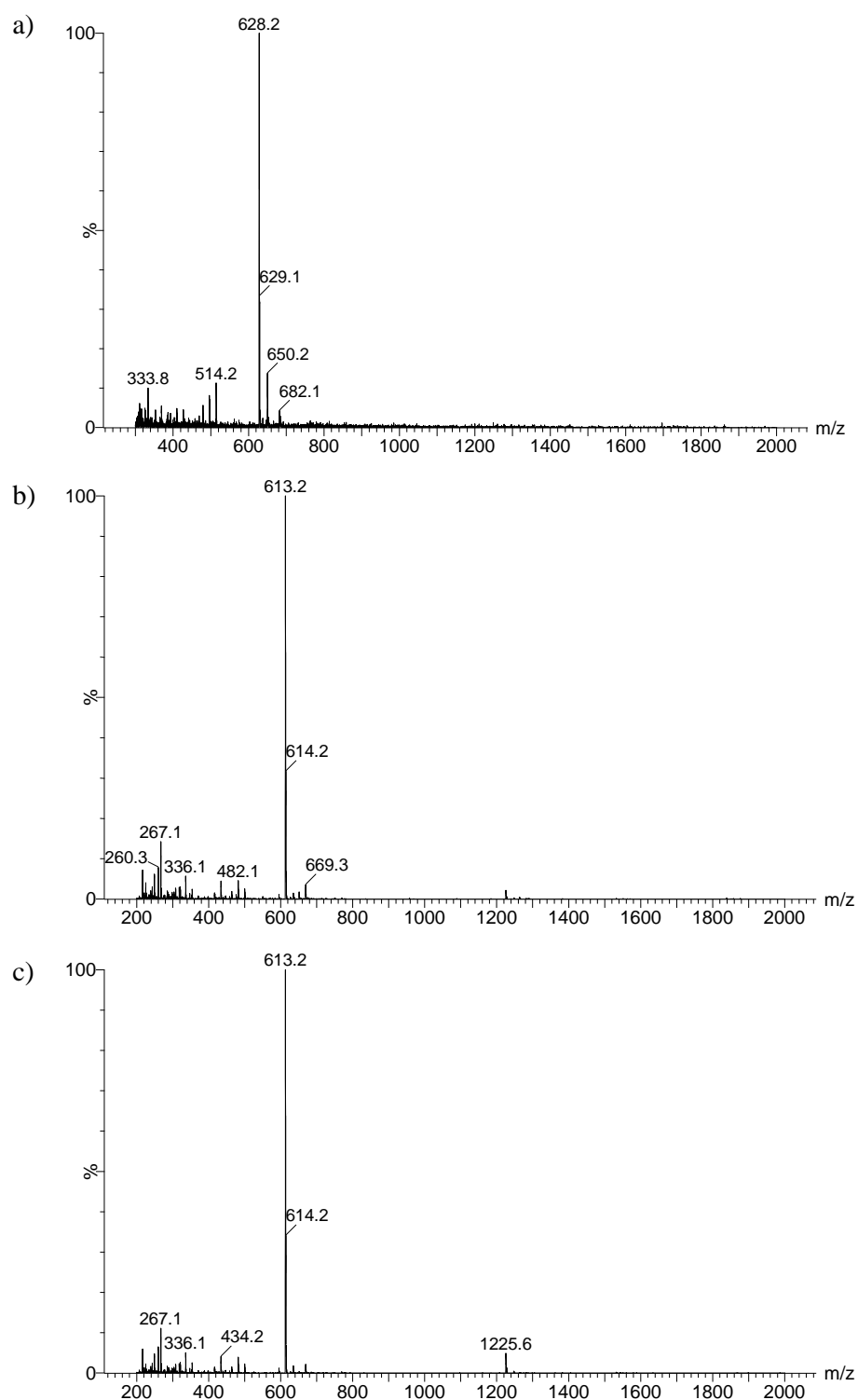


**Figure 90:** ESI-MS spectra of a) peptide sequence 1: Ac-KQQSP-NH<sub>2</sub>, (theoretical [M+H]<sup>+</sup> m/z ratio = 628.34) b) peptide sequence 2: Ac-HSSKL-COOH (theoretical [M+H]<sup>+</sup> m/z ratio = 613.33) and c) peptide sequence 3: Ac-hsskl-COOH (theoretical [M+H]<sup>+</sup> m/z ratio = 613.33) after synthesis.

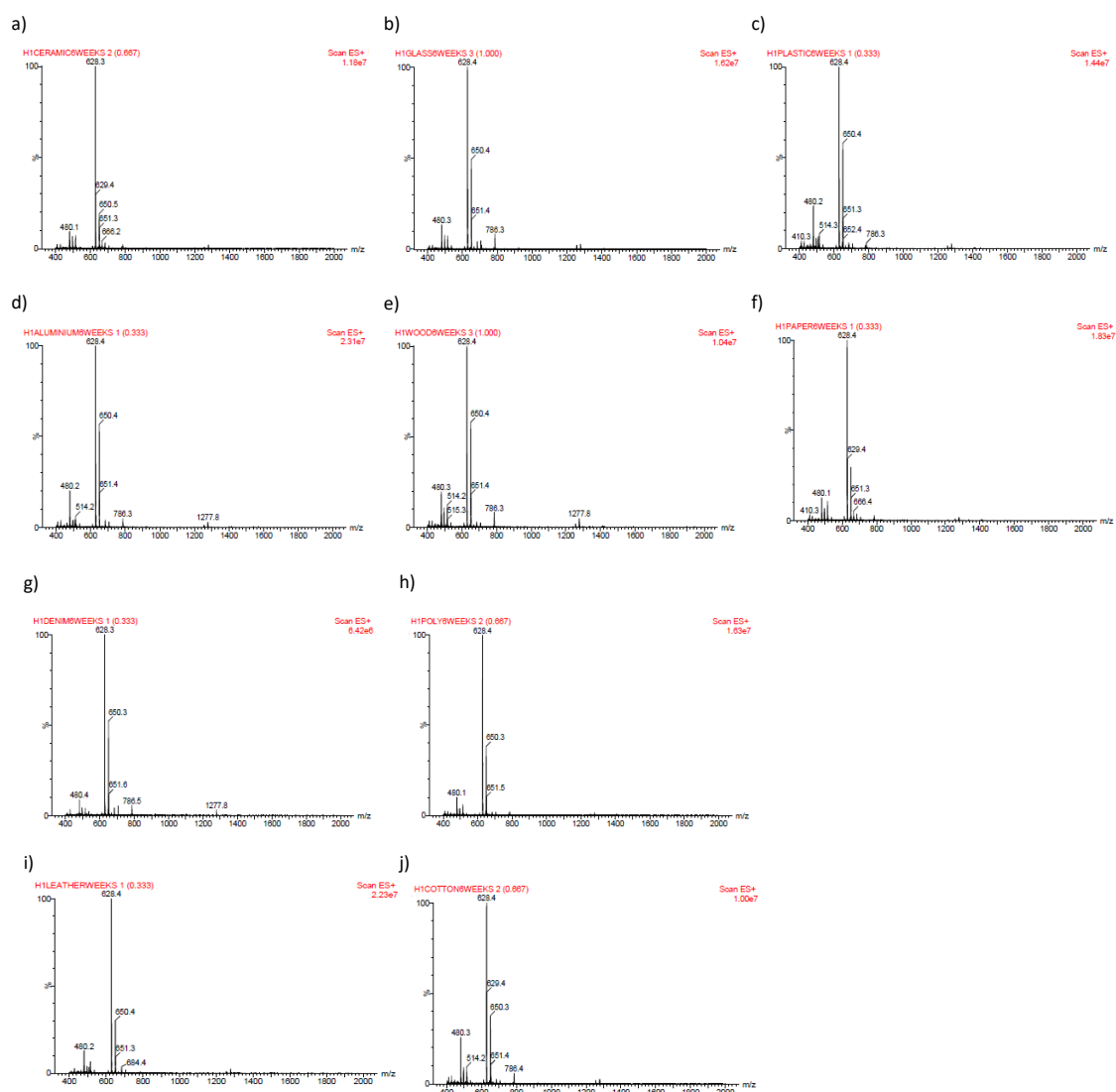


**Figure 91:** ESI-MS spectra of peptide sequence 1: Ac-KQQSP-NH<sub>2</sub>, (theoretical [M+H]<sup>+</sup> m/z ratio = 628.34) reagent samples extracted six weeks after application to surfaces: a) ceramic, b) glass, c) plastic, d) aluminium, e) wood, f) paper, g) denim, h) polyester, i) leather, j) cotton. Similar results were obtained for all previous time point extractions.

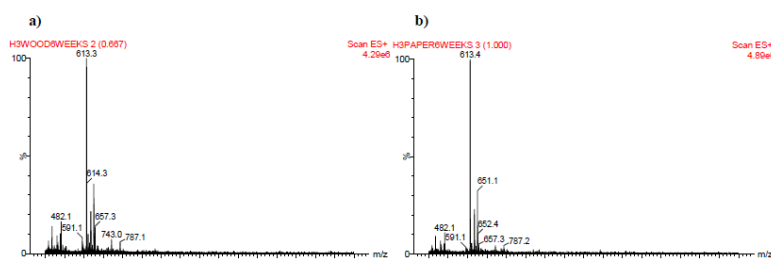
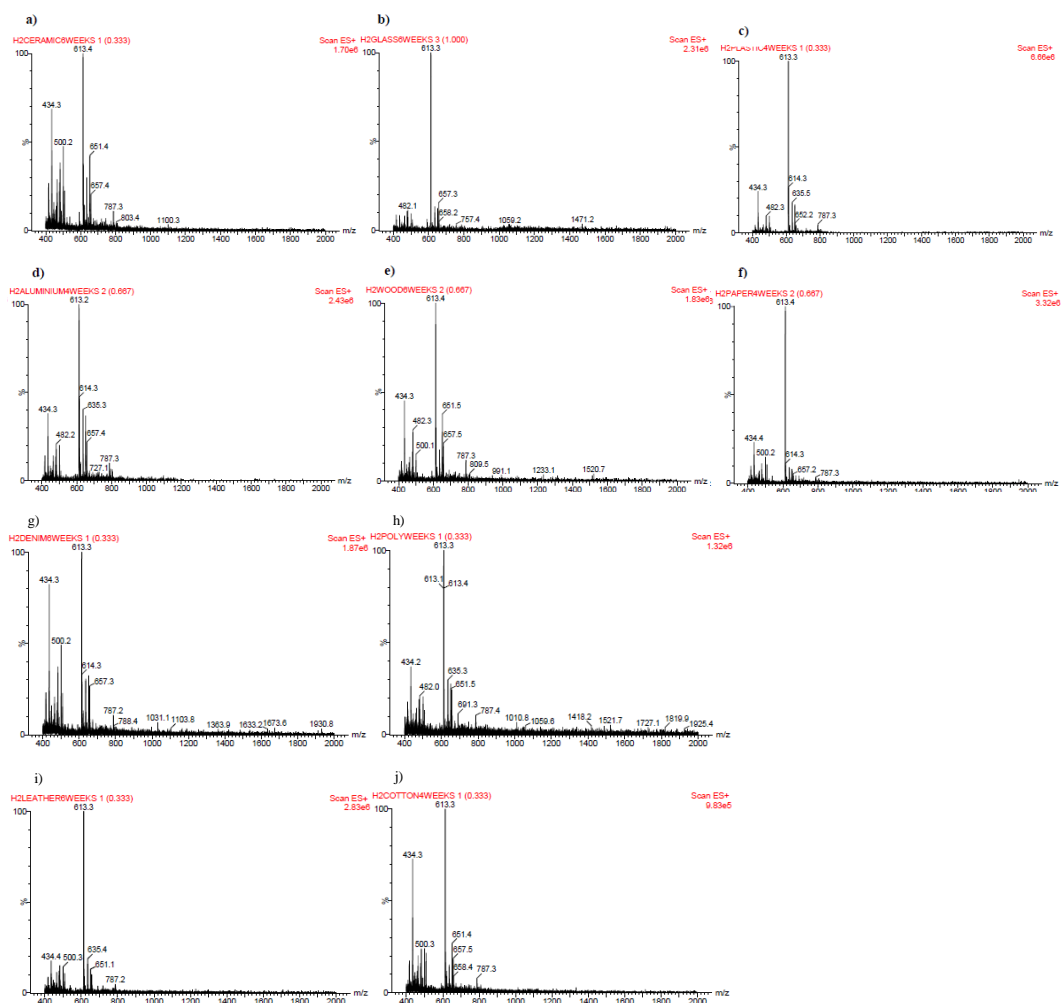
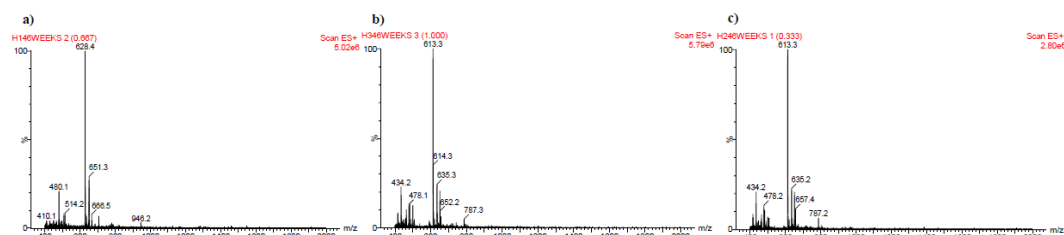


**Figure 92:** ESI-MS spectra of peptide sequence 2: Ac-HSSKL-COOH (theoretical [M+H]<sup>+</sup> m/z ratio = 613.33) reagent samples extracted six weeks after application to surfaces: a) wood, b) paper. Similar results were obtained for all previous time point extractions.





FRIDGE (4°C)



INCUBATOR (37.39°C)

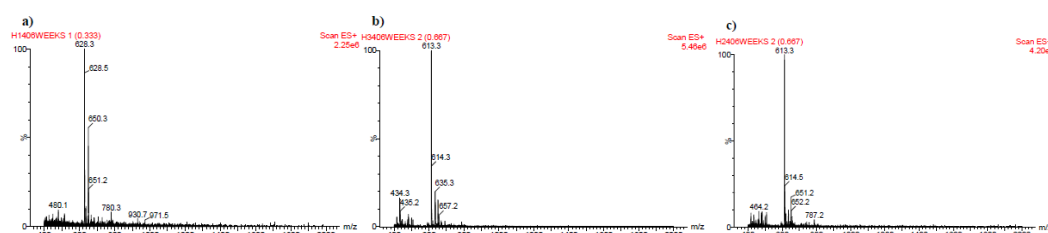
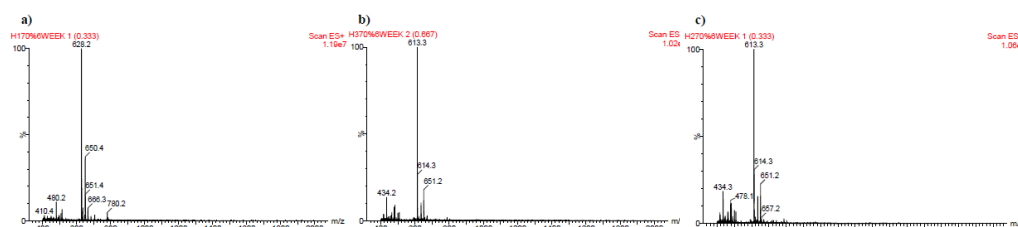


**Figure 94:** ESI-MS spectra of a) peptide sequence 1: Ac-KQQSP-NH<sub>2</sub>, (theoretical [M+H]<sup>+</sup> m/z ratio = 628.34) b) peptide sequence 2: Ac-HSSKL-COOH (theoretical [M+H]<sup>+</sup> m/z ratio = 613.33) and c) peptide sequence 3: Ac-hsskl-COOH (theoretical [M+H]<sup>+</sup> m/z ratio = 613.33) reagent samples extracted after exposure to 4°C or 39°C for six weeks. Similar results were obtained for all previous time point extractions.

70% HUMIDITY



90% HUMIDITY

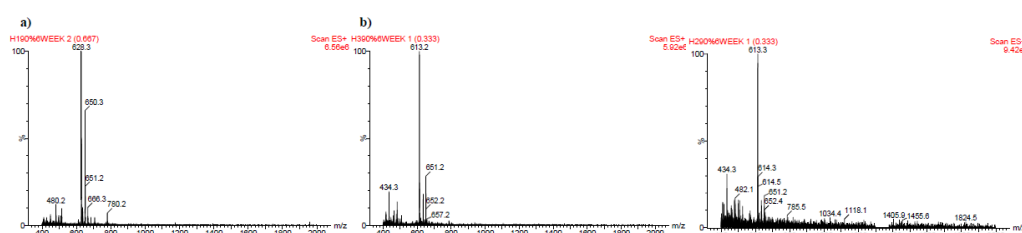


**Figure 95:** ESI-MS spectra of a) peptide sequence 1: Ac-KQQSP-NH<sub>2</sub>, (theoretical [M+H]<sup>+</sup> m/z ratio = 628.34) b) peptide sequence 2: Ac-HSSKL-COOH (theoretical [M+H]<sup>+</sup> m/z ratio = 613.33) and c) peptide sequence 3: Ac-hsskl-COOH (theoretical [M+H]<sup>+</sup> m/z ratio = 613.33) reagent samples extracted after exposure to 70% or 90% humidity for six weeks. Similar results were obtained for all previous time point extractions

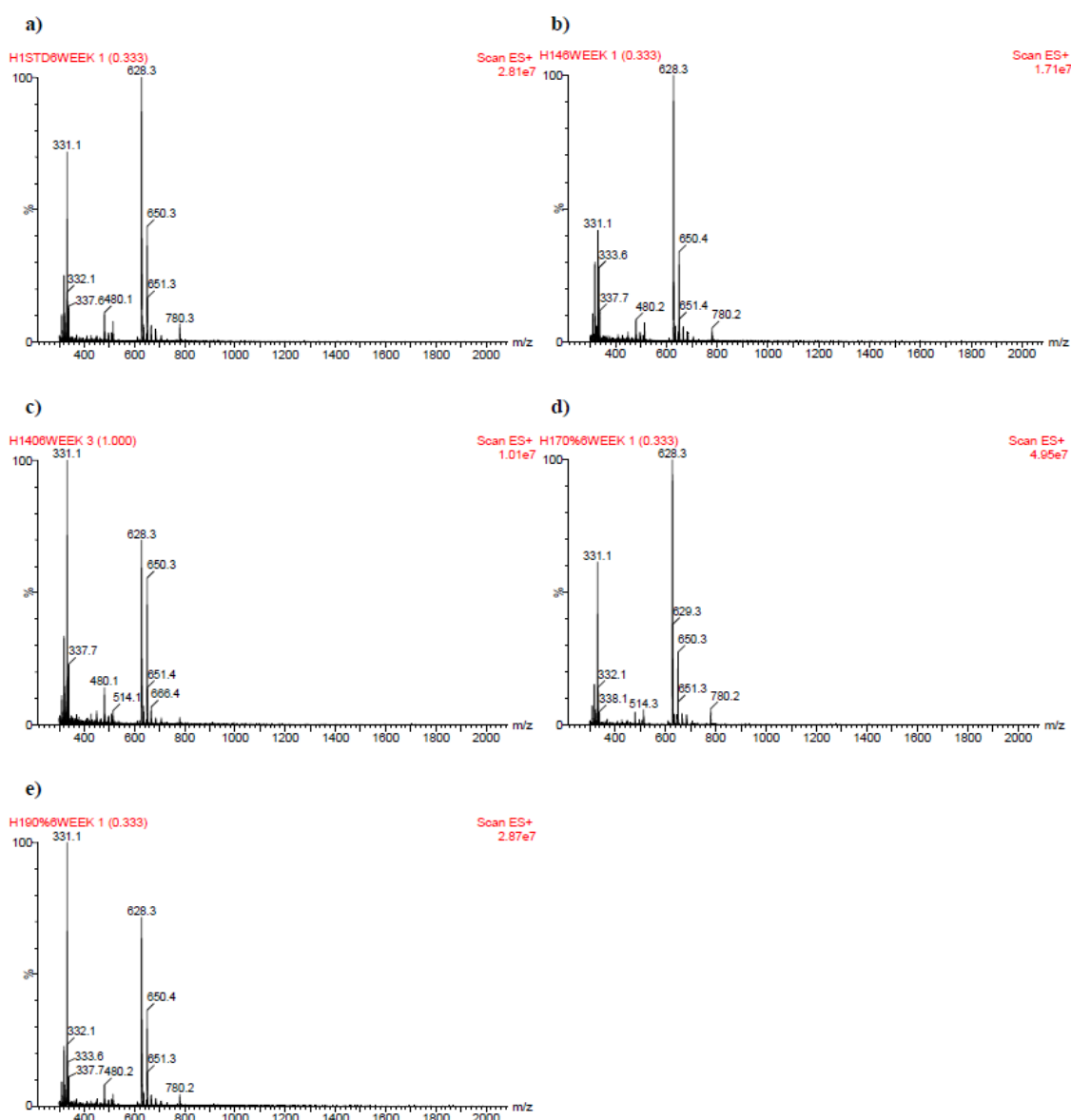


**Figure 96:** ESI-MS spectra of peptide sequence 1: Ac-KQQSP-NH<sub>2</sub>, (theoretical [M+H]<sup>+</sup> m/z ratio = 628.34) and Rhodamine 110 (theoretical [M+H]<sup>+</sup> m/z ratio = 331.11) samples extracted after exposure to all experimental conditions: a) standard laboratory conditions, b) 4°C, c) 39°C, d) 70% humidity, e) 90% humidity for six weeks. Similar results were obtained for all previous time point extractions.

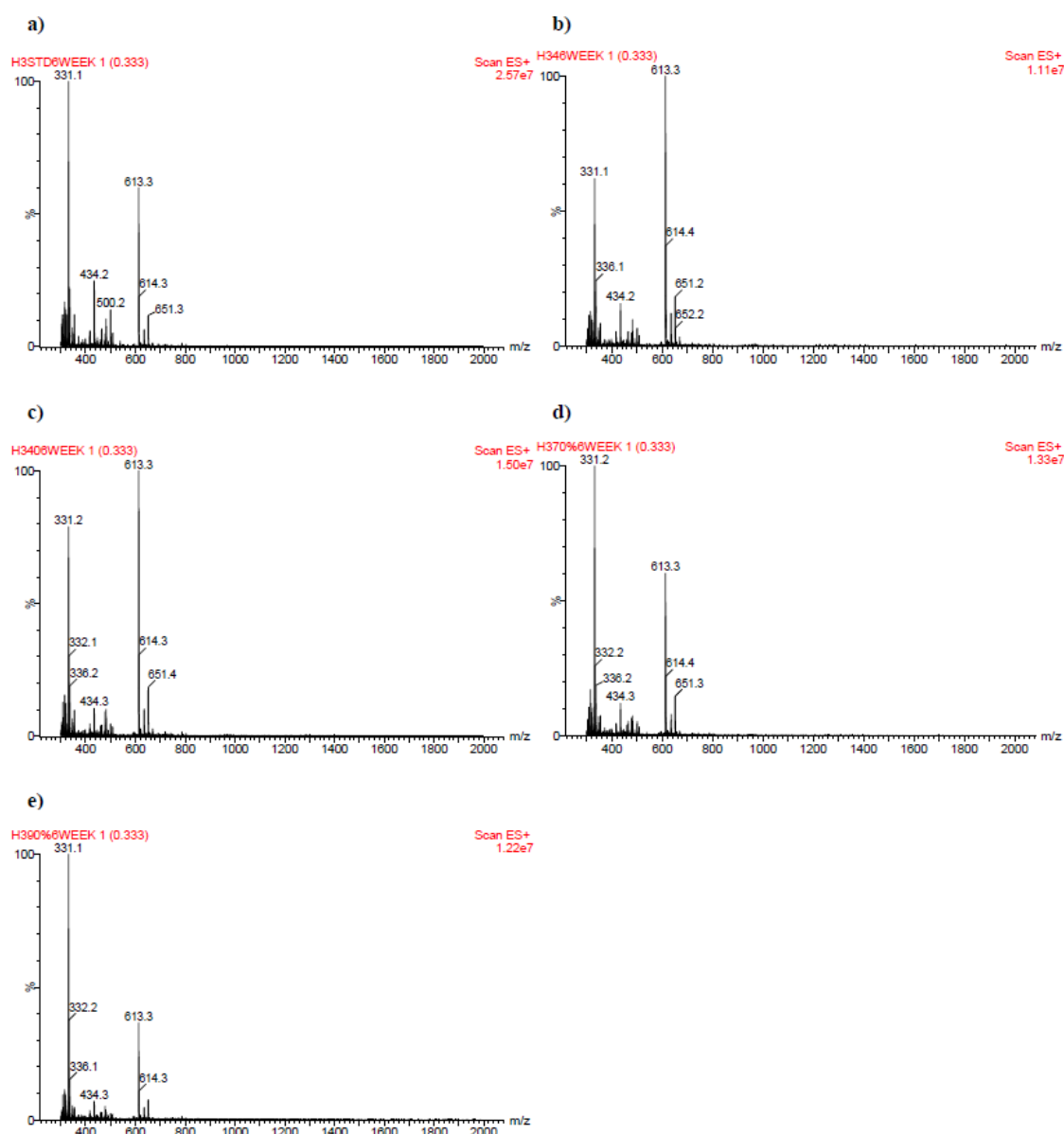


**Figure 97:** ESI-MS spectra of peptide sequence 2: Ac-HSSKL-COOH (theoretical [M+H]<sup>+</sup> m/z ratio = 613.33) and Rhodamine 110 (theoretical [M+H]<sup>+</sup> m/z ratio = 331.11) samples extracted after exposure to all experimental conditions: a) standard laboratory conditions, b) 4°C, c) 39°C, d) 70% humidity, e) 90% humidity for six weeks. Similar results were obtained for all previous time point extractions.

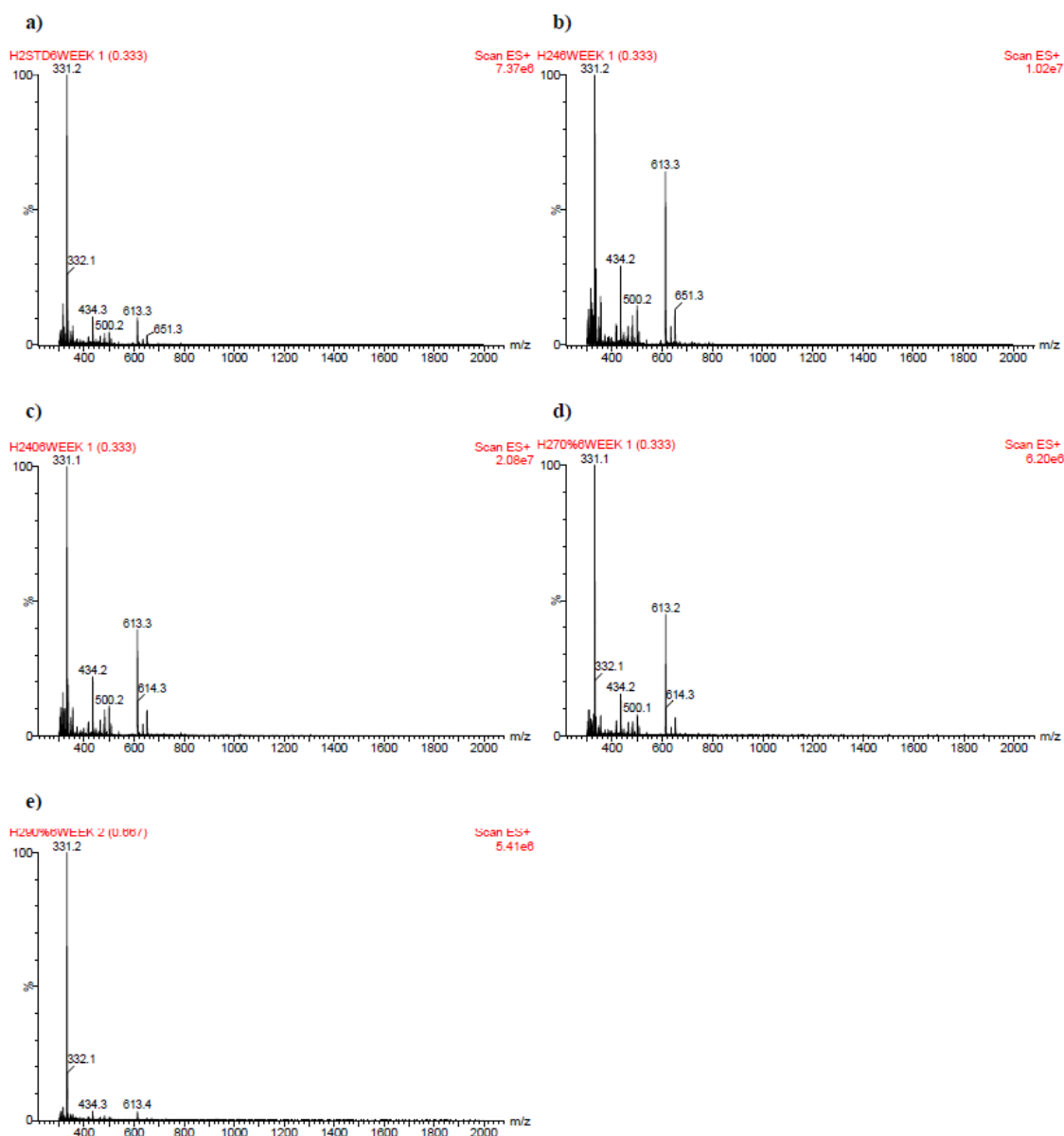


**Figure 98:** ESI-MS spectra of peptide sequence 3: Ac-hsskl-COOH (theoretical  $[M+H]^+$   $m/z$  ratio = 613.33) and Rhodamine 110 (theoretical  $[M+H]^+$   $m/z$  ratio = 331.11) samples extracted after exposure to all experimental conditions: a) standard laboratory conditions, b) 4°C, c) 39°C, d) 70% humidity, e) 90% humidity for six weeks. Similar results were obtained for all previous time point extractions.

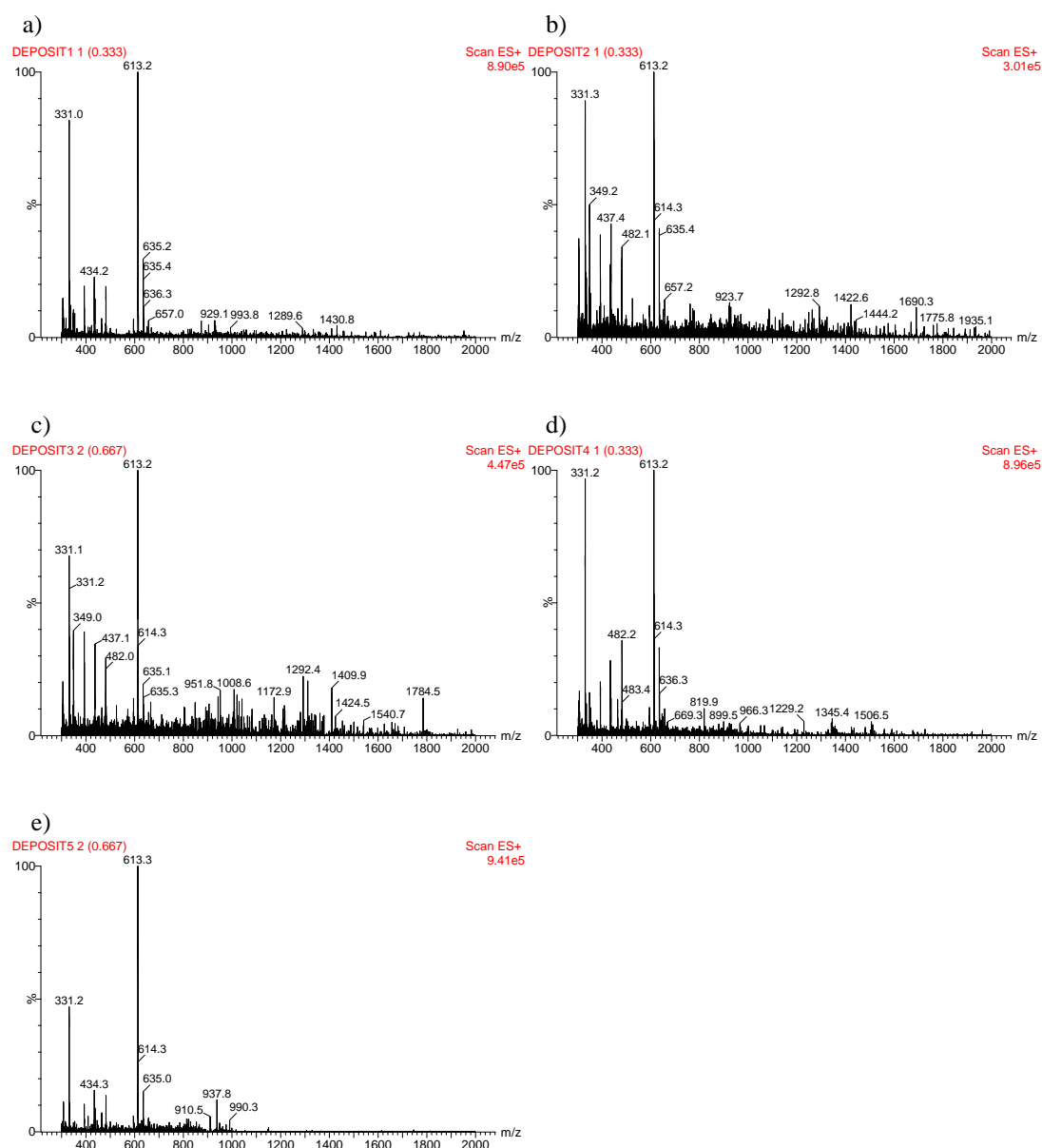


**Figure 99:** ESI-MS spectra of peptide sequence 2: Ac-HSSKL-COOH (theoretical  $[M+H]^+$   $m/z$  ratio = 613.33) and Rhodamine 110 (theoretical  $[M+H]^+$   $m/z$  ratio = 331.11) samples extracted from the surface of a finger after a) one, b) two, c) three, d) four and e) five additional contacts.

# **| Published Articles**



# Application of fluorescent substrates to the *in situ* detection of prostate specific antigen

James Gooch, Barbara Daniel, Nunzianda Frascione\*

Department of Forensic and Analytical Science, King's College London, Franklin-Wilkins Building, 150 Stamford Street, London SE1 9NH, UK



## ARTICLE INFO

### Article history:

Received 5 November 2013

Received in revised form

4 February 2014

Accepted 10 February 2014

Available online 12 March 2014

### Keywords:

Fluorogenic substrate

*In situ* testing

PSA

## ABSTRACT

The forensic identification of body fluids frequently presents an important source of genetic material and investigative interpretation. However, presumptive testing techniques presently employed in the discrimination of biological fluids are subject to criticism for poor specificity, lack of fluid localisation ability and detrimental effects on DNA recovery rates. The recognition of fluid-specific biomarkers by fluorogenic substrates may provide a novel resolution to these issues but research has yet to establish any pertinent *in situ* fluid detection applicability. This study therefore utilises a fluorogenic substrate (Mu-HSSKLQ-AFC) specific to the seminal protein prostate specific antigen in an effort to detect human semen deposited on a number of surfaces typical to criminal investigation. The ability of fluorescent fluorogenic substrates to simultaneously identify and visualise biological fluids *in situ* is demonstrated for the first time, whilst the production of complete STR profiles from fluid sources is also confirmed to be completely unaffected by substrate application.

© 2014 Elsevier B.V. All rights reserved.

## 1. Introduction

Locating and identifying body fluids such as semen, blood and saliva can often aid the progression of criminal investigation by providing intelligence on the nature and circumstance of an offence and may additionally associate or exonerate a suspect through the isolation of genetic material.

A number of 'presumptive' screening assays exist to rapidly exclude or indicate fluid presence, employing simple biochemical processes in order to generate colorimetric changes within a given substrate. Those indicating the presence of blood rely on the oxidation of haem to catalyse substrate-specific reactions [1–3], whilst intra-fluidic enzyme activity provides the basis for the testing of semen and saliva [4,5]. However, previous validation studies have established limitations in the usefulness and evidential strength of these assays. With the exception of the chemiluminescence phenomenon exploited in the detection of blood by Luminol, presumptive tests cannot be used to localise fluid depositions, thereby necessitating time-consuming visual searches prior to analysis. Furthermore, the molecular targets examined by these tests are not fluid-specific, often leading to false positives between different fluid types and other non-fluid substances [6–8]. Detrimental effects on the recovery of DNA from fluid depositions have also been demonstrated after some presumptive test applications [9,10].

Currently the most widely used presumptive test for semen identification is the Brentamine assay for the detection of acid phosphatase, an enzyme secreted into semen by the prostate gland [4]. However, the requirement of specialist knowledge and equipment often makes this test problematic. Results are subject to a high level of expert interpretation [11–13], whilst Brentamine toxicity also necessitates use of a fume hood.

Recent improvements in fluid assay specificity have utilised immunological testing strips for the detection of fluid-endogenous protein biomarkers [14–16]. However, these testing processes do not allow for the retention of fluids following application, potentially sacrificing a valuable source of material for genetic profiling [17].

Our research group has made initial efforts in the design of novel body fluid analysis techniques, developing a fluorescent biosensor complex specific to Glycophorin A, an erythrocyte membrane protein used in the identification of human blood [18]. However, whilst demonstrating effective glycophorin detection via decreases in fluorescence intensity, the 'turn-off' nature of signalling restricts the use of this sensor in visualising discrete fluid depositions *in situ*. A 'turn-on' fluorescence based assay is therefore preferable for simultaneous identification and localisation purposes.

The proteolytic digestion of peptide substrates to release fluorescent by-products within the same molecular unit may be considered an attractive signalling mechanism for *in situ* fluid detection. High specificities make enzyme recognition elements ideal candidates for fluid analysis, whilst 'turn-on' increases in fluorescence

\* Corresponding author. Tel.: +4420 7848 4978.

E-mail address: [nunzianda.frascione@kcl.ac.uk](mailto:nunzianda.frascione@kcl.ac.uk) (N. Frascione).



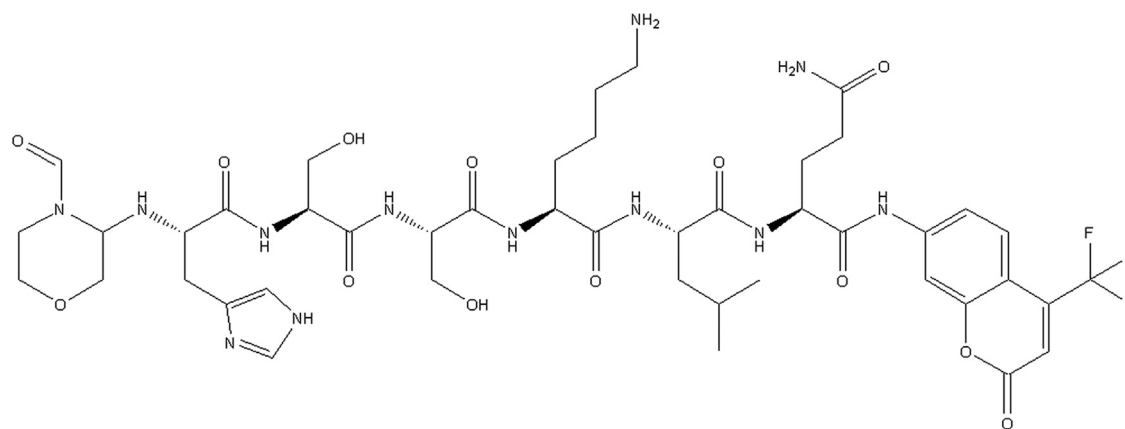


**Fig. 1.** PSA fluorogenic substrate – a hexapeptide consisting of amino acid sequence HSSKLQ, terminally labelled with a fluorescent coumarin derivative. Specific digestion of the peptide by PSA yields highly fluorescent 7-amino-4-trifluoromethylcoumarin.

intensity upon target interaction may allow the visualisation of *in situ* fluid depositions. Furthermore, unlike irreversible antibody-based reactions, enzyme targets may interact with multiple substrate molecules to amplify signal production. Simultaneous detection of multiple fluid enzymes may also potentially be achieved by exploiting fluorophores of differing wavelengths in a single multiplex assay.

A central appeal of fluorogenic substrates as an alternative to current presumptive assays is that DNA-degrading oxidative processes, such as those exploited by Luminol and Leucomalachite green, are not required to generate a positive response [6]. With research yet to explore the effect of substrates on genetic material, investigation into the possible interference of reagents with DNA amplification, quantitation or profiling may be considered pertinent.

This study therefore explores the use of fluorogenic peptide substrates specific to prostate specific antigen (PSA) for the simultaneous visualisation and identification of human seminal fluid. PSA is a semen-endogenous protein responsible for proteolysis of gel-forming Semenogelin 1 and 2 [19]. The unique expression level of PSA within seminal fluid, often produced in milligram levels per millilitre [19], has established its wide acceptance as a forensic biomarker for semen identification.

Denmeade et al. [20] produced 12 peptide substrates for monitoring PSA activity based on amino acid sequences directly adjacent to mapped PSA cleavage sites of Semenogelin 1 and 2. These substrates utilise 7-amino-4-methylcoumarin fluorophores, which after amide bond conjugation to peptides undergo excitation and emission wavelength shifts, restricting fluorescence output. Subsequent separation of the fluorophore from the peptide by serine protease hydrolysis occurs in the presence of PSA and restores fluorescence.

The particular substrate MU-HSSKLQ-AFC (Fig. 1) displayed the highest specificity for PSA, arising from its resistance to similar proteolytic enzymes found within body fluids. Whilst this substrate has found routine use in the recognition of prostate cancer markers, it has yet to be applied towards the detection of human semen.

The fluorescence response of substrate MU-HSSKLQ-AFC to dilutions of semen within solution, as well as to whole semen extracted from *in situ* swabs, was measured via spectrofluorometry to determine the ability of the fluorogenic substrate to detect free PSA within seminal fluid. Further *in situ* detection ability was examined, testing substrate performance against semen deposits on glass slides and a number of surfaces typically encountered within forensic casework. Assay reagent was also applied to depositions of blood, saliva and urine to confirm substrate specificity. MU-HSSKLQ-AFC was lastly applied to semen samples for subsequent SGM plus profiling to assess reagent effect on each stage of the profiling process.

## 2. Materials and methods

### 2.1. Reagents

#### 2.1.1. Fluorogenic PSA substrate

Lyophilised Prostate Specific Antigen Fluorogenic Substrate (Mu-HSSKLQ-AFC) was purchased from EMD Millipore (Massachusetts, USA) and dissolved in 109.5  $\mu$ l DMSO to make an 8 mM stock solution before dilution in PBS to a working concentration of 400  $\mu$ M.

#### 2.1.2. Body fluid collection and storage

Blood, semen, saliva and urine samples were taken after informed consent. Blood samples were drawn by venipuncture and stored in a BD Vacutainer® Plus tube (Oxford, UK) containing 3.2% sodium citrate coagulation preservative. All tissue samples were stored at 4 °C until analysis.

### 2.2. Instrumentation and procedures

#### 2.2.1. Spectrofluorometry

Fluorescence measurements were conducted on a BioTek Synergy HT spectrophotometer (Vermont, USA). Dilution curves were constructed through the addition of 100  $\mu$ l of diluted semen (1:1, 1:2, 1:4, 1:8, 1:16, 1:32, 1:64) in a 96-well microplate to 100  $\mu$ l of 400  $\mu$ M PSA fluorogenic substrate and measured with appropriate blank (200  $\mu$ l PBS) and negative controls (100  $\mu$ l PBS, 100  $\mu$ l assay reagent). Swabs taken from *in situ* semen depositions were extracted in 100  $\mu$ l of PBS and added to 100  $\mu$ l of working concentration substrate. All fluorescence emissions were recorded at room temperature in duplicate using Ex400/Em528  $\pm$  20 nm wavelengths (for the measurement of emissions at 508 nm) immediately after mixing.

#### 2.2.2. Slide microscopy

Fluorogenic PSA reagent was tested against seminal dilutions (1:25, 1:50, 1:100, 1:200, 1:500, 1:1000) deposited on glass slides as a demonstration of *in situ* substrate sensitivity. Semen volumes of 10  $\mu$ l were applied to the centre of each slide before the direct 10  $\mu$ l addition of substrate. Duplicates of each dilution were performed. Negative reagent-only controls were applied on the same slide as a measure of background reagent fluorescence, whilst blank controls consisting of semen-only applications were also used to monitor possible analyte auto-fluorescence. The simulation of dry depositions was achieved through the application of 10  $\mu$ l of seminal fluid to glass slides, which were subsequently allowed to dry overnight. Reagent was then applied directly at the point of analysis.

Images were taken in the dark immediately after application on an Olympus SZX12 fluorescence microscope (Tokyo, Japan) and internal CCD camera. BV filtration (Ex 400–440 nm) was used for substrate excitation, whilst all additional microscopy parameters were kept constant (hue=359, saturation=255, white balance=64, contrast=0, brightness=1023, gamma=10, magnification= × 8.5) in order to restrict result variation.

Investigations into substrate specificity were also undertaken with application to depositions of whole blood, urine and saliva on slides in order to exclude the possibility of inter-fluidic cross-reaction.

### 2.2.3. Surface microscopy.

Eight different surfaces consisting of cotton, denim, felt, leather, paper, plastic, polyester and wood were chosen to reflect materials on which body fluids are commonly deposited within criminal investigations. All surfaces were cut to fit the size of a microscope slide. In a similar manner as commercial assay testing, 10 µl depositions of human semen were applied to the surfaces and allowed to dry overnight. PSA substrate was applied directly to depositions in 10 µl volumes with the same negative and blank controls previously described.

Images were once again recorded on an Olympus SZX12 fluorescence microscope utilising BV filtration (Ex 400–440 nm). All measurements were performed in duplicate.

200 µl of working concentration substrate was lastly dispersed directly over a semen deposition on leather using a common atomising spray bottle to reflect ideal future application methods.

### 2.3. DNA profiling

50 µl of PSA substrate at working concentration was added to 150 µl of human semen to observe effects on DNA recovery after application. DNA was extracted using the QIAmp® DNA Mini kit (Qiagen, Manchester, UK) according to the supplied protocol and quantified with the Quant-iT™ PicoGreen® dsDNA Assay Kit (Invitrogen, Paisley, UK). Samples were diluted to 0.1 ng/µl prior to amplification with the AmpFISTR® SGM Plus® PCR Amplification Kit (Applied Biosystems, Paisley, UK) using a Perkin-Elmer 9700 thermal cycler (Cambridge, UK). STR amplicons were resolved on an ABI3130 genetic analyser and evaluated using GeneMapper® software. Generated profiles were compared to a semen reference profile to examine potential inhibition.

## 3. Results and discussion

### 3.1. Spectrofluorometry

Whilst regularly demonstrating detection of purified PSA protein within solution [20,21], this fluorogenic substrate has never been used to target the native PSA contained within seminal fluid. The potential for reagent inhibition or physical fluorescence screening by other biomolecules present in a complex matrix makes it pertinent to investigate whether a positive signal can be generated from whole semen.

Appropriate fluorescence intensity changes to varying dilutions of seminal fluid were observed through spectrofluorometry. Constructed calibration curves were found to be consistent with those demonstrated by Niemelä et al. [21] for the detection of PSA within solution and established a quantitative linear relationship between semen concentration and substrate fluorescence (Fig. 2).

A commonplace practice within forensic investigation is to swab potential fluid depositions that require analysis at a later point. It is consequently vital that substrates react to material extracted from these swabs in the same manner as whole fluid.

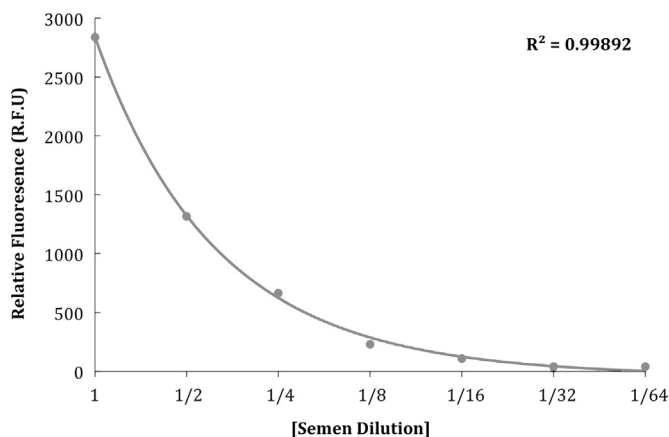


Fig. 2. Dilution curve demonstrating the relationship between seminal concentration and fluorogenic PSA substrate emission.

Swabs were therefore taken of semen deposited on a leather surface prior to extraction in PBS via brief vortexing. The collected material was analysed using the same procedure as whole fluid and did not display any differentiation in fluorescence response from its neat fluid counterpart (results not shown).

### 3.2. Slide microscopy

The main benefit of many presumptive tests is their ability to be performed at the point of fluid discovery. It is important that substrate reagents designed to detect biological fluids may do so *in situ* with only basic instrumental assistance for fluorescence observation, such as a portable alternative light source.

Human semen was deposited both on to glass slides prior to the direct application of PSA substrate. Any changes in fluorescence intensity were observed using standard fluorescence microscopy. Positive substrate reactions successfully identified all semen depositions, even at sensitive 1:1000 dilutions (Fig. 3). Similar results were obtained using simulated dry depositions.

Fluorescence emissions occurred immediately upon substrate application, promising potential for rapid fluid screening without extended incubation times. Background reagent fluorescence was not observed at any point during negative control testing, allowing for the visualisation of discrete fluid areas.

Additional studies of inter-fluidic substrate specificity were also undertaken with reagent applied to wet and dry depositions of whole blood, saliva and urine. In all cases, the PSA substrate did not generate a positive reaction, thereby demonstrating both high semen specificity, as well as resistance to proteases that may be present within other body fluids (results not shown).

### 3.3. Surface microscopy

The successful detection of semen by this substrate clearly confirms the high performance of fluorogenic substrates in the simultaneous identification and localisation of biological fluids *in situ*.

Nevertheless, clean glass slides are not representative of surfaces encountered within forensic casework. Surfaces on which fluids are typically deposited may potentially prevent the success of fluorescent substrates via absorption, movement restriction and physical screening effects. Furthermore, surfaces may contain a number of unknown substances that could inhibit substrate–target interaction. Fluorogenic PSA substrate was therefore applied, utilising the same slide testing procedure, to dry semen depositions on eight surfaces relevant to criminal investigation.

Despite the difficult nature of surface testing, positive results were generated on each of the eight surfaces, identifying and

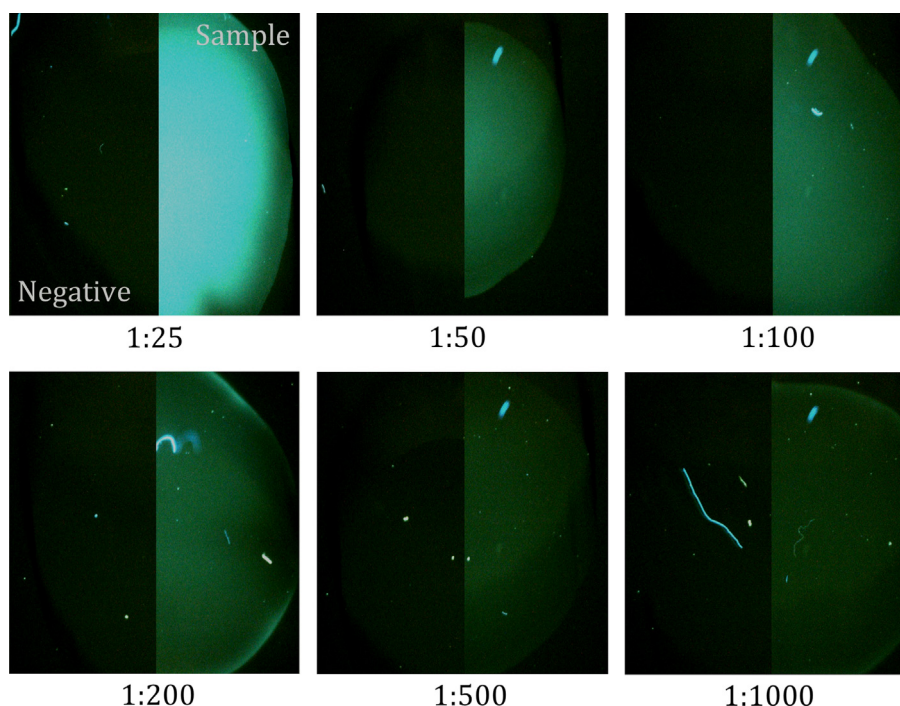


**Fig. 3.** Demonstration of *in situ* substrate testing of seminal depositions upon glass slides across a range of five dilutions. Duplicate measurements were taken and also displayed expected results.

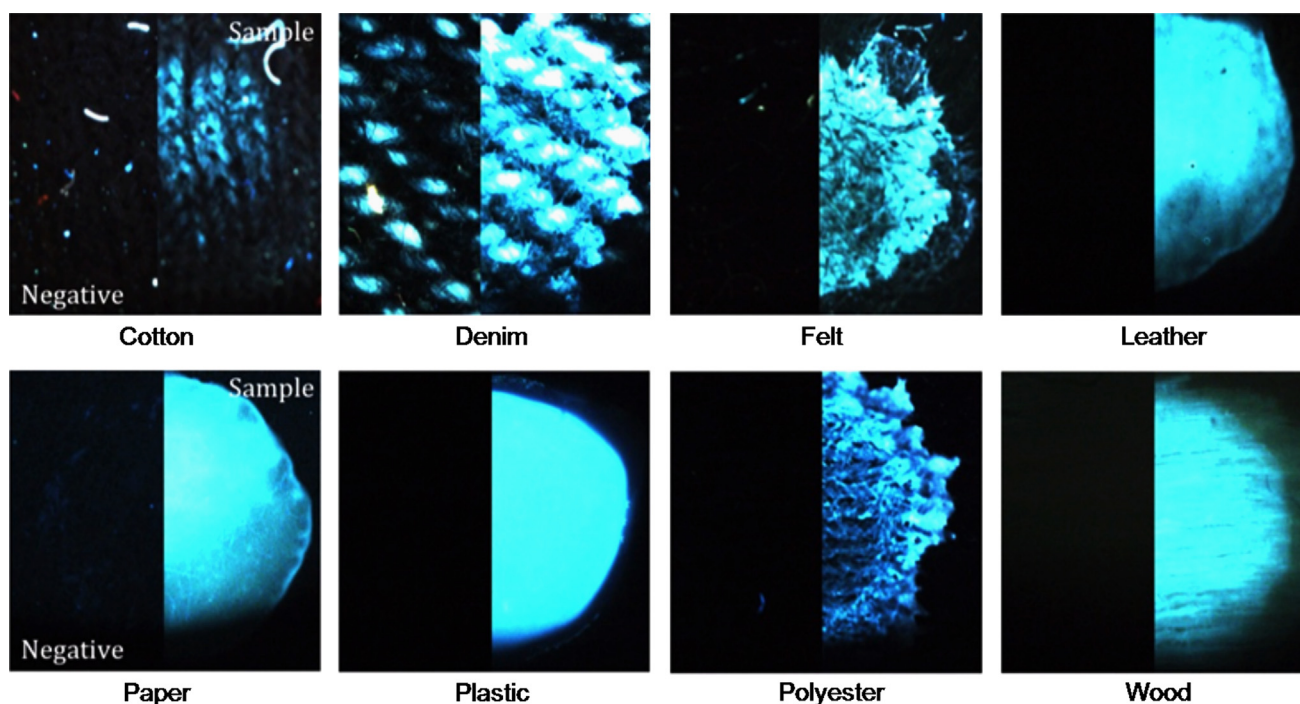


**Fig. 4.** Successful detection of human semen across eight forensically relevant surfaces by fluorogenic PSA substrate. Reagent-only negative controls are provided on the left side of each image.

visualising all semen deposits (Fig. 4). Once again, substrate-only negative controls did not exhibit any observable fluorescence upon application. Furthermore, surface material had little effect on the ability of the substrate to generate positive results, with no assay interference occurring during testing.

The direct spray dispersal of reagent over a large evidential surface may be considered the most efficient process of localising fluid deposits. 200  $\mu$ l of substrate was applied to seminal depositions on leather using a common 1 ml atomising spray bottle in

order to examine the viability of this method. Positive substrate emissions easily localised all semen depositions, elucidating discrete staining areas and confirming the validity of this technique (results not shown).

### 3.4. DNA profiling

Validation studies by Tobe et al. [10] have previously demonstrated a significantly reduced recovery of high molecular weight



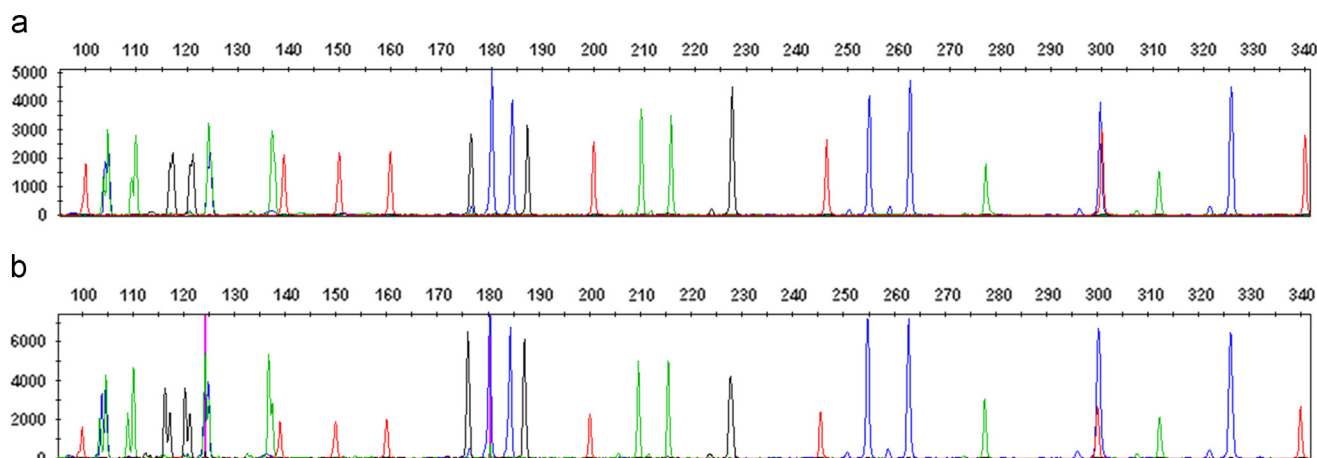


Fig. 5. Genetic profiles generated from (a) semen reference profile and (b) semen sample with applied PSA substrate. Profiles display no significant differences.

STR loci from biological fluids after some presumptive testing applications. Furthermore, the physical application process of the seminal acid phosphatase test has been shown to limit the amount of spermatozoa, and thus DNA, available for genetic profiling [13].

PSA substrate was applied to semen samples, which underwent extraction, quantification, amplification and profiling according to standard forensic protocols to examine the effects of assay application on the recovery of genetic material from biological fluids. Comparisons were then made to reagent-less semen standard (Fig. 5).

Successful genetic recovery from substrate-applied semen was established by Picogreen quantification, with an average concentration of 8.99 ng/μl DNA per sample extraction falling within expected values. Furthermore, full STR profiles were obtained from all assay applications, with no detrimental effects on high molecular weight loci. Differentiation of reagent-applied samples from their reference profiles was not observed at any stage of the profiling process outside the limits of normal experimental variation.

#### 4. Conclusion

This study successfully demonstrates for the first time the ability of fluorescent substrates to identify biological fluid depositions *in situ*. Human semen was detected across a range of surfaces typical to forensic investigation with additional visualisation via a direct spraying application.

This particular substrate exhibited ideal increases in fluorescence intensity upon target interaction, even at sensitive 1:1000 seminal dilutions, giving opportunity for its use in contaminated fluid depositions or those washed in removal attempts.

Importantly, substrates were found to have no effect on DNA profiling processes after application to biological fluids and thereby negate the potential forfeit of fluid identification in order to maximise genetic material recovery.

An ideal application of fluid-specific substrates would likely exploit a number of different peptide sequences, each with separate emission wavelengths for simultaneous enzyme detection within several fluid types in a multiplex sensing system.

Displaying both an immediate and specific response to analyte presence, fluorogenic substrates have the potential to prevent month-long visual evidence searches by localising fluid depositions within a matter of seconds. Serious thought should therefore be given to the development of fluorogenic substrates as replacements to current presumptive testing techniques.

#### Acknowledgements

This work was carried out in a joint venture between King's College London and the Metropolitan Police Forensic Services Directorate. The authors would like to thank the Metropolitan Police Service for providing financial assistance throughout the project.

#### References

- [1] J. Glaister, Br. Med. J. 1 (1926) 650–652.
- [2] M. Grodsky, K. Wright, P.L. Kirk, J. Crim. Law Criminol. 42 (1951) 95–104.
- [3] W. Specht, Angew. Chem. 50 (1937) 155–157.
- [4] S. Kaye, J. Crim. Law Criminol. 41 (1951) 834–835.
- [5] G.M. Willott, Sci. Justice 14 (1974) 341–344.
- [6] M. Cox, J. Forensic Sci. 36 (1991) 1503–1511.
- [7] A. Castelló, F. Francés, F. Verdú, Talanta 77 (2009) 1555–1557.
- [8] M. Bancirova, Sci. Justice 52 (2012) 102–105.
- [9] B.C.M. Pang, B.K.K. Cheung, J. Forensic Sci. 53 (2008) 1117–1122.
- [10] S.S. Tobe, N. Watson, N. Nic-Daeid, J. Forensic Sci. 52 (2007) 102–109.
- [11] P. Redhead, M.K. Brown, Sci. Justice 53 (2013) 187–191.
- [12] A.F. Schiff, J. Forensic Sci. 23 (1978) 833–844.
- [13] G. Davidson, T.B. Jalowiecki, Sci. Justice 52 (2012) 106–111.
- [14] B.C. Pang, B.K. Cheung, Forensic Sci. Int. 169 (2007) 27–31.
- [15] D.G. Casey, J. Price, Forensic Sci. Int. 194 (2010) 67–71.
- [16] S. Turrina, G. Filippini, R. Atzei, E. Zaglia, D. De Leo, Forensic Sci. Int. Genet. 1 (2008) 74–75.
- [17] R. Thorogate, J.C. Moreira, S. Jickells, M.M. Miele, B. Daniel, Forensic Sci. Int. Genet. 2 (2008) 363–371.
- [18] N. Frascione, V. Pinto, B. Daniel, Anal. Bioanal. Chem. 404 (2012) 23–28.
- [19] M. Yokota, T. Mitani, H. Tsujita, T. Kobayashi, T. Higuchi, A. Akane, M. Nasu, Legal Med. 3 (2001) 171–176.
- [20] S.R. Denmeade, W. Lou, J. Lovgren, J. Malm, H. Lilja, J.T. Isaacs, Cancer Res. 57 (1997) 4924–4930.
- [21] P. Niemela, J. Lovgren, M. Karp, H. Lilja, K. Pettersson, Clin. Chem. 48 (2002) 1257–1264.

Cite this: *Analyst*, 2016, **141**, 2392

Received 22nd March 2016,

Accepted 24th March 2016

DOI: 10.1039/c6an00686h

www.rsc.org/analyst

## Solid-phase synthesis of Rhodamine-110 fluorogenic substrates and their application in forensic analysis†

J. Gooch,<sup>a</sup> V. Abbate,<sup>b</sup> B. Daniel<sup>a</sup> and N. Frascione<sup>\*a</sup>

**A novel synthetic route for the rapid and efficient preparation of fluorogenic substrates utilizing Rhodamine-110 or similar fluorophores is reported. Applicability of the synthesized peptide substrate within a forensic casework context is also presented.**

Last year, over 10 000 exhibits were submitted to the Evidence Recovery Unit (ERU) of the Metropolitan Police Service. Body fluid stains such as blood, semen and saliva are often the most important forms of biological evidence encountered in forensic casework. Determining the identity of such deposits can be used to further a criminal investigation as it may provide information on both the nature of the offence and the genetic origin of the fluid (through DNA profiling).<sup>1</sup> Consequently, over 90% of these submitted exhibits required examination for the presence of biological fluids.

However, with meticulous visual examination by trained personnel being the most common method of detection, determining the presence and location of any fluid deposits may be very challenging, especially with small, or latent traces on dark backgrounds which may be easily overlooked.<sup>1</sup> Long wave UV or violet light sources may aid detection by exploiting the auto-fluorescent properties of some intra-fluidic molecules but their use is restricted to a select number of surface types.<sup>2</sup> The colorimetric presumptive assays used in order to identify the type of fluid present are also considered by many in the forensic community to be limited by issues of specificity,<sup>3</sup> safety,<sup>4</sup> and their detrimental effects on DNA recovery.<sup>5</sup> Developing a fast, dependable and specific method of fluid detection would save time and money. Biosensors that simultaneously detect and identify body fluids could represent a cost and time efficient alternative to present day techniques. The development of fluorogenic peptide substrates specific to each body

fluid type could improve body fluid search efficiency through the identification of fluid-specific proteases *in situ* via fluorescence emission.<sup>6,7</sup>

Rhodamine-110 (Rh-110) is a xanthene-based fluorescent dye containing two aromatic amine moieties, the symmetric or asymmetric modification of which may shift the existing equilibrium of the molecule from a highly fluorescent quinoid towards a colorless lactone formation, quenching fluorescence emission.<sup>8</sup> This has cemented Rhodamine-110 as a popular pro-fluorophore for use within many protease substrates *via* the direct attachment of specific amino acid chains (with a positive fluorescence signal achieved *via* the proteolytic separation of peptide and fluorophore in the presence of a target enzyme).<sup>8</sup> The physical and spectral characteristics of Rho-110 are considered highly desirable for biological fluid detection, as they display a high quantum yield and are relatively pH insensitive. Moreover, Rho-110 based substrates exhibit an almost non-existent emission upon peptide conjugation, preventing background fluorescence and ensuring high enzymatic assay sensitivities.<sup>8</sup>

However, all reported symmetric and asymmetrically labeled Rh-110 peptide substrates have so far been synthesized through solution chemistry, a task that is made problematic due to the poor nucleophilicity of the Rh-110 aromatic amines,<sup>9</sup> and often leads to inefficient peptide-fluorophore acylations. Final product yields are inevitably very low, as each intermediate must undergo substantial purification.<sup>10</sup> This makes the cost of Rh-110-based substrates high and since the aim of the research is to produce a spray that could be used directly on forensic evidence, this cost would be unacceptable.

We surmised that preparing large quantities of peptide substrates in a rapid and efficient manner could be achieved *via* the direct attachment of Rh-110 to a solid support. In this procedure (Fig. 1), it is envisioned that one of the aromatic amine groups of Rh-110 may be anchored to a functionalized solid support, keeping the remaining amine group available for the subsequent stepwise incorporation of amino acids by standard Fmoc-SPPS. This route offers advantages over typical solution-phase conjugation techniques by allowing the incubation of

<sup>a</sup>Analytical & Environmental Sciences Division, King's College London, 150 Stamford Street, Waterloo, SE19NH, London. E-mail: nunzianda.frascione@kcl.ac.uk

<sup>b</sup>Institute of Pharmaceutical Science, King's College London, 150 Stamford Street, Waterloo, SE19NH, London

†Electronic supplementary information (ESI) available: Detailed experimental methods, compound synthesis and characterization (HPLC and MS), substrate testing. See DOI: 10.1039/c6an00686h

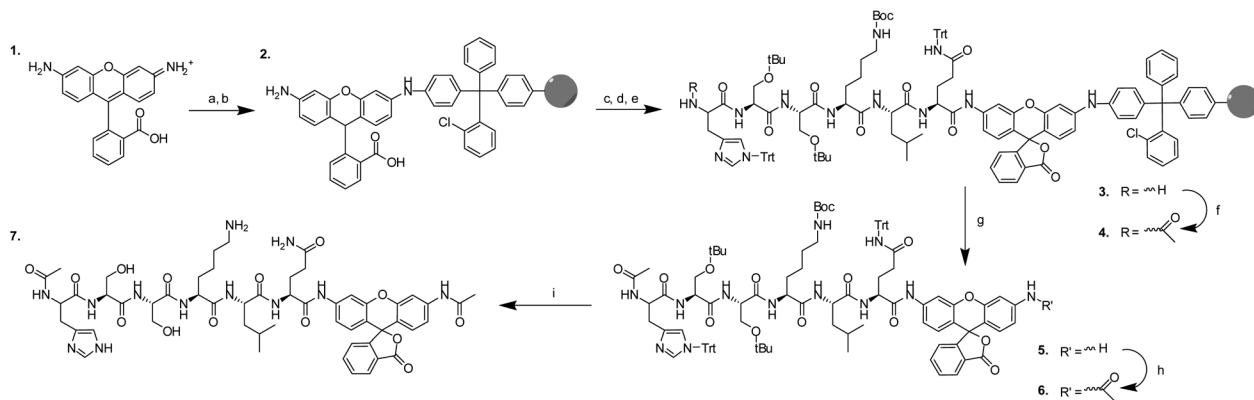


**Fig. 1** Schematic of Rh-110 PSA substrate development: (a) 2-ct resin (0.27 mmol), DCM, DIPEA, 24 h, (b) MeOH, 10 min, (c) Fmoc-Gln(Trt)-OH (3 mmol), DMF/pyridine, EDC (2.5 mmol), 24 h,  $\times 2$ , (d) 20% piperidine/DMF, 30 min, (e) 6  $\times$  AA, oxyma, DIC, DMF, 1 h, (f) 10  $\times$  (CH<sub>3</sub>CO)<sub>2</sub>O, DIPEA, DMF, 1 h, (g) AcOH : TFE : DCM, 1 h, (h) CH<sub>3</sub>COCl, DIPEA, DMF, 48 h, (i) TFA : TIPS : TA : phenol.

fluorophores with large molar excesses of any desired amino acid residue, which may be removed without extensive liquid-liquid extraction and chromatographic purification steps, thereby increasing overall product yield. Instead, excess amino acids, coupling reagents and other by-products may be removed by simple resin wash and filtration processes. Therefore, a fluorogenic substrate for the purpose of detecting seminal fluid within a forensic casework framework was constructed through the sequential coupling of immobilized Rh-110 to amino acids HSKLQ, a sequence previously reported by Denmeade *et al.*<sup>11</sup> as a proteolytic cleavage site of seminal fluid-specific protease prostate specific antigen (PSA).

Rh-110 was successfully anchored to the 2-chlorotrityl chloride resin (known to react with aromatic amines in the presence of a base such as pyridine or *N,N*-diisopropylethylamine (DIPEA))<sup>12</sup> in the first step towards substrate preparation. Upon reaction, the resin exhibited a deep red coloration that was retained after extensive washing, indicating successful dye incorporation. Cleavage of a small portion of the acid-labile resin, followed by ESI-MS analysis confirmed the presence of free Rh-110 (Fig. S1, ESI†).

With a number of workers previously reporting the unsuccessful conjugation of bulky peptides to Rh-110 within solution,<sup>13</sup> product 3 was instead assembled *via* the stepwise addition of single amino acids in a series of individual reactions. Multiple large excesses of Fmoc-protected glutamine were first incubated with Rh-110-attached resin 2 in order to ensure complete coupling (which was confirmed *via* ESI-MS analysis after 'soft' cleavage of a small portion of resin (Fig. S2, ESI†)), with successive amino acids incorporated through standard SPPS deprotection-wash-coupling-wash cycling to form a PSA-specific peptide backbone. Acetylation of the histidine N-terminus was performed to prevent substrate degradation from environmental aminopeptidase activity.<sup>14</sup>

As previously mentioned, many substrates utilizing Rh-110 fluorophores are bis-substituted, having been synthesized through the symmetric conjugation of identical peptides to both aromatic amines in order to quench fluorescence.

However, in such substrates, a two-step enzymatic hydrolysis is required in order to cleave both peptide chains before a full fluorescence signal is restored, consequently limiting the dynamic linear range of the assay.<sup>15</sup> As a result, the majority of fluorogenic Rh-110 peptide substrates now produced are mono-substituted, with secondary aromatic amines 'capped' through amide, carbamate or urea modifications.<sup>8</sup> This not only permits the assay to be completed within a single hydrolysis step, but also produces the same complete emission quenching effects as bis-peptide modification.<sup>16</sup> Therefore, a 'soft' cleavage of the resin was performed under mild acidic conditions to generate 5 from the solid support, allowing all *tert*-butoxycarbonyl and trityl amino acid side-chain protecting groups to remain intact (preventing accidental amino acid side-chain modification) during the capping of the remaining Rh-110 aromatic amine by acetylation. Liquid-liquid extraction was then performed to separate aqueous-reactive acetyl chloride from organic-soluble products, which were subsequently treated with TFA and precipitated in ether to remove acid-labile side-chain protecting groups. RP-HPLC and high-resolution mass spectrometry were used to confirm the purity and identity of final substrate product 7 respectively (Fig. S3 and S4, ESI†).

Spectrofluorometry was employed to observe the emission response of 7 quantitatively towards its intended enzymatic target. Whilst the final goal of this substrate is to identify the presence of whole semen, it is important to confirm that a fluorescence response is only elicited as a result of PSA hydrolysis and not from interaction with any other molecule within the seminal fluid matrix. Therefore in addition to dilutions of seminal fluid, substrate 7 was incubated with varying concentrations of purified PSA protein. Immediate fluorescence signal increases upon the addition of both PSA (Fig. 2a) and seminal fluid (Fig. 2b) successfully demonstrated cleavage between Rh-110-Ac and the attached glutamine residue, consequently establishing the potential use of this substrate as a semen-specific biosensor. Responses generated by seminal fluid were found to be much higher compared to that of tested purified protein concentrations, which was expected considering

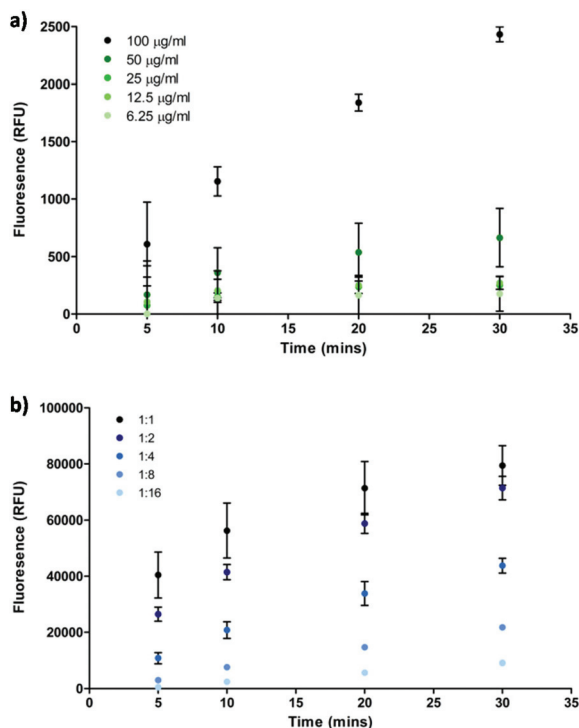


Fig. 2 Fluorescence response of final substrate 7 to (a) concentrations of purified PSA protein and (b) seminal fluid dilutions over time.

the significantly larger levels of PSA usually contained within whole semen (approximately  $0.5\text{--}3.0\text{ mg ml}^{-1}$ ).<sup>17</sup> As it is important to determine the proteolytic specificity of fluorogenic substrates prior their application (especially within the context of forensic casework, in which a false-positive signal may represent an incorrect evidential identification), final substrate 7 was also incubated with identical concentrations of trypsin, proteinase K and aminopeptidase M as a measure of PSA selectivity. In all cases the substrate did not exhibit a positive response, thereby demonstrating a high specificity towards seminal fluid, as well as an inherent resistance to protease enzymes present within other body fluids or the surrounding environment (Fig. S5, ESI†).

With one of the advantages of this assay over current forensic testing techniques being the ability to simultaneously locate and identify fluid stains *in situ* via fluorescence, it is pertinent to establish that a positive substrate emission will not be affected by the physical nature of the evidential surface on which a body fluid is deposited. Substrate 7 was therefore applied to small volumes of semen deposited on six surfaces routinely examined within criminal investigation, with subsequent signal responses observed by fluorescence microscopy. Upon reagent application, all deposits were successfully visualised, with surface material displaying little effect on resulting substrate emission (Fig. 3). Similar visualization was also achieved *via* the use of a hand-held Crime-lite® portable excitation source. As an additional method of observing reagent specificity, substrate 7 was also incubated with

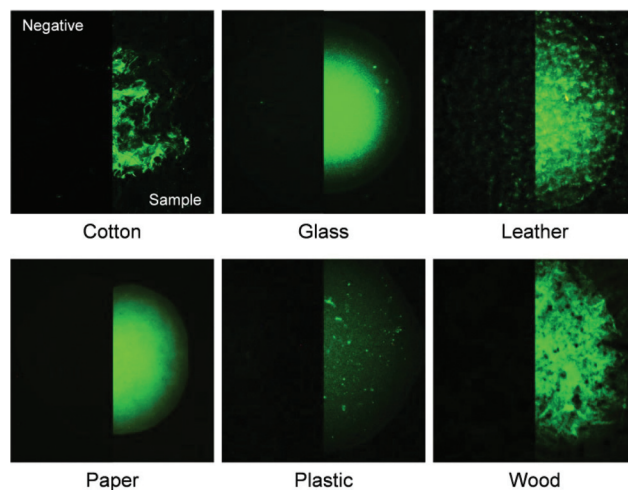


Fig. 3 Detection of semen across six surfaces by substrate 7. Seminal fluid-only negative controls are provided on the left side of each image.

volumes of blood and saliva *in situ*. No signal was observed upon application (Fig. S6, ESI†).

The identification of seminal fluid by PSA detection is currently achieved through absorption of a reconstituted suspect stain onto an immunochromatographic testing strip.<sup>18</sup> However, this technique is not only unable to locate the position of stains upon an evidential item but furthermore, consumes the fluid during the testing process, preventing further DNA analysis. An *in situ* PSA detection assay that allows downstream genetic profiling would consequently be considered advantageous. Therefore, substrate 7 was applied to a volume of seminal fluid deposited on a glass slide, with the resultant mixture being recovered by use of a cotton swab. Samples then underwent standard DNA extraction, quantification, amplification and capillary electrophoresis according to forensic protocols. Comparisons were then made to an untreated but identically processed reference sample to examine the effects of substrate application on genetic recovery. Differentiation of samples was not observed at any stage of the profiling process with the DNA concentrations of reagent-applied fluid and reference sample calculated at  $0.66$  and  $0.61\text{ ng }\mu\text{l}^{-1}$  respectively. A full STR profile from both samples was also obtained (Fig. S7, ESI†).

In summary, we have described a versatile detailed a synthetic route for the simple, rapid and inexpensive preparation of Rh-110-based fluorogenic substrates. Moreover, a substrate produced by this method has already shown great potential as a replacement for currently employed forensic body fluid testing techniques. This substrate allowed the specific detection of seminal fluid traces both within solution and *in situ*, without compromising subsequent genetic profiling processes. Future work will centre on the use of this method to produce fluorogenic substrates towards other biological fluids and latent fingerprints (something that has not currently been achieved). However, with fluorogenic substrates routinely employed in a variety of industrial and

biomedical applications, the disclosed synthetic protocol is also likely to have a much larger implication beyond the field of forensic science.

The authors would like to thank the Metropolitan Police Service Forensic Science Directorate and the UK Home Office for the financial support of this project through the Police Innovation Fund. Additional thanks are given to Dr Athena Vidaki and Gabriella Mason-Buck for their help with DNA profiling.

## Notes and references

- 1 K. Virkler and I. K. Lednev, *Forensic Sci. Int.*, 2009, **188**, 1–17.
- 2 N. Vandenberg and R. A. H. van Oorschot, *J. Forensic Sci.*, 2006, **51**, 361–370.
- 3 T. I. Quickenden and J. I. Creamer, *Luminescence*, 2001, **16**, 295–298.
- 4 J. L. Webb, J. I. Creamer and T. I. Quickenden, *Luminescence*, 2006, **21**, 214–220.
- 5 S. S. Tobe, N. Watson and N. N. Daéid, *J. Forensic Sci.*, 2007, **52**, 102–109.
- 6 N. Frascione, J. Gooch and B. Daniel, *Analyst*, 2013, **138**, 7279–7288.
- 7 J. Gooch, B. Daniel and N. Frascione, *Talanta*, 2014, **125**, 210–214.
- 8 M. Beija, C. A. M. Afonso and J. M. G. Martinho, *Chem. Soc. Rev.*, 2009, **38**, 2410–2433.
- 9 L. M. Wysocki, J. B. Grimm, A. N. Tkachuk, T. A. Brown, E. Betzig and L. D. Lavis, *Angew. Chem., Int. Ed.*, 2011, **50**, 11206–11209.
- 10 Z.-Q. Wang, J. Liao and Z. Diwu, *Bioorg. Med. Chem. Lett.*, 2005, **15**, 2335–2338.
- 11 S. R. Denmeade, W. Lou, J. Lovgren, J. Malm, H. Lilja and J. T. Isaacs, *Cancer Res.*, 1997, **57**, 4924–4930.
- 12 J. G. Park, K. J. Langenwalter, C. A. Weinbaum, P. J. Casey and Y.-P. Pang, *J. Comb. Chem.*, 2004, **6**, 407–413.
- 13 L. Jixiang, M. Bhalgat, C. Zhang, D. Zhenjun, B. Hoyland and D. H. Klaubert, *Bioorg. Med. Chem. Lett.*, 1999, **9**, 3231–3236.
- 14 K. M. Carvalho, G. Boileau, A. C. Camargo and L. Juliano, *Anal. Biochem.*, 1996, **237**, 167–173.
- 15 H.-Z. Zhang, S. Kasibhatla, J. Guastella, B. Tseng, J. Drewe and S. X. Cai, *Bioconjugate Chem.*, 2003, **14**, 458–463.
- 16 L. D. Lavis, T.-Y. Chao and R. T. Raines, *ACS Chem. Biol.*, 2006, **1**, 252–260.
- 17 M. Yokota, T. Mitani, H. Tsujita, T. Kobayashi, T. Higuchi, A. Akane and M. Nasu, *Leg. Med.*, 2001, **3**, 171–176.
- 18 M. N. Hochmeister, B. Budowle, O. Rudin, C. Gehrig, U. Borer, M. Thali and R. Dirnhofer, *J. Forensic Sci.*, 1999, **44**, 1057–1060.





## Fluorogenic substrates for the detection of saliva

James Gooch<sup>a</sup>, Chang Rong Chua<sup>b</sup>, Vincenzo Abbate<sup>a</sup>, Nunzianda Frascione<sup>a,\*</sup>

<sup>a</sup> King's Forensics, Analytical & Environmental Sciences Division, King's College London, 150 Stamford Street, London, SE1 9NH, UK

<sup>b</sup> Department of Biological Sciences, National University of Singapore, 14 Science Drive 4, 117543, Singapore

### ARTICLE INFO

#### Keywords:

Fluorogenic substrates

Saliva detection

Body fluids

### ABSTRACT

The potential of fluorogenic substrates to detect and identify human saliva *in situ* was first explored using commercially available substrate Boc-VPR-AMC. The substrate was applied to a range of saliva dilutions deposited on glass microscope slides. A positive fluorescence response was observed immediately after application against each deposit up to a 1:8 dilution. In an attempt to improve assay sensitivity, a novel substrate Ac-VPR-Rho110-Ac, utilising a Rhodamine-110 fluorophore, was prepared using a solid-phase peptide synthesis protocol previously reported by our research group. Application of Ac-VPR-Rho110-Ac to saliva deposits demonstrated a successful increase in assay sensitivity limits, allowing stains of up to 1 in 128 dilution to be detected.

### 1. Introduction

The Office for National Statistics estimates that in 2016/2017 alone, over 5 million criminal offences occurred within the UK [1]. Of these offences, almost 50% remain unsolved with no recorded suspect [2]. As the vast majority of criminal identifications made by forensic means involve the use of DNA, there is continuing pressure to develop rapid and sensitive techniques capable of detecting and identifying genetic material deposited as biological fluid traces during a criminal act.

At present, the most widely used methods to identify deposits of saliva include the Phadebas<sup>®</sup> test, the RSID<sup>™</sup>-Saliva test and the SALigAE<sup>®</sup> test, all of which exploit reactions with the single most abundant salivary enzyme,  $\alpha$ -amylase [3]. Although these tests have proven effective within a casework scenario, they often suffer from caveats of low specificity [4] and lack of ability to localise fluids and attribute their tissue type at the same time.

Our research group has recently demonstrated the use of fluorogenic peptide substrates as successful assays for the simultaneous detection and identification of body fluid targets *in situ* [5]. These substrates utilise fluorophores that are quenched as a result of conjugation to an amino acid chain. Incubation of the substrate with a body fluid-specific protease results in the separation of the peptide-fluorophore bond and emission of fluorescence. These assays were shown to possess both high target specificity and sensitivity, whilst a 'turn-on' fluorescence signal allowed for the visualisation of discrete fluid staining areas. Furthermore, this fluorescence approach was shown to be highly compatible with current DNA profiling processes.

In the course of testing a number of commercially available

fluorogenic substrates against different biological fluids in solution, it was observed that substrate Boc-VPR-AMC exhibited a strong positive reaction in the presence of saliva. This substrate utilises a 7-amino-4-methylcoumarin (AMC) fluorophore, which is liberated upon target interaction to produce a fluorescence emission at 440 nm (Fig. 1).

This study therefore documents the use of Boc-VPR-AMC, to visualise *in situ* deposits of saliva within a forensic context, as well as the synthesis of a novel substrate (Ac-VPR-Rho110-Ac) based on the same reactive amino acid sequence, in an attempt to increase testing sensitivity.

### 2. Materials and methods

#### 2.1. Materials

Saliva was collected upon informed consent from three donors (KCL Ethics BDM/13/14-26). Substrate Boc-VPR-AMC was purchased from R & D Systems (Abingdon, UK) and diluted to a working concentration of 100  $\mu$ M. All amino acids and coupling reagents were purchased from Sigma-Aldrich Ltd (Dorset, UK), while Rhodamine-110 (Rho110) was purchased from Fisher Scientific Ltd (Loughborough, UK).

#### 2.2. Ac-VPR-Rho110-Ac synthesis

Substrate Ac-VPR-Rho110-Ac was prepared using a solid-phase peptide synthesis protocol previously reported [6]. Electrospray Ionisation Mass Spectrometry (ESI-MS) on a Waters/Micromass (Manchester, UK) ZQ mass spectrometer was used to confirm the identity of the

\* Corresponding author.

E-mail address: [nunzianda.frascione@kcl.ac.uk](mailto:nunzianda.frascione@kcl.ac.uk) (N. Frascione).

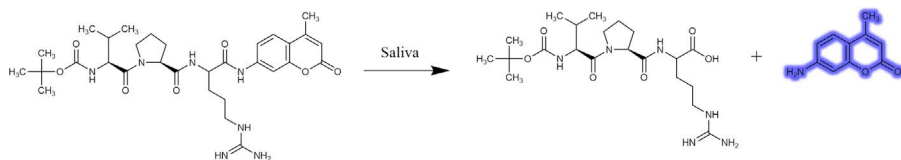


**Fig. 1.** Boc-VPR-AMC – A short peptide chain (VPR) terminally labelled with a fluorophore, creating a non-fluorescent substrate system. Resulting protease activity relieves quenching to release highly fluorescent 7-amino-4-methylcoumarin.

product at each key step of the synthesis (data not shown).

### 2.3. Microscopy

Saliva dilutions (1:1, 1:2, 1:4, 1:8, 1:16, 1:32, 1:64, 1:128) were applied in duplicate to glass slides in 5  $\mu$ l deposits and allowed to dry. Working concentration Boc-VPR-AMC (100  $\mu$ M) or Ac-VPR-Rho110-Ac (500  $\mu$ M) was pipetted in 5  $\mu$ l volumes onto the dried saliva. Fluorescence response of the substrates was recorded immediately after application by an Olympus SZX12 fluorescence microscope using UV (Ex 330–385/Em 420 nm) or GFP (Ex 460–490/Em 510 nm) filters for the commercial and synthesized substrates respectively. Negative reagent-only and saliva-only controls were also utilised and recorded in the same manner.

### 3. Results and discussion

Immediate ‘turn-on’ signal responses of substrate Boc-VPR-AMC

were observed against all saliva deposits up to a 1:8 dilution (Fig. 2a). Stains beyond this limit could not be visualised successfully. The use of negative controls also demonstrated the inherent lack of fluorescence emission of both saliva deposits and unreacted substrate.

Our research group recently reported the development of a solid-phase peptide synthesis protocol for the construction of fluorogenic substrates using the fluorophore Rhodamine-110 [6]. Such substrates are likely to be more sensitive than those using coumarin dyes due to Rhodamine-110’s superior spectral characteristics. Attempts were therefore made to improve assay performance through the construction of a novel substrate Ac-VPR-Rho110-Ac. After confirming the success of substrate synthesis by mass spectrometry, Ac-VPR-Rho110-Ac was applied to saliva deposits in the same manner as commercial substrate testing. Successful visualisation of all *in situ* saliva samples up to a 1:128 dilution, demonstrated a significant increase in assay detection limits (Fig. 2b).

During the application of Ac-VPR-Rho110-Ac, it was noted that the substrate solution exhibited some background fluorescence. However,

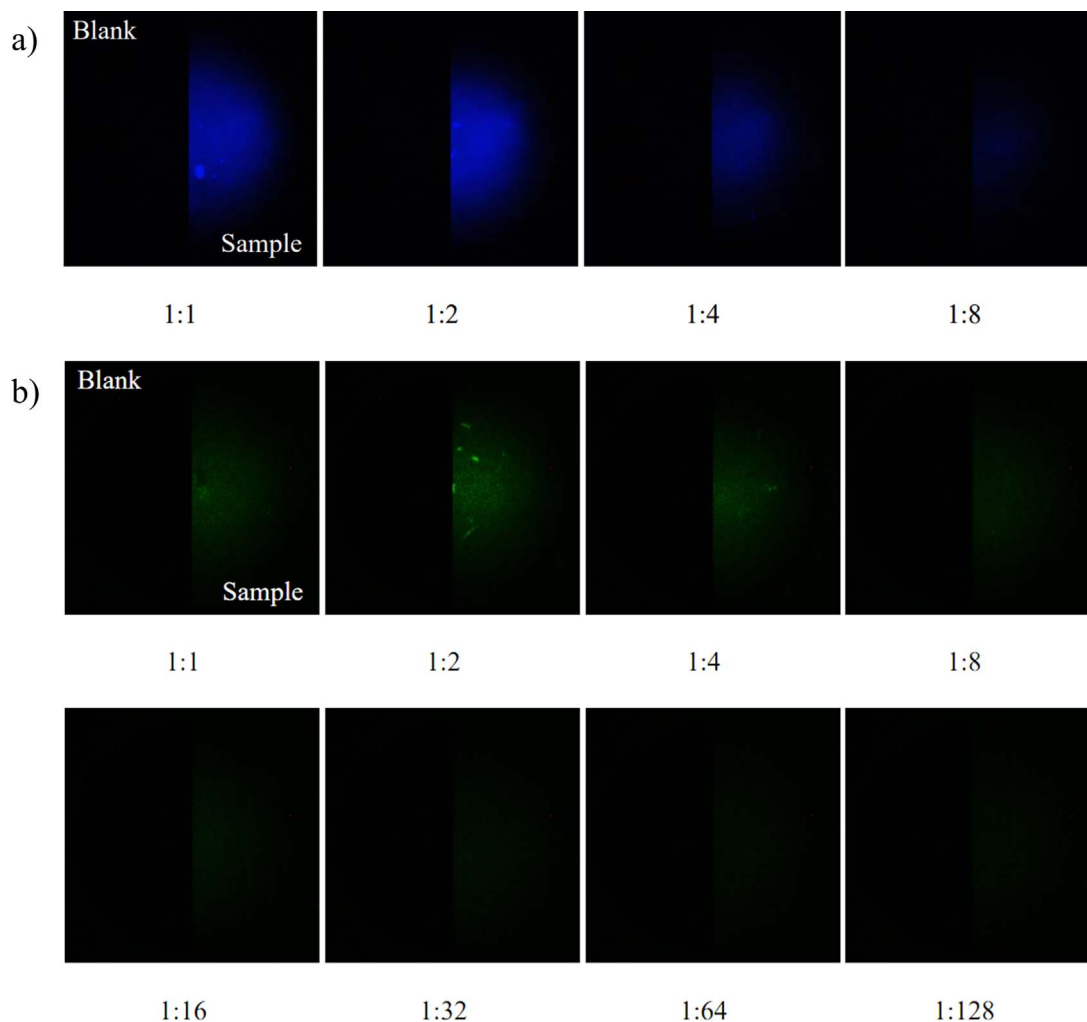


**Fig. 2.** Fluorescence response of (a) Boc-VPR-AMC and (b) Ac-VPR-Rho110-Ac to saliva dilutions deposited on glass slides. Negative saliva-only controls are provided on the left side of each image.

this was successfully corrected for through changes to microscope parameters. This background signal is likely to originate from dye molecules that were not completely conjugated during synthesis. Further purification to remove any free Rhodamine-110 from the substrate product should therefore be undertaken to prevent potential limitations to assay sensitivity.

#### 4. Conclusion

This proof-of-concept study has demonstrated the potential of fluorogenic substrates as a rapid, portable and simple method for the visualisation of saliva. Commercially available Boc-VPR-AMC was first utilised to detect deposited saliva *in situ* before assay sensitivity was increased through the construction of synthetic substrate Ac-VPR-Rho110-Ac. With substrates now designed by our group for the detection of both semen and saliva, future work is likely to focus on the development of a multiplex substrate system for the detection of multiple fluid types simultaneously.

#### Funding source

King's College London.

#### Conflict of interest

None.

#### References

- [1] Crime in England and Wales: Year Ending March 2017, Office for National Statistics, 2017.
- [2] Crime Outcomes in England and Wales 2016/17, Home Office, 2017.
- [3] K. Virkler, I.K. Lednev, Analysis of body fluids for forensic purposes: from laboratory testing to non-destructive rapid confirmatory identification at a crime scene, *Forensic Sci. Int.* 188 (1) (2009) 1–17.
- [4] B.C.M. Pang, B.K.K. Cheung, Applicability of two commercially available kits for forensic identification of saliva stains, *J. Forensic Sci.* 53 (5) (2008) 1117–1122.
- [5] J. Gooch, B. Daniel, N. Frascione, Application of fluorescent substrates to the *in situ* detection of prostate specific antigen, *Talanta* 125 (2014) 210–214.
- [6] J. Gooch, V. Abbate, B. Daniel, N. Frascione, Solid-phase synthesis of Rhodamine-110 fluorogenic substrates and their application in forensic analysis, *Analyst* 141 (8) (2016) 2392–2395.



## Developing aptasensors for forensic analysis



James Gooch, Barbara Daniel, Mark Parkin, Nunzianda Frascione\*

Analytical and Environmental Sciences Division, King's College London, 150 Stamford Street, London, SE1 9NH, UK

### ARTICLE INFO

#### Article history:

Available online 1 August 2017

#### Keywords:

Aptasensors  
Aptamers  
Biosensors  
Forensic  
Analytical science  
DNA

### ABSTRACT

Aptamer-based biosensors may be of significant benefit to forensic analysis by allowing the rapid, sensitive and specific detection of molecular targets relevant to criminal investigation. However, despite the production efficiency, stability and cost effectiveness of aptamer recognition moieties, aptasensors have yet to find commercial employment within any area of forensic science. This review therefore attempts to encourage aptasensor development by initially identifying the methods of selection, sequence analysis and affinity measurement most appropriate for the discovery of suitable aptamers against analytes of forensic interest. A range of optical, electrochemical and mass-sensitive transduction platforms that may be considered amenable to current forensic testing procedures are then discussed. The specific analytical disciplines in which aptasensing technology is likely to be of greatest value, including forensic drug analysis, forensic toxicology and biological evidence and explosives detection are lastly highlighted to stimulate researchers to consider the development of sensors towards these particular target types.

© 2017 Elsevier B.V. All rights reserved.

### 1. Introduction

Forensic science may be considered one of the broadest analytical disciplines due to the extensive spectrum of analytes and sample types used to add value to a criminal investigation. For example, in the field of human identification alone, examinable material may range from simplistic visual patterns (e.g. fingerprints) to complex biological molecules (e.g. DNA) [1]. Challenges associated with the growing variety of analytical techniques and instrumentation required by forensic laboratories to meet comprehensive testing demands have prompted the search for new and flexible methods that are able to detect, identify and quantify analytes of forensic interest.

Immunological analysis methods have long been an integral part of forensic serological and toxicological screening processes [2]. However, with the recent discovery of aptamer-based recognition, research groups are beginning to question the efficiency of the ELISA and lateral flow strip testing strategy's currently employed by forensic laboratories. Nucleic acid aptamers are short single-stranded DNA or RNA sequences that are able to undergo selective antigen association as a result of three-dimensional structure formation [3]. These structures (usually a combination of k-turn, loop, pseudoknot and quadruplex motifs) facilitate

intermolecular interaction with targets via van der Waal forces, hydrogen bonding and aromatic ring stacking [4]. Through the *in vitro* enrichment of random oligonucleotide libraries (consisting of approximately  $10^{12}$ – $10^{15}$  individual sequences) aptamers may be developed towards almost any small molecule [5], virus [6], large protein [7] or whole-cell target [8], giving potential for their use as recognition moieties in the analysis of diverse forensic samples.

While analogous to antibodies in terms of binding affinity (often displaying  $K_d$  values in the nanomolar or picomolar range [9]), aptamers possess a number of key advantages over their protein counterparts. Once selected, aptamer sequences can be mass-produced using automated solid-phase synthesis techniques, resulting in the production of highly purified oligonucleotides within a number of hours and at a fraction of the cost of biological antibody generation methods [10]. Aptamers also display greater thermal stability affording long shelf-lives without loss of activity, easy transport and storage and ability to return to a native conformation being subjected to high-temperature assay conditions [11].

Although demonstrating success as effective therapeutic agents [12], aptamers, since their discovery, have been predominately developed as recognition molecules for use in a range of biological chemical analysis techniques. This has mainly focused on the use of immobilized aptamers within traditional ELISA, western blot, flow cytometry and lateral flow assays as replacements for expensive and cumbersome antibody moieties [10]. In addition, aptamers have also found beneficial application with the field of separation science, having been used to successfully resolve enantiomeric

\* Corresponding author.

E-mail address: [nunzianda.frascione@kcl.ac.uk](mailto:nunzianda.frascione@kcl.ac.uk) (N. Frascione).

molecules within High Performance Liquid Chromatography (HPLC) systems by the inclusion stereo specific aptamers on solid chromatographic supports [13].

Nevertheless, Hamaguchi et al. argue that the most powerful application of nucleic acid aptamers is within analytical biosensing platforms [14]. Biosensors are compact devices capable of the real-time transduction of biological interaction events into a number of measurable signal outputs [15]. Some authors have recently recognized the potential of biosensors to provide the highly specific detection and quantification of forensically relevant materials (such as body fluids, drugs, explosives and toxins) without the need for extensive sample processing steps [16–18]. Displaying significant conformational changes upon target binding and allowing an extensive range of chemical modifications (including the incorporation of various optical, electrochemical or nanoparticle reporters [19]) at various sites without loss of binding affinity, aptamers may be considered as ideal recognition moieties for use within molecular sensing purposes [20].

Despite great promise, aptasensors (or indeed any form of aptamer technology) have yet to find commercial employment within the field of forensics. This lack of success has been attributed to a number of factors, including the limited number of aptamer sequences raised against analytically relevant targets [20], the need for further investigation into the use of developed sensors within complex matrices [17] and the high investment already made by analytical laboratories in antibody-based testing methods [30]. This review therefore attempts to outline the current state of aptasensor development processes, with a specific focus on those techniques most likely to aid the construction of forensic analyte sensing devices. Recent advances in aptamer selection, sequencing and affinity testing are first explored, along with signal transduction mechanisms most amenable to current forensic testing capabilities. A number of forensic disciplines liable to benefit from aptasensor application are lastly identified in the hope of encouraging experts within the field of biosensor design to produce aptasensors towards valuable evidential targets.

## 2. Aptamer development

### 2.1. Aptamer selection

In recent years, a substantial number of modifications have been made to the SELEX (Systematic Evolution of Ligands by EXponential enrichment) protocol initially developed by Gold's [31] and Szostak's [32] groups. While generally based on the same library incubation, target binding and sequence amplification principles exploited within the original method, these modified techniques differ in their approach to the separation and removal of non-specific ligands [33]. By altering the means in which aptamer-target complexes are partitioned from unbound oligonucleotides, aptamers may be selected against particular target types with a higher specificity and affinity than would be possible using conventional SELEX protocols [34]. As the physical properties of forensically relevant targets are extremely diverse, it is vital that an optimal selection method is chosen and carried out prior to aptasensor development. A summary of SELEX protocols that may be useful in the selection of aptamers against forensically relevant targets can be found in Table 1.

These modifications are especially pertinent in the selection of aptamers towards low-molecular weight forensic analytes (e.g. toxic chemicals and explosives), where separation is problematic due to the similar masses of bound complexes and unbound nucleic acid sequences [35]. The immobilization of such targets to a solid support surface (e.g. sepharose, agarose or magnetic beads) may be used to increase separation efficiency but can also result in the

amplification of non-specific sequences that bind to the support matrix or immobilization linkers [5]. Furthermore, the creation of a chemical link between the small molecule target and the solid support can introduce an unfavourable selection bias through the removal of least one potential aptamer binding site. Fortunately, a number of SELEX processes that allow for the selection of aptamers against small-molecules without the need for target immobilization have recently been developed.

Capture-SELEX (also known as structure-switching SELEX), involves the conjugation of oligonucleotide libraries themselves to DNA-functionalized magnetic particles by use of a complimentary 'docking' sequence [22,36]. When incubated with a target molecule, sequences that undergo conformational changes as a result of binding are displaced from the beads (which can then be removed with unbound ligands through the application of a magnetic field). Aptamers isolated using this capture method may be considered particularly attractive recognition moieties for use in analytical biosensing platforms due to their significant structure-switching abilities [37].

Another immobilization-free method, GO-SELEX, makes use of the ability of graphene oxide (GO) to bind single stranded DNA through  $\pi$ - $\pi$  stacking interactions [25]. In this technique, target molecules are first incubated with an oligonucleotide library in solution, allowing binding to occur. Unbound sequences are then adsorbed onto the surface of the graphene oxide, allowing separation from aptamer-target complexes via centrifugation. Ethanol precipitation is finally used to purify and recover bound ssDNA sequences. As partitioning is purely based on interaction between DNA libraries and graphene, GO-SELEX is largely independent of target size (and has already been successfully employed to produce aptamer sequences towards low-molecular weight pesticide compounds [38]). One class of forensic analytes that may also benefit from aptamer-sensing application is that of whole-cells. The immunological analysis of cellular material is currently undertaken by forensic laboratories as a method of confirming the identity of biological fluid deposits left behind at crime scenes [2]. Unlike conventional SELEX procedures, the selection of aptamers against whole-cells does not require the use of a single highly purified (or even known) target. First described by Morris et al., Cell-SELEX instead involves concurrent binding of library oligonucleotides to multiple biomarkers exposed on the surface of intact live cells [23]. As a result, this approach generates a panel of aptamer sequences (each targeting a particular membrane protein or lipid) that can then be used for cell recognition purposes [39]. The use of live targets within Cell-SELEX ensures that aptamers are raised towards the native conformational structure of such membrane molecules, allowing for the high-affinity binding of natural cellular material during subsequent analysis [8]. In comparison to other selection protocols, the partitioning of unbound nucleotides within Cell-SELEX is relatively simplistic and may be achieved by basic centrifugation or washing steps [40]. A counter-selection stage, in which enriched libraries are incubated with a negative control cell line, is also often included in cell-selection protocols to remove non-specific ligands that bind to universally shared membrane motifs [41]. Cell-SELEX techniques have in fact already been used to produce aptamers against sperm [42] and red-blood cell targets [23], which may already be of potential use within forensic assays for the analysis of biological fluids.

### 2.2. Sequence analysis

Following sufficient enrichment, aptamer pools are sequenced in order to elucidate the nucleotide structures of high-affinity binders [33]. Conventionally, this process was performed via the ligation of selected sequences into commercially available cloning



**Table 1**

SELEX protocols that may be used in the selection of aptamers against forensic targets.

Protocol	Mechanism	Advantages	Reference
Capillary-Electrophoresis SELEX	Aptamer-target complexes are separated from unbound nucleotide sequences according to electrophoretic mobility.	- Selection may be completed within 2–4 rounds.	[21]
Capture-SELEX	Library sequences are displaced from magnetic beads by target binding. Unbound ligands are then removed magnetically.	- Useful for small molecule targets.	[22]
Cell-SELEX	A panel of membrane biomarker-specific aptamer sequences is produced as a result of exposure to live cell targets.	- Aptamers display large structural changes.	[23]
FluMag SELEX	Complexes formed between bead-immobilized analytes and fluorescent library sequences are collected magnetically.	- Useful for small molecule targets.	[24]
Graphene Oxide (GO) SELEX	Graphene oxide is used to adsorb and separate unbound ssDNA sequences from aptamer-target complexes in solution.	- Counter-selection used to increase specificity.	[25]
<i>In-Silico</i> SELEX	Theoretical oligonucleotide libraries are screened against a target using computational tools to identify potential binders.	- Selection rounds and dissociation values may be quantified by fluorescence measurement.	[26]
Microfluidic (M) SELEX	Ligands bound to magnetic or sol-gel bead-conjugated targets are purified by continuous washing within a microchannel.	- Requires less than 5 rounds of selection.	[27]
MonoLEX	Affinity columns used to partition aptamer-target complexes are physically segregated to elute highest affinity sequences.	- Useful for small molecule targets.	[28]
NanoSelection	High affinity aptamers are detected and recovered via the use of fluorescence and Atomic Force Microscopy (AFM).	- Atomic-level mechanisms of nucleotide-target binding can easily be determined.	[29]

vectors, which are then transformed into competent bacterial cell colonies. Approximately 50–100 individual clones (each possessing one aptamer sequence) are then recovered before plasmids are extracted and subjected to standard Sanger sequencing [43]. However, whilst able to indicate the most abundant aptamers present within an enriched pool, these cloning techniques only involve the sequencing of a small fraction of the total binders obtained during selection (which may be up to 1,000,000 sequences) [44]. As a result, the majority of new aptamer development protocols now make use of next generation sequencing (NGS) platforms for the comprehensive analysis of potential binding candidates [45]. Such high-throughput methods not only allow the discovery of millions of sequences from enriched pools without laborious cloning processes, but can also be used to shorten selection processes by identifying aptamers during early SELEX rounds [46].

Commercially available NGS platforms previously used for aptamer discovery include Ion Torrent's Personal Genome Machine (PGM) [47] Illumina's Genome Analyzer/HiSeq system [48,49], Roche's GS FLX system [50,51] and Applied Biosystem's SOLiD

system [52]. However, with extensive sequence reads and higher total read lengths, a greater level of detail on the structural features of target binders may be provided by Illumina instruments, making them the most preferable choice for aptamer sequencing (Fig. 1) [43]. Furthermore, these platforms, based upon the principle of cyclic reversible termination, are already widely used within the forensic community for the analysis of human genomic material [53] and may therefore be readily applied by forensic researchers to determine aptamer sequences for the recognition of forensic analytes.

While NGS use may significantly enhance the resolution and sampling depth of enriched aptamer pools, additional computational bioinformatic tools are currently required to process the sheer quantity of raw sequence data obtained [45]. Web-based and offline preprocessing software, such as Galaxy [54], cutadapt [55] and AptaTools [56] are often used to first isolate variable aptamer regions of a defined length by removing adapter and constant region sequences. Further programs are then employed to filter this data in order to narrow down aptamer candidates for subsequent experimental testing. The FASTaptamer toolkit achieves such

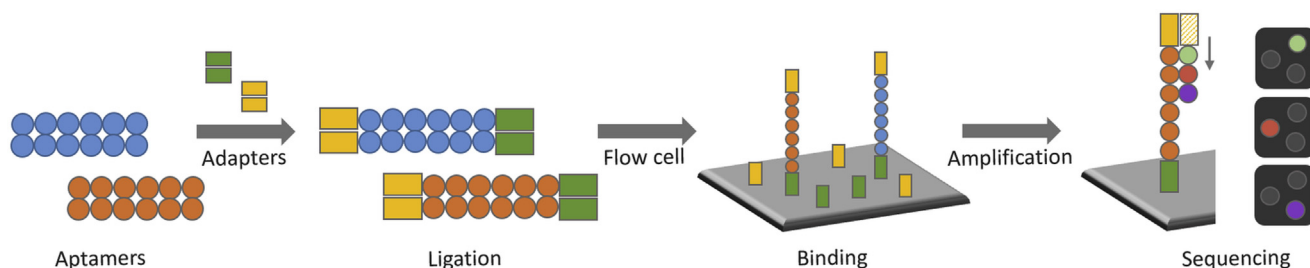


**Fig. 1.** Workflow of the Illumina sequencing-by-synthesis approach – Specialist adapter sequences are first ligated to the end of aptamers obtained from SELEX-enriched pools. These adapters aid the anchoring of selected oligonucleotides to the surface of a flow cell, allowing solid-phase bridge amplification. Fluorescently labelled nucleotides are then added to the cell, which is imaged after the incorporation of each base into DNA strands. The emission wavelengths of each nucleotide dye are then monitored in order to determine aptamer sequences.

filtering by monitoring the relative enrichment of specific aptamer sequences between selection rounds [57], whereas APTANI examines both the total read counts of each sequence as well as shared structural homology between sequences [58]. After aptamer discovery has taken place, sequences may be further analysed by programs such as *mfold* [59] to provide more information on secondary oligonucleotide structure.

### 2.3. Affinity measurement

In order to ensure adequate aptasensor performance, it is vital that integrated aptamers demonstrate strong affinity towards target molecules [60]. Aptamer affinity is usually expressed in terms of a dissociation constant ( $K_d$ ), the value of which may be determined by a range of separation-based, mass-sensitive, spectroscopic or other label-free techniques [5]. A summary of methods that may be able to assess the performance of aptamers with potential use in forensic testing may be found in Table 2.

Variations in the size and physical properties of forensically relevant analytes make the evaluation of aptamer-target affinities challenging. Much like similar SELEX processes, measuring  $K_d$  via the separation of unbound ligands from aptamer-target complexes is often problematic for compounds of a smaller molecular weight than nucleotide binding sequences. Other techniques, such as fluorescence polarization or surface plasmon resonance (SPR), are additionally disadvantaged by the chemical labelling or immobilization of aptamers or targets, which may reduce  $K_d$  calculation accuracy by altering binding interactions [5].

A resolution to these issues may be provided by isothermal titration calorimetry (ITC), a label-free solution-based method that allows the characterization of binding energy by monitoring temperature increases during complex formation [72]. ITC methods are currently considered the 'gold standard' for quantifying biomolecular interactions and have already been used to assess the affinity of aptamers towards several forensically relevant targets, including cocaine [73] and organophosphate pesticides [74]. In this

**Table 2**  
Techniques that may be used to determine the affinity of aptamers against forensic targets.

Technique	Type	Mechanism	Reference
Affinity chromatography	Separation	- Binding is measured after labelled aptamers or target molecules are incubated with corresponding components that are conjugated to a solid support (typically agarose or magnetic beads).	[61]
Capillary electrophoresis	Separation	- Concentrations of aptamers, targets and aptamer-target complexes are determined after size and charge-based separation. Fluorescent labelling of each component is often required for detection.	[21]
Equilibrium dialysis	Separation	- Unbound ligands within an aptamer-target mixture are allowed to diffuse through a semi-permeable membrane before being quantified.	[62]
Gel Electrophoresis	Separation	- Like capillary electrophoresis, binding components are separated by size and charge but by a non-denaturing agarose or polyacrylamide gel. Visualization is required to observe isolated components.	[63]
Ultrafiltration	Separation	- Unbound ligands are measured after partitioning across a membrane (typically nitrocellulose) under applied pressure, vacuum or centrifugation.	[64]
Back-Scattering Interferometry (BSI)	Spectroscopic	- Changes in the refractive index of a sample through the association of aptamer-target complexes are detected within a microfluidic channel.	[65]
Circular Dichroism (CD)	Spectroscopic	- Differences in the absorption of left and right circularly polarized light are monitored during the titration of DNA against increasing concentrations of target.	[66]
Fluorescence Intensity	Spectroscopic	- The increase/decrease in fluorescence intensity of targets or labelled aptamers as a result of complex formation is measured via spectrofluorometry.	[67]
Fluorescence Polarization	Spectroscopic	- The rotational diffusion of fluorescent dyes conjugated to aptamers or targets is decreased as a result of binding. Subsequent increases in signal polarization are then monitored.	[68]
UV–Vis Absorption	Spectroscopic	- Affinity is inferred from variations in the wavelength or intensity of UV–Vis absorption of aptamers or targets upon binding.	[7]
Quartz Crystal Microbalance	Mass-Based	- Accumulation of aptamer-target complexes on the surface of functionalized piezoelectric crystals results in a measurable decrease in resonance frequency.	[69]
Surface Plasmon Resonance	Mass-Based	- Ligands immobilized on a sensor flow cell are subjected to an aqueous flow of binding partners. The formation of target complexes then results in a change in refractive index near the sensor surface.	[70]
DNase Footprinting	Other	- The relative levels of aptamers protected from digestion (by association with varying concentrations of target molecules) are determined after treatment with DNase I enzymes.	[71]
Isothermal Titration Calorimetry (ITC)	Other	- The amount of energy required to maintain the temperature of a cell is monitored during exothermic aptamer-complex binding.	[72]

technique, targets are titrated into a cell containing an aptamer of interest and allowed to react. Heat released as a result of exothermic binding processes is monitored and compared to an identical reference cell containing buffer or water. Power required by the calorimeter to maintain equal temperature between the cells at each molar ratio of target/aptamer may then be used to construct a binding isotherm, allowing affinity to be determined [75]. However, while ITC may provide detailed information on the thermodynamic parameters of aptamer-target interactions (such as changes in entropy, enthalpy and Gibbs's energy), relatively high amounts of target are required for detectable amounts of heat to be generated [7]. This may be considered problematic for some forensic analytes that are expensive to purchase or only available from commercial providers in low concentrations (although micro and nano-ITC instruments may be utilised to overcome these challenges).

### 3. Biosensing platforms

#### 3.1. Optical

Reported by Kleinjung et al. in 1998, the first biosensor to use aptamers as moieties for target recognition involved the competitive binding of L-adenosine and FITC-labelled analogues to an RNA ligand immobilized on the surface of an optical fibre [76]. As a result, the vast majority of early aptasensing platforms also focused on the use of optical methods to signal biological interaction occurrence [77]. Such sensing generally relies on the structural transitions that aptamers undergo during target binding to create measurable variations in the spectroscopic properties of optical transduction components [19]. These components (typically organic dyes, luminophores, nanoparticles or conjugated polymers) may be incorporated into conformationally labile regions of oligonucleotide sequences by covalent attachment or as 'label-free' reporters by indirect intercalation [78]. Subsequent alterations in the microenvironment of these reporters as a result of aptamer folding may then prompt changes in the intensity, wavelength or anisotropy of label emissions [20]. Alternatively, multiple reporters can be used to achieve transduction through distance-dependent fluorescence (FRET) or chemiluminescence (CRET) resonance energy transfer processes [79].

Two popular forms of optical aptasensing include aptamer-beacons and hybridized DNA displacement assays [80]. Based on the conventional molecular-beacon format for the detection of specific DNA molecules, aptamer-beacons are constructed by the addition of short complementary nucleotides (alternately labelled

with a fluorophore or quencher) to each end of a specific aptamer sequence [14]. Under normal conditions these nucleotides allow the aptamer to take on a closed hairpin structure, bringing the quencher and fluorophore moieties within close proximity and restricting fluorescence output. However, in the presence of target molecules, aptamer interaction causes the hairpin to unfold, resulting in the production of a 'signal-on' fluorescence emission [80]. Hybridized DNA displacement assays (Fig. 2a) work via a similar premise but instead employ a separate quencher-labelled antisense sequence bound to fluorescent aptamers through Watson-Crick base pairing that then dissociates in the presence of higher affinity target analytes [81].

One of the main advantages of optical sensing is the ability to offer real-time analyte detection without extensive sample processing steps or specialized equipment [82]. Such advantages may give the potential for optical aptasensors to be used as chemical reagents for the simultaneous detection and identification of latent (i.e. non-visible) evidence deposited at crime scenes or on evidential items. This concept has already been explored within Li et al. in which two aptamers labelled with emitting gold nanoparticles (Au-NPs) reassembled in the presence of cocaine doped within latent fingerprints [83]. While the adherence of the nanoparticles themselves to deposited marks was sufficient to visualize identifiable ridge detail, aggregation of the Au-NPs as a result of cocaine binding also resulted in a shift in emission wavelength of scattered light from 550 to 580 nm.

#### 3.2. Electrochemical

Cho et al. note that despite the significant amount of optical detection platforms reported during the early stages of aptasensor research, greater attention is now being paid to the use of electrochemical strategies for the transduction of aptamer interactions [20]. Biosensing assays incorporating such methods are becoming increasingly attractive to researchers due to their relative portability, ease of operation, robustness and low cost (to both develop and operate) [84]. Electrochemical aptasensors are further benefitted by excellent sensitivities and can be used in conjunction with a number of electrical signal amplification techniques (such as biocatalytic labelling) to provide extremely low limits of analyte detection [85]. For example, Hanson et al. employed the use of a single-step replacement aptasensor exploiting electrochemical nanoparticle stripping-based signal amplification for the measurement of thrombin at ultrasensitive attomole levels [86].

While electrochemical aptasensors may make use of amperometric, potentiometric, conductometric, impedimetric and

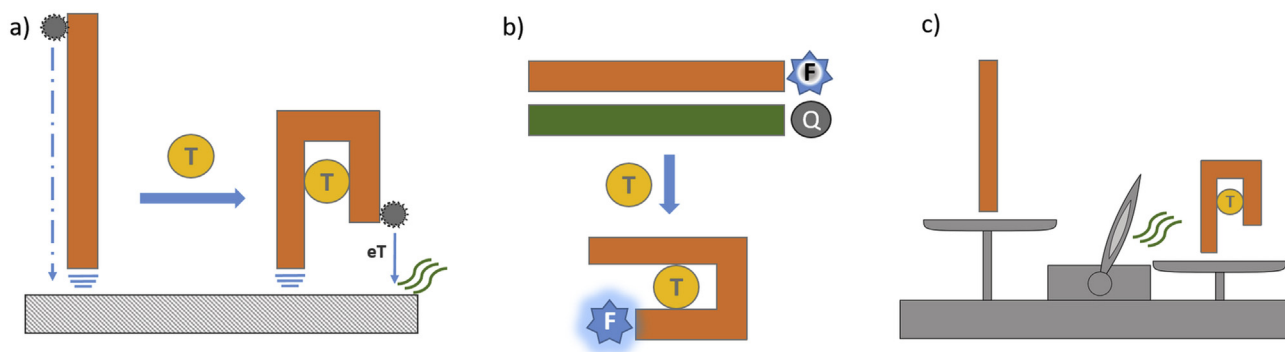


**Fig. 2.** Schema of aptamer-based sensing formats – a) Optical transduction. Aptamers labelled with fluorescence reporters (F) are hybridized to quencher (Q)-conjugated DNA sequences, which absorb emission via FRET. Upon binding to targets (T), aptamers separate from complimentary strands, allowing fluorescence to be restored. b) Electrochemical transduction. Changes in aptamer conformation as a result of target interaction allow redox-active labels to interact with the surface of electrodes to produce an electrical signal. c) Mass-sensitive. An increase in the mass of surface-immobilized binders through aptamer-target complex formation is detected either optically or electrically.



semiconductor field-effect principles, signals are generally derived from changes in electric current as a result of aptamer-mediated redox reactions occurring at the surface of an electrode [84]. Much like optical aptasensing mechanisms, these reactions are generated by reporter molecules incorporated within aptamer sequences, which are then brought closer to or further away from electrodes as a result of target binding interactions [79]. Popular reporters for electrochemical aptasensors include methylene blue (MB), ferrocene, ferricyanide, ruthenium complexes, enzymes, quantum dots (QDs) and metal nanoparticles [87].

According to Han et al., electrochemical aptasensor assays may be designed in four broad formats: target-induced structure switching (TISS), sandwich, target-induced displacement (TID) or competitive replacement [88]. TISS assays exploit the ability of surface-immobilized aptamers to form rigid tertiary structures in the presence of analytes in order to change the proximity of signalling moieties in relation to an electrode (Fig. 2b). Sandwich assays conversely involve the assembly of a complex between an immobilized primary aptamer, a target, and a second reporter-labelled recognition molecule (which may be an aptamer or an antibody). In TID sensors, complementary nucleotide sequences are instead immobilized and are used to anchor labelled aptamers to electrodes via base pairing. Upon target interaction these aptamers dissociate, causing a decrease in electron transfer (eT) signals. Competitive replacement lastly involves the incubation of targets with reporter-attached analytes, which then compete for aptamer binding space. As a result, signal intensities obtained from competitive replacement assays are inversely proportional to the amount of target present within a sample.

Electrochemical detection platforms may be considered especially amenable to forensic analysis due to their excellent performance in turbid matrices [89]. Such sensing platforms are able to negate the effects of optically absorbing and fluorescent molecules present within complex samples (that often interfere with spectroscopic analysis) and therefore represent great potential as toxicological assays for the detection of trace compounds within biological matrices. Work conducted by Baker et al. has already proven this capability through the production of an electrochemical TISS aptasensor that was successfully able to detect micromolar concentrations of cocaine in saliva and blood serum samples [90].

### 3.3. Mass-sensitive

Unlike both optical and electrochemical transduction mechanisms, mass-sensitive aptasensing techniques do not utilise the conformational changes that aptamers undertake in order to indicate biological interaction events [20]. Instead, sequences are tethered to a variety of solid supports and used as simple capture ligands to create discernible increases in mass at sensor surfaces upon target binding (Fig. 2c). As a result, such methods do not require the use of molecular reporters to generate detectable signals and are therefore classified as 'label-free' techniques [79]. Popular mass-based aptasensing formats include: SPR, surface acoustic wave (SAW), quartz crystal microbalance (QCM) and microcantilever assays [79].

Employing the same principles for the characterization of binding affinity constants, SPR methods have also found use as platforms for the aptamer-based detection of numerous target compounds [91]. One of the most frequently used instruments for SPR sensing is the Biacore™ system manufactured by GE Healthcare [92]. In this system, aptamers are first covalently immobilized onto a thin gold film attached to a glass slide, which is then illuminated by monochromatic p-polarised light. Solutions containing an analyte of interest are then introduced into the sensor at a continuous flow through microfluidic channels. As these analytes

interact with aptamer sequences, increases in mass bound to the film surface cause changes in the refractive index of incident light, which is then registered by the instrument [93].

SAW and QCM-based aptasensors both involve the generation and detection of acoustic waves by electrodes patterned on the surface of aptamer-functionalized piezoelectric crystals [94]. The propagation speed of such waves (either on the surface or in the bulk of crystals for QCM and SAW respectively) is highly influenced by mass associated with the crystal itself. Increases in this mass as a result of aptamer-target binding subsequently cause a reduction in crystal resonance frequencies, which are then observed by electrical means [20]. Whilst these devices are normally only applicable for the sensing of large analytes such as proteins or cells (which provide more measurable mass changes) a number of modified protocols, such as QCM with dissipation monitoring (QCM-D), have been developed to allow the aptamer-based detection of lower molecular weight analytes [35].

Microcantilever assays typically consist of thin silicon or polymer-based micromechanical beams (approximately one micron thick), which respond to changes in physical stress [95]. A gold coating is often applied to one side of the beam in order to allow the immobilization of biological receptors, including aptamers, onto cantilever surfaces [96]. The binding of target molecules to these receptors creates stress differences between the functionalized and non-functionalized sides of the surface, causing the cantilever to bend by a matter of nanometres [97]. The degree of bending (also known as cantilever deflection or  $\Delta\chi$ ) is then detected optically and compared to a reference cantilever containing non-interacting nucleotide sequences [98]. As this deflection is directly proportional to the amount of target present within a sample, microcantilever methods represent a great opportunity for the quantitative sensing of forensically relevant analytes.

## 4. Aptasensor applications

### 4.1. Biological evidence

Chemical reagents used for the detection and identification of biological evidence (i.e. body fluids and fingerprints) are currently limited by issues of low specificity and sensitivity, environmental and safety concerns, ease of application and effect on downstream DNA profiling processes [16,99]. Other antibody-based devices (such as immunochromatographic test cartridges) are conversely able to provide absolute confirmation of body fluid identity with a sufficient degree of sensitivity and safety, but cannot be used to locate latent stains on evidential surfaces [100]. As previously mentioned, optical aptasensing strategies may have the opportunity to overcome these challenges by allowing the simultaneous detection and highly specific identification of biological evidence *in situ*.

Furthermore, a number of optical aptasensors have already been constructed towards biomarkers that may be (or currently are) used for the confirmation of body fluid presence. For example, Kong et al. recently reported the production of a fluorescent aptasensor towards prostate specific antigen (PSA), a serine protease enzyme already used in forensic analysis for the immunological detection of seminal fluid [102]. In this assay, fluorophore-labelled aptamers adsorbed onto the surface of emission-quenching MoS<sub>2</sub> nanosheets were used to detect sub-nanogram concentrations of PSA after dissociation upon target binding.

Since its isolation by Bock et al. in 1992, the thrombin-binding aptamer has become one of the most commonly exploited DNA receptor sequences for the construction of new aptamer-based sensing platforms [103]. As a result, a number of these aptasensing assays may find application in the specific detection of

thrombin for the purposes of identifying bloodstains deposited on evidential surfaces. One such sensor, developed by Wang et al., involves the use of aptamer-functionalized upconverting phosphors, which are initially quenched by the binding of carbon nanoparticles to DNA strands through  $\pi$ – $\pi$  stacking interactions (Fig. 3). In the presence of thrombin, these nanoparticles dissociate from ligand sequences, relieving FRET quenching effects and producing 'signal-on' fluorescence emission [101].

#### 4.2. Forensic drug analysis

Routinely employed methods for detecting trace quantities of illicit drugs include presumptive chemical tests, immunoassays and a wide selection of chromatographic techniques [104]. With a high sensitivity, selectivity and reliability, gas chromatography coupled with mass spectrometry (GC-MS) or liquid chromatography coupled with mass spectrometry (LC-MS) is currently considered the 'gold-standard' for the forensic analysis of bulk drug samples. However, such approaches are costly and may be considered inappropriate for high-throughput analysis due to extensive run times. Rapid, cheap and portable drug-screening assays based on aptasensor technology are therefore likely to be welcomed by the forensic community.

Much like the thrombin-binding sequence previously discussed, a cocaine-specific aptamer constructed by Stojanovic et al. [106] has also been extensively used as a model ligand for proof-of-concept aptasensing assays. Demonstrated by Hilton et al., a particularly sensitive example of such assays involved the target-induced displacement of Dabcyl quencher-attached complementary oligonucleotides from carboxyfluorescein (FAM) labelled aptamers immobilized within microfluidic channels. This assay was subsequently shown to enable the detection of cocaine at picomolar levels, without the need for sample cleanup and derivatization processes required for GC-MS analysis [107].

Beyond cocaine-based assays, initial explorations are also being made into the use of aptasensing platforms for the detection of amphetamine derivatives. Yarbakht and Nikkhah recently exploited the ability of single stranded aptamers to shield Au-NPs from salt-induced aggregation in order to allow the colourimetric signalling of MA and MDMA presence [105]. In this sensor (Fig. 4), an aptamer able to bind both MA and MDMA is incubated with a given sample. If target molecules are contained within the sample, conformational changes in the aptamer take place as a result of binding. Such changes prevent the association of aptamer sequences with Au-NPs, which then aggregate upon salt addition, turning the colour of sample solutions from red to blue. If target molecules are absent

from the sample, aptamers are instead able to interact freely with AuNPs, protecting them from aggregation.

In an alternative transduction approach, Huang et al. [108] were able to successfully develop an electrochemical biosensor based on Au-mesoporous silica nanoparticles (Au-MSN) after selecting a 37-mer aptamer sequence against the opiate alkaloid codeine. Here, thiolated codeine aptamers were conjugated to Au-MSN's immobilized on the surface of a glassy carbon electrode. Changes in electrical impedance at the electrode surface associated with aptamer-target binding were used to monitor codeine concentrations across a linear range of 10 pM–100 nM. Furthermore, denaturation of the aptamer sequences by incubation with heated distilled water allowed the sensor to be reused for subsequent measurements.

With relatively fast selection and isolation times compared to antibodies (i.e. a matter of weeks), nucleic acid aptamers also represent a great opportunity to rapidly develop forensic assays for the detection of new psychoactive substances (NPS). These substances (typically scheduled drugs slightly modified to circumvent legal restrictions) are emerging at an unprecedented rate, with over 450 new compounds identified by the EU early warning system since 2005 [109]. At present, the majority of NPS compounds are poorly or not detected by standard immunoassay tests, forcing analysts to rely on mass-spectrometry techniques [110]. Despite the excellent potential of aptasensor platforms as drug-screening assays, aptamers selected towards any NPS target have yet to be reported in the literature.

#### 4.3. Forensic toxicology

The synthetic nature of SELEX protocols means that aptamer recognition moieties may be selected against toxic compounds that would likely kill animal hosts during standard *in vivo* antibody-generation methods [111]. Such moieties may be therefore of great benefit to toxicology practices, where determining cause of death is often dependent upon the detection and quantitation of hazardous substances. This branch of forensic chemistry heavily relies on the use of expensive and labour-intensive analytical techniques to confirm the identify of various poisons and toxins [112].

Ochratoxin A (OTA) is a toxic metabolite secreted by *aspergillus* and *penicillium* fungi species that can exert severe nephrotoxic, immunotoxic, and carcinogenic effects [114]. As such toxins represent a threat to health through the contamination of commercialized food systems, significant efforts have been made towards the development of a simple and flexible sensing platform

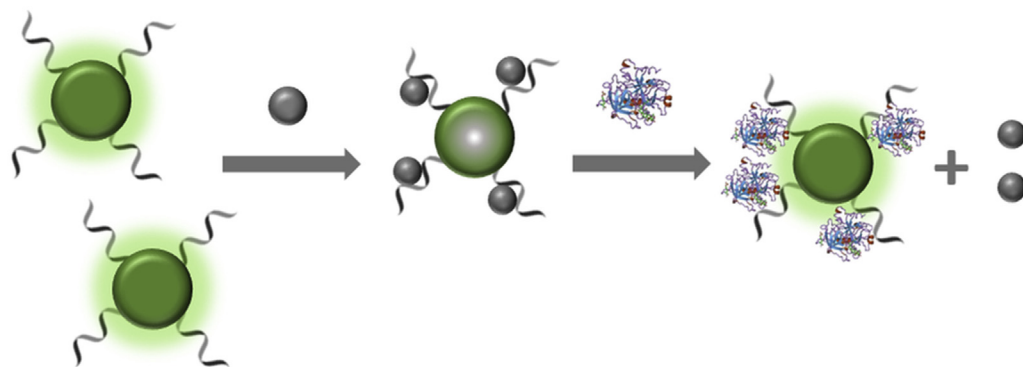


**Fig. 3.** Schema of a FRET-based aptasensor for the detection of thrombin developed by Wang et al. [101]. Here, 5' amino-modified aptamer sequences are first covalently linked to poly-acrylic acid (PAA)-functionalized up-conversion phosphors (UCP's). Subsequent incubation with carbon nanoparticles results in quenching of the sensor through aptamer-bridged fluorescence resonance energy transfer (FRET). This sensor demonstrated a linear detection range of 0.5–20 nM and was even used to detect Thrombin concentrations of 0.25 nM within spiked human serum samples.

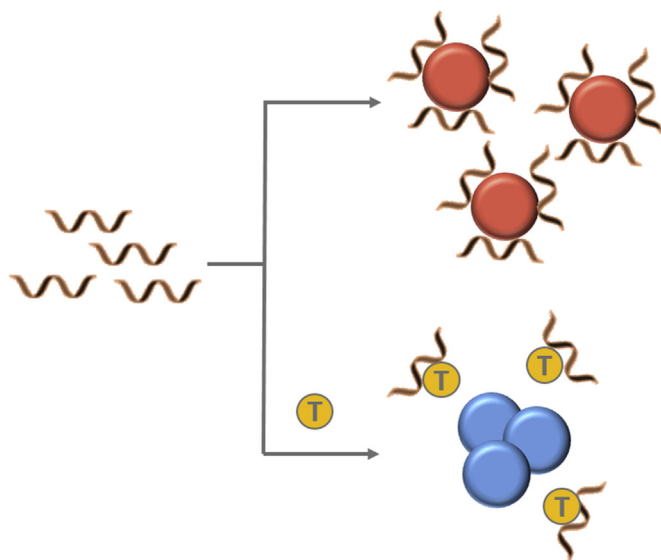


**Fig. 4.** Schema of a colourimetric Au-NP aptasensor for the detection of methamphetamine developed by Yarbakht and Nikkhah [105]. In this assay, aptamers are initially adsorbed onto the surface of gold nanoparticles (Au-NPs) through hydrophobic and electrostatic interactions to stabilize them within solution. However, in the presence of methamphetamine (MA) or 3,4-Methylenedioxymethamphetamine (MDMA), alterations in the structural conformation of the aptamers allow salt-induced aggregation of the particles to occur, prompting surface plasmon resonance-based colour changes. A purely visual detection of MA was found to occur at concentrations as low as 5 mM.

for the detection of OTA compounds [115]. In a strategy designed by Sheng et al. (Fig. 5), this sensing was achieved by the use of FAM-modified aptamers which, in the absence of OTA, are adsorbed onto a basal plane of graphene oxide and quenched [113]. However, in the presence of target molecules, aptamers are induced into particular three-dimensional conformations and resist adsorption, allowing fluorescence to be monitored.

In an extension of the Au-NP aggregation assay exploited by Yarbakht and Nikkhah for the detection of amphetamines, Wu et al. also utilised an aptamer-based sensor for the detection of arsenic within aqueous solutions [116]. In this method, a cationic surfactant Hexadecyltrimethylammonium bromide (CTAB) was employed instead of salts to stimulate nanoparticle aggregation, allowing the colourimetric detection of arsenic concentrations in the range of 1–500 parts per billion.

Work from Lamont et al. resulted in the selection of an aptamer (SSRA1) specific to the B-chain of ricin [117]. Ricin, a cytotoxic protein of biological origin, is considered as a potential threat agent for terrorist use because of its high toxicity and relative availability.

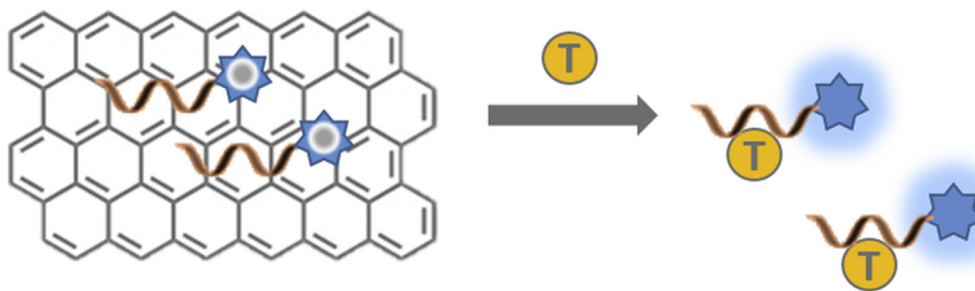


**Fig. 5.** Schema of a graphene-quenching fluorescence aptasensor for the detection of ochratoxin A developed by Sheng et al. [113]. Here, aptamers are made initially fluorescent via 5' labelling with 6-carboxyfluorescein (6-FAM). Under normal conditions, these aptamers are readily adsorbed onto the basal plane of PVP-protected graphene oxide, which subsequently quenches 6-FAM emission by energy transfer. However, in the presence of ochratoxin A, antiparallel G-quadruplex formation prevents such adsorption and fluorescence signals are generated. Using this sensor, Sheng et al. were able to monitor ochratoxin A with high selectivity in a linear range from 50 to 500 nM.

The selected aptamer displayed superior detection capabilities compared to a commercially available ELISA kit for ricin. Following this study, attempts have been made in order to embed the SSRA1 aptamer into a biosensing platform for rapid and sensitive ricin detection. Esteban-Fernández de Ávila et al. reported on a micro-motor sensing strategy for the fluorescent detection of ricin [118]. Self-propelled reduced graphene-oxide (rGO)/platinum (Pt) micromotors were synthesized and were modified with the ricin-specific aptamer tagged with a fluorescent dye. The resulting complex is non-fluorescent due to the quenching effect of the graphene surface. In the presence of the target toxin, the aptamer is displaced from the graphene-oxide quenching motor surface and its fluorescence is restored. By this method, real-time detection of trace amounts of ricin toxin could be achieved in biological and environmental samples. Li et al. further developed a detection system for ricin based on isothermal strand-displacement polymerase reaction [119]. The ricin-specific aptamer SSRA1 was first hybridized with a single stranded DNA blocker and then it was immobilized on the surface magnetic beads. When ricin binds to the aptamer, the blocker is released and it hybridizes to with a dye-modified hairpin probe triggering an isothermal strand-displacement polymerase reaction. The fluorescent double stranded DNA product cannot be quenched as it does not interact with the graphene oxide surface, resulting in an increase of the fluorescence intensity.

Scientific efforts have been made in the forensic field towards the development of new methods for the detection of chemical weapon agents with emphasis been placed on the real-time, on-site analysis of nerve agents (e.g. sarin). Zhao et al. developed a cantilever-based aptasensor for dimethyl methylphosphonate (DMMP), a nerve agent simulant [120]. The piezoresistive cantilever sensor was designed with four cantilevers (two sensing and two reference cantilevers). A biotinylated anti-DMMP aptamer was immobilized on the surface of the sensing cantilevers. In the presence of DMMP, binding takes place between the immobilised aptamers and the target; this results in a surface stress and a bending of the sensing cantilevers which can be recorded and measured. The method resulted in sensitive (50 nM–1.0 μM) and specific detection of DMMP in aqueous solutions.

#### 4.4. Explosives

The development of rapid, cost-effective and reliable assays for the detection of explosive molecules in both aqueous and gaseous samples is a high priority for forensic investigators, counter-terrorism agencies and global de-mining projects [121]. Ehrenreich-Förster et al. argue that aptamers are likely to make ideal recognition moieties for such assays, as immunological methods

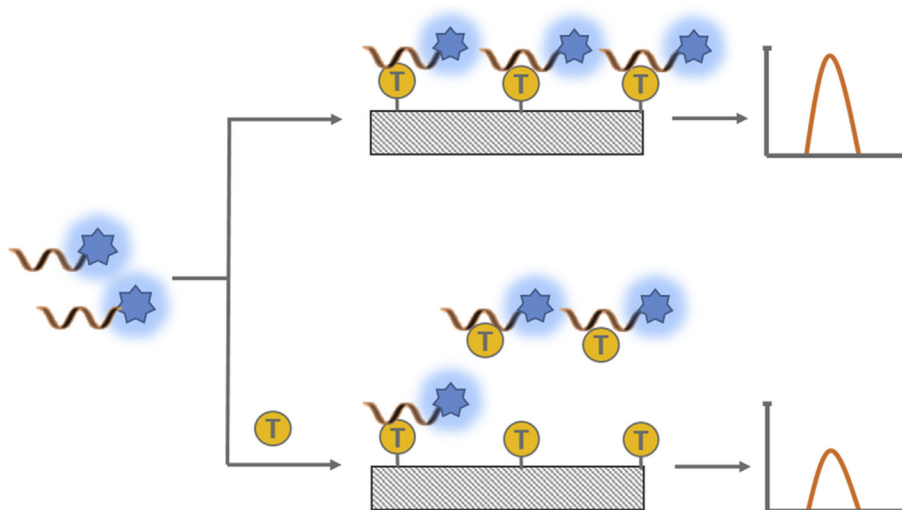


**Fig. 6.** Schema of an optical fibre-based aptasensor for the detection of TNT developed by Ehrentreich-Förster et al. [122]. Silanised optical fibres functionalized with TNT competitors are first embedded within the surface of a flow cell. Under normal conditions, a sample solution containing fluorescently labelled aptamers is introduced into the cell, which subsequently bind to the competitive analogues. Excitation by a laser at 480 nm allows the detection of aptamer presence on the fibre. However, a reduction in signal occurs when free TNT molecules present within the sample solution capture available aptamers, preventing interaction with the surface-attached analogues.

are often disadvantaged by the poor specificity of antibodies raised against low molecular weight explosive analytes [122]. Furthermore, aptamers are known to retain their activity in a number of organic solvents (such as methanol and acetonitrile) commonly used for the solubilisation and detection of explosive compounds.

To prove this concept the same group demonstrated the construction of an optical aptasensor towards the detection of 2,4,6-trinitrotoluene (TNT). In this sensing strategy, activated TNT derivatives are first immobilized on the surface of silanised optical fibres. TNT-specific aptamers mixed within sample solutions are then introduced into the flow cell and bind to the surface-bound analytes unless already captured by TNT present within the sample itself (Fig. 6). Nanobeads covalently attached to these aptamer sequences are then used to report the amount of ligands bound to the fibre (with emission intensities inversely proportional to the concentration of TNT present in measured samples).

Whilst aptasensing assays towards explosive targets other than TNT remain extremely limited, it is hoped that this review will encourage researchers in the field explosives research to consider their use for the detection for compounds such as hexahydro-1,3,5-trinitro-1,3,5-triazine (RDX).

## 5. Conclusions

Challenges associated with the immunological and instrumental analysis methods currently employed within both crime scene and laboratory-based testing procedures have resulted in the demand for new techniques able to allow the rapid, sensitive and specific detection of forensically relevant analytes. In this review, we have highlighted the potential of biosensing technology that incorporates aptamer recognition moieties to address this demand. Moreover, we have reported on a wide range of aptasensors that, although being successfully developed for use in other analytical disciplines, could be readily adapted to forensic analysis.

Whilst research in the development of aptasensors for forensic purposes is extremely limited, it is hoped that recent technological advances (e.g. NGS) will make aptamer-based sensor development more accessible to researchers working within the field of forensic science.

## References

- [1] T. Thompson, S. Black, *Forensic Human Identification: an Introduction*, CRC Press, 2006.
- [2] K. Virkler, I.K. Lednev, Analysis of body fluids for forensic purposes: from laboratory testing to non-destructive rapid confirmatory identification at a crime scene, *Forensic Sci. Int.* 188 (1–3) (2009) 1–17.
- [3] T. Hermann, D.J. Patel, Adaptive recognition by nucleic acid aptamers, *Science* 287 (5454) (2000) 820–825.
- [4] B. Strehlitz, et al., Aptamers for pharmaceuticals and their application in environmental analytics, *Bioanal. Rev.* 4 (1) (2012) 1–30.
- [5] M. McKeague, M.C. DeRosa, Challenges and opportunities for small molecule aptamer development, *J. Nucleic Acids* 2012 (2012) 1–20.
- [6] Z. Balogh, et al., Selection and versatile application of virus-specific aptamers, *FASEB J.* 24 (11) (2010) 4187–4195.
- [7] M. Jing, M.T. Bowser, Methods for measuring aptamer-protein equilibria: a review, *Anal. Chim. Acta* 686 (1) (2011) 9–18.
- [8] K.-T. Guo, et al., Cell-SELEX: novel perspectives of aptamer-based therapeutics, *Int. J. Mol. Sci.* 9 (4) (2008) 668–678.
- [9] A.B. Iliuk, L. Hu, W.A. Tao, Aptamer in bioanalytical applications, *Anal. Chem.* 83 (12) (2011) 4440–4452.
- [10] K.M. Song, S. Lee, C. Ban, Aptamers and their biological applications, *Sensors* 12 (1) (2012) 612–631.
- [11] H. Sun, Y. Zu, A highlight of recent advances in aptamer technology and its application, *Molecules* 20 (7) (2015) 11959–11980.
- [12] A.D. Keefe, S. Pai, A. Ellington, Aptamers as therapeutics, *Nat. Rev. Drug Discov.* 9 (7) (2010) 537–550.
- [13] M. Michaud, et al., A DNA aptamer as a new target-specific chiral selector for HPLC, *J. Am. Chem. Soc.* 125 (28) (2003) 8672–8679.
- [14] N. Hamaguchi, A. Ellington, M. Stanton, Aptamer beacons for the direct detection of proteins, *Anal. Biochem.* 294 (2) (2001) 126–131.
- [15] A.P. Turner, Biosensors: sense and sensibility, *Chem. Soc. Rev.* 42 (8) (2013) 3184–3196.
- [16] N. Frascione, J. Gooch, B. Daniel, Enabling fluorescent biosensors for the forensic identification of body fluids, *Analyst* 138 (24) (2013) 7279–7288.
- [17] P. Yáñez-Sedeño, et al., Biosensors in forensic analysis. A review, *Anal. Chim. Acta* 823 (2014) 1–19.
- [18] N. Frascione, et al., Fluorogenic displacement biosensors for PSA detection using antibody-functionalised quantum dot nanoparticles, *RSC Adv.* 5 (9) (2015) 6595–6598.
- [19] P. Hong, W. Li, J. Li, Applications of aptasensors in clinical diagnostics, *Sensors* 12 (2) (2012) 1181–1193.
- [20] E.J. Cho, J.W. Lee, A.D. Ellington, Applications of aptamers as sensors, *Annu. Rev. Anal. Chem.* 2 (2009) 241–264.
- [21] S.D. Mendonsa, M.T. Bowser, In vitro evolution of functional DNA using capillary electrophoresis, *J. Am. Chem. Soc.* 126 (1) (2004) 20–21.
- [22] R. Nutiu, Y. Li, In vitro selection of structure-switching signaling aptamers, *Angew. Chem. Int. Ed.* 44 (7) (2005) 1061–1065.
- [23] K.N. Morris, et al., High affinity ligands from in vitro selection: complex-targets, *Proc. Natl. Acad. Sci. U. S. A.* 95 (6) (1998) 2902–2907.



- [24] R. Stoltenburg, C. Reinemann, B. Strehlitz, FluMag-SELEX as an advantageous method for DNA aptamer selection, *Anal. Bioanal. Chem.* 383 (1) (2005) 83–91.
- [25] J.-W. Park, et al., Immobilization-free screening of aptamers assisted by graphene oxide, *Chem. Commun.* 48 (15) (2012) 2071–2073.
- [26] Y. Chushak, M.O. Stone, In silico selection of RNA aptamers, *Nucleic Acids Res.* 37 (12) (2009) e87.
- [27] X. Lou, et al., Micromagnetic selection of aptamers in microfluidic channels, *Proc. Natl. Acad. Sci. U. S. A.* 106 (9) (2009) 2989–2994.
- [28] A. Nitsche, et al., One-step selection of Vaccinia virus-binding DNA aptamers by MonoLEX, *BMC Biotechnol.* 7 (1) (2007) 1–12.
- [29] L. Peng, et al., A combined atomic force/fluorescence microscopy technique to select aptamers in a single cycle from a small pool of random oligonucleotides, *Microsc. Res. Tech.* 70 (4) (2007) 372–381.
- [30] J.G. Bruno, Predicting the uncertain future of aptamer-based diagnostics and therapeutics, *Molecules* 20 (4) (2015) 6866–6887.
- [31] C. Tuerk, L. Gold, Systematic evolution of ligands by exponential enrichment: RNA ligands to bacteriophage T4 DNA polymerase, *Science* 249 (4968) (1990) 505–510.
- [32] A.D. Ellington, J.W. Szostak, In vitro selection of RNA molecules that bind specific ligands, *Nature* 346 (6287) (1990) 818–822.
- [33] R. Stoltenburg, C. Reinemann, B. Strehlitz, SELEX—a (r) evolutionary method to generate high-affinity nucleic acid ligands, *Biomol. Eng.* 24 (4) (2007) 381–403.
- [34] S.C.B. Gopinath, Methods developed for SELEX, *Anal. Bioanal. Chem.* 387 (1) (2007) 171–182.
- [35] A. Ruscito, M.C. DeRosa, Small-molecule binding aptamers: selection strategies, characterization, and applications, *Front. Chem.* 4 (14) (2016) 1–14.
- [36] R. Stoltenburg, N. Nikolaus, B. Strehlitz, Capture-SELEX: selection of DNA aptamers for aminoglycoside antibiotics, *J. Anal. Methods Chem.* 2012 (2012) 1–14.
- [37] J.A. Martin, et al., A Method for selecting structure-switching aptamers Applied to a colorimetric gold nanoparticle assay, *J. Vis. Exp.* (96) (2015) e52545.
- [38] V.-T. Nguyen, et al., Multiple GO-SELEX for efficient screening of flexible aptamers, *Chem. Commun.* 50 (72) (2014) 10513–10516.
- [39] Y. Kim, C. Liu, W. Tan, Aptamers generated by Cell SELEX for biomarker discovery, *Biomarkers Med.* 3 (2) (2009) 193–202.
- [40] K. Sefah, et al., Development of DNA aptamers using Cell-SELEX, *Nat. Protoc.* 5 (6) (2010) 1169–1185.
- [41] S. Ohuchi, Cell-SELEX technology, *Biores. Open Access* 1 (6) (2012) 265–272.
- [42] E. Katilius, et al., Sperm Capture Using Aptamer Based Technology, 2014.
- [43] A. Ozer, J.M. Pagano, J.T. Lis, New technologies provide quantum changes in the scale, speed, and success of SELEX methods and aptamer characterization, *Mol. Ther. Nucleic Acids* 3 (2014) e183.
- [44] R.C. Conrad, S. Baskerville, A.D. Ellington, In vitro selection methodologies to probe RNA function and structure, *Mol. Divers.* 1 (1) (1995) 69–78.
- [45] M. Yüce, N. Ullah, H. Budak, Trends in aptamer selection methods and applications, *Analyst* 140 (16) (2015) 5379–5399.
- [46] M. Blind, M. Blank, Aptamer selection technology and recent advances, *Mol. Ther. Nucleic Acids* 4 (2015) e223.
- [47] K.R. Riley, et al., Combining capillary electrophoresis and next-generation sequencing for aptamer selection, *Anal. Bioanal. Chem.* 407 (6) (2015) 1527–1532.
- [48] T. Schütze, et al., Probing the SELEX process with next-generation sequencing, *PLoS One* 6 (12) (2011) e29604.
- [49] M. Cho, et al., Quantitative selection of DNA aptamers through microfluidic selection and high-throughput sequencing, *Proc. Natl. Acad. Sci. U. S. A.* 107 (35) (2010) 15373–15378.
- [50] D. Van Simaey, et al., Study of the molecular recognition of aptamers selected through ovarian cancer Cell-SELEX, *PLoS One* 5 (11) (2010) e13770.
- [51] R. Wilson, et al., Single-step selection of bivalent aptamers validated by comparison with SELEX using high-throughput sequencing, *PLoS One* 9 (6) (2014) e100572.
- [52] L.A. Bawazer, et al., Efficient selection of biomineralizing DNA aptamers using deep sequencing and population clustering, *ACS Nano* 8 (1) (2014) 387–395.
- [53] C. Børsting, N. Morling, Next generation sequencing and its applications in forensic genetics, *Forensic Sci. Int. Genet.* 18 (2015) 78–89.
- [54] W.H. Thiel, P.H. Giangrande, Analyzing HT-SELEX data with the Galaxy project tools – a web based bioinformatics platform for biomedical research, *Methods* 97 (2016) 3–10.
- [55] M. Martin, Cutadapt removes adapter sequences from high-throughput sequencing reads, *EMBnet. J.* 17 (1) (2011) 10–12.
- [56] J. Hoinka, et al., Large scale analysis of the mutational landscape in HT-SELEX improves aptamer discovery, *Nucleic Acids Res.* 43 (12) (2015) 5699–5707.
- [57] K.K. Alam, J.L. Chang, D.H. Burke, FASTAptamer: a bioinformatic toolkit for high-throughput sequence analysis of combinatorial selections, *Mol. Ther. Nucleic Acids* 4 (3) (2015) e230.
- [58] J. Caroli, et al., APTANI: a computational tool to select aptamers through sequence-structure motif analysis of HT-SELEX data, *Bioinformatics* 32 (2) (2015) 161–164.
- [59] M. Jo, et al., Development of single-stranded DNA Aptamers for specific bisphenol A detection, *Oligonucleotides* 21 (2) (2011) 85–91.
- [60] A.L. Chang, et al., Kinetic and equilibrium binding characterization of aptamers to small molecules using a label-free, sensitive, and scalable platform, *Anal. Chem.* 86 (7) (2014) 3273–3278.
- [61] M. Sassanfar, J.W. Szostak, An RNA motif that binds ATP, *Nature* 364 (6437) (1993) 550–553.
- [62] J.R. Lorsch, J.W. Szostak, In vitro selection of RNA aptamers specific for cyanocobalamin, *Biochemistry* 33 (4) (1994) 973–982.
- [63] M. Fried, D.M. Crothers, Equilibria and kinetics of lac repressor-operator interactions by polyacrylamide gel electrophoresis, *Nucleic Acids Res.* 9 (23) (1981) 6505–6525.
- [64] B. Hall, et al., In vitro selection of RNA aptamers to a protein target by filter immobilization, *Curr. Protoc. Mol. Biol.* 24 (2009) 1–24.
- [65] I.R. Olmsted, et al., Measurement of aptamer-protein interactions with back-scattering interferometry, *Anal. Chem.* 83 (23) (2011) 8867–8870.
- [66] S. Nagatoishi, Y. Tanaka, K. Tsumoto, Circular dichroism spectra demonstrate formation of the thrombin-binding DNA aptamer G-quadruplex under stabilizing-cation-deficient conditions, *Biochem. Biophys. Res. Commun.* 352 (3) (2007) 812–817.
- [67] C. Baugh, D. Grate, C. Wilson, 2.8 Å crystal structure of the malachite green aptamer, *J. Mol. Biol.* 301 (1) (2000) 117–128.
- [68] J.A. Cruz-Aguado, G. Penner, Fluorescence polarization based displacement assay for the determination of small molecules with aptamers, *Anal. Chem.* 80 (22) (2008) 8853–8855.
- [69] T. Hianik, et al., Influence of ionic strength, pH and aptamer configuration for binding affinity to thrombin, *Bioelectrochemistry* 70 (1) (2007) 127–133.
- [70] A.L. Chang, M. McKeague, C.D. Smolke, Facile characterization of aptamer kinetic and equilibrium binding properties using surface plasmon resonance, *Methods Enzymol.* 549 (2014) 451–466.
- [71] K.D. Connaghan-Jones, A.D. Moody, D.L. Bain, Quantitative DNase footprint titration: a tool for analyzing the energetics of protein–DNA interactions, *Nat. Protoc.* 3 (5) (2008) 900–914.
- [72] J.E. Sokolowski, S.E. Dombrowski, P.C. Bevilacqua, Thermodynamics of ligand binding to a heterogeneous RNA population in the malachite green aptamer, *Biochemistry* 51 (1) (2012) 565–572.
- [73] M.A.D. Neves, et al., Defining the secondary structural requirements of a cocaine-binding aptamer by a thermodynamic and mutation study, *Biophys. Chem.* 153 (1) (2010) 9–16.
- [74] Y.S. Kwon, et al., Detection of Iprufenos and Edifenphos using a new multi-aptasensor, *Anal. Chim. Acta* 868 (2015) 60–66.
- [75] A. Velázquez-Campoy, et al., Isothermal Titration Calorimetry, in *Current Protocols in Cell Biology*, John Wiley & Sons, Inc, 2001.
- [76] F. Kleinjung, et al., High-affinity RNA as a recognition element in a biosensor, *Anal. Chem.* 70 (2) (1998) 328–331.
- [77] T. Hianik, J. Wang, Electrochemical aptasensors—recent achievements and perspectives, *Electroanalysis* 21 (11) (2009) 1223–1235.
- [78] C. Feng, S. Dai, L. Wang, Optical aptasensors for quantitative detection of small biomolecules: a review, *Biosens. Bioelectron.* 59 (2014) 64–74.
- [79] S. Song, et al., Aptamer-based biosensors, *Trends Anal. Chem. Trac.* 27 (2) (2008) 108–117.
- [80] Y.S. Kim, M.B. Gu, *Advances in Aptamer Screening and Small Molecule Aptasensors, in Biosensors Based on Aptamers and Enzymes*, Springer, 2013, pp. 29–67.
- [81] Z. Tang, et al., Aptamer switch probe based on intramolecular displacement, *J. Am. Chem. Soc.* 130 (34) (2008) 11268–11269.
- [82] F. Long, A. Zhu, H. Shi, Recent advances in optical biosensors for environmental monitoring and early warning, *Sensors* 13 (10) (2013) 13928–13948.
- [83] K. Li, et al., Nanoplasmonic imaging of latent fingerprints and identification of cocaine, *Angew. Chem. Int. Ed.* 52 (44) (2013) 11542–11545.
- [84] A. Hayat, J.L. Marty, Aptamer based electrochemical sensors for emerging environmental pollutants, *Front. Chem.* 2 (41) (2014) 1–9.
- [85] E. Torres-Chavolla, E.C. Alocilja, Aptasensors for detection of microbial and viral pathogens, *Biosens. Bioelectron.* 24 (11) (2009) 3175–3182.
- [86] J.A. Hansen, et al., Quantum-Dot/aptamer-based ultrasensitive multi-analyte electrochemical biosensor, *J. Am. Chem. Soc.* 128 (7) (2006) 2228–2229.
- [87] A. Sassolas, L.J. Blum, B.D. Leca-Bouvier, Electrochemical aptasensors, *Electroanalysis* 21 (11) (2009) 1237–1250.
- [88] K. Han, Z. Liang, N. Zhou, Design strategies for aptamer-based biosensors, *Sensors* 10 (5) (2010) 4541–4557.
- [89] D. Grieshaber, et al., Electrochemical biosensors – sensor principles and architectures, *Sensors* 8 (3) (2008) 1400–1458.
- [90] B.R. Baker, et al., An electronic, aptamer-based small-molecule sensor for the rapid, label-free detection of cocaine in adulterated samples and biological fluids, *J. Am. Chem. Soc.* 128 (10) (2006) 3138–3139.
- [91] C.-H. Weng, C.-J. Huang, G.-B. Lee, Screening of aptamers on microfluidic systems for clinical applications, *Sensors* 12 (7) (2012) 9514–9529.
- [92] S.C. Gopinath, Biosensing applications of surface plasmon resonance-based Biacore technology, *Sens. Actuator B Chem.* 150 (2) (2010) 722–733.
- [93] P. Schuck, Use of surface plasmon resonance to probe the equilibrium and dynamic aspects of interactions between biological macromolecules, *Annu. Rev. Biophys.* 26 (1) (1997) 541–566.
- [94] M.V. Voinova, On mass loading and dissipation measured with acoustic wave sensors: a review, *J. Sensors* 2009 (2009) 1–13.
- [95] R. Datar, et al., Cantilever sensors: nanomechanical tools for diagnostics, *MRS Bull.* 34 (06) (2009) 449–454.

- [96] W. Mok, Y. Li, Recent progress in nucleic acid aptamer-based biosensors and bioassays, *Sensors* 8 (11) (2008) 7050–7084.
- [97] H. Hou, et al., Aptamer-based cantilever array Sensors for oxytetracycline detection, *Anal. Chem.* 85 (4) (2013) 2010–2014.
- [98] S.K. Vashist, A review of microcantilevers for sensing applications, *J. Nanotechnol.* 3 (2007) 1–15.
- [99] M. Wood, et al., Selective targeting of fingerprints using immunogenic techniques, *Aust. J. Forensic Sci.* 45 (2) (2013) 211–226.
- [100] R. Thorogate, et al., A novel fluorescence-based method in forensic science for the detection of blood in situ, *Forensic Sci. Int. Genet.* 2 (4) (2008) 363–371.
- [101] Y. Wang, et al., Aptamer biosensor based on fluorescence resonance energy transfer from upconverting phosphors to carbon nanoparticles for thrombin detection in human plasma, *Anal. Chem.* 83 (21) (2011) 8130–8137.
- [102] R.-M. Kong, et al., A novel aptamer-functionalized MoS<sub>2</sub> nanosheet fluorescent biosensor for sensitive detection of prostate specific antigen, *Anal. Bioanal. Chem.* 407 (2) (2015) 369–377.
- [103] B. Deng, et al., Aptamer binding assays for proteins: the thrombin – example-a review, *Anal. Chim. Acta* 837 (2014) 1–15.
- [104] F. Smith, *Handbook of Forensic Drug Analysis*, Academic Press, 2004.
- [105] M. Yarbakt, M. Nikkhah, Unmodified gold nanoparticles as a colorimetric probe for visual methamphetamine detection, *J. Exp. Nanosci.* 11 (7) (2016) 593–601.
- [106] M.N. Stojanovic, P. de Prada, D.W. Landry, Aptamer-based folding fluorescent sensor for cocaine, *J. Am. Chem. Soc.* 123 (21) (2001) 4928–4931.
- [107] J.P. Hilton, et al., A microfluidic affinity sensor for the detection of cocaine, *Sens. Actuator B-Chem.* 166 (2) (2011) 241–246.
- [108] L. Huang, et al., A label-free electrochemical biosensor based on a DNA aptamer against codeine, *Anal. Chim. Acta* 787 (2013) 203–210.
- [109] A. Cunningham, European Monitoring Centre for Drugs and Drug Addiction: New Psychoactive Substances in Europe: an Update from the EU Early Warning System, 2015. Available from: <http://www.emcdda.europa.eu/system/files/publications/65/TD0415135ENN.pdf>.
- [110] C. Bell, et al., Development of a rapid LC-MS/MS method for direct urinalysis of designer drugs, *Drug Test. Anal.* 3 (7–8) (2011) 496–504.
- [111] V. Thiviyanathan, D.G. Gorenstein, Aptamers and the next generation of diagnostic reagents, *Proteomics Clin. Appl.* 6 (0) (2012) 563–573.
- [112] M.L. Smith, et al., Modern instrumental methods in forensic toxicology, *J. Anal. Toxicol.* 31 (5) (2007) 237–239.
- [113] L. Sheng, et al., PVP-coated graphene oxide for selective determination of ochratoxin A via quenching fluorescence of free aptamer, *Biosens. Bioelectron.* 26 (8) (2011) 3494–3499.
- [114] G. Cooper, A. Negrusz, *Clarke's Analytical Forensic Toxicology*, Pharmaceutical Press, 2013.
- [115] T.H. Ha, Recent advances for the detection of ochratoxin a, *Toxins* 7 (12) (2015) 5276–5300.
- [116] Y. Wu, et al., Ultrasensitive aptamer biosensor for arsenic (III) detection in aqueous solution based on surfactant-induced aggregation of gold nanoparticles, *Analyst* 137 (18) (2012) 4171–4178.
- [117] E.A. Lamont, et al., A single DNA aptamer functions as a biosensor for ricin, *Analyst* 136 (19) (2011) 3884–3895.
- [118] B. Esteban-Fernández de Ávila, et al., Aptamer-modified graphene-based catalytic micromotors: off-on fluorescent detection of ricin, *ACS Sens.* 1 (3) (2016) 217–221.
- [119] C.H. Li, et al., A graphene oxide-based strand displacement amplification platform for ricin detection using aptamer as recognition element, *Biosens. Bioelectron.* 91 (2017) 149–154.
- [120] R. Zhao, et al., Cantilever-based aptasensor for trace level detection of nerve agent simulant in aqueous matrices, *Sens. Actuators B Chem.* 238 (2017) 1231–1239.
- [121] S. Singh, Sensors—an effective approach for the detection of explosives, *J. Hazard Mater.* 144 (1–2) (2007) 15–28.
- [122] E. Ehrentreich-Förster, et al., Biosensor-based on-site explosives detection using aptamers as recognition elements, *Anal. Bioanal. Chem.* 391 (5) (2008) 1793–1800.



## Taggant materials in forensic science: A review

James Gooch<sup>a</sup>, Barbara Daniel<sup>a</sup>, Vincenzo Abbate<sup>b</sup>, Nunzianda Frascione<sup>a,\*</sup>

<sup>a</sup> Analytical and Environmental Sciences Division, King's College London, 150 Stamford Street, London SE1 9NH, UK

<sup>b</sup> Institute of Pharmaceutical Science, King's College London, 150 Stamford Street, London SE1 9NH, UK



### ARTICLE INFO

#### Keywords:

Taggant  
Forensic  
Identification  
Security  
Fluorescence  
DNA  
Peptide  
Mass Spectrometry

### ABSTRACT

The use of taggant technology to mark objects for the purpose of identification is becoming a significant part of national crime reduction strategies. Taggants may be able to prevent or monitor criminal offences by associating an object with a specific piece of information. While the material properties of a taggant will largely vary between application purposes, a specific 'coding' element will generally be incorporated to infer marker uniqueness. With the speed, simplicity and accuracy of coding component analysis largely determining the overall efficacy of taggants, continuing advances in portable in-field analysis, nanotechnology and material science should have allowed for the development of new and improved forensic marking agents. However, the limited amount of recent research in this area suggests that this is not the case. This critical review therefore examines the current state of presently available taggants before attempting to offer insight into the future direction of forensic marking technology.

© 2016 Elsevier B.V. All rights reserved.

### Contents

1. Introduction .....	49
2. Current technology .....	50
2.1. Physical taggants .....	50
2.2. Spectroscopic taggants .....	51
2.3. Chemical taggants .....	52
2.4. DNA taggants .....	52
3. Future perspectives .....	52
4. Conclusions .....	53
References .....	53

### 1. Introduction

Costing approximately £24 billion a year, the social and economic effect of organised criminal activity in the UK is substantial. Offences related to the trafficking of illicit drugs (£10.7 billion), organised fraud (£8.9 billion) and acquisitive crime (£1.8 billion) are reported to be the largest sources of criminal revenue [1]. With actual costs likely to be even greater (as such estimates are only based on data from recorded crimes), developing strategies that are able to prevent or aid in the investigation of these offences is a significant priority of the forensic science community.

Among the number of products made commercially available for the purpose of reducing criminal activity, forensic taggants may be seen as one of the most successfully employed. Taggant materials

have been widely accepted for use as evidence within the UK court system since 2008, with certain marking agents having aided in the conviction of over one thousand criminal offenders since that time. Based on statistics published by the Metropolitan Police Service, household burglary across London was decreased by nearly 30% in areas where forensic taggants were applied (i.e. SmartWater®). Taggants are a class of materials that can be applied to or incorporated within an object in order to make it identifiable [2]. This is achieved by producing each 'batch' of taggant in an entirely unique formulation, allowing the particular molecular composition to be registered against a specific piece of information. Once recovered at a later date, this composition can be analysed in order to reveal the identity of the taggant and thus, the object it is marking [3].

A forensic taggant displaying entirely ideal characteristics should be of low cost to produce, have high coding capacity, be non-toxic to individuals and the surrounding environment, be simplistic and inexpensive to detect and analyse via non-destructive means and be of a complex enough nature to prevent duplication. The

\* Corresponding author. Tel.: +44 20 7848 4978.

E-mail address: [nunzianda.frascione@kcl.ac.uk](mailto:nunzianda.frascione@kcl.ac.uk) (N. Frascione).



Fig. 1. The four main applications utilising forensic taggants.

majority of taggant manufacturers claim that their products are versatile enough to be applied in a broad range of circumstances. However, forensic marking materials are most extensively utilised for four distinct purposes (Fig. 1):

- **Property marking** – Taggants may be applied upon valuable items such as vehicles and electronics in order to associate them with a specific owner. If that property becomes subject to theft but is later recovered, it may be returned to the original purchaser [4, 5]. Property taggants are usually invisible to the naked eye in order to prevent spoiling the item's aesthetic or to avoid detection by offenders.
- **Anti-counterfeiting** – Industries at risk of counterfeiting activities (pharmaceuticals, clothing, currency, etc.) may choose to incorporate taggants into their products to distinguish them from potential forgeries [6]. Marking agents used for this application are typically non-visible and have replaced traditional barcoding and hologram anti-counterfeit technologies, which are more easily duplicated [7].
- **Tracking** – Materials used in the manufacture of hazardous or potentially illegal products may be tagged by law enforcement agencies to aid detection or track initial origin. Such marking agents are predominantly applied during the production of industrial explosives that are susceptible to illicit use [8]. Robust taggants able to survive detonation may be detected to reveal information regarding type of explosive, supplier or batch ID. Taggants may also be covertly added to bulk volumes of illegal narcotics, allowing their distribution to be monitored [9].
- **Monitoring** – Taggants may be placed on exterior surfaces of houses, commercial properties or objects of value. As a result of criminal activity (such as trespassing or out-of-hours burglary), these taggants may be transferred to an individual, providing strong physical evidence to associate them with that offence [10]. Additional information of the suspect's subsequent activity can also be gained if the taggant undergoes a secondary object-to-person-to-object transfer.

The physical characteristics of a taggant will depend largely upon which of these four purposes it is being used for (Fig. 2). For example, markers utilised to stain currency stolen during a CViT (Cash-and-valuables-in-transit) robbery should remain permanent after application and should not be easily removed [5]. Conversely, a forensic coating applied to firearms and cartridge casings in an attempt to establish handling, should be designed to be as transferrable as possible [11]. The range of taggant formulations is therefore extensive. Markers may be dispersed within a medium such as grease,

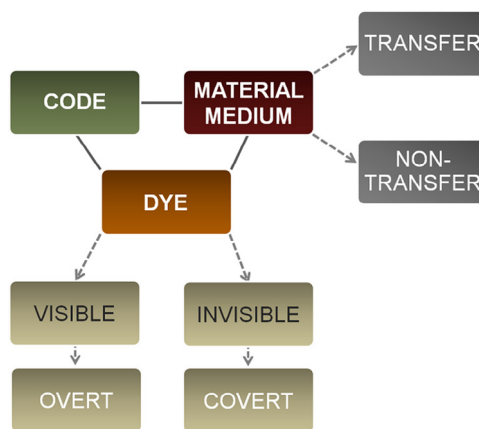


Fig. 2. Forensic taggants may include different components (i.e. code, dye and material/medium), which can determine its physical characteristics.

paint or ink, sprayed via aerosol, applied directly as a powder or embedded into materials during manufacturing processes [12].

Taggants designed to be covertly applied (in order to avoid destruction or discovery by offenders) may also include an additional component to allow detection at a later time point. Being invisible to the naked eye, these taggants require localization in order to be successfully recovered for analysis. This is most often achieved by adding fluorescent compounds to the taggant, which will then emit light when excited at certain wavelengths of the UV or visible spectrum [13]. Other detection methods involve the inclusion of volatile chemicals for vapour identification [14] or radioactive isotopes [3].

While these detection constituents may not always be required within a taggant, all forensic markers will include a main 'coding' element in order to infer a required statistical uniqueness. By creating a formulation that is unable to be duplicated, a taggant may effectively 'store' information regarding the object it is marking [13].

As the success of a taggant will be largely influenced by the ability of this code to be recovered and analysed, all marker coding methods produced within the UK are subject to validation by the British Standards Institution (BSI) under Publicly Available Specification 820:2012 (PAS 820:2012). In this process, taggants are exposed to a number of accelerated UV light, temperature and humidity conditions in order to simulate the longevity of coding materials within a variety of circumstances.

Despite the extensive commercialisation of taggant technology (Table 1), detailed information regarding the synthesis and manufacturing procedures of such marking agents is extremely limited within academic literature. Whilst publishing such protocols within the public domain may result in a decrease in taggant efficiency (by allowing offenders to become familiar with such materials), it is still pertinent to conduct a thorough exploration into the different encoding methods used in commercially established forensic marking agents (Fig. 3). This critical review therefore attempts to examine these coding mechanisms, as well as explore recent research that may indicate how forensic taggant technology is likely to progress within the near future.

## 2. Current technology

### 2.1. Physical taggants

Renowned for being one of the earliest existing forensic marking materials; physical taggants possess coding systems that are based on the simple morphological properties of their components. These



**Table 1**  
Commercially available forensic taggants

Coding Type	Manufacturers	Taggants Produced	Analysis Method	Uses
Physical	Alpha•Dot	Alpha•Dot [15]	Optical microscopy	Property marking, vehicle marking
	DataDot	DataDots® [16]	Optical microscopy	Property marking, anti-counterfeiting
Spectroscopic	Microtrace	Microtaggant® [17]	Optical microscopy	Anti-counterfeiting, explosives detection
	DNA Technologies	SmartDye™ [18]	Spectrofluorometry	Anti-counterfeiting
	Luminex	MagPlex® spheres [19]	Flow Cytometry	Anti-counterfeiting, biological labeling
	Microtrace	Spectral Taggant™ [20]	Spectrofluorometry	Currency marking, security printing
Chemical	Spectra Systems	SpectraFluor™ [21]	Spectrofluorometry	Currency marking, product tracking
	Authentix	Authentix [22]	Immunoassay, GC-MS	Fuel Adulteration, anti-counterfeiting
	SmartWater	SmartWater® [4]	LA-ICP-MS	Property Marking, activity monitoring
	Polysecure	Brandproof® [23]	XRF spectroscopy	Anti-counterfeiting
DNA	Applied DNA Sciences	SigNature® [24]	DNA sequencing	Property marking, anti-counterfeiting, CViT
	DataDot	dDotDNA® [25]	DNA sizing analysis	Property marking, anti-counterfeiting
	DNA Technologies	DNA Matrix™ [26]	DNA sequencing	Anti-counterfeiting
	SelectaMark	SelectaDNA® [27]	DNA sequencing	Property marking, activity monitoring
	TraceTag	CypherMark™ [28]	DNA sequencing	Property marking, anti-counterfeiting

taggants are generally made unique by exploiting solid particles of a specific size, appearance or structural arrangement [29]. Such encoding mechanisms may also be described as ‘graphical’, as analysis is usually achieved by basic visual methods such as low-power microscopy [13].

One coding element commonly used in physical taggants is the microdot, a small polymer disc between 2–1000 µm in size containing minute photographic information. Text or images etched onto microdots are usually too small to be observed by the naked eye alone but may be revealed upon optical magnification [30]. Although initially developed as a covert means of transferring data during World War II, companies such as DataDot and Microtrace have taken advantage of microdot technology by including them in a number of ink and varnish based suspensions [3]. The dots within these suspensions are then able to act as simplistic tagging mechanisms by being imprinted with a unique numeric code, which is then registered against a particular owner on an electronic database [16].

Another physical tagging approach pioneered in the 1970’s by the US company 3M, focuses on the use of small plastic particles, constructed using a number of different proprietary coloured materials. These materials are combined in a sequence of layers, the order of which will be specific to each formulation of taggant produced [17]. A visual inspection of the layers is then reveals the identity of the marker and the batch from which it originated. The robust nature of the materials used in layer construction has resulted in these particles becoming a predominant tagging agent for the identification of post-detonation explosive materials [31].

However, in a number of circumstances the utilisation of physical type taggants may be considered disadvantageous. Marking agents based on graphical identification strategies will generally have very little ‘space’ in which coding can take place [2]. This consequently limits the amount of statistically unique particles (and thus

taggant formulations) that may be produced. Applications such as property marking, which necessitate a continuous stream of distinct codes, may benefit better from the use of molecular-based tagging agents, which have a higher coding capacity. Other drawbacks include the easy observability of physical taggants due to the relatively large size of incorporated solid particles, limiting their use within covert situations [12].

## 2.2. Spectroscopic taggants

In spectroscopic taggants, a number of molecules possessing differing optical qualities are combined together to create a single mixture with a spectrally unique signature. These taggants utilise multi-component encoding strategies, achieving their individuality from a precise combination of different emission wavelengths or intensities [13]. However, in certain taggant designs, these optically distinct molecules may be enclosed together within solid particles (to increase taggant stability or simplify analysis) and may thus be described as single-component systems [32]. Determining the identity of these marking agents is usually performed via the analysis of overall emission signature by simple spectrophotometry techniques.

The materials most often utilised within spectroscopic taggants are simple non-toxic organic dyes that fluoresce in different regions of the visible spectrum [33]. Companies such as Luminex and Spectra Systems manufacture a number of marking agents based on the integration of several cyanine, phthalocyanine or squaraine-based fluorophores [19, 21]. The low cost and wide availability of organic dyes ensures that the production of spectroscopic markers remains inexpensive, but may also result in the illegal reproduction of taggants themselves if fluorophores are recognised and acquired by counterfeiters [7]. Organic dyes are also disadvantaged by broad spectral emission overlaps, short fluorescence lifetimes and sensitivity to photobleaching [12].

Industrial and academic research has attempted to overcome these challenges by developing spectroscopic taggants that include more sophisticated optical components. Guillo *et al.* recently reported the development and commercialisation of a large array of spectroscopic coding materials based on non-toxic lanthanide ion complexes [34]. The unique temporal and spectral characteristics associated with these complexes are considered extremely difficult to duplicate by materials available to forgers, which may significantly deter potential attempts at taggant duplication. The narrow emission bands of rare-earth materials may also serve to increase the discriminatory power of a taggant by allowing more optically distinct components to be added to a marker without spectral overlap [13]. As the number of existing lanthanide elements is

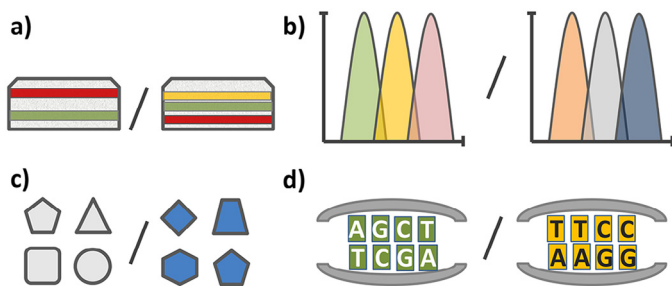


**Fig. 3.** Code uniqueness provided by differences in: a) physical characteristics (i.e. multiple coloured layer particles); b) optical spectra; c) chemical composition; d) DNA sequences.

limited, varying the emission intensity ratios as well as the wavelengths of rare-earth materials is often used to further increase this statistical discrimination.

### 2.3. Chemical taggants

Much like spectroscopic markers, inorganic taggants rely on a multiplex of molecules within a specific combination to infer identity. However, instead of optical signature detection, chemical encoding is achieved from a fixed set of trace materials, which may be either present or absent from a mixture [35]. Each of these materials is tested for on an individual basis, essentially creating a form of 'binary string' data in which each position of the string represents a different compound. The presence of a particular trace may be indicated by a "1" in that position of the string, whilst its absence may be denoted by a "0" [36]. Taggant identity is determined by the comparison of binary sequence data generated from trace analysis with a list of strings registered on a database.

The UK's largest manufacturer of forensic marking technology SmartWater, bases the majority of their commercially available reagents on this premise. In these taggants rare-earth lanthanides are also utilised but are identified by their individual mass through laser ablation inductively coupled plasma mass spectrometry (LA-ICP-MS) rather than fluorescence emission [4]. A method of using isotopic materials as chemical encoding components for the authentication of fuels, consumer products and agrochemicals has also been developed by U.S. firm Authentix. These trace elements usually consist of deuterated organic or inorganic compounds that are then detected by either gas-chromatography mass spectrometry (GC-MS) or multiplex immunoassay systems [22, 37]. The increased sensitivity of chemical analysis methods over spectroscopic techniques allows coding materials to be included at much lower quantities (as little as parts per billion) than other taggant types. This in turn prevents the physical properties of a marker from being altered (unlike those containing large insoluble particles, which may appear more 'granular' in nature) and may thus lower the risk of unwanted detection.

Once again, these taggant classes are not without limitations. Binary string data can be compromised if one or more components within a mixture is removed or destroyed, or if extraneous material are added (for example, by accidental mixing of two different taggant formulations) [35]. Chemical multi-component encoding may also not be compatible with highly transferrable marking agents as the different underlying chemical structures of tracing elements may cause them to be transferred at dissimilar rates, leading to incomplete recovery and subsequent erroneous identification.

### 2.4. DNA taggants

Discovered in the early 1950's as the foundation of information storage for all known life forms, the immense coding ability of deoxyribonucleic acid (DNA) has been recognised for a considerably long period [38]. Since that time, a range of methods have been developed for the storage of non-genetic data within DNA molecules [13]. As a result, manufacturers such as Selectamark Security Systems [27], TraceTag [28] and Applied DNA Sciences [24] now produce forensic marking agents that can infer identity via the use of unique oligonucleotide sequences. Such sequences may be naturally occurring, entirely synthetic or a combination of both (e.g. botanical DNA shuffled into a random arrangement) [39]. The order of single nucleotide units comprising a sequence will be individual to each formulation of taggant produced, allowing separate batches to be distinguished.

The benefits of near-unlimited coding capacity, straightforward synthesis and low toxicity of genetic material have ensured

that DNA taggants are one of the most prevalent forms of forensic marking agents commercially available. However, challenges regarding the application of DNA-based tagging approaches are twofold. Sequencing techniques employed for the analysis of oligonucleotides are typically more cost, reagent and labour-intensive than methods used to identify other types of taggant coding components [40]. As the genetic material recovered from a taggant also requires amplification by the polymerase chain reaction (PCR) prior to testing, this method of analysis can be especially expensive [2].

Furthermore, DNA is a relatively sensitive molecule and can degrade under the normal temperature, oxidation, radiation and chemical and enzymatic activity levels associated with ambient environmental conditions [41, 42]. While DNA damages caused by these stresses may be repaired by a number of processes within living organisms, the same cannot be said of the synthetic oligonucleotides included within forensic taggants. Concerns have therefore been raised over the general stability of DNA-based tagging materials and the subsequent compromise of genetic coding sequences [2, 13, 43]. However, encapsulation of nucleotides within silica microbeads [44] or plant materials [45] may be carried out in order to protect against this potential degradation.

## 3. Future perspectives

Each of the commercially available taggant mechanisms included within this review displays a distinct set of strengths and weaknesses, either in terms of coding capacity, covert usage, overall stability or method of analysis (Table 2). These disadvantages currently prevent a single taggant type from being used as a universal product identification system, necessitating the application of separate marking methods for different purposes [3]. However, it must also be noted that major practical innovations in the fields of nanotechnology, material science and analytical instrument portability have occurred since the scientific technologies behind these coding mechanisms were established. These advances are now being exploited by a number of research groups in an attempt to develop forensic tagging reagents that can identify any object, regardless of situation or circumstance.

Much of the research surrounding the design of globally applicable marking systems has focused on the use of nanomaterial-based encoding strategies. Nanoscale particles, wires and tubes all show great potential as next generation tagging mechanisms due to their small size (preventing detection and the physical alteration of marker properties), range of potential analysis methods and ease of formulation within traditional marking reagent media [12].

Semi-conductive quantum dot nanoparticles are currently being utilised to create spectroscopic taggants with optical qualities superior to those employing organic dyes or lanthanide ion complexes [46]. With narrow emission wavelengths, colour-tuneable signals and environmental-independent fluorescence properties, quantum dots may represent an excellent opportunity to improve the multi-component spectral encoding mechanisms presently utilised by

**Table 2**

Summary of the advantages and disadvantages of commercially available forensic taggants

Coding Type	Advantages	Disadvantages
Physical	Simplistic analysis Inexpensive	Limited coding capacity Less covert
Spectroscopic	Simplistic analysis Inexpensive	Subject to counterfeiting Limited coding capacity
Chemical	Analysis sensitivity More covert	Prone to misidentification Incomplete recovery
DNA	High coding capacity Low toxicity	Expensive analysis Possible degradation

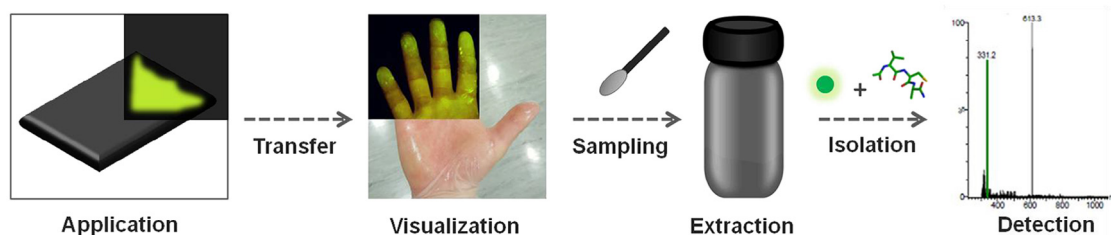


Fig. 4. Schematic of peptide-based taggant application and analysis. Adapted from [56].

spectroscopic taggants [13, 47]. Commercialisation of this technology may have been hindered by the relative cytotoxicity of metal ions used in the synthesis of quantum dot particles [48]. Efforts to reduce these potential damages to human health and the surrounding environment are currently underway through the development of heavy metal-free quantum dots [49].

However, there has been debate over whether fluorescent molecules should be included within tagging materials at all, as many offenders are now familiar with optical anti-counterfeit methods and are able to identify markers with obvious visible emissions [12]. In an attempt to resolve this issue, a number of taggants have recently been produced that can only be analysed via the use of Raman spectroscopy [50, 51]. Much like other forms of spectroscopic coding mechanisms, these reagents comprise compounds mixed in a specific combination to produce a unique spectral fingerprint (which in this case, is generated through the inelastic scattering of monochromatic laser light). The main advantage of this method is that Raman spectroscopy may also be used for the initial detection of tagging materials as well as identification, avoiding the requirement of additional tracing components that may result in unwanted discovery [12]. The sensitivity of such detection may also be greatly increased through the phenomenon of surface enhanced Raman scattering (SERS) by the direct conjugation of Raman-active compounds to a number of metallic nanoparticles [52].

Another coding technique designed by Duong et al. utilises the properties of nanomaterials beyond fluorescence involves deriving the individual melting-temperatures of a panel of solid particles within a taggant mixture to provide it with a unique thermal barcode [2]. The presence or absence of these so called 'phase-change' nanoparticles within a taggant is assessed using differential scanning calorimetry (DSC) in a linear thermal scan, which generates a specific melting-point peak for each component [7]. However, only a limited selection of nanoparticles has currently been developed for this purpose [53]. It is likely that this number will have to be increased in order for this system to possess the level of statistical differentiation required from a universal tagging system.

Aside from nanoparticle-based encoding methods, recent developments in novel tagging technology have also been achieved by the use of synthetic polypeptide sequences [54]. The principle of inferring identity through the unique order of successive amino acids has been theorised since the early 1980's [55]. However, only within the last year have methods been realised for their practical application and analysis within forensic marking materials [56]. Fig. 4 demonstrates this process, in which an oil-based medium containing hydrophilic peptide molecules is first applied onto the surface of an object. As a result of handling during criminal activity, this reagent is transferred to an individual, associating them with the offence. Detection by added fluorescence tracers is performed to permit recovery of the taggant by targeted swabbing. Hydrophilic peptides may be then isolated from the medium by simple liquid-liquid extraction, allowing their mass (and therefore sequence) to be determined by electrospray ionisation mass spectrometry (ESI-MS).

As an alternative form of single-component biomolecular coding, peptide taggants possess a number of advantages over current commercially available DNA-based marking systems. The statistical coding capacity of polypeptide chains is significantly greater than that of oligonucleotides, owing to the 22 different natural amino acids that may be used as individual sequence units (compared to the four bases possessed by DNA) [57]. Kydd reports that a string of 10 random amino acids can code up to  $4 \times 10^{13}$  unique sequences [55]. ESI-MS methods are also quicker than DNA sequencing (with processes from detection to analysis able to be completed in less than one hour) and are becoming increasingly more portable, which could allow the point-of-care testing of peptide tagging reagents. Peptides are additionally easy to produce at low cost, are environmentally harmless and relatively inert (with stability being further increased by simple chemical modifications) [57].

#### 4. Conclusions

By authenticating objects, deterring theft and monitoring illegal activity, forensic taggants continue to play a pivotal role in the reduction of criminal enterprise. This review has attempted to highlight the significant abilities of tagging materials to infer identity in an enormous range of products, as well as document the most prominent commercially available coding mechanisms used for achieving this aim.

Whilst it is quite clear that none of the commercial marking methods available currently possess every single one of the qualities demanded of a universally applicable forensic taggant, the recent research covered within this article demonstrates that concerted efforts towards taggant improvement are occurring.

The myriad of surfaces, environments and time-frames in which a taggant may be applied makes the technical innovation and validation of forensic marking materials relatively challenging. Only through continuing advances in material science, nanotechnology and instrumental analysis, can steps be made towards the development of a single versatile platform for object identification. It is hoped that this review will encourage researchers working within the field of analytical chemistry to take interest in taggant technology and engage with this development in order to make universal marking systems a reality.

#### References

- [1] H. Mills, S. Skodbo, P. Blyth, *Understanding organised crime: estimating the scale and the social and economic costs*, Research Report 73, 2013.
- [2] B. Duong, H. Liu, L. Ma, M. Su, Covert thermal barcodes based on phase change nanoparticles, *Sci. Rep.* 4 (2014) 5170.
- [3] J.J. Plimmer, Choosing the correct forensic marker(s) in currency, document, and product protection, *Proc. SPIE* 6075 (2006) 60750–60759.
- [4] S.H. Wise, J.R. Almirall, Chemical taggant detection and analysis by laser-induced breakdown spectroscopy, *Appl. Opt.* 47 (2008) G15–G20.
- [5] B.K. Mead, J. Hayward, B. Liang, M. Wan, T. Benson, J. Karp, The role of DNA-stained currency in gang robberies within the United Kingdom, *J. Forensic Sci.* 59 (2014) 264–267.



- [6] H.J. Bae, S. Bae, C. Park, S. Han, J. Kim, L.N. Kim, et al., Biomimetic microfingerprints for anti-counterfeiting strategies, *Adv. Mater.* 27 (2015) 2083–2089.
- [7] B. Duong, H. Liu, C. Li, W. Deng, L. Ma, M. Su, Printed multilayer microtaggants with phase change nanoparticles for enhanced labeling security, *ACS Appl. Mater. Interfaces* 6 (2014) 8909–8912.
- [8] J.W. Grate, R.G. Ewing, D.A. Atkinson, Vapor-generation methods for explosives-detection research, *Trends Anal. Chem.* 41 (2012) 1–14.
- [9] N. Kaish, J. Fraser, V. Otugen, S. Popovic, Method for remote detection of volatile taggant, Google Patents, 2000.
- [10] C. Smith, S. Strauss, L. DeFrancesco, DNA goes to court, *Nat. Biotech.* 30 (2012) 1047–1053.
- [11] P.A. Sermon, M.P. Worsley, Y. Cheng, L. Courtney, V. Shinar-Bush, O. Ruzimuradov, et al., Deterring gun crime materially using forensic coatings, *Forensic Sci. Int.* 221 (2012) 131–136.
- [12] M. Wang, B. Duong, H. Fenniri, M. Su, Nanomaterial-based barcodes, *Nanoscale* 7 (2015) 11240–11247.
- [13] D. Paunescu, W.J. Stark, R.N. Grass, Particles with an identity: tracking and tracing in commodity products, *Powder Technol.* 291 (2016) 344–350.
- [14] J.M. Perr, K.G. Furton, J.R. Almirall, Solid phase microextraction ion mobility spectrometer interface for explosive and taggant detection, *J. Sep. Sci.* 28 (2005) 177–183.
- [15] C.D. Loving, Composite microdot and method of forming the same, Google Patents, 1994.
- [16] G.F. Swiegers, B.W. Bootle, G.M. George, Method and system for identifying items, Google Patents, 2012.
- [17] P.K. Lee, Method of tagging with color-coded microparticles, Google Patents, 1977.
- [18] C. Outwater, Product authentication system, Google Patents, 2002.
- [19] D.J. Chandler, B.A. Lambert, J.J. Reber, S.L. Phipps, Precision fluorescently dyed particles and methods of making and using same, Google Patents, 2003.
- [20] W.J. Kerns, B. Brogger, J.L. Esterberg, Identification particles and system and method for retrospective identification using spectral codes, Google Patents, 2006.
- [21] N. Lawandy, A. Smuk, L. Olson, C. Zepp, Multi wavelength excitation/emission authentication and detection scheme, Google Patents, 2014.
- [22] T.G. Wilkinson, E. Dorland, Marking fuel for authentication, Google Patents, 2010.
- [23] T. Baque, Method of authenticating and/or identifying an article, Google Patents, 2013.
- [24] L. Jung, J.A. Hayward, M.B. Liang, DNA marking of previously undistinguished items for traceability, Google Patents, 2014.
- [25] G.M. George, Article marking system, Google Patents, 2009.
- [26] C.L. Butland, B. Baggot, Labeling technique for countering product diversion and product counterfeiting, Google Patents, 2000.
- [27] J. Brown, B. Reichert, Compositions for use in security marking, Google Patents, 2012.
- [28] R. Sleat, G. Van Lint, A marking apparatus for nucleic acid marking of items, Google Patents, 2012.
- [29] A.K. Deisingh, Pharmaceutical counterfeiting, *Analyst* 130 (2005) 271–279.
- [30] M.R. Whitehead, R. Peakall, Microdot technology for individual marking of small arthropods, *Agric. For. Entomol.* 14 (2012) 171–175.
- [31] L. Husáková, J. Šrámková, J. Staňková, P. Němec, M. Večeřa, A. Krejčová, et al., Characterization of industrial explosives based on the determination of metal oxides in the identification particles by microwave digestion and atomic absorption spectrometry method, *Forensic Sci. Int.* 178 (2008) 146–152.
- [32] H.H. Pham, I. Gourevich, J.E. Jonkman, E. Kumacheva, Polymer nanostructured material for the recording of biometric features, *J. Mater. Chem.* 17 (2007) 523–526.
- [33] N.H. Finkel, X. Lou, C. Wang, L. He, Barcoding the microworld, *Anal. Chem.* 76 (2004) 352–359.
- [34] O. Guillou, C. Daiguebonne, G. Calvez, K. Bernot, A long journey in lanthanide chemistry: from fundamental crystallogenes studies to commercial anticounterfeiting taggants, *Acc. Chem. Res.* 49 (2016) 844–856.
- [35] P. Przybylowicz, Black and Smokeless Powders, Technologies for Finding Bombs and the Bomb Makers, National Academy Press, Washington DC, 1998.
- [36] M. Cleary, Method of identifying a surface, Google Patents, 1998.
- [37] D.W. Britton, M.J. Wraith, Detection of chemicals by immunoassay, Google Patents, 1999.
- [38] L. Hood, D. Galas, The digital code of DNA, *Nature* 421 (2003) 444–448.
- [39] J.A. Hayward, J. Meraglia, DNA to safeguard electrical components and protect against counterfeiting and diversion, *Proc. ISTFA 4* (2011) 238–241.
- [40] J.P.L. Cox, Long-term data storage in DNA, *Trends Biotechnol.* 19 (2001) 247–250.
- [41] D. Paunescu, M. Puddu, J.O.B. Soellner, P.R. Stoessel, R.N. Grass, Reversible DNA encapsulation in silica to produce ROS-resistant and heat-resistant synthetic DNA 'fossils', *Nat. Protocols* 8 (2013) 2440–2448.
- [42] T. Lindahl, Instability and decay of the primary structure of DNA, *Nature* 362 (1993) 709–715.
- [43] A. Glover, N. Aziz, J. Pillmoor, D.W.J. McCallien, V.B. Croud, Evaluation of DNA as a taggant for fuels, *Fuel* 90 (2011) 2142–2146.
- [44] M. Puddu, D. Paunescu, W.J. Stark, R.N. Grass, Magnetically recoverable, thermostable, hydrophobic DNA/silica encapsulates and their application as invisible oil tags, *ACS Nano* 8 (2014) 2677–2685.
- [45] P. Reep, M.H. Liang, J.J. Sheu, System and method for authenticating multiple components associated with a particular product, Google Patents, 2006.
- [46] M. Zhou, S. Chang, C.P. Grover, Cryptography based on the absorption/emission features of multicolor semiconductor nanocrystal quantum dots, *Opt. Express* 12 (2004) 2925–2931.
- [47] G.M. Williams Jr., T. Allen, C. Dupuy, T. Novet, D. Schut, Optically coded nanocrystal taggants and optical frequency IDs, *Proc. SPIE* 7673 (2010) 76730–76744.
- [48] R. Hardman, A toxicologic review of quantum dots: toxicity depends on physicochemical and environmental factors, *Environ. Health Perspect.* 114 (2006) 165–172.
- [49] H. Li, W.Y. Shih, W.-H. Shih, Non-heavy-metal ZnS quantum dots with bright blue photoluminescence by a one-step aqueous synthesis, *Nanotechnology* 18 (2007) 205604.
- [50] R. Li, Y. Zhang, J. Tan, J. Wan, J. Guo, C. Wang, Dual-mode encoded magnetic composite microsphere based on fluorescence reporters and raman probes as covert tag for anticounterfeiting applications, *ACS Appl. Mater. Interfaces* 8 (2016) 9384–9394.
- [51] K.D. Osberg, M. Rycenga, G.R. Bourret, K.A. Brown, C.A. Mirkin, Dispersible surface-enhanced raman scattering nanosheets, *Adv. Mater.* 24 (2012) 6065–6070.
- [52] M. Natan, S. Norton, R. Freeman, S. Penn, I. Walton, Nanoparticles as covert taggants in currency, bank notes, and related documents, Google Patents, 2007.
- [53] D.C. Hyun, N.S. Levinson, U. Jeong, Y. Xia, Emerging applications of phase-change materials (PCMs): teaching an old dog new tricks, *Angew. Chem. Int. Ed. Engl.* 53 (2014) 3780–3795.
- [54] J. Gooch, C. Koh, B. Daniel, V. Abbate, N. Frascione, Establishing evidence of contact transfer in criminal investigation by a novel 'peptide coding' reagent, *Talanta* 144 (2015) 1065–1069.
- [55] P.H. Kydd, Polypeptides as chemical tagging materials, Google Patents, 1982.
- [56] J. Gooch, H. Goh, B. Daniel, V. Abbate, N. Frascione, Monitoring criminal activity through invisible fluorescent "peptide coding" taggants, *Anal. Chem.* 88 (2016) 4456–4460.
- [57] G. Dollinger, Nonbiological applications, in: K. Mullis, F. Ferre, R. Gibbs (Editors), *The Polymerase Chain Reaction*, Springer, Boston, 1994, pp. 265–274.



# Establishing evidence of contact transfer in criminal investigation by a novel 'peptide coding' reagent



James Gooch<sup>a</sup>, Clarissa Koh<sup>a</sup>, Barbara Daniel<sup>a</sup>, Vincenzo Abbate<sup>b</sup>, Nunzianda Frascione<sup>a,\*</sup>

<sup>a</sup> Analytical & Environmental Sciences Division, King's College London, Franklin Wilkins Building, 150 Stamford Street, London SE1 9NH, UK

<sup>b</sup> Institute of Pharmaceutical Science, King's College London, Franklin Wilkins Building, 150 Stamford Street, London SE1 9NH, UK

## ARTICLE INFO

### Article history:

Received 22 April 2015

Received in revised form

30 June 2015

Accepted 4 July 2015

Available online 6 July 2015

### Keywords:

Taggants

Forensic

Fluorophore

Peptide

Mass spectrometry

Coding reagent

## ABSTRACT

Forensic investigators are often faced with the challenge of forming a logical association between a suspect, object or location and a particular crime. This article documents the development of a novel reagent that may be used to establish evidence of physical contact between items and individuals as a result of criminal activity. Consisting of a fluorescent compound suspended within an oil-based medium, this reagent utilises the addition of short customisable peptide molecules of a specific known sequence as unique owner-registered 'codes'. This product may be applied onto goods or premises of criminal interest and subsequently transferred onto objects that contact target surfaces. Visualisation of the reagent is then achieved via fluorophore excitation, subsequently allowing rapid peptide recovery and analysis. Simple liquid–liquid extraction methods were devised to rapidly isolate the peptide from other reagent components prior to analysis by ESI–MS.

© 2015 Elsevier B.V. All rights reserved.

## 1. Introduction

The Home Office estimates that billions of pounds in social and economic costs arise every year as a direct result of organised criminal activity within the UK [1], the majority of which may be attributed to physical crimes, including significant theft and drug trafficking offences. Consequently the reduction of this activity remains a high priority for the UK government and its criminal investigators. This has been recently reflected by the growing number of commercially available forensic 'taggants', chemical reagents which may be applied to a particular surface in order to monitor items of criminal interest or associated activity [2,3]. These products, usually consisting of a coloured compound mixed within an oil-based medium, are easily transferred onto persons or objects that come into contact with marked surfaces. The subsequent detection of these compounds may then be used to form a logical association between an individual and the object in question, providing strong evidence of criminal intent. For 'covert' operations, in which indication of transfer should remain hidden from the offender, coloured materials may be replaced by fluorescent ones, the presence of which is only revealed through excitation with specialist light sources [4]. For example, the US based company Sirchie has developed several visible and fluorescent transferrable products designed for home and business owners to

protect their property from trespassers and to mark valuable goods that are likely to be the subject of theft. However, the disadvantage of such products is that they are comprised of a single standard formulation and cannot be used to differentiate the source of two separate objects on which the same medium has been applied, thereby limiting investigative potential.

Others have sought to address this problem by inserting a unique 'code' within the medium itself, which may be traced back to the original owner upon analysis. Many of the UV–vis emitting products developed by Cleary [5] contain a mixture of trace metals and organic moieties, with coding achieved by the unique combination in which the materials are present. Subsequent analysis of reagent samples recovered from individuals or stolen goods may then be able to determine the address to which that particular elemental composition is registered. However, the disadvantage of using a large variety of compounds within a single formulation is twofold; first that differences in chemical structure will cause molecules to be transferred at different rates. An incomplete or erroneous code may therefore be given in cases in which only trace amounts of medium are recovered that may not contain a full range of materials added to the formulation. This is further dependant on the type of surface on which the medium has been applied, making the estimation of transfer unpredictable. Furthermore, the relative stability of each molecule is also governed by these same structural differences, which will be different for each additive. Incorrect codes may once again be given if certain compounds break down prior to recovery and analysis. This would

\* Corresponding author.

E-mail address: [nunzianda.frascione@kcl.ac.uk](mailto:nunzianda.frascione@kcl.ac.uk) (N. Frascione).

be especially pertinent in scenarios where media have been applied on a long-term basis.

In recent years, Brown and Reichert [6] have made attempts to avoid using a coding system based upon multiple identifying additives by synthesising a number products that contain a unique synthetic DNA sequence. Despite negating differential transfer rates by using a single molecular identification system, the labile nature of DNA in exposed environmental conditions is well documented [7,8], making overall reagent stability a cause of concern. Moreover, sequencing DNA to determine its associated address can be expensive and time consuming, requiring trained personnel and large-size laboratory based instrumentation, as well as specific procedures for sample collection and preservation. This also applies to DNA synthesis itself, in which pure sequences are difficult to achieve in a high yield [9]. Although circumvention of this issue may be achieved through the PCR amplification of low amounts of starting material, extensive extraction procedures are likely to be required in order to remove any additional materials that may cause downstream inhibition.

We therefore present the development of a novel reagent used to establish evidence of contact transfer in order to provide a more robust method of monitoring items associated with criminal activity. The proposed reagent, like those previously described, is comprised of a fluorescent compound dispersed within an oil-based medium that is transferred to an offender or object that comes into contact with a marked surface. However, this reagent employs an innovative single molecule coding system based on the addition of a unique synthetic peptide. This peptide, made up of a short known sequence of amino acids, is specific to every formulation of the reagent produced, allowing its registration to an individual or address. Once transferred as a result of criminal activity, this product may be visualised by excitation with a specialist light source to produce fluorescence.

Unlike other DNA based coding systems, peptides can be isolated from the rest of the reagent components via a simpler liquid-liquid workup procedure. Analysis of the sequence may then be rapidly achieved via standard Electrospray Ionisation Mass Spectrometry, with each peptide generating a specific  $m/z$  ratio that can be used to determine its identity (Fig. 1). Such analysis affords significant advantages over time-consuming and costly DNA sequencing processes. Amino acids are also amenable to a wide array of structural modifications [10], which can either be used to further increase stability or increase the exclusivity of a coded sequence.

There are numerous potential applications for this reagent. In addition to linking a person to a target surface via primary transfer (i.e. surface-to-person), it may also be possible to deduce their subsequent activity by tracking secondary transfer (i.e. surface-to-

person-to-object). For example, if a person handles a specific item (i.e. a package or document) after coming into contact with the reagent, it may be possible to also link them to that item through secondary transfer.

This study focuses on the reagent design and investigating optimum conditions for its successful detection and analysis. The in-field stability of the final reagent was also monitored over a six-week period via application to a number of surfaces routinely encountered within forensic casework.

## 2. Materials and methods

### 2.1. Medium selection

Glycerol (Sigma Aldrich, UK), castor oil (Holland and Barrett, UK), a mixed hydrocarbon formulation (MHF) (Vaseline, UK) and a lithium-based lubricant (Comma, US) were spread evenly in 100 mg amounts on 2.5 cm<sup>2</sup> areas of aluminium foil, ceramic, plastic and glass. Surfaces were contacted after 24 h with a white vinyl gloved index finger at a standardised force of 30 g. A brief qualitative visual examination was used to establish the two media displaying greatest transfer. A quantitative indication of MHF and lubricant transference was achieved through the process described above but with surfaces weighed before and after contact to calculate deposited media.

### 2.2. Peptide synthesis

Peptide Ac-HSSKL was manually synthesised by Fmoc-Solid Phase Peptide Synthesis using 2-chlorotritylchloride resin (Sigma Aldrich, UK), which was swollen in dichloromethane (DCM) for 10 min prior to coupling. Acylation steps were conducted using six equivalents of Fmoc amino acids, pre-activated with N,N'-diisopropylcarbodiimide (DIPCDI) and ethyl (hydroxyimino)cyanoacetate (oxyma) in anhydrous N,N-dimethylmethanamide (DMF). Coupling reactions were conducted for 1 h and monitored by the picrylsulphonic acid test. Fmoc deprotection of coupled amino acids was achieved by treatment with 20% (v/v) piperidine in DMF for 10 min and confirmed by the picrylsulfonic acid test. Impurities and excess reagents were removed by washing at each stage with DMF, methanol and dichloromethane. Capping acetylation was performed by the addition of ten equivalents of acetic anhydride and twenty equivalents of N,N-diisopropylethylamine (DIPEA) in DMF. Resin cleavage was achieved through treatment with a 95:0.5:0.5:0.5:0.25 solution of trifluoroacetic acid (TFA): water: phenol: thioanisole (TA): triisopropylsilane (TIPS) for 3 h at room temperature. Next, the filtrate was concentrated under nitrogen at

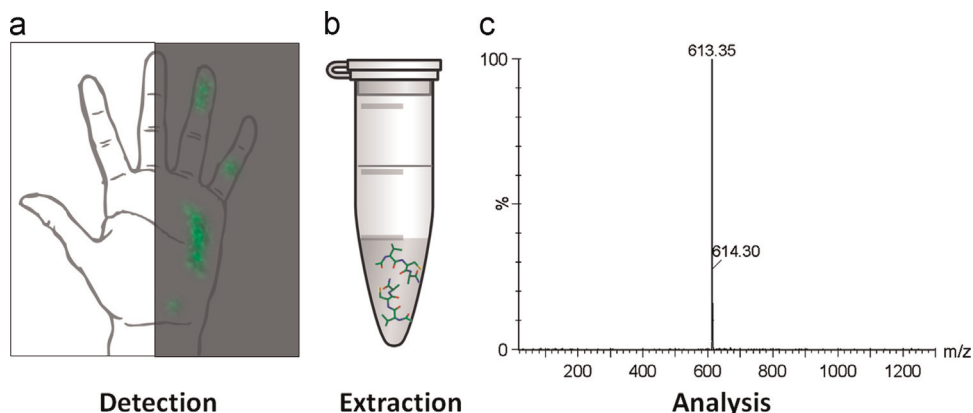


**Fig. 1.** Demonstration of peptide recovery and analysis: (a) the reagent is visualised through wavelength excitation, (b) the collected medium undergoes liquid-liquid extraction to isolate coding peptide, and (c) peptides are analysed and unique  $m/z$  value generated to identify sequence.

40 °C. Ice cold diethyl ether was added to precipitate peptides which were washed several times with diethyl ether, dissolved in 50% acetonitrile in water containing 0.1% TFA and finally freeze-dried for 24 h. The purity and correct mass of the final peptides were confirmed by analytical reverse-phase high-performance liquid chromatography (RP-HPLC) and ESI-MS, respectively. All peptide synthesis reagents were purchased from Bachem, UK and used as received.

### 2.3. Peptide concentration selection

Synthesised peptide in 1 mg, 2.5 mg and 5 mg quantities was mixed into 100 mg of MHF, which was subsequently spread evenly on a 2.5 cm<sup>2</sup> area of a glass microscope slide. Slides were contacted with a gloved finger as previously described (refer to the Medium Selection section). Portions of gloves containing transferred media were removed and placed in a 2 ml Eppendorf tube. A liquid–liquid extraction to isolate the peptide for analysis was performed through the addition of 1 ml hexane and 0.5 ml distilled water. Samples were vortexed and glove fragments removed before centrifugation at 13,000 rpm for two minutes. Aqueous phases were placed into a fresh tube. The original sample was then further extracted with an additional 0.5 ml of distilled water. Both aqueous layers were combined before undergoing counter extraction with 1 ml of hexane. After removal of hexane layer, formic acid was added to the aqueous phase at a final concentration of 0.1% v/v prior to ESI-MS analysis using a Waters ZQ micromass 2000 mass spectrometer.

### 2.4. Fluorophore studies

Rhodamine 110 (Sigma Aldrich, UK) and 7-amino-4-trifluoromethylcoumarin (AFC) (Santa Cruz Biotechnology, US) fluorophores were reconstituted in methanol to concentrations of 10 mg/mL, 1 mg/mL and 0.1 mg/mL. 50 µl of each fluorophore concentration was added to 100 mg of MHF and mixed thoroughly before being spread evenly on a 2.5 cm<sup>2</sup> area of a glass microscope slide. Samples were visualized in the dark using an Olympus SZX12 fluorescence microscope (Tokyo, Japan) and photographed with an internal CCD camera. Photostability of both fluorophore-containing media was monitored once a week over a six week period. Lastly, 50 µl of 0.1 mg/mL rhodamine solution was added to 100 mg of peptide-mixed media before extraction and ESI-MS analysis.

### 2.5. Stability studies

40 mg of peptide-mixed medium was applied to surfaces of aluminium foil, ceramic, plastic and glass, cotton, polyester, leather and denim. Liquid–liquid extractions were performed as previously described in order to isolate peptides for ESI-MS analysis. Extractions were performed from each surface once a week for a period of six weeks.

## 3. Results and discussion

### 3.1. Transferability studies

The initial priority of every forensic taggant reagent design is the selection of an appropriate medium in which fluorophore and coding additives are dispersed. It is crucial that the medium transfers well by itself so that identification components carried within it will be of a high enough concentration for subsequent analysis. Additionally, media should not dry out, allowing them to be applied over extended periods of time, as well as transparent,

to avoid detection within covert investigation.

Glycerol, castor oil, MHF and a lithium-based lubricant were chosen to be investigated as potential media due to their low volatility, odourless and colourless properties. Each medium was applied to four surfaces that are often encountered within forensic casework (i.e. plastic, ceramic, glass and metal) before being contacted with a gloved finger after a period of 24 h (ESI Fig. S1). This was carried out to ensure that the final reagent is able to operate efficiently in a range of environments where it is likely to be applied.

Both castor oil and glycerol samples showed significant decreases in transfer after a 24 h time period, which was especially evident in samples taken from the glass and metal surfaces. This may be due to the fact that both substances are known to undergo a high degree of hydrogen bonding [11,12]. Whilst theoretically the high viscosity caused by this bonding should allow for greater transfer, it is possible that the extensive intermolecular interaction also caused molecules to aggregate, leading to a more uneven transfer. In contrast, both semi-solid MHF and lubricant media showed greatest and most consistent transferability over time, likely benefiting from fixed molecular arrangements. These substances were therefore taken forward for further quantitative indication of transfer efficiency, in which the average percentage of media transferred was calculated by recording of surface weight before and after contact (Fig. 2).

Quantitative studies confirmed transfer efficiency in both semi-solid media. Whilst a two-way ANOVA test determined transfer rates between lubricant and MHF were not statistically significant ( $P$ -value=0.178309), a slightly higher percentage transfer on average across the majority of surfaces selected MHF as the basis for further reagent development. Whilst the use of a gloved finger allowed us to conduct this study within the remit of existing ethical approval, further studies are currently in progress to assess this transfer via skin contact.

### 3.2. Peptide sequence selection

With non-polar hydrocarbon-based MHF chosen as the basis for this reagent, use of a hydrophilic peptide coding sequence would allow for its rapid isolation via a simple liquid–liquid extraction. Amino acid sequence HSSKL was therefore synthesised after GenScript peptide property calculator analysis determined its suitable hydrophilicity through the inclusion of histidine and lysine residues. N-terminal acetylation was also performed to enhance peptide solubility during extraction. This peptide length was

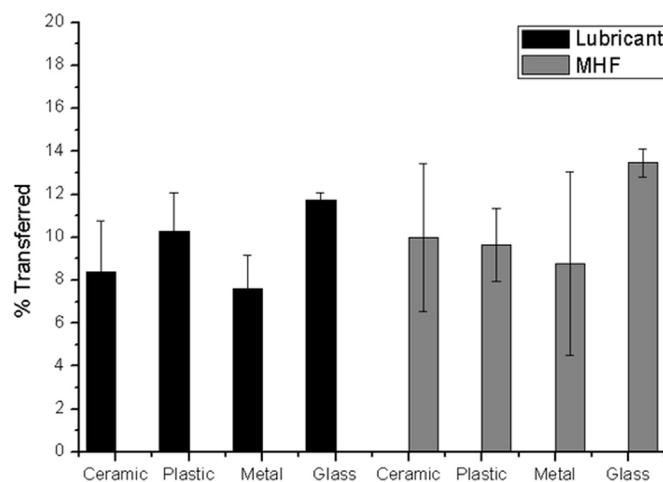
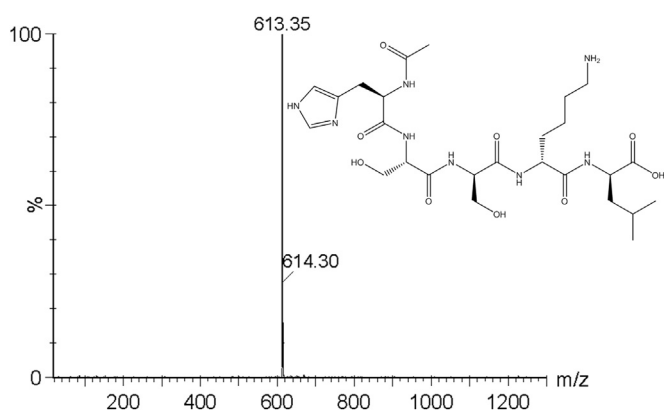


Fig. 2. Quantitative analysis of MHF and lubricant transfer rates from forensically relevant surfaces through touch contact (error bars represents standard deviation between replicates).





**Fig. 3.** Positive ESI-MS spectrum of synthesised peptide Ac-HSSKL and inset: peptide structure and calculated  $m/z$  ratio 612.32.

chosen such that synthesis would be rapid and inexpensive, while allowing enough variability to ensure unique coding. Additionally, a search of the RCSB Protein Databank yielded no results for this sequence, thus reducing the risk of generating false positive results from naturally occurring peptides.

RP-HPLC analysis was performed to cheque for peptide purity (data not shown) and an analysis via ESI-MS was conducted to confirm that the desired product had been obtained (Fig. 3). Extraction protocols were subsequently devised with hexane and distilled water selected to isolate the peptide in an aqueous phase and separate the remainder of the non-polar medium prior to further analysis.

### 3.3. Peptide concentration selection

With competing interests in designing a reagent that allows for maximum sequence detectability, whilst simultaneously being inexpensive to produce, it is crucial to determine the most suitable concentration of peptide required for successful MS analysis. After confirming identity, 5 mg of synthesised peptide was mixed into MHF (100 mg) and spread on glass slides. Liquid-liquid extraction was conducted on the traces of reagent obtained from primary transfer onto a glove, and the extract was analysed via ESI-MS. All samples and replicates generated positive results with peptides still remaining easily detectable in concentrations reduced to 2.5 mg and even 1 mg (ESI, Fig. S2). Based on the results obtained in the transferability studies, following liquid-liquid extraction an aqueous solution of the peptide at a concentration of  $\sim 150 \mu\text{g/ml}$  (corresponding to the lowest amount of peptide employed in the present study) was used for the ESI-MS analysis. Our research group is currently engaged in establishing the lowest amount of peptide that may be added to a reagent in which full detection may be achieved. This is focusing on the application of High Resolution Mass spectrometry, which, in many cases, has detected a number of similar peptides to a femtomolar concentration [13].

### 3.4. Fluorophore studies

Ideally, fluorophores incorporated into forensic taggants should allow for easy visualisation as well as an increased resistance to exposed environmental conditions. Rhodamine 110 and AFC, both noted for their fluorescence lifetimes, quantum yield and photostability [14,15] were therefore investigated as additives for the overall visualisation of the reagent upon transfer. In this study, fluorophores were added independent to peptide concentration to provide end users with more flexibility over how the reagent is applied.

Both fluorophores were mixed into MHF as stock solutions

starting at 10 mg/ml concentrations. While all samples displayed an intense emission under appropriate fluorescence microscopy filtration (ESI, Fig. S3), unexcited formulations still exhibited an obvious visual colouration inappropriate for marking surfaces within a covert scenario. Thus, both solutions were diluted to a concentration of 0.1 mg/ml in which no colour was observed under visible light but fluorescence remained highly detectable. This fluorescence was qualitatively monitored over a period of six weeks and was found to remain detectable.

With appropriate fluorophore concentrations established, Rhodamine 110 was added to a sample of peptide-mixed media to test final reagent performance, before being successfully extracted and analysed by ESI-MS as previously described (ESI, Fig. S4). Rhodamine is consequently present in the final mass spectrum due to its affinity for the analysed aqueous extraction phase. As an identical fluorophore is added to every formulation of reagent produced, rhodamine presence will not add value to the unique coding system provided by the peptide. However, the detection of a water-soluble fluorophore may infer added confidence that a successful extraction has taken place. Whilst advantageous stability and emission properties selected Rhodamine-110 for use within the scope of this study, any fluorescent compound exhibiting desirable properties may be used as a replacement detection element, further increasing the versatility of a final reagent for surface application.

### 3.5. Stability studies

As the majority of forensic taggants are applied to surfaces for extensive periods of time, it is important that coding peptides stored within a reagent remain stable. This is especially pertinent in those that are left within exposed environmental conditions. Samples of peptide-mixed medium were therefore applied once again to aluminium foil, ceramic, plastic and glass, and left without the application of atmospheric or temperature controls (laboratory temperature and humidity:  $23 \pm 2^\circ\text{C}$ ,  $25 \pm 5\%$ ) for a period of six weeks before undergoing extraction and analysis at one week intervals. Furthermore, as high coding sequence stability is crucial in the period between surface contact and reagent recovery, the same procedure was repeated on cotton, denim, polyester and leather substrates to simulate typical contact with clothing. All peptides proved to be detectable over the six week period on all eight surfaces with no evidence of deterioration (ESI, Fig. S5). Whilst the scope of this particular study aimed to assess the possibility of peptide breakdown as a result of time, subsequent research examining the effect of temperature and moisture upon reagent persistence is needed to ensure full validation, and is currently being undertaken by our research group. A larger validation study will be able to investigate resistance of the reagent to harsh environmental conditions so that the efficiency of the technique may be fully demonstrated.

## 4. Conclusion

We have successfully designed and developed a reagent for the rapid and specific determination of contact transfer arising as a result of criminal activity. When applied to surfaces this reagent becomes virtually undetectable to the naked eye, rendering it particularly useful within covert investigation. A novel two-step identification system was employed; firstly the area in which the reagent has been deposited is initially visualised through fluorescence excitation, before being subsequently recovered for standard MS analysis to reveal the identity of a unique registered peptide sequence. This process offers extremely rapid results compared to currently available reagents, with recovery, extraction and analysis



performed in less than two hours. Analysis time is further likely to be decreased considering continuing advances in portable MS techniques. Environmental stability of the reagent was also proven over a six-week period.

Our research group is currently investigating a number of further refinements to this reagent, including the use of a combination of fluorophores which emit at different wavelengths to confer added discrimination against possible background fluorescence. This is centred upon the application of compounds emitting in the IR region of the electromagnetic spectrum which offenders, now knowledgeable of UV-based marking, would be unable to detect. While naturally occurring amino acids were used within this study, investigation has been undertaken to examine the benefits of incorporating unnatural or modified peptide sequences. This would not only serve to increase sequence distinctiveness but is also likely to enhance peptide resistance to hydrolytic enzymes present in biological fluids [16].

### Acknowledgements

This work was conducted in collaboration with the National Crime Agency (NCA), UK.

### Appendix A. Supplementary material

Supplementary data associated with this article can be found in the online version at <http://dx.doi.org/10.1016/j.talanta.2015.07.014>

### References

- [1] M. Levi, Thinking about organised crime, *RUSI J.* 159 (2014) 6–14.
- [2] M. Puddu, D. Paunescu, W.J. Stark, R.N. Grass, Magnetically recoverable, thermostable, hydrophobic DNA/silica encapsulates and their application as invisible oil tags, *ACS Nano* 8 (2014) 2677–2685.
- [3] B. Duong, H. Liu, L. Ma, M. Su, Covert thermal barcodes based on phase change nanoparticles, *Sci. Rep.* 4 (2014).
- [4] L. Li, Technology designed to combat fakes in the global supply chain, *Bus. Horiz.* 56 (2013) 167–177.
- [5] C. Michael, Google Patents, 1998.
- [6] J. Brown, B. Reichert, Google Patents, 2012.
- [7] R. Alaeddini, S.J. Walsh, A. Abbas, Forensic implications of genetic analyses from degraded DNA—a review, *Forens. Sci. Int.: Genet.* 4 (2010) 148–157.
- [8] K. Bender, et al., Preparation of degraded human DNA under controlled conditions, *Forens. Sci. Int.* 139 (2004) 135–140.
- [9] R. Carlson, The changing economics of DNA synthesis, *Nat. Biotechnol.* 27 (2009) 1091.
- [10] E. Baslé, N. Joubert, M. Pucheault, Protein chemical modification on endogenous amino acids, *Chem. Biol.* 17 (2010) 213–227.
- [11] D.S. Ogunniyi, Castor oil: a vital industrial raw material, *Bioresour. Technol.* 97 (2006) 1086–1091.
- [12] R. Chelli, P. Procacci, G. Cardini, S. Califano, Glycerol condensed phases Part II. A molecular dynamics study of the conformational structure and hydrogen bonding, *Phys. Chem. Chem. Phys.* 1 (1999) 879–885.
- [13] R. Kiyonami, M. Zeller, V. Zabrouskov, Quantifying Peptides in Complex Mixtures with High Sensitivity and Precision Using a Targeted Approach with a Hybrid Linear Ion Trap-Orbitrap Mass Spectrometer.
- [14] M. Beija, C.A. Afonso, J.M. Martinho, Synthesis and applications of rhodamine derivatives as fluorescent probes, *Chem. Soc. Rev.* 38 (2009) 2410–2433.
- [15] R.E. Smith, E.R. Bissell, A.R. Mitchell, K.W. Pearson, Direct photometric or fluorometric assay of proteinases using substrates containing 7-amino-4-trifluoromethylcoumarin, *Thromb. Res.* 17 (1980) 393–402.
- [16] J. Frackenpohl, P.I. Arvidsson, J.V. Schreiber, D. Seebach, The outstanding biological stability of  $\beta$ - and  $\gamma$ -peptides toward proteolytic enzymes: an in vitro investigation with fifteen peptidases, *ChemBioChem* 2 (2001) 445–455.

# Monitoring Criminal Activity through Invisible Fluorescent “Peptide Coding” Taggants

James Gooch,<sup>†</sup> Hilary Goh,<sup>‡</sup> Barbara Daniel,<sup>†</sup> Vincenzo Abbate,<sup>§</sup> and Nunzianda Frascione<sup>\*,†</sup>

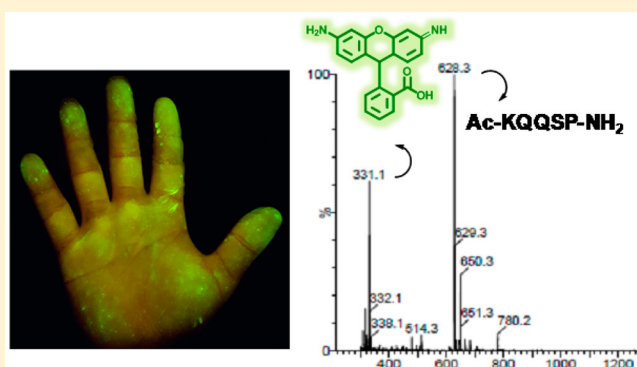
<sup>†</sup>Analytical and Environmental Sciences Division, King's College London, 150 Stamford Street, London, U.K., SE1 9NH

<sup>‡</sup>Department of Biological Sciences, National University of Singapore, 14 Science Drive 4, Singapore, 117543

<sup>§</sup>Institute of Pharmaceutical Science, King's College London, 150 Stamford Street, London, U.K., SE1 9NH

## Supporting Information

**ABSTRACT:** Complementing the demand for effective crime reduction measures are the increasing availability of commercial forensic “taggants”, which may be used to physically mark an object in order to make it uniquely identifiable. This study explores the use of a novel “peptide coding” reagents to establish evidence of contact transfer during criminal activity. The reagent, containing a fluorophore dispersed within an oil-based medium, also includes a unique synthetic peptide sequence that acts as a traceable “code” to identify the origin of the taggant. The reagent is detectable through its fluorescent properties, which then allows the peptide to be recovered by swabbing and extracted for electrospray ionization-mass spectrometry (ESI-MS) analysis via a simple liquid–liquid extraction procedure. The performance of the reagent in variable conditions that mimic the limits of a real world use are investigated.



Continuing efforts to reduce the substantial costs of crime on society have in recent years produced a number of highly effective criminal prevention technologies. The invention of forensic “taggants” is a successful example of such advances. Taggants are defined as materials that may act as a means of physically or chemically marking an item in a way that allows it to become uniquely identifiable.<sup>1</sup> Usually consisting of three molecular components, taggants will include a “coding” element (to infer uniqueness in the taggant), a system that allows the taggant to be visually detected, and a medium where these molecules are dispersed.

There are largely four forensic purposes for such materials. The first attempts to combat counterfeiting activities via the addition of a taggant to products (medicines, bank notes, official documents, etc.) to signify that they are of a genuine origin.<sup>2</sup> The second aims at marking valuable property (vehicles, electronic items) to associate them with a particular owner and discourage theft.<sup>3</sup> The third involves the surreptitious addition of taggants into illicit substances (illegal drugs, explosives), so that their distribution or use may be monitored by law enforcement agencies.<sup>4</sup> The last comprises the covert transfer of taggants to individuals during criminal activity in order to link them to a specific offense (e.g., handling firearms, trespassing).<sup>5</sup> The physical nature of a taggant reagent will be highly dependent on which of the above purposes it is required. For example, taggants employed in covert operations should be invisible to the naked eye, to avoid undesired detection by the offenders.<sup>3</sup> The medium of each taggant will

also vary depending on whether it needs to be easily transferred to an individual or remain anchored upon the product it is marking.<sup>3</sup> Only the coding element remains largely consistent across all tagging purposes.

One of the most popular methods to obtain this taggant coding is through the inclusion of unique DNA markers. Companies such as Applied DNA Sciences, Obiex, and SelectaDNA produce taggants containing either botanically derived or synthetic DNA oligonucleotides. The specific sequence of these oligonucleotides is then registered to a particular owner via an internal database.<sup>6</sup> When required, the taggant may be recovered to extract and “match” DNA to the owner’s information. While DNA taggants have been shown to decrease the number of Cash and Valuables in Transit (CViT) offenses,<sup>6</sup> limitations in their analysis have been identified. The extraction, amplification, and sequencing methods employed to isolate and match DNA are expensive and time-consuming. Moreover, the labile nature of DNA has raised significant concerns over the general stability of DNA taggants.<sup>7</sup> Research into the their use in monitoring fuel adulteration determined that short sequences of DNA within taggants had poor stability and were often susceptible to erroneous identification.<sup>8</sup>

Another recently emerging method of encoding focuses on the use of varying trace elements to identify taggants. Reagents

Received: January 20, 2016

Accepted: March 24, 2016

Published: March 24, 2016

produced by the U.K. manufacturer Smartwater contain a number of rare elements that are combined in unique formulations, allowing each taggant to be registered against a specific owner ID. After a reagent is detected (via the use of an incorporated fluorescent dye), laser ablation-inductively coupled plasma-mass spectrometry (LA-ICP-MS) is used to determine the individual formulation of the taggant and the owner that it is registered to (once again via internal database).<sup>1</sup> However, much like DNA-based coding systems, these tracer taggants are once again limited in their analysis. The use of multiple elements within a single taggant carries the potential of the formulation being incompletely recovered, which could then lead to erroneous identification. This problem stems from the differing transfer rates and stability of each individual tracer component, resulting from their chemical differences.

The development of a forensic taggant that is stable and can be rapidly and completely recovered is therefore critical to advancing crime reduction. In light of this, our research group recently suggested a novel “peptide coding” reagent (or peptide taggant) as an alternative to inefficient taggant analysis procedures.<sup>9</sup> This reagent has been designed to be covert and transferrable so that it may be used to mark an individual or object during criminal activity without the knowledge of the offender. Like the majority of taggants, our reagent comprises three distinct components. The base medium consists of a mixed hydrocarbon formulation (MHF) which is easily transferred to persons or clothing. Detection is achieved by Rhodamine-110 fluorophores, added in such a concentration as to make the taggant invisible under normal lighting conditions but highly fluorescent upon excitation by an appropriate light source. The specificity of this reagent (and main advantage over currently available taggants) is derived from the insertion of a unique peptide, where the amino acid sequence acts as an identifiable code for that particular taggant. The wide variety of natural and unnatural amino acids available ensures that the peptide may be sufficiently individual, without extensive length. Once the reagent is transferred as a result of criminal activity, it may be easily and rapidly recovered. First, areas of taggant presence may be indicated through fluorescence excitation, allowing complete recovery of the reagent by targeted swabbing. The peptide may then be isolated from the oil-based medium and swab via simple liquid–liquid extraction. The mass-to-charge ratio of the amino acid sequence is then revealed via electrospray ionization-mass spectrometry (ESI-MS), identifying the particular taggant.

While developed as an initial proof of concept, this taggant may have the potential to be used within criminal investigation to establish evidence of primary (object-to-person) and possibly even secondary (object-to-person-to-object) contact transfer. This work therefore involves a comprehensive investigation into the ability of peptide coding reagents to operate effectively within a real-world setting. Significant examination of the transfer, detection, recovery and stability of multiple peptide reagents was undertaken to demonstrate their advantages over currently available forensic taggants.

## ■ EXPERIMENTAL SECTION

**Peptide Synthesis.** Peptides Ac-KQQSP-NH<sub>2</sub> (sequence 1), Ac-HSSKL-COOH (sequence 2), and Ac-hsskl-COOH (sequence 3) were manually synthesized by Fmoc-solid phase peptide synthesis. NovaPEG rink amide (Merck Chemicals Ltd., U.K.) and 2-chlorotriyl chloride (Sigma-Aldrich, U.K.) resins were used to prepare sequences 1 and 2–3, respectively.

Resins were swollen in dimethylformamide (DMF) inside empty fritted polypropylene tubes for 30 min prior to coupling. All amino acid coupling steps for sequence 1 were performed using 4 equiv of Fmoc amino acids with *N,N'*-diisopropylcarbodiimide (DIC) and ethyl (hydroxyimino)cyanoacetate (Oxyma) in DMF in a molar ratio of 1:1:1 of amino acid, DIC, and Oxyma, respectively. The first coupling step for sequences 2–3 was performed using 1 equiv of Fmoc amino acid with 5 equiv of *N,N*-diisopropylethylamine (DIPEA) in dichloromethane (DCM). Subsequent coupling steps were performed using the same procedure utilized in the assembly of sequence 1. Coupling reactions were allowed to take place for 1 h with successful conjugation monitored by the picrylsulfonic acid test. After coupling, Fmoc deprotection of all amino acids was achieved via treatment with 20% (v/v) piperidine in DMF for 30 min and confirmed by the picrylsulfonic acid test. Impurities and excess reagents were removed at each stage via multiple washes using DCM and DMF. The N-terminus of each peptide was acetylated using 10 equivalents of acetic anhydride and 20 equivalents of DIPEA in DMF for 1 h. Resins were last treated with a solution of trifluoroacetic acid (TFA)–distilled water–phenol–thioanisole (TA)–triisopropylsilane (TIPS)–2,2'-(ethylenedioxy)diethanethiol in a 90:5:5:5:2.5:2.5 molar ratio for 3 h at room temperature to remove the completed peptides from the solid support. The filtrate was then concentrated under nitrogen at 40 °C before the addition of 10 equiv of ice cold diethyl ether to precipitate the peptides. The wash and precipitation process was repeated several times before the final obtained peptide pellets were freeze-dried for 24 h. The identities of the synthesized peptides were confirmed using a Waters/Micromass (Manchester, U.K.) ZQ ESI-mass spectrometer in positive ionization mode prior to use.

**Experimental Conditions.** The effects of four experimental conditions, (i) surface material, (ii) temperature, (iii) humidity, and (iv) fluorophore addition, on reagent stability were investigated. For monitoring the effect of surface material, peptide sequences 1–3 were mixed into MHF medium (Vaseline, U.K.) at a concentration of 2.5:100 mg of peptide–medium. Mixtures containing sequence 1 and 3 were then applied in 40 mg deposits onto 10 different surfaces (ceramic, glass, plastic, aluminum foil, wood, paper, denim, polyester, leather, and cotton) cut into 2 cm × 2 cm squares. The mixture in sequence 2 was applied in the same method to surfaces of wood and paper (as the stability of this sequence on the other 8 surfaces was already proven within the previous proof of concept study). The surfaces were then left exposed to standard laboratory conditions (temperature and humidity, 23 ± 2 °C; 40 ± 5%), constantly monitored using a data logger. Liquid–liquid extractions were then performed to isolate the peptides for ESI-MS analysis at time points of 2 weeks, 4 weeks, and 6 weeks for a total period of 6 weeks.

For experimental condition studies (ii), (iii), and (iv), the same concentration of peptide-MHF medium was applied to glass slides and exposed to their respective conditions. The effect of temperature was assessed via incubation of slides at both 4 and 39 °C and extracted at time points of 6 h, 24 h, 1 week, and 6 weeks. For the effect of humidity, surfaces were left in containers of 70% and 90% (as monitored by a hygrometer) and were once again extracted at the same time points as the temperature study. Humidity containers were prepared by enclosing wet paper towels within plastic boxes.



The effect on fluorophore presence on peptide detection was observed through the addition of Rhodamine-110 (Sigma-Aldrich, U.K.) to peptide-MHF at a concentration of 0.25:100 mg fluorophore–peptide-medium. This mixture was then applied in 40 mg deposits on glass slides, which were then exposed to the standard temperature and humidity conditions previously investigated. Extractions of fluorophore-peptide-MHF reagent were undertaken at time points of 3 weeks and 6 weeks for a total period of 6 weeks.

**Taggant Extraction and Analysis.** Extraction surfaces were placed into a 30 mL multipurpose container (Greiner Bio-One, U.K.) before the addition of 1 mL of hexane. Samples were vortexed for 1 min and the surfaces were removed using sterile forceps prior to the addition of 0.5 mL of distilled water. The samples were vortexed again and allowed to settle before the aqueous phase was removed into a fresh container via pipet. The original organic phase was then further extracted with an additional 0.5 mL of distilled water before both aqueous layers were pooled together. Counter extraction against the pooled aqueous layers was next performed with 1 mL of hexane. The final aqueous layer was then isolated into an Eppendorf tube before the addition of 0.1% v/v formic acid to enhance ionization. ESI-MS analysis of the samples was conducted using a Waters ZQ micromass 2000 mass spectrometer in positive ionization.

**Casework Application.** A thin layer of peptide reagent (containing sequence 2) was spread across a 25 cm × 25 cm glass tile to mimic a real-world application to a known surface. A transparent latex glove worn over the hand (with the glove preweighted) was then used to contact the surface at a standardized force of ~20 N (monitored by analytical balance). Transferred reagent was visualized using a Crime-lite hand-held light source (Foster and Freeman, U.K.) at an excitation wavelength of 460–510 nm and a supplied 495 nm viewing filter. The glove was then reweighed to assess the amount of taggant transferred upon physical contact.

**Depletion Series.** To establish the overall sensitivity of the reagent and determine its persistence after multiple contact transfers, a depletion series was prepared. A thin layer of peptide reagent (containing sequence 2) was once again spread over a glass tile before being contacted by a single gloved finger at a standardized force of ~10 N. A series of contacts after the initial reagent transfer were then performed by successively touching either 1, 2, 3, 4, or 5 clean glass slides with the glove. A sterile cotton swab of the entire surface of the finger was used to collect any taggant remaining at the end of each depletion series. Peptide sequence 2 was last extracted from all of the swabs and analyzed using the methods previously described.

## RESULTS AND DISCUSSION

**Peptide Synthesis.** Three different peptides were used to demonstrate the flexibility of the reagents coding system. These sequences were chosen due to their hydrophilicity, allowing them to be easily isolated from the nonpolar MHF medium by simple liquid–liquid extraction. The properties of each peptide, including hydrophilicity, were derived from GenScript's peptide property calculator (Table 1).

The sequences were also ensured to be non-naturally occurring using UniProt's BLAST function, thereby reducing the possibility of generating false positive results from ubiquitous environmental peptides.

Developing a coding system that is able to remain stable and recoverable over extended periods of time is a crucial aspect of

**Table 1. Summary of Peptide Characteristics Obtained from GenScript's Peptide Property Calculator**

<b>Peptide Sequence 1: Ac-KQQSP-NH<sub>2</sub> (L-amino acids)</b>	
GenScript PPC	MW = 627.69, attribute = basic (hydrophilic)
<b>Peptide Sequence 2: Ac-HSSKL-COOH (L-amino acids)</b>	
GenScript PPC	MW = 612.68, attribute = basic (hydrophilic)
<b>Peptide Sequence 3: Ac-hsskl-COOH (D-amino acids)</b>	
GenScript PPC	MW = 612.68, attribute = basic (hydrophilic)

taggant design. We therefore decided to explore the effect of a number of modifications on our peptide sequences, with the ideal aim of maximizing code detection post taggant recovery. N-terminal acetylation was carried out on all peptides to increase resistance to degradation by aminopeptidase activity.<sup>10</sup>

Further protection against enzymatic destruction was conferred by the C-terminal amidation<sup>11</sup> of sequence 1 (Ac-KQQSP-NH<sub>2</sub>) and the introduction of D-amino acids in peptide sequence 3 (Ac-hsskl-COOH). ESI-MS analysis was used to confirm the identity of the synthesized products, which all exhibited correct masses (see Figure S1).

**Experimental Conditions.** With popular uses in marking vehicles, objects, fabrics, and premises, the nature of the surface on which a taggant may be applied can be highly variable. It is consequently crucial that newly developed taggants demonstrate sufficient robustness to be detected and identified over extended periods of time, without being affected by the material on which they are deposited. The stability of all three peptide-MHF formulations was therefore monitored by their application on 10 different surfaces routinely encountered during forensic casework. All taggants were then left in standard laboratory conditions (temperature and humidity, 23 ± 2 °C; 40 ± 5%) before being extracted at several time points over a period of 6 weeks. Figure 1 shows the mass spectra of analyzed reagent samples containing peptide sequences 1, 2, and 3 from paper at the 6-week time point. The same results were achieved across all peptide, surface, and time combinations, with no observable reagent degradation (see Figures S2–S4).

Another facet of forensic taggant application that is highly variable is the environmental conditions to which a reagent may be exposed.<sup>12</sup> By marking items both outside and in sheltered locations, taggants are often subjected to a wide range of temperatures and humidities. However, the effect of such conditions on the detection and identification a taggant should ideally remain negligible. To establish the environmental resistance of our peptide coding reagent, formulations containing sequences 1–3 were deposited on glass slides and incubated over 6 weeks in temperatures of 4 and 39 °C or in humidities of 70% and 90%. Extraction and analysis of the reagents at various time points demonstrated that all peptides remained detectable despite incubation conditions, with no differentiation in the achieved mass spectra being displayed between samples (see Figures S5 and S6).

The foremost purpose of Rhodamine-110 addition to the peptide-MHF formulation is to allow taggants to be detected via fluorescence emission after transfer. This fluorescence not only quickly establishes evidence of contact between an object and a suspect but may also be used for a more targeted swabbing by indicating where identifying peptides are likely to be present. Moreover, as water-soluble Rhodamine-110 is coextracted with peptides into the same aqueous phase, a dual detection of the reagent is provided by the presence of both fluorophore and peptide ion peaks in the ESI-MS spectrum.

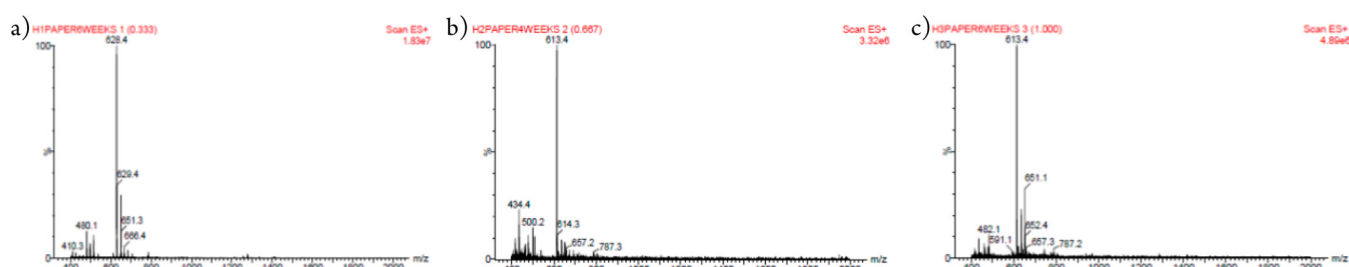


**Figure 1.** ESI-MS spectra of (a) peptide sequence 1, Ac-KQQSP-NH<sub>2</sub>, (theoretical  $[M + H]^+$   $m/z$  ratio = 628.34); (b) peptide sequence 2, Ac-HSSKL-COOH (theoretical  $[M + H]^+$   $m/z$  ratio = 613.33); and (c) peptide sequence 3, Ac-hsskl-COOH (theoretical  $[M + H]^+$   $m/z$  ratio = 613.33) reagent samples extracted 6 weeks after application to paper. Similar results were seen on all other surfaces.

To establish this dual-detectability, three final fluorophore-peptide-MHF formulations for each of the peptide sequences utilized were prepared and deposited on glass slides in the same manner previously described. Slides were exposed over 6 weeks to the standard laboratory temperature and humidity conditions already explored and were once again extracted and analyzed at a number of time points. Figure 2 displays both

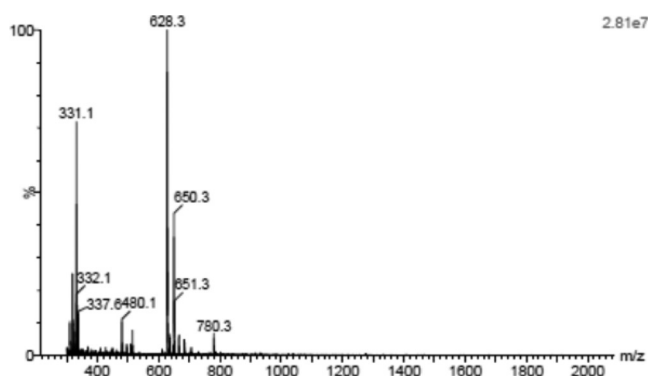


**Figure 2.** ESI-MS spectrum of sequence 1, Ac-KQQSP-NH<sub>2</sub> (theoretical  $[M + H]^+$   $m/z$  ratio = 628.34, theoretical  $[M + Na]^+$   $m/z$  ratio = 650.32) and Rhodamine-110 (theoretical  $[M + H]^+$   $m/z$  ratio = 331.11) extracted from full reagent samples applied to glass slides and incubated for 6 weeks in standard laboratory conditions.

fluorophore and peptide components detected by ESI-MS after extraction of final reagent (containing peptide sequence 1) after 6 weeks of standard laboratory exposure. In all cases, similar results were achieved regardless of peptide or environmental condition, with no observable fluorophore or peptide degradation (see Figures S7–S9).

**Casework Application and Depletion Series.** To successfully operate in the field, touch contacts must result in enough fluorophore and peptide transfer to ensure taggant visualization and identification, respectively. Demonstration of the reagents practical use in a real world scenario was therefore achieved by applying a thin layer of fluorophore-peptide-MHF formulation over a large glass tile, which was subsequently contacted by a transparent glove worn over the hand. As expected, the reagent remained imperceptible under natural light but was easily viewed upon the hand after illumination with a portable light source (Figure 3). Approximately 0.44 mg of taggant was transferred to each cm<sup>2</sup> of the glove's surface.

While this rate of transfer may be considered ideal after an initial contact, the amount of taggant recovered in a practical setting may actually be far less, depending upon the subsequent activity of the offender. For example, it is possible that the reagent may be removed if a suspect contacts other surfaces



**Figure 3.** Peptide coding reagent successfully transferred upon physical contact. Left: prior to visualization. Right: fluorescence emission upon excitation.

after touching a marked object, thereby diminishing the amount of peptide available for analysis. Designing a taggant to persist on an individual even after multiple contacts is therefore important. A depletion series was created to measure the overall retention of our reagent by contacting the tile previously prepared with a gloved finger. Taggant was then collected and recovered from the entire surface of the finger by direct swabbing and liquid–liquid extraction, respectively. This process was then repeated but with additional secondary contacts on clean glass slides (increasing from 1 to 5 contacts) prior to reagent recovery. ESI-MS analysis successfully detected the presence of both peptide and fluorophore ion peaks within all samples, establishing the excellent persistence of our reagent (see Figure S10).

## CONCLUSIONS

The ability of a novel “peptide coding” taggant to monitor contact transfer during criminal activity has been successfully established. The reagent is invisible to the naked eye but highly fluorescent when excited by an appropriate light source. If recovered from an individual, this reagent has the power to physically link a person to a specific object or offense through uniquely identifying amino acid sequences. The high transferability of the employed medium allows these peptides to persist on a person even after five additional contacts with other surfaces.

Remaining detectable and recoverable over a period of 6 weeks, our developed peptide taggant has proven to be successfully stable and resistant to all variable experimental conditions. A greater degree of confidence can therefore be given in the taggants efficacy to operate over extended periods of time on different surfaces and in a range of environments.

This reagent promises significant advantages over currently available forensic taggants; liquid–liquid extraction allows

coding sequences to be rapidly isolated with little expense. Taggant analysis via ESI-MS is also significantly less time-consuming than sequencing techniques used in DNA-based taggants and may be completed within 1 h of reagent recovery. Continuing advances in portable mass spectrometry technology are likely to result in this time being further reduced, by allowing analysis to be performed at the point of taggant discovery.

While not explored further within this study, this taggant was designed with a high intrinsic flexibility so that it may be easily adapted for application in a variety of crime reduction strategies. This is likely to center on the substitution of the reagents individual components to suit a specific purpose. For example, the replacement of Rhodamine-110 with a near-infrared fluorophores may provide enhanced contrast against certain colored or autofluorescent surfaces.<sup>13</sup> The discriminatory power of the taggants code may also be further increased by the use amino acids that feature unnatural modifications. While this reagent was developed for observing physical contact transfer during criminal activity, many taggants are designed to remain immobile upon the object they mark. Our peptide coding system may also be utilized in such an application by a simple change of dispersal media.

## ■ ASSOCIATED CONTENT

### ■ Supporting Information

The Supporting Information is available free of charge on the ACS Publications website at DOI: [10.1021/acs.analchem.6b00263](https://doi.org/10.1021/acs.analchem.6b00263).

ESI-MS spectra (Figure S1) of synthesized peptides and extracted reagent samples (Figures S2–S10) (PDF)

## ■ AUTHOR INFORMATION

### Corresponding Author

\*E-mail: [nunzianda.frascione@kcl.ac.uk](mailto:nunzianda.frascione@kcl.ac.uk). Phone: +442078484978.

### Notes

The authors declare no competing financial interest.

## ■ REFERENCES

- (1) Wise, S. H.; Almirall, J. R. *Appl. Opt.* **2008**, *47*, 15–20.
- (2) Plimmer, J. J. *Proc. SPIE* **2006**, 60750X.
- (3) Wang, M.; Duong, B.; Fenniri, H.; Su, M. *Nanoscale* **2015**, *7*, 11240–11247.
- (4) Duong, B.; Liu, H.; Ma, L.; Su, M. *Sci. Rep.* **2014**, *4*, 5170.
- (5) Sermon, P. A.; Worsley, M. P.; Cheng, Y.; Courtney, L.; Shinar-Bush, V.; Ruzimuradov, O.; Hopwood, A. J.; Edwards, M. R.; Gashi, B.; Harrison, D.; Xu, Y. *Forensic Sci. Int.* **2012**, *221*, 131–136.
- (6) Mead, B. K.; Hayward, J.; Liang, B.; Wan, M.; Benson, T.; Karp, J. *J. Forensic Sci.* **2014**, *59*, 264–267.
- (7) Puddu, M.; Paunescu, D.; Stark, W. J.; Grass, R. N. *ACS Nano* **2014**, *8*, 2677–2685.
- (8) Glover, A.; Aziz, N.; Pillmoor, J.; McCallien, D. W. J.; Croud, V. *B. Fuel* **2011**, *90*, 2142–2146.
- (9) Gooch, J.; Koh, C.; Daniel, B.; Abbate, V.; Frascione, N. *Talanta* **2015**, *144*, 1065–1069.
- (10) Carvalho, K. M.; Boileau, G.; Camargo, A. C. M.; Juliano, L. *Anal. Biochem.* **1996**, *237*, 167–173.
- (11) Rink, R.; Arkema-Meter, A.; Baudoin, I.; Post, E.; Kuipers, A.; Nelemans, S. A.; Akanbi, M. H. J.; Moll, G. N. *J. Pharmacol. Toxicol. Methods* **2010**, *61*, 210–218.
- (12) Penn, S. G.; Norton, S. M.; Walton, I. D.; Freeman, R. G.; Davis, G. *Proc. SPIE* **2004**, 5310, 337–340.
- (13) Umezawa, K.; Citterio, D.; Suzuki, K. *Anal. Sci.* **2014**, *30*, 327–49.